DOC.
E 1.20:
0026-DS/v.2/v 2

DOE/EIS-0026-DS

DRAFT SUPPLEMENT ENVIRONMENTAL IMPACT STATEMENT

Waste Isolation Pilot Plant

Volume 2 of 2

April 1989

U.S. DEPARTMENT OF ENERGY
Assistant Secretary for Defense Programs

UNIVERSITY OF
ILLINOIS LIBRARY
AT URBANA-CHAMPAIGN
BOOKSTACKS

DOE/EIS-0026-DS

DRAFT SUPPLEMENT ENVIRONMENTAL IMPACT STATEMENT

Waste Isolation Pilot Plant

Volume 2 of 2

April 1989

U.S. DEPARTMENT OF ENERGY
Assistant Secretary for Defense Programs
Washington, D.C. 20585

THIS DRAFT SEIS SHOULD BE SAVED BECAUSE PORTIONS THAT ARE NOT SIGNIFICANTLY REVISED WILL NOT BE REPRINTED IN THE FINAL SEIS

TABLE OF CONTENTS

VOLUME 2

Appendix	
A	WASTE ISOLATION PILOT PLANT WASTE ACCEPTANCE CRITERIA
B	WASTE CHARACTERISTICS
C	TRANSPORTATION EMERGENCY PLANNING
D	TRANSPORTATION AND TRANSPORTATION-RELATED RISK ASSESSMENTS
E	PERMEABILITY MEASUREMENTS AND BRINE INFLOW RATES
F	RADIOLOGICAL RELEASE AND DOSE MODELING FOR PERMANENT DISPOSAL OPERATIONS
G	TOXICITY PROFILES, RISK ASSESSMENT METHODOLOGY, AND MODELS FOR CHEMICAL HAZARDS
H	PUBLIC INFORMATION AND INTERGOVERNMENTAL AFFAIRS
I	METHODS AND DATA USED IN LONG-TERM CONSEQUENCE ANALYSES
J	BIBLIOGRAPHY
K	DOE READING ROOMS AND PUBLIC LIBRARIES

DOC.
E1.20
0026-DS/v.2

APPENDIX A

WASTE ISOLATION PILOT PLANT
WASTE ACCEPTANCE CRITERIA

TABLE OF CONTENTS

Section		Page
A.1	INTRODUCTION	A-1
	REFERENCES FOR APPENDIX A	A-9

LIST OF TABLES

Table		Page
A.1.1	Summary of WIPP Waste Acceptance Criteria	A-3

A.1 INTRODUCTION

The DOE has established waste acceptance criteria (WAC) for the safe handling and long-term disposal of TRU radioactive waste at the WIPP (FEIS Subsection 5.1). These criteria provide limits for the physical, radiological, and chemical composition of the waste in addition to specifications for waste packaging. Prior to any waste shipment departing any generator or storage facility, the shipment will be certified to meet the WAC. Similarly, the certification of shipments received at the WIPP will be verified prior to emplacement.

The WAC were established with the assumption that the radiological hazards of TRU mixed waste containing hazardous materials listed in 40 CFR Part 261, subparts C and D, are much greater than any hazards from associated chemical constituents (SEIS Appendix B). Therefore, the WAC focus on the radiological properties of the waste, and the chemical criteria of the WAC is primarily for the prevention of immediate hazards such as fire and explosion. The labeling and data package criteria of the WAC also provide for the identification of hazardous waste.

To ensure compliance with the WAC, the DOE has established the WIPP Waste Acceptance Criteria Certification Committee (WACCC) and requires that each facility certify that the WIPP-bound waste meets the WAC. Certification is directed by the following documents:

DOE 5820.2, "Radioactive Waste Management"

WIPP-DOE-069, "TRU Waste Acceptance Criteria for the Waste Isolation Pilot Plant"

WIPP-DOE-114, "TRU Waste Certification Compliance Requirements for Acceptance of Newly Generated Contact-Handled Wastes to be Shipped to the WIPP"

WIPP-DOE-120, "Quality Assurance Requirements for Certification of the TRU Waste for Shipment to WIPP"

WIPP-DOE-137, "TRU Waste Certification Compliance for Acceptance of Contact-Handled Wastes Retrieved from Storage to be Shipped to the WIPP"

WIPP-DOE-157, "Data Package Format for Certified Transuranic Waste for the Waste Isolation Pilot Plant (WIPP)"

WIPP-DOE-158, "TRU Waste Certification Compliance Requirements for Remote-Handled Wastes for Shipment to the WIPP"

SOP 6.6, "Quality Assurance Audit Program".

These documents may be reviewed in the DOE WIPP Project Office, Carlsbad, New Mexico and all DOE reading rooms.

Each waste-generating or storage site will prepare a TRU Waste Certification Plan that describes the Site Certification Program and how that program meets the WAC and the requirements of the documents listed above. Each facility will also prepare a TRU Waste Quality Assurance Plan that describes their QA program designed to meet the requirements of WIPP-DOE-120. Both of these plans must be approved by the WACCC.

Following the formal approval of Certification and Quality Assurance Plans for the waste generator or storage facility, a compliance verification audit will be performed by the WACCC. Subsequent periodic audits will be performed to verify that the facility is following the approved plans. Audit frequency will be determined by the Chairperson of the WACCC, in consideration of systematic requirements and facility certification status, but will generally be conducted on an annual basis at all facilities. The management of the generator or storage facility is expected to respond to findings and recommendations noted in the audit report, indicating the corrective action taken (or to be taken) to preclude recurrence. If subsequent site audits determine that corrective action has not been satisfactorily implemented, the WACCC will decertify the waste so that it cannot be accepted at the WIPP.

Since publication of the FEIS, the WAC have been modified twice, and these modifications are summarized in SEIS Subsection 2.3.1. A detailed discussion of the WAC and the basis for these criteria are provided in the TRU Waste Acceptance Criteria for the WIPP (DOE, 1989); a summary of the current WAC is provided in Table A.1.1.

Table A.1.1 Summary of WIPP Waste Acceptance Criteria

Criterion	Contact-handled TRU waste	Remote-handled TRU waste
Waste Containers	Waste containers for emplacement at the WIPP shall be noncombustible and meet all the applicable requirements of 49 CFR Part 173.412 for Type A packaging. Waste containers of various sizes shown to meet DOT Type A requirements by the methods detailed in the DOE Evaluation Document for DOT Type 7A, Type A Packaging (DOE, 1987) are acceptable to the WIPP. In addition, they shall have a design life of at least 20 yr from the date of certification. Any waste containers that appear to be bulged or otherwise damaged shall be recontainerd or overpacked in a container meeting the above requirements.	RH TRU waste containers shall be noncombustible and meet, as a minimum, the structural requirements and design conditions for Type A packaging contained in 49 CFR Part 173.412. Due to the special characteristics and application of the RH TRU canister, the compression test requirement in 49 CFR Part 173.465 (d) is not applicable. In addition, all RH TRU waste containers shall be certified to a WIPP approved specification to have a design life of at least 20 yr from the date of certification.
Waste Container Size	CH TRU waste containers or container assemblies shall not exceed 12 by 8 by 8.5 ft in overall length by width by height dimensions.	RH TRU waste containers shall be no larger than a nominal 26 inches in diameter with a maximum length of 10 ft, 1 inch including the pintle.
Waste Container Handling	All waste containers shall be provided with cleats, offsets, chains, or skids for handling by means of fork trucks, cranes, or similar handling devices. Lifting rings and other auxiliary lifting devices on the containers, if provided, shall be recessed, offset, or hinged in a manner which does not inhibit stacking the containers.	RH TRU waste containers shall be equipped with an axial lifting pintle of a design acceptable to the WIPP. The containers shall have no other lifting devices.
Specific Activity of Waste	For purposes of TRU waste certification, the 100 nCi/g TRU waste limit shall be interpreted as 100 nCi/g of waste matrix. The weight of added external shielding and the containers should be subtracted prior to performing the nCi/g calculation.	Same as CH TRU waste.
Waste Container Weight	CH TRU waste containers or container assemblies shall weigh no more than 21,000 lbs.	RH TRU waste containers shall weigh no more than 8,000 lbs.

Table A.1.1 Continued

Criterion	Contact-handled TRU waste	Remote-handled TRU waste
Nuclear Criticality	The fissile or fissionable radionuclide content for CH TRU waste containers shall be no greater than the following values, in Plutonium-239 fissile gram equivalents: 200 g/55-gal drum 100 g/30-gal drum 500 g/DOT 6M container 5 g/ft^3 in boxes, up to 350 g maximum For materials other than Plutonium-239, Uranium-235, and Uranium-233 which shall be treated as equivalent, fissile equivalents shall be obtained using ANSI/ANS-8. For materials other than Plutonium-239, U-235, and U-233 which shall be treated as equivalent, fissile equivalents shall be obtained using ANSI/ANS-8.15-1981.	The fissile or fissionable radionuclide content of RH TRU waste shall not exceed 1.9 g per liter (averaged over any 5 liters with a maximum 50 percent void space). If such reasonable distribution cannot be ensured, then the canister is limited to 240 g total (in Plutonium-239 fissile gram equivalents). The canister may be loaded with 17C or 17H drums, which will provide internal positioning and increase the limits to 100 g each for 30-gallon drums and 200 g each for 55-gallon drums.
Plutonium-239 Equivalent Activity[a]	Waste containers shall not exceed 1,000 Ci of Plutonium-239 equivalent activity (Plutonium Equivalent Curies or PE-Ci).	Same as CH TRU waste.
Surface Dose Rate	Waste containers shall have a maximum surface dose rate at any point no greater than 200 mRem/hr. Neutron contributions of greater than 20 mRem/hr to the total container dose rate shall be reported separately in the data container.	RH TRU waste containers shall have a surface dose rate at any point no greater than 1,000 Rem/hr. Neutron contributions are limited to 270 mRem/hr. Neutron contributions of greater than 20 mRem/hr to the total container dose rate shall be reported in the data container. WIPP prior approval is required before RH TRU canisters with a dose rate in excess of 100 Rem/hr but less than 1,000 Rem/hr may be shipped to the WIPP.
Surface Contamination	CH TRU waste containers or container assemblies shall have a removable surface contamination no greater than 50 pCi/100 cm^2 for alpha emitting radionuclides and 450 pCi/100 cm^2 for beta-gamma-emitting radionuclides.	Same as CH TRU waste.

Table A.1.1 Continued

Criterion	Contact-handled TRU waste	Remote-handled TRU waste
Thermal Power	Individual CH TRU waste containers in which the average thermal power density exceeds 0.1 watt per cubic foot (W/ft^3) shall have the thermal power recorded in the data container.	The thermal power generated by waste materials in any RH TRU waste container shall not exceed 300 W. The thermal power shall be recorded in the data container.
Gas Generation	Waste containers containing waste forms known or suspected of gas generation, such that a combination of overpressure and explosive mixtures might damage the container in the long term, shall be provided with an appropriate method of pressure relief. Any liner other than plastic bagging shall be provided with positive gas communication to the outer container. Each CH TRU waste shipper shall provide the following data for each waste container: ▪ Total activity (alpha Ci) ▪ Waste form description (from Certification Plan) ▪ Mass and volume percent of organic content For purposes of transportation and emplacement (short term), there will be no mixture of gases or vapors in any container which could, through any credible spontaneous increase of heat or pressure, or through an explosion, significantly reduce the effectiveness of the packaging.	All RH TRU waste containers shall be vented.
Labeling	In addition to DOT labeling requirements, each waste container shall be uniquely identified by means of a label permanently attached in a conspicuous location. The container identification number (to be standardized) shall be in medium to low density Code 39 bar code symbology per MIL-ST-1189 in characters at least 1 inch high, and alpha-numeric characters at least 1/2 inch high.	Each RH TRU waste container shall be uniquely identified by means of an identification number permanently attached to the container in a conspicuous location using characters at least 2 inches high. The label must be reasonably expected to remain legible and affixed to the container for a period of 10 yr under anticipated conditions of interim storage before shipment to the WIPP and emplacement underground.

Table A.1.1 Continued

Criterion	Contact-handled TRU waste	Remote-handled TRU waste
	The label must be reasonably expected to remain legible and affixed to the container for a period of 10 yrs under anticipated conditions of interim storage before shipment to the WIPP and emplacement underground.	
Data Package	There shall be transmitted to the WIPP operator in advance of shipment, a Data Package/Certification attesting to the fact that the waste container meets the requirements of these criteria. This Data Package/Certification shall be based upon a quality assurance program subject to audit and verification and shall provide information on the items specified below: ▪ Container identification number ▪ Container assembly identification number (if applicable) ▪ Date of waste container certification ▪ WAC exception number (if applicable) ▪ Waste generation site ▪ Date of packaging (closure date) ▪ Maximum surface dose rate in mRem/hr and specific neutron dose rate if greater than 20 mRem/hr. ▪ Weight (in kilograms) ▪ Container type ▪ Physical description of waste form (content code) ▪ Assay information, including PE-Ci, alpha Ci, and Plutonium-239 fissile gram equivalent content ▪ Radionuclide information including radionuclide symbol, quantity, and measure (in g or Ci) ▪ Radioactive mixed waste [identity and quantity of hazardous waste characteristic(s)] ▪ Weight and volume percent of organic materials content ▪ Measured or calculated thermal power (if over 0.1 W/ft^3)	The data package requirements for RH TRU waste shipments are the same as those for CH TRU waste shipments with the following exceptions: ▪ The container assembly identification requirement does not apply to RH TRU waste shipments. ▪ The cask number shall be used in place of the TRUPACT number.

Table A.1.1 Continued

Criterion	Contact-handled TRU waste	Remote-handled TRU waste
	▪ Shipment number ▪ Date of shipment ▪ Vehicle type ▪ TRUPACT number(s) ▪ Other information considered significant by the shipper ▪ Name of certifying official who approves the Data Package	
Activity Density	No criterion.	The maximum activity concentration for a RH TRU waste container shall not exceed 23 Curies/liter (Ci/l). The concentration may be averaged over the waste container.
Immobilization	Powders, ashes and similar particulate waste materials shall be immobilized if more than 1 weight percent of the waste matrix in each container is in the form of particles below 10 microns in diameter, or if more than 15 weight percent is in the form of particles below 200 microns in diameter.	Same as CH TRU waste.
Liquid Wastes	CH TRU waste shall not be in free-liquid form. Minor liquid residues remaining in well drained bottles, cans, and other containers are acceptable.	Same as CH TRU waste.
Pyrophoric Materials	Pyrophoric materials, other than radionuclides, shall be rendered safe by mixing with chemically stable materials (e.g., concrete, glass, etc.) or processed to remove their hazardous properties. No more than 1 percent by weight of the waste in each container may be pyrophoric forms of radionuclides, and these shall be generally dispersed in the waste.	Same as CH TRU waste.
Explosives and Compressed Gases	CH TRU waste shall contain no explosives or compressed gases as defined by 49 CFR Part 173, Subparts C and G.	Same as CH TRU waste.

Table A.1.1 Concluded

Criterion	Contact-handled TRU waste	Remote-handled TRU waste
Radioactive Mixed Waste	CH TRU wastes shall contain no hazardous wastes unless they exist as co-contaminants with transuranics. Waste containers containing hazardous materials shall be identified with the appropriate DOT label. TRU-contaminated corrosive materials shall be neutralized, rendered non-corrosive, or containerd in a manner to ensure container adequacy through the design lifetime. Hazardous materials to be reported are listed in 40 CFR Part 261, Subparts C and D.	Same as CH TRU waste.

[a] The Plutonium Equivalent Curies (PE-Ci) concept is described in Appendix F.

REFERENCES FOR APPENDIX A

DOE (U.S. Department of Energy), 1989. "TRU Waste Acceptance Criteria for the Waste Isolation Pilot Plant," WIPP-DOE-069, Revision 3, U.S. Department of Energy, Carlsbad, New Mexico.

DOE (U.S. Department of Energy), 1987. The DOE Evaluation Document for DOT Type 7A, Type A Packaging, MIL 3245/DOE/DP 0053-HI, Mound Applied Technology, Dayton, Ohio.

APPENDIX B

WASTE CHARACTERISTICS

TABLE OF CONTENTS

Section		Page
B.1	INTRODUCTION	B-1
B.2	TRANSURANIC RADIONUCLIDE INVENTORY	B-2
	B.2.1 Inventory	B-2
	B.2.2 Characteristics	B-7
B.3	HAZARDOUS CHEMICAL CONSTITUENTS	B-22
	B.3.1 CH TRU Mixed Waste	B-22
	B.3.2 RH TRU Mixed Waste	B-24
REFERENCES FOR APPENDIX B		B-28

LIST OF TABLES

Table		Page
B.2.1	Projected total radionuclide inventories	B-3
B.2.2	Estimated quantity of CH TRU waste in retrievable storage or projected to be generated through the year 2013	B-4
B.2.3	Estimated quantity of RH TRU waste in retrievable storage or projected to be generated through the year 2013	B-5
B.2.4	Retrievably-stored and newly generated TRU waste	B-6
B.2.5	Summary of average TRU waste characteristics	B-8
B.2.6	Average CH TRU waste trailer-load radioactivity (Curies)	B-9
B.2.7	Average RH TRU waste trailer-load radioactivity (Curies)	B-10
B.2.8	Total estimated activity (Curies) of CH TRU per trailer-load for Rocky Flats Plant	B-12
B.2.9	Total estimated activity (Curies) of RH TRU per trailer-load for Los Alamos National Laboratory	B-13
B.2.10	Representative radionuclide content of CH TRU waste drum	B-16
B.2.11	Representative radionuclide content of CH TRU waste Standard Waste Box (SWB)	B-17
B.2.12	Representative radionuclide content of RH TRU waste container	B-18
B.2.13	Initial CH waste inventory for long-term performance analysis	B-19
B.2.14	Modified inventory used in long-term performance analysis	B-20
B.3.1	Estimated quantities of TRU mixed waste (by waste form) from the Rocky Flats Plant in Colorado	B-25
B.3.2	Estimated maximum concentrations of hazardous chemical constituents in CH TRU mixed waste from the Rocky Flats Plant in Colorado	B-26

B.1 INTRODUCTION

Since 1980, a concerted effort has been made to more accurately characterize DOE TRU waste, resulting in a better knowledge of the waste forms and quantities at the generator and storage sites. This effort is continuing particularly with regard to RH TRU waste. This appendix describes the estimated volumes, estimated curie content, radionuclide distribution, and hazardous chemical constituents of the TRU waste that may be received at the WIPP as best as these characteristics are known currently.

The WAC differentiates between contact-handled (CH) and remote-handled (RH) TRU wastes. CH TRU waste must have a surface radiation dose rate below 200 mrem/hr at the package surface. This waste can be handled directly by personnel without excessive radiation exposure. RH TRU waste has surface radiation dose rates between 200 mrem/hr and 1000 rem per hour.

B.2 TRANSURANIC RADIONUCLIDE INVENTORY

Sampling and measurement of waste by radiography, nuclear assaying, and other methods and more stringent tracking and record keeping requirements have resulted in a more accurate definition of the TRU waste that may be shipped to the WIPP. In addition, the definition of TRU waste has changed. Prior to 1982, TRU waste was defined as having greater than 10 nCi/g of alpha-emitting radionuclides; TRU waste is presently defined as having greater than 100 nCi/g of alpha-emitting radionuclides. This change has resulted in reclassification of a considerable amount of TRU waste to low-level waste that is not eligible for shipment to the WIPP.

The source term (i.e., the actual amount of radiation released) for a particular release scenario is the material-at-risk times the fraction of that material which is released (release fraction) into the environment. Material-at-risk is any TRU waste material and any surface contamination on a TRU waste package that is subject to potential releases. Changes in the inventory, material-at-risk, and/or release fraction directly affect the potential environmental impacts of WIPP operations.

B.2.1 INVENTORY

As mentioned in Section 3.0 of this SEIS, in 1980 the WIPP was designed to receive approximately 6.2 million ft^3 of CH and 250,000 ft^3 of RH waste. DOE annually publishes an Integrated Data Base (IDB) summarizing the total projected radionuclide waste inventory and volume.

From the 1987 IDB (DOE,1987), it is anticipated that approximately 5.6 million ft^3 of CH TRU and 93,000 ft^3 of RH TRU waste are presently in retrievable storage or will be newly-generated through the year 2013. The currently projected total radionuclide inventories (Curies) for the 5.6 million ft^3 of CH and 93,000 ft^3 of RH are presented in Table B.2.1. Waste volumes are shown by site in Tables B.2.2 and B.2.3.

In order to conservatively bound the potential impacts, the maximum assumed volume of TRU waste of 6.45 million ft^3 (CH and RH TRU) has been utilized for analysis in this SEIS. Table B.2.4 projects the site-by-site assumed scale-up of stored and newly-generated waste volumes for this 6.45 million ft^3.

Prior to departing generator sites and transportation to the WIPP, waste must be certified to meet the WIPP WAC (DOE, 1989). These criteria have been refined as a result of further analyses of potential hazards associated with long-term waste storage and according to NRC and DOT regulatory requirements. The original criteria were described in Section 5.0 of the FEIS; the current WAC are summarized in SEIS Section 2.0 and Appendix A. Other aspects of the WAC that are relevant to the radionuclide source term include:

TABLE B.2.1 Project total radionuclide inventories (Curies)

CH waste site	Retrievably stored	Newly-generated	Total
		CH TRU waste	
Idaho National Engineering Laboratory	$3.86 \times 10^{+5}$	$7.23 \times 10^{+2}$	$3.87 \times 10^{+5}$
Rocky Flats Plant		$1.14 \times 10^{+6}$	$1.14 \times 10^{+6}$
Hanford Reservation	$8.30 \times 10^{+5}$	$9.28 \times 10^{+5}$	$1.76 \times 10^{+6}$
Savannah River Plant	$6.18 \times 10^{+5}$	$3.08 \times 10^{+6}$	$3.70 \times 10^{+6}$
Los Alamos National Laboratory	$4.32 \times 10^{+5}$	$1.62 \times 10^{+6}$	$2.05 \times 10^{+6}$
Oak Ridge National Laboratory	$2.68 \times 10^{+4}$	$3.02 \times 10^{+4}$	$5.70 \times 10^{+4}$
Nevada Test Site Laboratory	$4.27 \times 10^{+2}$		$4.27 \times 10^{+2}$
Argonne National Laboratory-East		$7.20 \times 10^{+2}$	$7.20 \times 10^{+2}$
Lawrence Livermore National Laboratory		$6.88 \times 10^{+4}$	$6.88 \times 10^{+4}$
Mound		$4.80 \times 10^{+2}$	$4.80 \times 10^{+2}$
Subtotals	$2.29 \times 10^{+6}$	$6.87 \times 10^{+6}$	$9.16 \times 10^{+6}$
		RH TRU waste	
Idaho National Engineering Laboratory	$1.23 \times 10^{+3}$	$2.23 \times 10^{+4}$	$2.36 \times 10^{+4}$
Hanford Reservation	$1.57 \times 10^{+5}$	$3.24 \times 10^{+5}$	$4.81 \times 10^{+5}$
Los Alamos National Laboratory	$2.50 \times 10^{+3}$	$2.42 \times 10^{+2}$	$2.74 \times 10^{+3}$
Oak Ridge National Laboratory	$7.97 \times 10^{+3}$	$4.70 \times 10^{+2}$	$8.44 \times 10^{+3}$
Argonne National Laboratory East		$1.00 \times 10^{+3}$	$1.00 \times 10^{+3}$
Subtotals	$1.69 \times 10^{+5}$	$3.48 \times 10^{+5}$	$5.17 \times 10^{+5}$
Totals	$2.46 \times 10^{+6}$	$7.22 \times 10^{+6}$	$9.68 \times 10^{+6}$

TABLE B.2.2 Estimated quantity of CH TRU waste in retrievable storage or projected to be generated through the year 2013

Generator or storage facility	Retrievably-stored[b]	Newly-generated[c]	Total
Idaho National Engineering Laboratory[d]	1,073,686	9,923	1,083,609
Rocky Flats Plant[e]	0	2,037,582	2,037,582
Hanford Reservation[d]	293,247	537,762	831,009
Savannah River Plant[d]	91,463	615,947	707,410
Los Alamos National Laboratory[d]	250,905	302,253	553,158
Oak Ridge National Laboratory[d]	19,176	41,953	61,129
Nevada Test Site[d]	21,294	0	21,294
Argonne National Laboratory-East[e]	0	3,814	3,814
Lawrence Livermore National Laboratory[e]	0	259,346	259,346
Mound[e]	0	40,046	40,046
Totals	1,749,771	3,848,626	5,598,397

[a] Estimated volumes correspond to the Integrated Data Base for 1987 (DOE, 1987). Volumes of waste used for the environmental analysis in this SEIS are higher and are based on the WIPP design capacity.

[b] From Table 3.5 (DOE, 1987).

[c] From Table 3.16 (DOE, 1987).

[d] These sites have been designated as TRU waste storage sites.

[e] These sites generate but do not store TRU waste.

TABLE B.2.3 Estimated quantity of RH TRU waste in retrievable storage or projected to be generated through the year 2013

Generator or storage facility	Retrievably-stored[b]	Newly-generated[c]	Total
Idaho National Engineering Laboratory	989	4,873	5,862
Hanford Reservation	848	28,604	29,452
Los Alamos National Laboratory	1,024	212	1,236
Oak Ridge National Laboratory	45,484	10,594	56,078
Argonne National Laboratory-East[d]	0	283	283
Totals	48,345	44,566	92,911

[a] Estimated volumes correspond to the Integrated Data Base for 1987 (DOE, 1987). The estimated volumes of waste used for the environmental analysis in this SEIS are higher and are based on the design capacity of the WIPP.

[b] From Table 3.5 Integrated Data Base for 1987: Spent Fuel and Radioactive Waste Inventories, Projections and Characterizations, DOE/RW-0006, Revision 3 (DOE, 1987).

[c] From Table 3.16 Integrated Data Base for 1987: Spent Fuel and Radioactive Waste Inventories, Projections and Characterizations, DOE/RW-0006, Revision 3 (DOE, 1987).

[d] This site generates but does not store RH TRU waste.

TABLE B.2.4 Retrievably-stored and newly-generated TRU waste

Facility	Total Base (1987 IDB)	Volume Scale-up (ft^3)	Total Volume (ft^3)
CH Waste			
Idaho National Engineering Laboratory	$1.1x10^6$	$3.8x10^5$	$1.5x10^6$
Rocky Flats Plant	$2.0x10^6$	0	$2.0x10^6$
Hanford Reservation	$8.3x10^5$	$1.0x10^5$	$9.4x10^5$
Savannah River Plant	$7.1x10^5$	$3.2x10^4$	$7.4x10^5$
Los Alamos National Laboratory	$5.5x10^5$	$8.8x10^4$	$6.4x10^5$
Oak Ridge National Laboratory	$6.1x10^4$	$6.8x10^3$	$6.8x10^4$
Nevada Test Site	$2.1x10^4$	0	$2.1x10^4$
Argonne National Laboratory-East	$3.8x10^3$	0	$3.8x10^3$
Lawrence Livermore National Laboratory	$2.6x10^5$	0	$2.6x10^5$
Mound Laboratory	$4.0x10^4$	0	$4.0x10^4$
TOTAL - CH	$5.6x10^6$	$6.1x10^5$	$6.2x10^6$
RH Waste			
Idaho National Engineering Laboratory	$5.9x10^3$	0	$5.9x10^3$
Hanford Reservation	$2.9x10^4$	0	$2.9x10^4$
Oak Ridge National Laboratory	$5.6x10^4$	$1.6x10^5$	$2.1x10^5$
Argonne National Laboratory-East	$2.8x10^2$	0	$2.8x10^2$
Los Alamos National Laboratory	$1.2x10^3$	0	$1.2x10^3$
TOTAL - RH	$9.3x10^4$	$1.6x10^5$	$2.5x10^5$
Total - All Waste	$5.7x10^{+6}$	$7.7x10^{+5}$	$6.4x10^{+6}$

- Surface contamination on CH or RH TRU waste packages may not exceed 5.0 percent of the limits specified in DOT regulations in 49 CFR Part 173.442.

- The thermal power or heat-generating capacity of a package of CH TRU waste must be labeled if it exceeds 0.1 W/ft^3. RH TRU waste may not have a thermal power in excess of 300 W per canister.

An upper limit of 350 g or 113 W has been established for the 4 by 4 by 7 ft DOT Type 7A boxes or DOE SWBs. In addition, the total PE-Ci are limited to 1,000 per package. A discussion of the PE-Ci concept is provided in Appendix F. In order to ensure that criticality events (i.e., self-sustaining atomic chain reactions) will not occur, total fissile material is limited to no more than 200 g per 55-gal drum or 350 g for SWBs. Finally, fissile material concentrations are restricted to a maximum of 5 g/ft^3.

B.2.2 CHARACTERISTICS

Transuranic radionuclide mixes (elements and weight fractions), quantities (Pu and total alpha-TRU Curies), and volumes (Table B.2.4) used in the transportation analysis, the WIPP operations assessment and the WIPP long-term performance assessment are based on the 1987 IDB and WIPP-WEC-88-049 (WIPP, 1989). Information in the IDB is collected for both stored and newly generated CH and RH TRU waste from each generator/storage site. Since that document was published, additional information has been obtained from the sites regarding fission product fractions, total quantities of radionuclides (Curies) and numbers of actual waste containers in storage and projected through 2013. This additional information has been drafted as a report and is in the process of being finalized as WIPP-WEC-88-049 (WIPP, 1989). These two documents constitute the fundamental basis for analyses reported in this SEIS and in the WIPP FSAR. Table B.2.5 summarizes the differences in waste characteristics between the WIPP FEIS and FSAR. Analysis of the impacts of transportation operations, operational safety, and long-term performance assessment presented in this SEIS incorporate differing elements of the basic TRU waste inventory and characteristics presented above. The following paragraphs describe the development of the inventory bases for the transportation operations, operational safety, and long-term performance assessment calculations.

B.2.2.1 Transportation

Site specific radionuclide mixes for transuranics (DOE, 1987) and fission products (WIPP, 1989) were used to specify radionuclide weight fractions for each waste stream (stored and newly generated) at the site. Specific activities were multiplied by these weight fractions to obtain activity fractions for the radionuclide mixes. Those activity fractions were renormalized to 100% and were used to calculate a site-specific quantity of radionuclides (Curies) per TRUPACT II or RH canister. This quantity is the volumetric average of all of the specific TRU waste streams at the site. From this, average site-specific transportation trailer-loads of radionuclides (Ci/package) were calculated. These serve as the source term for calculating amounts of respirable nuclides released in transportation accident events (Tables B.2.6 and B.2.7). An example of this calculational

TABLE B.2.5 Summary of average TRU waste characteristics

Characteristic	CH TRU waste		RH TRU waste	
	FEIS[a]	FSAR[b]	FEIS[a]	FSAR[b]
Surface dose rate[c]				
Drum	3.1	14		
DOT Type 7A Box	1.0	14		
Canister			200-100,000	30,000
Thermal power[d]				
Drum	0.5	0.5		
DOT Type 7A Box	0.8	0.8		
Canister			70	60
Curies[e]				
Drum	3.4	20.6		
DOT Type 7A Box	5.5	77		
Canister			512	37[f]
Total plutonium[g]				
Drum	8	15.5		
DOT Type 7A Box	13	86.3		
Canister			12.8	120
Fissile material[h]				
Drum	7.5	17		
DOT Type 7A Box	12.2	90		
Canister			12	110

[a] DOE, 1980.
[b] DOE, 1987.
[c] The radiation exposure rate at the outside surface of the package in mrem/hr.
[d] The heat generating capacity of the radionuclides in W.
[e] The special unit of activity in Ci; one Ci equals 3.7×10^{10} nuclear transformations per second.
[f] Daughter products are not included. Average Ci/container as reported by sites. Maximum Pu-equivalent Ci per container is 1000 Curies (WIPP-WAC).
[g] Total plutonium mass in grams (g).
[h] Expressed as the Pu-239 Equivalent Fissile Content in g. For materials other than PU-239, U-235, and U-233, which are treated as equivalent, fissile equivalents shall be obtained using ANSI/ANS-8.15-1981.

TABLE B.2.6 Average CH TRU waste trailer-load radioactivity (Curies)[a]

Radionuclide	ANLE	HANF	INEL	LANL	LLNL	MOUND	NTS	ORNL	RFP	SRP
Th-232			0.00011							
U-233			0.163	0.0444				75.2		
U.235				0.000226						
Np-237										0.00406
Pu-238	5.77	8.1	11.55	201.9	1.27	0.0146	0.0408	50.04	0.573	1956
Pu-239	3.65	35.1	6.3	94.3	30.6	0.0126	0.69	221.4	19.5	2.27
Pu-240	1.67	12.5	1.54	22	29.9	0.00333	0.164		4.44	0.939
Pu-241	33.3	636.0	48.78	130.8	291	0.00127	6.15		139	70.8
Pu-242				0.00585	0.000621					
Am-241	15.10		41.7	281.1	164			18.03	0.918	0.195
Cm-244								60.15		
Cf-252								9.6		

[a] Three cylindrical TRUPACT-IIs per trailer-load; truck mode: 1 trailer-load/shipment; rail mode: 2 trailer-loads/shipment

TABLE B.2.7 Average RH TRU waste trailer-load radioactivity (Curies)[a]

Radionuclide	Facility				
	Hanford Reservation	Idaho National Engineering Laboratory	Los Alamos National Laboratory	Oak Ridge National Laboratory	Argonne National Laboratory-East
Sr-90	[b]	2.35×10^{0}	8.11×10^{0}	9.99×10^{-1}	
Ru-106			6.41×10^{0}		
Sb-125			1.98×10^{-1}		
Cs-137		3.34×10^{0}	6.30×10^{0}	3.96×10^{-2}	8.83×10^{0}
Ce-137			$6.31 \times 10^{+1}$		
Eu-155			3.19×10^{-1}		
U-233				5.55×10^{-3}	
U-235		1.41×10^{-3}	1.38×10^{-5}	7.00×10^{-7}	
U-238		4.04×10^{-4}		1.00×10^{-6}	
Pu-238	6.30×10^{-1}	9.41×10^{-3}		1.05×10^{-3}	
Pu-239	3.85×10^{0}	8.81×10^{-2}	7.51×10^{-1}	4.53×10^{-2}	2.52×10^{-1}
Pu-240	1.96×10^{0}	3.45×10^{-2}	9.99×10^{-1}		9.30×10^{-2}
Pu-241	TBD[c]		$1.14 \times 10^{+1}$		
Pu-242	6.00×10^{-2}				
Am-241		1.88×10^{-3}		2.30×10^{-2}	
Cm-244				2.06×10^{-1}	
Cf-252				3.61×10^{-1}	

[a] 1 RH cask/trailer load; for truck mode: 1 trailer load/shipment; for the rail mode, multiply radioactivity by 2

[b] Blanks = radionuclide not in facility waste stream

[c] TBD = To be determined

procedure is shown in Table B.2.8 for RFP CH waste and in Table B.2.9 for LANL RH waste which consists of two waste streams, i.e., stored and newly generated.

Incident-free transportation radiological risks depend upon the radiation field produced by the waste at the surface of the transportation package. The Transport Index (TI) is a measure of this field (dose rate in mrem/hr at 1 meter from the package surface) and is the source for calculating normal transport radiation exposures. The TI's are extremely sensitive to gamma-producing isotopes which are typically difficult to characterize in small quantities such as are found in TRU waste. For the SEIS, the IDB data and the updated radionuclide data in WIPP, 1989 were further updated through discussions with sites to develop a site-by-site stratified listing of actual waste containers versus radiation field. From this information, an average (based on weighted fraction of containers) radiation field for containers from a site was calculated. For conservatism, it was assumed that this field resulted entirely from radionuclides emitting 1 MeV photons. Shielding models of the TRUPACT II and RH cask were then developed to calculate TI's from the 1MeV radiation fields. In some cases, lack of waste-specific information (e.g. Hanford RH waste) necessitated an assumption regarding the waste radiation field. For this SEIS, Hanford waste was assumed to produce a field of 100 R/hr of 1 MeV photons (100R/hr is the maximum nonexempt shipment limit for RH TRU according to the WIPP-WAC). This very conservative assumption resulted in a high TI for Hanford RH shipments compared to other sites.

To estimate shipments of TRU waste to WIPP for this various SEIS alternative, volumes reported in the 1987 IDB (95.6 m ft^3 CH and 93,000 ^{3} ft RH) were used. These volumes are comprised of waste in storage as of 12/31/86 and that projected to be generated from 1987-2013 at the rates reported in the IDB. For conservatism, these volumes were scaled (at storage sites only) to the WIPP maximum emplacement volume of 6.45 M Cu ft (CH and RH). Numbers of CH truck shipments from each site were estimated by the following:

$$\#\ \text{shipments CH} = \frac{\text{Stored + newly generated volume } (m^3)}{(0.2\ m^3/\text{drum})\ (0.80)\ 42\ \text{drums/shipment}}$$

(3 TRUPACTS
per shipment
for truck)

Rail shipments assumed 6 TRUPACTS per shipment for sites with rail access. RH truck shipments were calculated as follows:

$$\#\ \text{shipments RH} = \frac{\text{Stored \& newly generated volume } (m^3)}{(0.89\ m^3/\text{cask})\ (1\ \text{cask/shipment})}$$

(1 cask
per shipment)

Rail shipments assumed 2 casks per shipment for sites with rail access. The waste transported in the shipments calculated above was assumed to be identical in characteristics to that used in the Ci/package and TI calculations.

TABLE B.2.8 Total estimated activity (Curies) of CH TRU per trailer-load for Rocky Flats Plant

	Newly generated				
CH TRU	Number of Containers	Total Volume (m^3)	Total Activity (Ci)	Total Pu (Ci)	Total Alpha-TRU (Ci)
	$1.29 \times 10^{+5}$	$6.26 \times 10^{+4}$	$1.14 \times 10^{+6}$	$1.08 \times 10^{+6}$	$2.22 \times 10^{+5}$

Radionuclide	Weight Fraction	Activity Fraction	Renorm. Fraction	Ci/pkg	Trailer-load Ci/pkg
Pu-238	0.0001	0.002	0.035	1.91×10^{-1}	5.73×10^{-1}
Pu-239	0.9300	0.058	0.1186	6.49×10^{0}	$1.95 \times 10^{+1}$
Pu-240	0.0580	0.013	0.0271	1.49×10^{0}	4.44×10^{0}
Pu-241	0.0040	0.412	0.8452	$4.62 \times 10^{+1}$	$1.39 \times 10^{+2}$
Am-241	0.0008	0.003	0.0056	3.06×10^{-1}	9.18×10^{-1}
Other	0.0070				
Total	1.000	0.488	1.000	$5.5 \times 10^{+1}$	$1.6 \times 10^{+2}$

$$\text{Ci/pkg} = \sum_{i=1}^{n,\ \text{nuclides}} \left(\frac{\text{Total Activity}}{\text{Total Volume}}\right) \times \frac{3\ m^3}{\text{TRUPACT}} \times (\text{Renorm. Fraction})_i$$

$$= \sum_{i=1}^{R} \left(\frac{1.14 \times 10^{+6}}{6.26 \times 10^{+4}}\right) \times (3)(RF)_i$$

TABLE B.2.9 Total estimated activity (Curies) of RH TRU per Trailer-load for Los Alamos National Laboratory

From Storage

RH TRU	Number of Containers	Total Volume (m^3)	Total Activity (Ci)	Total Pu (Ci)	Total Alpha-TRU (Ci)
Canisters	$2.20 \times 10^{+1}$	$1.98 \times 10^{+4}$	$2.50 \times 10^{+3}$	$3.99 \times 10^{+2}$	$5.70 \times 10^{+1}$

Radionuclide	Weight Fraction	Activity Fraction	Renorm. Fraction	Ci/pkg stored
Sr-90	0.0009	0.1271	0.0816	6.16
Ru-106	0.0000	0.1005	0.0645	4.87
Sb-125	0.0000	0.0031	0.0020	0.151
Cs-137	0.0011	0.0984	0.0632	4.77
Ce-144	0.0003	0.9896	0.6356	48.01
Eu-155	0.0000	0.0049	0.0032	0.242
U-235	0.7480	0.0000	0.0000	0.000
Pu-239	0.2270	0.0141	0.0091	0.687
Pu-240	0.0206	0.0047	0.0030	0.227
Pu-241	0.0021	0.2144	0.1377	10.40
Total	1.000	1.5568	1.000	75.5

TABLE B.2.9 Concluded
Los Alamos National Laboratory

RH TRU	Number of Containers	Total Volume (m^3)	Total Activity (Ci)	Total Pu (Ci)	Total Alpha-TRU (Ci)
		Newly Generated			
Canisters	6.00×10^{0}	5.40×10^{0}	$2.42 \times 10^{+2}$	$1.20 \times 10^{+1}$	1.00×10^{0}

Radionuclide	Weight Fraction	Activity Fraction	Renorm. Fraction	Ci/pkg stored	Ci/pkg Newly-generated	Ci/pkg Trailer-load
Sr-90	0.0031	0.4232	0.0914	6.2×10^{0}	1.9×10^{0}	8.1×10^{0}
Ru-106	0.0001	0.3348	0.0723	4.9×10^{0}	1.5×10^{0}	6.4×10^{0}
Sb-125	0.0000	0.0103	0.0022	1.5×10^{-1}	4.7×10^{-2}	2.0×10^{-1}
Cs-137	0.0038	0.3273	0.0707	4.8×10^{0}	1.5×10^{0}	6.3×10^{0}
Ce-144	0.0010	3.2880	0.7098	4.8×10^{1}	1.5×10^{1}	6.3×10^{1}
Eu-155	0.0000	0.0165	0.0036	2.4×10^{-1}	7.7×10^{-2}	3.2×10^{-1}
U-235	0.7440	0.0000	0.0000	0.000	0.000	0.000
Pu-239	0.2250	0.0140	0.0030	6.9×10^{-1}	6.4×10^{-2}	7.5×10^{-1}
Pu-240	0.0205	0.0047	0.0010	2.3×10^{-1}	2.1×10^{-2}	1.0×10^{-1}
Pu-241	0.0021	0.2134	0.0461	1.0×10^{1}	9.8×10^{-1}	1.1×10^{1}
Total	0.9996	4.6323	1.0000	$7.5 \times 10^{+1}$	$2.1 \times 10^{+1}$	$3.9 \times 10^{+1}$

(Trailer-load)

$$\text{Ci/trailer-load} = \sum_{i=1}^{n,\ \text{nuclides}} \left(\frac{\text{Total Activity}}{\text{Total Volume}}\right) \times \frac{.89\ m^3}{\text{cask}} \text{ (Volume Fraction)(Renorm. Fraction)}_i$$

$$\text{Volume Fraction: } \frac{\text{Stored Volume}}{\text{Total Volume}} = .78$$

$$\frac{\text{Newly generated volume}}{\text{Total volume}} = .22$$

B.2.2.2 Operational Analysis

Operational impacts of waste handling and storage at WIPP in this SEIS were abstracted from the WIPP FSAR. The FSAR, like the SEIS transportation analysis, was based on waste inventories reported in the 1987 IDB and updated by WIPP, 1989. This updated information provides total quantities of radionuclides (Curies), volumes and numbers of containers (55-gal drums, standard waste boxes, other waste packages) for various waste streams from each site. From this, average representative CH drums and CH standard waste boxes and RH containers were developed as shown in Tables B.2.10, B.2.11, and B.2.12. Operational impacts at WIPP developed in the FSAR involving accidents used these average containers (Ci/package). Exposures to workers handling waste at WIPP were based on the same radiation fields produced by individual site's wastes as were used to calculate transportation TI's.

B.2.2.3 Long Term Performance Assessment

As reported by SNL (Lappin et al., 1989), the long-term performance assessment for WIPP (undisturbed and intruder scenarios) was based on the same CH radionuclide inventory as was reported by the 1987 IDB and updated by WIPP, 1989. This total inventory of approximately $9.2 \times 10^{+6}$ Ci (Table B.2.13) was modified to account for decay of short-lived nuclides and build-up of daughter products with high radiotoxicity. In addition, radioisotopes having low radiotoxicity were eliminated from the inventory. This modified inventory (Table B.2.14) amounts to approximately $5.2 \times 10^{+6}$ Ci. RH TRU waste was not included in the performance assessment inventory. As discussed by SNL, RH TRU inventory information is uncertain, emplacement procedures at WIPP will minimize degradation of RH TRU canisters, and many of the short-lived radionuclides (which typically result in RH-TRU waste being so categorized) will have minimal consequences over the long term.

B.2.2.4 High Curie Waste

Heat is primarily generated by the interaction of alpha radiation, from the decay of plutonium isotopes, with waste materials and package walls. The amount of heat generated depends on the quantities of radioactive materials present and the energy of the radiation released. Specific activity is a measure of the energy available for interaction for a particular radionuclide. Pu-238 has a specific activity 100 to 1,000 times greater than other plutonium isotopes in the waste. Thus, waste containing large concentrations of Pu-238 is designated as high specific activity waste or high-curie waste. Due to its greater heat-generating capacity, it is also referred to as heat source plutonium.

Pu-238 is a major contributor to the total radionuclide content of CH TRU waste, primarily due to waste generated at the Savannah River Plant in South Carolina. This waste has a higher curie content and heat-generating capacity than the waste used in the FEIS analyses. Typically, the average Pu-238 content reported in the FEIS was 1.2 percent of the total radioactivity content of CH TRU waste. TRU waste from the Savannah River Plant increases the Pu-238 contribution to the radioactivity of all CH TRU waste to 17 percent. The higher proportion of Pu-238 in the total waste has modi-

TABLE B.2.10 Representative radionuclide content of CH TRU waste drum

Radionuclide	Mass present (g per drum)		Activity (Ci per drum)	
	FEIS[a]	FSAR[b]	FEIS[a]	FSAR[b]
Thorium-232	NP	6.0×10^{0}	NP	6.6×10^{-7}
Uranium-233	NP	1.7×10^{0}	NP	1.7×10^{-2}
Uranium-235	NP	4.0×10^{-1}	NP	8.8×10^{-7}
Uranium-238	NP	1.0×10^{1}	NP	3.5×10^{-6}
Neptunium-237	NP	3.1×10^{-2}	NP	2.2×10^{-5}
Plutonium-238	2.5×10^{-3}	6.2×10^{-1}	4.2×10^{-2}	1.1×10^{1}
Plutonium-239	7.5×10^{0}	1.4×10^{1}	4.6×10^{-1}	8.5×10^{-1}
Plutonium-240	5.0×10^{-1}	8.5×10^{-1}	1.1×10^{-1}	1.9×10^{-1}
Plutonium-241	2.7×10^{-2}	6.6×10^{-2}	2.8×10^{0}	6.8×10^{0}
Plutonium-242	2.4×10^{-3}	7.8×10^{-3}	9.4×10^{-6}	3.1×10^{-5}
Americium-241	1.5×10^{-3}	4.9×10^{-1}	5.2×10^{-3}	1.7×10^{0}
Curium-244	NP	4.2×10^{-4}	NP	3.4×10^{-2}
Californium-252	NP	1.0×10^{-5}	NP	5.4×10^{-3}
TOTAL	8.0×10^{0}	3.4×10^{1}	3.4×10^{0}	2.1×10^{1}

[a] DOE, 1980. NP indicates that data were not provided in the FEIS.

[b] DOE, 1987.

TABLE B.2.11 Representative radionuclide content of CH TRU waste Standard Waste Box (SWB)

Radionuclide	Mass present (g per drum)		Activity (Ci per drum)	
	FEIS[a]	FSAR[b]	FEIS[a]	FSAR[b]
Thorium-232	NP	1.2×10^{1}	NP	1.3×10^{-6}
Uranium-233	NP	6.7×10^{0}	NP	6.5×10^{-2}
Uranium-235	NP	9.6×10^{-1}	NP	2.1×10^{-6}
Uranium-238	NP	2.5×10^{1}	NP	8.3×10^{-6}
Neptunium-237	NP	4.4×10^{-4}	NP	3.1×10^{-7}
Plutonium-238	4.0×10^{-3}	4.2×10^{-2}	6.8×10^{-2}	7.2×10^{-1}
Plutonium-239	1.2×10^{1}	7.9×10^{1}	7.5×10^{-1}	4.9×10^{0}
Plutonium-240	8.1×10^{-1}	6.5×10^{0}	1.8×10^{-1}	1.5×10^{0}
Plutonium-241	4.4×10^{-2}	6.7×10^{-1}	4.5×10^{0}	6.9×10^{1}
Plutonium-242	3.9×10^{-3}	7.5×10^{-2}	1.5×10^{-5}	2.9×10^{-4}
Americium-241	2.5×10^{-3}	2.1×10^{-1}	8.4×10^{-3}	7.3×10^{-1}
Curium-244	NP	8.6×10^{-5}	NP	7.0×10^{-3}
Californium-252	NP	2.1×10^{-6}	NP	1.1×10^{-3}
Total	1.3×10^{1}	1.3×10^{2}	5.5×10^{0}	7.7×10^{1}

[a] DOE, 1980. NP indicates that data were not provided in the FEIS.

[b] DOE, 1987.

TABLE B.2.12 Representative radionuclide content of RH TRU waste container

Radionuclide	Activity (Ci per container) FEIS[a]	FSAR[b,c]
Cobalt-60	1.6×10^{0}	1.7×10^{-1}
Strontium-90	2.5×10^{2}	5.1×10^{0}
Ruthenium-106	2.2×10^{0}	3.5×10^{-2}
Antimony-125	NP	1.1×10^{-3}
Cesium-137	1.2×10^{0}	4.3×10^{0}
Cerium-144	NP	3.4×10^{-1}
Europium-155	NP	1.7×10^{-3}
Uranium-233	NP	5.5×10^{-3}
Uranium-235	NP	3.0×10^{-3}
Uranium-238	NP	1.5×10^{-3}
Plutonium-238	6.5×10^{-2}	5.7×10^{0}
Plutonium-239	7.5×10^{-1}	6.8×10^{0}
Plutonium-240	1.8×10^{-1}	2.2×10^{0}
Plutonium-241	4.6×10^{0}	$1.2 \times 10^{+1}$
Plutonium-242	NP	3.8×10^{-4}
Americium-241	1.2×10^{-2}	2.1×10^{-1}
Curium-244	NP	1.6×10^{-1}
Californium-252	NP	2.8×10^{-1}
Total	2.6×10^{2}	3.7×10^{1}

[a] DOE, 1980. NP indicates that data were not provided in the FEIS.

[b] DOE, 1987.

[c] Daughter products not included.

TABLE B.2.13 Initial CH waste inventory for long-term performance analysis

Radionuclide	half-life(yr)	Curies
Th-232	1.41×10^{10}	2.74×10^{-1}
U-233	1.59×10^{5}	7.72×10^{3}
U-235	7.04×10^{8}	3.70×10^{-1}
U-238	4.47×10^{9}	1.47
Np-237	2.14×10^{6}	8.02
Pu-238	8.77×10^{1}	3.90×10^{6}
Pu-239	2.41×10^{4}	4.25×10^{5}
Pu-240	6.54×10^{3}	1.05×10^{5}
Pu-241	1.44×10^{1}	4.08×10^{6}
Pu-242	3.76×10^{5}	1.80×10^{1}
Am-241	4.32×10^{2}	6.37×10^{5}
Cm-244	1.81×10^{1}	1.27×10^{4}
Cf-252	2.64	2.03×10^{4}
Total		9.2×10^{6}

Source: Lappin et al., 1989

TABLE B.2.14 Modified inventory used in long-term performance analysis

Radionuclide	half-life(yr)	Curies	Grams
Pu-238	8.77×10^{1}	3.90×10^{6}	2.28×10^{5}
Pu-239	2.41×10^{4}	4.25×10^{5}	6.84×10^{6}
Pu-240	6.54×10^{3}	1.05×10^{5}	4.61×10^{5}
U-233	1.59×10^{5}	7.72×10^{3}	8.15×10^{5}
U-234	2.44×10^{5}	0	0
U-235	7.04×10^{8}	3.70×10^{-1}	1.71×10^{5}
U-236	2.34×10^{7}	0	0
Am-241	4.32×10^{2}	7.75×10^{5}	2.26×10^{5}
Np-237	2.14×10^{6}	8.02	1.14×10^{4}
Th-229	7.43×10^{3}	0	0
Th-230	7.70×10^{4}	0	0
Ra-226	1.60×10^{3}	0	0
Pb-210	2.23×10^{1}	0	0
Total		5.2×10^{6}	

Source: Lappin et al., 1989

fied the average radionuclide composition of the source term used to evaluate radiation dose consequences in this SEIS. High-curie waste will be subject to the same surface dose equivalent rate restrictions as other waste; therefore, no unique handling or storage procedures or precautions will be required for the high-curie waste.

B.2.2.5 High-Neutron Waste

Since publication of the FEIS, it has been determined that the Oak Ridge National Laboratory in Tennessee may be contributing a small amount of waste containing californium-252 (Cf-252) which decays by neutron emission (DOE, 1988). Almost 0.03 percent of the total CH TRU waste radioactivity will be composed of Cf-252. Neutron-emitting (high-neutron) waste may be subject to the same surface dose equivalent rate restrictions as other waste; therefore, no unique handling or storage procedures or precautions will be required for the high-neutron waste.

B.3 HAZARDOUS CHEMICAL CONSTITUENTS

TRU radioactive waste that also contains hazardous chemical constituents is termed TRU mixed waste. The FEIS addressed only the impacts of the radioactive component of TRU waste. Since that time,it has been determined that TRU waste is subject to dual regulation under the Atomic Energy Act (AEA) and Resource Conservation and Recovery Act (RCRA). TRU mixed waste is defined as TRU waste that is co-contaminated with hazardous chemical constituents. The TRU mixed waste that may be shipped to the WIPP is generated by the ten DOE defense facilities, and hazardous chemical waste constituents are often commingled with TRU waste from these operations. Approximately 60 percent of the TRU waste that may be shipped to the WIPP is TRU mixed waste.

Until recently, few records were required to document the hazardous chemical constituents in the TRU waste. Due to the complex waste matrices and potential for unacceptable radiation exposure to personnel, the waste was and is not routinely sampled and analyzed. The TRU mixed waste has been characterized using knowledge of the waste and/or the industrial processes from which it is generated. The requirements for strict product quality and concerns for safety in handling radioactive materials results in highly structured production and research activities. The ingredients entering a given process cannot be substituted and the process conditions are highly controlled. This precision requires extensive knowledge about the ingredients and the processes involved and allows the characterization of TRU mixed waste.

B.3.1 CH TRU MIXED WASTE

The DOE facilities that may ship waste to the WIPP site have very conservatively characterized their CH TRU mixed waste to facilitate preparation of the permit application to operate the WIPP as an "interim status" facility under the RCRA. This information was reported in the "WIPP RCRA TRU Mixed Waste Characterization Data Base" (WEC, 1989), and represents a conservative upper bound in classifying the waste. In other words, if a chemical is present in the waste, it is identified even though its concentration in the waste may be below the regulatory limit.

The identification of the hazardous chemical constituents in CH TRU mixed waste is based on newly-generated waste from the Rocky Flats Plant in Colorado and waste from the Rocky Flats Plant that is currently in retrievable storage at the Idaho National Engineering Laboratory in Idaho. It is estimated that the Rocky Flats Plant waste represents approximately 50 percent of the total CH TRU waste proposed to be emplaced in the WIPP. The Rocky Flats Plant generates many different forms of waste from a variety of processes. Other DOE facilities generate smaller quantities of TRU mixed waste, fewer waste forms, and waste that contains a narrower range of hazardous chemical constituents (WEC, 1989). Therefore, the use of information for the Rocky Flats Plant waste that is currently generated and in retrievable storage at the

Idaho National Engineering Laboratory represents a conservative upper bound for the potential risks associated with the chemical components of the CH TRU mixed waste.

CH TRU waste is segregated into groups based on the physical characteristics of the materials in the waste. Each DOE facility has categorized its waste into specific waste categories or "forms." Each waste form must be certified by the DOE for compliance with the WIPP WAC (SEIS Subsection 2.0 and Appendix A) before shipment to the WIPP. The waste forms that have been identified by the Rocky Flats Plant as containing hazardous chemical constituents are cemented and uncemented aqueous and organic wastes, immobilized process and laboratory solids, combustible waste, metal and filter wastes, inorganic solids, and leaded rubber waste. Descriptions of these waste forms are as follows:

- Cemented and Uncemented Aqueous Waste. Aqueous process wastes are treated by a precipitation process involving neutralization, precipitation, flocculation, clarification, filtration, and immobilization. This waste form consists of a wastewater treatment sludge that is precipitated at a pH of 10 to 12. Currently, the waste is solidified with Portland cement. Prior to 1984, this waste was not cemented and exists today as a damp solid. Alcohols and halogenated organics in the sludge are derived from the cleaning of equipment and glassware and the degreasing of metal. Some aqueous process waste may also contain metals such as cadmium and lead although no analysis has been performed to determine specific concentrations.

- Cemented and Uncemented Organic Waste. Organic waste containing oil and halogenated organic solvents is solidified using Envirostone cement and an emulsifier. Prior to 1984, this waste form was not solidified with cement; it is a damp solid. Organic waste consists of lathe coolants and degreasing solvents used in plutonium fabrication.

- Immobilized Process and Laboratory Solids. This waste form consists of anion and cation resins and incinerator ash that are neutralized and immobilized with Portland cement. Solvents in this waste are from plutonium recovery operations.

- Combustible Waste. This waste form consists of paper and cloth (dry and damp); various plastics such as polyethylene and polyvinyl chloride; wood; and filters contaminated with trace quantities of halogenated organic solvents. These materials are generated in plutonium recovery and fabrication processes and analytical laboratories.

- Metal Waste. Lead, tantalum, stainless steel, and aluminum constitute the majority of this waste form. These metallic wastes include equipment, tools, crucibles, and molds. Residual halogenated organic solvents may also be found in this waste form.

- Filter Waste. This waste form consists of FulFlo (polypropylene) and HEPA filters as well as processed filter media. Portland cement is added to absorb any residual liquid and neutralize residual acids. Exhaust stream filters may

be contaminated with volatile organic solvents used in plutonium fabrication and recovery processes.

- Inorganic Solid Waste. Materials such as firebrick, Oil Dri, concrete, and soil are included in this waste form. This waste is generated from the decontamination and decommissioning of plutonium recovery areas. Oil Dri, concrete, and soil may be contaminated with residual halogenated organic solvents.

- Leaded Rubber Waste. Leaded rubber dry-box gloves and aprons which are used throughout the plutonium processing areas make up this waste form. It is considered a RCRA-regulated hazardous waste according to the EPA Extraction Procedure (EP) toxicity test (40 CFR Part 261) for lead although no analysis has been done to establish the lead concentrations. The EP toxicity test is an extraction procedure that is used to characterize wastes as hazardous under RCRA.

The estimated quantity of each waste form is given in Table B.3.1. The descriptions indicate that the majority of the organic solvents are present in residual quantities from the cleaning of equipment, plastics, glassware, and filters. A major constituent in CH TRU mixed waste is lead that is present predominantly as shielding, dry-box parts, and lead-lined gloves and aprons.

The types and estimated maximum concentrations of hazardous chemical constituents in the CH TRU mixed waste forms are provided in Table B.3.2. These concentrations, as estimated by the Rocky Flats Plant (Rockwell International, 1988), are very conservative and represent the maximum concentrations possible in the waste forms. Because the DOT requires generators to document the concentrations of hazardous materials over reportable quantities (49 CFR Part 172.101) on the shipping documents that accompany the waste during transport, the Rocky Flats Plant has reported the maximum possible concentrations based on process knowledge. The data indicate a broad range of concentrations of the various constituents both within and between waste forms. The data also indicate that the majority of the waste forms contain less than 1 percent by weight of any of the identified hazardous chemical constituents.

B.3.2 RH TRU MIXED WASTE

RH TRU waste represents a much smaller portion of the total waste that may be shipped to the WIPP site (SEIS Subsections 1.2 and 2.3). It is estimated that a maximum of 4,000 to 5,000 canisters of RH TRU waste may be placed in the repository. Oak Ridge National Laboratory generates a majority of the RH TRU waste that may be sent to the WIPP and reported the following two major waste forms in the "TRU Mixed Waste Characterization Data Base" for preparation of the RCRA permit application to operate the WIPP as an "interim status" facility:

- Solid RH TRU Mixed Waste. This waste contains mixtures of combustibles (e.g., paper, polyvinyl chloride, polypropylene, polyethylene, and neoprene)

TABLE B.3.1 Estimated quantities of TRU mixed waste (by waste form) from the Rocky Flats Plant in Colorado[a,b]

Description	Quantity (Kg)
Cemented and uncemented aqueous waste	13,502,156
Cemented and uncemented organic waste	3,268,296
Immobilized process and laboratory solids	338,396
Combustible waste	6,662,118
Metal waste	9,654,088
Filter waste	2,210,912
Inorganic solid waste	415,480
Leaded rubber waste	363,655
Total	36,415,101

[a] Westinghouse Electric Corporation, 1989. "Radioactive Mixed Waste Compliance Manual," Appendix 6.4.1, WP-02-07, Rev. 0, WIPP, Carlsbad, New Mexico.

[b] Quantities include waste projected to be generated through the year 2013, as well as waste currently in retrievable storage at the Idaho National Engineering Laboratory.

TABLE B.3.2 Estimated maximum concentrations of hazardous chemical constituents in CH TRU mixed waste from the Rocky Flats Plant in Colorado[a]

Hazardous chemical constituent[b]	Waste form							
	Aqueous waste[c]	Organic waste[c]	Process and laboratory solids[d]	Combustible waste	Metal waste	Filter waste	Inorganic solids	Leaded rubber waste
1,1,1-trichloroethane	75	150,000	200	2,000	15	150	900	0
Carbon tetrachloride	25	50,000	25	750	10	150	100	0
1,1,2-trichloro-1,2,2-trifluoroethane	100	50,000	200	1,500	75	100	8,000	0
Methylene chloride	700	0	100	750	200	50	700	0
Methyl alcohol	25	0	15	0	0	0	0	0
Xylene	50	0	50	0	0	0	0	0
Butyl alcohol	10	0	10	0	0	0	0	0
Cadmium	10	0	0	0	0	0	0	0
Lead	10	0	400	10	$1x10^6$	0	0	$6x10^5$

[a] Estimated maximum concentrations in milligrams per kilogram (mg/kg) (Rockwell International, 1988).

[b] The hazardous chemical constituents were determined by knowledge of the processes used in generating the waste. The estimated maximum concentrations represent extremely conservative quantities that may be present in the specific waste forms. No analytical data are available for the hazardous chemical constituents in these waste forms.

[c] Cemented and uncemented sludges.

[d] Neutralized and immobilized (cemented) solids.

and noncombustibles (e.g., laboratory equipment, tools, and small electric motors) that were removed from the Alpha Gamma Hot Cell Facility. This waste will not contain free liquids or particulates.

- Sludges. Fuel and process sludges currently stored in tanks will be solidified (i.e., cemented or microwaved). This waste will be a solid monolith packaged in lead-shielded canisters.

The primary hazardous chemical constituent of RH TRU mixed waste is lead packaging which is used as gamma shielding in most of the waste packages. Trace quantities of mercury, barium, chromium, and nickel have also been reported in some of the sludges.

REFERENCES FOR APPENDIX B

DOE (U.S. Department of Energy), 1989. TRU Waste Acceptance Criteria for the Waste Isolation Pilot Plant, WIPP-DOE-069, Revision 3, Carlsbad, New Mexico.

DOE (U.S. Department of Energy), 1988. Final Safety Analysis Report, Waste Isolation Pilot Plant (Draft), DOE/WIPP 88-XXX, Carlsbad, New Mexico.

DOE (U.S. Department of Energy), 1987. Integrated Data Base for 1987: Spent Fuel and Radioactive Waste Inventories, Projections, and Characteristics, DOE/RW-0006, Rev. 3.

DOE (U.S. Department of Energy), 1980. Final Environmental Impact Statement, Waste Isolation Pilot Plant, WIPP-DOE-0026, Volumes 1 and 2, Carlsbad, New Mexico.

Rockwell International, 1988. "Hazardous Constituents of Rocky Flats Transuranic Waste", Internal Letter for distribution from J. K. Paynter, May 24, 1988, WCP02-31, Golden, Colorado.

WEC (Westinghouse Electric Corporation), 1989. "Radioactive Mixed Waste Compliance Manual," Appendix 6.4.1, WP-02-07, Rev. 0, Waste Isolation Pilot Plant, Carlsbad, New Mexico.

WIPP-WEC, 1989. "Draft Radionuclide Source Term for the WIPP, 1989, 88-049, Carlsbad, New Mexico.

APPENDIX C

TRANSPORTATION EMERGENCY PLANNING

TABLE OF CONTENTS

Section		Page
C.1	INTRODUCTION	C-1
C.2	EMERGENCY RESPONSE TRAINING	C-2
	C.2.1 Introduction	C-2
	C.2.2 Emergency Response (ER) Training	C-2
	C.2.3 Examples of Emergency Response	C-7

C.1 **INTRODUCTION**

Emergency response programs have been initiated far in advance of any waste transportation to the WIPP. Several Federal and state agencies across the country have been involved in developing and implementing effective emergency response programs. These efforts require a variety of interfaces in twenty-three states and involves contacts with the public, and local, state, Federal, and Indian tribal government agencies.

This appendix describes the emergency response training programs, and examples of DOE responses to past accidents involving radioactive wastes.

C.2 EMERGENCY RESPONSE TRAINING

C.2.1 INTRODUCTION

The Safety, Security, and Environmental Programs (SS&EP) of the DOE WIPP Project Office have the responsibility for developing and conducting emergency response training to corridor states and Indian Tribes. The purpose is: 1) to provide accurate information regarding the WIPP to enhance hazardous materials response capabilities along the transport corridor routes, 2) to provide specific response protocols to responders along TRU waste routes, 3) to provide states and local jurisdictions with the framework to build radiological materials response programs, 4) to provide responders with skills necessary to assess impacts of an accident involving a WIPP shipment, and 5) to provide states with independent response and monitoring capabilities.

C.2.2 EMERGENCY RESPONSE (ER) TRAINING

In late 1987, agreement was reached with the State of New Mexico to provide WIPP-related emergency response (ER) training to the state. As a result of this decision, the States Training and Education Program (STEP) was created.

Training is team-taught by experienced primary and secondary instructors. Primary instructors include experienced emergency medical personnel, fire fighters, law enforcement personnel, and incident commanders. Secondary instructors include professional health physicists and personnel experienced in radiation protection. The ER training is an ongoing program and will continue over the active life of the WIPP Project using the "train-the-trainer" approach. Provision is made for training materials to be given to state agencies for their instructors and for the evaluation of state instructors by STEP officials before certification. Instructors must be state certified before attending the STEP.

In addition, detailed plans and procedures have been developed to guide emergency response to a transportation accident. These include:

- Waste Isolation Division Transportation Plan: Reporting Transportation Accidents or Incidents
- WIPP Waste Transportation Manual: Emergency Responses and Reporting
- WIPP Central Coordination Center (CCC) Transportation Monitoring Responsibilities
- TRANSCOM Tracking System Emergency Response
- Defense Transuranic Waste Program Management and Operation Plan: Emergency Response

- Emergency Responses That Have Utilized The Regional Radiological Assistance Program.

These may be examined at the WIPP Project Office in Carlsbad, New Mexico.

C.2.2.1 **Emergency Response Courses**

Training materials and aids that are needed or recommended varies for level and type of instruction. These include TRUPACT-II models, radiation monitoring equipment, scale models or maps of cities and towns, simulated accident scenes and response techniques, a WIPP overview and description, DOE capabilities, and the transportation tracking system.

Four separate training programs have been developed.

- First Responder Course - A one-day, eight-hour class that provides an overview of the WIPP and basic radiation and radiation protection principles. This course is intended for fire, law enforcement, and emergency medical personnel to ascertain accident severity before a command center can be established.

  The following is a synopsis of the actions necessary for a responder to follow to insure the protection of himself, the victims, and the public as is taught in the STEP classes.

  1. Remain calm. Do not be overly concerned with the presence of radioactive material or allow it to disrupt usual emergency response activities.

  2. Perform life-saving rescue and emergency first aid. Delay other first aid until victims can be removed from the vicinity of any potentially hazardous materials. Notify receiving medical facilities of possible contamination for radiation exposure of the injured.

  3. Establish a control zone. The perimeter of this zone will be determined by the accident scene conditions. If there is no chance of release of radioactive material, a minimum distance of 150 ft is recommended. If containers are breached and dispersal is possible, the minimum distance may be 200 ft or more, depending on the quantity of material, its radiotoxicity, the weather and atmospheric conditions, or as required by other hazardous materials.

  4. Notify radiological assistance and other emergency service agencies as needed.

  5. Remove personnel from the immediate downwind area. Detain personnel in the immediate area and cordon off items with possible contamination until they can be checked by radiological monitors.

6. Keep upwind of fumes or smoke.

7. Limit time near radioactive shipping package to the minimum necessary.

8. Obtain information concerning the cargo from placards, labels, shipping documents, and other immediately available sources from the appropriate state office.

9. Note conditions that may indicate damage to shipping packages. Cover spilled radioactive material to limit dispersal and identify the area.

10. Avoid direct contact with radioactive materials where possible. Utilize protective clothing and anything available for remote handling (e.g., shovels, branches, ropes), if available.

11. Wrap and label or separate clothing, tools, etc., used during the emergency and retain them until they can be monitored for radiation.

12. Make detailed records of actions and findings, including times, names, locations, etc. This information will assist in reconstructing the accident and estimating radiation exposures, if any.

13. Perform radiological monitoring if so equipped and trained to do so.

14. Do not allow eating, drinking, smoking, or other activities within contaminated areas that might lead to intake of radioactive material.

- Command and Control Center - This is a two-and-one-half day course intended for individuals who may be in command at the scene of a transportation accident involving TRU waste. Explanation of protocol for radiological response teams, actions for the first responders, scene and crowd control (including media interface) are discussed thoroughly. Students are also instructed in basic health physics and radiation protection principles to assist in decision making. Simulated table-top exercises are included to challenge the students and ascertain their ability to respond correctly to a postulated accident.

- Mitigation Course - This is a one-day, eight-hour course intended for health physics and environmental professionals from the states. This course covers: 1) the health physics and characteristics of TRU waste, 2) the DOE's Radiological Response Team's capabilities and duties, 3) interfaces between state and local authorities and the DOE, 4) media interfaces, 5) sampling techniques applicable to TRU waste accidents, and 6) assessment of the effectiveness of recovery operations.

- Train-the-Trainer Program - This is a 16-hour course intended for individuals currently certified or authorized to conduct training of law enforcement, fire, or medical personnel within their state or local jurisdictions. Methods, information and materials to instruct trainers are provided to effectively

transmit this information to their students. Slides, lesson plans, and sample handouts are provided to these instructors at the completion of the course.

These four courses are available to local responders approximately every sixty miles along transportation routes and will be taught one to four months prior to initial TRUPACT-II shipments. Training in the first transportation corridor, from the Idaho National Engineering Laboratory and Rocky Flats Plant to the WIPP, was completed in October 1988. Training for state personnel along the Southern Transportation Corridor, from the Savannah River Plant to the WIPP (South Carolina, Georgia, Alabama, Mississippi, Louisiana, and Texas) is scheduled to start in April 1989 and finish in August 1989. Refresher training will be offered to the first corridor states of Idaho, Utah, Wyoming, Colorado, and New Mexico commencing in June 1989 with completion in October 1989.

C.2.2.2 Emergency Response Scenario

To illustrate the course content and to provide the reader with graphic examples of emergency response, an accident situation involving a transporter destined for the WIPP is described in the following scenario. Explanation of actions taken by responders and the time elements involved in controlling and mitigating the accident scene are provided.

Preface: It is impossible to envision every detail in any accident scenario. The following gives an upper bound accident scenario in which a release of TRU waste from a TRUPACT-II has occurred. The average response times of various agencies are projected in this scenario as well as the personnel and equipment which typically would respond.

Scenario: At approximately 10:45 p.m., a TRUPACT-II shipment with 42 barrels of TRU waste is travelling a two-lane U.S. Highway in northern New Mexico, proceeding to the WIPP. It is raining and as the vehicle tops the crest of a hill, a car attempts to pass a second vehicle and collides head-on with the transporter. The transporter goes off the road and rolls into an adjacent arroyo that is approximately 20 ft deep and 15 ft off the roadway. The truck driver and the passengers in the car are seriously injured.

A passerby stops and assesses the nature of the injuries. He leaves the accident scene and drives 11 miles to the nearest telephone where help is summoned by calling the New Mexico State Police. It is assumed that the passerby did not note the radioactive placarding and therefore, the fact that the vehicle carried radioactive material was not relayed to the New Mexico State Police.

Approximately 15 minutes later, the first New Mexico State Police car arrives at the scene and parks approximately 50 feet from the TRUPACT-II tractor/trailer in the arroyo. The New Mexico State Police officer, utilizing a spotlight, identifies the radioactive placard and immediately instructs bystanders to move back from the area, a minimum of 150 ft upwind; get into their vehicles; and remain there until such time as the vehicles can be surveyed.

The state police officer at this time would assess the extent of injuries to the best of his ability. The officer would then radio Santa Fe Control and inform them that he has a hazardous material accident involving radioactive materials in which several people have

been injured and requires immediate medical response. Additionally, due to gasoline and diesel fuel at the scene and the precarious positioning of the TRUPACT-II trailer with the drivers still in the cab of their tractor, he requires fire and rescue response in addition to backup law enforcement for scene security.

A volunteer fire department covers this area and requires 24 minutes from time of notification to mobilize and respond to the scene. The ambulance service arrives approximately 20 minutes before the fire-rescue units. Immediately, the emergency medical personnel proceed to check in with the state policeman, who is the on-scene commander. He informs them of the situation and the number of injured he has observed.

The emergency medical personnel proceed to the vehicles and render aid to the victims. In preparation for handling the victims, additional Emergency Medical Technicians (EMTs) and fire personnel prepare the stretchers and ambulance interior to minimize or eliminate the possibility of contamination spread from the scene to the EMTs and then to the hospital.

Additional law enforcement officers arrive at this time and begin to cordon off the area and secure a minimum distance of 150 ft in all directions which includes blockage of the highway. Fire personnel utilize standard operating procedures for control of flammable and combustible liquids at the scene and the possibility of electrical fires within the vehicles.

Since fire personnel will be spending significant time around the scene, they have donned their fire fighting clothing (bunker clothes) and self-contained breathing apparatus to preclude any possibility of contamination or uptake of material. Santa Fe Control has now notified the Environmental and Health Department of the State of New Mexico that an incident has occurred involving a TRUPACT-II transporter with unconfirmed release of radioactive materials and likewise notifies the DOE, Albuquerque Operations Office. Albuquerque Operations Office notifies the nearest DOE facility, Los Alamos National Laboratory, which immediately begins to activate a radiological response team. The radiological response team from Los Alamos National Laboratory arrives at the accident scene approximately 1 hour and 45 minutes after the first notification was made to the state police. In the meantime, the state team from Santa Fe has already arrived and is in the process of making preliminary surveys for any gross contamination or release.

It is determined that a TRUPACT-II container has been damaged, after surveys have been concluded by the State and the DOE radiological response team. Damage is the result of the container striking large, sharp, jagged rocks in the arroyo. A small amount of the radioactive waste has escaped from a small rip in the side of the container. Concern for human life and health is paramount and radiation surveys are immediately made of all bystanders, law enforcement officers, firefighters, and rescue personnel still at the scene to immediately address the problem of potential contamination. Contamination is found on firefighters' boots and the shoes of one state police officer still at the scene. Their footwear is removed and placed in plastic bags and given to the DOE team for decontamination. The remainder of the personnel are surveyed and no contamination is found. Those personnel no longer needed at the scene are

released after personal data are recorded for any follow up. The DOE will be responsible for cleanup and full mitigation of all consequences of the accident.

The DOE, in cooperation with the state Environmental and Health team, will upright the TRUPACT-II containers, and repair them if possible. If the damage is not repairable, the material will be transloaded into another TRUPACT-II container to be delivered in approximately eight hours. The soil around the area would be surveyed, retrieved, containerized, and transported to the WIPP site. All possible modes of contamination spread would be evaluated. Samples of water and vegetation would be taken and continuous air monitors would be set up in the area. When the DOE and the New Mexico State Police Officer verify all radiation levels are at normal background, the State will release the DOE from the scene with possible follow-up sampling in the general area in the weeks or months to come. Samples taken at the scene will be evaluated independently by the State and the DOE. Results of the samples would be compared. The DOE and the State will cooperate on the preparation of a report outlining actions taken. The DOE will assist the State in the actual accident investigation. Materials such as fire hoses, boots, blankets, etc. that were contaminated at the scene and do not lend themselves to easy decontamination will be replaced at the expense of the DOE.

DOE, State and hospital representatives with radiological monitoring expertise will respond to the hospital to which the injured were taken. The State and DOE health physics personnel will cooperate and coordinate with the physician in charge in assessing the possibility of contamination. Any contaminated clothing or materials which can not be decontaminated, will be taken into DOE possession for disposal and replaced at the cost of the DOE.

C.2.3 EXAMPLES OF EMERGENCY RESPONSE

The following summaries provide examples of past incidents and response times for various DOE responses to specific incidents. These responses are similar to those that would occur during accidents of trucks or trains carrying TRU waste to the WIPP.

C.2.3.1 Radiological Assistance Response - Burley, Idaho - October 12, 1986

At 5:25 p.m. on October 12, 1986, the Idaho Warning Communications Center arranged a conference call between the Idaho Department of Health and Welfare (IHW), and the DOE Idaho Operations Office, Region 6 Radiological Assistance Coordinator. It was reported that a tractor-trailer containing radioactive materials had been involved in an accident with other vehicles on Interstate 84 near Burley, Idaho, and had plunged into the Snake River. The radioactive shipment was enroute from the RMI Company Ashtabula Extrusion Plant, Ashtabula, Ohio, to the United Nuclear Company, Hanford Site, Richland, Washington. IHW staff were preparing to proceed to the scene of the accident (about 130 miles from Boise, Idaho, and about 120 miles from Idaho Falls, Idaho) to assist law enforcement personnel at the scene.

A Radiological Assistance Team (RAT) of the DOE Idaho Operations was placed on alert pending a request for services. Following a review of the accident, the five-man RAT (with eight RAT kits and special survey instruments) was dispatched to the Burley airport by helicopter. Ground transportation to the accident scene was provided by the Idaho State Police and the Cassia County Sheriff's Office. Following an inspection of

the accident scene by the RAT and a determination that the radioactive shipment posed no immediate threat to public health and safety, a meeting was held in Twin Falls, Idaho, with state and local authorities to formulate a plan of action to be implemented as soon as daylight permitted.

The Idaho National Engineering Laboratory Emergency Response Van arrived at Burley to function as a mobile command post, communications center, and health physics laboratory. A second RAT arrived by helicopter at the Burley airport to provide assistance at the accident scene. The truck driver and relief driver had sustained injuries that required their hospitalization. The tractor-trailer cargo consisted of: 1) 20 wooden packages loaded with 3-5 billets of low enrichment uranium metal weighing 250-285 pounds each, and 2) 73 empty wooden packages. Radiological surveys of the cargo, vehicle, handling personnel, and the environment by the State of Idaho health and physics personnel and the RAT demonstrated that no detectable radioactivity was released from the radioactive shipment.

Local, regional, and national news media coverage of this accident was intense. Local and state authorities at the scene requested that the DOE coordinate radio commentaries, television coverage, and newspaper articles. This action ensured that information about the accident was timely, factual, and consistent among the various reports of the accident. Timely notifications, with appropriate updates, were made throughout the response to DOE management, the DOE Headquarters Emergency Operations Center, the shipper, the receiver, state and local officials, and other officials.

By October 13, 1986, a firm in Twin Falls, Idaho, commenced salvage operations to retrieve the tractor/trailer cargo of loaded and empty containers. The last package was lifted out by crane that afternoon. The salvaged containers were placed in large water-tight metal containers. In addition, a structural engineer provided guidance to the RAT and the salvage operator, relative to the effects of water (river) pressure on the trailer during load recovery operations. Late on October 13, 1986, two trucks, one loaded with empty containers and the other carrying loaded containers, arrived at the Idaho National Engineering Laboratory.

On October 14, 1986, the tractor-trailer was towed from the Snake River and transported to a salvage yard in Twin Falls, Idaho. Later on October 14, 1986, following radiological surveys of the vehicle and the environment, the area was released for unrestricted use. A close-out was held at the accident scene by participants in the response. A critique of the accident response was held at the Idaho State Police Office in Twin Falls.

C.2.3.2 Radiological Assistance Response - Pocatello, Idaho - October 10, 1985

On October 7, 1985, the Idaho Warning Communications Center (WCC) was contacted by Union Pacific Railroad Operations Division, Omaha, Nebraska, regarding a radioactive placarded ATMX railcar observed to be leaking at the Union Pacific Rail Terminal in Pocatello, Idaho.

The WCC was provided details by the Region 6, Radiological Assistance Coordinators with a followup call to the shipping department at Rocky Flats Plant, Colorado, from which the shipment originated. It was confirmed that the subject car was carrying

plutonium contaminated waste. A radiological assistance team (RAT) was formally requested by the Union Pacific Railroad.

Immediate actions that evening at the site were to monitor (frisk) the five personnel who had visited the railcar in question. No contamination was detected during the personnel alpha surveys. Then, samples were taken in the immediate railcar area. Weather conditions prior to and during the surveys were generally windy with a mixture of snow and rain. Samples were taken of the dripping liquid and smears taken in the immediate railcar area. The smears were allowed to dry, scanned (frisked) with alpha and beta gamma instruments, and then counted. Followup smears were taken of the observed wide crack on the underside of the ATMX car. No contamination was detected and it was concluded that leakage was weather-related without any radioactive release.

APPENDIX D

TRANSPORTATION AND TRANSPORTATION-RELATED RISK ASSESSMENTS

TABLE OF CONTENTS

Section		Page
D.1	INTRODUCTION	D-1
D.2	TRANSPORTATION OF WASTE TO THE WIPP	D-2
D.2.1	Background	D-2
D.2.2	TRU Waste Transportation Package: Regulatory Authorities and Responsibilities	D-3
D.2.2.1	Regulatory Authorities	D-3
D.2.2.2	Responsibilities	D-3
D.2.3	Transportation Modes	D-3
D.2.3.1	Truck Transport	D-3
D.2.3.2	Rail Transport	D-9
D.2.4	Transportation Routes	D-9
D.2.4.1	Truck Transport	D-9
D.2.4.2	Rail Transport	D-36
D.2.5	Transportation Planning and Responsibilities	D-37
D.2.6	Vehicle Tracking System	D-40
D.3	RADIOLOGICAL RISK OF TRANSPORTATION	D-42
D.3.1	Introduction	D-42
D.3.2	Incident-Free Risks	D-45
D.3.2.1	Incident-Free Radiological Risk Method	D-45
D.3.2.2	Incident-Free Radiological Risk Results	D-51
D.3.3	Radiological Risks of Transportation Accidents	D-57
D.3.3.1	Method for Calculating Radiological Risks of Transportation Accidents	D-57
D.3.3.2	Accident Radiological Risk Results	D-79
D.3.4	Radiological Consequences of Bounding-Case Transportation Accident	D-82
D.3.4.1	Assumptions - Bounding-Case Accident	D-82
D.3.4.2	Results - Bounding-Case Accident	D-86
D.4	NONRADIOLOGICAL AND NONCHEMICAL CONSEQUENCES OF TRANSPORTATION	D-89
D.4.1	Introduction	D-89
D.4.2	Method	D-89
D.4.3	Results	D-89
D.4.4	Traffic Accidents and Statistics	D-103
D.4.4.1	State Traffic Statistics	D-103
D.4.4.2	State Traffic Accidents	D-103
REFERENCES FOR APPENDIX D		D-117

LIST OF FIGURES

Figure		Page
D.2.1	Typical tractor-trailer combination for TRU waste transport	D-6
D.2.2	Proposed TRU waste truck transportation routes	D-14
D.2.3	Indian tribes along proposed TRU waste truck transportation routes	D-15
D.2.4	Proposed TRU waste truck transportation routes in New Mexico	D-16
D.2.5	Proposed TRU waste truck transportation routes from eastern DOE facilities to the New Mexico border	D-17
D.2.6	Proposed TRU waste truck transportation routes from western DOE facilities to the New Mexico border	D-21
D.2.7	Proposed mainline railroad routes for TRU waste transportation to the WIPP	D-38
D.3.1	Truck Accident Severity Category Classification Scheme	D-63
D.3.2	Railroad Accident Severity Category Classification Scheme	D-64
D.3.3	Possible Pathways to Man from Radionuclide Release	D-77

LIST OF TABLES

Table		Page
D.2.1	Road segments of concern	D-23
D.3.1	Year 2013 projected retrievably-stored and newly-generated TRU waste	D-46
D.3.2	Projected CH TRU and RH TRU waste shipments from generating and storage facilities to the WIPP	D-47
D.3.3	Average CH TRU waste trailer load radioactivity	D-48
D.3.4	Average RH TRU waste trailer load radioactivity	D-49
D.3.5	Transport index values	D-50
D.3.6	Average distances to the WIPP and percent of travel in various population zones	D-51
D.3.7	RADTRAN general input data	D-53
D.3.8	Radiological risk per CH TRU shipment	D-54
D.3.9	Radiological risk per RH TRU shipment	D-55
D.3.10	Lifetime radiological risk of incident-free transportation of CH TRU waste	D-56
D.3.11	Summary of lifetime radiological risks between Proposed Action and Alternative Action, CH TRU incident-free occupational risk	D-58
D.3.12	Summary of lifetime radiological risks between Proposed Action and Alternative Action, CH TRU incident-free nonoccupational risk	D-59
D.3.13	Summary of lifetime radiological risks for incident-free transportation of RH TRU waste (person-rems): Proposed Action and the Alternative Action	D-60
D.3.14	Hypothetical maximum exposure to an individual from incident-free transportation during Test Phase and Disposal Phase (25 years)	D-61

D.3.15 Fractional occurrences for truck accidents by accident severity category and population density zone D-66

D.3.16 Fractional occurrences for train accidents by accident severity category and population density zone D-67

D.3.17 Estimate of potential accident release fractions for CH and RH TRU waste shipments D-69

D.3.18 Release algorithm parameters D-70

D.3.19 CH TRU waste package release fractions: truck D-73

D.3.20 CH TRU waste package release fractions: rail D-74

D.3.21 RH TRU waste package release fractions: truck D-75

D.3.22 RH TRU waste package release fractions: rail D-76

D.3.23 Per shipment radiological risk of CH TRU waste shipments (mrem) . . . D-80

D.3.24 Lifetime radiological risk for accident transportation of CH TRU waste (mrem) D-81

D.3.25 Summary of lifetime radiological risk changes between Proposed Action and Alternative Action: CH TRU accident nonoccupational risk (mrems) D-83

D.3.26 Per shipment radiological risk of RH TRU shipments (mrem) D-84

D.3.27 Lifetime radiological risk for accidents during transportation of RH TRU waste (mrem): Proposed Action and Alternative Action D-85

D.3.28 Bounding case accident scenario assumptions D-87

D.4.1 Estimated CH TRU and RH TRU waste shipments from generating and storage sites to the WIPP D-90

D.4.2 Average distances to the WIPP and percent of travel in various population zones D-91

D.4.3 Air pollutant unit consequence factors D-92

D.4.4 Nonradiological and nonchemical unit risk factors D-92

D.4.5 Per shipment nonradiological risk of waste shipments D-93

D.4.6 Total transportation risk for Proposed Action Alternative, CH truck mode D-95

D.4.7 Total transportation risk for Proposed Action Alternative, CH rail mode D-97

D.4.8.Total transportation risk for Alternative Action, CH truck mode D-99

D.4.9. Total transportation risk for Alternative Action, CH rail mode D-100

D.4.10 Total transportation risk for Proposed Action and the Alternative Action, RH truck mode D-101

D.4.11 Total transportation risk for Proposed Action and the Alternative Action, RH rail mode D-102

D.4.12 Traffic statistics segment analysis: Savannah River Plant to the WIPP D-104

D.4.13 Traffic statistics segment analysis: Argonne National Laboratory to the WIPP D-105

D.4.14 Traffic statistics segment: Mound Laboratory to the WIPP D-106

D.4.15 Traffic statistics segment analysis: Nevada Test Site to the WIPP . . . D-107

D.4.16 Traffic statistics segment analysis: Idaho National Engineering Laboratory to the WIPP D-108

D.4.17 Traffic statistics segment analysis: Rocky Flats Plant to the WIPP . . . D-109

D.4.18 Traffic statistics segment: Los Alamos National Laboratory to the WIPP D-110

D.4.19 Traffic statistics segment: Lawrence Livermore National Laboratory to the WIPP D-111

D.4.20 Traffic statistics segment analysis: Hanford Reservation to the WIPP D-112

D.4.21 Traffic statistics segment analysis: Oak Ridge National Laboratory to the WIPP D-113

D.4.22 Traffic statistics - accidents by segments D-114

D.1 **INTRODUCTION**

This appendix provides additional detail and background information for Sections 3.1.4 and 5.4.3 on the transportation modes under consideration (truck and maximum rail transportation); the DOE proposed transportation routes; the risks and accidents associated with radiological pathways; and nonradiological and nonchemical risks. Each section provides the reader with the various changes in analyses that have developed since the FEIS was published in 1980.

The DOE has contacted each of the 23 corridor states for current highway and rail transportation data in order to update the highway analyses provided in the FEIS. Additionally, each of the states was asked to provide qualitative information on road segments that were perceived to be hazardous.

D.2 TRANSPORTATION OF WASTE TO THE WIPP

D.2.1 BACKGROUND

Since the FEIS was prepared in 1980, many changes have been made in plans and systems required to transport TRU waste to the WIPP. In addition, substantial development work has been accomplished on the required components, systems, and facilities for transport. In this section, the details of these are described.

There are four major areas of changes between transportation analysis in the 1980 FEIS and those presented in this SEIS.

First, there are ten facilities currently from which TRU waste may be shipped. Originally, only transportation of TRU waste from the Idaho National Engineering Laboratory and the Rocky Flats Plant to the WIPP was analyzed. A comprehensive analysis of the activities and consequences of handling and moving this waste from these ten facilities is now provided.

Second, the volumes, quantities, locations, and characteristics of the TRU waste currently planned for shipment are different from that reported in the 1980 FEIS. For this study, a comprehensive analysis of the new data is now available and has been provided in other sections of this SEIS (see SEIS subsections 1.1, 3.1 and Appendix B).

Third, design, testing, and NRC certification of CH and RH transportation packaging has advanced. The design of the CH waste package is new, the result of 7 years of an intense, iterative process of redesign, testing, and certification. Work on design and testing the RH waste package is progressing.

Fourth, as directed by law (P.L. 96-164), substantive discussions were initiated with the State of New Mexico on a wide variety of WIPP subjects including transportation of TRU waste across the State. A supplemental Stipulated Agreement (SSA) with New Mexico was developed as a result. The DOE has also initiated discussions with the other states through which TRU waste will be transported. All western TRU waste corridor states belong to the Western Interstate Energy Board (WIEB), which includes Arizona, California, Colorado, Idaho, Nevada, Oregon, Utah, Washington, and Wyoming. The remaining affected states are organized into a Southern States Energy Board (SSEB). Each state provides one representative to attend Board meetings. Numerous meetings have been held with representatives of the WIEB and the SSEB to discuss WIPP-related transportation issues. Several agreements have been reached on the training of personnel (sheriffs, police, firemen, and ambulance attendants) for transportation emergency response programs and for local Command and Control operations (see SEIS Appendix C).

D.2.2 TRU WASTE TRANSPORTATION PACKAGE REGULATORY AUTHORITIES AND RESPONSIBILITIES

D.2.2.1 Regulatory Authorities

The NRC is the certifying authority for the WIPP TRU waste containers that would be used for truck or rail transportation. To date, TRUPACT-IIs have undergone extensive testing and design modification that will continue until NRC requirements have been satisfied, prior to any WIPP-related transportation. The DOE will apply for NRC certification under 10 CFR 71 once package testing is complete. Additionally, the DOE is developing and testing packaging for RH TRU waste (NUPAC 72B) that will also meet all NRC requirements prior to use. In addition to NRC certification requirements, TRUPACT-II and NUPAC 72B must also satisfy DOT requirements as defined in 49 CFR 173.465 and 173.466 (packaging tests for Type A containers) and 49 CFR 173.469 (packaging tests for Type B containers). TRUPACT-II and NUPAC 72B are described in detail in SEIS Subsection 3.1.4.

D.2.2.2 Responsibilities

In addition to regulatory requirements specific to the TRU waste containers, responsibilities related to the shipments have been defined by the DOE and are given below by governing entity:

Defense facility responsibilities

- Complying with package certification criteria
- Preparing WIPP WAC data package
- Transmitting WIPP WAC data package to WIPP
- Transmitting bill of lading to TRANSCOM
- Receiving and inspecting empty packages

WIPP responsibilities

- Dispatching empty packages
- Maintaining transport packages
- Decontaminating packages as required
- Reporting package availability status.

D.2.3 TRANSPORTATION MODES

D.2.3.1 Truck Transport

The WIPP is capable of receiving truck or train TRU waste shipments. Current plans are to ship wastes by truck, however, wastes may be shipped by train in the future. As previously noted, TRU waste transportation will be accomplished in two phases. The first phase is the Test Phase which will span up to five years. During this time TRU shipments will be by truck. Under the proposed action, up to a maximum of ten

percent of the TRU waste would be transported during the Test Phase. The next phase will span twenty years, and could utilize either trucks or trains.

D.2.3.1.1 Scope of work. In 1988, the DOE awarded a contract to a commercial carrier for the first five years of truck transport of TRU wastes from the storage and generator facilities to the WIPP (DOE, 1988b). This contract contains numerous provisions for safe and efficient transport of TRU waste and for response to transportation emergencies. Key provisions of the contract include, but are not limited to:

- The contractor will provide tractors wholly dedicated to contract requirements and provide technically qualified and experienced drivers for the life of the contract period. The DOE will operate a transportation operations control center called the Central Coordination Center (CCC) 24 hours a day, seven days a week. This center will be the day-to-day contact for the contractor carrier and drivers (see SEIS Subsection D.2.6).

- Tractors are to be domiciled and maintained within a 50-mile radius of the WIPP, and will be dispatched with a DOE-owned trailer and empty packaging.

- At high volume origins, the driver will drop the trailer and packaging at the loading location designated by each facility and will be provided a return loaded trailer for the shipment back to the WIPP. At low volume origins, the driver will drop the trailer and packaging at the loading location designated by each facility and wait for the facility to load the container and trailer and release it to the driver for the return trip to the WIPP.

- Upon reaching the WIPP, the driver will drop the trailer and loaded packages at the facility's designated location and return to the terminal.

- The contractor will be required to perform verifiable routine maintenance and inspections on tractors and trailers before and after each movement.

- DOE will be responsible for any maintenance and repairs to the packaging. If repair of the packaging needs to be performed while enroute, the contractor will take appropriate corrective steps after receiving CCC approval.

- The contractor will be required to meet Federal regulatory requirements for the transportation of radioactive and hazardous materials, including driver training in accordance with 10 CFR and 49 CFR, as amended, and the Commercial Motor Vehicles Safety Act of 1986 and subsequent amendments.

- The contractor is required to provide a Traffic Manager who will act as a single point of contact for the DOE's Technical Representative in dealing with dispatching and scheduling of shipments, and coordinating and resolving problems associated with shipments.

D.2.3.1.2 Tractor equipment. Listed below are the minimum specifications for tractors required to haul TRU waste in a safe and efficient manner:

- The tractor will be a Type II truck tractor with a conventional, 6 x 4-ft cab sleeper. The gross tractor weight, completely equipped per requirements, including fuel, safety equipment, tractor spare, and drivers' personal items will not exceed 18,000 lb (Figure D.2.1).

- The tractor will be equipped with full-time power steering.

- The tractor will be equipped with a mobile telephone (industry standard) for two-way communication. The telephone system will be Motorola Model T5023 or its equivalent.

- The tractor will be equipped with an in-dash plug or other adaptation for a two-way digital communication device.

- The tractor will contain a 40-channel two-way citizens band (CB) transceiver.

- The tractor will be equipped with an alpha-beta-gamma radiation detection meter and a beta-gamma radiation detection meter.

- Parking brakes will be required on rear axles, and an auxiliary braking system will be required.

- The tractor will have full diesel power of at least 400 HP.

- The tractor will be equipped with spray guards and mud flaps for the rear and front wheels.

- A heavy duty, 36-inch sliding fifth wheel will be required on the tractor.

- Tire chains will be carried at all times.

- Tires will be sufficient to meet maximum weight limitations.

- The tractor will be equipped with an air ride suspension that maximizes torsional stability.

The DOE has not requested an exemption for TRU waste transport through any of the corridor states and will meet applicable Federal regulations.

The tractor/trailer combination will meet state required weight distributions and dimension requirements. The overall length of the tractor and the trailer will not exceed 60 ft.

D.2.3.1.3 Driver Qualifications. Drivers will meet the driver licensing, training, and physical qualification requirements set forth in 49 CFR Parts 177.825 and 391, the Commercial Motor Vehicle Safety Act of 1986 and subsequent amendments. Additional qualifications include:

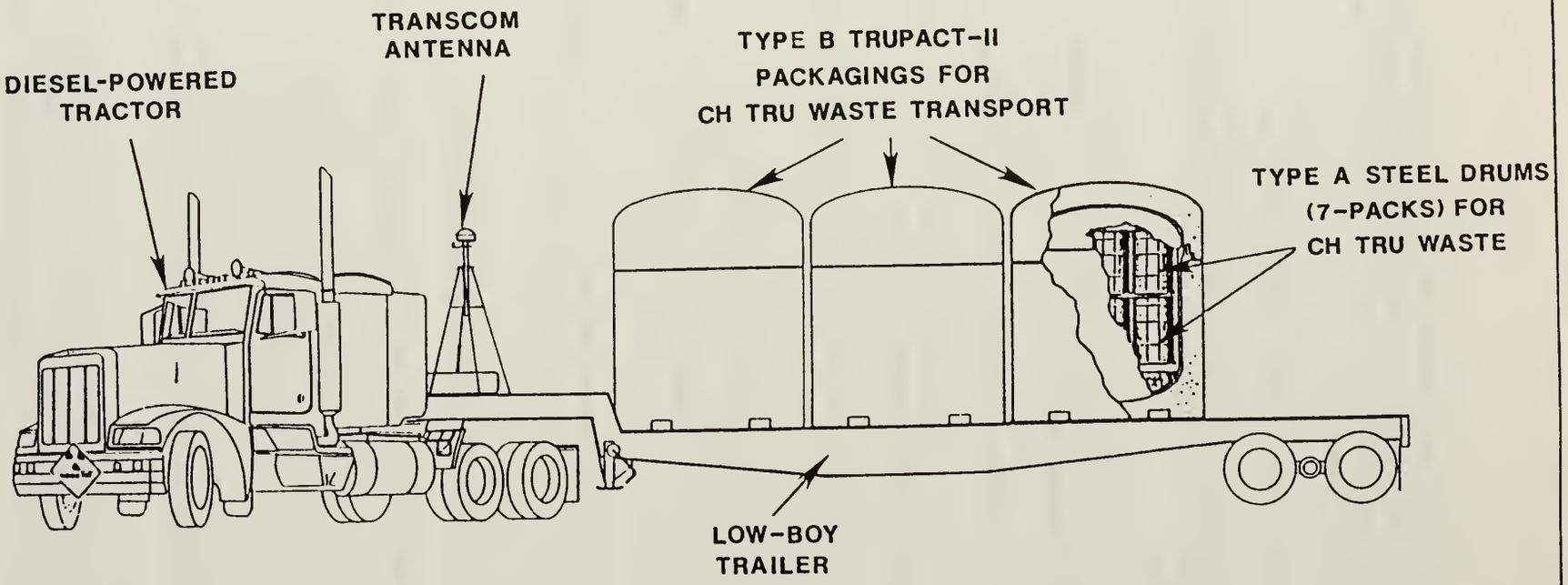

NOT TO SCALE

FIGURE D.2.1

TYPICAL TRACTOR-TRAILER COMBINATION FOR TRU WASTE TRANSPORT

- Drivers will be at least 25 years of age.

- Drivers will have logged a minimum of 100,000 miles in semi-tractor/trailer combination.

- Drivers will have at least two years of uninterrupted semi-tractor/trailer commercial driving experience during the last five years.

- Drivers will be tested for drugs as part of their hiring physical and are subject to retesting at any time during the contract.

D.2.3.1.4 Driver Training Program. Drivers will be trained to the requirements set forth in 49 CFR Part 177.825 which states: 1) the driver has received within the two preceding years, written training on: i) requirements in Parts 172, 173, and 177 of this subchapter (49 CFR) pertaining to the radioactive materials being transported, and the properties and hazards of the radioactive materials being transported.

Training for the drivers on the radioactive materials being transported to WIPP includes the properties and hazards of the transuranic materials being shipped, basic radiation and radiation protection principles, and the use and understanding of the radiation detection instruments carried on the transport vehicles for routine checks and emergencies.

The DOE will provide accident or other emergency training as required under 49 CFR 177.825 (d)(1)(iii) (see SEIS Appendix C).

D.2.3.1.5 Driver Inspections. Drivers are required to make routine visual safety inspections of the tractor, trailer, and container every 100 miles as required by 49 CFR 397.17.

D.2.3.1.6 Dual Drivers. Two qualified drivers are required to accompany each shipment of TRU waste. If a driver becomes incapacitated in route, the alternate driver must receive appropriate instructions through the CCC before proceeding.

D.2.3.1.7 Constant Surveillance. Constant Surveillance Service (CSS) shall be provided for loaded shipments. Constant Surveillance Service is defined as follows:

- Continuous responsibility for constant surveillance and custody of shipments in transit. Such attendance and surveillance shall prevent tampering, pilfering, sabotage, including, insofar as humanly possible, all manner of unusual circumstances, such as wreck, delay, flood, or violent disturbances.

- A vehicle must be attended at all times by a driver or qualified representative of the contractor. A vehicle is "attended" when at least one driver is in the tractor, awake, not in a sleeper berth, or is within 100 ft of the vehicle and has the vehicle within their constant unobstructed view.

- When circumstances require extended stops in route, the shipment will be parked only at a CCC designated parking area. When this occurs, a driver must keep the shipment in full view and stay within 100 ft of the shipment at all times unless released by CCC.

- The trailer and package must always be connected to the designated tractor during shipment except when stopped at a DOE facility for loading, unloading, enroute maintenance, or as approved by the CCC.

D.2.3.1.8 Driver Call-In. Prior to the operation of the satellite tracking system, the driver will provide a two-hour call-in check while drivers are enroute. This call-in will be made to the CCC by the on-board communication devices in the contractor's tractors.

D.2.3.1.9 Detention Rules for Tractors and Drivers. Detention rules for contractor's tractors and drivers include:

- Drivers will arrive at the WIPP for pick-up of the trailer and packaging when specified by the CCC on a 24-hour, seven days-a-week basis.

- Drivers will provide two hours of detention time at the WIPP and high volume shipment origins.

- Drivers must arrive at the defense facilities for loading when specified by facility personnel between the hours of 8:00 a.m. and 4:00 p.m., Monday through Friday. Other times will be approved by the CCC prior to arrival.

- Drivers will provide 24 hours of detention time at locations other than the WIPP and at the high-volume origins.

D.2.3.1.10 Maintenance and Inspection. A maintenance facility will be provided and located within a 50-mile radius of the WIPP. Maintenance will be performed in accordance with tractor and trailer manufacturer's recommendations. The facility will be of sufficient size to allow provisions for recordkeeping, parts storage, dispatching, and associated management functions. In addition, a maintenance plan will be maintained that addresses the following elements:

- Pre-trip inspection requirements, procedures and proposed maintenance schedules for each tractor and trailer utilized.

- A verifiable maintenance, inspection, and repair record on each tractor and trailer, after each loaded movement and prior to being dispatched on each run.

- Nationwide maintenance agreements or arrangements to address equipment breakdowns, replacements, or operating difficulties route between origin and destination. Plan must address capability of replacing route tractors within eight hours.

- Procedures for maintaining an annual, per tractor and trailer, 2 percent or less "DOWN TIME RATE," (i.e., the annual percent relationship of scheduled time that a tractor is not safely operable versus the time that it is in actual operating mode).

- Security measures to prevent public access to maintenance facilities. Public access to maintenance facility shall be denied on a 24-hour basis by appropriate security measures.

- Qualifications and training of maintenance personnel.

D.2.3.2 Rail Transport

Current plans call for waste transport by truck for at least five years rail transport details and specifications have yet to progress in a commensurate manner for example, a rail car design for the transportation of TRU waste has not been agreed upon by the rail companies and the DOE. It is unknown when certifiable packaging would be available for rail use. The present TRUPACT-II design may to be modified for proper tie-down on a rail car. It may be possible that the tractor-trailer with TRUPACT-II containers could be placed on flat bed cars with only additional supporting features. A decision to pursue rail certification, design modifications, other feature modifications, and safety specification for rail transport of CH and RH TRU waste will be made in the future as necessary.

D.2.4 TRANSPORTATION ROUTES

D.2.4.1 Truck Transport

D.2.4.1.1 Regulatory Authorities. TRU waste shipments must comply with the rules, regulations, and orders promulgated by the DOE, the NRC, the ICC, and the DOT. The major responsibilities and regulations, by governing entity, are summarized below.

- DOE. The DOE governs the protection of the public health and safety during transport of radioactive materials by requiring compliance with applicable DOT and NRC regulations. In particular, the following DOE Orders assure such compliance:

  DOE Order 1540.1. Order 1540.1 governs materials transportation and traffic management and defers to the DOT and NRC regulations; the Interstate Commerce Act (49 U.S.C.); and the Hazardous Materials Transportation Act (49 U.S.C. 1801 et. seq.).

  DOE Order 5820.2. Order 5820.2 establishes policies, guidelines, and minimum requirements by which the DOE manages its radioactive and mixed waste and contaminated facilities, including the transportation of waste; shipment of low-level waste defers to Order 1540.1.

- NRC. As the regulator of the commercial nuclear industry, the NRC must assure the safety of commercial nuclear operations, specifically, the transfer of by products, source, and special nuclear materials. For the transport of nuclear materials, the NRC regulations apply primarily to shippers and, in particular, to the packaging of materials. 10 CFR 71 (Packaging and Transportation of Radioactive Material) sets packaging standards for radioactive materials and defers to DOT 49 CFR 177 for regulating the transport of these materials on public highways.

- ICC. The Interstate Commerce Commission has jurisdiction over the economic (cost) aspects of shipping radioactive material, such as regulating carrier rates. ICC regulations are not considered further, since the primary concern of this document is environment, health, and safety.

- DOT. The DOT has the primary responsibility for regulating the transportation of radioactive materials. The DOT responsibilities related to the WIPP project, truck transportation option are defined primarily in 49 CFR 171 and 177, which are summarized as follows:

  49 CFR 171.8 defines a "state-designated route" as a preferred route selected in accordance with the U.S. DOT "Guidelines for Selecting Preferred Highway Routes for Highway Route Controlled Quantities of Radioactive Materials" or an equivalent routing analysis which adequately considers overall risk to the public. Designation must have been preceded by substantive consultation with affected local jurisdictions and with any other affected States to ensure consideration of impacts and continuity of designated routes.

  "State routing agency" means an entity (including a common agency of more than one State such as one established by Interstate compact) which is authorized to use a State legal process pursuant to Part 177.825 of this subchapter to impose routing requirements, enforceable by State agencies, on carriers of radioactive materials without regard to intrastate jurisdictional boundaries. This term also includes Indian tribal authorities which have police power to regulate and enforce highway routing requirements within their lands.

  49 CFR 177.825 provides: "Routing and training requirements for radioactive materials", which is excerpted for the reader as follows:

  (a) The carrier shall ensure that any motor vehicle which contains a radioactive material for which placarding is required is operated on routes that minimize radiological risk. The carrier shall consider available information on accident rates, transit time, population density and activities, time of day, and day of week during which transportation will occur. In performance of this requirement, the carrier shall tell the driver that the motor vehicle contains radioactive materials and shall indicate the general route to be taken. This requirement does not apply when--

1) There is only one practicable highway route available, considering operating necessity and safety, or

2) The motor vehicle is operating on a preferred highway under conditions described in paragraph (b) of this section.

(b) Unless otherwise permitted by this section, a carrier and any person who operates a motor vehicle containing a package of highway route controlled quantity radioactive materials as defined in Part 173.403(l) of this subchapter shall ensure that the vehicle operates over preferred routes selected to reduce time in transit, except that an Interstate System bypass or beltway around a city shall be used when available.

1) A preferred route consists of:

(i) An Interstate System highway for which an alternative route is not designated by a State routing agency as provided in this section, and

(ii) A State-designated route selected by a State routing agency (see Part 171.8 of this subchapter) in accordance with the DOT "Guidelines for Selecting Preferred Highway Routes for Shipments of Large Quantity Radioactive Materials."

2) When a deviation from a preferred route is necessary (including emergency deviation, to the extent time permits), routes shall be selected in accordance with paragraph (a) of this section. A motor vehicle may deviate from a preferred route under any of the following circumstances:

(i) Emergency conditions that would make continued use of the preferred route unsafe.

(ii) To make necessary rest, fuel, and vehicle repair stops.

(iii) To the extent necessary to pick up, deliver, or transfer a highway route controlled quantity package of radioactive materials.

(c) A carrier (or high agent) who operates a motor vehicle which contains a package of highway route controlled quantity radioactive materials as defined in Part 173.403(l) of this subchapter shall prepare a written route plan and supply a copy before departure to the motor vehicle driver and a copy to the shipper (before departure for exclusive use shipments, or otherwise within fifteen working days following departure). Any variation between the route plan and routes actually used, and the reason for it, shall be reported in an amendment to the route plan delivered to the shipper as soon as practicable but within 30 days following the deviation.

D.2.4.1.2 Selection Criteria. Traditionally, the choice of the highway routes used for the transportation of hazardous materials has been the prerogative of the carrier. The choice was determined by the routes authorized in the carrier's Interstate Commerce Commission (ICC) Certificate or subsequent carrier's certificates. However, due to the perceived risks associated with the transport of radioactive materials, various local governmental units began to ban or limit the movements of radioactive materials through their jurisdictions. Since there are many such local units, given a proliferation of this process, the nation would be faced with a potential breakdown of the transport system.

To forestall such an occurrence, the DOT (the regulating Federal agency) undertook a rule-making action to examine the relative roles of Federal, state, and local agencies in establishing the routes to be used in transporting placarded shipments of radioactive materials. An Advance Notice of Proposed Rule Making was published on August 17, 1978. The final rule was published on January 19, 1981. The content of the final rule can be summarized as:

1. The primary safety mechanism imposed on the transport of radioactive materials is the highly regulated packaging requirements (NRC: 10 CFR 71). Properly packaged radioactive materials can be transported with the same degree of safety as other hazardous materials.

2. Recognizing the increased safety features inherent in the Federal Interstate Highway System, movement of radioactive materials should be routed on Interstate Highways, including Interstate bypasses around population centers.

3. If a different route choice provides a demonstrated added degree of safety, an individual state may make that determination and enforce the use of the designated preferred route. The DOT has chosen the State government for this role over country and local government because it results in a reasonably small number of government units (there are approximately 23,000 county and local government units), and because the State is sufficiently large to achieve an overall approach to routing determinations.

4. However, the DOT recognizes that highway safety considerations can be and are highly local concerns. Therefore, the DOT specifically requires that the process of designating preferred routes be designed to involve participation by local government representatives and members of the general public.

5. Finally, reflecting the position expressed in Item 1, State and local governments must not interfere with the movements of radioactive material shipments from points of origin along direct access to Interstate Highways, or from the Interstates to specific destinations. Similarly, normal use of non-Interstate roads for purposes of refueling, rest stops, repairs, etc., may not be denied.

As a result of the above-stated DOT policies, the proposed WIPP transportation routes have been chosen to make maximum use of the Interstate Highway System. Several states have expressed an interest in providing an alternative route segment for evaluation. The DOE and carrier will work with any state who can provide timely, reasonable alternatives to the proposed route.

D.2.4.1.3 Proposed Routes. The general proposed routes for transporting TRU waste from the defense facility of origin to the WIPP are shown on Figure D.2.2. The various Indian tribes along the proposed routes are shown on Figure D.2.3, and Figures D.2.4 through D.2.6 provide additional details on the routes. These routes were selected based on the use of interstate highways and other criteria previously presented (Subsection D.2.4.1.2).

To ensure that road segments of state concern are identified corridor states have provided a qualitative assessment of relatively hazardous road conditions that may be present along the proposed routes (Table D.2.1). Segments of concern were found to be primarily related to winter driving conditions in the mountains and bridges icing up in the winter, and interchanges in urban areas. These road segments and potential problems will be noted on logs provided to the carrier. In areas having the potential for sudden winter storms, parking areas will be designated in concert with the corridor state. The following text provides additional details.

- State of New Mexico. As shown in Figure D.2.4, all transportation routes converge in New Mexico and for that reason, New Mexico is addressed separately. Because all radioactive waste bound for WIPP must be routed through New Mexico, transportation and routing within the state have been identified in several agreements with the State of New Mexico. The most relevant of these is the "Supplemental Stipulated Agreement Resolving Certain State Off-Site Concerns Over WIPP," which was entered into by the State of New Mexico and the DOE in December 1982.

  The specifications of the Agreement recognized that movements between incoming interstates and the relatively remote WIPP would involve conventional highways. A corollary consideration was that, as New Mexico is the host State, these highways would see relatively concentrated service. Therefore, the DOE agreed to support the State in efforts to obtain from Congress the funds necessary to repair and upgrade the routes designated in the Agreement. Additionally, in New Mexico, there are two highway sectors that have been identified in the Supplemental Stipulated Agreement as alternate routes. These would be used during severe weather conditions. As shown in Figure D.2.3, east-bound trucks on I-40 would interchange onto I-25 in Albuquerque and continue east on I-25 to the US-285 interchange, just west of Glorietta, New Mexico. They would then continue south on US-285 to the WIPP. West bound trucks on I-40 would remain on I-40 to Clines Corners and then continue south on US-285.

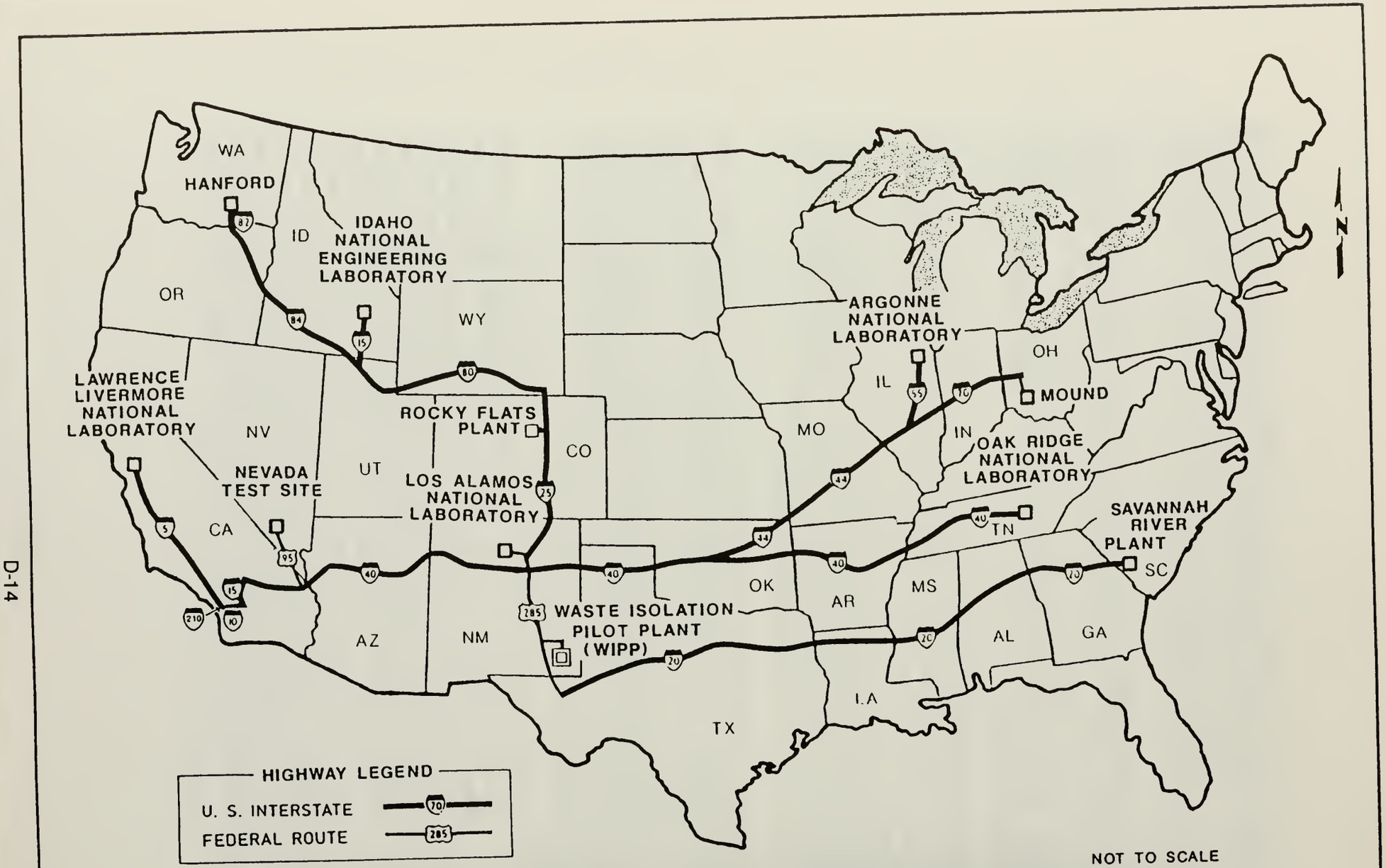

FIGURE D.2.2
PROPOSED TRU WASTE TRUCK TRANSPORTATION ROUTES

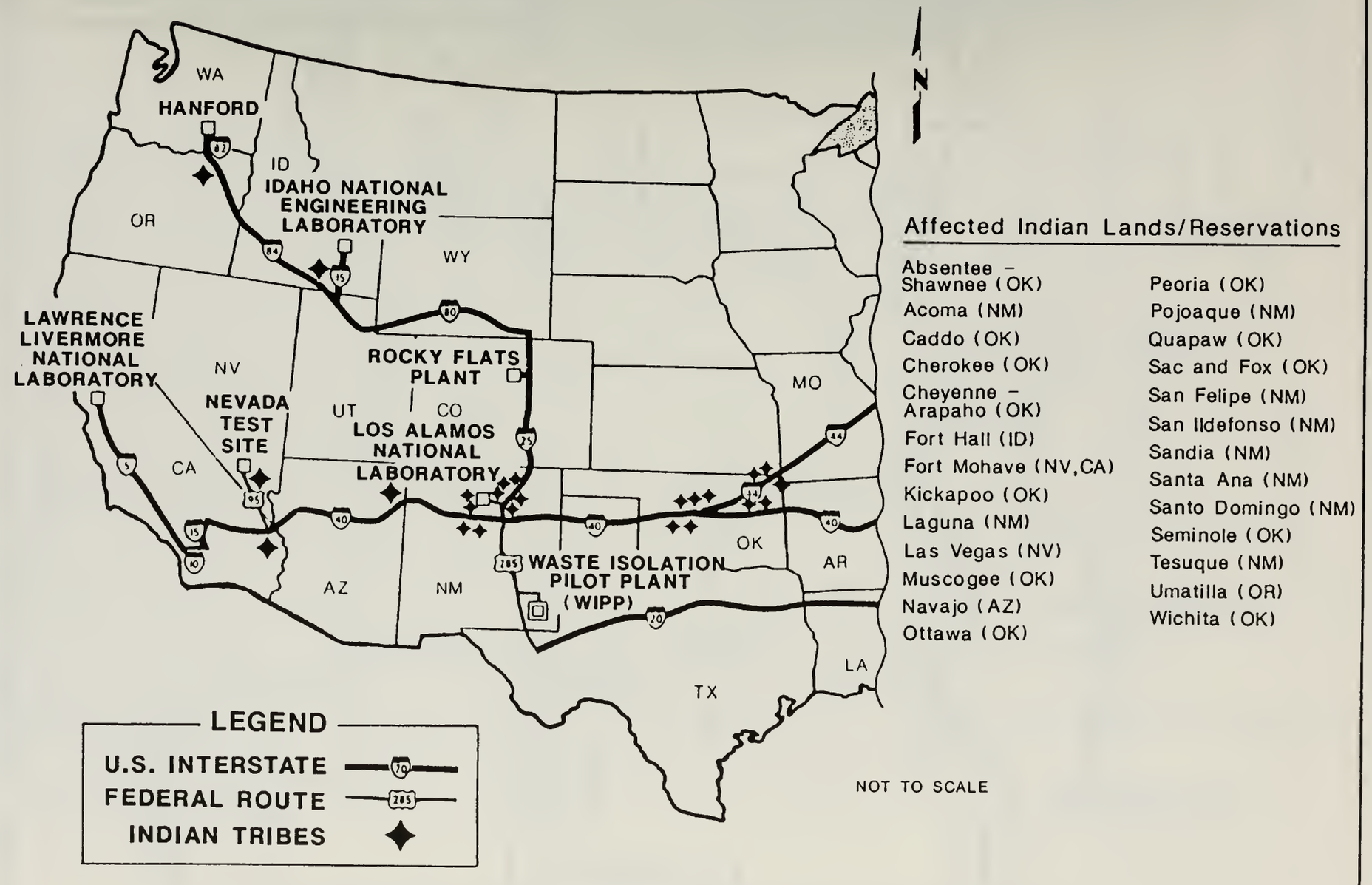

Affected Indian Lands/Reservations

Absentee – Shawnee (OK)
Acoma (NM)
Caddo (OK)
Cherokee (OK)
Cheyenne – Arapaho (OK)
Fort Hall (ID)
Fort Mohave (NV,CA)
Kickapoo (OK)
Laguna (NM)
Las Vegas (NV)
Muscogee (OK)
Navajo (AZ)
Ottawa (OK)
Peoria (OK)
Pojoaque (NM)
Quapaw (OK)
Sac and Fox (OK)
San Felipe (NM)
San Ildefonso (NM)
Sandia (NM)
Santa Ana (NM)
Santo Domingo (NM)
Seminole (OK)
Tesuque (NM)
Umatilla (OR)
Wichita (OK)

FIGURE D.2.3
INDIAN TRIBES ALONG PROPOSED TRU WASTE TRUCK TRANSPORTATION ROUTES

FIGURE D.2.4

PROPOSED TRU WASTE TRUCK TRANSPORTATION ROUTES IN NEW MEXICO

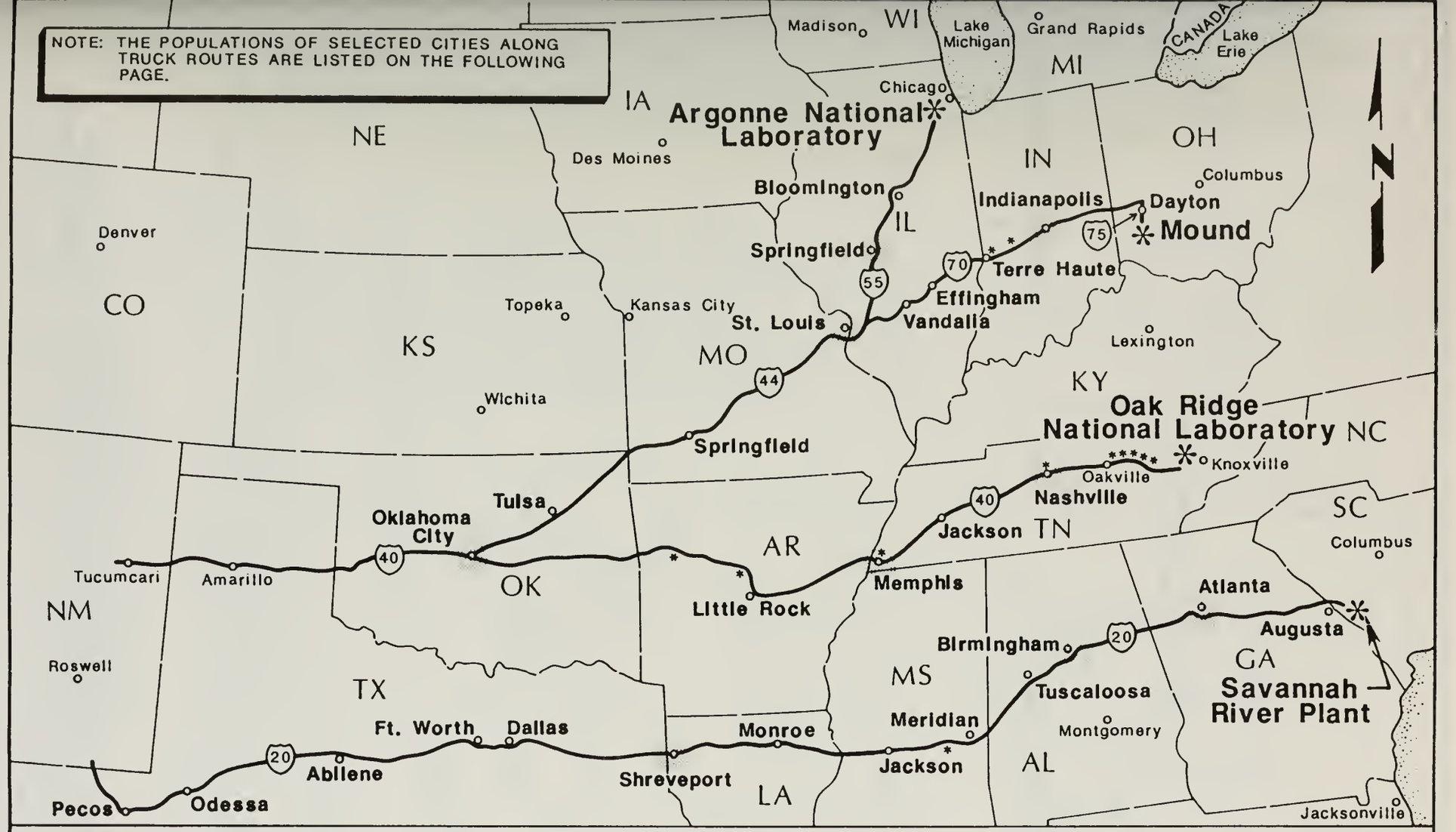

FIGURE D.2.5
PROPOSED TRU WASTE TRUCK TRANSPORTATION ROUTES FROM EASTERN DOE FACILITIES TO THE NEW MEXICO BORDER

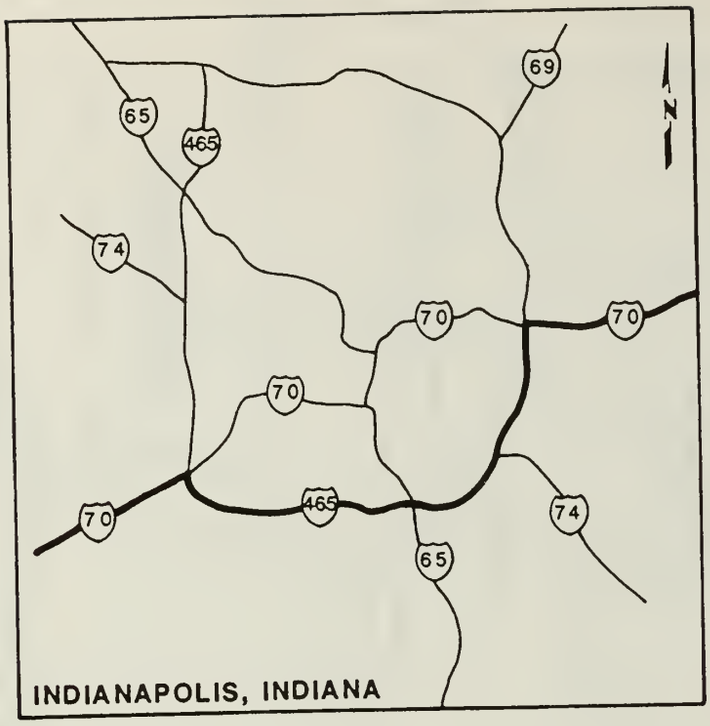

INDIANAPOLIS, INDIANA

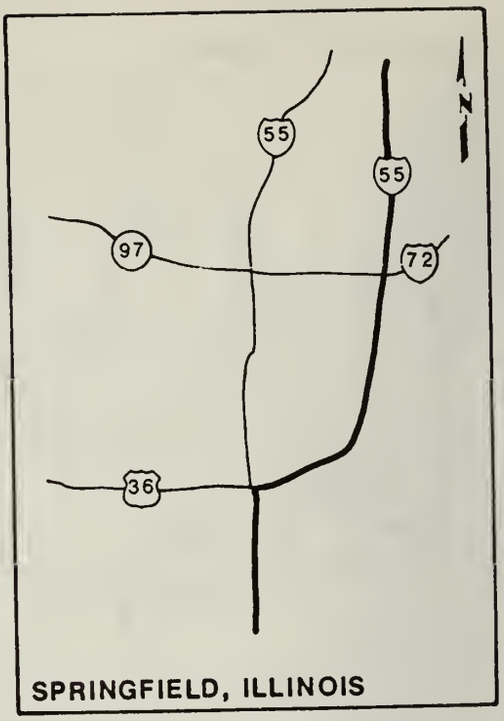

SPRINGFIELD, ILLINOIS

ST. LOUIS, MISSOURI

Populations of Selected Cities

Abilene, Texas	98,315
Amarillo, Texas	149,230
Atlanta, Georgia	425,022
Augusta, Georgia	47,532
Birmingham, Alabama	284,413
Bloomington, Illinois	44,189
Dallas, Texas	904,078
Dayton, Ohio	203,588
Effingham, Illinois	11,270
Fort Worth, Texas	385,141
Indianapolis, Indiana	700,807
Jackson, Mississippi	202,895
Jackson, Tennessee	49,131
Little Rock, Arkansas	158,461
Memphis, Tennessee	646,356
Meridian, Mississippi	46,577
Monroe, Louisiana	57,597
Nashville, Tennessee	455,651
Odessa, Texas	90,027
Oklahoma City, Oklahoma	403,213
Pecos, Texas	14,618
Shreveport, Louisiana	205,815
Springfield, Illinois	99,637
Springfield, Missouri	133,116
St. Louis, Missouri	453,085
Terra Haute, Indiana	61,125
Tulsa, Oklahoma	470,593
Tuscaloosa, Alabama	75,143
Vandalia, Illinois	5,338

NOTE: THIS FIGURE SHOWS THE HIGHLIGHTED CITY BYPASSES ALONG ROUTES FROM THE ARGONNE NATIONAL LABORATORY AND MOUND TO OKLAHOMA CITY, OKLAHOMA.

NOT TO SCALE

REF: RAND McNALLY, 1987.

FIGURE D.2.5 (CONTINUED)
PROPOSED TRU WASTE TRUCK TRANSPORTATION ROUTES FROM EASTERN DOE FACILITIES TO THE NEW MEXICO BORDER

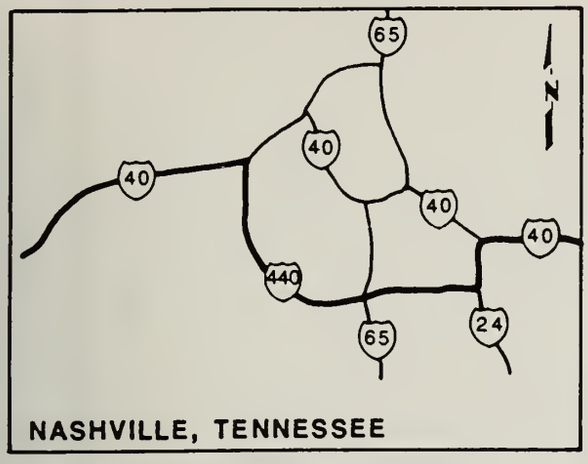

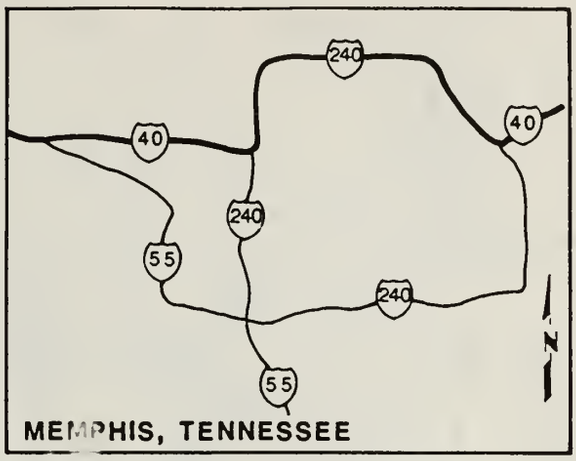

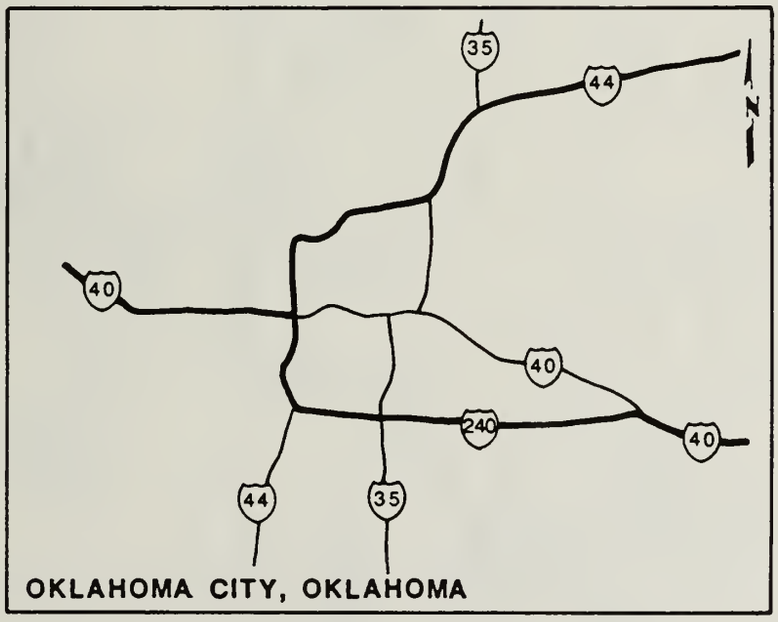

NOT TO SCALE

NOTE: THIS FIGURE SHOWS THE HIGHLIGHTED CITY BYPASSES ALONG THE ROUTE FROM OAK RIDGE NATIONAL LABORATORY TO THE NEW MEXICO BORDER.

REF: RAND McNALLY, 1987.

FIGURE D.2.5 (CONTINUED)
PROPOSED TRU WASTE TRUCK TRANSPORTATION ROUTES
FROM EASTERN DOE FACILITIES TO THE NEW MEXICO BORDER

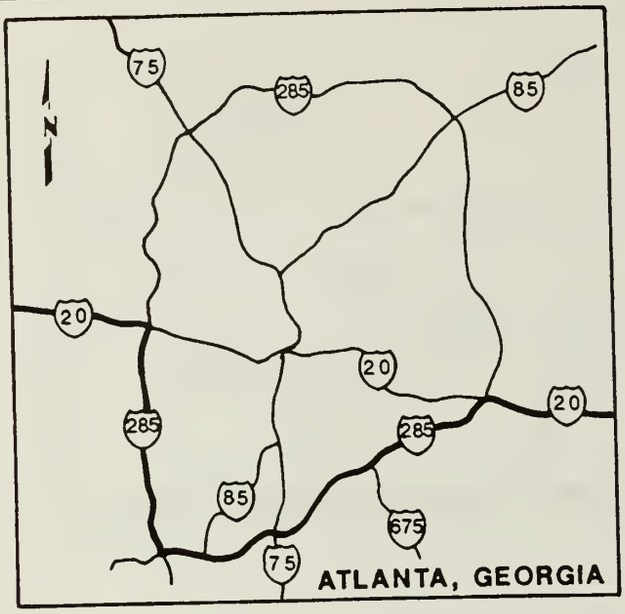

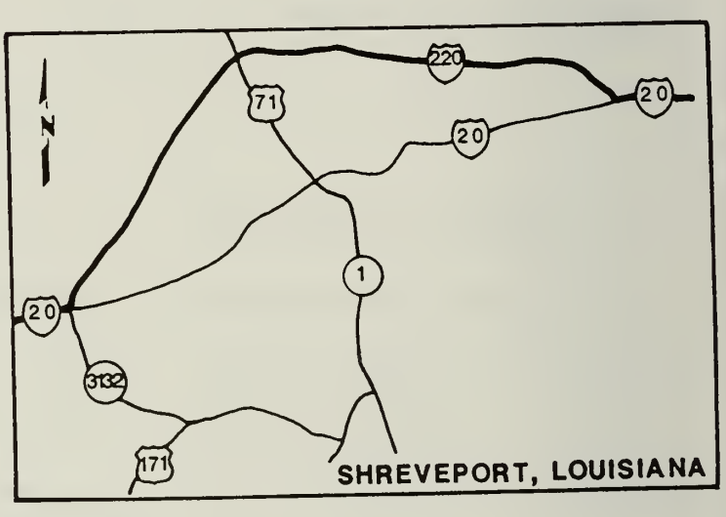

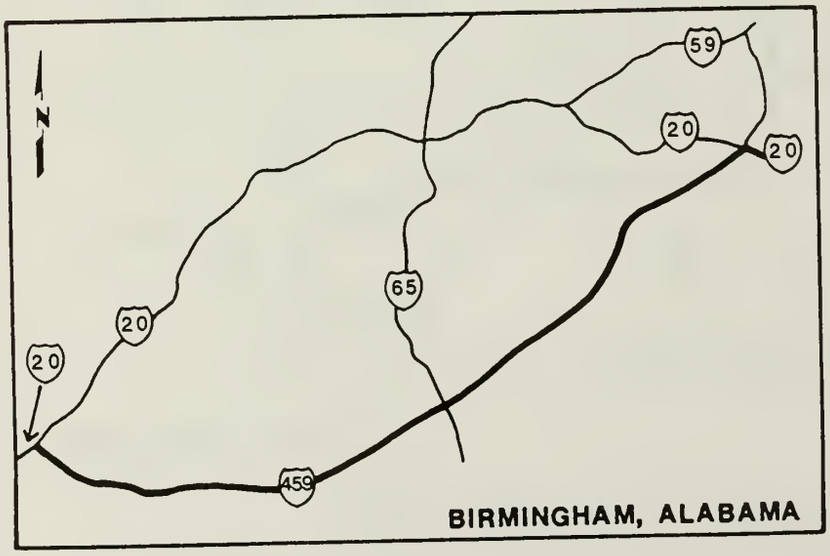

NOT TO SCALE

NOTE: THIS FIGURE SHOWS THE HIGHLIGHTED CITY BYPASSES ALONG THE ROUTE FROM THE SAVANNAH RIVER PLANT TO THE NEW MEXICO BORDER.

REF: RAND McNALLY, 1987.

FIGURE D.2.5 (CONCLUDED)
PROPOSED TRU WASTE TRUCK TRANSPORTATION ROUTES FROM EASTERN DOE FACILITIES TO THE NEW MEXICO BORDER

LEGEND

*** SEGMENT OF CONCERN

SEE NEXT PAGE FOR ENLARGEMENT OF AREA

0 100 200

SCALE IN MILES

REF: RAND McNALLY, 1987.

FIGURE D.2.6

PROPOSED TRU WASTE TRUCK TRANSPORTATION ROUTES FROM WESTERN DOE FACILITIES TO THE NEW MEXICO BORDER

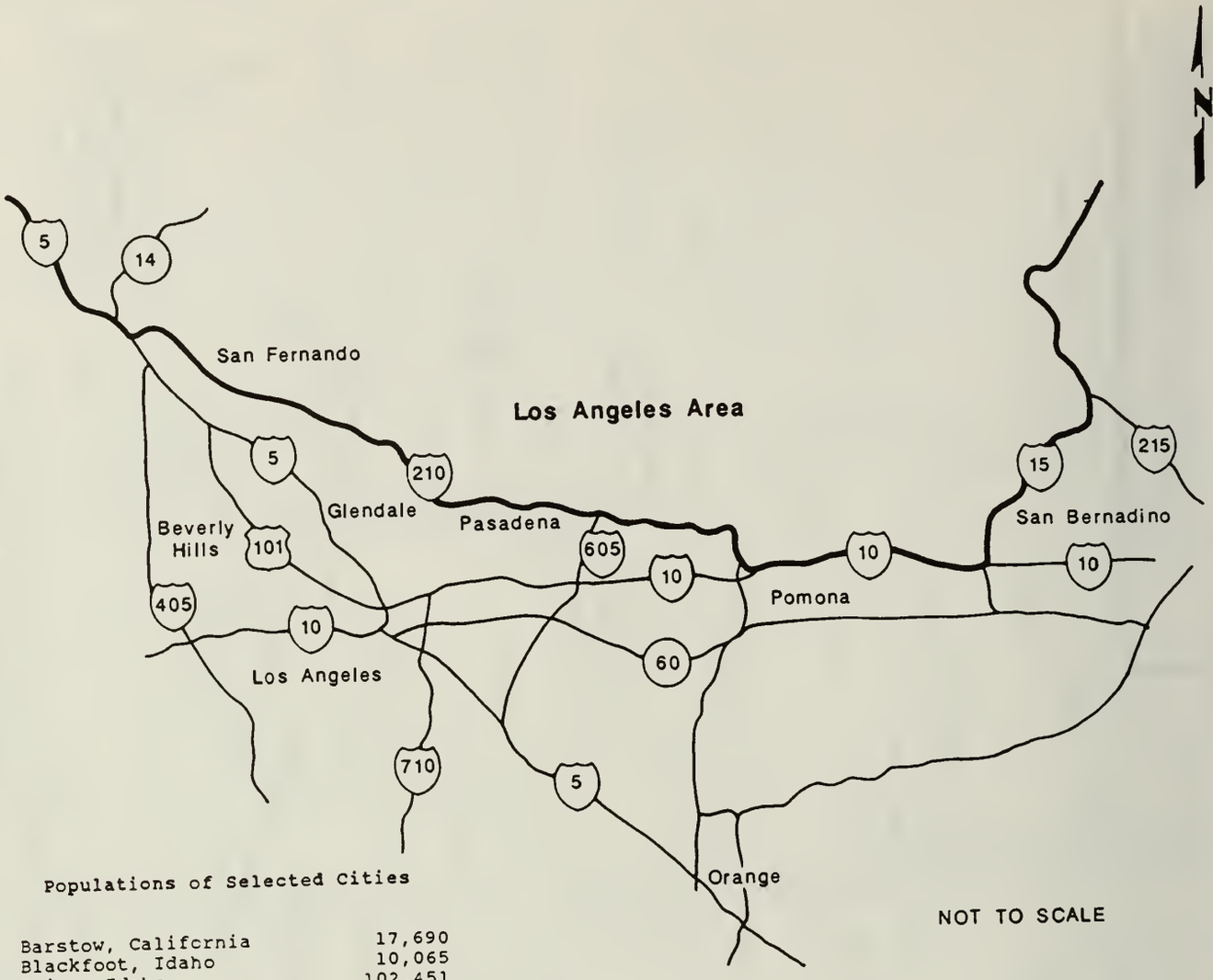

NOT TO SCALE

Populations of Selected Cities

Barstow, California	17,690
Blackfoot, Idaho	10,065
Boise, Idaho	102,451
Boulder City, Nevada	9,590
Cheyenne, Wyoming	47,283
Colorado Springs, Colorado	215,150
Denver, Colorado	491,396
Flagstaff, Arizona	34,641
Glenns Ferry, Idaho	1,374
Holbrook, Arizona	5,785
La Grande, Oregon	11,354
Laramie, Wyoming	24,410
Las Vegas, Nevada	164,674
Los Angeles, California	2,966,763
Ogden, Utah	64,407
Ontario, Oregon	8,814
Pasco, Washington	17,944
Pendleton, Oregon	11,354
Pocatello, Idaho	46,340
Pueblo, Colorado	101,686
Rawlins, Wyoming	11,547
San Bernadino, California	118,057
Trinidad, Colorado	9,663
Twin Falls, Idaho	26,209
Yuma, Arizona	42,433

REF: RAND McNALLY, 1987.

NOTE: THIS FIGURE SHOWS THE HIGHLIGHTED BYPASS ALONG THE ROUTE FROM LAWRENCE LIVERMORE NATIONAL LABORATORY TO THE NEW MEXICO BORDER.

FIGURE D.2.6 (CONCLUDED)
PROPOSED TRU WASTE TRUCK TRANSPORTATION ROUTES FROM WESTERN DOE FACILITIES TO THE NEW MEXICO BORDER

TABLE D.2.1 Road segments of concern[a]

Defense Facility/Route	Milepost[b]	Geographic Description	Description of Concern
Mound Laboratory, Ohio[c]			
I-70 (Indiana)	34-33	Approximately seven miles west of Cloverdale, Indiana	Water in east-bound lane may puddle causing trucks to hydroplane
I-70 (Indiana)	18-17	Near Terre Haute, Indiana	Overpass bridge on curve will ice
I-70 (Indiana)	11	State Highway 46 interchange, Near Terre Haute, Indiana.	High volume interchange
I-70 (Indiana)	7-6	US-41 Interchange, near Terre Haute, Indiana.	High volume interchange
Oak Ridge National Laboratory, Tennessee			
I-40 (Tennessee)	330-287	Highway segment between Crab Orchard and Cookeville, Tennessee	Mountain driving, ice on highway during winter storms, may be impassable
I-40 (Tennessee)	210 0.00	Nashville and Memphis, Tennessee.	Interchanges are busy during rush hour traffic
I-40 (Arkansas)	69.61	Just east of Clarksville, Arkansas	Flat curve in west-bound lane
I-40 (Arkansas)	125.11	Just west of Conway, Arkansas	Flat curve in east-bound lane

TABLE D.2.1 Continued

Defense Facility/Route	Milepost[b]	Geographic Description	Description of Concern
Oak Ridge National Laboratory, Tennessee (continued)			
I-40 (New Mexico)	373-358	Just east of San Jon, New Mexico	Pavement is concrete and will freeze first.
I-40 (New Mexico)	326-324	Palma Hill, west of Tucumcari, New Mexico	Ices in winter
I-40 (New Mexico)	310	West of Tucumcari, New Mexico	Bad curve, accident area
I-40 (New Mexico)	291-281	East of Santa Rosa, New Mexico.	Windy, drifting snow conditions
Savannah River Plant, South Carolina			
I-20 (Mississippi)	100-92	Approximately 30 mi. west of Meridian, Mississippi.	Ground shifting breaks up pavement, road under construction
I-20 (Mississippi)	100	Approximately 30 mi. west of Meridian, Mississippi.	Long, gradual curve

TABLE D.2.1 Continued

Defense Facility/Route	Milepost[b]	Geographic Description	Description of Concern
Hanford Reservation, Washington			
I-82 (Washington)	96.6 - 132.6	Interstate from Richland, Washington south to Oregon border.	Subject to freezing rain late fall to early spring
I-84 (Oregon)	208.00 - 378.00	Pendleton to Ontario, Oregon	Majority of I-84 in northeastern Oregon has hazardous winter driving conditions; mountainous driving
I-84 (Oregon)	213.00 - 225.00	Approximately five miles east of Pendleton, Oregon	Fog in winter and steep grades on hill
I-84 (Oregon)	268.00 - 280.00	Approximately eight miles east of La Grande, Oregon (Ladd Canyon)	Mountain driving; snow and ice. winter driving conditions in canyon
I-84 (Idaho)[d]	0.00 - 25.00	Western Idaho border to Caldwell, Idaho	"Black ice" conditions in winter
I-84 (Idaho)	50.00 - 90.00	Boise to Mountain Home, Idaho	"Black ice" conditions in winter
I-84 (Idaho)	100.00 - 121.00	East of Mountain Home, to Glenns Ferry, Idaho	When wet, concrete paving may cause trucks to jackknife
I-84 (Idaho)	222.00 - 275.65	I-84/I-86 interchange in Idaho to Utah border	Low visibility due to blowing snow or dust in early spring and winter; in general, subject to poor weather conditions

TABLE D.2.1 Continued

Defense Facility/Route	Milepost[b]	Geographic Description	Description of Concern
Hanford Reservation, Washington (continued)			
I-84 (Utah)	87.70 - 111.70	Nine miles east of Ogden, Utah	Mountain driving; Wever Canyon is subject to high winds and blowing snow
I-84/I-80 (Utah)	168.00	Interchange in Utah	High speed on curve can cause trucks to overturn
I-80 (Utah)	168.00 - 180.00	From interchange east-bound on I-80, Utah	Mountain driving; curves and shady areas with ice in winter; history of vehicles sliding off road
I-80 (Utah)	186.00 - 198.00	I-80 in Utah to Wyoming border	Pavement changes to concrete and freezes in winter; problems with vehicles sliding off road
I-80 (Wyoming)	68.97 - 212.54	Between Little America and Rawlins, Wyoming	Icy roads and strong cross winds; may have concurrent ground blizzard conditions
I-80 (Wyoming)	235.00 - 300.00	Elk Mountain area, Wyoming	Many long and steep grades may have ice, blowing snow and blizzard conditions
I-80 (Wyoming)	323.05 - 359.98	Happy Jack Summit to Cheyenne, Wyoming	Icy roads and strong cross winds; have concurrent ground blizzard conditions
I-25 (Colorado)	298.9 - 272.4	Southern Wyoming border to Fort Collins, Colorado	Hazardous storms with high winds, ground blizzards, and ice conditions

TABLE D.2.1 Continued

Defense Facility/Route	Milepost[b]	Geographic Description	Description of Concern
Hanford Reservation Washington (continued)			
I-25 (Colorado)	221 - 197.2	Between 104th St. to Avapahoe Rd., Denver, Colorado	Rush hour traffic 6:00 a.m. to 9:00 a.m.
I-25 (Colorado)	221 - 197.2	38th St. exit and the Alameda exit south to University Ave., Denver, Colorado	During heavy rain storms, segments segments may flood several feet
I-25 (Colorado)	221 - 197.2	Broadway viaduct near Santa Fe Dr. in Denver, Colorado	Has restricted access because it is elevated and may be subject to ice conditions
I-25 (Colorado)	174	Monument Hill, 17 miles north of Colorado Springs, Colorado	Subject to severe weather with high winds, heavy rain, icy conditions, and snow blizzards. I-25 in this location often closed for weather
I-25 (Colorado)	157.1	Colorado Springs, Colorado	Rush hour traffic conditions
I-25 (Colorado)	141.8	Bejew St. exit, Colorado Springs, Colorado	Unique curves and turns may be hazardous during weather or high-speed conditions
I-25 (Colorado)	103.5	Pueblo, Colorado.	Rush hour traffic conditions

TABLE D.2.1 Continued

Defense Facility/Route	Milepost[b]	Geographic Description	Description of Concern
Hanford Reservation, Washington (continued)			
I-25 (Colorado)	100	Near Colorado Fuel & Iron Plant, Pueblo, Colorado	Unique curves and turns that may be dangerous during weather or high-speed conditions
I-25 (Colorado)	15.6	Elevated portion of I-25 in Trinidad, Colorado	Has restricted access because it is elevated and may be subject to ice conditions
I-25 (Colorado)	0.0	Entire I-25 corridor in Colorado	Severe weather conditions may result in white outs and heavy winds
I-25 (New Mexico)	454-460	Raton Pass, New Mexico	Moutain pass area, may be closed because of weather conditions
I-25 (New Mexico)	434	North of Maxwell, New Mexico	Curves and overpass may ice up
I-25 (New Mexico)	426-413	Between Maxwell and Springer, New Mexico.	Winter ski traffic packs snow on road
I-25 (New Mexico)	374-369	South of Wagon Mound, New Mexico.	Hill ices up in winter
I-25 (New Mexico)	323-307	South of Las Vegas, New Mexico.	Icy hills with snow drifts in winter

TABLE D.2.1 Continued

Defense Facility/Route	Milepost[b]	Geographic Description	Description of Concern
Hanford Reservation, Washington (concluded)			
I-25 (New Mexico)	314	South of Wagon Mound, New Mexico.	Hills can ice up
I-25 (New Mexico)	300-299	Glorietta Pass, New Mexico.	Ices up with drifting snow
U.S.-285 (New Mexico)	276	White Lakes area, New Mexico.	Hills, icy
U.S.-285 (New Mexico)	264-250	Clines Corners area, New Mexico.	May have drifting snow with zero visibility, high winds
U.S.-285 (New Mexico)	239-238	South of Clines Corners, New Mexico	Hills, icy
U.S.-285 (New Mexico)	205-175	South of Vaughn, New Mexico.	Snow pack, icy, windy
U.S.-285 (New Mexico)	135	20-Mile Hill, 30 mi north of Roswell, New Mexico	Long hill, weather change area
Rocky Flats Plant, Colorado			
SH-128; U.S.-36 (Colorado)	48 - 57.2	Segment from Rocky Flats Plant to I-25, Colorado	Area is subject to high winds and severe snow blizzards; portions of road are two-lane

TABLE D.2.1 Continued

Defense Facility/Route	Milepost[b]	Geographic Description	Description of Concern
Idaho National Engineering Laboratory, Idaho			
SH 26/20 (Idaho)	272.00 - 306.00	Entire length of state road to I-15 interchange	Road is two-lane with old pavement. Severe weather may close road. Blowing snow and wind gusts exceeding 40-60 mph are not uncommon in winter
I-15 (Idaho)	92.50 - 00.00	Entire I-15 segment from Blackfoot, Idaho to Utah border.	Mountain driving; winter closures for weather of blowing snow and high wind gusts of 40-60 mph. Also, segments 3 to 10 miles in length on I-15 will be under construction until 1995
I-15 (Utah)	397.5 - 381	Plymouth to Tremonton, Utah	Mountain driving, two lanes; under construction until 1992 or 1993
Lawrence Livermore National Laboratory, California			
I-580 (California)	1.48 - 8.29	Altamont Pass, San Joaquin County	Steep grades
I-5 (California)	[e]	From I-580 to Tejon Pass, in San Joquin Valley	Subject to heavy fog, particularly months of Dec., Jan., and Feb., clearing by 10:00 a.m. Steep grades on Tejon Pass, may close for ice or snow conditions

TABLE D.2.1 Continued

Defense Facility/Route	Milepost[b]	Geographic Description	Description of Concern
Lawrence Livermore National Laboratory, California (concluded)			
I-5, I-210, I-10 (California)	[f]	Freeway interchanges in Los Angeles area	Extremely hazardous, multiple freeway interchanges
I-10, I-15 (California)	[g]	I-10 to I-15 interchange	Hazardous freeway interchange. May have high winds
I-15 (California)	[h]	Cajon Pass in San Bernadino Mountains	Steep mountain road grades, may have ice and snow road closures
I-15 (California)	[i]	Near Victorville, California	Steep downhil grade with curve
Nevada Test Site, Nevada			
U.S.-95 (Nevada)	86.65 - 70	Between Rancho Rd. and Boulder Highway in Las Vegas, Nevada.	Dangerous intersections
U.S.-95 (Nevada)	64.89 - 11.37	Junction of U.S.-93 in Las Vegas to Henderson	High speeds at intersections, construction until 1995
I-40 (New Mexico)	36-47; 63-68	Between Gallup and Grants, New Mexico	Rapid snow, ice accumulation
I-40 (New Mexico)	80-100	Between Grants and Laguna, New Mexico	Rapid snow and ice accumulation

TABLE D.2.1 Continued

Defense Facility/Route	Milepost[b]	Geographic Description	Description of Concern
Nevada Test Site, Nevada (concluded)			
I-40 (New Mexico)	104	West of Laguna, New Mexico	Wind, rapid snow and ice accumulations, steep hill
I-40 (New Mexico)	114	Near Laguna, New Mexico	Curves, high accident area
I-40 (New Mexico)	115	Laguna area, New Mexico	Wind, steep hill, accident area
I-40 (New Mexico)	126-128	East of Laguna area, New Mexico.	Interchanges
I-40 (New Mexico)	149	Nine Mile Hill, west of Albuquerque, New Mexico	Sharp exit
I-40 (New Mexico)	160	Albuquerque, New Mexico "Big I" interchange.	All ramps ice fast
I-40 (New Mexico)	170-184	Tijeras Canyon, east of Albuquerque, New Mexico	Icy, winds, poor visibility; road may be closed for weather
I-40 (New Mexico)	179-183	West of Edgewood, New Mexico.	Long hill can ice up
I-40 (New Mexico)	194	West end of Moriarity, New Mexico.	Bad curve, accident area, fog will settle over area

TABLE D.2.1 Concluded

Defense Facility/Route	Milepost[b]	Geographic Description	Description of Concern

[a] The states of Arizona, Illinois, Louisiana, Missouri, Ohio, Oklahoma, South Carolina and Texas did not report segments of concern.

[b] Estimated.

[c] Ssegments of concern reported along interstate by defense facility until routes merge (e.g., I-40 in Oklahoma is confluence of Mound Laboratory route I-70 and Oak Ridge National Laboratory route I-40).

[d] Also route from Idaho National Engineering Laboratory to the WIPP.

[e] From milepost 28.06 in Stanislaus County to milepost 11.0 in Kern County, California.

[f] From milepost 46.58 to 42.44 (on I-10) in Los Angeles County, California.

[g] Milepost 9.95 on I-10 in San Bernadino County, California.

[h] Milepost 15 to 34 in San Bernadino County, California.

[i] Milepost 55 in San Bernadino County, California.

- Route from Mound Laboratory, Ohio. Figure D.2.5 provides the route WIPP trucks would take from the Mound Laboratory, Ohio, to the New Mexico border. The proposed route is described as follows:

  Mound Avenue (W)
  First Street (N), .5 mi
  State 725 (E), .4 mi
  I-75 (N) to I-70
  I-70 (W) to I-74/465 (S) Indianapolis, Indiana
  I-74/465 (S) to I-70 (W) I-70/55 (W) to I-255 (S)
  I-255 (S) to I-270 (W)
  I-270 (W) to I-44 St. Louis, Missouri
  I-44 (W) to I-40 Oklahoma City, Oklahoma
  I-40 to US-54 (S) Santa Rosa, New Mexico
  US-54 (S) to Vaughn, New Mexico
  US 285 (S) to Carlsbad, New Mexico
  US 62/180 (E), 32 mi
  State 31 (North Access Rd.), 13 mi

  Between the Mound Laboratory and New Mexico, several highway segments of concern in Indiana have been identified; these are shown on Figure D.2.4 and further described in Table D.2.1. Major populated areas with their populations are also provided on Figure D.2.4. WIPP traffic would use the beltway around St. Louis, Mo.

- Route from Argonne National Laboratory, Illinois. Figure D.2.5 provides the proposed WIPP transportation route from the Argonne National Laboratory south of Chicago to the New Mexico border. From the Argonne National Laboratory, trucks would take the Northgate Entrance Road (NE) for 0.25 mi to Cass Avenue and go north 0.1 mi to I-55. Once on I-55, they would continue south until they intersected with I-70, east of St. Louis, Missouri.

- Route from Oak Ridge National Laboratory, Tennessee. Figure D.2.5 shows the proposed transportation route from the Oak Ridge National Laboratory, southwest of Knoxville, Tennessee to the New Mexico border. The following provides a more detailed route description:

  Bethel Valley Road (W), 1.1 mi
  Tennessee State Route 95 (S), 3.3 mi
  I-40 to I-240 (southern bypass) Oklahoma City, Oklahoma
  I-240 to I-44 (N)
  I-44 to I-40
  I-40 to US-54 (S) Santa Rosa, New Mexico
  US-54 (S) to US 285 Vaughn, New Mexico
  US-285 (S) to US-62/180, Carlsbad, New Mexico
  US-62/180 (E), 32 mi
  State 31 (North Access Rd), 13 mi

Several hazardous road segments of concern were identified in Tennessee and Arkansas and are shown on Figure 2.5 as well as further explained in Table D.2.1. WIPP traffic would use established by-passes of major cities as shown on Figure D.2.4.

- Route from Savannah River Plant, South Carolina. The Savannah River Plant is located southwest of Columbia, South Carolina just east of the border with Georgia. The proposed TRU waste transportation route from the Savannah River Plant to the WIPP follows I-20 for the majority of the route. Figure D.2.5 shows the proposed route with major cities, by-passes, and segments of concern. The route is described in more detail as follows:

  The local route from the Savannah River Plant to I-20 has not yet been determined.

  I-20 (W) to I-285 (southern bypass) Atlanta, Georgia
  I-285 to I-20 (W)
  I-20 to I-459 (W) Birmingham Bypass
  I-459 (W) to I-20 (W)
  I-20 to US-285 (N), Pecos, Texas
  US-285 (N) to US-62/180, Carlsbad, New Mexico
  US-62/180 (E) for 32 mi
  State 31 (North Access Rd.), 13 mi

- Route from Hanford Reservation, Washington. The Hanford Reservation facility is north of the tri-cities area in south-central Washington. Figure D.2.6 shows the proposed route to transport TRU waste materials from the Hanford defense facility to the New Mexico border. Major cities, road segments of concern are provided. The route would pass through mountainous areas of Oregon, Idaho, Utah, Wyoming, and Colorado. A brief description of the route follows:

  SR-240 (S), 3.4 mi
  I-182 (E), 5-10 mi
  I-82 (E) to I-84 (Oregon, Idaho, Utah)
  I-84 to I-80 (Utah)
  I-80 to I-25 (Wyoming, Colorado, New Mexico)
  NM US-285 to NM US-62/180
  State 31 (North Access Rd.), 13 mi

- Route from Idaho National Engineering Laboratory (INEL), Idaho. The INEL is west of Idaho Falls in southeastern, Idaho. Figure D.2.6 shows the proposed highway route from INEL to where it will intersect with the Hanford Reservation transportation corridor. US-26 will be used to access I-15.

- Route from Rocky Flats Plant, Colorado. The Rocky Flats Plant is between Golden and Boulder, Colorado, west of Denver, Colorado. TRU waste shipment to the WIPP in New Mexico would follow the transportation corridor in Colorado shown for the Hanford Reservation facility on Figure D.2.6. Access from the plant to I-25 would be as follows:

  East Gate of Plant to Indiana Avenue
  Indiana Avenue (N) to State Highway 128
  State Highway 128 (E) to US Highway 36
  US Highway 36 (S) to I-25

- Route from Los Alamos, New Mexico. The Los Alamos National Laboratory is not shown on Figure D.2.4. The route from Los Alamos to the WIPP is not described because the DOE has agreed to construct a by-pass around Santa Fe, New Mexico, and the final route had not been selected at this time.

- Route from Lawrence Livermore National Laboratory, California. The Lawrence Livermore National Laboratory is located just west of Stockton, California. Figure D.2.6 shows the proposed route to transport TRU waste materials to the New Mexico border. The State of California is in the process of evaluating additional routes in California and plans to propose an alternate route in 1989 for WIPP-related use. No TRU waste shipment is planned from the Lawrence Livermore National Laboratory during the first five years of the WIPP program. Major cities are shown on Figure D.2.5. Route segments are further described in Table D.2.1. The following describes in more detail the proposed TRU waste route from the Lawrence Livermore National Laboratory.

  South Exit 0.5 mi on East Avenue
  Right on Vasco 3.0 mi on I-580
  I-580 South 35 mi to I-5
  I-5 to I-210
  I-210 to I-10
  I-10 to I-15
  I-15 to I-40
  I-40 to NM US-285
  NM US-285 to NM US-62/180, Carlsbad, New Mexico
  State 31 (North Access Rd.), 13 mi

- Route from Nevada Test Site, Nevada. Highway access from the Nevada Test Site is northwest of Las Vegas. TRU waste will be transported on US-95 to I-40; Figure D.2.6 shows the proposed route to the New Mexico border.

D.2.4.2 Rail Transport

D.2.4.2.1 Regulatory Authorities. Transportation by rail is regulated by the DOT under 49 CFR 100-399. In particular, parts 172.200-204 (shipping papers); 172.300 (marking); 172.400 (labeling); 172.500 (placarding); and 173.401i-.478 (packaging) relate to various packaging requirements that would apply to TRU waste. Regulations specific to rail

transportation are found in 49 CFR 174, Carriage by Rail. This part provides details on carrier responsibilities, inspections of cars, special handling of various substances such as explosives, gases, or flammable liquids. Further regulation of railroad carriers is provided in 49 CFR 200-399. These parts provide detailed regulation of track standards, service, and operation of carriers and do not directly affect TRU waste shipment.

There are no regulatory requirements related to the selection of routes to be used for rail shipment of TRU waste (or any other material). However, the Federal Railroad Administration (FRA), which is the delegated enforcement arm of the DOT, does request to be informed of any hazardous materials shipments and will provide an evaluation of the proposed rail route for the shipper. Additionally, the FRA will provide regular (e.g. each six months) safety inspections of the route.

D.2.4.2.2 Proposed Rail Routes. Six mainline rail companies have rail lines that would directly access eight defense facilities. These are a) the Atchison-Topeka Santa Fe (now known as Santa Fe Railroad), b) the Union Pacific (which also owns the Missouri Pacific), c) Mid-South, d) CSX Transportation, e) Norfolk-Southern and f) Denver, RIO Grand. The two defense facilities that are not readily accessible to mainline railroads or that would require truck transportation to a rail spur are the Nevada Test Site and Los Alamos National Laboratory. Figure D.2.7 shows the proposed rail routes and mainline companies. As noted on the figure, only Argonne National Laboratory would be able to transport directly to the WIPP without transferring rail companies; between one and five transfers would be required for transporting TRU waste from the other defense facilities.

D.2.5 TRANSPORTATION PLANNING AND RESPONSIBILITIES

The truck transportation system will consist of the shippers (the sites), the carrier (the trucking contractor), and the receiver (WIPP). Overall management of the transportation system will be conducted at the WIPP at the Central Communications Center (CCC).

Transportation planning tasks will be coordinated by DOE personnel. These offices will direct the transportation strategy, planning, and the implementation of TRU waste shipments.

An overall schedule will be developed by Transportation Operations in cooperation with the TRU Waste and Integration Department. A strategy will be developed for the optimum employment of available TRUPACTs. The schedule will be redeveloped at the end of each fiscal year to reflect current transportation system operating experience and revised waste projections. A midyear update will be provided. A short-range schedule reflecting a six-week projection will be developed in close cooperation with the waste shipper traffic managers. This schedule will be developed to implement the long-term schedule.

With respect to transportation, the defense facilities will be responsible for implementing the following transportation activities:

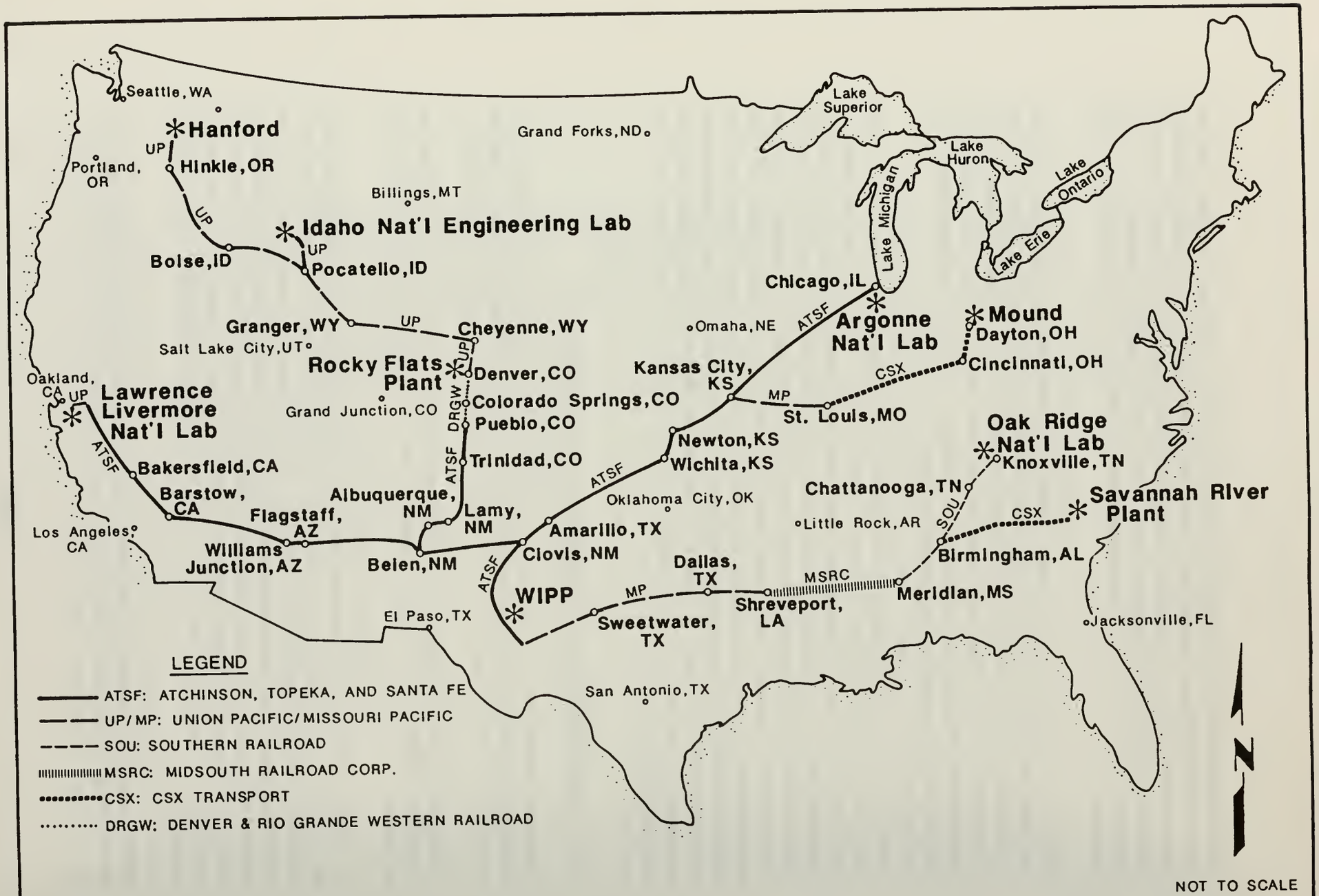

FIGURE D.2.7
PROPOSED MAINLINE RAILROAD ROUTES FOR TRUWASTE TRANSPORTATION TO THE WIPP

- Interacting with WIPP and involved states on institutional issues
- Certifying TRU waste to meet the WIPP WAC
- Meeting the WIPP/site traffic manager coordinated shipment schedule
- Inspecting vehicles and trailers
- Reporting TRUPACT-II and NUPAC 72B status to the CCC
- Loading TRU waste into TRUPACT-IIs and NUPAC 72Bs
- Meeting DOT and RCRA shipping paper requirements
- Dispatching loaded TRUPACT-IIs and NUPAC 72Bs
- Notifying CCC of shipments
- Following on-site emergency response procedures for TRU waste loading accidents.

The Carrier will be responsible for aspects related to the actual physical movement of the TRUPACT-IIs and NUPAC 72Bs between the facilities and the WIPP. This participant will be a contract carrier that will provide a dedicated tractor fleet, dedicated drivers, and a dedicated manager for this contract. See Subsection D.2.3.1.2 for carrier responsibilities related to their vehicles.

The carrier will be responsible for the following transportation tasks:

- Filing accident and incident reports as outlined in the WIPP Waste Transportation Manual
- Maintaining up to $5.0 million liability insurance for non-radiological related accidents including property damage, injury, or death. The statutory indemnity contained in Section 170 of the Atomic Energy Act of 1954, as amended, the "Price Anderson Act" applies to radiological liabilities associated with TRU waste transportation.
- Furnishing the shipper and the CCC with routes and alternate routes for TRU waste shipments.

The DOE will be responsible for the following transportation tasks:

- Interfacing on institutional issues with other Federal, State, and local agencies in conjunction with TRU waste storage/generator facilities and local DOE field offices
- Coordinating with sites
- Planning TRU waste transportation

- Translating DOE policies into operating procedures
- Establishing and operating the CCC
- Administering the carrier contract
- Budgeting transportation operations
- Procuring transport packages and trailers with placard holders
- Scheduling shipments in coordination with the site traffic managers
- Receiving shipments
- Maintaining communications equipment
- Complying with procedures and reporting requirements
- Reporting routine activities and nonroutine incidents
- Monitoring and evaluating carrier performance.

D.2.6 VEHICLE TRACKING SYSTEM

The CCC at WIPP will use TRANSCOM, the designated vehicle tracking system, to track TRU waste shipments. This system will be operated by the Oak Ridge Operations Office and linked to the WIPP at the CCC. TRANSCOM will utilize a land-based LORAN-C positioning system to obtain longitude/latitude information. This information will be calculated by a LORAN-C receiver carried in the cab of the truck with the transporter antenna attached to the trailer. Signals will be transmitted via satellite to a commercial ground station and then to the TRANSCOM Control Center (TCC). The TRANSCOM transportation will be mounted on the trailer. The satellite communications system will allow direct digital communication between the driver and the CCC at the WIPP. The CCC will be able to communicate directly with the enroute carrier by mobile telephone. The TCC will provide access to the tracking system to those Indian tribes, states, and sites that need to monitor TRU waste shipments.

The location of the tracked vehicle will be monitored by the CCC so as to detect any deviation from the authorized shipment route. Frequency of detection is limited by the frequency of vehicle location transmissions to the TCC. For TRU waste shipments, the frequency will be approximately every fifteen minutes.

In New Mexico, as elsewhere, the officials of the states and the Indian tribes will also have access to limited functions of TRANSCOM. The appropriate software training will be provided to enable them to receive data regarding TRU waste shipments passing through their jurisdictions.

Integrated with the Defense TRU Waste Shipment System will be a set of activities that function to deter, protect, detect, and respond to unauthorized possession, use, or sabotage of TRU waste shipments. These activities will include:

1. Close, continued surveillance of the enroute package by use of a computerized vehicle tracking and two-way communications system.

2. Minimize intermediate stops for a shipment.

3. Constant surveillance of unit and cargo during transit. One of the drivers in the two-person truck crew will remain with the unit at all times, including refueling, food, and relief stops. A vehicle will be considered to be under surveillance when one driver is in the vehicle, awake, and not in the sleeper berth, or is within one hundred feet of the vehicle and has the vehicle within his unobstructed field of view.

4. The use of an escort vehicle would be a decision made by the appropriate State agency, with due consideration for DOT regulations. The DOE does not plan to use any escorts as an escort vehicle could do little, except react to an accident situation. With real-time tracking of shipments, accident situations would be identified and communications with the vehicle would take place almost immediately.

D.3 RADIOLOGICAL RISK OF TRANSPORTATION

D.3.1 INTRODUCTION

The radiological risk assessment results presented in this Appendix and summarized in Subsection 5.0 were originally published in DOE (1986) and subsequently updated. DOE also addressed recent changes in the waste packaging system, current waste characterization data, and inventory projections. Radiological and nonradiological shipment risk estimates were developed on an individual site and systemwide basis. The risk estimates encompassed off-site travel and activities, but did not address any impacts resulting from on-site transportation.

The risk of radiological hazards during shipment of radioactive wastes is evaluated in this SEIS by considering the probability of an accident occurring, and the potential consequences of that accident. Shipping risk analyses include the following steps:

1. a system description;
2. an identification of potential releases or accidents;
3. a probability to be assigned to release or accident scenarios;
4. an estimate of the amount and type of material released for each scenario; and
5. an evaluation of the consequences of the scenarios, most often in terms of exposure or dose to the worker or the public, or in terms of latent cancer fatalities.

Additionally, a credible evaluation of the consequences must factor in variations in shipping routes, population density along the shipping routes, and weather characteristics that could affect risk calculations. Risk assessments are obtained by considering accident occurrence probabilities and estimated consequences.

The analytical models or codes used in this analysis have been extensively documented elsewhere (Peterson, 1984; Joy et al., 1982; NRC, 1977; Taylor and Daniel, 1977; AEC, 1972). The RADTRAN code, used to calculate the radiological risk, is the product of about 15 years of development. The base code and its subsequent improvements were used to prepare a number of documents, including the Environmental Assessment used in the ICC hearings on the issue of shipping radioactive materials by special-use trains; the Final Environmental Impact Statement on the Transportation of Radioactive Material by Air and Other Modes, NUREG-0170 (NRC, 1977); the shipping risk analysis presented in the 1980 FEIS; and subsequent environmental and technical documentation for shipping TRU waste to the WIPP.

RADTRAN II (Taylor and Daniel, 1982), a revision of the RADTRAN code (Taylor and Daniel, 1977), is a flexible analytical tool for calculating both routine operational and

accident related impacts of transporting radioactive materials. In routine operational transport, waste shipments are assumed to arrive on schedule and without release of contaminants to the environment. Public and worker radiation exposures occur only from direct radiation at levels allowed by transportation regulations. Even though radiation shielding is incorporated into package designs where needed, the workers, vehicle crew members, and the public along the transportation routes will be exposed to direct radiation at very low dose rates under routine conditions.

In the RADTRAN model, the consequences of accidents during shipments are apportioned among severity classes and calculated for truck and rail transport. The model divides accidents into eight severity categories, each with an associated release fraction and probability of occurrence. These categories are related to fire and crush impact, and puncture forces encountered in an accident. Specific accident scenarios are not described for the severity classes. Instead, they are associated with increasing impact crush force, increasing fire duration, or a combination. The package release model combines the user specified fraction of material which is released with the fraction of material which becomes airborne and the fraction of the release that is of respirable size. These latter fractions are based on material characteristics and release mechanisms.

It is possible to characterize in general terms the nature of the human populations or ecological systems at risk along the transportation routes to the WIPP. Therefore, only general population data were used in the modeling as were generalized ecological characteristics. However, this type of uncertainty with respect to population and ecological parameters was offset by the conservative assumptions employed in the model.

The radiological accident risk (probability times consequence summed over postulated accidents) was calculated in terms of radiation exposures to population, early population dose fatalities, early morbidities, and latent cancer fatalities. Inhalation and direct exposure dose pathways were modeled to calculate the radiological health risks from accidents. Economic impacts were evaluated based on costs for emergency response, cleanup, evacuation, income loss, and land use impacts. RADTRAN input parameters include:

- Waste package type
- Transport index (external radiation levels)
- Transport mode (truck or rail)
- Transport mode characteristics (crew size, speeds, dimensions)
- Route characteristics (length, number of stops, population density)
- Number of shipments
- Release fractions (for accidents).

The above information was used to compute total dose in person-rem for accident free transport. Dose impacts were distributed along the route by weighting average population in urban, suburban, and rural areas by the proportion of the route through each. Major input parameters are summarized in SEIS Section 5.0

In the absence of historical data for container response to accidents of varying severity, certain assumptions were required for this assessment. An average release fraction for each severity category was estimated, and containers in the Type B packaging (TRUPACT-II) were assumed to respond the same way in an accident regardless of actual waste contents or waste form. It was further assumed that there would be no release from accidents falling within the limits of severity class one or two for which Type B packaging is certified.

Releases from crush impacts were expected to be limited to the interior of the TRUPACT-II with no subsequent release for accidents below severity category six. Releases were assumed to be possible from the TRUPACT-II during accidents involving fires in category three or above. Subsequent release fractions were increased for succeeding accident severity categories. The release fractions for each severity category were combined with the accident rates for each category, the probability of a fire or impact event, the distance per shipment, and the fraction of travel through each population density zone to determine a cumulative, probability weighted dose consequence for each shipment.

The major revisions to RADTRAN from the earlier RADTRAN version used in the FEIS include:

Incident Free Model

- Shielding options in urban and suburban areas
- Checks for regulatory consistency
- Addition of rail crew doses
- Inclusion of rail travel through urban areas
- Revision of dose-while-stopped model
- Three package-size discriminators for handlers
- Pedestrian dose evaluated in cities

Accident Model

- Groundshine dose evaluated
- Cloudshine dose evaluated
- Economic impacts included
- Early morbidities evaluated
- Genetic effects evaluated
- Building dose factors included
- Inclusion of urban pedestrian inhalation dose
- Addition of Pasquill stability category option
- Expanded material dispersibility classes

General

- Redesign of input and output.

D.3.2 INCIDENT FREE RISKS

D.3.2.1 Incident Free Radiological Risk Method

The radiological risk assessment of the TRU transportation system using RADTRAN requires the volumes and characteristics of the waste to be transported. Volumes of both retrievably-stored and projected newly-generated CH and RH TRU waste through the year 2013 were estimated from the 1987 Integrated Data Base (IDB) (see SEIS Subsection 3.1) (DOE, 1988). These volumes of waste at storage sites were scaled up to consider the maximum amount of waste which could be emplaced at WIPP (approximately 6.45 million ft^3). These quantities constitute the volumes used in this analysis. These volumes are shown in Table D.3.1. The analysis assumed for truck shipments that the inventory of CH TRU waste was packaged in Type A 55-gallon drums in TRUPACT-IIs (3 TRUPACTs per trailer with 2 seven-packs of drums per TRUPACT or 42 drums per shipment). RH TRU waste is packaged and transported in RH casks (1 cask per shipment). Under these conditions, the number of shipments to WIPP was calculated as shown in Table D.3.2. For rail shipments, a total of six TRUPACT-IIs on a single railcar constitutes a CH shipment, and a total of two RH casks on a railcar constitutes an RH shipment.

For incident free shipments, the waste characteristics of interest are the specific radionuclides and the total amount (Curies) of each radionuclide transported per shipment. Using waste characteristics presented in the 1987 IDB, the radioactive characteristics of average truck or rail shipments of CH TRU waste from each of the sites were determined and were used to calculate the risks from an accident. The values are shown in Table D.3.3 for CH TRU waste and Table D.3.4 for RH TRU waste. These waste characteristics in addition to an estimated fission products fraction were further used to determine site-specific Transport Index (TI) values for a typical shipment of CH and RH TRU waste. These TI values were developed through coordination with WIPP and generator/storage site personnel. The TI depends upon waste density, distribution of radionuclides, quantity of radionuclides per shipment, mix of waste types, waste self shielding, and shielding due to the TRUPACT-II package or RH cask and is very sensitive to small quantities of fission product gamma-producing waste such as Co-60 and Cs-137. The TI represents the radiation dose rate at 1 meter (3.28 ft) from the surface of the transportation package (TRUPACT-II with a load of 42 drums of waste or 1 RH cask). TI values for typical shipments from each facility are shown in Table D.3.5. The radiation dose rate represented by the TI serves as the source term for calculation of radiation exposures to populations affected by truck or rail shipments (i.e., crew, waste handlers, people living or traveling along shipment routes, and people in the vicinity of the shipment while it is stopped).

Affected populations living along shipment routes were classified into urban, suburban, and rural fractions with respective population densities of 3861 persons/km^2, 719 persons/km^2 and 6 persons/km^2 as specified by NRC, 1977. These population densities are quite typical of urban, suburban, and rural environments. For example, using statistics from the Denver Regional Council of Governments, along I-25 through Denver, only a small area around downtown Denver has a population density exceeding RADTRAN's urban figure (3997 persons/km^2 for Denver vs 3861 persons/km^2 assumed

TABLE D.3-1 Year 2013 projected retrievably-stored and newly-generated TRU waste

Facility	1987 IDB 12/31/86 Stored (ft^3)	1987 IDB Amount Generated Thru 2013 (ft^3)	Total Base (ft^3)	Volume Scale-up (ft^3)	Total Max Volume Case (ft^3)
Contact-Handled					
Idaho National Engineering Laboratory	1.07×10^6	9.92×10^3	1.08×10^6	3.79×10^5	1.46×10^6
Rocky Flats Plant	0	2.04×10^6	2.04×10^6	0	2.04×10^6
Hanford Reservation	2.93×10^5	5.38×10^5	8.31×10^5	1.04×10^5	9.35×10^5
Savannah River Plant	9.15×10^4	6.16×10^5	7.07×10^5	3.20×10^4	7.39×10^5
Los Alamos National Laboratory	2.51×10^5	3.02×10^5	5.53×10^5	8.82×10^4	6.41×10^5
Oak Ridge National Laboratory	1.91×10^4	4.19×10^4	6.11×10^4	6.78×10^3	6.79×10^4
Nevada Test Site	2.13×10^4	0	2.13×10^4	0	2.87×10^4
Argonne National Laboratory-East	0	3.81×10^3	3.81×10^3	0	3.81×10^3
Lawrence Livermore National Laboratory	0	2.59×10^5	2.59×10^5	0	2.59×10^5
Mound Laboratory	0	4.00×10^4	4.00×10^4	0	4.00×10^4
TOTAL	1.75×10^6	3.85×10^6	5.6×10^6	6.09×10^5	6.21×10^6
Remote-Handled					
Idaho National Engineering Laboratory	9.90×10^2	4.87×10^3	5.86×10^3	0	5.86×10^3
Hanford Reservation	8.47×10^2	2.86×10^4	2.94×10^4	0	2.94×10^4
Oak Ridge National Laboratory	4.55×10^4	1.06×10^4	5.61×10^4	1.57×10^5	2.13×10^5
Argonne National Laboratory-East	0	2.82×10^2	2.82×10^2	0	2.82×10^2
Los Alamos National Laboratory	1.02×10^3	2.11×10^2	1.24×10^3	0	1.24×10^3
TOTAL	4.83×10^4	4.46×10^4	9.29×10^4	1.57×10^5	2.50×10^5

TABLE D.3.2 Projected CH TRU and RH TRU waste shipments from generating and storage facilities to the WIPP

Facility	Number of shipments 100% Truck	Maximum Rail
Contact-Handled[a,b]		
Idaho National Engineering Laboratory	6162	3081
Rocky Flats Plant	8586	4293
Hanford Reservation	3939	1970
Savannah River Plant	3116	1558
Los Alamos National Laboratory	2703	2703[c]
Oak Ridge National Laboratory	286	143
Nevada Test Site	121	121[c]
Argonne National Laboratory-East	16	8
Lawrence Livermore National Laboratory	1093	547
Mound Laboratory	169	85
TOTAL	26191	14509
Remote-Handled[a]		
Idaho National Engineering Laboratory	187	94
Hanford Reservation	937	467
Los Alamos National Laboratory	39	39
Oak Ridge National Laboratory	6781	3392
Argonne National Laboratory-East	9	5
TOTAL	7953	3997

[a] Shipments based on 3 TRUPACT-IIs per truck shipment and 6 TRUPACT-IIs per railcar shipment

[b] Shipments calculated from a drum volume of $0.2m^3$ x (0.80) x 14 drums/TRUPACT-IIs

[c] LANL and NTS do not have access to rail, thus truck shipments are included in the maximum rail case.

TABLE D.3.3 Average CH TRU Waste Trailer-Load Radioactivity (curies)[a]

Radionuclide Radioactivity, Curies (Ci)	ANEL	HANF	INEL	LANL	LLNL	Mound	NTS	ORNL	RFP	SRP
Th-232			1.10×10^{-4}							
U-233			1.63×10^{-1}	4.44×10^{-2}				$7.52\times10^{+1}$		
U-235										
U-238				2.26×10^{-4}						
Np-237										4.06×10^{-3}
Pu-238	5.77×10^{0}	8.10×10^{0}	$1.16\times10^{+1}$	$2.02\times10^{+2}$	1.27×10^{0}	1.46×10^{-2}	4.08×10^{-2}	$5.00\times10^{+1}$	5.73×10^{-1}	$1.96\times10^{+3}$
Pu-239	3.65×10^{0}	$3.51\times10^{+1}$	6.30×10^{0}	$9.43\times10^{+1}$	$3.06\times10^{+1}$	1.26×10^{-2}	6.90×10^{-1}	$2.21\times10^{+2}$	$1.95\times10^{+1}$	2.27×10^{0}
Pu-240	1.67×10^{0}	$1.25\times10^{+1}$	1.54×10^{0}	$2.20\times10^{+1}$	$2.99\times10^{+1}$	3.33×10^{-3}	1.64×10^{-1}		4.44×10^{0}	9.39×10^{-1}
Pu-241	$3.33\times10^{+1}$	$6.36\times10^{+2}$	$4.88\times10^{+1}$	$1.31\times10^{+2}$	$2.91\times10^{+2}$	1.27×10^{-3}	6.15×10^{0}		$1.39\times10^{+2}$	$7.08\times10^{+1}$
Pu-242				5.585×10^{-3}	6.21×10^{-4}					
Am-241	$1.51\times10^{+1}$		$4.17\times10^{+1}$	$2.81\times10^{+2}$	$1.64\times10^{+2}$			$1.80\times10^{+1}$	9.18×10^{-1}	1.95×10^{-1}
Cm-244								$6.02\times10^{+1}$		
Cf-252								9.60×10^{0}		

[a] 3 Cylindrical TRUPACT-IIs per Trailer Load; Truck Mode: 1 Trailer Load/Shipment; Rail Mode: 2 Trailer Loads/Shipment

[b] Blanks = radionuclide not in facility waste stream

TABLE D.3.4 Average RH TRU waste trailer-load radioactivity (Curies)[a]

Radionuclide	Facility				
	Hanford Reservation	Idaho National Engineering Laboratory	Los Alamos National Laboratory	Oak Ridge National Laboratory	Argonne National Laboratory-East
Sr-90	[b]	2.35×10^{0}	8.11×10^{0}	9.99×10^{-1}	
Ru-106			6.41×10^{0}		
Sb-125			1.98×10^{-1}		
Cs-137		3.34×10^{0}	6.30×10^{0}	3.96×10^{-2}	8.83×10^{0}
Ce-137			$6.31 \times 10^{+1}$		
Eu-155			3.19×10^{-1}		
U-233				5.55×10^{-3}	
U-235		1.41×10^{-3}	1.38×10^{-5}	7.00×10^{-7}	
U-238		4.04×10^{-4}		1.00×10^{-6}	
Pu-238	6.30×10^{-1}	9.41×10^{-3}		1.05×10^{-3}	
Pu-239	3.85×10^{0}	8.81×10^{-2}	7.51×10^{-1}	4.53×10^{-2}	2.52×10^{-1}
Pu-240	1.96×10^{0}	3.45×10^{-2}	9.99×10^{-1}		9.30×10^{-2}
Pu-241	TBD[c]		$1.14 \times 10^{+1}$		
Pu-242	6.00×10^{-2}				
Am-241		1.88×10^{-3}		2.30×10^{-2}	
Cm-244				2.06×10^{-1}	
Cf-252				3.61×10^{-1}	

[a] 1 RH cask/trailer load; Truck mode: 1 trailer load/shipment; Rail mode: multiply radioactivity by 2

[b] Blanks = radionuclide not in facility waste stream

[c] TBD = To be determined

TABLE D.3.5 Transport index values[a]

Facility	CH TRU waste	RH TRU waste
Idaho National Engineering Laboratory	1.0	4.98
Rocky Flats Plant	1.5	
Hanford Reservation	0.7	16.04
Savannah River Plant	2.7	
Los Alamos National Laboratory	4.1	8.86
Oak Ridge National Laboratory	11.0	3.21
Nevada Test Site	1.2	
Argonne National Laboratory-East	7.5	2.52
Lawrence Livermore National Laboratory	0.4	[b]
Mound Laboratory	0.41	

[a] mrem/hr at 1 meter from transporter surface

[b] Blanks = RH TRU waste not stored at facility

by RADTRAN). Other segments through Denver have much lower population densities than the RADTRAN urban value. Fifteen miles south of downtown, population densities along I-25 approach the rural value of 6 persons/km^2.

For TRU truck shipments, the HIGHWAY model (Joy et al., 1982) was used to estimate trip lengths from various sites to the WIPP and corresponding population density fractions along these routes. Routes selected generally follow interstate highways as specified by the DOT for shipments of route-controlled quantities of radioactive materials. For TRU rail shipments, the INTERLINE model (Peterson, 1984) was used to estimate trip lengths and population density fractions for the routes. Selected routes follow Class A/Class B main lines. These distances and population fractions are summarized in Table D.3.6. Other major input parameters to RADTRAN are summarized in Table D.3.7. These parameters and the characteristic data for each facility and shipment discussed above are used by RADTRAN to calculate incident-free transportation risks.

D.3.2.2 Incident-free Radiological Risk Results

The radiation doses to affected populations from incident-free transport by truck and rail of CH and RH TRU waste as calculated by RADTRAN are shown in Tables D.3.8 and D.3.9. These doses are summarized for occupational (crew, waste handlers, shipment inspectors) and nonoccupational populations (i.e., travelers sharing the transportation pathway, people living along the shipment route, and people in the vicinity of the shipment while it is stopped). Radiological risks are presented on a per-shipment basis for each site in these tables and are given in doses (person-rems) to the exposed populations for each shipment. These per-shipment risks are used to calculate incident-free transportation risks for the proposed action and the two alternatives. Table D.3.10 shows the lifetime radiological risk for incident-free transportation of CH TRU waste by truck or rail modes from each of the storage and generator facilities to the WIPP. The proposed action corresponds to a five-year Test Phase period during which up to 10 percent of the waste is shipped to the WIPP by truck and a subsequent 20-year Disposal Phase during which the remainder of the waste is shipped by either truck or rail. Cumulative risks for the entire campaign are the sum of the total risks from Test Phase truck shipments and Disposal Phase (truck or rail modes).

The No Action Alternative does not involve transportation to the WIPP and therefore has no incident-free radiological risks of transportation.

The Alternative Action assumes no major shipments of waste during a five-year Test Phase with all waste then shipped to the WIPP during a subsequent 20-year period (truck or rail shipments as shown in Table D.3.2). During the Test Phase for the Alternative Action, approximately 300 drums of CH TRU waste will be shipped from the Rocky Flats Plant to the Idaho National Engineering Laboratory to conduct bin storage tests. Using TRUPACT-IIs, approximately seven truck shipments (three TRUPACT-IIs per shipment) would be required for this Alternative. Assuming a per-shipment incident-free risk which is the ratioed difference (based on Transport Index) between the per-shipment risks for the Idaho National Engineering Laboratory to the WIPP and the

TABLE D.3.6 Average distances to the WIPP and percent of travel in various population zones[a]

	Average distance	Population zone		
	Miles	R	S	U
Truck				
Idaho National Engineering Laboratory	1521	85.0	13.8	1.2
Rocky Flats Plant	874	82.3	15.7	2.0
Hanford Reservation	1913	85.7	13.4	0.9
Savannah River Plant	1585	74.3	25.1	0.6
Los Alamos National Laboratory	343	90.1	9.9	0.0
Oak Ridge National Laboratory	1350	78.6	20.7	0.7
Nevada Test Site	1286	86.8	11.2	2.0
Argonne National Laboratory-East	1387	78.1	21.8	0.1
Lawrence Livermore National Laboratory	1458	86.2	10.1	3.7
Mound Laboratory	1472	75.4	24.1	0.5
Rail				
Idaho National Engineering Laboratory	1761	89.5	9.8	0.7
Rocky Flats Plant	1098	86.7	11.6	1.7
Hanford Reservation	2296	87.8	11.5	0.7
Savannah River Plant	1915	76.0	22.4	1.6
Oak Ridge National Laboratory	1630	79.8	18.9	1.3
Argonne National Laboratory-East	1469	81.6	17.0	1.4
Lawrence Livermore National laboratory	1873	85.0	14.3	0.8
Mound Laboratory	1677	76.8	21.3	1.9

[a] Mean population densities are utilized and correspond to:
R = Rural (6 persons/km^2)
S = Suburban (719 persons/km^2)
U = Urban (3861 persons/km^2)

Source: Madsen et al., 1983

TABLE D.3.7 RADTRAN general input data[a]

Parameter	CH TRU waste		RH TRU waste	
	truck	rail	truck	rail
Package Type	TRUPACT-II		Cask	
Package Waste Volume, m^3	2.8	2.8	1.0	1.0
Packages/Shipment	3	6	1	2
Transport Index (TI), mrem/hr	(Site specific, See Table D.3.5)			
Package Length Dimension, m	7.32	7.32	3.61	3.61
Number of Crewmen	2	5	2	5
Distance from Source to Crew, m	4	152	5	152
Speed, km/hr				
Urban Population Zone	24	24	24	24
Suburban Population Zone	40	40	40	40
Rural Population Zone	88	64	88	64
Stop Time per Kilometer, hr/km	.011	.0036	.011	.0036
No. of People Exposed while Stopped	50	100	50	100
No. of People per Vehicle	2	3	2	3
Population Density, people/km^2				
Urban Population Zone	3861	3861	3861	3861
Suburban Population Zone	719	719	719	719
Rural Population Zone	6	6	6	6
Avg. Rad./Trailer-Load of Pkgs., Ci	(Site Specific, See Tables D.3.3 and D.3.4)			
Accident Release Fractions	(See Tables D.3.17 through D.3.22)			

[a] Source: Madsen et al., 1983

TABLE D.3.8 Radiological risk per CH TRU shipments (person-rems)[a,b,c]

	Truck		Rail	
Facility	Occupational	Nonoccupational	Occupational[d]	Nonoccupational
Idaho National Engineering Laboratory	5.0×10^{-2}	2.0×10^{-2}	2.9×10^{-4}	3.0×10^{-2}
Rocky Flats Plant	4.0×10^{-2}	1.0×10^{-2}	2.7×10^{-4}	2.0×10^{-2}
Hanford Reservation	4.0×10^{-2}	2.0×10^{-2}	2.6×10^{-4}	4.0×10^{-2}
Savannah River Plant	1.4×10^{-1}	7.0×10^{-2}	8.4×10^{-4}	1.2×10^{-1}
Los Alamos National Laboratory	3.0×10^{-2}	1.0×10^{-2}	e	e
Oak Ridge National Laboratory	1.3×10^{-1}	2.1×10^{-1}	2.1×10^{-3}	2.0×10^{-1}
Nevada Test Site	5.0×10^{-2}	2.0×10^{-2}	e	e
Argonne National Laboratory-East	1.3×10^{-1}	1.4×10^{-1}	1.8×10^{-3}	1.9×10^{-1}
Lawrence Livermore National Laboratory	2.0×10^{-2}	1.0×10^{-2}	1.2×10^{-4}	2.0×10^{-2}
Mound Laboratory	2.0×10^{-2}	1.0×10^{-2}	1.1×10^{-4}	1.0×10^{-2}

[a] Risks per waste shipment are expressed in equivalent whole body dose and are tabulated in units of person-rem.

[b] Values for rail are expressed per railcar shipment.

[c] Risks per waste shipment are presented as a function of the Transport Index (TI) which is defined as the dose rate in mrem/hr at 1 meter from the waste package. Calculations are based on three TRUPACT-IIs per truck and six per railcar.

[d] Rail occupational risks resulting from normal transportation include the impact of DOT inspection activities (.01 X Total Stop Time (hr) X TI)

[e] No railheads present

TABLE D.3.9 Radiological risk per RH TRU shipment (person-rems)[a,b,c]

	Truck		Rail	
Shipment Origin Site	Occupational	Nonoccupational	Occupational[d]	Nonoccupational
Idaho National Engineering Laboratory	1.0×10^{-1}	8.0×10^{-2}	1.3×10^{-3}	1.3×10^{-1}
Hanford Reservation	1.7×10^{-1}	3.3×10^{-1}	3.5×10^{-3}	2.9×10^{-1}
Los Alamos National Laboratory	3.0×10^{-2}	1.0×10^{-2}	e	e
Oak Ridge National Laboratory	6.0×10^{-2}	4.0×10^{-2}	7.7×10^{-4}	7.0×10^{-2}
Argonne National Laboratory-East	5.0×10^{-2}	4.0×10^{-2}	5.5×10^{-4}	5.0×10^{-2}

[a] Risks per waste shipment are expressed in equivalent whole body dose and are tabulated in units of person-rem.

[b] Values for rail are expressed per railcar shipment.

[c] Risks per waste shipment are presented as a function of the Transport Index (TI) which is defined as the dose rate in mrem/hr at 1 meter from the waste package. Calculations are based on three TRUPACT-IIs per truck and six per railcar.

[d] Rail occupational risks resulting from normal transportation include the impact of DOT inspection activities (.01 X Total Stop Time (hr) X TI)

[e] No railheads present

TABLE D.3.10 Lifetime radiological risk of incident-free transportation of CH TRU waste (person-rem)

Shipment origin site	Proposed Action						Alternative Action			
	Test Phase (5 yr)[a]		Disposal Phase (20 yr)				Disposal Phase (20 yr)			
	100% truck		100% truck		Max. rail		100% truck		Max. rail	
	Occ[b]	Non Occ[c]	Occ	Non Occ	Occ	Non Occ	Occ	Non Occ	Occ	Non Occ
Idaho National Engineering Laboratory	3.1×10^{1}	1.2×10^{1}	2.8×10^{2}	1.1×10^{2}	8.0×10^{-1}	8.3×10^{1}	3.1×10^{2}	1.2×10^{2}	8.9×10^{-1}	9.2×10^{1}
Rocky Flats Plant	3.4×10^{1}	8.6×10^{0}	3.1×10^{2}	7.7×10^{1}	1.0×10^{0}	7.7×10^{1}	3.4×10^{2}	8.6×10^{1}	1.2×10^{0}	8.6×10^{1}
Hanford Reservation	1.6×10^{1}[d]	7.9×10^{0}	1.4×10^{2}	7.1×10^{1}	4.7×10^{-1}	7.1×10^{1}	1.6×10^{2}	7.9×10^{1}	5.2×10^{-1}	7.9×10^{1}
Savannah River Plant	4.4×10^{1}	2.2×10^{1}	3.9×10^{2}	2.0×10^{2}	1.2×10^{0}	1.7×10^{2}	4.4×10^{2}	2.2×10^{2}	1.3×10^{0}	1.9×10^{2}
Los Alamos National Laboratory[e]	8.1×10^{0}	2.7×10^{0}	7.3×10^{1}	2.4×10^{1}	7.3×10^{1}	2.4×10^{1}	8.1×10^{1}	2.7×10^{1}	8.1×10^{1}	2.7×10^{1}
Oak Ridge National Laboratory	3.8×10^{0}	6.1×10^{0}	3.3×10^{1}	5.4×10^{1}	2.7×10^{-1}	2.7×10^{1}	3.7×10^{1}	6.0×10^{1}	3.0×10^{-1}	2.9×10^{1}
Nevada Test Site[e]	6.0×10^{-1}	2.4×10^{-1}	5.5×10^{0}	2.2×10^{0}	5.5×10^{0}	2.2×10^{0}	6.1×10^{0}	2.4×10^{0}	6.1×10^{0}	2.4×10^{0}
Argonne National Laboratory-East	2.6×10^{-1}	2.8×10^{-1}	1.8×10^{0}	2.0×10^{0}	1.3×10^{-2}	1.3×10^{0}	2.1×10^{0}	2.2×10^{0}	1.4×10^{-2}	1.5×10^{0}
Lawrence Livermore National Laboratory	2.2×10^{0}	1.1×10^{0}	2.0×10^{1}	9.8×10^{0}	5.9×10^{-2}	9.8×10^{0}	2.2×10^{1}	1.1×10^{1}	6.6×10^{-2}	1.1×10^{1}
Mound Laboratory	3.4×10^{-1}	1.7×10^{-1}	3.0×10^{0}	1.5×10^{0}	3.4×10^{-3}	7.6×10^{-1}	3.4×10^{0}	1.7×10^{0}	9.4×10^{-3}	8.5×10^{-1}
Total	1.4×10^{2}	6.1×10^{1}	1.3×10^{3}	5.5×10^{2}	8.2×10^{1}	4.7×10^{2}	1.4×10^{3}	6.1×10^{2}	9.1×10^{1}	5.2×10^{2}

[a] Test Phase assumes 10% of shipments; all by truck

[b] Occupational population—quantifies doses received by transportation crews

[c] Nonoccupational population

[d] Population group risks are calculated by multiplying the risk/shipment identified in Table D.3.8 by the total number of shipments to the WIPP by truck or rail, as determined from the projections in Table D.3.2. Rail occupational risks resulting from normal transportation include the impact of inspection activities.

[e] Waste shipments are limited to truck mode. Rail risks are thus the same as truck risks.

Rocky Flats Plant to the WIPP (see Table D.3.8), the estimated occupational and nonoccupational incident-free risks of these shipments are 0.035 person-rems and 0.02 person-rems, respectively.

Tables D.3.11 and D.3.12 summarize the differences in CH TRU incident-free risks for occupational and nonoccupational populations between the Proposed Action and the Alternative Action.

Table D.3.13 shows the lifetime radiological risk for incident-free transportation of RH TRU waste from generating and storage facilities to the WIPP. There are no RH TRU shipments during the Test Phase for either the Proposed Action or Alternative Action. However, RH TRU waste may be shipped to the WIPP during the Disposal Phase. Table D.3.13 shows incident-free risks of the Disposal Phase shipments by truck or rail modes.

For illustrative purposes, the maximum hypothetical doses expected for the 25-year shipping campaign (Test Phase and Disposal Phase) for the Proposed Action for a person living near each facility (100 ft from shipment path) are given in Table D.3.14. The totals on this table represent the doses expected to a person living near the WIPP which is exposed to every arriving truck or rail shipment. For Alternative Action, these maximum hypothetical doses would be identical except that they would be received over a 20-year period.

D.3.3 RADIOLOGICAL RISKS OF TRANSPORTATION ACCIDENTS

D.3.3.1 Method for Calculating Radiological Risks of Transportation Accidents

D.3.3.1.1 Severity Categories. CH TRU and RH TRU shipments to the WIPP will be made in NRC-certified Type B containers (TRUPACT-II and RH cask). The certification standards ensure that these packages will withstand virtually all typical accident conditions without releasing radioactive contents to the environment. For example, as shown in the WIPP FEIS (page 6-27) for impact, 99.5 percent of truck and 99.6 percent of rail accidents are less severe than the regulatory criteria. Similarly, for fire related accidents, 99.9 percent of truck and 99.8 percent of rail accidents are less severe than the regulatory criteria. Thus, the probability of a TRU waste shipment accident occurring that exceeds regulatory criteria and potentially releases a portion of the contents is extremely small. However, the radiological risks from these very low probability events are considered by RADTRAN to determine the overall probabilistic transportation risk.

The amount of radioactive material released in an accident depends upon the severity of the accident and the waste package capabilities. Minor accidents are unlikely to cause any release, but very severe accidents (much more severe than regulatory standards for Type B packages) may release some of the radioactive materials. Thus, the distribution of accidents according to severity must be determined in addition to the overall accident rate. In this subsection, the accident severity classification scheme used in this assessment is discussed. The distribution of accidents according to severity is presented for truck and rail shipping modes.

TABLE D.3.11 Summary of lifetime radiological risks between Proposed Action and Alternative Action: CH TRU incident-free occupational risk

(person-rems)

	Proposed Action		Alternative Action	
Facility	Truck	Rail	Truck	Rail
Idaho National Engineering Laboratory	3.1×10^{2}	3.2×10^{1}	3.1×10^{2}	8.9×10^{-1}
Rocky Flats Plant	3.4×10^{2}	3.5×10^{1}	3.4×10^{2}	1.2
Hanford Reservation	1.6×10^{2}	1.6×10^{1}	1.6×10^{2}	5.2×10^{-1}
Savannah River Plant	4.3×10^{2}	4.5×10^{1}	4.4×10^{2}	1.3
Los Alamos National Laboratory	8.1×10^{1}	8.1×10^{1}	8.1×10^{1}	8.1×10^{1}
Oak Ridge National Laboratory	3.7×10^{1}	4.1×10^{0}	3.7×10^{1}	3.0×10^{-1}
Nevada Test Site	6.1×10^{0}	6.1×10^{0}	6.1×10^{0}	6.1×10^{0}
Argonne National Laboratory-East	2.1×10^{0}	2.7×10^{-1}	2.1×10^{0}	1.4×10^{-2}
Lawrence Livermore National Laboratory	2.2×10^{1}	2.2×10^{0}	2.2×10^{1}	6.6×10^{-2}
Mound Laboratory	3.3×10^{0}	3.4×10^{-1}	3.4	9.4×10^{-3}
TOTAL	1.4×10^{3}	2.2×10^{2}	1.4×10^{3}	9.1×10^{1}

TABLE D.3.12 Summary of lifetime radiological risks between Proposed Action and the Alternative Action: CH TRU incident-free nonoccupational risk

(person-rems)

	Proposed Action		Alternative Action	
Facility	Truck	Rail	Truck	Rail
Idaho National Engineering Laboratory	1.2×10^{2}	9.5×10^{1}	1.2×10^{2}	9.2×10^{1}
Rocky Flats Plant	8.6×10^{1}	8.6×10^{1}	8.6×10^{1}	8.6×10^{-1}
Hanford Reservation	7.9×10^{1}	7.9×10^{1}	7.9×10^{1}	7.9×10^{1}
Savannah River Plant	2.2×10^{2}	1.9×10^{2}	2.2×10^{2}	1.9×10^{2}
Los Alamos National Laboratory	2.7×10^{1}	2.7×10^{1}	2.7×10^{1}	2.7×10^{1}
Oak Ridge National Laboratory	6.0×10^{1}	3.3×10^{1}	6.0×10^{1}	2.9×10^{1}
Nevada Test Site	2.4×10^{0}	2.4×10^{0}	2.4×10^{0}	2.4×10^{0}
Argonne National Laboratory-East	2.3×10^{0}	1.6×10^{0}	2.2×10^{0}	1.5×10^{0}
Lawrence Livermore National Laboratory	1.1×10^{1}	1.1×10^{1}	1.1×10^{1}	1.1×10^{1}
Mound Laboratory	1.7	9.3×10^{-1}	1.7	8.5×10^{-1}
TOTAL	6.1×10^{2}	5.3×10^{2}	6.1×10^{2}	5.2×10^{2}

TABLE D.3.13 Summary of lifetime radiological risks for incident-free transportation of RH TRU waste (person-rems): Proposed Action and the Alternative Action

	Disposal Phase (20 years)[a]			
	100% Truck		Maximum Rail	
Facility	Occ[b]	Non Occ[c]	Occ	Non Occ
Idaho National Engineering Laboratory	1.9×10^{1}[d]	1.5×10^{1}	1.2×10^{-1}	1.2×10^{1}
Hanford Reservation	1.6×10^{2}	3.1×10^{2}	1.6×10^{0}	1.4×10^{2}
Los Alamos National Laboratory[e]	1.2×10^{0}	3.9×10^{-1}	1.2×10^{0}	3.9×10^{-1}
Oak Ridge National Laboratory	4.1×10^{2}	2.7×10^{2}	2.6×10^{0}	2.4×10^{2}
Argonne National Laboratory-East	4.5×10^{-1}	3.6×10^{-1}	2.7×10^{-3}	2.5×10^{-1}
TOTAL	5.9×10^{2}	6.0×10^{2}	5.5×10^{0}	3.9×10^{2}

[a] No RH TRU is shipped to the WIPP during the Test Phase for any alternative

[b] Occupational population—quantifies doses received by transportation crews

[c] Nonoccupational population

[d] Population group risks are calculated by multiplying the risk/shipment identified in Table D.3.8 by the total number of shipments to WIPP by truck or rail, as determined from the projections in Table D.3.2, rail occupational risks resulting from normal transportation include the impact of inspection activities

[e] Waste shipments from this facility are limited to the truck mode. Rail risks are thus the same as truck risks

TABLE D.3.14 Hypothetical maximum exposure to an individual from incident-free transportation during Test Phase and Disposal Phase (25 yrs) (rems)

	100% truck		Maximum rail	
Facility	CH	RH	CH	RH
Idaho National Engineering Laboratory	2.3×10^{-4}	2.4×10^{-5}	2.2×10^{-4}	2.5×10^{-5}
Rocky Flats Plant	4.7×10^{-4}		4.7×10^{-4}	
Hanford Reservation	1.0×10^{-4}	4.0×10^{-4}	1.0×10^{-4}	4.0×10^{-4}
Savannah River Plant	3.1×10^{-4}		3.1×10^{-4}	
Los Alamos National Laboratory[a]	4.0×10^{-4}	9.4×10^{-6}	4.0×10^{-4}	9.4×10^{-6}
Oak Ridge National Laboratory	1.1×10^{-4}	5.8×10^{-4}	1.1×10^{-4}	5.8×10^{-4}
Nevada Test Site[a]	5.3×10^{-6}		5.3×10^{-6}	
Argonne National Laboratory-East	4.3×10^{-6}	6.1×10^{-7}	4.4×10^{-6}	8.0×10^{-7}
Lawrence Livermore National Laboratory	1.6×10^{-5}		1.6×10^{-6}	
Mound Laboratory	2.5×10^{-6}		2.6×10^{-5}	
TOTAL	1.6×10^{-3}	1.0×10^{-3}	1.6×10^{-3}	1.0×10^{-3}

[a] Waste shipments are limited to the truck mode. Rail risks are the same as truck risks.

Accident severity is a means of categorizing the seriousness of an accident in terms of mechanical and thermal loads. Many methods may be utilized to classify accidents using mechanical and thermal parameters. Relevant mechanical parameters may include impact speed, impact force, impact location and orientation, impact surface hardness, and impact puncture characteristics. Thermal characteristics may include flame temperature, fire duration, fire source size and orientation with respect to the packaging, and heat transfer properties (such as flame emissivity and convection coefficients).

NRC (1977) assigned eight accident severity categories for each transportation mode. This study was performed to assess the adequacy of radioactive material shipment regulations. The first two accident categories were defined to be less serious than the 10 CFR 71 hypothetical accident conditions for testing Type B packaging, such as TRUPACT-II and the RH cask. These tests simulate very severe transportation accidents, with the packaging sequentially subjected to drop, puncture, thermal, and water immersion tests. Thus, accidents within severity categories 1 and 2 are very unlikely to cause any release to the environment.

The NRC (1977) classification scheme for truck accidents is illustrated in Figure D.3.1, and uses crush force and fire duration to determine the seriousness of an accident. The crush force may result from either an internal (e.g., container crushed upon impact by other containers in load) or static load (e.g., container crushed beneath vehicle). The classification approach used for train accidents is shown in Figure D.3.2. While fire duration is retained as the thermal parameter, it was decided to use puncture and impact speed as the mechanical measure of accident severity. This was done since potential crush forces resulting from the interaction of other cargo was considered less relevant for rail shipments.

This assessment retains the severity classification scheme utilized in NRC (1977). In order to place the accident severities into perspective, two accident events which fall within categories 1 and 2 are described:

> Known as the I-80 bridge accident, a tractor-trailer rig was struck by a pickup truck while on an overpass bridge on I-80 near San Francisco, California. The tractor-trailer rig veered into the bridge railing and fell to a soil surface 64 feet below. NRC (1987) determined that a comparable accident involving a Type B certified package would fall within its design accident conditions and thus, would not be expected to have any significant release.
>
> A truck fire accident occurred in the Caldecott Tunnel near Oakland, California. The accident resulted from a collision involving a gasoline truck, a bus, and a car. The gasoline truck carried approximately 8,800 gallons of gasoline which acted as the fire source; a resulting peak flame temperature of 1900°F was estimated. While it took about 2 hours and 42 minutes to completely extinguish the fire, burning of the majority of gasoline occurred in less than 40 minutes. It was also concluded in NRC (1987) that the response of a Type B packaging would be within its design capabilities.

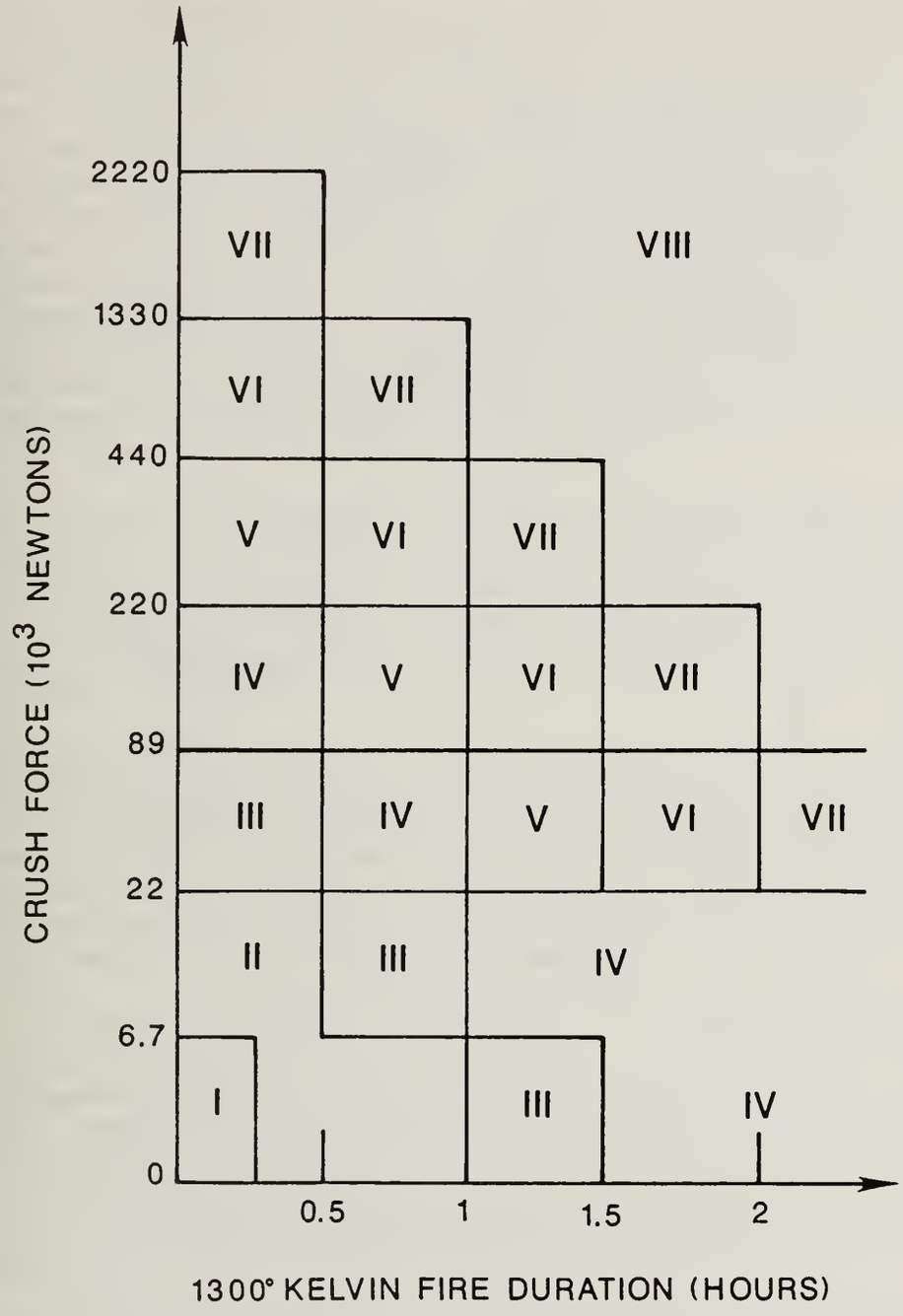

REF: NRC, 1977.

FIGURE D.3.1
TRUCK ACCIDENT SEVERITY CATEGORY CLASSIFICATION SCHEME

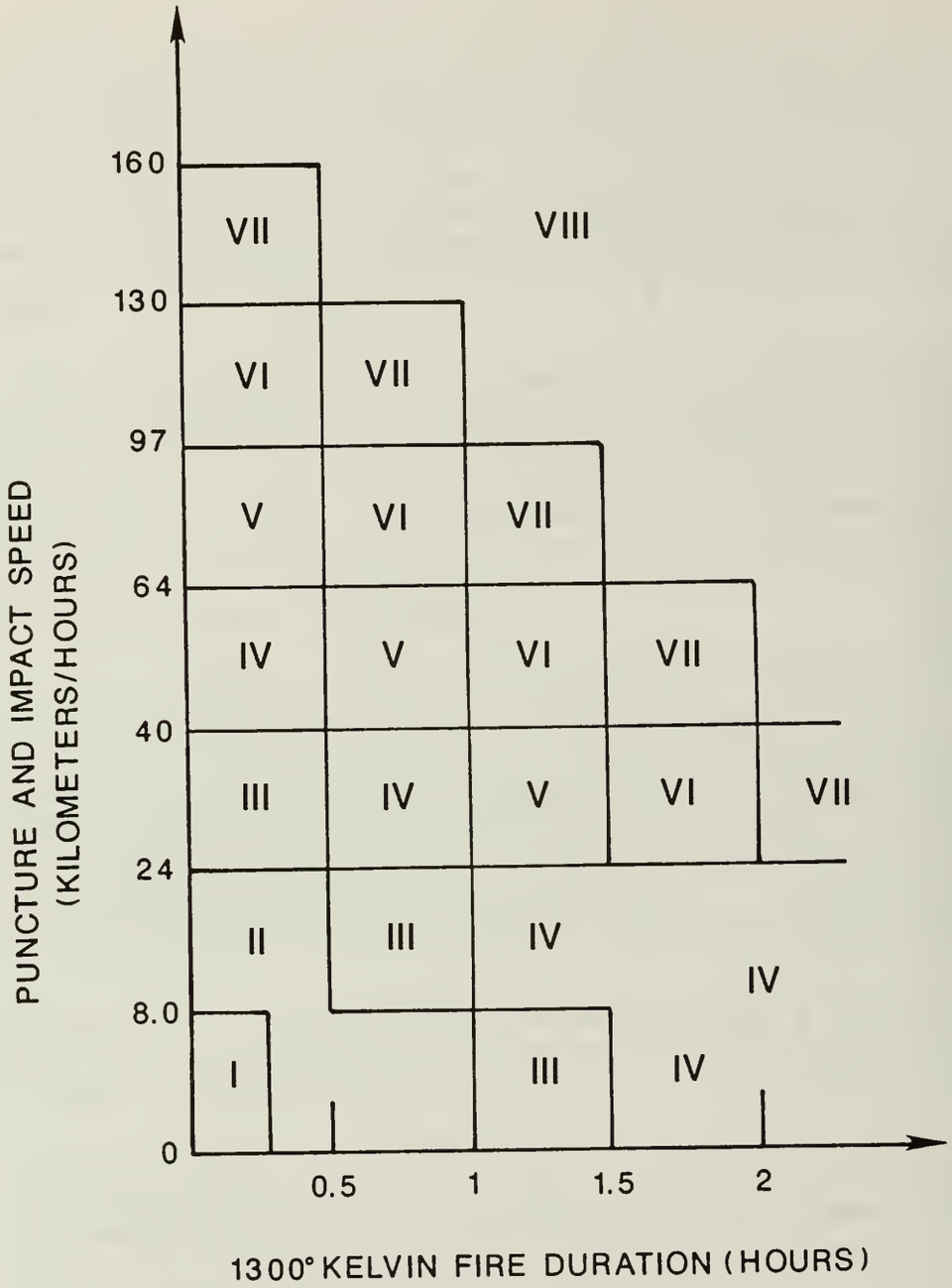

REF: NRC, 1977.

FIGURE D.3.2
RAILROAD ACCIDENT SEVERITY CATEGORY CLASSIFICATION SCHEME

For higher accident severities, there is an incremental increase in mechanical and thermal loads. At the highest severity category, impact forces can be 100 times greater than those within category 2 and fire durations in excess of 1.5 to 2.0 hours. For example, a 40 ft diameter engulfing fire involving a truck shipment would require approximately 17,000 gallons of hydrocarbon fuel to sustain a fire having a duration of 2 hours. This would require the very unlikely probability of involving three tanker trucks in the incident, since a typical tanker will carry approximately 5,000 gallons of hydrocarbons (Wolff, 1984). At a minimum, at least two full 10,000 gallon tanker trucks would need to be involved. For a rail incident, the average fire pool size is 2,000 ft^2 (50 ft diameter) (Wolff, 1984); over 27,000 gallons of hydrocarbon fuel would be required to maintain a fire of this magnitude for 2 hours. The large majority of truck (99.90 percent) and rail (99.83 percent) accidents that involve fires, however, have durations less than 30 minutes (Wolff, 1984). The probability that such accidents occur diminishes as their severity increases, as already noted.

Table D.3.15 presents the fractional occurrences of truck accidents in each of the eight severity categories. The dominant accident effect is crush rather than impact. This assessment assumes an overall accident rate of 1.1×10^{-6} accidents/kilometer (NRC, 1977). The fraction of accidents within each severity category and the fraction of accidents within each population zone relevant to TRU waste shipments to the WIPP are presented in Table D.3.15.

Table D.3.16 presents the fractional occurrence of train accidents in each of the eight accident severity categories. The dominant accident effect in a train accident is impact rather than crush force. The predominant mode of damage in severe accidents is puncture. The overall accident rate is 9.3×10^{-7} rail car accidents/railroad-kilometer, assuming an average train length of 70 cars and an average of 10 cars involved in each accident (NRC, 1977). The more severe accidents are assumed to occur in lower-population-density zones where travel speeds are higher.

D.3.3.1.2 Release Fractions. To assess the risk of a truck accident, one must be able to predict the package response to an accident of a given severity. For a given accident severity, one needs to know how much of the total package contents will be released. Additionally, the actual release from a number of packages in the same accident severity class would vary from no release to, for example, a 10 percent release. For this assessment, it was assumed that all packages, without regard to waste form or type, release an average release fraction for each accident severity class, and each waste container responds the same in an accident.

The containment designs for the CH and RH TRU waste packaging systems are described in Subsection D.2 of this appendix. These Type B packages are designed to comply with the hypothetical accident release limits described in 10 CFR 71.51 and DOE Order 5480.3. These regulations specify that the amount of radioactive material released under hypothetical accident conditions must not exceed A_2 curies in one week, where A_2 is the maximum activity of radioactive material which is permitted in a Type A package. A_2 values are tabulated in Appendix A of 10 CFR 71 by radionuclide.

TABLE D.3.15 Fractional occurrences[a] for truck accidents by accident severity category and population density zone

Accident severity category	Fractional occurences	Fractional occurrences according to population density zones		
		Low	Medium	High
I	.55	.1	.1	.8
II	.36	.1	.1	.8
III	.07	.3	.4	.3
IV	.016	.3	.4	.3
V	.0028	.5	.3	.2
VI	.0011	.7	.2	.1
VII	8.5×10^{-5}	.8	.1	.1
VIII	1.5×10^{-5}	.9	.05	.05

[a] Overall accident rate = 1.1×10^{-6} accidents/kilometer (4.6×10^{-7} accidents/kilometer for ICVs)

TABLE D.3.16 Fractional occurrences[a] for train accidents by accident severity category and population density zone

Accident severity category	Fractional occurences	Fractional occurences according to population density zones		
		Low	Medium	High
I	.50	.1	.1	.8
II	.30	.1	.1	.8
III	.18	.3	.4	.3
IV	.018	.3	.4	.3
V	.0018	.5	.3	.2
VI	1.3×10^{-4}	.7	.2	.1
VII	6.0×10^{-5}	.8	.1	.1
VIII	1.0×10^{-5}	.9	.05	.05

[a] Overall accident rate = 9.3×10^{-7} railcar accidents/railcar-kilometer

The current release fraction analysis retains the use of eight accident severity categories as defined by NRC (1977) for truck and rail shipments. Due to the limited data for package response to accidents, a prior analysis (DOE, 1986) assumed that for CH TRU waste shipments, a release corresponding to a fractional value of the A_2 quantity would occur for severity category 3, which represents a loss of package integrity for an accident that slightly exceeds Type B packaging regulatory limits. Subsequent release fractions were increased by an order of magnitude for each succeeding accident severity class. For RH TRU waste shipments, release fractions were estimated using the Model II values for 1975 Type B packages listed in Table 5-8 of NRC, 1977. The current approach estimates the release of radionuclides from the waste container to the cavity of the shipping package and subsequent release to the environment using available test data and analysis provided in literature.

There are multiple release mechanisms and pathways that determine the amount of airborne radioactive material that may be released to the environment following a severe accident. Release mechanisms may be evaluated on the basis of the initiating accident event-impact event, thermal event, or a combination of both. Specific impact release mechanisms include waste container failure, fragmentation of solid waste, particulate suspension, and aerodynamic entrainment of particles to the environment upon failure of packaging containment. Thermal release mechanisms include thermally induced failures of the waste containers; aerosolization of particulates by combustion, gas generation, or heating of contaminated surfaces; potential volatilization of selected radionuclides; and subsequent aerodynamic entrainment of particles and aerosols to the environment upon loss of package containment.

The following assumptions were utilized in order to estimate release fractions:

- Waste is packaged in Type A drums.
- A major breach of the Type B packaging system is not credible; thus, slight damage (e.g., puncture) limits air/oxygen and internal combustion.
- Loss of packaging containment will result in a 100 percent release to the environment of airborne particulates and aerosols present in the packaging cavity.
- Radioactive contamination is evenly distributed throughout the waste volume.

The third assumption adds conservatism to the analysis since the assumption does not take credit for the accident specific nature of mitigating factors such as particulate settling, plateout, and filtration effects.

Table D.3.17 summarizes the algorithm used to estimate the total respirable release fraction (TRRF) for impact and thermal events. The algorithm assumes that accidents involving a fire will have an associated impact event and that the releases associated with both event types are additive. Table D.3.18 summarizes the values for the release algorithm parameters and their bases. Release fractions for truck and rail shipments differ due to the higher probability of a thermal event for rail shipments. Tables D.3.19

TABLE D.3.17 Estimate of potential accident release fractions for CH and RH TRU waste shipments

Total respirable release fraction (TRRF)	=	Impact release fraction (IRF) + Thermal release fraction (TRF)
Impact release fraction	=	(FFC x FMRC) (FMAI + FMEI)FMRPI
Thermal release fraction	=	FAT ((FMC x FMAC) + (FMAT)FMRPT)

where:

FFC	=	Fraction of failed waste containers
FMRC	=	Fraction of material released from failed containers into package cavity
FMAI	=	Fraction of material aerosolized from impact
FMEI	=	Fraction of material entrained during impact event
FMRPI	=	Fraction of material released from packaging during impact event
FAT	=	Fraction of accidents involving a thermal event
FMC	=	Fraction of material consumed by combustion
FMAC	=	Fraction of material aerosolized by combustion
FMAT	=	Fraction of material aerosolized by thermal event
FMRPT	=	Fraction of material released from packaging during thermal event

TABLE D.3.18 Release algorithm parameters

Parameters	Value	Basis/Reference
FFC	.2728 lnF -2.814 (Where F is accident severity breach force)	Reference Slurley, 1983 and Huerta, 1983
FMRC	Varies with accident severity case	Conservatively assumed using Reference Huerta, 1983 and NRC, 1977 for guidance
FMAI	(KxVV)/(AxW) Where: K = Resuspension Factor $= 2x10^{-2}m_{-1}$ VV = Void Volume $= 6m^3$(CH-TRU) $= 1.1m^3$(RH-TRU) A = Area/Units Mags $= .5m^2/kg$ W = Waste Weight = 3175 kg (CH-TRU) = 907 kg (RH-TRU)	Reference NRC, 1980 The mechanical action of vigorous sweeping is used to estimate respirable air-borne contamination resulting for material released from the failed waste containers.
FMEI	1.5E = -4 (.0024 + .000038 + .00075 + .00087)(.15)/4	Reference Mishima and Schwendeman, 1973 Aerodynamicentrainment of respirable particles results from a potential pressure buildup from gas generation and subsequent depressurization upon accident induced packaging containment failure. The average entrainment value for 4 surfaces was used with an airflow of 2.5 mph for 30 minutes.

TABLE D.3.18 Concluded

Parameters	Value	Basis/Reference
FMRPI	Accident Severity 1-4: 0.0 Accident Severity 5-8: 0.0	Estimate based on packaging system design and Reference NRC, 1977
FAT	.017 (Truck) .068 (Rail)	Reference Fisher et al., 1987
FMC	Accident Severity 1-2: 0.0 (CH/RH-TRU) Accident Severity 3-8: 9.E-4 (CH-TRU) 6.E-4 (RH-TRU)	Reference NRC, 1980
FMAC	5.E-4	Reference Mishima and Schwendeman, 1973 Maximum observed respirable airborne particle release during the burning of contaminated wastes
FMAT	Accident Severity 1-2: 0.E + 0(CH/RH-TRU) Accident Severity 3: 2.E - 8(CH/RH-TRU) Accident Severity 4-8: 1.E - 5(CH-TRU) 9.E - 6(RH-TRU)	Reference NRC, 1980
FMRPT	Accident Severity 1-2: 0.0 Accident Severity 3-8: 1.0	Assumed based on accident severity category definitions (Reference NRC, 1977) and Type B Packaging design requirements

through D.3.22 present the release fractions for accident severity categories for CH and RH TRU truck and rail shipments.

Lorenz et al. (1980) was utilized to assess the extent that fission products present in RH TRU waste may volatilize at elevated temperatures during accident events involving fires. Table 50 of the cited reference shows that releases of cesium, antimony, and ruthenium in vapor form increase at elevated temperatures. Testing was conducted at temperature ranging from 500°C to 1200°C in both steam and air environments. Ruthenium releases were considerably more significant in dry air. This was also true for cesium at 700°C. Testing was conducted with fuel rod segments in a quartz tube furnace. Assuming that release mechanisms for RH TRU waste would be similar, and using test results corresponding to 700°C, it was concluded that cesium, antimony, and ruthenium vapor releases would be comparable to the values estimated for respirable particulate releases. Consequently, the analysis retains the particulate-based estimates to describe releases for these three radionuclides.

D.3.3.1.3 Dispersal Conditions. The dispersion of airborne radioactive material from an accident is controlled by the winds. The airborne radioactive material moves downwind from the scene of the accident and is additionally influenced by the degree of atmospheric turbulence. For this analysis, the materials are assumed to move downwind and disperse. As the radioactive cloud disperses, persons in its path will be exposed to external radiation, internal radiation due to inhalation, or internal radiation due to ingestion. For inhalation and ingestion, the degree of exposure depends on the amount of material retained in the lungs or other organs of the exposed persons.

Airborne transport and diffusion can disperse radioactive materials over large areas. The degree of dispersion is influenced by many factors such as: season (which influences atmospheric turbulence), time of day, degree of cloud cover, land surface features and characteristics, and other meteorological parameters. Dispersed material can expose people in many ways as shown in Figure D.3.3. Gamma emitters' principle effect to people is a direct external or internal dose. Material that emits alpha or beta radiation when aerosolized and inhaled by people produces the largest consequence. Figure D.3.3 illustrates that radioactive materials can also be incorporated in the food chain. Radiation doses to the population through the food chain pathway are usually more significant if a continuous release exists.

One of the pathways of note is resuspension. This occurs when deposited particulate material becomes airborne as a result of pedestrians, vehicles, plowing, etc., or wind. The resuspended material then becomes available for inhalation and can cause additional dose that accumulates with time.

Two effects can be estimated when the downwind concentrations and deposition patterns are known. The first effect and the most important is the inhalation of the material by the population exposed. The method of calculation for this effect is given in NRC, 1977 and the interested reader is referred to that document. The level of surface contamination is the second effect and is also determined by the dispersion pattern.

TABLE D.3.19 CH TRU waste package release fractions: truck

Impact Release Fraction (IRF)

Accident severity category	FFC	FMRC	FMAI	FMEI	FMPRI	IRF
1	0	0	0	0	0	0
2	0	0	0	0	0	0
3	3.0×10^{-1}	1.0×10^{-1}	8.0×10^{-5}	0	0	0
4	5.0×10^{-1}	3.0×10^{-1}	8.0×10^{-5}	0	0	0
5	7.0×10^{-1}	5.0×10^{-1}	8.0×10^{-5}	1.5×10^{-4}	1.0	8.0×10^{-5}
6	1.0	7.0×10^{-1}	8.0×10^{-5}	1.5×10^{-4}	1.0	2.0×10^{-4}
7	1.0	1.0	8.0×10^{-5}	1.5×10^{-4}	1.0	2.0×10^{-4}
8	1.0	1.0	8.0×10^{-5}	1.5×10^{-4}	1.0	2.0×10^{-4}

Thermal Release Fraction (TRF)

Accident severity category	FAT	FMC	FMAC	FMAT	FMRPT	TRF
1	1.7×10^{-2}	0	0	0	0	0
2	1.7×10^{-2}	0	0	0	0	0
3	1.7×10^{-2}	9.0×10^{-4}	5.0×10^{-4}	2.0×10^{-8}	1.0	8.0×10^{-9}
4	1.7×10^{-2}	9.0×10^{-4}	5.0×10^{-4}	1.0×10^{-5}	1.0	2.0×10^{-7}
5	1.7×10^{-2}	9.0×10^{-4}	5.0×10^{-4}	1.0×10^{-5}	1.0	2.0×10^{-7}
6	1.7×10^{-2}	9.0×10^{-4}	5.0×10^{-4}	1.0×10^{-5}	1.0	2.0×10^{-7}
7	1.7×10^{-2}	9.0×10^{-4}	5.0×10^{-4}	1.0×10^{-5}	1.0	2.0×10^{-7}
8	1.7×10^{-2}	9.0×10^{-4}	5.0×10^{-4}	1.0×10^{-5}	1.0	2.0×10^{-7}

Total Respirable Release Fraction (TRRF)

Accident severity category	IRF	TRF	TRRF
1	0	0	0
2	0	0	0
3	0	8.0×10^{-9}	8.0×10^{-9}
4	0	2.0×10^{-7}	2.0×10^{-7}
5	8.0×10^{-5}	2.0×10^{-7}	8.0×10^{-5}
6	2.0×10^{-4}	2.0×10^{-7}	2.0×10^{-4}
7	2.0×10^{-4}	2.0×10^{-7}	2.0×10^{-4}
8	2.0×10^{-4}	2.0×10^{-7}	2.0×10^{-4}

TABLE D.3.20 CH TRU waste package release fractions: rail

Impact Release Fraction (IRF)

Accident severity category	FFC	FMRC	FMAI	FMEI	FMPRI	IRF
1	0	0	0	0	0	0
2	0	0	0	0	0	0
3	3.0×10^{-1}	1.0×10^{-1}	8.0×10^{-5}	0	0	0
4	5.0×10^{-1}	3.0×10^{-1}	8.0×10^{-5}	0	0	0
5	7.0×10^{-1}	5.0×10^{-1}	8.0×10^{-5}	1.5×10^{-4}	1.0	8.0×10^{-5}
6	1.0	7.0×10^{-1}	8.0×10^{-5}	1.5×10^{-4}	1.0	2.0×10^{-4}
7	1.0	1.0	8.0×10^{-5}	1.5×10^{-4}	1.0	2.0×10^{-4}
8	1.0	1.0	8.0×10^{-5}	1.5×10^{-4}	1.0	2.0×10^{-4}

Thermal Release Fraction (TRF)

Accident severity category	FAT	FMC	FMAC	FMAT	FMRPT	TRF
1	6.8×10^{-2}	0	0	0	0	0
2	6.8×10^{-2}	0	0	0	0	0
3	6.8×10^{-2}	9.0×10^{-4}	5.0×10^{-4}	2.0×10^{-8}	1.0	3.0×10^{-8}
4	6.8×10^{-2}	9.0×10^{-4}	5.0×10^{-4}	1.0×10^{-5}	1.0	7.0×10^{-7}
5	6.8×10^{-2}	9.0×10^{-4}	5.0×10^{-4}	1.0×10^{-5}	1.0	7.0×10^{-7}
6	6.8×10^{-2}	9.0×10^{-4}	5.0×10^{-4}	1.0×10^{-5}	1.0	7.0×10^{-7}
7	6.8×10^{-2}	9.0×10^{-4}	5.0×10^{-4}	1.0×10^{-5}	1.0	7.0×10^{-7}
8	6.8×10^{-2}	9.0×10^{-4}	5.0×10^{-4}	1.0×10^{-5}	1.0	7.0×10^{-7}

Total Respirable Release Fraction (TRRF)

Accident severity category	IRF	TRF	TRRF
1	0	0	0
2	0	0	0
3	0	3.0×10^{-8}	3.0×10^{-8}
4	0	7.0×10^{-7}	7.0×10^{-7}
5	8.0×10^{-5}	7.0×10^{-7}	8.0×10^{-5}
6	2.0×10^{-4}	7.0×10^{-7}	2.0×10^{-4}
7	2.0×10^{-4}	7.0×10^{-7}	2.0×10^{-4}
8	2.0×10^{-4}	7.0×10^{-7}	2.0×10^{-4}

TABLE D.3.21 RH TRU waste package release fractions: truck

Impact Release Fraction (IRF)

Accident severity category	FFC	FMRC	FMAI	FMEI	FMPRI	IRF
1	0	0	0	0	0	0
2	0	0	0	0	0	0
3	3.0×10^{-1}	1.0×10^{-1}	5.0×10^{-5}	0	0	0
4	7.0×10^{-1}	3.0×10^{-1}	5.0×10^{-5}	0	0	0
5	1.0	5.0×10^{-1}	5.0×10^{-5}	1.5×10^{-4}	1.0	1.0×10^{-4}
6	1.0	7.0×10^{-1}	5.0×10^{-5}	1.5×10^{-4}	1.0	1.0×10^{-4}
7	1.0	1.0	5.0×10^{-5}	1.5×10^{-4}	1.0	2.0×10^{-4}
8	1.0	1.0	5.0×10^{-5}	1.5×10^{-4}	1.0	2.0×10^{-4}

Thermal Release Fraction (TRF)

Accident severity category	FAT	FMC	FMAC	FMAT	FMRPT	TRF
1	1.7×10^{-2}	0	0	0	0	0
2	1.7×10^{-2}	0	0	0	0	0
3	1.7×10^{-2}	7.0×10^{-4}	5.0×10^{-4}	2.0×10^{-8}	1.0	6.0×10^{-9}
4	1.7×10^{-7}	7.0×10^{-4}	5.0×10^{-4}	9.0×10^{-6}	1.0	2.0×10^{-7}
5	1.7×10^{-2}	7.0×10^{-4}	5.0×10^{-4}	9.0×10^{-6}	1.0	2.0×10^{-7}
6	1.7×10^{-2}	7.0×10^{-4}	5.0×10^{-4}	9.0×10^{-6}	1.0	2.0×10^{-7}
7	1.7×10^{-2}	7.0×10^{-4}	5.0×10^{-4}	9.0×10^{-6}	1.0	2.0×10^{-7}
8	1.7×10^{-2}	7.0×10^{-4}	5.0×10^{-4}	9.0×10^{-6}	1.0	2.0×10^{-7}

Total Respirable Release Fraction (TRRF)

Accident severity category	IRF	TRF	TRRF
1	0	0	0
2	0	0	0
3	0	6.0×10^{-9}	6.0×10^{-9}
4	0	2.0×10^{-7}	2.0×10^{-7}
5	1.0×10^{-4}	2.0×10^{-7}	1.0×10^{-4}
6	1.0×10^{-4}	2.0×10^{-7}	2.0×10^{-4}
7	2.0×10^{-4}	2.0×10^{-7}	2.0×10^{-4}
8	2.0×10^{-4}	2.0×10^{-7}	2.0×10^{-4}

TABLE D.3.22 RH TRU waste package release fractions: rail

Impact Release Fraction (IRF)

Accident severity category	FFC	FMRC	FMAI	FMEI	FMPRI	IRF
1	0	0	0	0	0	0
2	0	0	0	0	0	0
3	3.0×10^{-1}	1.0×10^{-1}	5.0×10^{-5}	0	0	0
4	7.0×10^{-1}	3.0×10^{-1}	5.0×10^{-5}	0	0	0
5	1.0	5.0×10^{-1}	5.0×10^{-5}	1.5×10^{-4}	1.0	1.0×10^{-4}
6	1.0	7.0×10^{-1}	5.0×10^{-5}	1.5×10^{-4}	1.0	1.0×10^{-4}
7	1.0	1.0	5.0×10^{-5}	1.5×10^{-4}	1.0	2.0×10^{-4}
8	1.0	1.0	5.0×10^{-5}	1.5×10^{-4}	1.0	2.0×10^{-4}

Thermal Release Fraction (TRF)

Accident severity category	FAT	FMC	FMAC	FMAT	FMRPT	TRF
1	6.8×10^{-2}	0	0	0	0	0
2	6.8×10^{-2}	0	0	0	0	0
3	6.8×10^{-2}	7.0×10^{-4}	5.0×10^{-4}	2.0×10^{-8}	1.0	2.0×10^{-8}
4	6.8×10^{-2}	7.0×10^{-4}	5.0×10^{-4}	9.0×10^{-6}	1.0	7.0×10^{-7}
5	6.8×10^{-2}	7.0×10^{-4}	5.0×10^{-4}	9.0×10^{-6}	1.0	7.0×10^{-7}
6	6.8×10^{-2}	7.0×10^{-4}	5.0×10^{-4}	9.0×10^{-6}	1.0	7.0×10^{-7}
7	6.8×10^{-2}	7.0×10^{-4}	5.0×10^{-4}	9.0×10^{-6}	1.0	7.0×10^{-7}
8	6.8×10^{-2}	7.0×10^{-4}	5.0×10^{-4}	9.0×10^{-6}	1.0	7.0×10^{-7}

Total Respirable Release Fraction (TRRF)

Accident severity category	IRF	TRF	TRRF
1	0	0	0
2	0	0	0
3	0	2.0×10^{-8}	2.0×10^{-8}
4	0	2.0×10^{-7}	2.0×10^{-7}
5	1.0×10^{-4}	2.0×10^{-7}	1.0×10^{-4}
6	1.0×10^{-4}	2.0×10^{-7}	1.0×10^{-4}
7	2.0×10^{-4}	2.0×10^{-7}	2.0×10^{-4}
8	2.0×10^{-4}	2.0×10^{-7}	2.0×10^{-4}

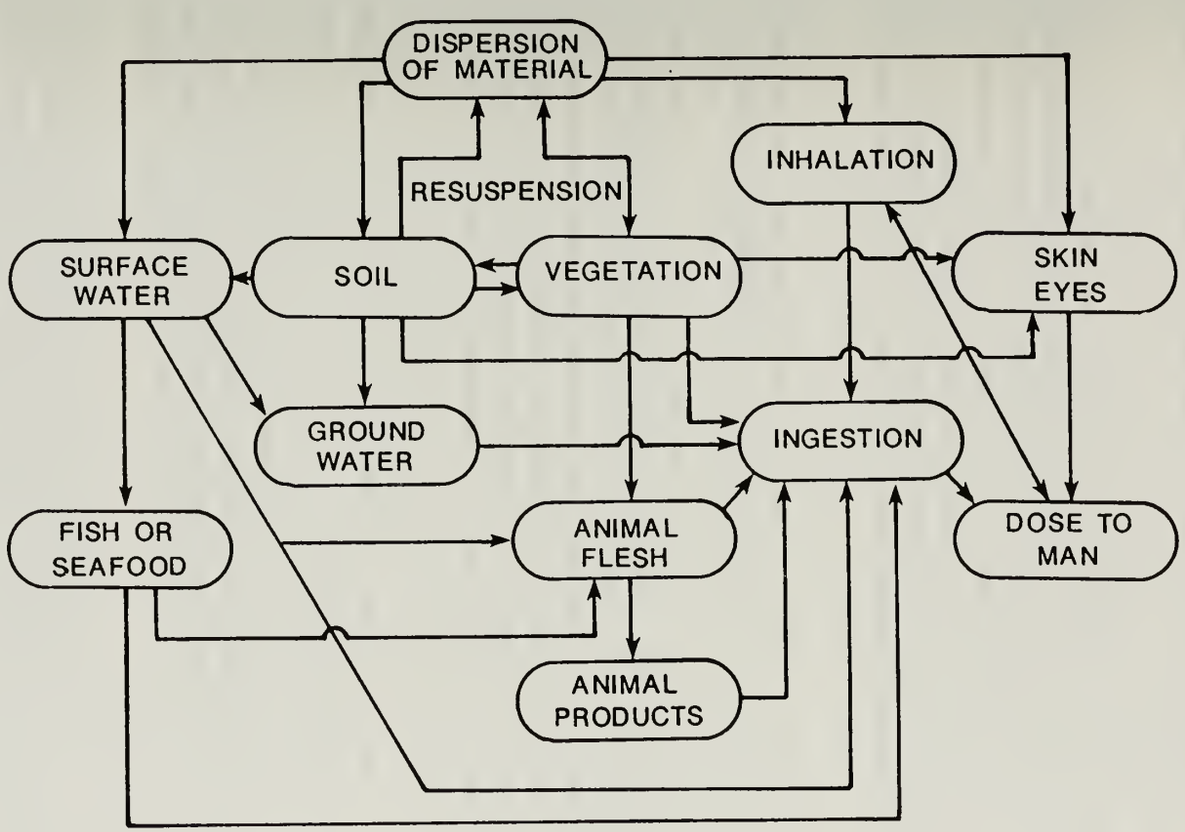

REF: NRC, 1977.

FIGURE D.3.3
POSSIBLE PATHWAYS TO MAN FROM RADIONUCLIDE RELEASE

D.3.3.1.4 Pathways and Exposed Populations. RADTRAN, or similar analytical tools, can be used to evaluate the radiological impacts of transporting radioactive materials under accident conditions. As input to RADTRAN, the exposure pathways must be identified and the size of exposed populations must be estimated. Transportation accidents may be divided into those accidents in which no package failure (and therefore no release of radioactive materials) occurs, and those accidents in which package integrity is compromised. The exposure pathways and the exposed population subgroups are discussed below.

In an accident that does not compromise the containment of the package, the exposure pathway is limited to direct exposure by penetrating radiation from the intact package. Dose to any member of an exposed population is evaluated in the same manner as the exposure from incident-free transportation, with adjustments made for duration of exposure and distance between the package and the exposed individuals. The exposed populations include truck or rail crew, occupants of other vehicle(s) involved in the accident, bystanders and pedestrians, occupants of nearby buildings, and members of emergency response crews.

In an accident that results in package failure and possible release of radioactive material, exposures may result from both nondispersible and dispersible materials.

The exposure pathway from accidents involving packaging failure with nondispersible materials is direct exposure resulting from loss of shielding of the package contents. Certain radioactive materials are not dispersible due to chemical or physical form, such as irradiated steel hardware; these materials may nevertheless result in exposure by penetrating radiation. Doses to exposed individuals are evaluated in the same manner as other direct exposures, with adjustments made for increased dose rates resulting from shielding loss, as well as exposure time and distance adjustments. The exposed populations are the same as identified above.

Four exposure pathways may result from accidents that include failure of the packages transporting dispersible radioactive materials:

- Cloudshine: the exposure from cloudshine is the direct *external* dose from the passing cloud of dispersed material. Dispersion is a function of the meteorological conditions at the accident scene, as well as the fraction of failed packages and the fraction of material released from failed packages that becomes airborne.

- Groundshine: the exposure from groundshine is the direct *external* dose from material that has deposited on the ground after being dispersed from the accident site. Deposition is a function of the material being deposited (i.e., how fast does the dispersed material settle out) and of the amount of dispersed material available to settle out (i.e., how much material from the original release has dispersed far enough to deposit on the area of interest).

- Inhalation: the exposure from inhalation is the *internal* exposure that results from breathing aerosolized material. Exposure from inhalation ia a function of the package failure fraction, the fraction of material that becomes airborne,

the aerosol fraction of respirable size, the dose per curie inhaled, the dilution factor of radioactive material in the surrounding air, and the breathing rate of the exposed individual.

- Resuspension: the exposure from resuspension is the *internal* exposure that results from inhalation of material that was dispersed, deposited at a distance from the accident scene, then resuspended as an aerosol and inhaled. Evaluating exposure from resuspension combines evaluating the mechanisms of dispersion, deposition and inhalation described above, as well as evaluating the fraction of deposited material that is resuspended. (Resuspension may occur by changing meteorological conditions, eg., change in wind speed or direction, or by otherwise disturbing deposited material (e.g., traffic through a deposition area.) Note that exposure by ingestion pathways is not included in evaluating radiological impacts of accidents, since it is assumed that emergency response and governmental authorities would intervene to impound foodstuffs, provide alternate water supply, and clean up contaminated land.

The population subgroups that are exposed by an accident that results in dispersion of radioactive material include those individuals directly exposed at the accident scene and those individuals within the areas over which dispersion occurs.

D.3.3.2 **Accident Radiological Risk Results**. The radiological risks associated with truck or rail shipping accidents involving CH TRU waste are expressed as a risk per shipment and as a cumulative risk over the shipping campaign relevant to the alternative being considered. The risk is the sum of the products of the probability of a given severity class accident times the consequences of such an accident for each of the severity classes. The radiological risks from an accident carrying CH TRU waste are expressed in equivalent whole body dose and are tabulated in units of person-rem and assume three TRUPACT-IIs per truck shipment and six TRUPACT-IIs per rail shipment. Table D.3.23 presents the risk per shipment for each site shipping CH TRU waste and the total per shipment risk for all sites for truck or rail shipments. Table D.3.24 presents the cumulative risk for all facilities shipping CH TRU waste to WIPP. This table presents radiological accident risks for the proposed action which includes the Test Phase (only CH TRU shipments of 10 percent of the waste by truck mode) and the following Disposal Phase using truck or rail modes and the shipment estimates as shown in Table D.3.2.

No accident radiological risks related to shipment to the WIPP are calculated for the no action alternative because no shipments to the WIPP would occur.

Accident radiological risks for Alternative Action for all truck shipments are the sum of the Test Phase and Disposal Phase risks shown on Table D.3.24. However, these risks are incurred in a continuous 20-year period following a five-year Test Phase during which no waste is shipped to the WIPP but during which approximately seven CH TRU TRUPACT truck shipments from the Rocky Flats Plant to the Idaho National Engineering Laboratory occur to support bin tests. The accident contribution for these shipments is calculated by subtracting the per-shipment accident radiological risks (Table D.3.23) for an Idaho National Engineering Laboratory to WIPP shipment from that for a Rocky

TABLE D.3.23 Per shipment radiological risk of CH TRU waste shipments (person-rem)[a,b,c]

Facility	Nonoccupational Accident Contribution	
	Truck	Rail
Idaho National Engineering Laboratory	7.9×10^{-4}	5.7×10^{-4}
Rocky Flats Plant	2.0×10^{-4}	1.9×10^{-4}
Hanford Reservation	5.6×10^{-4}	9.4×10^{-4}
Savannah River Plant	4.2×10^{-2}	4.0×10^{-2}
Los Alamos National Laboratory	1.2×10^{-3}	[d]
Oak Ridge National Laboratory	5.9×10^{-3}	5.7×10^{-3}
Nevada Test Site	8.9×10^{-6}	[d]
Argonne National Laboratory-East	4.9×10^{-4}	3.5×10^{-4}
Lawrence Livermore National Laboratory	2.1×10^{-3}	3.3×10^{-3}
Mound Laboratory	6.2×10^{-7}	5.4×10^{-7}

[a] Risks per waste shipment are expressed in equivalent whole body dose and are tablulated in units of person-rem

[b] Values for rail are expressed per railcar shipment

[c] Risks per waste shipment are presented as a function of the Transport Index (TI) which is defined as the dose rate in mrem/hr at 1 meter from the waste package

[d] No railheads present

TABLE D.3.24 Lifetime radiological risk for accident transportation of CH TRU waste (person-rems)[a]

	Proposed Action			Alternative Action	
	Test Phase	Disposal Phase (20 yr)		Disposal Phase (20 yr)	
Facility	Truck	Truck	Max. Rail	Truck	Max. Rail
Idaho National Engineering Laboratory	4.9×10^{-1}	4.4	1.6	4.7	1.7
Rocky Flats Plant	1.7×10^{-1}	1.5	7.3×10^{-1}	1.7	8.2×10^{-1}
Hanford Reservation	2.2×10^{-1}	2.0	1.7	2.2	1.7
Savannah River Plant	$1.3 \times 10^{+1}$	$1.2 \times 10^{+2}$	$5.5 \times 10^{+1}$	$1.3 \times 10^{+2}$	$6.2 \times 10^{+1}$
Los Alamos National Laboratory[d]	3.3×10^{-1}	2.1	2.9	3.3	3.3
Oak Ridge National Laboratory	1.7×10^{-1}	1.5	7.3×10^{-1}	1.7	8.1×10^{-1}
Nevada Test Site[d]	1.1×10^{-4}	9.7×10^{-4}	9.7×10^{-4}	1.1×10^{-3}	1.1×10^{-3}
Argonne National Laboratory-East	9.7×10^{-4}	6.8×10^{-3}	2.5×10^{-3}	7.8×10^{-3}	2.2×10^{-3}
Lawrence Livermore National Laboratory	2.3×10^{-1}	2.1	1.6	2.3	1.9
Mound Laboratory	1.0×10^{-5}	9.4×10^{-5}	4.1×10^{-5}	1.0×10^{-4}	4.6
Total	$1.5 \times 10^{+1}$	$1.3 \times 10^{+2}$	$6.4 \times 10^{+1}$	$1.5 \times 10^{+2}$	$7.2 \times 10^{+1}$

[a] Population group risks are calculated by multiplying the risk/shipment identified in Table D.3.21 by the total number of shipments to the WIPP by truck or rail, as determined from the projection in Table Ds.3.2

[b] Test Phase assumes 10% of shipment completed by truck

[c] Nonoccupational population

[d] Waste shipments from this site are limited to truck mode, thus rail risks are the same as truck risks

Flats Plant to WIPP shipment. This difference, which represents the Idaho National Engineering Laboratory to Rocky Flats Plant transportation segment risk, is multiplied by the number of shipments to arrive at the transportation risk for the bin tests. Thus, an accident contribution of approximately 5.90×10^{-4} person-rem is expected due to bin test shipments. Rail accident radiological risks differ between the Proposed Action and Alternative Action as shown on Table D.3.25, which summarizes the differences in CH TRU shipment accident radiological risk for nonoccupational populations between the Proposed Action and Alternative Action.

The radiological risks from an accident involving a truck or railcar carrying RH TRU waste are expressed in equivalent whole body dose and are tabulated in units of person-rem and assume one RH TRU cask per truck shipment and two RH casks per rail shipment. Table D.3.26 presents the risk per shipment for each site shipping RH TRU waste by truck or rail and the total risk for all sites. Table D.3.27 presents the cumulative risk for all sites shipping RH TRU waste to WIPP. These lifetime radiological risks due to accidents involving transportation of RH TRU waste by truck or rail are shown in Table D.3.27 and assume a 20-year shipping period. No RH TRU shipments occur during the Test Phase of the Proposed Action or the Alternative Action; no accident risk contributions result therefore. Radiological risks of RH TRU shipments are identical for the Proposed Action and Alternative Action.

D.3.4 RADIOLOGICAL CONSEQUENCES OF BOUNDING CASE TRANSPORTATION ACCIDENT

D.3.4.1 Assumptions—Bounding Case Accident

As discussed in Section 5.0, a "bounding case" transportation accident scenario was developed for this SEIS. This scenario was used to calculate the impact of a very severe accident in the higher population areas along the WIPP-preferred transportation routes. The postulated accident involved a truck carrying three TRUPACT-II containers. Each is loaded with fourteen 55-gallon Type A drums filled with the mean activity level mix of CH TRU waste originating from the Rocky Flats Plant. The accident is assumed to be of the highest severity category (category eight) and occurs in the urbanized portion of a non-specific large (greater than one million population) urban area. A rail mode bounding case accident scenario (six TRUPACT-IIs) was also assumed as an alternative. Since current shipment plans primarily rely on the truck transportation mode, however, this analysis focuses on the truck mode accident scenario.

During the accident, all TRUPACT-IIs were assumed to be equally breached and subsequently engulfed in fire for two hours (it is estimated that at least 17,000 gallons of fuel would be required to provide sufficient fuel to sustain a two-hour fire). External air/oxygen sources were assumed to be limited (internal combustion is limited) since a major breach of the Type B TRUPACT-II transporters is not credible. Radioactive contamination and hazardous chemicals were assumed to be evenly distributed throughout the waste volume and 0.02% of the hazardous and radioactive particulate materials were postulated to be released in a respirable form (less than ten micron particle size). The accident was assumed to occur during a period having very stable

TABLE D.3.25 Summary of lifetime radiological risk changes between Proposed Action and Alternative Action: CH TRU accident nonoccupational risk (person-rems)

	Proposed action		Alternative Action	
Facility	Truck	Rail	Truck	Rail
Idaho National Engineering Laboratory	3.2	3.2	3.3	3.3
Rocky Flats Plant	1.0×10^{-4}	5.1×10^{-5}	1.0×10^{-4}	4.6×10^{-5}
Hanford Reservation	4.9	2.1	4.9	1.7
Savannah River Plant	1.7	9.0×10^{-1}	1.7	8.2×10^{-1}
Los Alamos National Laboratory	1.7	9.0×10^{-1}	1.7	8.1^{-1}
Oak Ridge National Laboratory	2.3	1.8	2.3	1.8
Nevada Test Site	7.3×10^{-3}	3.5×10^{-3}	7.8×10^{-3}	2.8×10^{-3}
Argonne National Laboratory-East	2.2	1.9	2.2	1.9
Lawrence Livermore National Laboratory	$1.3 \times 10^{+2}$	$6.8 \times 10^{+1}$	$1.3 \times 10^{+2}$	$6.2 \times 10^{+1}$
Mound Laboratory	1.1×10^{-3}	1.1×10^{-3}	1.1×10^{-3}	1.1×10^{-3}
Total	$1.5 \times 10^{+2}$	$7.9 \times 10^{+1}$	$1.5 \times 10^{+2}$	$7.2 \times 10^{+1}$

TABLE D.3.26 Per shipment radiological risk of RH TRU shipments (person-rem)[a,b,c]

Facility	Nonoccupational Accident Contribution	
	Truck	Rail
Idaho National Engineering Laboratory	1.8×10^{-6}	1.5×10^{-6}
Hanford Reservation	6.2×10^{-2}	6.3×10^{-2}
Los Alamos National Laboratory	4.4×10^{-6}	[d]
Oak Ridge National Laboratory	5.9×10^{-6}	6.4×10^{-6}
Argonne National Laboratory-East	6.4×10^{-6}	5.2×10^{-6}

[a] Risks per waste shipment are expressed in equivalent whole body dose and are tablulated in units of person-rem

[b] Values for rail are expressed per railcar shipment

[c] Risks per waste shipment are presented as a function of the Transport Index (TI) which is defined as the dose rate in mrem/hr at 1 meter from the waste package. Calculations are based on three TRUPACT-II waste packages per truck and six per railcar shipment

[d] No railheads present

TABLE D.3.27 Lifetime radiological risk for accidents during transportation of RH TRU waste (person-rems): Proposed Action and Alternative Action

Facility	100% truck	Maximum rail
Idaho National Engineering Laboratory	3.4×10^{-4}	1.4×10^{-4}
Hanford Reservation	$5.8 \times 10^{+1}$	$2.9 \times 10^{+1}$
Los Alamos National Laboratory	1.7×10^{-4}	1.7×10^{-4}
Oak Ridge National Laboratory	4.0×10^{-2}	5.7×10^{-3}
Argonne National Laboratory-East	5.8×10^{-5}	2.6×10^{-5}
Total	$5.8 \times 10^{+1}$	$2.9 \times 10^{+1}$

[a] Population group risks are calculated by multiplying the risk/shipment identified in Table D.3.21 by the total number of shipments to WIPP by truck or rail, as determined from the projection in Table D.3.2. Rail occupational risks resulting from normal transportation include the impact of inspection activities.

[b] No RH shipments assusmed during Test Phase

[c] Nonoccupational populations

[d] Waste shipments from the site are limited to truck mode. Rail risks are thus the same as the truck risks

atmospheric meteorological conditions, as stable meteorological conditions limit dispersion or breakup of the plume and tend to maximize radiation doses and hazardous chemical concentrations.

The accident risk analysis method discussed in Subsections D.3.1 and D.3.2 relies on the probabilistic approach in RADTRAN to determine cumulative risks of a series of increasingly less probable but more severe accident scenarios. To determine the accident consequences of this "bounding case" accident scenario, a probability of 100 percent was specified. The specific conditions assumed for this bounding case accident (CH TRU truck shipment) are summarized in Table D.3.28. The "bounding case accident" scenario has an extremely low likelihood of occurring.

The probability of breaching all three TRUPACT-IIs (in a truck accident scenario) or all six TRUPACT-IIs (in a rail accident scenario) and engulfing them in a two hour fire (requiring the fuel equivalent of two fully-loaded fuel transports) in an urban area during adverse meteorological conditions is very small. The probability would be a small fraction of the fraction, $0.05 \times 1.5 \times 10^{-5}$ for a truck shipment or a small fraction of $0.05 \times 1.0 \times 10^{-5}$ for a rail shipment (Tables D.3.15 and D.3.16). Additional conservatism in the analysis included the use of a range population densities higher than currently exist along most WIPP transportation corridors, including Atlanta, Georgia; Denver, Colorado; and Albuquerque, New Mexico.

These conditions were input to the RADTRAN computer code to determine radiological consequences of this bounding case. These radiological consequences measure the potential to cause immediate and delayed health effects on the affected population including early fatalities, early morbidities, latent cancer fatalities, and genetic effects from the inhalation, resuspension, groundshine, and cloudshine of the aerosol cloud of the released radionuclides.

D.3.4.2 Results—Bounding Case Accident

The RADTRAN computer code was used to predict the consequences of the upper bounding case accident scenario. As previously discussed, health impacts may result from external exposure (e.g., cloudshine, groundshine) and internal exposure (e.g., inhalation, resuspension, and ingestion) to the dispersed radioactive material. Since it is assumed that the accident occurs within an urban area, ingestion impacts associated with contamination of agricultural products were not applicable and were ignored.

The analysis assumed that stable to extremely stable atmospheric conditions predominated. This assumption conservatively predicted high airborne radioactive contaminant concentrations and limited the dispersion of the contaminants to outlying areas. In an urban area, surface irregularities and thermal anomalies will tend to preclude the probability of a prevailing stable atmospheric condition.

The analysis predicted that no early fatalities or early morbidities would result. The collective population committed effective dose equivalent (CEDE) was estimated to be 1,240 mrem, which includes the continuing exposure from resuspended radioactive material for a period of fifty years following the accident.

TABLE D.3.28 Bounding case accident scenario assumptions

The waste shipment is assumed to be three fully-loaded TRUPACT-II transporters on a tractor-trailer combination vehicle from the Rocky Flats Plant, containing three times 14 or 42 55-gallon drums of CH TRU waste with the following radionuclides, plutonium 238, plutonium 239, plutonium 240, plutonium 241, and americium 241.

All waste is packaged in Type A drums.

A major breach of any of the three Type B TRUPACT transporters that compose a trailer-load CH TRU shipment is not credible, limiting external air/oxygen sources.

Loss of packaging containment will result in .0002 fraction of the radioactive waste material in the three TRUPACTs being released to the environment in a respirable form. These respirable materials are airborne particulates and aerosols, which are all less than 10 microns aerodynamic diameter in size.

Radioactive contamination is evenly distributed throughout the waste volume.

The highest accident severity category, category eight, is assumed, with a fire duration of two hours.

All three TRUPACTs on the trailer are equally breached.

The accident occurs in the urbanized portion of a non-specific large (greater than one million population) metropolitan area with a mean population density of 3,861 persons per km^2 in the subarea immediately surrounding the accident site.

An aerosol cloud of respirable radionuclides is dispersed downwind in an elliptical pattern with a Gaussian distribution rate of concentration diffusion.

Inhalation of the initially dispersed and subsequently resuspended radionuclide particulates was the primary exposure pathway to the public. Inhalation of resuspended particulates accounts for 82 percent of the total collective CEDE.

The CEDE received by a hypothetical, maximally exposed individual was estimated to be 0.0879 rem, which is from the initial inhalation of the cloud contaminants resulting from the accident. This assumed that the individual was present for the full duration of the time required for the cloud of contaminants to pass overhead. This individual would receive an additional exposure of 0.398 rem for a total exposure of 0.486 rem, if he/she continued to reside in the area for fifty years. This additional exposure resulted from the inhalation of particulates released from the original accident that have been deposited on the ground and buildings and then resuspended later as airborne particulates. An average resident was estimated to receive a CEDE of 0.0774 rem. This assumed that this resident continued to live within the affected area for the remainder of his/her lifetime (fifty years) and included the exposure from inhalation of resuspended particulates.

For a bounding case accident scenario assuming a rail shipment of Rocky Flats Plant CH TRU waste with six loaded TRUPACT-IIs that are breached, the radiological consequences would be doubled. Bounding case accident scenarios for truck and rail shipments of mean activity level RH TRU waste from Idaho National Engineering Laboratory resulted in much lower impacts than the CH TRU truck shipment accident scenario, because of the much smaller volume of waste per shipment. Thus, the RH TRU truck mode and RH TRU rail mode accident scenarios were discarded from further consideration as a maximum bounding case.

D.4 NONRADIOLOGICAL AND NONCHEMICAL CONSEQUENCES OF TRANSPORTATION

D.4.1 INTRODUCTION

The nonradiological and nonchemical consequences of transportation of radioactive waste to the WIPP are discussed in this subsection. These nonradiological and nonchemical impacts are the same as those resulting from transporting non-nuclear materials. In other words, nonradiological and nonchemical impacts do not consider the characteristics of the cargo.

There are two types of nonradiological and nonchemical risks associated with projected TRU waste shipments to WIPP. They are normal (i.e., incident-free) risks and accident condition risks. The normal risks include the health risks in urban areas caused by the generation of nonradiological air pollutants by the carrier vehicles during waste shipments. The accident condition risks include the risks of injuries and fatalities from shipments that are totally unrelated to radiological and hazardous chemical risks resulting from projected accidents.

D.4.2 METHOD

Risks were calculated on a per shipment basis and a cumulative basis. Estimates of per shipment risk included the probability of adverse urban area pollutant health effects and accident related injuries and fatalities of a single TRU waste shipment (round trip) to the WIPP. Cumulative risk estimates were determined by multiplying per shipment risks by average annual shipments for the initial five-year Test Phase and for the approximate 20-year Disposal Phase of the WIPP. The estimated total number of shipments, both truck and rail are summarized in Table D.4.1.

The average distance and population zone fraction from Table D.4.2 are used with Table D.4.3 (Air Pollutant Unit Consequence Factors) and Table D.4.4 (Nonradiological and Nonchemical Unit Risk Factors) to calculate the per shipment nonradiological and nonchemical risk of CH TRU and RH TRU waste shipments from each facility for truck and rail alternatives. The air pollutant unit consequence factors represent the estimated additional urban area health effects from particulates and sulfur dioxide truck diesel or locomotive diesel emissions generated by the truck or locomotive during a shipment.

D.4.3 RESULTS

Calculated per shipment nonradiological and nonchemical risks for CH TRU and RH TRU shipments to WIPP are summarized in Table D.4.5. These risks include the impact of the return trip by either truck or rail from the WIPP to the generator or storage facility.

TABLE D.4.1 Estimated CH TRU and RH TRU waste shipments from generating and storage sites to the WIPP

CH TRU

Facility	Total Shipments[a] Truck	Rail
Idaho National Engineering Laboratory	6,162	3,081
Rocky Flats Plant	8,586	4,293
Hanford Reservation	3,939	1,970
Savannah River Plant	3,116	1,558
Los Alamos National Laboratory	2,703	2,703
Oak Ridge National Laboratory	286	143
Nevada Test Site	121	121
Argonne National Laboratory - East	16	8
Lawrence Livermore National Laboratory	1,093	547
Mound	169	85
Total	26,191	14,509

RH TRU

Facility	Total Shipments[a] Truck	Rail
Idaho National Engineering Laboratory	187	94
Hanford Reservation	937	467
Los Alamos National Laboratory	39	39
Oak Ridge National Laboratory	6,781	3,391
Argonne National Laboratory - East	9	5
Total	7,953	3,996

[a] Estimates from Draft Addendum to the Transuranic Assessment and Guidance Report, November 1988, by WEC-WIPP, based on 2.8 cubic meters/TRUPACT and three TRUPACTs per truck shipment and six TRUPACTs per railcar shipment.

[b] Estimates from Draft Addendum to the Transuranic Assessment and Guidance Report, November 1988, by WEC-WIPP, based on .89 cubic meter/RH-cask and one RH-cask per truck shipment and two RH-casks per railcar shipment.

TABLE D.4.2 Average distances to the WIPP and percent of travel in various population zones[a]

	Average distance	Population zone		
	Miles	R	S	U
Truck				
Idaho National Engineering Laboratory	1521	85.0	13.8	1.2
Rocky Flats Plant	874	82.3	15.7	2.0
Hanford Reservation	1913	85.7	13.4	0.9
Savannah River Plant	1585	74.3	25.1	0.6
Los Alamos National Laboratory	343	90.1	9.9	0.0
Oak Ridge National Laboratory	1350	78.6	20.7	0.7
Nevada Test Site	1286	86.8	11.2	2.0
Argonne National Laboratory-East	1387	78.1	21.8	0.1
Lawrence Livermore National Laboratory	1458	86.2	10.1	3.7
Mound Laboratory	1472	75.4	24.1	0.5
Rail				
Idaho National Engineering Laboratory	1761	89.5	9.8	0.7
Rocky Flats Plant	1098	86.7	11.6	1.7
Hanford Reservation	2296	87.8	11.5	0.7
Savannah River Plant	1915	76.0	22.4	1.6
Oak ridge National Laboratory	1630	79.8	18.9	1.3
Argonne National Laboratory-East	1469	81.6	17.0	1.4
Lawrence Livermore National laboratory	1873	85.0	14.3	0.8
Mound Laboratory	1677	76.8	21.3	1.9

[a] Mean population densities are utilized and correspond to:
R = Rural (6 persons/km^2)
S = Suburban (719 persons/km^2)
U = Urban (3861 persons/km^2)

Source: Madsen et al., 1983

TABLE D.4.3 Air pollutant unit consequence factors[a]

Source	Health Effects per Kilometer	
	Truck (LCF/Km)	Rail (LCF/Km)
Pollutants (Particulates & sulfur dioxide)	1.0×10^{-7} (urban travel only)	1.3×10^{-7} (urban travel only)

TABLE D.4.4 Nonradiological and nonchemical unit risk factors[a]

Mode	Zone	LCF/Km[a]	Injuries/Km[b]	Fatalities/Km[b]
Truck	Rural	0	8.28×10^{-7}	6.80×10^{-8}
	Suburban	0	3.83×10^{-7}	1.67×10^{-8}
	Urban	1.0×10^{-7}	3.83×10^{-7}	9.60×10^{-8}
Rail	Rural	0	2.97×10^{-7}	2.82×10^{-8}
	Suburban	0	2.97×10^{-7}	2.82×10^{-8}
	Urban	1.3×10^{-7}	2.97×10^{-7}	2.82×10^{-7}

LCF - Latent Cancer Fatalities

Sources:

[a] Rao, Ramana K., Edwin L. Wilmont, and Robert E. Luna, 1982. Nonradiological Impacts of Transporting Radioactive Material. SAND 81-1703, TTC-0236, Albuquerque, NM: Sandia National Laboratories.

[b] Cashwell, Jon W., et. al., 1986, Transportation Impacts of the Commercial RAdioactive Waste Management, Appendix 4, Tables 4-4A and 4-4B. SAND 85-2715, TTC-0663, Albuquerque, NM: Sandia National Laboratories. Nonradiological unit risk factors determined from US Dept. of Transportation, Research and Special Programs Administration, Transportation Systems Center, 1986, National Transportation Statistics, Annual Report, 1986, Report No. DOT-TSC-RSPA-86-3, "Truck Profile, Heavy Truck Category" and "Rail Profile, Class I Railroads Category," for 1983 and 1984 calendar year

TABLE D.4.5 Per shipment nonradiological risk of waste shipments (a)

		Truck			Rail		
		Normal transportation	Accident Case		Normal transportation	Accident Case	
Facility	Zone	LCF(c)	Fatalities	Injuries	LCF(c)	Fatalities	Injuries
INEL	Rural	0.00E+00	2.83E-04	3.44E-03	0.00E+00	1.43E-04	1.51E-03
	Suburban	0.00E+00	1.13E-05	2.59E-04	0.00E+00	1.57E-05	1.65E-04
	Urban	5.87E-06	5.64E-07	2.25E-05	5.16E-06	1.12E-06	1.18E-05
RFP	Rural	0.00E+00	1.57E-04	1.92E-03	0.00E+00	8.64E-05	9.09E-04
	Suburban	0.00E+00	7.38E-06	1.69E-04	0.00E+00	1.16E-05	1.22E-04
	Urban	5.63E-06	5.40E-07	2.16E-05	7.81E-06	1.69E-06	1.78E-05
HANF	Rural	0.00E+00	3.59E-04	4.37E-03	0.00E+00	1.83E-04	1.93E-03
	Suburban	0.00E+00	1.38E-05	3.16E-04	0.00E+00	2.40E-05	2.52E-04
	Urban	5.54E-06	5.32E-07	2.12E-05	6.72E-06	1.46E-04	1.54E-05
SRP	Rural	0.00E+00	2.58E-04	3.14E-03	0.00E+00	1.32E-04	1.39E-03
	Suburban	0.00E+00	2.14E-05	4.90E-04	0.00E+00	3.89E-05	4.10E-04
	Urban	3.06E-06	2.94E-07	1.17E-05	1.28E-05	2.78E-06	2.93E-05
LANL	Rural		6.76E-05	8.24E-04			
	Suburban	(d)	1.83E-06	4.19E-05	(e)	(e)	(e)
	Urban		0.00E+00	0.00E+00			
ORNL	Rural	0.00E+00	2.32E-04	3.83E-03	0.00E+00	1.18E-04	1.24E-03
	Suburban	0.00E+00	1.50E-05	3.44E-04	0.00E+00	2.80E-05	2.94E-04
	Urban	3.04E-05	2.94E-07	1.16E-05	8.87E-06	1.94E-06	2.03E-05
NTS	Rural	0.00E+00	2.44E-04	2.94E-03			
	Suburban	0.00E+00	7.74E-06	1.78E-04	(e)	(e)	(e)
	Urban	8.28E-07	7.94E-08	3.17E-06			
ANLE	Rural	0.00E+00	2.37E-04	2.89E-03	0.00E+00	1.09E-04	1.15E-03
	Suburban	0.00E+00	8.12E-06	3.73E-04	0.00E+00	2.27E-05	2.39E-04
	Urban	4.46E-07	4.28E+08	1.71E-06	8.60E-06	1.87E-06	1.97E-05
LLNL	Rural	0.00E+00	2.75E-04	3.35E-03	0.00E+00	1.44E-04	1.52E-03
	Suburban	0.00E+00	7.91E-05	1.82E-04	0.00E+00	2.43E-05	2.56E-04
	Urban	1.74E-05	1.67E-06	6.65E-05	5.49E-06	1.19E-06	1.25E-05
Mound	Rural	0.00E+00	2.75E-04	3.35E-03	0.00E+00	1.17E-04	1.52E-03
	Suburban	0.00E+00	1.91E-05	4.37E-04	0.00E+00	3.24E-05	3.41E-04
	Urban	2.37E-06	2.27E-07	4.53E-06	1.33E-05	2.89E-06	3.05E-05

(a) units are expressed in scientific notation 4.41-05 = 4.10×10^{-5}

Each travel mode alternative assumes the uniform maximum use of that mode by all sites. Therefore, the mode alternatives are labeled as 100 percent truck and maximum rail for those sites that have access to rail. Los Alamos National Laboratory and the Nevada Test Site do not have access to rail, and thus, they are listed with the maximum rail results for the purpose of cumulative risk.

The results show very small per shipment nonradiological and nonchemical risks for all facilities. The volumes of particulates and sulfur dioxide emitted by a single truck or rail shipment in an urban area is so small that one million or more similar pollutant generating shipments would be needed simultaneously for it to achieve the minimum required pollutant volume of particulates and sulfur dioxide to cause one latent cancer fatality (LCF). Assuming normalized odds, the probability of causing one injury from a traffic accident from a single shipment ranges from 1.7×10^{-6} to 4.4×10^{-3}. The probability of causing one fatality from a traffic accident ranges from 4.3×10^{-8} to 3.6×10^{-4}.

Calculated average annual nonradiological and nonchemical CH TRU shipment risks are summarized in Tables D.4.6 and D.4.7 for the Test Phase and 20-year Disposal Phase at the WIPP. Tables D.4.8 through D.4.11 summarized the corresponding results for Alternative Action.

Total individual site risks were calculated for the following 20 year in a like manner, multiplying the per shipment risk by total shipments for both truck and rail. For both the initial five-year Test Phase and the following Disposal Phase the results show that from very conservative assumptions of travel conditions, the resulting average annual nonradiological and nonchemical impacts to the affected population along the shipment routes to the WIPP are very small, reflecting the same small magnitude of transportation risk associated with any like number of shipments per kilometers of travel for regular nonradioactive goods.

Considering the systemwide total nonradiological and nonchemical risk totals for either truck or rail during the Test Phase as shown in Tables D.4.6 and D.4.7, it is estimated as a bounding condition that there would be approximately 79 injuries for the 100 percent truck mode and approximately 27 injuries for the maximum rail mode. Summing all risks for the Test Phase plus the Disposal Phase, one would expect approximately 7 fatalities for the CH truck mode and 2 fatalities for the maximum rail case. For the Alternative Action, approximately 6.1 fatalities and 79 injuries would occur from the shipment of CH TRU waste by truck to the WIPP. For shipping by rail for the Alternative Action, approximately 2 fatalities and 21 injuries would occur. For RH TRU truck shipments, approximately 2 fatalities and 27 injuries are estimated to occur. Slightly less than one fatality and 6.5 injuries would be estimated to occur from shipping RH TRU waste by rail.

TABLE D.4.6 Total transportation risk for proposed action alternative, CH truck mode

Facility	Zone	Test Phase[a] Number of shipments	Test Phase[a] Normal transportation LCFs	Test Phase[a] Accident Case Fatalities	Test Phase[a] Accident Case Injuries	Disposal Phase[b] Number of shipments	Disposal Phase[b] Normal transportation LCFs	Disposal Phase[b] Accident case Fatalities	Disposal Phase[b] Accident case Injuries
INEL	Rural	617	0	1.7×10^{-1}	2.1×10^{0}	5,545	0	1.6×10^{0}	1.9×10^{1}
	Suburban		0	7.0×10^{-3}	1.6×10^{-1}		0	6.3×10^{-2}	1.4×10^{0}
	Urban		3.6×10^{-3}	3.5×10^{-4}	1.4×10^{-2}		3.3×10^{-2}	3.1×10^{-3}	1.2×10^{-1}
RFP	Rural	859	0	1.3×10^{-1}	1.6×10^{0}	7,727	0	1.2×10^{0}	1.5×10^{1}
	Suburban		0	6.3×10^{-3}	1.5×10^{-1}		0	5.7×10^{-2}	1.3×10^{0}
	Urban		4.8×10^{-3}	4.6×10^{-4}	1.9×10^{-2}		4.4×10^{-2}	4.2×10^{-3}	1.7×10^{-1}
HANF	Rural	394	0	1.4×10^{-1}	1.7×10^{0}	3,545	0	1.3×10^{0}	1.5×10^{1}
	Suburban		0	5.4×10^{-3}	1.2×10^{-1}		0	4.9×10^{-2}	1.1×10^{0}
	Urban		2.2×10^{-3}	2.1×10^{-4}	8.4×10^{-4}		2.0×10^{-2}	1.9×10^{-3}	7.5×10^{-2}
SRP	Rural	312	0	8.0×10^{-2}	9.8×10^{-1}	2,804	0	7.2×10^{-1}	8.8×10^{0}
	Suburban		0	6.7×10^{-3}	1.5×10^{-1}		0	6.0×10^{-2}	1.4×10^{0}
	Urban		9.5×10^{-4}	9.2×10^{-5}	3.7×10^{-3}		8.6×10^{-3}	8.2×10^{-4}	3.3×10^{-2}
LANL	Rural	270		1.8×10^{-2}	2.2×10^{-1}	2,433		1.6×10^{-1}	2.0×10^{-1}
	Suburban			4.9×10^{-4}	1.1×10^{-2}			4.5×10^{-3}	1.0×10^{-2}
	Urban			0	0			0	0
ORNL	Rural	29	0	6.7×10^{-3}	8.2×10^{-2}	257	0	6.0×10^{-2}	7.3×10^{-1}
	Suburban		0	4.4×10^{-4}	1.0×10^{-3}		0	3.9×10^{-3}	8.8×10^{-2}
	Urban		8.8×10^{-5}	8.5×10^{-6}	3.4×10^{-4}		7.8×10^{-4}	7.5×10^{-5}	3.0×10^{-3}

TABLE D.4.6 Concluded

Facility	Zone	Test Phase[a] Number of shipments	Test Phase[a] Normal transportation LCFs	Test Phase[a] Accident case Fatalities	Test Phase[a] Accident case Injuries	Disposal Phase[b] Number of shipments	Disposal Phase[b] Normal transportation LCFs	Disposal Phase[b] Accident case Fatalities	Disposal Phase[b] Accident case Injuries
NTS	Rural	12	0	2.9×10^{-3}	3.6×10^{-2}	109	0	2.7×10^{-2}	3.2×10^{-2}
	Suburban		0	9.3×10^{-5}	2.1×10^{-3}		0	8.4×10^{-4}	1.9×10^{-3}
	Urban		9.9×10^{-6}	9.5×10^{-7}	3.8×10^{-5}		9.0×10^{-6}	8.7×10^{-6}	3.5×10^{-5}
ANLE	Rural	2	0	$4.7 \times 10^{-4,c}$	5.8×10^{-3}	14	0	3.3×10^{-3}	4.0×10^{-2}
	Suburban		0	1.6×10^{-5}	7.5×10^{-4}		0	1.1×10^{-4}	5.2×10^{-3}
	Urban		8.9×10^{-7}	8.6×10^{-8}	3.4×10^{-6}		6.2×10^{-6}	6.0×10^{-7}	2.4×10^{-5}
LLNL	Rural	109	0	3.0×10^{-2}	3.7×10^{-1}	984	0	2.7×10^{-1}	3.3
	Suburban		0	8.6×10^{-4}	2.0×10^{-2}		0	7.8×10^{-3}	1.8×10^{-1}
	Urban		1.9×10^{-3}	1.8×10^{-4}	7.2×10^{-3}		1.7×10^{-2}	1.6×10^{-3}	6.5×10^{-2}
Mound	Rural	17	0	4.1×10^{-3}	5.0×10^{-2}	152	0	3.7×10^{-2}	4.5×10^{-1}
	Suburban		0	3.2×10^{-4}	7.4×10^{-3}		0	2.9×10^{-3}	6.6×10^{-2}
	Urban		4.0×10^{-5}	3.9×10^{-6}	7.7×10^{-5}		3.6×10^{-4}	3.5×10^{-5}	6.9×10^{-4}
Total		2621	1.4×10^{-2}	6.1×10^{-1}	7.8×10^{0}	23570	1.2×10^{-1}	5.6×10^{0}	7.1×10^{1}

[a] The Test Phase assumes a five-year time frame and 10% waste implacement and shipment for the Test Phase.

[b] Operation assumes 20 years of rail shipment

[c] Numbers are expressed in scientific notation, 8.92x10-7 = 0.000000892.

TABLE D.4.7 Total transportation risk for proposed action alternative, CH rail mode

Facility	Zone	Test Phase[a] Number of shipments	Test Phase[a] Normal transportation LCFs	Test Phase[a] Accident case Fatalities	Test Phase[a] Accident case Injuries	Disposal Phase[b] Number of shipments	Disposal Phase[b] Normal transportation LCFs	Disposal Phase[b] Accident case Fatalities	Disposal Phase[b] Accident case Injuries
INEL	Rural	617	0	1.3×10^{-1}	2.1×10^{0}	2773	0	4.0×10^{-1}	4.2×10^{0}
	Suburban		0	7.0×10^{-4}	1.6×10^{-1}		0	4.4×10^{-2}	4.6×10^{-1}
	Urban		3.6×10^{-3}	2.6×10^{-4}	1.4×10^{-2}		1.5×10^{-2}	3.1×10^{-3}	3.3×10^{-2}
RFP	Rural	859	0	1.3×10^{-1}	1.6×10^{0}	3864	0	3.3×10^{-1}	3.5×10^{0}
	Suburban		0	6.3×10^{-3}	1.5×10^{-1}		0	4.5×10^{-2}	4.7×10^{-1}
	Urban		4.8×10^{-3}	4.6×10^{-4}	1.9×10^{-2}		3.0×10^{-2}	6.5×10^{-3}	6.9×10^{-2}
HANF	Rural	394	0	1.3×10^{-1}	1.7×10^{0}	1773	0	3.2×10^{-1}	3.4×10^{0}
	Suburban		0	5.4×10^{-3}	1.1×10^{-1}		0	4.3×10^{-2}	4.5×10^{-1}
	Urban		2.2×10^{-3}	1.9×10^{-4}	8.4×10^{-4}		1.2×10^{-2}	2.6×10^{-3}	2.7×10^{-2}
SRP	Rural	312	0	7.7×10^{-2}	9.8×10^{-1}	1402	0	1.9×10^{-1}	1.9×10^{0}
	Suburban		0	6.4×10^{-3}	1.5×10^{-1}		0	5.5×10^{-2}	5.7×10^{-1}
	Urban		9.5×10^{-4}	8.8×10^{-2}	3.7×10^{-3}		1.8×10^{-2}	3.9×10^{-3}	4.1×10^{-2}
LANL	Rural	270		1.6×10^{-2}	2.2×10^{-1}	2433		1.6×10^{-1}	2.0×10^{0}
	Suburban		[g]	4.3×10^{-4}	1.1×10^{-2}		[f]	4.5×10^{-3}	1.0×10^{-1}
	Urban			0	0			0	0
ORNL	Rural	29	0	6.0×10^{-3}	8.2×10^{-2}	129	0	1.5×10^{-2}	1.6×10^{-1}
	Suburban		0	3.9×10^{-4}	1.0×10^{-2}		0	3.6×10^{-3}	3.8×10^{-2}
	Urban		8.8×10^{-5}	7.6×10^{-6}	3.4×10^{-4}		1.1×10^{-3}	2.5×10^{-4}	2.6×10^{-3}

TABLE D.4.7 Concluded

Site	Zone	Test Phase[a] Number of Shipments	Test Phase[a] Normal transportation LCFs	Test Phase[a] Accident Case Fatalities	Test Phase[a] Accident Case Injuries	Disposal Phase[b] Number of Shipments	Disposal Phase[b] Normal transportation LCFs	Disposal Phase[b] Accident Case Fatalities	Disposal Phase[b] Accident Case Injuries
NTS	Rural	12	0	2.9×10^{-3}	3.6×10^{-2}	109	0	2.7×10^{-2}	3.2×10^{-1}
	Suburban		0	9.3×10^{-5}	2.1×10^{-3}		0	4.7×10^{-4}	2.0×10^{-2}
	Urban		9.9×10^{-6}	9.5×10^{-7}	3.8×10^{-5}		9.0×10^{-6}	8.7×10^{-6}	3.5×10^{-4}
ANLE	Rural	2	0	4.7×10^{-4}	5.8×10^{-3}	7	0	7.6×10^{-4}	8.1×10^{-3}
	Suburban		0	1.5×10^{-5}	7.5×10^{-4}		0	1.6×10^{-4}	1.7×10^{-3}
	Urban		8.9×10^{-7}	8.6×10^{-8}	3.4×10^{-6}		6.0×10^{-5}	1.3×10^{-5}	1.4×10^{-4}
LLNL	Rural	109	0	3.0×10^{-2}	3.7×10^{-1}	492	0	7.1×10^{-2}	7.5×10^{-1}
	Suburban		0	8.6×10^{-4}	2.0×10^{-2}		0	1.2×10^{-2}	1.3×10^{-1}
	Urban		1.9×10^{-3}	1.8×10^{-4}	7.3×10^{-3}		2.7×10^{-3}	5.9×10^{-4}	6.2×10^{-3}
Mound	Rural	17	0	4.1×10^{-3}	5.0×10^{-2}	76	0	8.9×10^{-3}	9.3×10^{-2}
	Suburban		0	3.2×10^{-4}	7.4×10^{-3}		0	2.5×10^{-3}	2.6×10^{-2}
	Urban		4.0×10^{-5}	3.9×10^{-6}	7.7×10^{-5}		1.0×10^{-3}	2.2×10^{-4}	2.3×10^{-3}
Total		2,621	1.4×10^{-2}	6.1×10^{-1}	7.8	13,098	7.9×10^{-2}	1.8×10^{0}	1.9×10^{1}

[a] The Test Phase assures a five-year time frame and 10% waste implacement shipment for the Test Phase.

[b] Disposal Phase assumes 20 years of rail shipment

[c] Numbers are expressed in scientific notation 8.92x10-7 = 0.000000892.

TABLE D.4.8 Total transportation risk for alternative action, CH truck mode (a)

Facility	Zone	No. of shipments	Normal transportation LCFs	Accident Fatalities	Accident Injuries
INEL	Rural	6,162	0.0E+00	1.7E+00	2.1E+01
	Suburban		0.0E+00	7.0E-02	1.6E+00
	Urban		3.6E-02	3.5E-03	1.4E-01
RFP	Rural	8,586	0.0E+00	1.3E+00	1.7E+01
	Suburban		0.0E+00	6.3E-02	1.5E+00
	Urban		4.8E-02	4.6E-03	1.9E-01
HANF	Rural	3,939	0.0E+00	1.4E+00	1.7E+01
	Suburban		0.0E+00	5.4E+02	1.2E+00
	Urban		2.2E-02	2.1E-03	8.4E-02
SRP	Rural	3,116	0.0E+00	8.0E-01	9.8E+00
	Suburban		0.0E+00	6.7E-02	1.5E+00
	Urban		9.5E-03	9.2E-04	3.7E-02
LANL(b)	Rural	2,703		1.8E-01	2.2E+00
	Suburban		(c)	5.0E-03	1.1E-01
	Urban			0.0E+00	0.0E+00
ORNL	Rural	286	0.0E+00	6.6E-02	8.1E-01
	Suburban		0.0E+00	4.3E-03	9.8E-02
	Urban		8.7E-04	8.4E-05	3.3E-03
NTS	Rural	121	0.0E+00	3.0E-02	3.6E-01
	Suburban		0.0E+00	9.4E-04	2.2E-02
	Urban		1.0E-04	9.6E-06	3.8E-04
ANLE	Rural	16	0.0E+00	3.8E-03 (a)	4.6E-02
	Suburban		0.0E+00	1.3E-04	6.0E-03
	Urban		7.1E-06	6.9E-07	2.7E-05
LLNL	Rural	1,093	0.0E+00	3.0E-01	3.7E+00
	Suburban		0.0E+00	8.7E-03	2.0E-01
	Urban		1.9E-02	1.8E-03	7.3E-02
MOUND	Rural	169	0.0E+00	4.1E-02	5.0E-01
	Suburban		0.0E+00	3.2E-03	7.4E-02
	Urban		4.0E-04	3.8E-05	7.7E-04
	Total	26,191	1.4E-01	6.1E+00	7.9E+01

(a) units are expressed in scientific notation 1.4-01 = $4.10 \times 10^{-1} = 0.14$

TABLE D.4.9 Total transportation risk for alternative action, CH rail mode (a)

Facility	Zone	No. of shipments	Normal transportation LCFs	Accident Fatalities	Accident Injuries
INEL	Rural	3,081	0.0E+00	4.4E-01	4.7E+00
	Suburban		0.0E+00	4.8E-02	5.1E-01
	Urban		1.6E-02	3.5E-03	3.6E-02
RFP	Rural	4,293	0.0E+00	3.7E-01	3.9E+00
	Suburban		0.0E+00	5.0E-02	5.2E-01
	Urban		3.4E-02	7.3E-03	7.6E-02
HANF	Rural	1.970	0.0E+00	3.6E-01	3.8E+00
	Suburban		0.0E+00	4.7E-02	5.0E-01
	Urban		1.3E-02	2.9E-03	3.0E-02
SRP	Rural	1,558	0.0E+00	2.1E-01	2.2E+00
	Suburban		0.0E+00	6.1E-02	6.4E+00
	Urban		2.0E-02	4.3E-03	4.6E-02
LANL(b)	Rural	2,703		1.8E-01	2.2E+00
	Suburban		(c)	5.0E-03	1.1E-01
	Urban			0.0E+00	0.0E+00
ORNL	Rural	143	0.0E+00	1.7E-02	1.8E-01
	Suburban		0.0E+00	4.0E-02	4.2E-02
	Urban		1.3E-03	2.8E-04	2.9E-03
NTS	Rural	121	0.0E+00	3.0E-02	3.6E-01
	Suburban		0.0E+00	9.4E-04	2.2E-02
	Urban		1.0E-04	9.6E-06	3.8E-04
ANLE	Rural	8	0.0E+00	8.7E-04 (a)	9.2E-03
	Suburban		0.0E+00	1.8E-04	1.9E-03
	Urban		6.9E-05	1.5E-05	1.6E-04
LLNL	Rural	547	0.0E+00	7.9E-02	8.3E-01
	Suburban		0.0E+00	1.3E-02	1.4E-01
	Urban		3.0E-03	6.5E-04	6.8E-03
MOUND	Rural	85	0.0E+00	1.0E-02	1.1E-01
	Suburban		0.0E+00	2.8E-03	2.9E-02
	Urban		1.1E-03	2.5E-04	2.6E-03
	Total	14,509	8.8E-02	2.0E+00	2.1E+01

(a) units are expressed in scientific notation 8.8E-02 = $8.8 \times 10^{-2} = 0.088$

TABLE D.4.10 Total transportation risk for proposed action and the alterntive action, RH truck mode (a)

Facility	Zone	No. of shipments	Normal transportation LCFs	Accident Fatalities	Accident Injuries
INEL	Rural	187	0.0E+00	5.3E-02	6.4E-01
	Suburban		0.0E+00	2.1E-03	4.8E-02
	Urban		1.1E-03	1.1E-04	4.2E-03
HANF	Rural	937	0.0E+00	3.4E-01	4.1E+00
	Suburban		0.0E+00	1.3E-02	3.0E-01
	Urban		5.2E-03	5.0E-04	2.0E-02
LANL(b)	Rural	39		2.6E-03	3.2E+01
	Suburban		(c)	7.1E-05	1.6E-03
	Urban			0.0E+00	0.0E+00
ORNL	Rural	6,781	0.0E+00	1.6E+00	3.2E-02
	Suburban		0.0E+00	1.0E-01	1.6E+00
	Urban		2.1E-02	2.0E-03	7.9E-02
ANLE	Rural	9	0.0E+00	2.1E-03 (a)	2.6E-02
	Suburban		0.0E+00	7.3E-05	3.4E-03
	Urban		4.0E-06	3.9E-07	1.5E-05
	Total	7,953	2.7E-02	2.1E+00	2.7E+01

(a) units are expressed in scientific notation 2.7E-02 = 2.7 x 10^{-2} = 0.27

TABLE D.4.11 Total transportation risk for proposed action and the alternative action, RH rail mode (a)

Facility	Zone	No. of shipments	Normal transportation LCFs	Accident Fatalities	Accident Injuries
INEL	Rural	94	0.0E+00	1.3E-02	1.4E-01
	Suburban		0.0E+00	1.5E-03	1.6E-02
	Urban		4.9E-04	1.1E-04	1.1E-03
HANF	Rural	467	0.0E+00	8.6E-02	9.0E-01
	Suburban		0.0E+00	1.1E-02	1.2E-01
	Urban		3.1E-03	6.8E-04	7.2E-03
LANL(b)	Rural	39		2.6E-03	3.2E-02
	Suburban		(c)	7.1E-05	1.6E-03
	Urban			0.0E+00	0.0E+00
ORNL	Rural	3,391	0.0E+00	4.0E-01	4.2E+00
	Suburban		0.0E+00	9.5E-02	1.0E+00
	Urban		3.0E-02	6.5E-03	6.9E-02
ANLE	Rural	5	0.0E+00	5.5E-04 (a)	5.8E-03
	Suburban		0.0E+00	1.1E-04	1.2E-03
	Urban		4.3E-05	9.4E-06	9.9E-05
	Total	3,996	3.4E-02	6.2E-01	6.5E+00

(a) Numbers are expressed in abbreviated scientific notation 4.3E-04 = 4.3×10^{-5} = 0.0000430.

(b) Rail shipments are not available; truck shipments are included in this table for cumulative impacts.

These results are directly comparable to the results determined in the FEIS, Section 6.9, where only shipments between the WIPP and Rocky Flats Plant and Idaho National Engineering Laboratory were considered. It was calculated in the FEIS, using similar magnitude injury and fatality rates per kilometer, that there would be, as a bounding condition, .84 injuries per year or 21 injuries for 25 years and .08 fatalities per year or 2 fatalities for 25 years. Thus, the systemwide lifetime nonradiological and nonchemical consequences of shipping TRU waste to the WIPP for Rocky Flats Plant and the Idaho National Engineering Laboratory have remained approximately the same as was determined in the FEIS. These injuries and fatalities are the expected maximum adverse impacts that would occur with the addition of approximately 20,000 truck shipments or 10,000 rail shipments of any sort of cargo, whether radioactive or not, shipped by the type of carriers in Type B containers and with similar transporter vehicles as proposed for the TRU waste shipment program.

D.4.4 TRAFFIC ACCIDENTS AND STATISTICS

D.4.4.1 State Traffic Statistics

This section examines the impact of systemwide, 100 percent TRU truck shipments alongs preferred shipment routes from generator/storage facility to the WIPP (Figure D.4.1). No data were available for potential rail transportation routes to assess traffic volume impacts.

As shown in Tables D.4.12 through D.4.21, the total annual truck-kilometers, per segment, were calculated for each preferred route. Specific truck ADT (Average Daily Traffic) information was used when provided by the states. Along some segments, only total vehicle ADT data was available and an estimate of the total truck traffic was made, as shown in the notes to the tables.

The annual TRU truck-kilometers along these same segments were calculated using the maximum volume of TRU shipments from Appendix D, Table D.3.2.

The additional TRU shipment truck traffic, for most segments, is several orders of magnitude less than existing truck traffic and represents an insignificant impact on the highway system in most cases, as shown in the right-hand columns of each table which presents annual TRU traffic volume (truck-km) as a percentage of total segment traffic volume.

D.4.4.2 State Traffic Accidents

Data provided by state highway authorities regarding segment specific truck accidents, injuries, and fatalities is used in this section to compare to national accident statistics used to calculate nonradiological and nonchemical risks of TRU transportation. No data were available for potential rail transportation routes to assess accident rates.

Table D.4.22 outlines the nonradiological unit risk factors (accidents), injuries, fatalities) for truck traffic along segments of the preferred shipment routes. These accident data

TABLE D.4.12 Traffic Statistics Segment Analysis: Savannah River Plant to the WIPP

State	Segment Description	Miles	Km	Truck Annual ADT (a)	Truck ADT Est. Tech. (b)	Total Annual Truck-Km	Annual TRU Shipments	Total Annual TRU Truck-Km	TRU as % of Total Truck-Km
SC	SRP-I20								
GA	I20-I285	135.1	217.4	1.1E+06	1	2.28E+08	113	2.5E+04	0.011%
	I285-I20	26.1	42.0	3.3E+06	1	1.4E+08	113	4.8E+03	0.003%
	I20-I20 (AL)	50.9	81.9	2.0E+06	1	1.61E+08	113	9.3E+03	0.006%
AL	I20-I20 (MS)	212.5	341.9	2.1E+06	1	2.0E+06	113	3.9E+04	ERR
MS	I20-I20 (LA)	156.1	251.2	1.7E+06	1	1.2E+06	113	2.8E+04	ERR
LA	I20-I20 (TX)	186.2	299.6	2.0E+06	1	5.87E+08	113	3.4E+04	0.006%
TX	I20-US285				TBD	TBD	113		ERR
	US285-US285 (NM)				TBD	TBD	113		ERR
NM	US285-Carlsbad	32.0	51.5	7.3E+04	4	3.8E+06	113	5.8E+03	0.155%
	Carlsbad-WIPP	31.0	49.9	7.3E+04	4	3.6E+06	954 *	4.8E+04	1.307%

(a) ADT - Average Daily Traffic

(b) Truck ADT estimation technique
1) State supplied
2) 30% of total vehicle ADT
3) 20% of total vehicle ADT
4) 10% of total vehicle ADT

* Additional shipments from other sites included in this segment

TBD - to be determined: data not available

ERR - calculation not made due to lack of data

TABLE D.4.13 Traffic statistics segment analysis: Argonne National Laboratory to the WIPP

State	Segment Decription	Miles	Km	Truck Annual ADT (a)	Truck ADT Est. Tech (b)	Total Annual Truck-Km	Annual TRU Shipments	Total Annual TRU Truck-Km	TRU as % of Total Truck-Km
IL	Northgate-Cass	0.35	0.6	TBD		TBD	1		
	I55-155/70			TBD		TBD	1		ERR
	I70-I270			TBD		TBD	1		ERR
MO	I270-I44			TBD		TBD	7 *		ERR
	I44-I44 (OK)	297.0	477.9	1.9E+06	2	9.18E+08	7 *	3.3E+03	0.000%
OK	I44-I40			TBD		TBD	7 *		ERR
	I40-I40 (TX)			TBD		TBD	17 *		ERR
TX	I40-I40 (NM)			TBD		TBD	17 *		ERR
NM	I40-Santa Rosa	98.5	158.5	3.2E+05	1	5.1E+07	17 *	2.7E+03	0.005%
	Santa Rosa-Vaughn	41.0	66.0	2.6E+04	4	1.7E+06	17 *	1.1E+03	0.066%
	Vaughn-Carlsbad	164.0	263.9	8.1E+04	4	2.1E+07	841 *	2.2E+05	1.043%
	Carlsbad-WIPP	31.0	49.9	7.3E+04	4	3.6E+06	954 *	4.8E+04	1.307%

(a) ADT - average daily traffic

(b) Truck ADT estimation technique
1) State supplied
2) 30% of total vehicle ADT
3) 20% of total vehicle ADT
4) 10% of total vehicle ADT

* Additional shipments from other sites included in this segment

TBD - to be determined: data not available

ERR - calculation not made due to lack of data

TABLE D.4.14 Traffic statistics segment: Mound Laboratory to the WIPP

Segment Description	Miles	Km	Truck Annual ADT (a)	Truck ADT Est. Tech. (b)	Total Annual Truck-Km	Annual TRU Shipments	Total Annual TRU Truck-Km	TRU as % of Total Truck-Km
SR725-I75	1.8	3.0	2.9E+05	1	2.4E+03	6	1.8E+01	
I75-I70	16.1	25.8	4.4E+06	1	2.8E+05	6	1.5E+02	0.054%
I70-I70 (IN)	33.9	59.5	2.6E+06	1	5.8E+05	6	3.3E+02	0.057%
I70-I70 (IL)	155.9	250.8	3.5E+06	1	8.78E+08	6	1.5E+03	0.000%
I70-I270			TBD		TBD	7 *		ERR
I270-I44			TBD		TBD	7 *		ERR
I44-I44 (OK)	297.0	477.9	1.9E+06	2	9.18E+08	7 *	3.3E+03	0.000%
I44-I40			TBD		TBD	7 *		ERR
I40-I40 (TX)			TBD		TBD	17 *		ERR
I40-I40 (NM)			TBD		TBD	17 *		ERR
I40-Santa Rosa	98.5	158.5	3.2E+05	1	5.1E+07	17 *	2.7E+03	0.005%
Santa Rosa-Vaughn	41.0	66.0	2.6E+04	4	1.7E+06	17 *	1.1E+03	0.066%
Vaughn-Carlsbad	164.0	263.9	8.1E+04	4	2.1E+07	841 *	2.2E+05	1.043%
Carlsbad-WIPP	31.0	49.9	7.3E+04	4	3.6E+06	954 *	4.8E+04	1.307%

(a) ADT - average daily traffic

(b) Truck ADT estimation technique
1) State supplied
2) 30% of total vehicle ADT
3) 20% of total vehicle ADT
4) 10% of total vehicle ADT

* Additional shipments from other sites included in this segment

TBD - to be determined: data not available

ERR - calculation not made due to lack of data

TABLE D.4.15 Traffic statistics segment analysis: Nevada Test Site to the WIPP

State	Segment Description	Miles	Km	Truck Annual ADT (a)	Truck ADT Est. Tech. (b)	Total Annual Truck-Km	Annual TRU Shipments	Total Annual TRU Truck-Km	TRU as % of Total Truck-Km
NV	US35-I40	137.0	220.4	3.0E+05	1	6.6E+07	5	1.1E+03	0.002%
CA	I40-I40 (AZ)	21.9	35.2	1.6E+06	1	5.7E+07	5	1.8E+02	0.000%
AZ	I40-I40 (NM)	359.6	578.6	1.2E+06	1	6.8E+08	44 *	2.5E+04	0.004%
NM	I40-US285	218.0	350.8	6.0E+05	1	2.1E+08	44 *	1.5E+04	0.007%
	US285-Vaughn	44.0	70.8	6.4E+04	4	4.5E+06	384 *	2.7E+04	0.601%
	Vaughn-Carlsbad	164.0	263.9	8.1E+04	4	2.1E+07	841 *	2.2E+05	1.043%
	Carlsbad-WIPP	31.0	49.9	7.3E+04	4	3.6E+06	954 *	4.8E+04	1.307%

(a) ADT - Average Daily Traffic

(b) Truck ADT estimation technique
1) State supplied
2) 30% of total vehicle ADT
3) 20% of total vehicle ADT
4) 10% of total vehicle ADT

* Additional shipments from other sites included in this segment

TBD - to be determined: data not available

ERR - calculation not made due to lack of data

TABLE D.4.16 Traffic statistics segment analysis: Idaho National Engineering Laboratory to the WIPP

State	Segment Description	Miles	Km	Truck Annual ADT (a)	Truck ADT Est. Tech. (b)	Total Annual Truck-Km	Annual TRU Shipments	Total Annual TRU Truck-Km	TRU as % of Total Truck-Km
ID	US20/26-ID15	36.0	57.9	TBD		0	228	1.3E+04	ERR
	I15-I15 (UT)	92.7	149.2	5.4E+05	1	8.1E+07	228	3.4E+04	0.042%
UT	I15-I84	24.0	38.6	TBD		TBD	300 *	1.2E+04	ERR
	I84-I80	76.0	122.3	TBD		TBD	372 *	4.5E+04	ERR
	I80-I80 (WY)	33.0	53.1	TBD		TBD	372 *	2.0E+04	ERR
WY	I80-I25	359.6	578.6	9.8E+05	1	5.7E+08	372 *	2.2E+05	0.038%
	I25-I25 (CO)	8.8	14.2	5.5E+05	1	7.9E+06	372 *	5.3E+03	0.067%
CO	I25-I25 (NM)	298.9	480.9	3.5E+06	2	1.7E+09	597 *	2.9E+05	0.017%
NM	I25-US285	174.1	280.2	7.3E+04	1	2.0E+07	681 *	1.9E+05	0.935%
	US285-Vaughn	84.0	135.2	6.4E+04	4	8.6E+06	802 *	1.1E+05	1.255%
	Vaughn-Carlsbad	164.0	263.9	8.1E+04	4	2.1E+07	841 *	2.2E+05	1.043%
	Carlsbad-WIPP	31.0	49.9	7.3E+04	4	3.6E+06	954 *	4.8E+04	1.307%

(a) ADT - average daily traffic

(b) Truck ADT estimation technique
1) State supplied
2) 30% of total vehicle ADT
3) 20% of total vehicle ADT
4) 10% of total vehicle ADT

* Additional shipments from other sites included in this segment

TBD - to be determined: data not available

ERR - calculation not made due to lack of data

TABLE D.4.17 Traffic statistics segment analysis: Rocky Flats Plant to the WIPP

Segment Description	Miles	Km	Truck Annual ADT (a)	Truck ADT Est. Tech. (b)	Total Annual Truck-Km	Annual TRU Shipments	Total Annual TRU Truck-Km	TRU as % of Total Truck-Km
East GT-IN	0.0	0.0	TBD		TBD	309	0.0E+00	ERR
Indiana-HY128	1.5	2.4	TBD		TBD	309	7.5E+02	ERR
HY128-US36	3.9	6.3	2.2E+05	4	1.4E+06	309	2.0E+03	0.143%
US36-I25	12.3	19.8	4.4E+06	3	8.7E+07	309	6.1E+03	0.007%
I25-I25 (NM)	217.0	349.2	3.8E+06	2	1.3E+09	597 *	2.1E+05	0.016%
I25-US285	174.1	280.2	7.3E+04	1	2.0E+07	681 *	1.9E+05	0.935%
US285-Vaughn	84.0	135.2	6.4E+04	4	8.6E+06	802 *	1.1E+05	1.255%
Vaughn-Carlsbad	164.0	263.9	8.1E+04	4	2.1E+07	841 *	2.2E+05	1.043%
Carlsbad-WIPP	31.0	49.9	7.3E+04	4	3.6E+06	954 *	4.8E+04	1.307%

(a) ADT - average daily traffic

(b) Truck ADT estimation technique
1) State supplied
2) 30% of total vehicle ADT
3) 20% of total vehicle ADT
4) 10% of total vehicle ADT

* Additional shipments from other sites included in this segment

TBD - to be determined: data not available

ERR - calculation not made due to lack of data

TABLE D.4.18 Traffic statistics segment: Los Alamos National Laboratory to the WIPP

State	Segment Description	Miles	Km	Truck Annual ADT (a)	Truck ADT Est. Tech. (b)	Total Annual Truck-Km	Annual TRU Shipments	Total Annual TRU Truck-Km	TRU as % of Total Truck-Km
NM	LANL-I25	0.0	0.0	TBD		TBD	99		ERR
	I25-US285	0.0	0.0	TBD		TBD	99		ERR
	US285-Vaughn	84.0	135.2	6.4E+04	4	8.6E+06	802 *	1.1E+05	1.255%
	Vaughn-Carlsbad	164.0	263.9	8.1E+04	4	2.1E+07	841 *	2.2E+05	1.043%
	Carlsbad-WIPP	31.0	49.9	7.3E+04	4	3.6E+06	954 *	4.8E+04	1.307%

(a) ADT - average daily traffic

(b) Truck ADT estimation technique
1) State supplied
2) 30% of total vehicle ADT
3) 20% of total vehicle ADT
4) 10% of total vehicle ADT

* Additional shipments from other sites included in this segment

TBD - to be determined: data not available

ERR - calculation not made due to lack of data

TABLE D.4.19 Traffic statistics segment: Lawrence Livermore National Laboratory to the WIPP

Segment Description	Miles	Km	Truck Annual ADT (a)	Truck ADT Est. Tech. (b)	Total Annual Truck-Km	Annual TRU Shipments	Total Annual TRU Truck-Km	TRU as % of Total Truck-Km
East Avenue	0.5	0.8	TBD		TBD	39	3.1E+01	ERR
Vasco	3.0	4.8	TBD		TBD	39	1.9E+02	ERR
I580-I5	35.0	56.3	4.0E+06	1	2.3E+08	39	2.2E+03	0.001%
I5-I210	319.0	513.3	3.1E+06	1	1.6E+09	39	2.0E+04	0.001%
I210-I10	48.5	78.1	3.1E+06	1	2.4E+08	39	3.0E+03	0.001%
I10-I15	18.0	29.0	5.5E+06	1	1.6E+08	39	1.1E+03	0.001%
I15-I40	72.0	115.8	3.4E+06	1	4.0E+08	39	4.5E+03	0.001%
I40-I40 (AZ)	154.6	248.8	1.6E+06	1	4.0E+08	39	9.7E+03	0.002%
I40-I40 (NM)	359.6	578.6	1.2E+06	1	6.8E+08	44 *	2.5E+04	0.004%
I40-US285	218.0	350.8	6.0E+05	1	2.1E+08	44 *	1.5E+04	0.007%
US285-Vaughn	44.0	70.8	6.4E+04	4	4.5E+06	384 *	2.7E+04	0.601%
Vaughn-Carlsbad	164.0	263.9	8.1E+04	4	2.1E+07	841 *	2.2E+05	1.043%
Carlsbad-WIPP	31.0	49.9	7.3E+04	4	3.6E+06	954 *	4.8E+04	1.307%

(a) ADT - Average Daily Traffic

(b) Truck ADT estimation technique
1) State supplied
2) 30% of total vehicle ADT
3) 20% of total vehicle ADT
4) 10% of total vehicle ADT

* Additional shipments from other sites included in this segment

TBD - to be determined: data not available

ERR - calculation not made due to lack of data

TABLE D.4.20 Traffic statistics segment analysis: Hanford Reservation to the WIPP

Segment Description	Miles	Km	Truck Annual ADT (a)	Truck ADT Est. Tech. (b)	Total Annual Truck-Km	Annual TRU Shipments	Total Annual TRU Truck-Km	TRU as % of Total Truck-Km
SR 240	3.4	5.5	TBD		TBD	144	7.9E+02	ERR
I82-I82 (OR)	35.0	56.3	4.9E+05	3	2.8E+07	144	8.1E+03	0.029%
I82-I84	12.0	19.3	TBD		TBD	144	2.8E+03	ERR
I84-I84 (ID)	193.9	312.0	5.0E+05	3	1.54E+08	144	4.5E+04	0.029%
I84-I84 (UT)	275.6	443.5	7.7E+05	1	3.39E+08	258 *	1.1E+05	0.034%
I84-I80	109.0	175.4	TBD		TBD	372 *	6.5E+04	ERR
I80-I80 (WY)	33.0	53.1	TBD		TBD	372 *	2.0E+04	ERR
I80-I25	359.6	578.6	9.8E+05	1	5.7E+08	372 *	2.2E+05	0.038%
I25-I25 (CO)	8.8	14.2	5.5E+05	1	7.9E+06	372 *	5.3E+03	0.067%
I25-I25 (NM)	298.9	480.9	3.5E+06	2	1.7E+09	597 *	2.9E+05	0.017%
I25-US285	174.1	280.2	7.3E+04	1	2.0E+07	681 *	1.9E+05	0.935%
US285-Vaughn	84.0	135.2	6.4E+04	4	8.6E+06	802 *	1.1E+05	1.255%
Vaughn-Carlsbad	164.0	263.9	8.1E+04	4	2.1E+07	841 *	2.2E+05	1.043%
Carlsbad-WIPP	31.0	49.9	7.3E+04	4	3.6E+06	954 *	4.8E+04	1.307%

(a) ADT - average daily traffic

(b) Truck ADT estimation technique
1) State supplied
2) 30% of total vehicle ADT
3) 20% of total vehicle ADT
4) 10% of total vehicle ADT

* Additional shipments from other sites included in this segment

TBD - to be determined: data not available

ERR - calculation not made due to lack of data

TABLE D.4.21 Traffic statistics segment analysis: Oak Ridge National Laboratory to the WIPP

State	Segment Description	Miles	Km	Truck Annual ADT (a)	Truck ADT Est. Tech. (b)	Total Annual Truck-Km	Annual TRU Shipments	Total Annual TRU Truck-Km	TRU as % of Total Truck-Km
TN	Bethel V. Rd	1.1	1.8	TBD		TBD	10		
	TN RT 95	3.3	5.3	TBD		TBD	10		ERR
	I40-140 (AK)	334.2	553.9	1.7E+06	1	2.4E+06	10	5.5E+03	
AR	I40-140 (OK)	284.7	458.1	2.0E+06	1	9.07E+08	10	4.6E+03	0.001%
OK	I40-I240			TBD		TBD	10		ERR
	I240-I44			TBD		TBD	10		ERR
	I44-140			TBD		TBD	10		ERR
	I40-140 (TX)			TBD		TBD	17 *		ERR
TX	I40-140 (NM)			TBD		TBD	17 *		ERR
NM	I40-Santa Rosa	98.5	158.5	3.2E+05	1	5.1E+07	17 *	2.7E+03	0.005%
	Santa Rosa-Vaughn	41.0	66.0	2.6E+04	4	1.7E+06	17 *	1.1E+03	0.066%
	Vaughn-Carlsbad	164.0	263.9	8.1E+04	4	2.1E+07	841 *	2.2E+05	1.043%
	Carlsbad-WIPP	31.0	49.9	7.3E+04	4	3.6E+06	954 *	4.8E+04	1.307%

(a) ADT - average daily traffic

(b) Truck ADT estimation technique
1) State supplied
2) 30% of total vehicle ADT
3) 20% of total vehicle ADT
4) 10% of total vehicle ADT

* Additional shipments from other sites included in this segment

TBD - to be determined: data not available

ERR - calculation not made due to lack of data

TABLE D.4.22 Traffic statistics - accidents by segments

Title: Georgia-Trucks (I20 + I285) (1986 & 1987)

		Accidents		Injuries		Fatalities		Truck km
		# of	Rate/km	# of	Rate/km	# of	Rate/km	
Section 1	86	(40)	5.1E-07	(16)	2.0E-07	0	0.0E+00	7.860E+07
	87	(32)	4.1E-07	(22)	2.8E-07	0	0.0E+00	7.860E+07
Section 2	86	(117)	1.6E-06	(61)	8.2E-07	0	0.0E+00	7.430E+07
	87	(136)	1.7E-06	(57)	7.0E-07	(4)	4.9E-08	8.200E+07
Section 3	86	(164)	1.1E-06	(65)	4.4E-07	(6)	4.1E-08	1.473E+08
	87	(164)	1.2E-06	(75)	5.4E-07	(4)	2.9E-08	1.397E+08
Section 4	86	(54)	1.4E-06	(14)	3.7E-07	0	0.0E+00	3.740E+07
	87	(63)	1.4E-06	(12)	2.7E-07	(1)	2.2E-08	4.480E+07
Section 5	86	(69)	4.5E-07	(36)	2.4E-07	(1)	6.6E-09	1.517E+08
	87	(50)	2.7E-07	(27)	1.5E-07	(1)	5.4E-09	1.842E+08
Section 6	86	(12)	7.3E-07	(4)	2.4E-07	0	0.0E+00	1.650E+07
	87	(9)	5.5E-07	(4)	2.4E-07	0	0.0E+00	1.650E+07
Total	86	(456)	9.0E-07	(196)	3.9E-07	(7)	1.4E-08	5.058E+08
	87	(454)	8.3E-07	(197)	3.6E-07	(10)	1.8E-08	5.458E+08

Title: Wyoming-Trucks (I80) (1986 & 1987)

		Accidents		Injuries		Fatalities		Truck km
		# of	Rate/km	# of	Rate/km	# of	Rate/km	
Uinta Co	86	(54)	7.1E-07	(33)	4.3E-07	(1)	1.3E-08	7.620E+07
	87	(80)	8.1E-07	(36)	3.6E-07	(1)	1.0E-08	9.920E+07
Sweetwater Co	86	(139)	7.0E-07	(75)	3.8E-07	(2)	1.0E-08	1.998E+08
	87	(149)	6.3E-07	(86)	3.6E-07	(9)	3.8E-08	2.361E+08
Carbon	86	(120)	1.1E-06	(45)	4.1E-07	(1)	9.2E-09	1.087E+08
	87	(87)	6.8E-07	(26)	2.0E-07	0	0.0E+00	1.282E+08
Albany	86	(83)	1.2E-06	(43)	6.4E-07	(1)	1.5E-08	6.720E+07
	87	(61)	7.7E-07	(34)	4.3E-07	(1)	1.3E-08	7.940E+07
Lara. 1	86	(29)	1.4E-06	(11)	5.2E-07	0	0.0E+00	2.130E+07
	87	(49)	1.9E-06	(27)	1.1E-06	(2)	7.9E-08	2.520E+07
Lara. 2	86	(7)	9.0E-07	0	0.0E+00	0	0.0E+00	7.800E+06
	87	(9)	1.2E-06	(2)	2.6E-07	0	0.0E+00	7.800E+06
Total	86	(432)	9.0E-07	(207)	4.3E-07	(5)	1.0E-08	4.810E+08
	87	(435)	7.6E-07	(211)	3.7E-07	(13)	2.3E-08	5.759E+08

TABLE D.4.22 Concluded

Title: Louisiana-Trucks (I20) (1987)

	Accidents		Injuries		Fatalities		Truck km
	# of	Rate/km	# of	Rate/km	# of	Rate/km	
Section 1	(6)	3.7E-07	(3)	1.8E-07	0	0.0E+00	1.640E+07
Section 2	(236)	1.8E-06	(104)	7.9E-07	(2)	1.5E-08	1.312E+08
Section 3	(137)	5.2E-07	(99)	3.7E-07	(7)	2.7E-08	2.641E+08
Section 4	(57)	1.0E-06	(52)	9.4E-07	0	0.0E+00	5.530E+07
Section 5	(44)	2.7E-07	(38)	2.3E-07	(1)	6.2E-09	1.626E+08
Annual Stats for State	(508)	5.0E-07	(314)	3.1E-07	(10)	9.8E-09	1.025E+09

* Do not necessarily add from segments above

Title: Idaho-Trucks (I-15 + I-84) (1987)

		Accidents		Injuries		Fatalities		Truck km
		# of	Rate/km	# of	Rate/km	# of	Rate/km	
I-15	87	(19)	2.3E-07	(14)	1.7E-07	0	0.0E+00	8.12E+07
I-84	87	(93)	2.7E-07	(49)	1.4E-07	(1)	2.9E-09	3.39E+08
Total		(112)	5.1E-07	(63)	3.2E-07	(1)	2.9E-09	4.202E+08

Title: Oregon-Trucks (I-84) (1986 & 1987)

	Accidents		Injuries		Fatalities		Truck km
	# of	Rate/km	# of	Rate/km	# of	Rate/km	
86	(42)	3.0E-07	(50)	3.5E-07	(3)	2.1E-08	1.420E+08
87	(22)	1.4E-07	(35)	2.3E-07	0	0.0E+00	1.540E+08

Title: Mississippi-Trucks (I-30) (1987)

	Accidents		Injuries		Fatalities		Truck km
	# of	Rate/km	# of	Rate/km	# of	Rate/km	
87	Not Available		(8)	4.6E-06	(1)	8.2E-07	1.210E+06

Title: Tennessee-Trucks (I-40) (1987)

	Accidents		Injuries		Fatalities		Truck km
	# of	Rate/km	# of	Rate/km	# of	Rate/km	
87	(102)	5.9E-08	(57)	3.2E-07	(0)	0.0E+00	2.621E+08

were provided by the states of Wyoming, Oregon, Idaho, Georgia, and Louisiana for 1986 and/or 1987. These statistics were compared to the national average accident/km rate for trucks of 1.1×10^{-6} (NRC,1977) and the national average injury and fatality/km rates as presented in Table D.4.4. These national statistical averages are based on truck accident data from 1983 and 1984. The unit risk factors for segments of preferred TRU shipments routes, using state accident statistics from 1986 and 1987, compare favorably to the previously published national statistical averages.

REFERENCES FOR APPENDIX D

AEC (Atomic Energy Commission), December, 1972. Environmental Survey of Transportation of Radioactive Materials, to and from Nuclear Power Plants, WASH-1238, Directorate of Regulatory Standards, Washington, D.C.

Cashwell, J. W., et al., 1986. Transportation Impacts of the Commercial Radioactive Waste Management Program, Appendix 4, Tables 4-4A and 4-4B, SAND 85-2715, TTC-0663, Sandia National Laboratories, Albuquerque, New Mexico.

DOE (U.S. Department of Energy), July 1988. Draft Radionuclide Source Term for the WIPP, DOE/WIPP-88-049, Carlsbad, New Mexico.

DOE (U.S. Department of Energy), 1986. Transportation Assessment and Guidance Report, Carlsbad, New Mexico.

DOE (U.S. Department of Energy), 1980. Final Environmental Impact Statement, Waste Isolation Pilot Plant, DOE-EIS-0026, Vol. 1 and 2, Carlsbad, New Mexico.

Huerta, M., et al., 1983. Analysis, Scale Modeling, and Full-Scale Test of Low-Level Nuclear Waste Drum Response to Accident Environments, Sand 80-2517 Sandia National Laboratories, Albuquerque, New Mexico.

Joy, D. S., et al., 1982. Highway, a Transportation Routing Model: Program Description and User's Manual, ORNL/TM 84-19, Oak Ridge National Laboratory, Oak Ridge, Tennessee.

Lorenz, R. S. et al., April 1980. Fission Product Release From Highly Irradiated LWR Fuel, NUREG/CR-0772, Oak Ridge National Laboratory, Oak Ridge, Tennessee.

Madsen, M. M., et al., 1983. RADTRAN II User Guide, SAND 82-2681, TTC-0399, Sandia National Laboratories, Albuquerque, New Mexico.

Mishma, J. and Schwendiaman, L.C., 1973a. Some Experimental Measurements of Airborne Uranium (Representing Plutonium) in Transportation Accidents, BNWL-1732, Pacific Northwest Laboratories.

Mishma, J. and Schwendiaman, L.C., 1973b. Fractional Airborne Release of Uranium (Representing Plutonium) During the Burning of Contaminated Wastes, BNWL-1730, Pacific Northwest Laboratories.

NRC (Nuclear Regulatory Commission), 1987. Shipping Container Response to Severe Highway and Railway Accident Conditions, NUREG/CR-4829, Vol. 1 and 2, Lawrence Livermore National Laboratory, Livermore, California.

NRC (Nuclear Regulatory Commission), 1977. Final Environmental Statement on the Transportation of Radioactive Material by Air and Other Modes, NUREG-0170, Vol. 1, Office of Standards Development, Washington, D.C.

NRC (Nuclear Regulatory Commision), 1980. Accident Generated Particulate Materials and Their Characteristics - A Review of Background Information, NUREG/CR-2651, PNL-4154, Pacific Northwest Laboratory.

ORNL (Oak Ridge National Laboratory), 1988. Integrated Data Base for 1988: Spent Fuel and Radioactive Waste Inventories, Projections, and Characteristics, DOE/RW-0006, Rev. 4, for U.S. DOE.

Peterson, B. E., 1984. INTERLINE: A Railroad Routing Model, ORNL/TM-8944, Oak Ridge National Laboratory, Oak Ridge, Tennessee.

Rand McNally, 1988. Rand McNally Handy Railroad Atlas of the United States, Rand McNally & Company, 1988.

Rand McNally, 1987. Rand McNally Road Atlas, Rand McNally & Company, USA, 1987.

Rao, R. K., E. L. Wilmont, and R. E. Luna, 1982. Nonradiological Impacts of Transporting Radioactive Material, SAND 81-1703, TTC-0236, Sandia National Laboratories, Albuquerque, New Mexico.

Shirley, C. G., 1983. "A Simple Risk Analysis Tool for Estimating Release Fractions From Shipments of 55-Gallon Drums Involved in Transportation Accidents," Seventh International Symposium on Packaging and Transportation of Radioactive Materials (PATRAM 83), New Orleans, Louisiana.

Taylor, J. M. and S. L. Daniel, 1982. RADTRAN II: Revised Computer Code to Analyze Transportation of Radioactive Material, SAND 80-1943, TTC-0239, Sandia National Laboratories, Albuquerque, New Mexico.

Taylor, J. M. and S. L. Daniel, 1977. RADTRAN: A Computer Code to Analyze Transportation of Radioactive Material, SAND 75-0243, Sandia National Laboratories, Albuquerque, New Mexico.

Wilmot, E. L., M. M. Madsen, J. W. Cashwell, and D. S. Joy, 1983. A Preliminary Analysis of the Cost and Risk of Transporting Nuclear Waste to Potential Candidate Repository Sites, SAND 83-0867, TTC-0434, Sandia National Laboratories, Albuquerque, New Mexico.

Wolff, T. A., 1984. The Transportation of Nuclear Materials, SAND84-0062, TTC-0471, Sandia National Laboratory, Albuquerque, New Mexico.

APPENDIX E

PERMEABILITY MEASUREMENTS AND BRINE INFLOW RATES

TABLE OF CONTENTS

Section		Page
E.1	INTRODUCTION	E-1
E.2	BRINE INFLOW MEASUREMENTS (Deal and Case, 1987)	E-3
E.3	BRINE INFLOW MODEL (Nowak et al., 1988)	E-47
E.4	WIPP HORIZON GAS FLOW MEASUREMENT RESULTS SUMMARY THROUGH 1986 (Stormont et al., 1987)	E-59
E.5	1984 GAS FLOW MEASUREMENT TEST RESULTS (Peterson et al., 1985)	E-85
E.6	N1400 DRIFT GAS FLOW DATA ANALYSIS AND EVALUATION (Peterson et al., 1987)	E-123
E.7	WASTE HANDLING SHAFT PULSE TESTING DATA SUMMARY AND CONCLUSIONS (Saulnier and Avis, 1988)	E-151
E.8	REFERENCES FOR APPENDIX E	E-237

E.1 INTRODUCTION

Appendix E contains excerpts from published documents to support brine inflow rates and formation permeabilities defined in the text. This appendix is not intended to provide a complete understanding of the various tests, but is intended to provide enough data and interpretation to provide the reader with an understanding and information to verify the permeability values and brine inflow rates defined in the text.

For complete citations please see the Appendix E reference list.

E.2 **BRINE INFLOW MEASUREMENTS**

This subsection of Appendix E describes preliminary sampling and evaluations of brine occurrences at the WIPP facility horizon. Included is a discussion and description of sampling methodology, the manner in which the data were used, calculations made, and a location-by-location description of sampling results.

This subsection was excerpted from Appendix D of Deal and Case, 1987, Brine Sampling and Evaluation Program, Phase I Report. This subsection is included to provide evidence of brine inflow rates defined in the text.

APPENDIX D

PHASE I PRELIMINARY SAMPLING AND EVALUATION
OF BRINE OCCURRENCES AT THE WIPP REPOSITORY HORIZON

This appendix contains a discussion of the Task 2 sampling activities that were part of Phase I of the WIPP Brine Sampling and Evaluation Program (BSEP). Included in this discussion is a description of sampling methodology, the manner in which the data was handled and calculations made, and a location-by-location description of both the sampling and the sampling results. The data obtained during Task 2 of Phase I are presented in tabular form in Appendix E.

1.0 SAMPLING METHODOLOGY AND PROBLEMS

The general procedure for brine collection and inflow measurements was simply to provide for the accumulation of the small brine inflows, to collect those accumulations on a periodic basis (approximately once a week for initial collections), and to measure the volume that had accumulated since the previous sampling. These measurements were then recorded and tabulated as the average fractions of liters per day collected from each location.

A variety of field techniques were used, depending upon the specifics of each occurrence. They can be broken down into the following groups:

- Initial volume measurements, experimental pumping techniques, and water-level measurements
- Vacuum-assisted sampling probe for brine removal from downholes
- Hand-operated rotary suction pump
- Continuous, gravity-driven collecting installations
- Pressure-vacuum and vacuum moisture-sampler installations

Additional details concerning the brine sampling procedures is provided in WIPP Procedure WP 07-410.

Down-hole sampling was done with a variety of bailing devices, most of which relied on check valves to retain collected brine while the bailer was raised to the surface (the floor of the repository workings). These devices occasionally failed when debris (mostly salt crystals and other muck in the holes) prevented the valves from seating properly, allowing some brine to leak from the sampler and flow down the inside of the drill hole. The result was an anomalously small recorded value for brine withdrawn at that time, usually followed the next week by a larger than expected amount. In most cases, the average of those two values was consistent with the trend of earlier and later readings. The result is a "kick" in the data that is not representative of the actual, much more consistent, inflow rates. Such sampling problems were noted on the field data sheets.

The bailing techniques would remove most, but not all of the brine in the hole. The amount of brine remaining in the hole was a fairly consistent amount, so the values obtained for "brine removed" were very close to the amount that actually flowed into the hole during the period between evacuations. After sampling, a visual inspection was made of the bottom of the hole to see if the bottom was at least partially exposed. If a partially-dry bottom was not observed after initial evacuation, the sampler was lowered to the bottom again and the evacuation repeated. After bailing, the downholes were plugged just below the collar with a piece of plastic foam which was covered, in turn, by a metal lid. The plug and lid prevented the inadvertent introduction of foreign solids into the hole and reduced moisture loss by evaporation to the repository atmosphere.

Evaporation has played a significant role in reducing the measured amounts of brine inflow, especially from the upholes. Several techniques were used to seal the collar of the upholes, but none of the techniques completely controlled evaporation. The projected high temperatures that will eventually be reached in Rooms A1, A2, A3, and B required that some of the materials used in the initial phases of the study be removed (they might give off deleterious vapors at high temperatures) and caused the replacement of some plastic items with metal.

Occasionally large "kicks" are observed in the uphole data. Many of these are a result of the clearing of a temporary blockage in the plastic tube leading from the collecting device at the hole collar to the collecting container. It was not uncommon for pieces of clay to slough from the clay seams exposed in the holes and for clay to fall down into the collecting device. The clay, in addition to pieces of salt that either fall from the sides of the hole or accumulate by the evaporation of brine, occasionally completely plugged the devices.

The result of these conditions and disruptions are that the data from the upholes should be considered as providing only minimum inflow data. Additionally, the effects of heat, the presence of metal, and the close proximity of many other holes need to be considered when evaluating the data from the A rooms and Room B.

2.0 DATA HANDLING AND CALCULATIONS

The data collected as part of the BSEP were initially recorded on field data sheets and then transferred to a computerized data base using an IBM XT microcomputer. Standard software programs (dBase III Plus and Lotus 1-2-3) were used for storage and calculations. Samples were collected about once a week except for special circumstances discussed later. The amount of brine removed was measured to the nearest hundredth of a liter and recorded, along with the date and time of collection, on the field data sheets. Brine levels were also measured and recorded. An approximation of the volume of brine in the downholes can be calculated from the height of the column of brine in the hole and the average diameter of the hole. The result of this calculation is less accurate than actually measuring the volume of brine removed, but the brine level was routinely measured prior to attempting evacuation of the accumulated brine. In a few instances, the brine level data were used to resolve apparent anomalies in the brine volume measurements that resulted from equipment failure or human error.

The dates and times at which collections were made were transformed into decimal days since an arbitrary reference date (January 1, 1985) and the elapsed time in decimal days between samples was used to calculate average brine inflow rates in terms of fractions of liters per day.

As described in Section 1.0, much of the variability in the quantity of brine collected resulted from limitations of the collecting techniques rather than variations in the actual inflow of brine from the bedrock into the collecting locations. As a result, plotting of the inflow data from the data tables (Appendix E) results in an irregular plot which implies variations in inflow that, in fact, do not exist. The graphed data included in this report were processed and plotted by a standard computer software program (STSC Statgraphics) on an IBM AT microcomputer, using a simple moving average to smooth the curves. A five-point moving average was used for the majority of the graphs. The smoothed result reflects trends that are representative of the brine inflow rates while still showing variations that are probably the result of collecting problems.

An alternative technique to smooth the data is to plot cumulative inflow against time, fit a curve to that plot, and then differentiate the best-fit equation to determine the flow rate. This technique may be attempted after more data has been acquired.

3.0 OBSERVATIONS

3.1 Room 1, Hole IG202

SPDV Test Room 1 was one of the first rooms excavated in the northern part of the WIPP underground (Figure D-1). Initial mining was finished on April 13, 1983, and a number of instrument holes were drilled in it during the following few weeks. One of those was downhole IG202, located near the west rib in the center of the room, which was drilled for use as an inclinometer observation location. It is lined with a 74 millimeter (2 7/8th inch) I.D. flexible PVC inclinometer guide tube that is not a normal well casing. Leaks may occur into the guide tube. This type of liner has flexible expansion joints that can transmit fluids and a plastic cap on the bottom that was not installed with the intent of preventing brine inflow.

IG202 was drilled using brine as the drilling fluid. On April 21, 1983, the PVC guide tube was installed in the hole and a small-diameter tremie pipe (plastic tubing) was used to grout the liner in place. It is likely that the grouting is incomplete and that vertical movement of fluid takes place in open, ungrouted spaces outside the guide tube. When the guide tube was installed, it was filled with fresh water to assist in sinking the guide tube to the bottom of the hole. The fluid in the guide tube was reportedly blown out with compressed air, but it is not known how complete that removal was. It is probable at least some fluid remained in the partially grouted space outside the guide tube and in pore spaces and fractures in the rock which drained into the bottom of the hole after it was "blown dry."

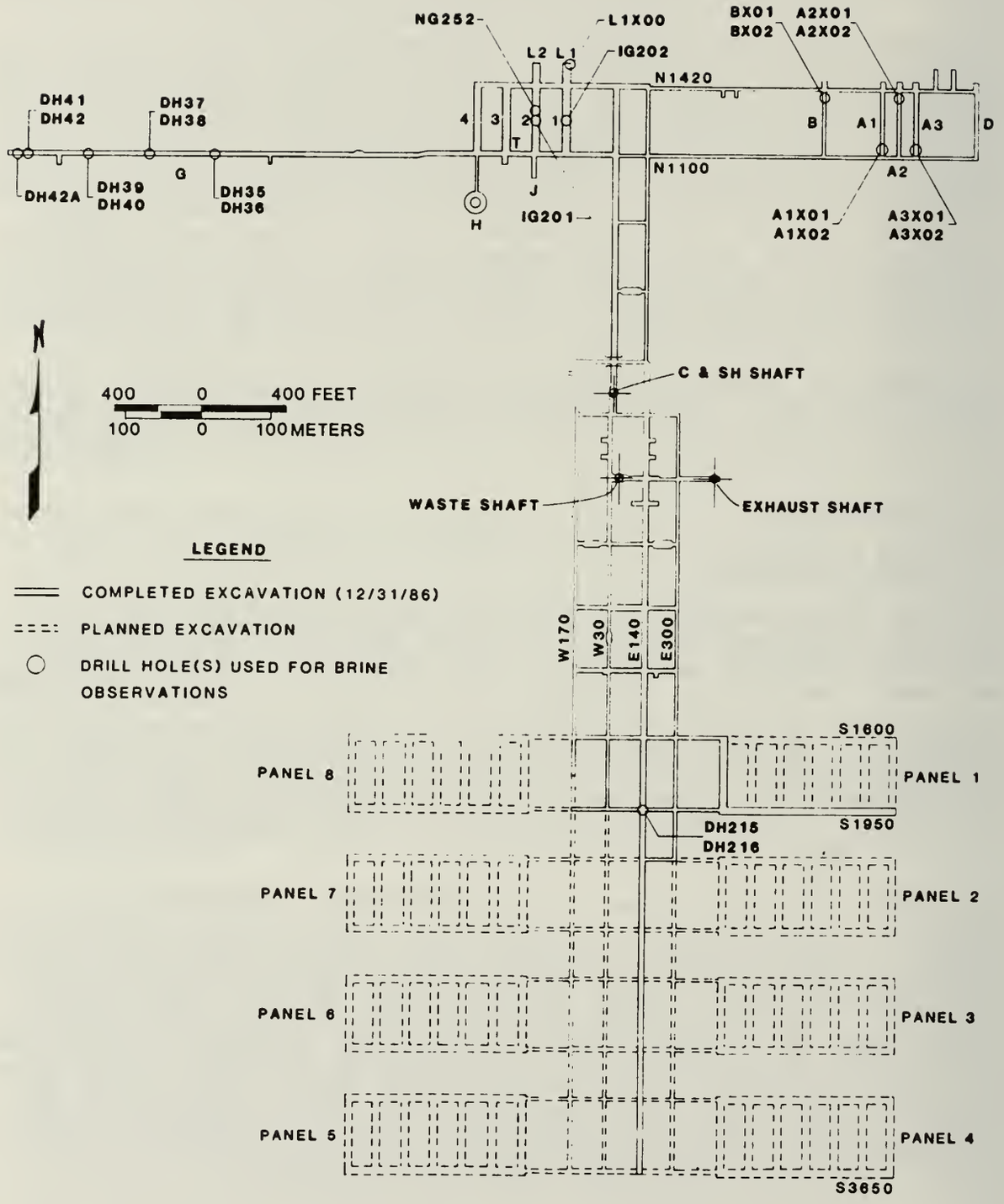

Figure D-1.

Map of the WIPP Underground Workings

On November 30, 1984, fluid filled the hole to within approximately two meters of the collar. It is known that fluids were introduced into this hole on at least two occasions (brine of unknown composition at the time of drilling and fresh water during guide-tube emplacement). The chemistry of fluids in this hole has certainly been affected by the materials and fluids introduced into the hole, especially the grout. Room 1 was also used by the mining contractor as an underground shop and lunchroom. As a result, the origin, quantity, and chemical composition of the fluid in the hole at the time of initial BSEP testing was probably not representative of naturally occurring, spontaneous inflows from the surrounding rocks.

This hole was the location of some of the initial experiments with air-jet pumping techniques. On November 30, 1984, over 52 liters of brine were removed from the hole and the inside of the guide tube was blown as dry as possible with high-pressure air. On January 8, 1985, an additional 12.6 liters was removed and the inside of the guide tube blown dry again. Some brine was lost during both of these evacuations, so those figures, although reasonably accurate, represent minimum figures for the amount of brine actually in the hole. Evacuation using the vacuum-assisted sampling system and measuring technique described in WIPP Procedure WP 07-410 began January 15, 1985, and continued until October 15, 1985, when the guide tube had become so distorted due to shear movement in the bedrock that sampling was discontinued for fear that the sampling device would become wedged in the hole. Most of the displacement is taking place along fractures in anhydrite interbed MB 139, which is about one to two meters below the floor of Room 2 (Figure D-2).

Relatively few data points exist for the inflow data for IG202. As a result, a four-point moving average was used to smooth this data (Figure D-3) instead of the five-point average used for most of the rest of the data.

Average inflow rates were on the order of 0.05 liters per day in early 1985, decreasing gradually for about 175 days (Table E.18; Figure D-3). Inflow rates leveled out to between 0.01 and 0.02 liters per day for the remainder of the sampling period with the fluctuations falling within the limit of error of the sampling and measuring techniques. A total of over 71 liters of brine was removed from hole IG202 between November 30, 1984 and August 24, 1986.

3.2 Room 2

SPDV Test Room 2 was also one of the first rooms excavated in the northern part of the WIPP underground (Figure D-1). Initial mining was finished March 17, 1983 and a number of test holes were drilled in it during the following few weeks. Two of these holes were included in Phase I of the BSEP: inclinometer hole IG201 and stressmeter hole NG252.

3.2.1 Hole IG201

IG201 was drilled for use as an inclinometer observation location and is located near the west rib in the center of Room 2. Brine was used as the drilling fluid. On March 28, 1983 a 74 millimeter (2 7/8th inch) I.D. PVC guide tube identical to the one in Hole IG202 was installed in the hole, and a small-diameter tremie pipe (plastic tubing) was used to grout the liner in

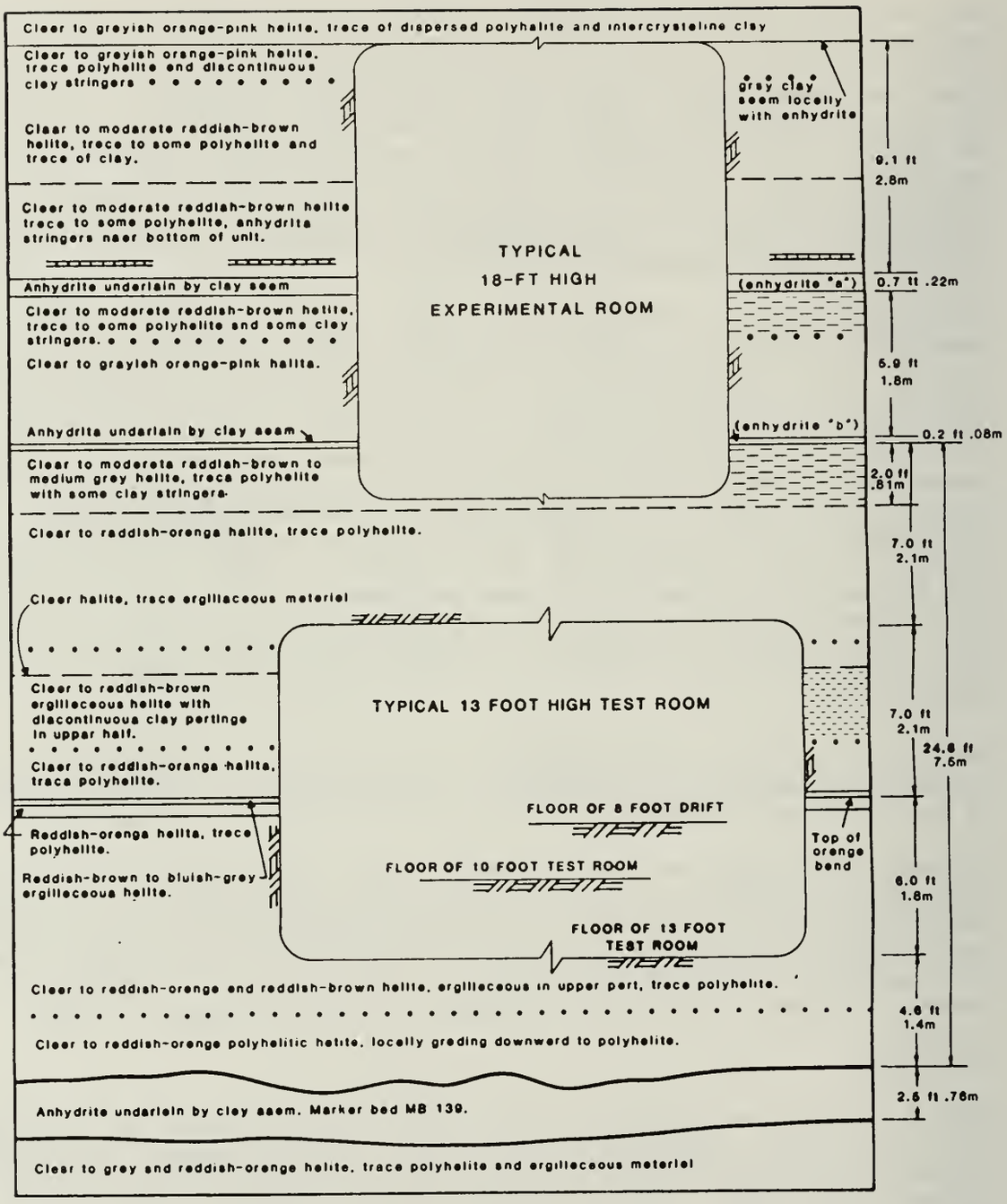

NOTES:

1. Dimensions and lithologic descriptions are derived primarily from corehole and geologic mapping data from the four test rooms and experimental area supplemented by geologic information from the remaining SPDV excavation.
2. Unit thicknesses are approximate and very slightly.
3. Room dimensions have changed with time due to salt-creep closure.

Figure D-2.

Geologic Cross Section of the Facility and Experimental Level

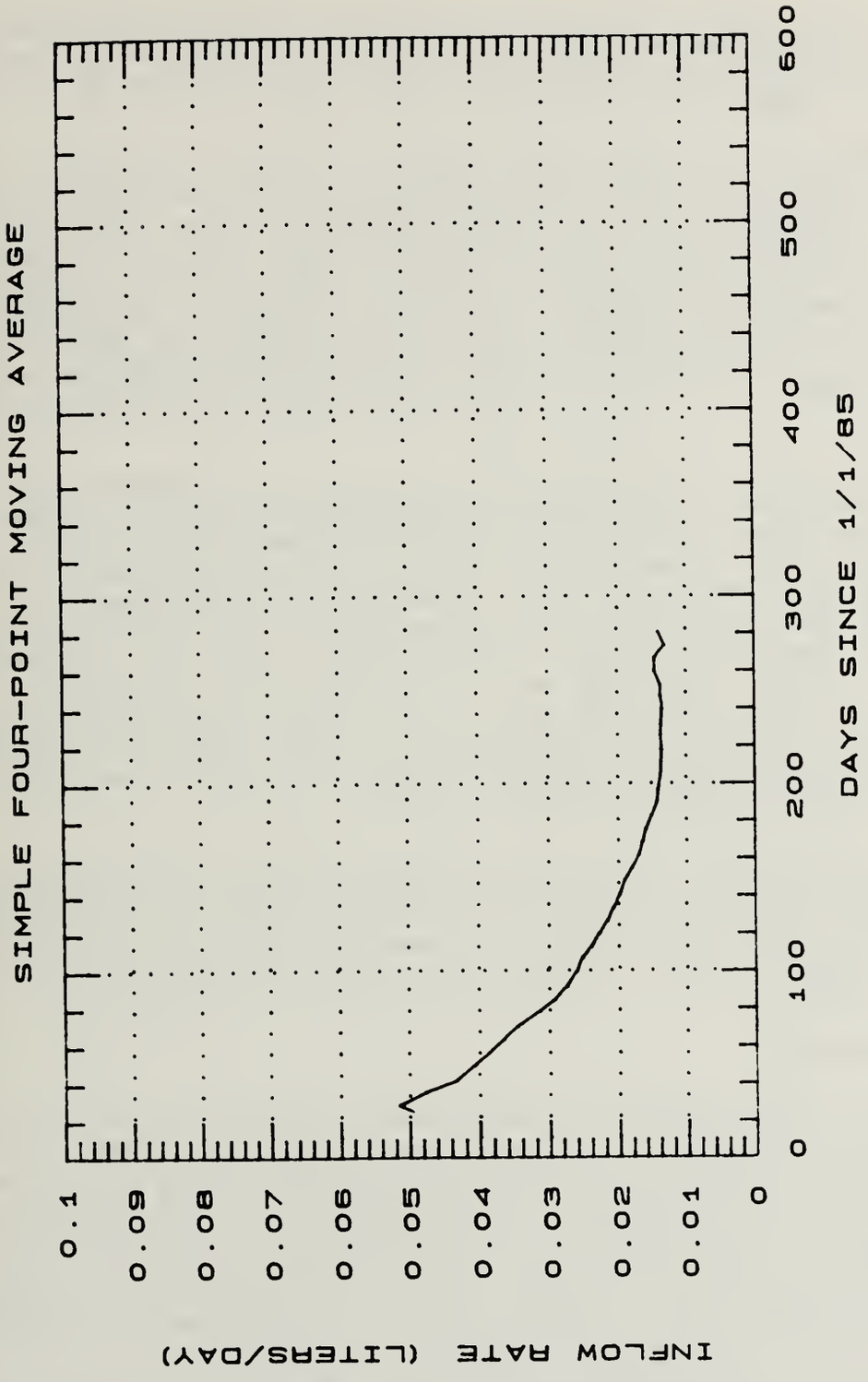

Figure D-3.

IG202 Inflow Rates

place. It is highly likely that the grouting is incomplete and that vertical movement of fluid takes place in open, ungrouted spaces outside the guide tube. When the guide tube was installed, it was filled with fresh water to assist in sinking the guide tube to the bottom of the hole.

On November 21, 1984 fluid filled the hole to within 1.23 meters (4.05 feet) of the collar. It is known that fluids were introduced into this hole on at least two occasions (brine of unknown composition at the time of drilling and fresh water during guide-tube emplacement). The chemistry of fluids in this hole has certainly been affected by the materials and fluids introduced into the hole, especially the grout. Room 2 was also used by the mining contractor as an underground storage area. The origin, quantity, and chemical composition of the fluid in the hole at the time of initial BSEP testing was probably not representative of naturally-occurring, spontaneous inflows from the surrounding rocks.

This hole was the location of some of the initial experiments with air-jet pumping techniques. On November 21, 1984, about 8.4 liters of brine had been removed from the hole when the experimental pumping system failed. On November 30, 1984, an additional 54.7 liters were removed and the inside of the guide tube was blown as dry as possible with high-pressure air. On January 8, 1985, 1.5 liters were removed before the check valve failed on a different experimental sampler. An additional 2.5 liters were removed on January 9, 1985. Some brine was lost during these evacuations, so those figures, although reasonably accurate, represent minimum figures for the amount of brine that was actually in the hole. Evacuation using the vacuum-assisted sampling system and measuring technique described in WIPP Procedure WP 07-410 began January 15, 1985.

Initial brine inflow rates were slightly greater than 0.05 liters per day, decreasing gradually to slightly less than 0.02 liters per day at the end of April, 1986 (Table E.17, Figure D-4). At that time, the guide tube had become so distorted from shear within the bedrock that sampling was discontinued. A total of over 81 liters of brine had been removed from hole IG201 over that period of time.

3.2.2 Hole NG252

Stressmeter downhole NG252 is located about 3 meters north of IG201 in SPDV Test Room 2. This hole has a fairly complicated history (Figure D-5). The initial 38 millimeters (1.5 inch) hole was drilled 2 meters (6.5 feet) deep in March 1983 with brine used as the drilling fluid. The stressmeter failed in December 1983 and on March 4, 1984, the instrument was over-cored with a 152-millimeter (6-inch) core barrel and removed. As a result, the upper 50 centimeters (1.5 feet) of this hole is 152 millimeters (6 inches) in diameter and the bottom 1.5 meters (5 feet) is 38 millimeters in diameter.

On November 21, 1984, this hole was found to be filled with both brine and muck. The top of the brine was 18 centimeters (7 inches) below the collar and the top of the salt muck was 28 centimeters below the collar. Approximately 1.3 liters of brine were removed on November 21, effectively evacuating the hole to the level of the top of the salt muck.

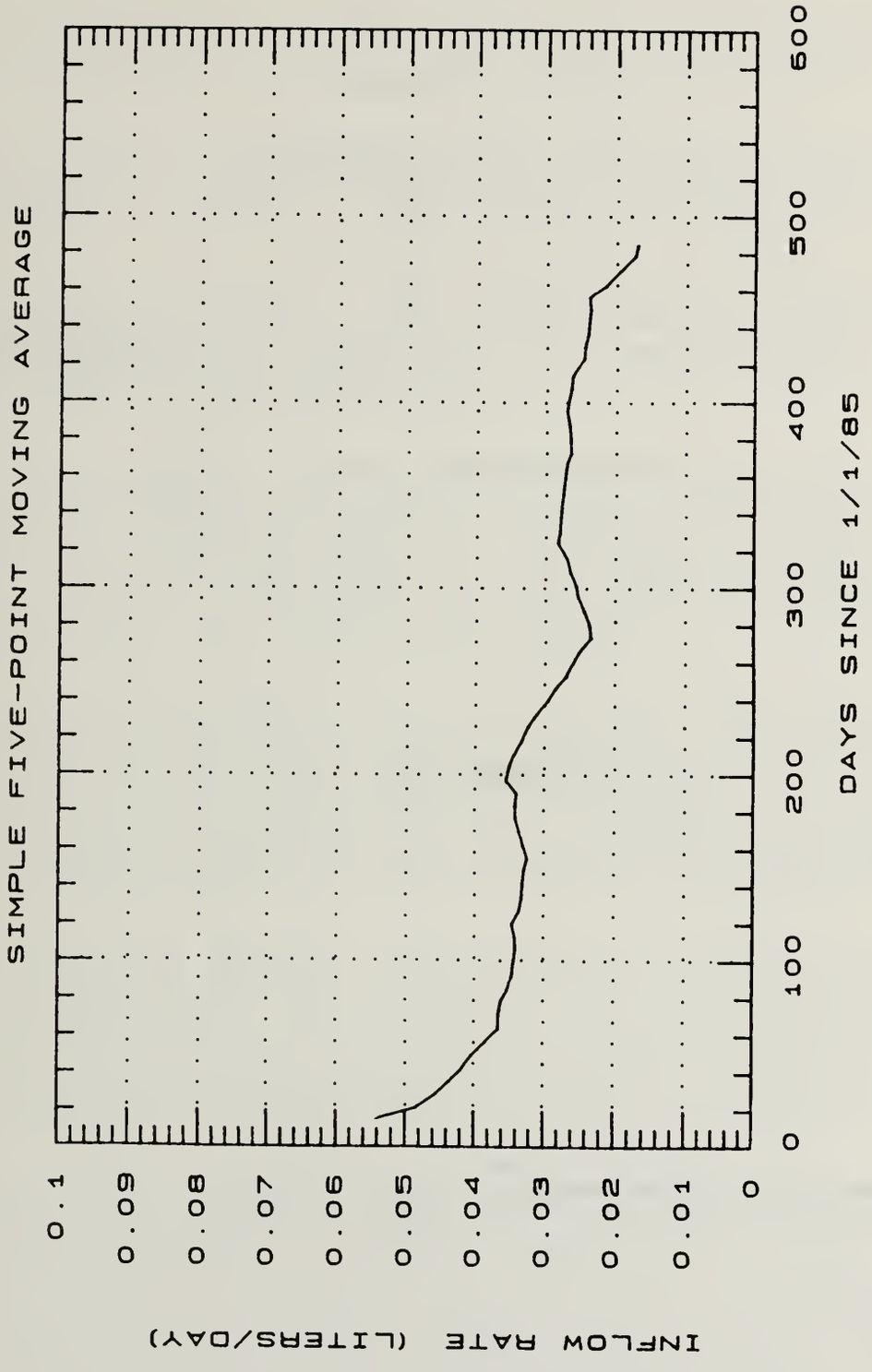

Figure D-4.

IG201 Inflow Rates

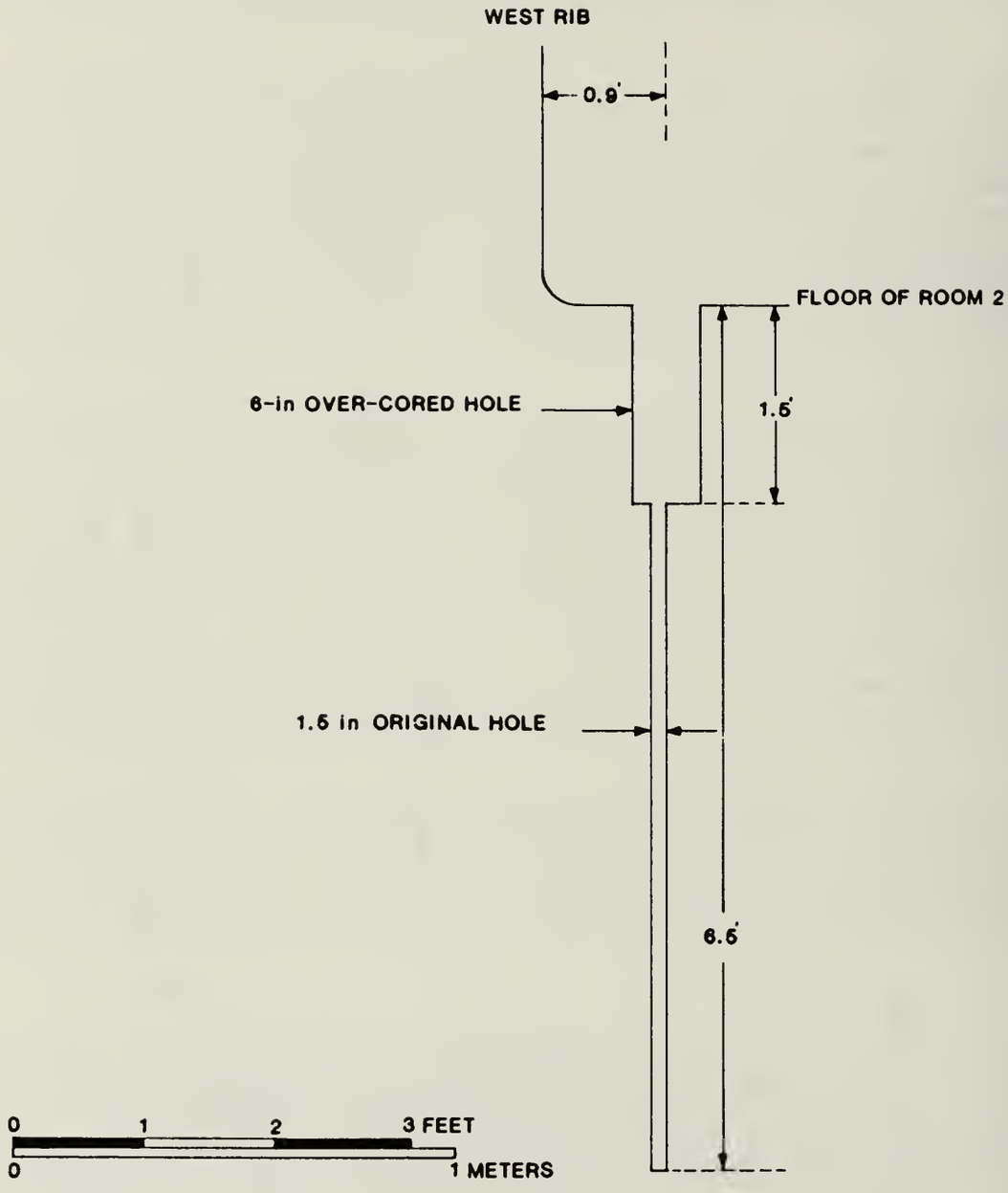

Figure D-5.

NG252 Configuration

Six days later, on November 27, 1984, the brine level had risen to 6.4 centimeters above the salt muck. About 0.76 liters of brine were evacuated, exposing the top of the salt muck. Later that day, the brine level was observed to have risen to completely cover the salt muck.

On November 29, 1984, compressed air was used to blow all the salt muck and accumulated brine out of NG252. The quantity of brine that was blown out was not measured, but it amounted to several liters. PVC casing with a cap was installed to prevent debris from entering and plugging the hole.

Twenty days later, on December 19, 1984, representatives of the Environmental Evaluation Group (EEG) collected a sample of brine from this location. On that date, the level of the brine surface had risen to approximately the level observed on November 21; 18 centimeters below the collar or about 50 centimeters below the top of the new PVC casing.

Since this hole was easily accessible, known to produce brine, and of small diameter, it was selected as the location for initial observations. The hole was evacuated and a short-term inflow test was performed following normal surface-well recovery analysis techniques. Initial brine levels were measured every hour. Intervals between measurements were lengthened as appropriate once initial inflow rates were determined. Measurements continued around the clock until the brine level stabilized (Table E.20).

The diameter of the hole enlarges from 38 to 152 millimeters at a point approximately 1.5 meters above the bottom of the hole. The inflow data was recorded as the increasing level of brine in the hole with time. To correct for the change in hole diameter, brine level was converted to approximate volume of brine in the hole by multiplying by the appropriate cross-sectional area. The calculations were made using Lotus 123 software. This figure is reported as equivalent volume in liters in Table E-20 and on Figures D-6 and D-7.

The data for the rise in static level was plotted both as an X-Y plot (Figure D-6) and as a semi-log plot (Figure D-7), the more conventional form for recovery graphs. These curves are not strictly analogous to "recovery tests," however, since the initial point for the curves probably does not represent a steady-state drawn-down condition. In addition, the distribution of potential energy (hydrologic regime) of the brine in the vicinity of the underground drill holes is still poorly understood.

Brine flowed into the evacuated hole from the fractures and pores close to the hole and, for a while, the hole actually filled faster the fuller it became. This can be seen on Figure D-6 between approximately 35 and 175 hours. Both graphs show an abrupt change-in-slope at a brine level of approximately 1.5 liters, where the hole diameter enlarged from 38 to 152 millimeters. Inflow ceased after the hole became filled with brine to a depth of approximately 6.1 feet. The floor of Room 2 slopes down toward the south, and it is probable that when Hole NG252 is filled to this level, additional inflow ceases because the brine discharges through some undetermined flow path into unconsolidated muck on the floor of Room 2. The conclusion reached was that this type of data, although interesting, is not very useful unless an equilibrium draw-down state is established prior to recording the rising brine level.

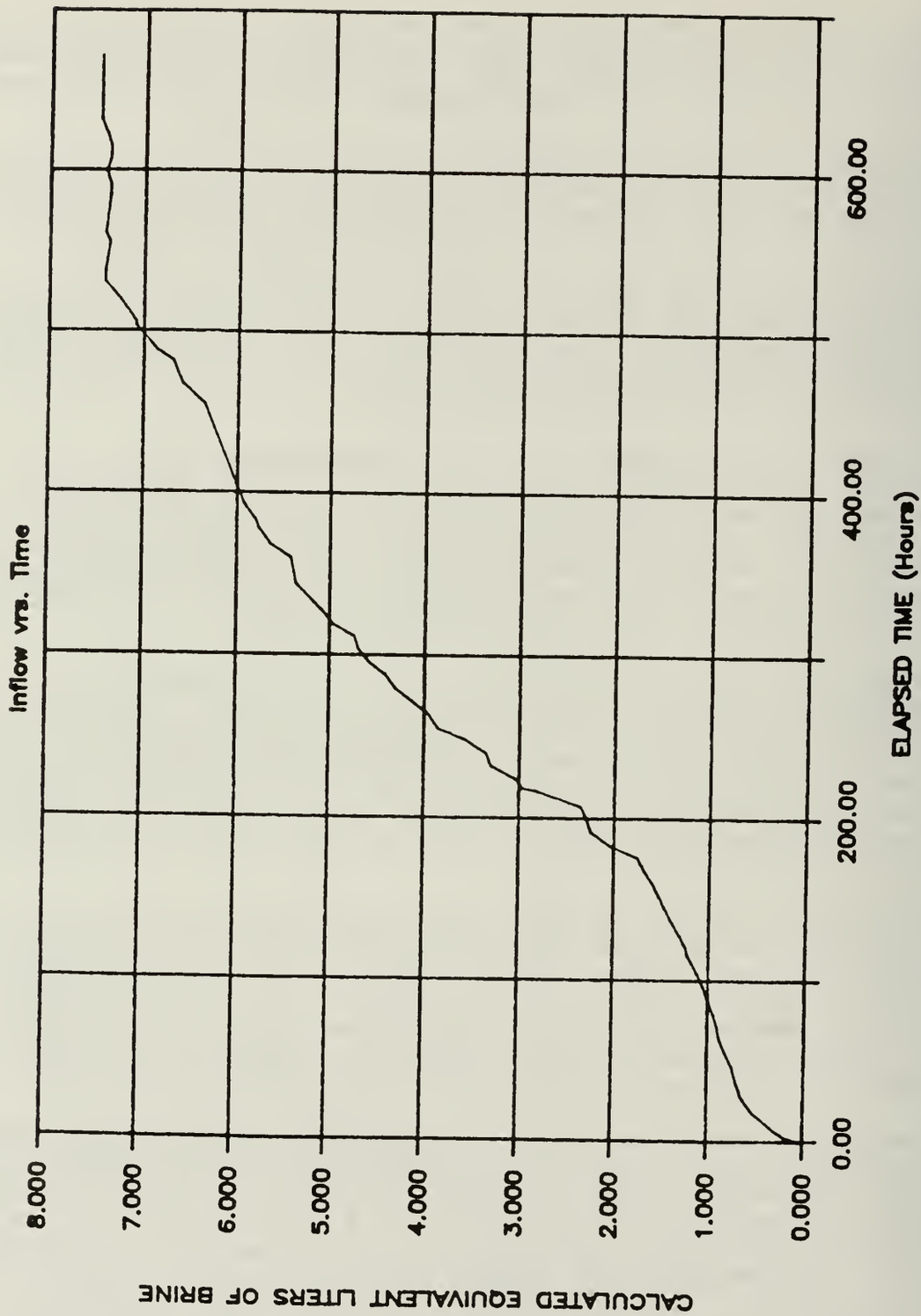

Figure D-6.

NG252 Short Term Inflow

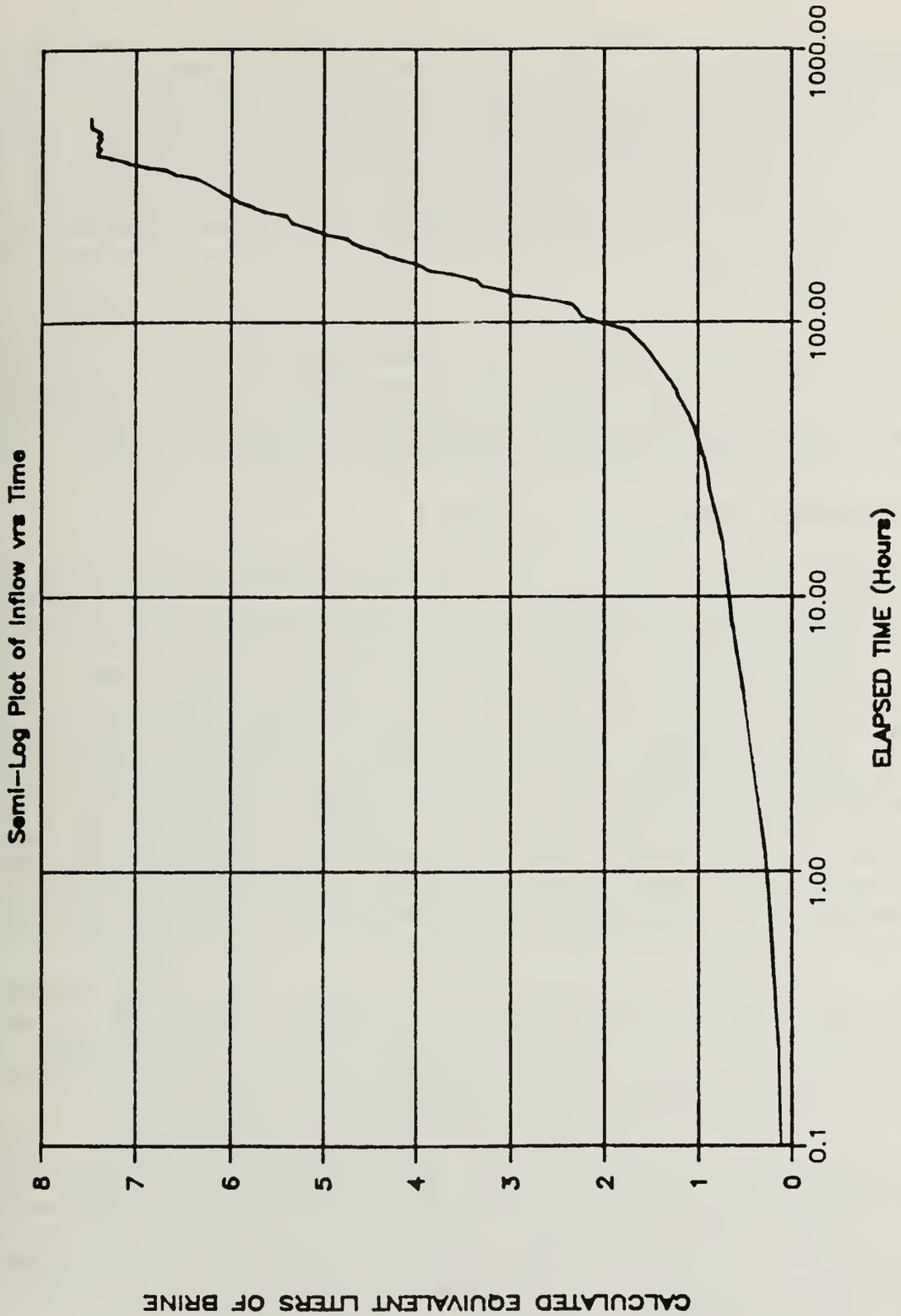

Figure D-7.

Semi-Log Plot of NG252 Short Term Inflow

Starting in February 1985, brine was bailed from NG252 on a regular basis (Table E.21; Figure D-8). Inflow rates were initially close to 0.6 liters per day, gradually declining to about 0.27 liters per day by August 19, 1986. Over 235 liters of brine had been removed from this hole by that date. Significant quantities of gas are associated with the brine inflow into NG252. Gas bubbles are almost always observed. Brine withdrawn from the hole effervesces immediately after bailing as it is poured from one container into another. NG252 penetrates anhydrite Marker Bed 139 and most of the brine flows into this hole from a fracture very close to the bottom of the hole, near the base of Marker Bed 139 (Figure D-2).

NG252 is the largest brine producer of any of the drill holes observed during Phase I of the BSEP, and appears to be something of an anomaly. It is located in close proximity to a completely dry downhole. The dry hole is approximately 4.7 meters east of NG252 on the centerline of Room 2, is 15 centimeters in diameter, is 1.65 meters deep, and penetrates into MB 139. It does not appear to completely penetrate MB 139, which may be the reason it is dry.

3.3 Experimental Rooms A1, A2, A3, and B

Experimental Rooms A1, A2, A3, and B are in the northeastern part of the WIPP underground workings (Figure D-1). Excavation of Room A1 was completed in October 1984, Room A2 in July 1984, Room A3 in November 1984, and Room B in June 1984. They are 5.5 meters (18 feet) high and are excavated in a zone about 6 meters (20 feet) stratigraphically higher than the rest of the workings (Figure D-2). As a result, the drill holes penetrate a slightly different stratigraphy, a fact that results in especially useful data. The end of 15-meter upholes typically penetrate rocks about seven meters stratigraphically above the end of other 15-meter upholes. Hole A1X02 is 18 meters long and penetrates an additional 3 meters, intersecting an anhydrite interbed not present in the other three upholes in Rooms A2, A3, and B. Downholes typically penetrate MB139 at depths of 7 to 7.6 meters. The data from these holes reflects both the sampling of different geological horizons and, perhaps, more importantly, interbeds such as MB 139 under different stress conditions than is encountered elsewhere in the facility.

These rooms all contain many experimental and instrument holes (Appendix A), almost all of which are inaccessible to the BSEP. In early 1985, a pair of stratigraphic observation holes were drilled in each of these rooms. These holes were drilled with air as the drilling fluid. Inflow to these pairs of holes have been monitored from the time they were drilled.

The A and B rooms are the location of the heated room experiments. Canisters containing electric heaters have been emplaced at the stratigraphic level of the facility, below the floor of the rooms. The power was turned on to the heaters in the A rooms on October 2, 1985 (day 274 after 1/01/85), and in Room B on April 23, 1985 (day 112 after 1/01/85). Since that time the rooms have been heating up, a factor that is expected to effect both the inflow of brine and the brine chemistry.

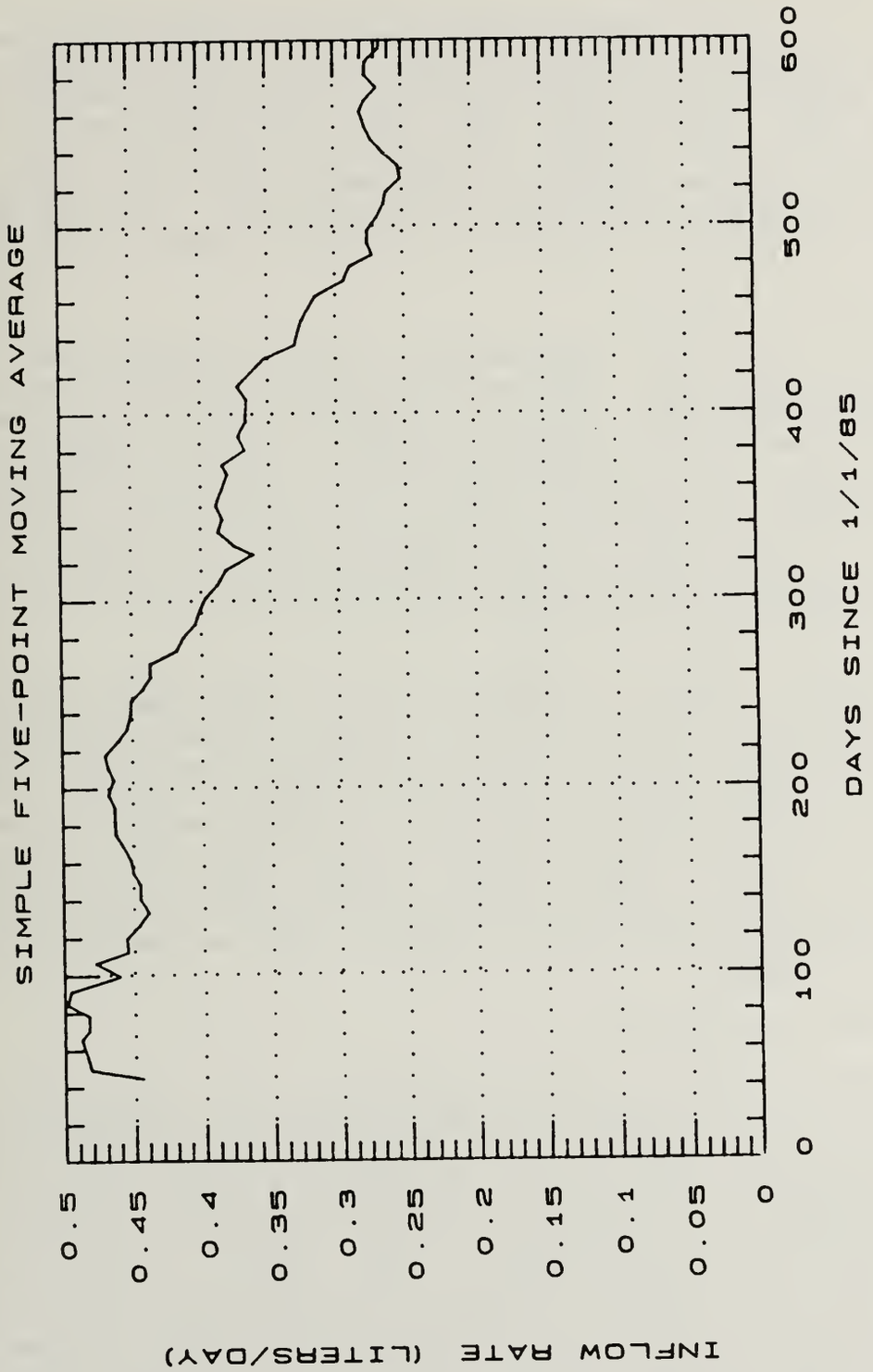

Figure D-8.

NG252 Inflow Rates

3.3.1 Room A1, Hole A1X01

Hole A1X01 is a downhole drilled in the south end of Room A1 on February 26, 1985. No brine or gas was noticed during drilling. Brine accumulations were noticed shortly after drilling. Brine was first removed from this hole on March 12, 1985. Inflow rates in April 1985, were on the order of 0.047 liters per day, gradually decreasing to slightly greater than 0.026 liters per day in October 1985. Inflow appeared to stabilized at that rate and remained quite constant through August 1986 (Table E.1, Figure D-9). A total of approximately 15.3 liters of brine had been removed from A1X01 by August 19, 1986.

3.3.2 Room A1, Hole A1X02

Hole A1X02 is an uphole completed March 7, 1985, in the south end of Room A1, directly over hole A1X01. The end of this hole penetrates beds that are stratigraphically higher than those penetrated by any of the other holes monitored as part of the BSEP, intersecting an additional anhydrite interbed. Drillers noted that brine entered the hole at a depth of 3.55 meters. The hole was reamed on February 28, 1985 to a 12.7 centimeters (5-inch) diameter for the first 3.7 meters to eliminate drilling problems caused by moist cuttings. A moist area was noted developing around the collar on March 7, 1985. On March 12, 1985 the moist area on the back (roof) extended for a third of a meter in all directions from the drill hole.

Several different types of collecting devices were installed, with successful collection of brine first occurring on April 2, 1985. Most of the irregularities in the data (Table E.2) are a result of collecting difficulties and evaporation losses, not real variations in brine inflow. Inflow rates were on the order of 0.02 liters per day between drilling and the end of October 1985, decreasing slightly between November 1985 through June 1986, followed by an increase to almost 0.04 liters per day in August 1986 (Figure D-10). A total of over 8.7 liters of brine had been collected from this hole by August 19, 1986. A significant, additional amount was certainly produced from the hole but lost by dissipation near the borehole collar and evaporation to the repository atmosphere.

3.3.3 Room A2, Hole A2X01

Hole A2X01 is a downhole completed February 9, 1985 in the north end of Room A2. No brine or gas inflows were noted during drilling, but moist, irregular vugs were observed in the core, usually in coarsely crystalline polyhalitic halite, clear halite, and halite containing some brown clay. Brine accumulations were noticed shortly after drilling. Brine-soaked muck containing some oil (contamination from the drilling operations) was first removed from this hole on February 19, 1985. Mixtures of brine and muck were also bailed from the hole on March 7, 1985 and March 12, 1985. On March 20, 1985, 0.52 liters of fairly clear brine were removed from the hole (Table E.3). Initial inflow rates in late March and early April 1985, were slightly greater than 0.05 liters per day, declining fairly rapidly to slightly less than 0.035 liters per day by mid-May. Inflow then remained quite steady, decreasing very gradually to about 0.025 liters per day in late August 1986 (Table E.3, Figure D-11). A total of approximately 16.8 liters of brine had been removed from A2X01 by August 19, 1986.

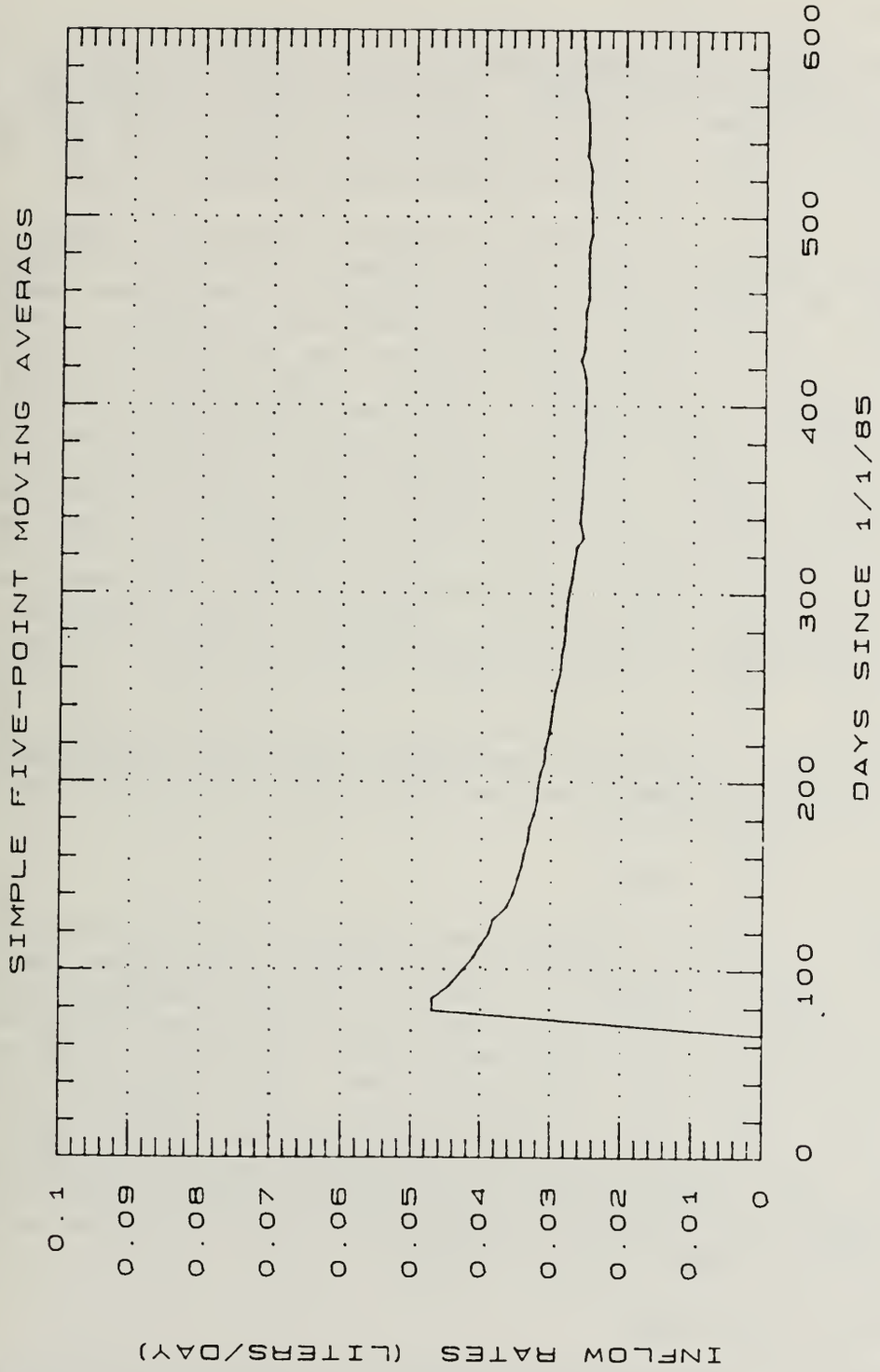

Figure D-9.

AlX01 Inflow Rates

3.3.4 Room A2, Hole A2X02

Hole A2X02 is an uphole completed February 20, 1985, in the north end of Room A2, directly over Hole A2X01. The drillers noted that the hole produced brine during drilling at both 3.5 meters and 7.7 meters. The hole was reamed on February 13, 1985, to a 12.7 centimeter (5-inch) diameter for the first 7.6 meters to eliminate drilling problems caused by moist cuttings.

A collecting device was installed on the hole February 19, 1985. The same difficulties described for Hole A1X02 were encountered, and the same cautions concerning the use of the data are applicable. A moist area immediately developed on the back (roof) around the hole and was about 1.5 meters in diameter on March 12, 1985. The irregularities in the data are mostly the result of problems in collecting the brine. A large amount of brine is known to have been lost by evaporation. Inflow rates were over 0.03 liters per day in March 1985, but then decreased to less than 0.01 liters per day (Table E.4, Figure D-12). Problems with the collecting device from April through August 1985 resulted in most of the brine inflows escaping and not being recorded, so the low readings during that time period do not reflect the fact that considerable brine flowed from Hole A2X02. Flow does appear to have been much lower during the winter of 1985-86, but shows an increase in the summer of 1986 to more than about 0.015 liters per day. Figure D-12 shows trends that roughly parallel the humidity measurements taken in the room, but the above-mentioned collecting uncertainties caution against drawing too strong a correlation.

Approximately 3.35 liters of brine had been collected from Hole A2X02 by August 19, 1986. A significant additional amount was certainly produced from the hole but lost by dissipation near the borehole collar and evaporation to the repository atmosphere.

3.3.5 Room A3, Hole A3X01

Hole A3X01 is a downhole completed on January 14, 1985 in the south end of Room A3. No brine or gas inflows were noted during drilling, but moist, irregular vugs were observed in the core, usually in coarsely crystalline polyhalitic halite, clear halite, and halite containing some brown clay. Brine accumulations were noticed shortly after drilling. Brine-soaked muck was noticed in this hole on February 5, 1985. Approximately 0.3 liters of brine, muck, and oil was removed from the hole on February 19, 1985 (Table E.5). Inflow rates in February and March were on the order of 0.03 liters per day, decreasing gradually through October 1985, and then maintaining a fairly constant inflow slightly greater than 0.02 liters per day through August 1986 (Table E.5, Figure D-13). Over 13.6 liters of brine had been removed from A3X01 by August 19, 1986.

3.36 Room A3, Hole A3X02

Hole A3X02 is an uphole completed January 22, 1985 in the south end of Room A3, directly over Hole A3X01. No brine or gas inflows were noted during drilling, but moist, irregular vugs were observed in the core, usually in coarsely crystalline polyhalitic halite, clear halite, and halite containing some brown clay. Brine accumulations were noticed shortly after drilling. A collecting device was installed February 5, 1985 and on February 19, 1985, over 0.1 liters of brine had accumulated in the collection container. The wet

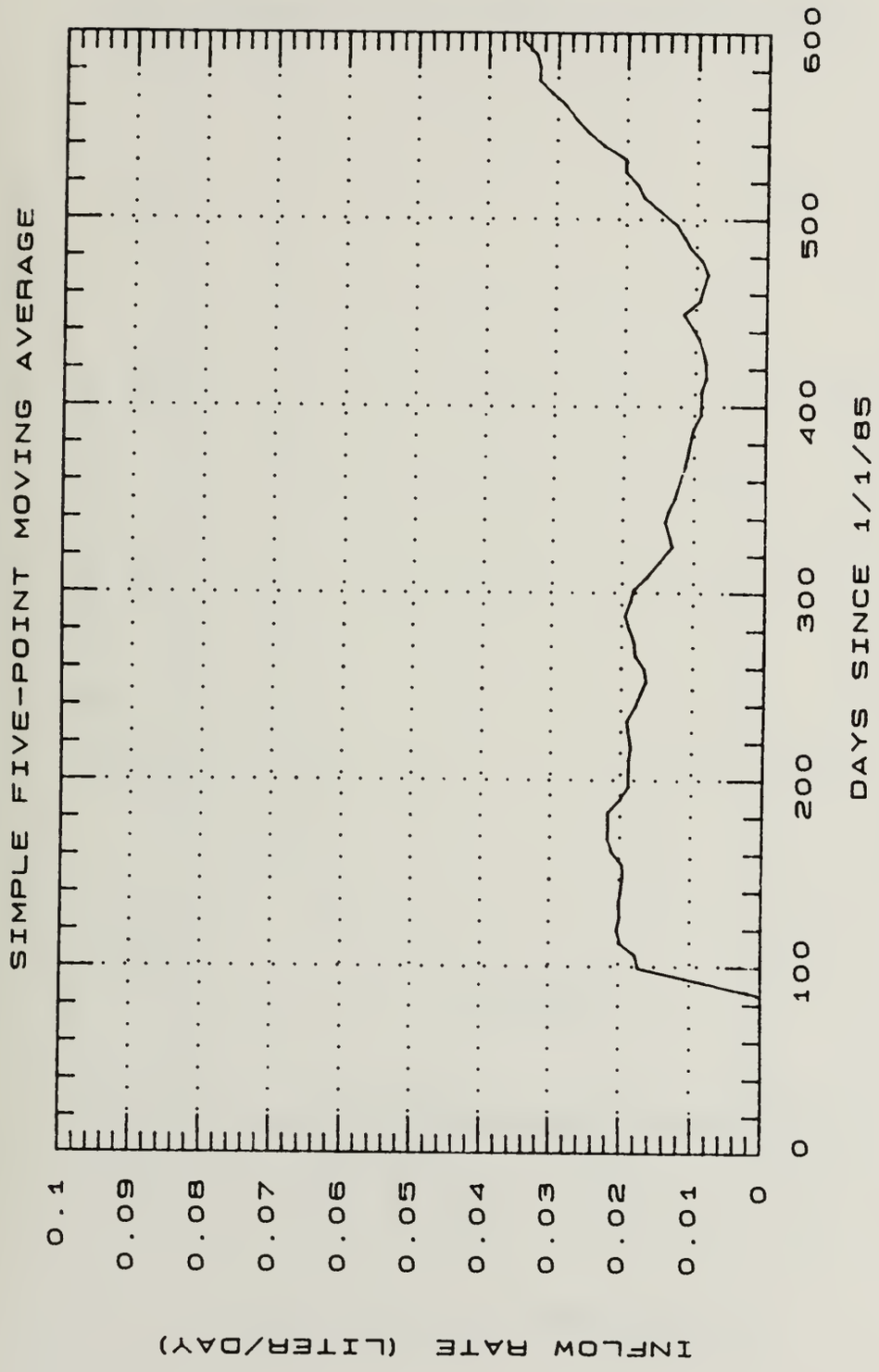

Figure D-10.

A1X02 Inflow Rates

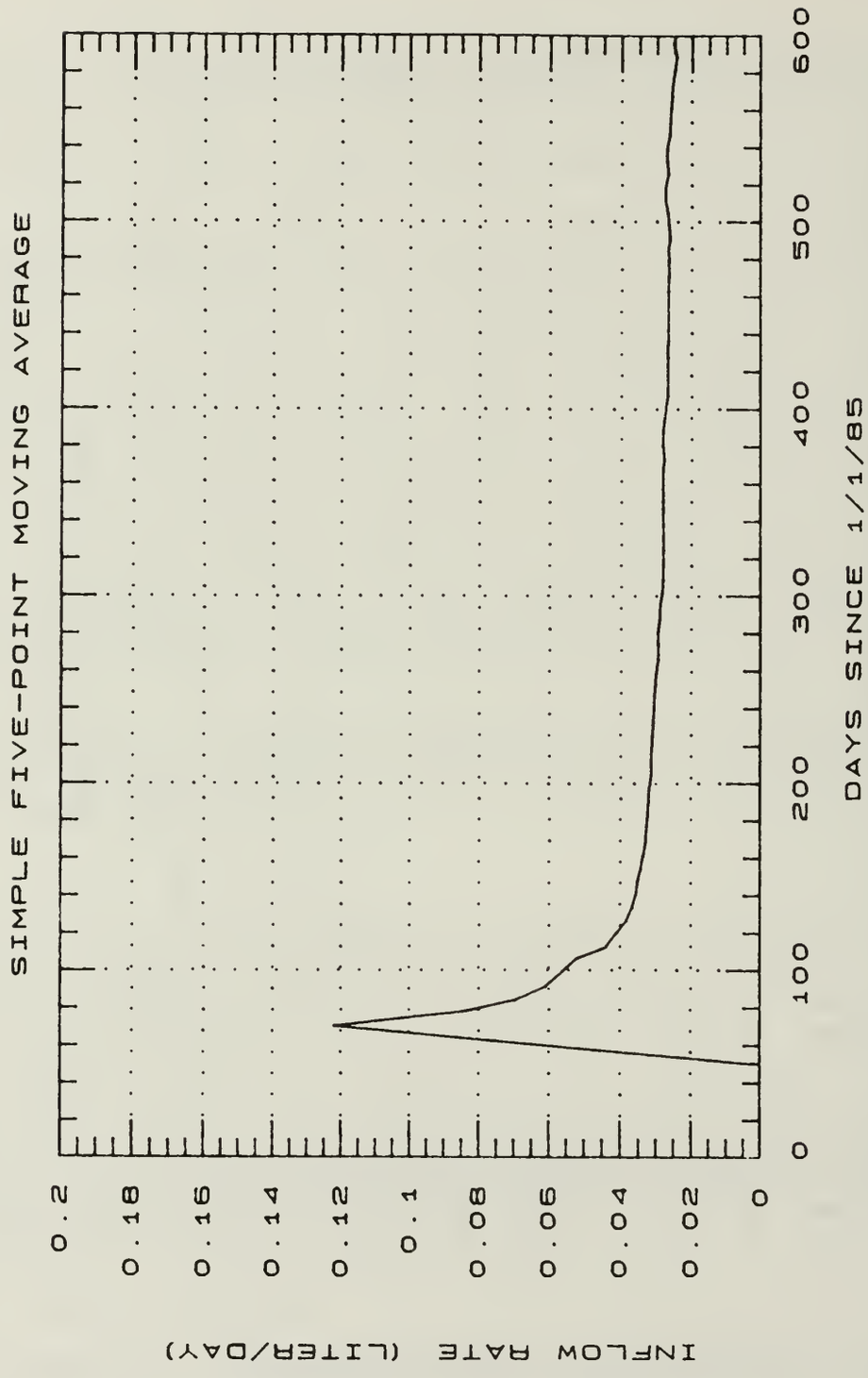

Figure D-11.

A2X01 Inflow Rates

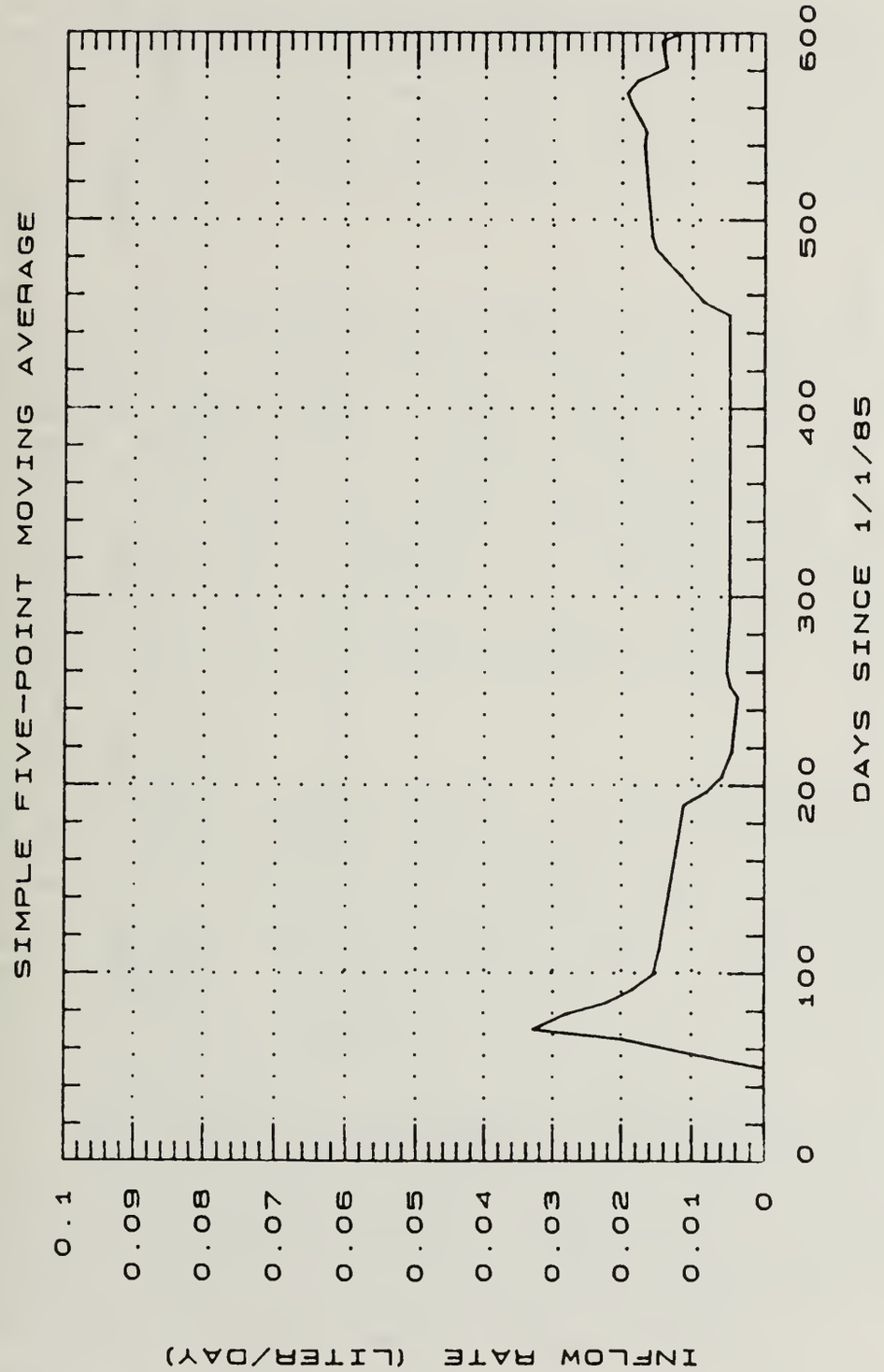

Figure D-12

A2X02 Inflow Rates

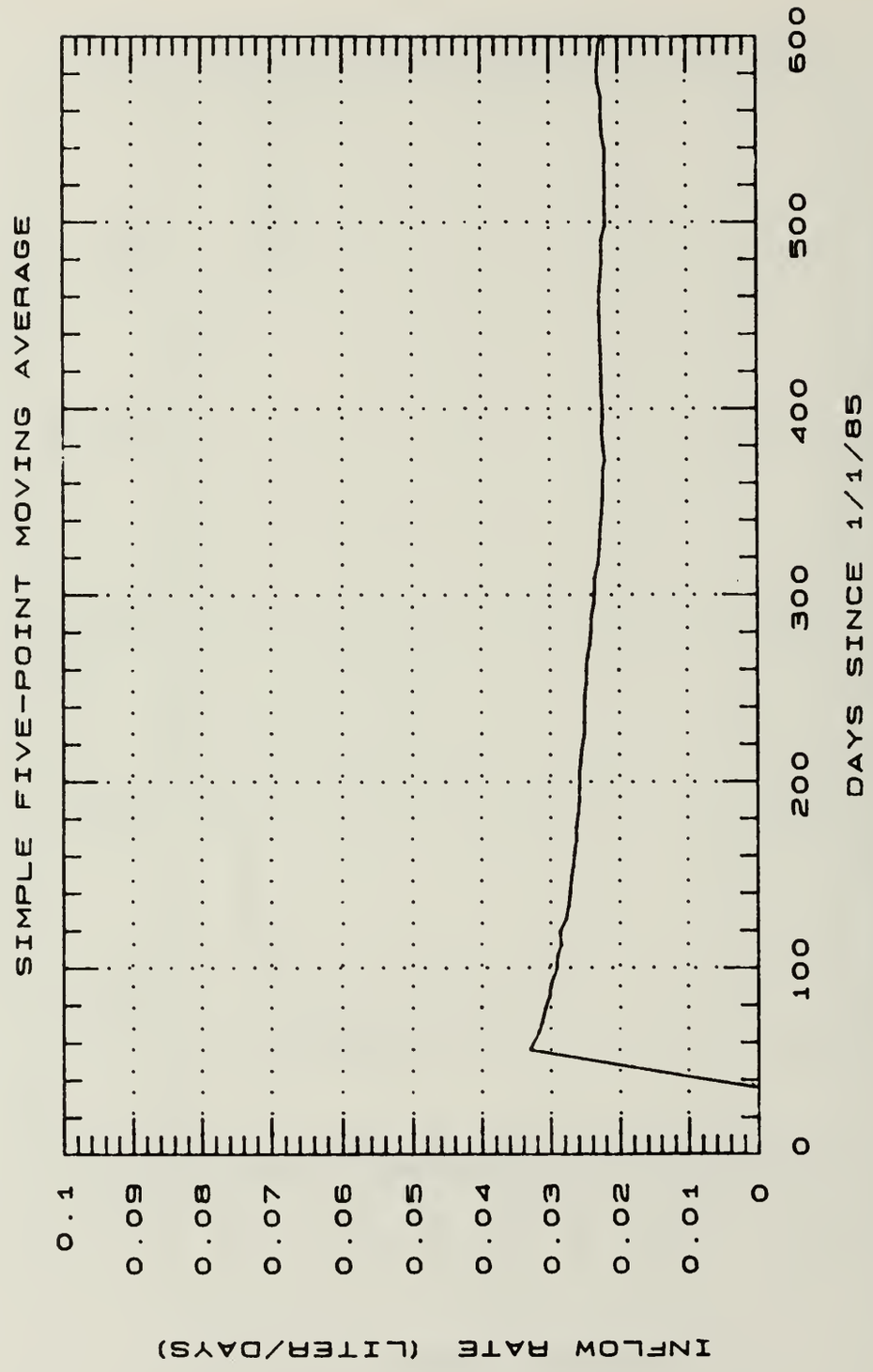

Figure D-13.

A3X01 Inflow Rates

area on the back (roof) was 3 feet in diameter by February 26, 1985. Inflow rates exceeded 0.02 liters per day in March 1985, declined slowly to about 0.01 liters per day in October 1985, and then declined more rapidly to trace amounts (0.01 liters per day or less) by the end of January 1986 (Table E.6, Figure D-14). A total of approximately 4.4 liters of brine had been collected by the end of January 1986, when significant inflows effectively ceased. An additional amount was certainly produced from the hole but lost by dissipation near the borehole collar and evaporation into the repository atmosphere.

3.3.7 Room B, Hole BX01

Hole BX01 is a downhole completed on January 27, 1985 in the north end of Room B. Marker Bed 139 was penetrated from 7.09 to 7.91 meters. When the core from 10.7 to 11.1 meters was removed from the core barrel, it was visibly wet with brine, and brine dripped from the fresh core. This interval consisted of clear to light reddish-orange, coarsely crystalline halite and polyhalitic halite. Moist, irregular vugs were observed in the core, usually in coarsely crystalline polyhalitic halite, clear halite, and halite containing some brown clay. Brine accumulations were noticed shortly after drilling. Approximately 0.4 liters of brine and muck were bailed from the hole on February 5, 1985 (Table E.7). Inflow rates in February 1985, were on the order of 0.1 liters per day, declining to about 0.06 liters per day by the end of April 1985 (Table E.7, Figure D-15). Inflow rates then continued through August 1986, showing only a slight decline to about 0.05 liters per day. A total of over 32 liters had been collected from BX01 by August 19, 1986.

3.3.8 Room B, Hole BX02

Hole BX02 is an uphole completed February 1, 1985 in the north end of Room B, directly over Hole BX01. Some moisture was noted on the core at 2.9 meters, but presented no problems to the drilling operations. The drillers noted that the hole was dry at completion of the drilling. Moist, irregular vugs were observed in the core, usually in coarsely crystalline polyhalitic halite, clear halite, and halite containing some brown clay. A collecting device was attached to the collar of the hole on February 5, 1985, and a few drops of brine were observed in the collecting container on March 12, 1985. On March 20, 1985, about 0.1 liter was removed from the collecting device (Table E.8). In April 1985, the inflow rate was on the order of 0.02 liters per day, declining gradually to about 0.015 liters per day in June 1985 (Table E.8, Figure D-16). Inflow then declined abruptly so that by the end of July 1985, only trace amounts were noticed. The evaporation problem has been exacerbated by the increasing air temperatures that began to develop in this room after the heaters were turned on. A total of about 1.75 liters of brine were collected from BX02 by the middle of January 1986. An additional amount was certainly lost by dissipation near the borehole collar and evaporation to the repository atmosphere, and the hole has been essentially dry since the end of January 1986.

3.4 Room G

Room G extends farther to the northwest than any of the rest of the WIPP underground workings (Figure D-1). It was excavated in November through December 1984. Four pairs of 15-meter up and down, vertical, stratigraphic observation holes were drilled to obtain geologic cores. These holes were

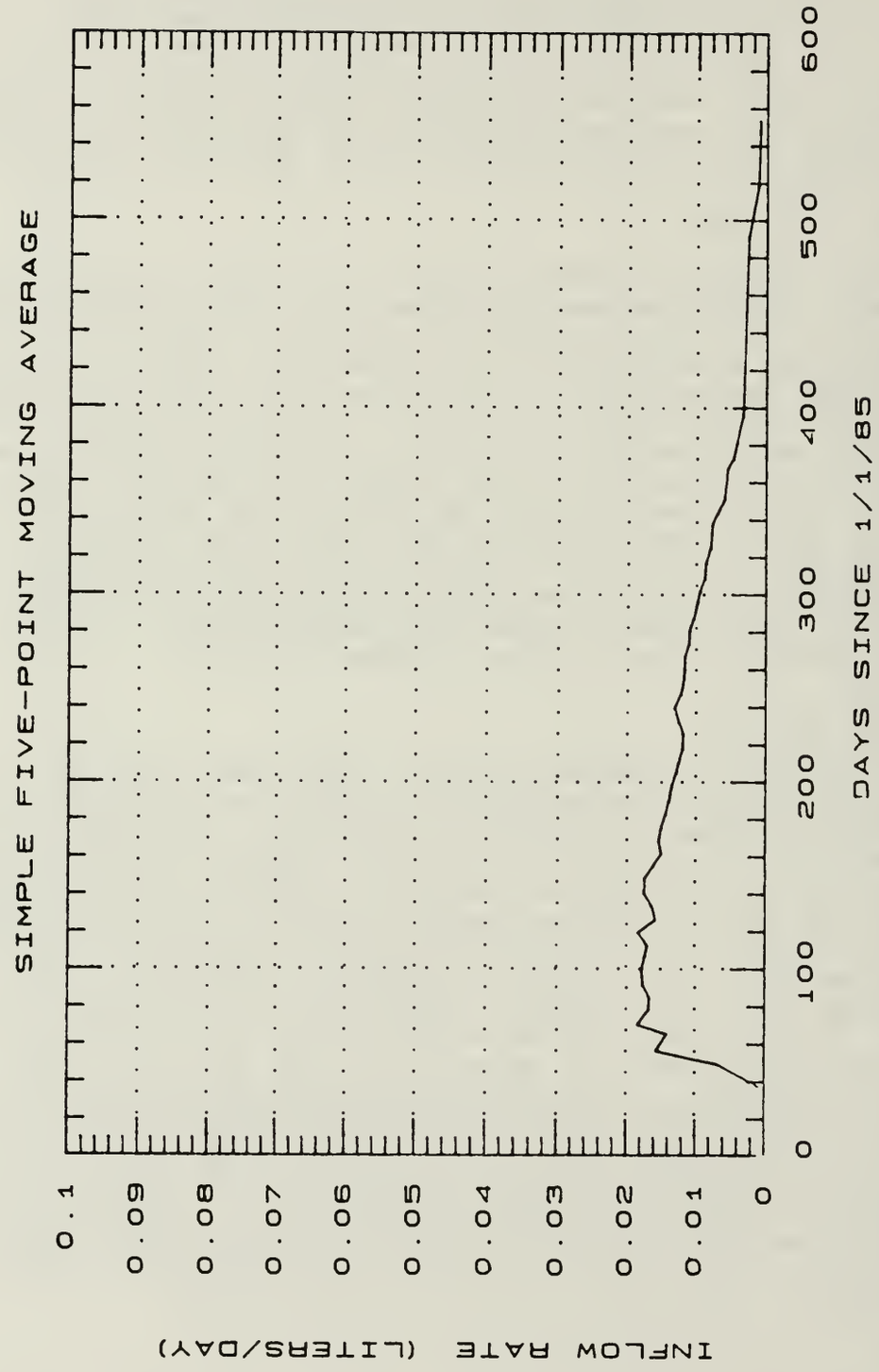

Figure D-14

A3X02 Inflow Rates

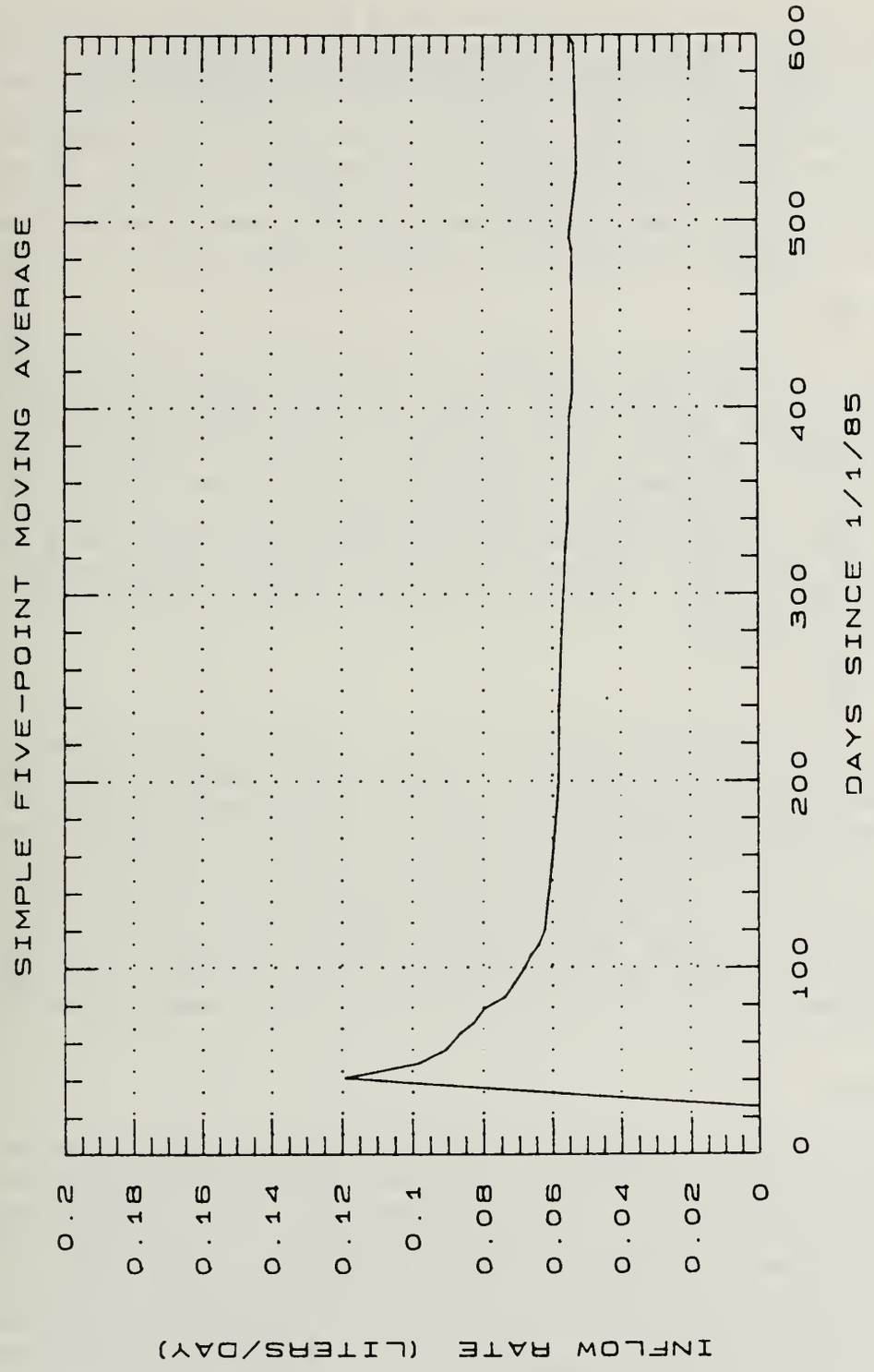

Figure D-15.

BX01 Inflow Rates

drilled with air as the drilling fluid. They were monitored from the time of drilling as part of the BSEP. The numbering system used assigned odd numbers to the upholes (DH35, DH37, DH39, and DH41) and even numbers to the corresponding downholes (DH36, DH38, DH40, and DH42). As a result of poor core recovery from the 6- to 12-meter interval in the westernmost downhole, DH42, an offset hole, DH42A, was drilled 12 meters deep, 2 meters west of DH42. It is interesting to note the striking difference in the inflow into this pair of holes, only 2 meters apart. Marker Bed 139 was generally intersected at depths of about 1.4 to 2 meters below the floor of Room G (Figure D-2).

3.4.1 Hole DH36

Hole DH36 is the easternmost downhole in Room G and was completed January 26, 1985. No brine or gas inflows were noted during drilling, but brine accumulations were noticed shortly after drilling. Moist muck was observed in the bottom of the hole on January 28, 1985 and 2.5 liters of brine, muck, and hydraulic fluid (contamination from drilling) were bailed from the hole on February 5, 1985 (Table E.10). Initial inflow rates were on the order of 0.25 liters per day and remained quite steady, decreasing only slightly through August 1986, when inflow rates still exceeded 0.2 liters per day (Table E.10, Figure D-17). Almost 125 liters of brine had been removed from DH36 by August 19, 1986.

3.4.2 Hole DH38

Hole DH38 is a downhole completed January 26, 1985 just east of the center of Room G. No brine or gas inflows were noted during drilling, but brine accumulations were noticed shortly after drilling. Moist muck was observed in the bottom of the hole on February 5, 1985 and 0.8 liters of brine and muck were bailed from the hole on February 19, 1985 (Table E.12). Initial inflow rates exceeded 0.1 liters per day in February 1985, but by mid-March had declined to less than 0.06 liters per day (Table E.12, Figure D-18). Inflow rates show a slightly increasing trend through October 1985, followed by a slightly decreasing trend through August 1986, but overall the inflow rate has been remarkably steady. Over 34 liters of brine had been removed from DH38 by August 19, 1986.

3.4.3 Hole DH40

Hole DH40 is a downhole completed January 25, 1985 just west of the center of Room G. No brine or gas inflows were noted during drilling, but brine accumulations were noticed shortly after drilling. Moist muck was observed in the bottom of the hole on February 5, 1985 and about a liter of brine, muck, and hydraulic fluid was bailed from the hole on April 17, 1985 (Table E.13). Calculated inflow rates in April 1985 exceeded 0.04 liters per day but quickly decreased to about 0.01 liters per day in May, then decreased only gradually through August 1986 (Table E.13, Figure D-19). A total of slightly more than 4.3 liters had been removed from DH40 by June 3, 1986.

3.4.4 Hole DH42

Hole DH42 is a downhole completed on January 23, 1985 at the west end of Room G. No brine or gas inflows were noted during drilling, but brine accumulations were noticed shortly after drilling. Moist muck was observed in the

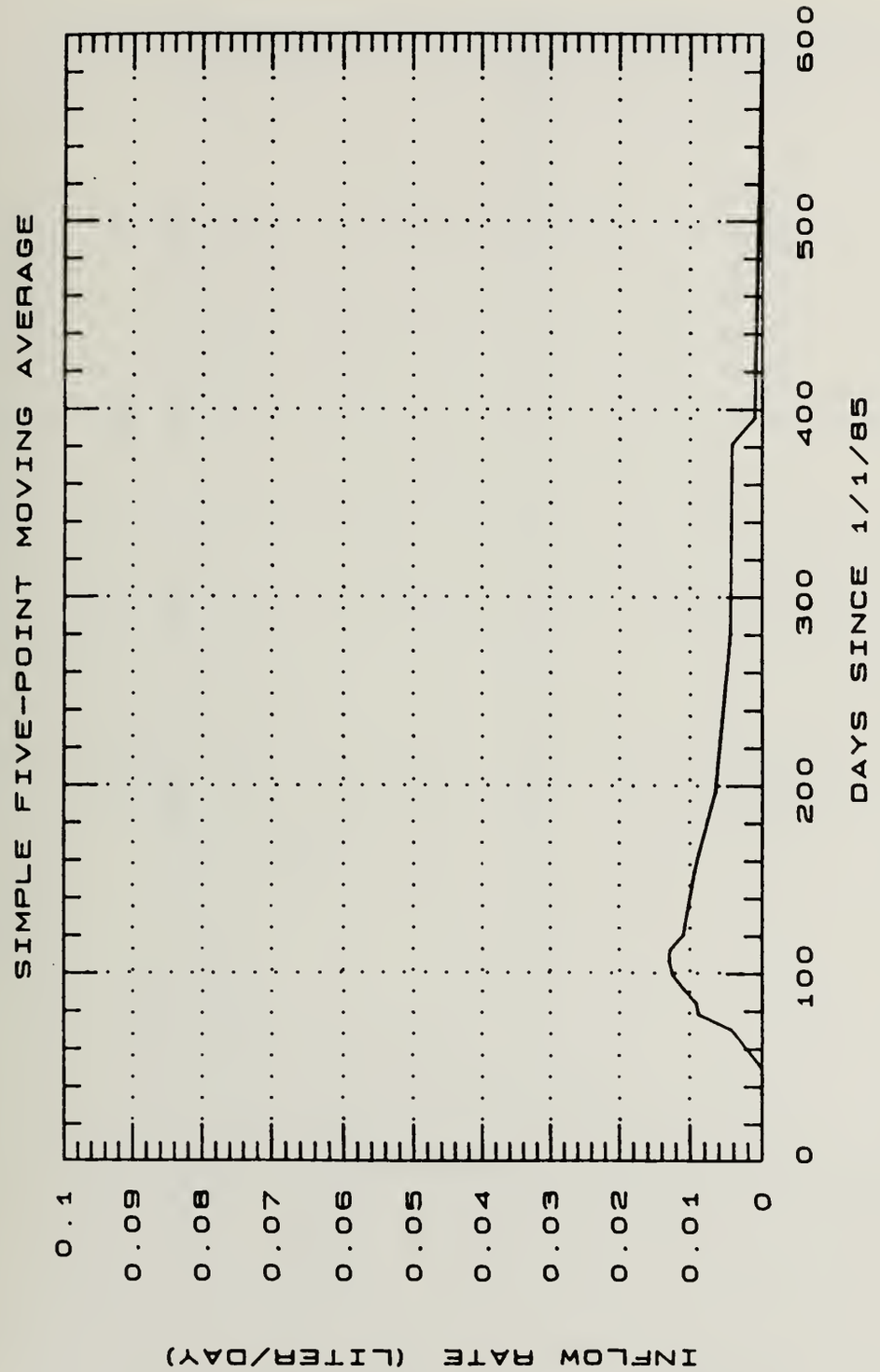

Figure D-16.

BX02 Inflow Rates

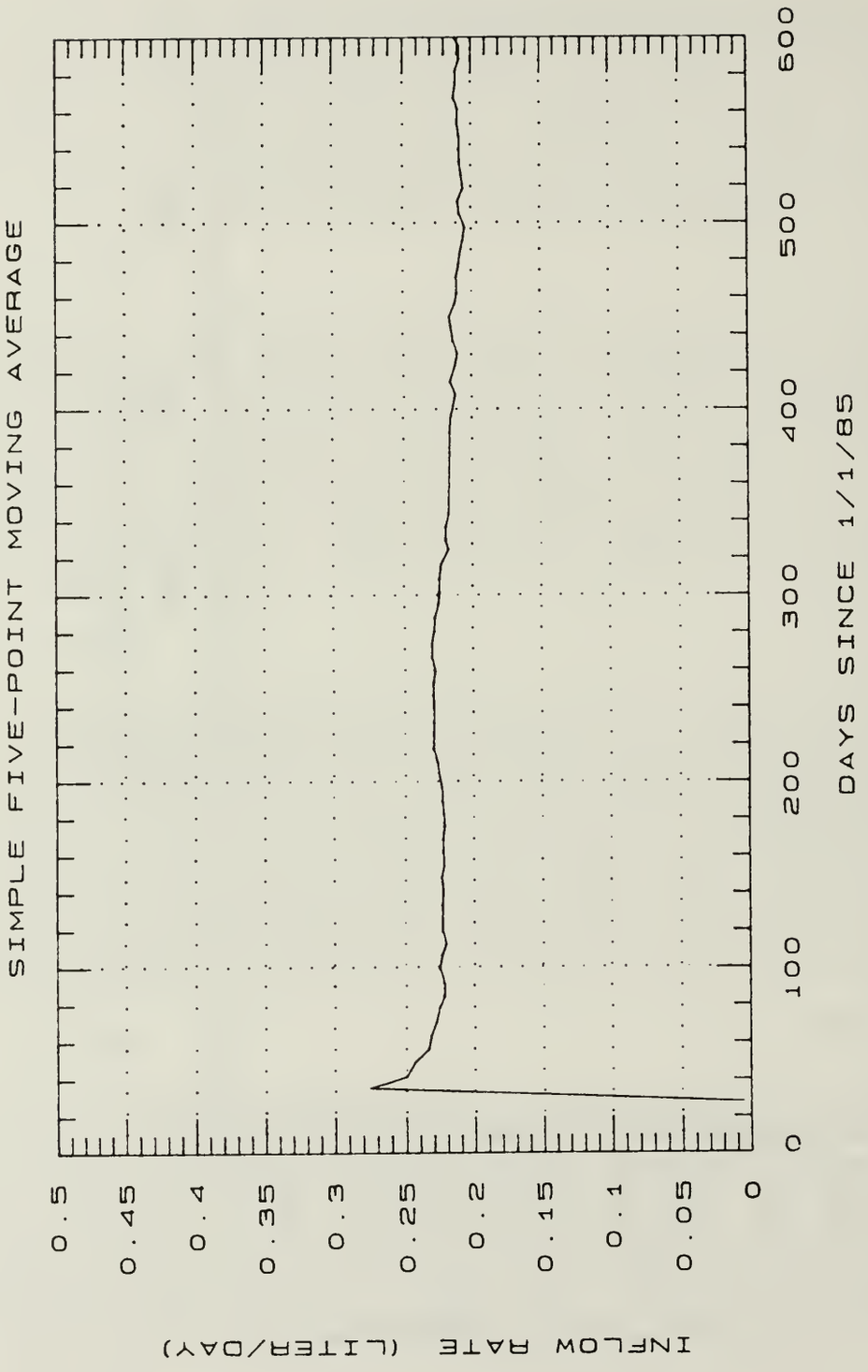

Figure D-17

DH36 Inflow Rates

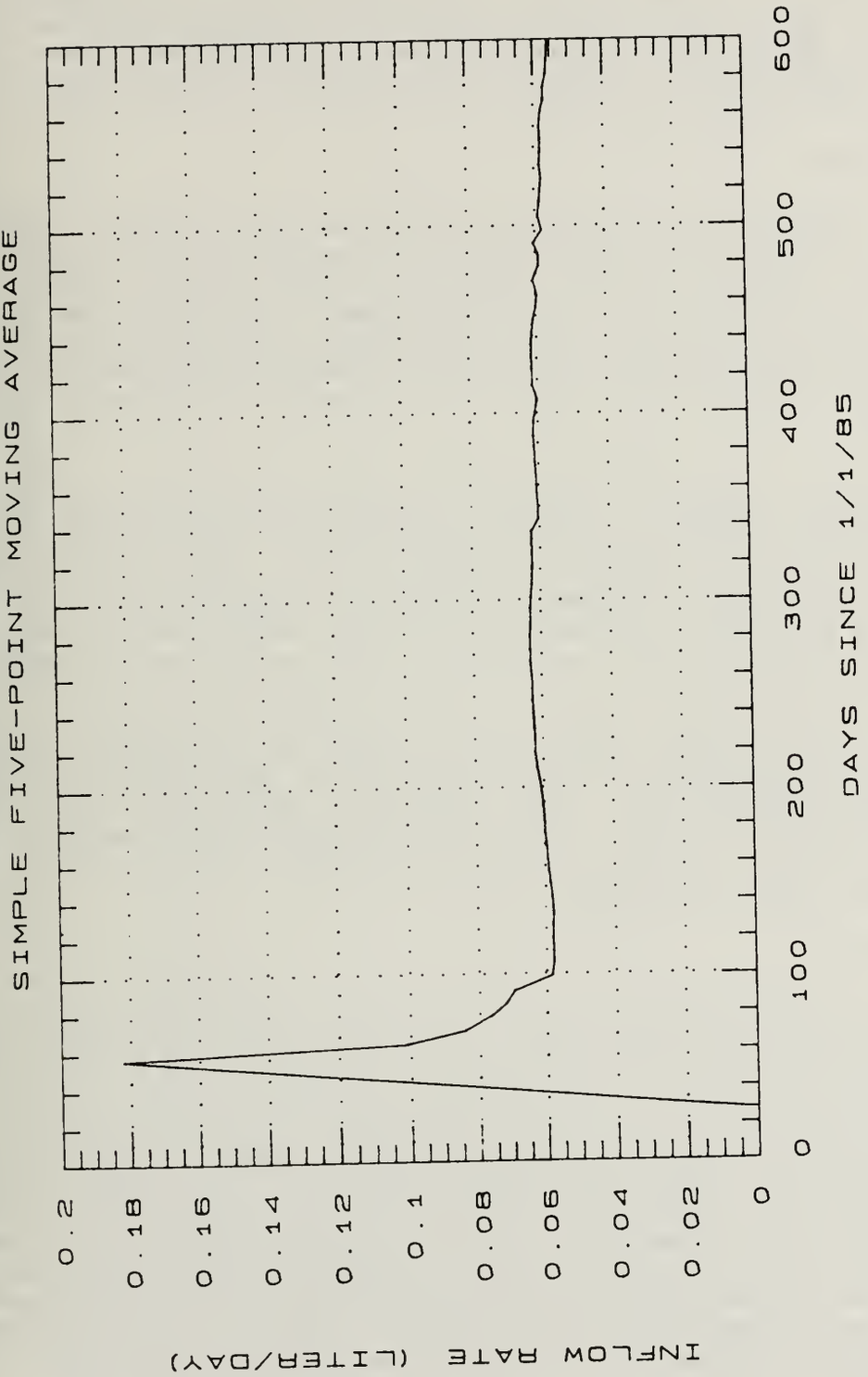

Figure D-18.

DH38 Inflow Rates

bottom of the hole on January 28, 1985 and about 0.3 liters of brine and muck was bailed from the hole on February 5, 1985 (Table E.14). Calculated inflow rates in mid-February 1985, were on the order of 0.05 liters per day and decreased only gradually to about 0.03 liters per day through August 1986 (Table E.14, Figure D-20). A total of approximately 19 liters had been removed from DH42 by August 19, 1986.

3.4.5 Hole DH42A

Hole DH42A is the westernmost downhole at the west end of Room G, 2 meters west of DH42. This hole was drilled because of poor core recovery from the 6- to 12-meter interval in DH42, which is 15.6 meters deep. DH42A was completed January 25, 1985 and is 12.3 meters deep. No brine or gas inflows were noted during drilling, but brine accumulations were noticed shortly after drilling. Brine was observed in the bottom of the hole on January 28, 1985 and 0.85 liters of brine were bailed from the hole on February 5, 1985 (Table E.15).

Calculated inflow rates in mid-February 1985, were on the order of 0.18 liters per day, increased gradually to about 0.2 liters per day in May 1985, and then began decreasing to about 0.1 liters per day in April 1986, where the inflow rate appeared to level out (Table E.15, Figure D-21). A total of approximately 75 liters of brine had been removed from DH42A by August 19, 1986. It is interesting to note that approximately four times as much brine flowed into DH42A than into DH42, which is 2 meters to the east and 3.3 meters deeper.

Most of the downholes studied showed an initial period of little or no inflow followed by a brief maximum inflow period lasting for a few days or a week or two, followed in turn by a decreasing inflow trend. Hole DH42A is the only location studied during Phase I that exhibited an early inflow trend that increased gradually over a much longer period of time (three months). The decreasing trend that followed also took much longer to begin to level out to a fairly steady inflow rate (Figure D-21).

3.4.6 Hole DH35

Hole DH35 was completed January 25, 1985 and is the easternmost uphole at the east end of Room G, above Hole DH36. No brine or gas inflows were noted during drilling, but brine accumulations were noticed shortly after drilling. Brine was observed dripping from the collar on February 5, 1985. A collecting device was installed under the collar on that date, and almost 0.2 liters was collected on March 5, 1985. Inflow rates were in excess of 0.02 liters per day in mid-March 1985, and decreased fairly steadily to 0.01 liters per day in May 1986 (Table E.9, Figure D-22). The lack of brine collected in late May and early April 1986, reflects the fact that the collecting device was broken, not that inflow ceased. However, a marked decrease in inflow did take place about that time. Calculated inflow rates in the summer of 1986 were less than 0.05 liters per day and seemed to be reduced to trace amounts by late August 1986. A total of approximately 4.3 liters was collected from DH35 by August 19, 1986.

3.4.7 Hole DH37

Hole DH37 was completed January 26, 1985 and is located just east of the center of Room G, above Hole DH38. No brine or gas inflows were noted during

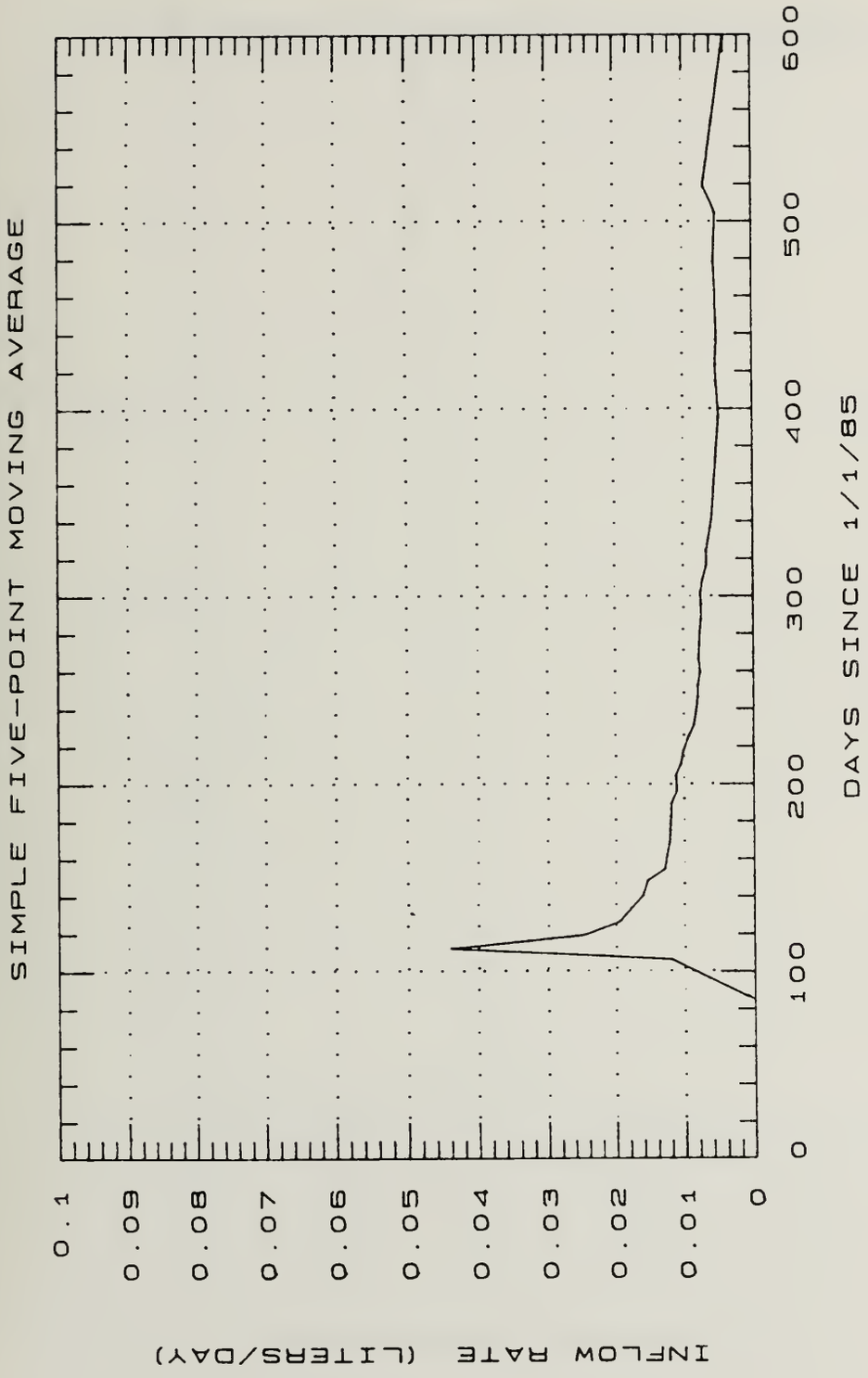

Figure D-19

DH40 Inflow Rates

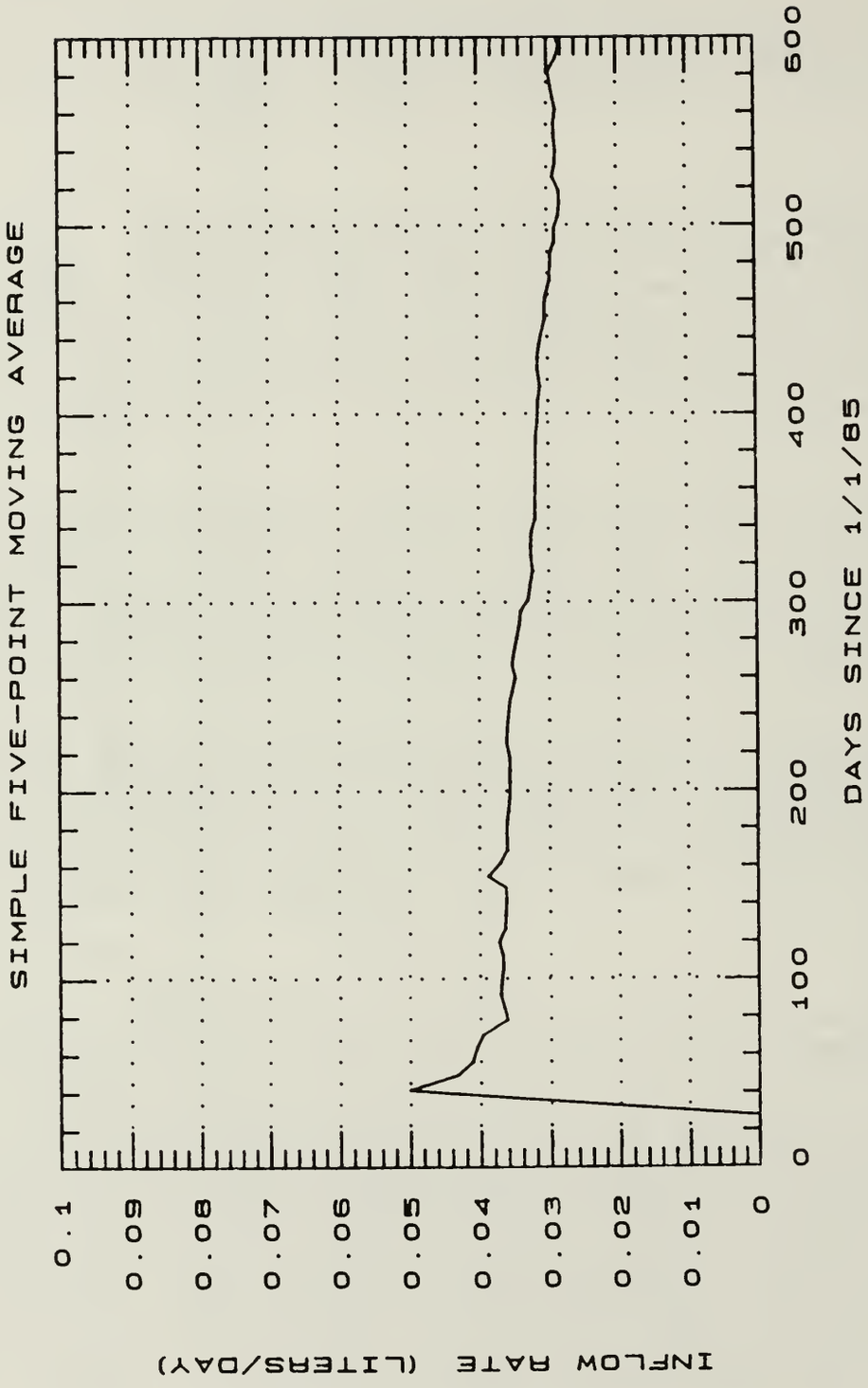

Figure D-20.

DH42 Inflow Rates

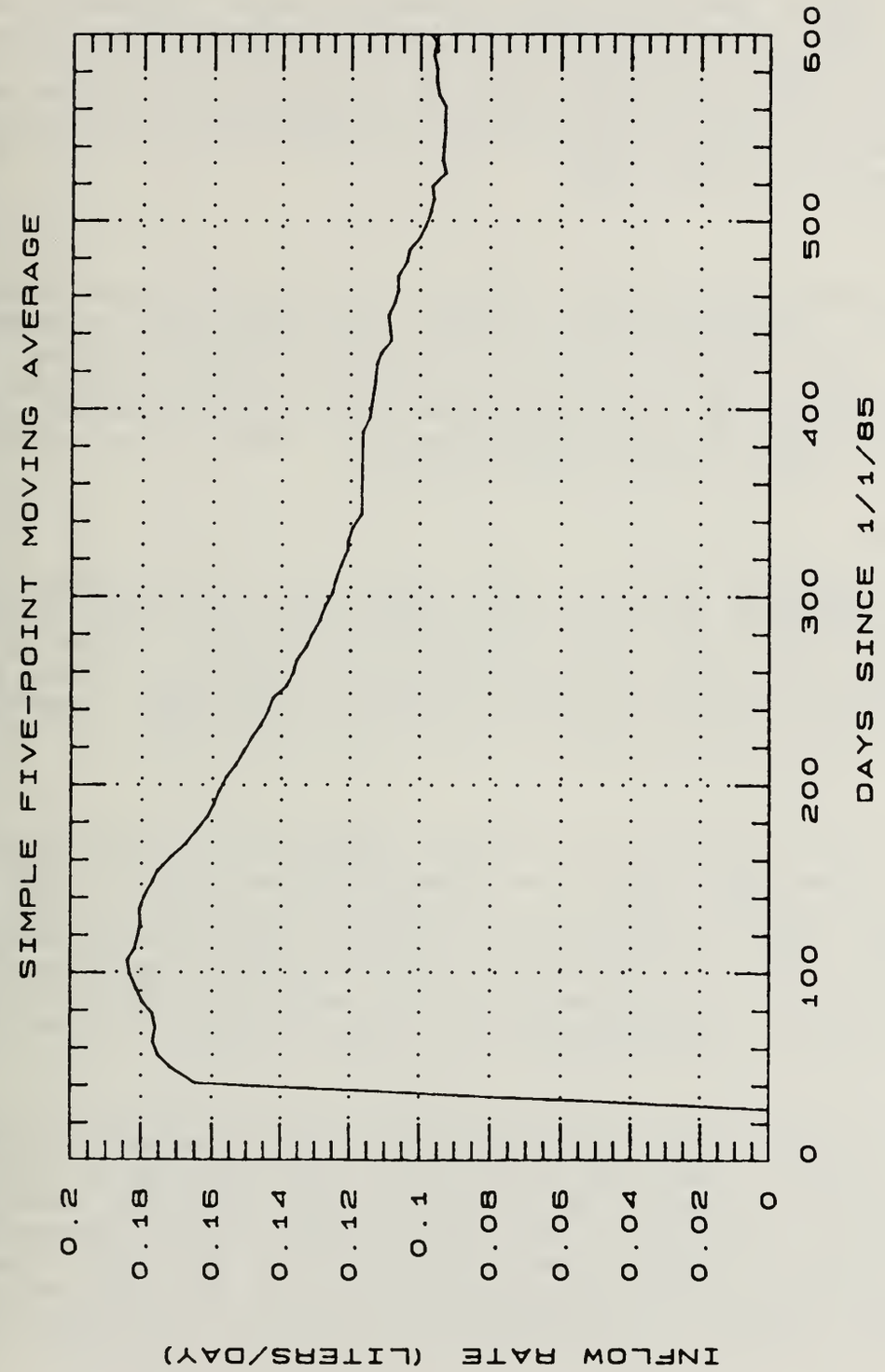

Figure D-21

DH42A Inflow Rates

drilling, but brine accumulations were noticed shortly after drilling. Brine was observed dripping from the collar on February 5, 1985. A collecting device was installed under the collar on that date, and approximately 0.06 liters was collected on March 5, 1985. Inflow rates were on the order of 0.01 liters per day through July 1985, decreasing to less than 0.005 through September 1985, and then decreased further to trace quantities accumulating in the collecting container (Table E.11; Figure D-23). A total of a little over 1.2 liters was collected from DH37 by July 1, 1986.

3.4.8 Hole DH39

Hole DH39 was completed January 24, 1985 and is located just west of the center of Room G, above Hole DH40. No brine or gas inflows were noted during drilling, but brine accumulations were noticed shortly after drilling. A moist area on the back (roof) around the collar was observed on February 5, 1985. A collecting device was installed under the collar on that date, and trace amounts of brine were collected in May 1985. Measurable quantities of brine did not accumulate in the collecting device.

3.4.9 Hole DH41

Hole DH41 was completed January 25, 1985 at the west end of the center of Room G, above Hole DH42. No brine or gas inflows were noted during drilling, but brine accumulations were noticed shortly after drilling. A moist area on the back (roof) around the collar was observed on February 5, 1985. A collecting device was installed under the collar on that date. Measurable quantities of brine did not accumulate in the collecting device.

3.5 Room J

Room J is the site of the Materials Interface Interactions Test (MIIT) and the Drum Durability Test (DDT). Room J was excavated in April 1984. A pit was excavated in the southwest floor of the room and a series of 1- to 2-meter deep drill holes were made in the north end of the room (Figure D-24; Morse and Hassinger, 1985). Brine flowed into Holes MIIT-2 and MIIT-4 during drilling, and began to seep into the pit immediately after excavation. The brine pit was cleaned and blown dry with compressed air on June 27, 1984. Five days later the pit had refilled to about one-half of its previous depth.

Forty shallow drill holes were made for the MIIT program. The fact that the brine levels in these closely-spaced drill holes were dramatically different was observed during the summer and fall of 1984. Holes partially or completely filled with brine were interspersed with dry or nearly dry holes, often less than a meter away. On October 26, 1984, the room and the brine accumulations were surveyed (Figure D-24; Morse and Hassinger, 1985). The brine levels in the drill holes were resurveyed on November 26, 1984. At that time, the floor of the room was observed to be contaminated by a variety of materials and fluids.

On November 29, 1984, the MIIT holes were evacuated and cleaned with compressed air, the DDT pit was cleaned, and the contaminants that were loose on the floor removed. Approximately 75 liters of brine and salt crystals were removed from

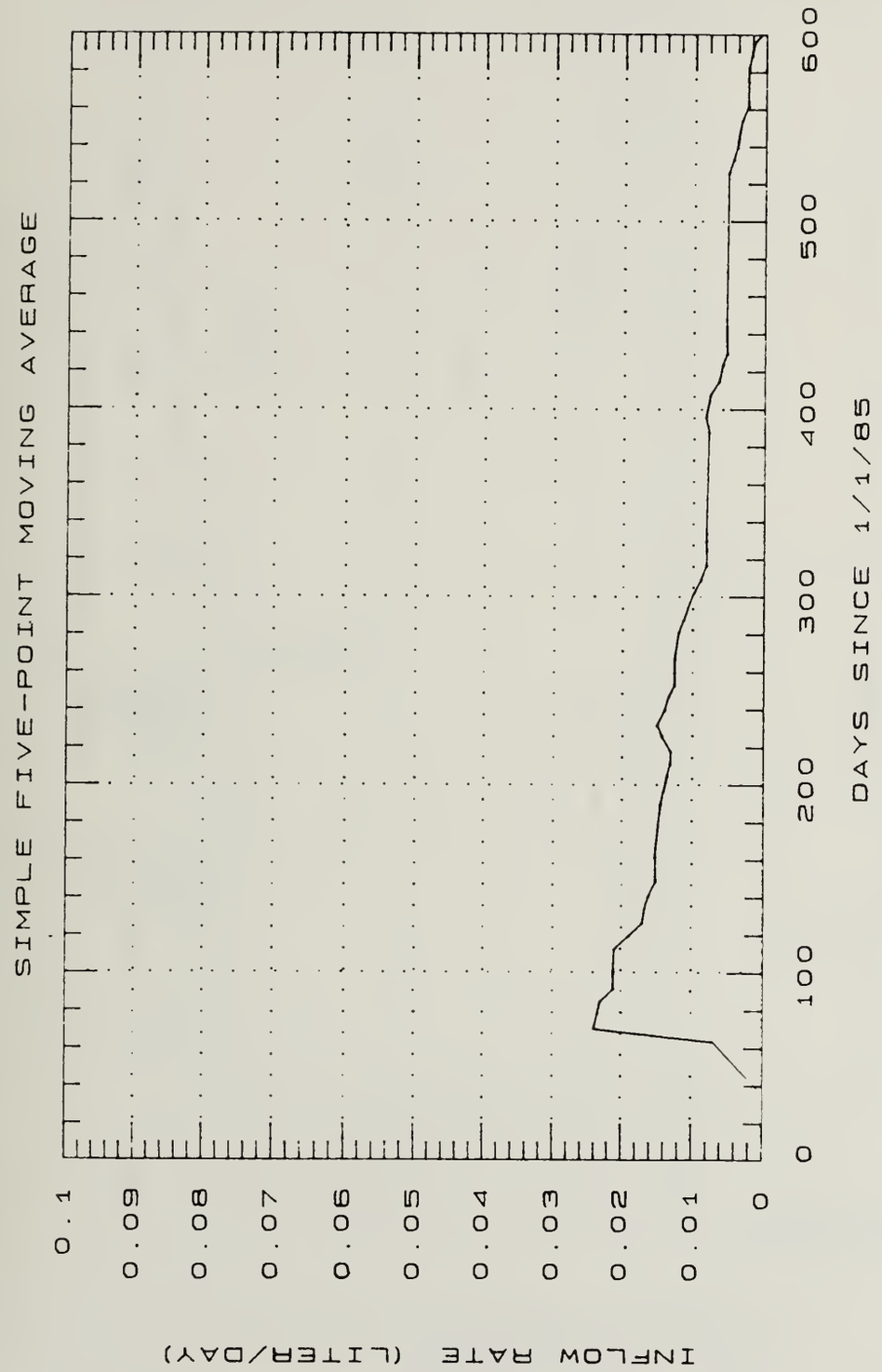

Figure D-22.

DH35 Inflow Rates

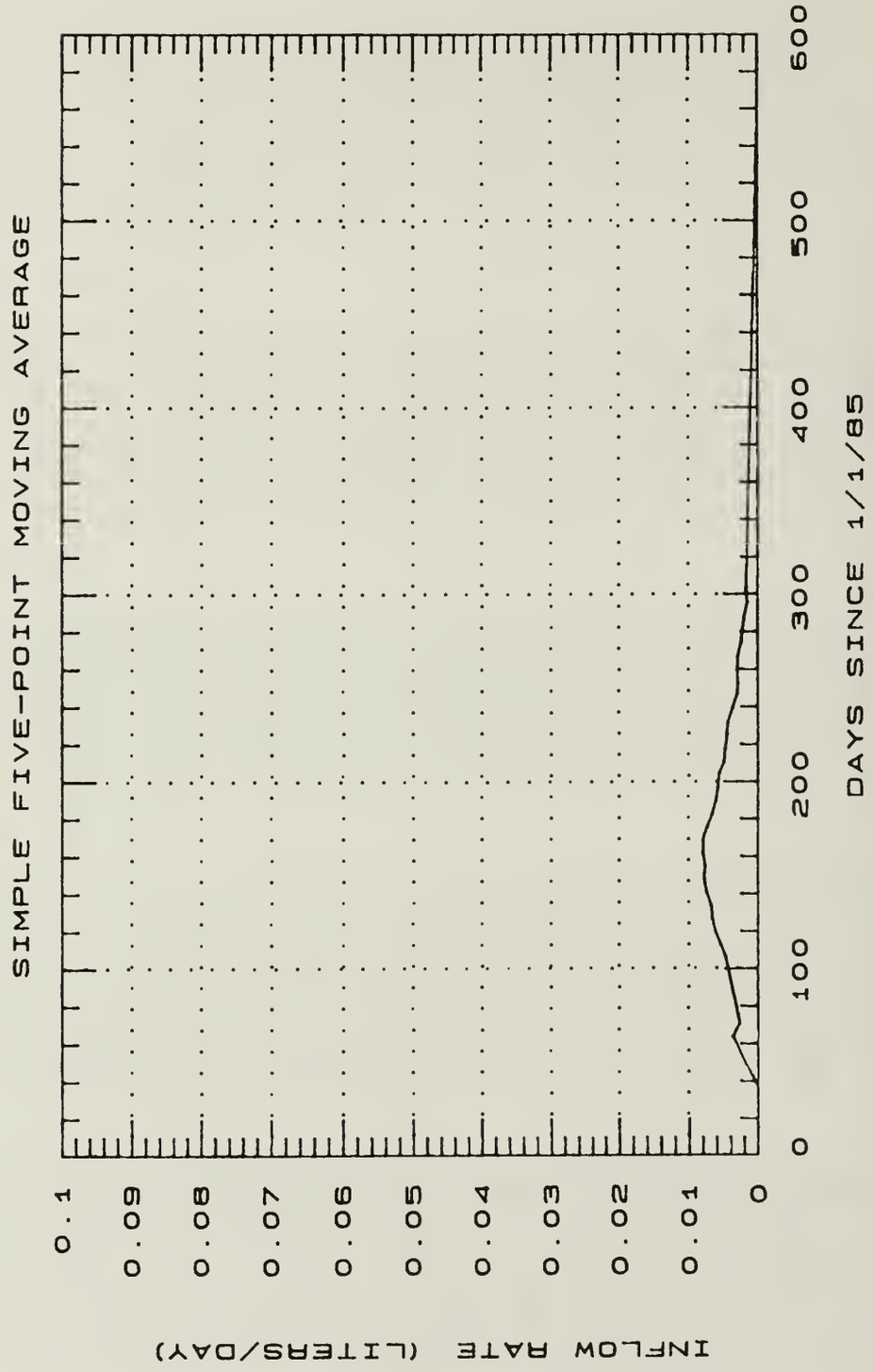

Figure D-23.

DH37 Inflow Rates

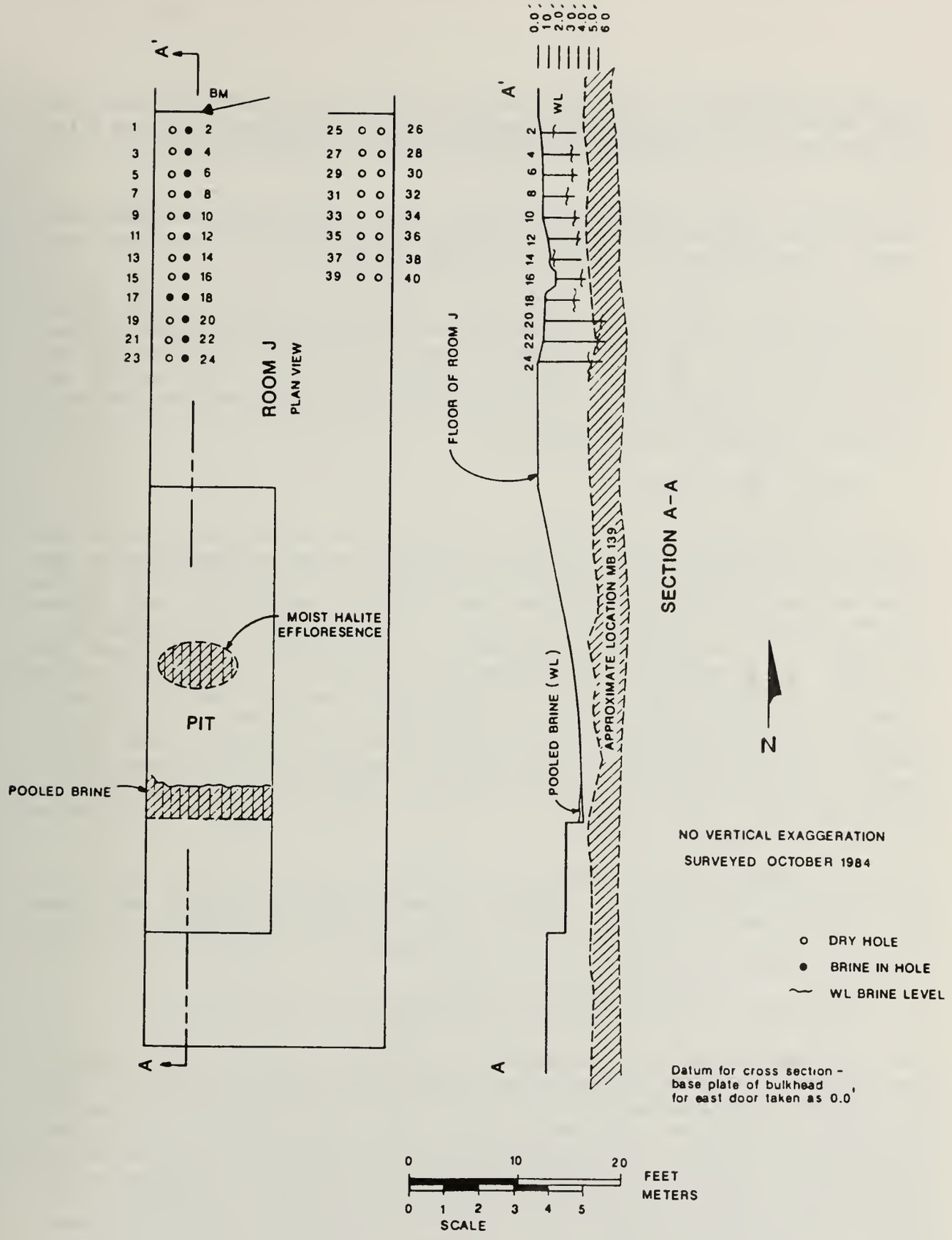

Figure D-24.

Room J Brine Survey, Plan and Cross Section
(After Morse and Hassinger, 1985)

the pit and about 17.5 liters were removed from the MIIT holes. Eighteen days later brine puddles had returned to the floor of the DDT pit and some brine had returned to all except one of the MIIT holes that had previously contained brine.

On January 8, 1985, the brine levels were again surveyed and the holes evacuated. Brine inflows were monitored through April 23, 1985, when Room J was closed to the BSEP in the course of the MIIT experiments.

The significance of the observations that were made in Room J is that drill holes less than a meter apart exhibited strikingly different brine inflows and the brine level in adjacent holes stood at strikingly different levels. Marker Bed 139 was obviously playing a significant role in the migration of brine to the MIIT holes and the brine pit (Figure D-24), and gas bubbles were associated with almost all occurrences. A total of over 18 liters of brine were removed from the MIIT holes.

3.6 Room L1, Hole L1X00

Room L1 was excavated in April 1984. Shortly after excavation, 11 holes were drilled in the floor across the north end of the room and approximately one foot of brine accumulated in each of these holes. On November 27, 1984 it was observed that 10 of the 11 holes had been filled and sealed with grout as part of the Plugging and Sealing test program. The remaining hole, L1X00, was still open and contained brine, and about 11 liters of brine were removed from the hole. On November 30, 1984 compressed air was used to completely evacuate the hole. On May 14, 1985 the hole was found to contain brine and an additional 11.46 liters were removed. Inflow rates at the end of May were calculated to be on the order of 0.03 liters per day, declining gradually to about 0.02 liters per day in early December 1985 (Table E.19, Figure D-25). Inflow rates then gradually increased through August 1986 returning almost to their May 1985, values. A total of over 23.5 liters of brine had been removed from L1X00 by August 19, 1986.

Thirty-six downholes, 10 centimeters in diameter, and 3.6 meters deep were drilled through MB 139 on a 1 meter by 1.5 meter grid in the north end of Room L1. Observations of brine inflows into some of these holes showed variations between holes that were similar to, but somewhat less dramatic than, those described above for the MIIT holes in Room J.

3.7 E140 Drift at S1950, Holes DH215 and DH216

The south exploratory drift was excavated at E140 in 1982 and 1983, reaching the southern end (S3666) of the planned underground facility January 29, 1983. The initial excavation was 2.4 meters high and 7.6 meters wide. The part of the drift at S1950 was mined on January 3, 1983. A pair of uphole and downholes (DH215 and DH216) were drilled shortly after excavation, and sonic-probe extensometers (GE247 and GE248) were installed in them. Both holes were drilled with brine as the drilling fluid and both encountered traces of pressurized gas during drilling. Hole DH215 is the uphole and is 15.8 meters deep. Hole DH216 is the downhole and is 16.5 meters long. Both holes began producing brine shortly after drilling and, partially because they were far removed from the observation holes in the northern, experimental part of the WIPP workings, were the location of early, informal, brine inflow observations.

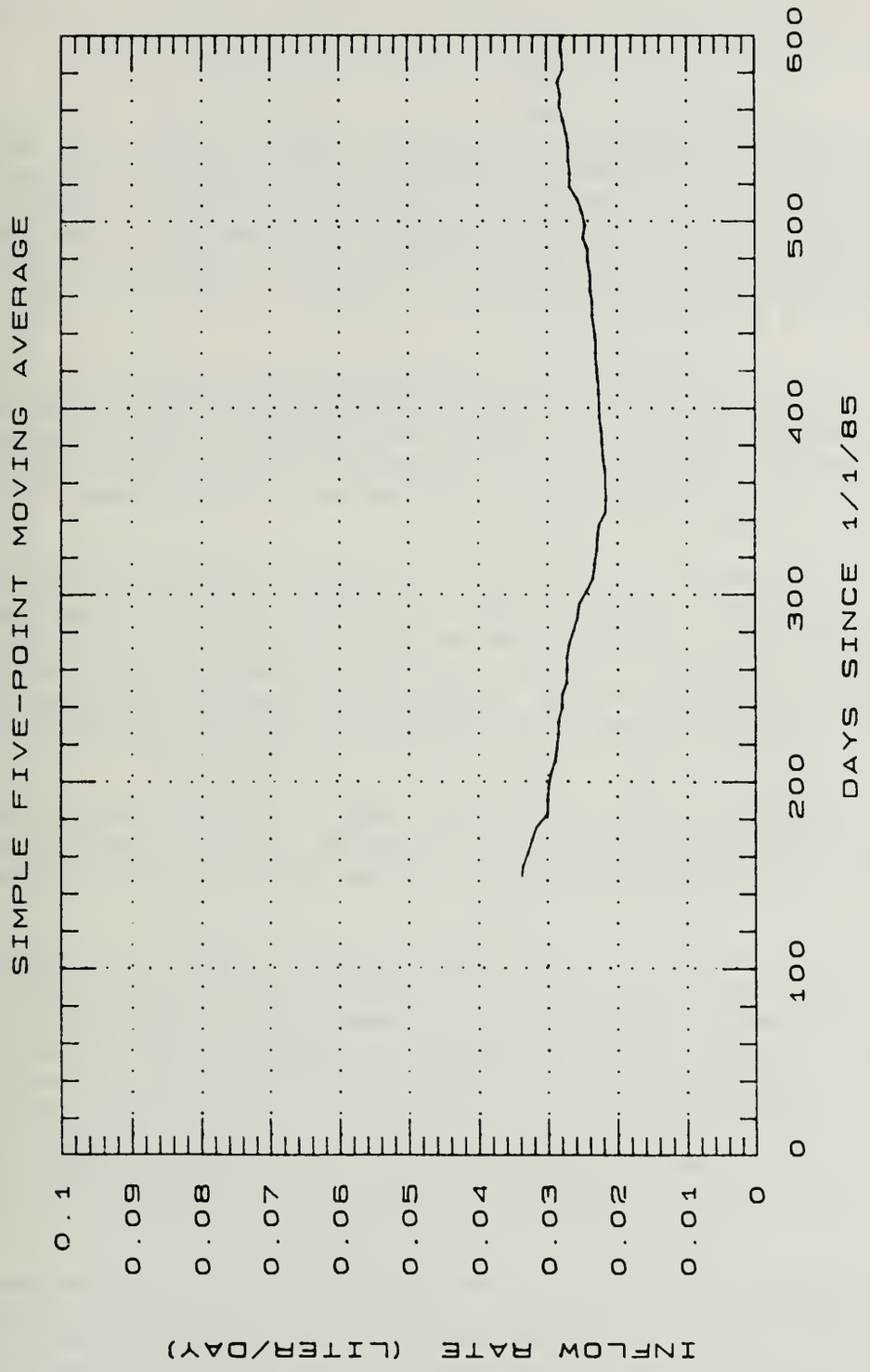

Figure D-25.

L1X00 Inflow Rates

The presence of instrumentation in both holes makes it difficult to obtain good quantitative data and probably effects any chemical data obtained from brine withdrawn from them.

In April 1984, the downhole was observed to be completely filled with brine, and brine was observed dripping into it from the uphole over it. It was not known how much of the 15.8 meters of brine in the downhole had been produced from the rocks exposed in the sides of the hole and how much had dripped into it from the uphole. It was further recognized that both holes had been drilled with brine and that water had been spread on the floor of the drift by the mining contractor for dust control, both possible sources of brine that may have accumulated in the downhole.

On April 20, 1984, a funnel and collecting device was installed on the uphole to collect the brine issuing from it, and the brine that filled the downhole was evacuated down to the level of the instrument head, approximately 0.55 meters below the collar. It was not possible to conveniently extract brine from below the instrument head, so a column of brine more than 15.2 meters long remained in the hole.

Three days later, on April 23, 1984, about an inch of brine had accumulated over the instrument head in the downhole (DH216), but no brine had been collected from the uphole (DH215). Gas bubbles were observed rising around the instrument head in DH216. By the end of April, small amounts of brine were collected from the uphole, and incidental observations throughout the summer and fall of 1984 documented that more brine was being produced from the downhole than from the uphole, but that both did yield brine.

Formal collections were initiated in January 1985, at which time the uphole seemed to be producing more brine than the downhole. Accurate data from the downhole (DH216) was difficult to obtain, and the collar was destroyed and the hole plugged by mining November 19, 1985.

Data from the uphole, DH215, is more complete (Table E.16) and is quite interesting (Figure D-26). Inflow rates in January 1985 were on the order of 0.01 liters per day and showed a gradual increase, almost doubling to 0.02 liters per day by November 1985. On November 19, 1985, the floor of E140 was lowered by 4 feet at S1950. On November 20, 1985, mining of the cross drift S1950 began, with mining to the east, toward E300. On January 29, 1986, the cross drift was extended to the west, toward W30. Hole DH215 was the uphole in the center of what then became the intersection of E140 and S1950. On February 28, 1986, additional mining took place at this intersection as the floor of E140 south of the intersection was lowered 1.2 meters.

Inflow rates increased three-fold, to approximately 0.06 liters per day, immediately following the lowering of the floor and the excavation of the cross drift to the east. It is highly probable that the change in the stress distribution in the vicinity of the intersection resulted in the increased inflow and that the sudden increase shown on Figure D-26 is a mining-induced transient effect. Inflow rates then declined steadily, perhaps beginning coincidentally with the additional mining at the intersection or perhaps related to that mining, through August 1986, to rates below those observed in January 1985.

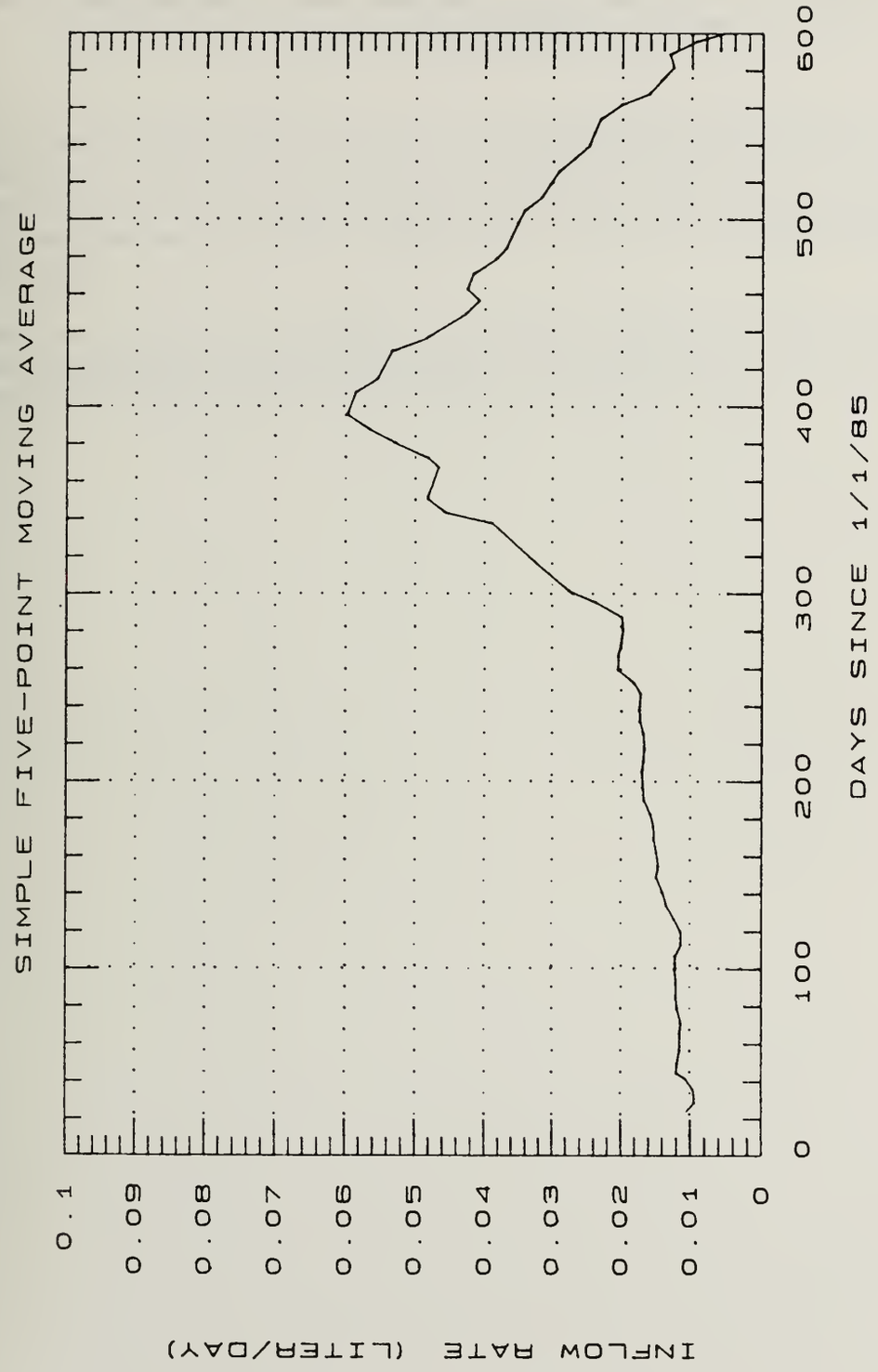

Figure D-26.

DH215 Inflow Rates

Over 15 liters of brine were collected from DH215 over the 600 days of collection. This figure is a minimum figure and much more brine had been produced from the hole, but not collected and measured, prior to January 1985.

E.3 **BRINE INFLOW MODEL**

This subsection of Appendix E presents and describes the WIPP Brine Flow Model for Darcian Flow. This model has been used to analyze brine-inflow rates to observed boreholes and moisture release experiments and is provided here to support brine inflow rates defined in the text. Included in this section are the assumptions inherent in the model.

This subsection has been completely excerpted from Chapters 2 and 3 of Nowak et al., 1988, Brine Inflow to WIPP Disposal Rooms: Data, Modeling, and Assessment. For additional information, please refer to the above referenced report.

2. WIPP BRINE FLOW MODEL

A brine transport model for both isothermal and non-isothermal conditions in bedded salt was developed with data from the WIPP large scale in situ experiments [25,28,29]. This model is for transient Darcy flow in a porous medium. Elastic responses of the salt and brine account for the "storage" of brine that supports transient flow, and thermal effects are accounted for by including the thermal expansion of the brine and the host rock salt.

Any model for transient flow of fluid in a porous medium requires the stipulation of a mechanism of ''storage,'' that is, local changes of fluid mass per unit volume of the medium. In a rigid porous medium, the only available mechanism is compression, or the local density change, of the fluid. In a deformable porous medium, storage can be accommodated by dilatation of the solid skeleton and local compression of the solid, as well. Dilatation of the porous skeleton is the principal mechanism of interest in soil and rock mechanics, and is the cornerstone of ''consolidation'' theory. Rock salt, of course, exhibits plastic as well as elastic properties. It is, however, plausible that the immediate, elastic response of the salt and brine and the subsequent relaxation of the pore pressure by flow to the excavation are the predominant mechanisms of brine storage and transport, at least over short time scales.

For a linearly elastic skeleton, Biot [36] generalized the consolidation theory, and Rice and Cleary [37] later recast it in terms with straightforward physical interpretations. An extension of this model to account for non-isothermal effects, allowing for thermal expansion of the fluid and solid, has been presented recently [38,39].

The essence of the model is embodied in a diffusion equation for the pore pressure that, in certain special cases, reduces to:

$$\frac{\partial p}{\partial t} - c\nabla^2 p = b'\frac{\partial \theta}{\partial t}, \qquad (1)$$

where p is the fluid pore pressure, c is the fluid diffusivity, b′ is a source coefficient, and θ is the temperature. The fluid diffusivity, c, depends upon the permeability, fluid viscosity, and the elastic properties of the solid and fluid (see Appendix A). The source coefficient, b′, depends upon the thermal expansivities of the solid and fluid (see Appendix A). For isothermal conditions, the right hand side of (1) vanishes, and the classical diffusion equation for Darcy flow is recovered. Various special cases widely considered in hydrologic modeling are embedded in this formulation [25]. For non-isothermal problems in which conduction heat transfer dominates (i.e., small Peclet number), as is certainly true in salt, the source term in (1), which represents the generation of pore pressure by thermal expansion, must be evaluated from the simultaneous solution of the heat equation:

$$\frac{\partial \theta}{\partial t} - \kappa \nabla^2 \theta = 0 , \qquad (2)$$

where κ is the thermal diffusivity. Extended discussion of this system of equations as well as various solutions to representative initial value problems can be found in [38,39].

The explicit relationships between properties of salt and brine and the coefficients appearing in equations (1) and (2) are given in APPENDIX A of this report. The host rock salt permeability, k, and other properties of the host rock and brine appear in the fluid diffusivity, c.

In the data analyses that are discussed here, permeability values, k, were chosen to match or bracket the brine inflow data. Other values for the host rock and brine properties in the diffusivity, c, were taken from known properties of salt and saturated brines. The permeability values thus obtained were used to calculate brine inflow to WIPP disposal rooms with this model.

2.1. Isothermal Flow

Consider now an idealized model for the introduction of a mined drift into a deeply buried region. The rock is assumed to be homogeneous and isotropic, and the undisturbed stress state is taken to be lithostatic, i.e., isotropic, compressive, and equal in magnitude to the overburden load. The initial pore pressure in the neighborhood of the tunnel is assumed to be constant:

$$p(r,0) = p_0 . \qquad (3)$$

The pressure p_0 is expected to be between hydrostatic (about 6 MPa) and lithostatic (about 15 MPa) [25]; this has been corroborated by field measurements from which pore pressures of 8.3 MPa and 10.3 MPa were estimated [31]. Superimposed on the hydrostatic pressure is a portion of the increased mean stress induced by the presence of the tunnel. The fluid pressure then relaxes by Darcy flow toward the tunnel, and the load is transferred to the solid skeleton.

The pressure field corresponding to this sequence is governed by (1) with the right-hand side zero and with the initial condition (3) and boundary conditions:

$$p(a,t)=0 , \qquad (4)$$

$$\lim_{r \to \infty} p(r,t) = p_0 , \qquad (5)$$

where a is the excavation or borehole radius. Equation (4) simply states that the fluid is free to flow to the ''drained'' face, which is maintained at atmospheric pressure.

The solution to (1) and (3) to (5) is well known (e.g., [40]); the flux at the tunnel wall, $q(a,t_*)$, follows immediately from Darcy's law by differentiation:

$$q(a,t_*) = - \frac{kp_o}{\mu a} \frac{4}{\pi^2} \int_0^\infty \frac{\exp(-u^2 t_*)}{J_o^2(u) + Y_o^2(u)} \frac{du}{u} \qquad (6)$$

where k is the permeability, μ is the fluid viscosity, $t_* = ct/a^2$ is the normalized time, and $J_o(x)$ and $Y_o(x)$ are zero-order Bessel functions of the first and second kind, respectively. Note that the sign of the flux is negative because it is in the (-r) direction. It is convenient also to introduce the asymptotic expansion for early time:

$$\lim_{t_* \to 0} q(a,t_*) = - \frac{kp_o}{\mu a} \left[\frac{1}{\sqrt{\pi}} t_*^{-1/2} + \frac{1}{2} - \frac{\sqrt{\pi}}{4} t_*^{1/2} + \frac{1}{8} t_* + \cdots \right] , \qquad (7)$$

and that for late time:

$$\lim_{t_* \to \infty} q(a,t_*) = - \frac{kp_o}{\mu a} \left[\frac{2}{\ln(4t_*) - 2\gamma} - \frac{2}{[\ln(4t_*) - 2\gamma]^2} + \cdots \right] , \qquad (8)$$

where $\gamma = 0.57722$ is Euler's constant. Values calculated with equations (6) - (8) are shown in Figure 1. Note that the flux falls off rapidly at early time, and changes only slowly for $t_* > 10$.

2.2. Flow to a Heated Borehole

Consider now the response of the salt and pore fluid to a constant heat flux delivered to a borehole wall. The appropriate initial and boundary conditions are then:

$$\theta(r,0) = \theta_o , \qquad (9)$$

$$\frac{\partial \theta}{\partial r}(a,t) = - \frac{q^h}{K} , \qquad (10)$$

$$\lim_{r \to \infty} \theta(r,t) = \theta_0 \ , \tag{11}$$

where θ_0 is the ambient temperature, q^h is the heat flux at the borehole wall, K is the thermal conductivity, and

$$p(r,0) = p(a,t) = \lim_{r \to \infty} p(r,t) = 0 \ . \tag{12}$$

The initial and far-field conditions on the pressure, equation (12), neglect the non-zero ambient pressure considered in the foregoing section.

The solution to the temperature field (equations 2, 9-11) is well known [41]; substitution into the right-hand side of (1) yields a diffusion equation for the pressure with a known source term. This, in turn, can be solved by Laplace transform [38] to give the flux at the borehole wall:

$$q(a,t_*) = - \frac{kb'q^h}{\mu KR(1 - R^2)} \frac{2}{\pi} \int_0^\infty \frac{\exp(-\omega^2 t_*)[\Phi J_1(\omega) - \Psi Y_1(\omega)]}{[J_1^2(R\omega) + Y_1^2(R\omega)][J_0^2(\omega) + Y_0^2(\omega)]} \frac{d\omega}{\omega} \ , \tag{13}$$

where

$$\Phi = J_0(\omega)\Lambda_1 + Y_0(\omega)\Lambda_2 \ , \quad \Psi = J_0(\omega)\Lambda_2 - Y_0(\omega)\Lambda_1 \ ,$$

$$\Lambda_1 = J_0(R\omega)Y_1(R\omega) - Y_0(R\omega)J_1(R\omega) \ ,$$

$$\Lambda_2 = J_0(R\omega)J_1(R\omega) + Y_0(R\omega)Y_1(R\omega) \ ,$$

and $R^2 = c/\kappa$ is the ratio of the fluid and thermal diffusivities, or ratio of characteristic times for transport of heat and fluid mass, respectively. The early-time, asymptotic expansion of (13) is given by

$$\lim_{t_* \to 0} q(a,t_*) = - \frac{kb'q^h}{\mu KR(1 + R)} \left[1 - \frac{1}{\sqrt{2\pi}R} t_*^{1/2} + \frac{3 + R}{8R^2} t_* \cdots \right] . \tag{14}$$

2.3. Assumptions Inherent in the Model

It is our judgement that uncertainties associated with the assumptions in the model introduce uncertainty in brine inflow predictions for waste disposal rooms of no more than about an order-of-magnitude. Both the Darcy model itself and some of the assumptions invoked in order to represent the practical problems of interest are idealizations of very complex systems. It can be anticipated that some of these idealizations are conservative, in the sense that they tend to lead to overpredictions of brine flow at the WIPP, and some are "liberal," in the sense that they probably lead to underpredictions. The directions of uncertainties that may arise from some of the other model assumptions are difficult to assess at this time.

Assumptions that are likely to lead to overpredictions of brine inflow (conservative) include the following:

There exists a network of interconnected porosity extending outward without bound. This assumption implies a limitless reservoir of brine.

The far-field brine pressure is lithostatic. Aside from the stress perturbation due to the presence of the excavations, it is difficult to imagine a mechanism by which the pressure could rise above lithostatic.

Brine flow is radially symmetric (two dimensional). The effect of the third dimension is to weaken the flow by geometric spreading of the disturbance.

The backpressure from the room contents is negligible. Any backpressure due to interaction of the salt with solid, fluid, or gas in the storage room will mitigate the flow to the room.

Inelastic dilatation of the salt is neglected (see also below). Dilatation of the salt near the excavations due to inelastic mechanisms, such as opening grain boundaries, tends to decrease the pore pressures that drive flow.

Assumptions that are likely to lead to underpredictions of brine inflow ("liberal") include the following:

The storage of available brine in the host rock is due entirely to elastic compression of the brine and salt. Additional (inelastic) storage mechanisms would decrease the brine diffusivity and, therefore, increase the decay time for the flux. Thus, integrated fluxes over long time would be larger. The magnitude of the initial (maximum) flux, however, is unaffected by the storage.

Inelastic dilatation of the salt is neglected (see also above). Dilatation of the salt near the excavations due to inelastic mechanisms such as opening grain boundaries tends to increase the permeability in that region. However, calculations that account for extreme increases in permeability near the wall (given in Section 4.3.4 of this report) show relatively small increases in the cumulative brine flux, because the flow over long periods of time is controlled by the far-field properties.

The directions of uncertainties about possible effects of inelastic, volumetric deformations and of heterogeneities in the host rock salt are now difficult to assess. Such effects have not been the focus of the laboratory testing program for host rock salt. Also, the effects of heterogeneity are difficult to anticipate. Some further work to reduce these uncertainties will be described below. However, these effects on predicted brine inflow values are not expected to exceed an order of magnitude.

3. WIPP BRINE FLOW CHARACTERISTICS DATA BASE

Data pertinent to WIPP brine inflow predictions are available from several sources. Brine accumulations were measured by periodic bailing in boreholes located over a wide area of the WIPP facility. These measurements were part of the WIPP Brine Sampling and Evaluation Program [30]. Brine inflow rates were also calculated from moisture release data obtained from isothermal and heated boreholes in the Moisture Release Experiment for Rooms A1 and B in the WIPP [29]. Host rock permeability values are available from WIPP in situ brine and gas flow measurements that support the WIPP Plugging and Sealing Program [31]. The data from these sources are described in the following sections.

3.1. WIPP Brine Sampling Data

Deal and Case [30] monitored 54 drillholes throughout the WIPP, most of them for about 500 days. They show graphical results for the time histories of the total flux for 20 holes. The flow rates to two of the holes, BX02 and DH37, fell essentially to zero after 600 days. The flow rates to the remaining 18 holes at the end of the reporting period are considered here (Table 1). Hole A1X02 exhibited a nearly monotonic decay in flow rate for nearly 400 days, but then experienced a steady increase in flow rate. The value entered in Table 1 for A1X02 hole corresponds to the value at the end of the period of declining rate. The recorded flow rates represent the integrated flux over the borehole surface areas, and are recorded in Table 1 in units of liters per day, i.e., a volume flow rate.

3.2. WIPP Moisture Release Data

Full-scale simulations of high-level waste repository environments [24] have been under way at the WIPP site since April, 1985 in two large (5.5 x 5.5 x 90 m) rooms, designated A1 and B. The rooms are at the WIPP waste disposal horizon in the bedded salt of the Salado Formation. In each of these rooms is an array of vertical boreholes, heated by electric resistance heaters. The boreholes are 0.38 m in radius, and the heated length is 3.10 m; the Room B hole designated B041 is an exception, with radius 0.46 m and heated length 3.45 m. The heaters in Room A1 are designed to simulate defense high-level waste at near-reference conditions of 18 W/m^2 thermal loading; each heater is operated nominally at 470 W. Room B simulates overtest conditions, at 1500 W per heater. Two of the heated holes in each room are instrumented to monitor temperatures and moisture release. Moisture from the borehole walls is removed continuously in the vapor phase by nitrogen circulated through the holes. The nitrogen is passed through cold traps and desiccant canisters, and the mass of water collected is recorded. Details of the experimental setup and procedures are given in [25,26].

Prior to the start of heating, the initial moisture release rate for each of the four test boreholes fell within the range of 5 to 15 g/day. Upon heating, the 470 W holes in Room A1 yielded peaks of 15 to 17 g/day

within about 10 days, and the flow rates declined subsequently to about 10 g/day after 100 days. Flow to the 1500 W holes in Room B continued to increase over a longer period, rising to peak rates of 80 to 90 g/day after 100 days, and slowly decreasing throughout the remainder of the test. Cumulative quantities of water were 4.3 kg at 441 days from Room A1 boreholes and 36 to 38 kg at 600 days from Room B boreholes. These moisture release data will be compared with calculations from the model to establish a credible permeability range that represents brine transport in the host rock.

3.3. WIPP Host Rock Permeabilities from Independent In Situ Flow Measurements

Permeability values in the range of 10^{-21} to 10^{-20} m^2 (1 to 10 nanodarcy) or lower have been derived for intact WIPP host rock from independent in situ measurements of brine flow during fluid transport experiments [31,42,43]. Independent measurements of the both gas and brine permeability of the salt at the WIPP facility horizon have been made using constant-pressure and pressure-decay methods in 6.5 cm radius boreholes [31,32,42]. These tests showed that permeabilities near the drift wall were mostly of the order of 10^{-20} to 10^{-18} m^2 (10 to 1000 nanodarcy) or higher in some cases. A few meters into the wall, permeabilities were of the order of 10^{-22} to 10^{-20} m^2 (0.1 to 10.0 nanodarcy). Measurements in the WIPP waste-handling shaft at levels above the proposed disposal horizon confirm the range of 10^{-21} to 10^{-20} m^2 (1 to 10 nanodarcy) for undisturbed host rock salt [43]. The permeability range implied by comparisons between model calculations and brine inflow measurements will be compared with these results.

3.4. Data Reduction

3.4.1. Radial Darcy Flow Model for Isothermal Data Reduction

An idealized model was introduced previously [25] to investigate the order-of-magnitude agreement of observed fluxes with the proposed Darcy flow mechanism. This model was described above. In particular, it was assumed that mined faces and boreholes introduce zero-pressure surfaces into a region of porous salt in which the brine is initially at hydrostatic pressure. (It is easy to argue that the initial pressure may be as large as lithostatic, but this changes the initial conditions only by a factor of about two. The uncertainty in the permeability is expected to be much greater.) In this case, the Darcy flux, q, to a circular borehole scales in the following fashion [25]:

$$q \propto \frac{kp_o}{\mu a} , \qquad (15)$$

where k is the permeability, p_o is the initial pressure, μ is the brine viscosity, and a is the borehole radius. This factor is multiplied by a

time-dependent function of order unity that represents the decay of the flux as the pressure disturbance propagates away from the hole. The characteristic time over which this decay takes place, t_o, is given by:

$$t_o = \frac{a^2}{c} , \tag{16}$$

where c is the fluid diffusivity. For elastic rock, the fluid diffusivity scales like:

$$c \propto \frac{kK}{\mu} , \tag{17}$$

where K is an elastic modulus for the porous skeleton. It can be argued from the model that, for WIPP salt, the appropriate modulus and viscosity yield a diffusivity of the order of

$$c \propto 1.1 \times 10^{14} k \quad m^2/s , \tag{18}$$

where the permeability is given in units of m^2.

Previous calculations [29,39] suggest that the brine diffusivity is of the order of 10^{-7} m^2/s. For a borehole of radius 0.05 m, then equation (16) gives a characteristic time of the order of 2.5×10^4 s, or about seven hours. Therefore, after 500 days, the drillholes in the WIPP can be expected to be in the asymptotic limit of ''late'' time. In this case, the flux can be approximated by the first term in the series given by equation (8):

$$|q| = \frac{kp_o}{\mu a} \frac{2}{\ln(4ct/a^2) - 2\gamma} , \tag{19}$$

where $\gamma \approx 0.57722$ is Euler's constant.

3.4.2. Permeabilities from Brine Sampling Data

Deal and Case [30] report the dimensions of the holes from which they collected and measured brine, so that it is simple to calculate the vertical wall area of each. These values are recorded in Table 2. The average Darcy flux (or "Darcy velocity") for each hole is easily calculated by dividing the integrated volume flux by the total borehole area. This step is not taken here, because the comparison can be misleading. If the flow does occur by a Darcy mechanism, then the Darcy velocity is expected to scale inversely with the borehole radius. Thus, the appropriate measure for a hole-to-hole comparison in this context is the product of the Darcy

flux and the borehole radius. The values of this product appear in the fifth column of Table 2, labeled "qa".

The values for the product of the Darcy flux times borehole radius, which are proportional to the total flow rates per unit length of borehole, center around 3 x 10^{-12} m^2/s. The maximum value is for hole NG252, at 2.1 x 10^{-10} m^2/s. This hole samples an anomaly in the WIPP host rock; consequences of this anomaly will be discussed below.

The apparent permeability was calculated for each borehole using values for "qa", the Darcy flux times the borehole radius, and equation (19). In particular, it was assumed that the initial pressure is p_o = 6.0 x 10^6 Pa, corresponding approximately to hydrostatic pressure for a depth of 600 m. The brine viscosity is taken to be 1.6 x 10^{-3} Pa·s. The time was assumed to be t = 4.32 x 10^7 s (500 days) for every hole. The diffusivity was assumed to be given by (18). Finally, for each drillhole, values for the flux times the radius, qa, are known (Table 2).

Thus, the only unknown parameter is the apparent permeability, k_{app}. The explicit relationships between the properties of salt and brine and the coefficients appearing in the above relationships are given in APPENDIX A of this report. Also given in that appendix are the typical properties for WIPP salt that were used.

The nonlinear relationship for "k_{app}", represented by equations (18) and (19) is then easily solved numerically. The results of this exercise are shown in the last column of Table 2. The values shown may be read directly as nanodarcies (10^{-21} m^2 = 1 nd).

Figure 2 shows a histogram of the logarithm of the apparent permeabilities given in Table 1. The mean of the log is -20.45 (k = 3.5 x 10^{-21} m^2, or about 3.5 nanodarcy), and the standard deviation of the logarithm of k_{app} is 0.81. Also shown is the lognormal distribution corresponding to these values. These limited data and the highly idealized model suggest a lognormal distribution for the apparent permeability. This is a common observation in other rocks.

The highest value of apparent permeability shown in Figure 2, 4.4 x 10^{-19} m^2, is likely to be anomalously high. That datum represents the brine inflow rate to borehole NG252, a borehole that is known to intersect a horizontal fracture associated with Marker Bed 139 [30]. Thus, the ideal smooth borehole model from which the apparent permeability was calculated can be expected to yield an anomalous value that does not correctly characterize the host rock salt. A fracture can introduce a large surface area for inflow; if this flow is then averaged over the borehole wall area only, the calculated flux and the apparent permeability will be erroneously large. A model that accounts explicitly for flow to both the borehole and a large intercepted fracture should yield a more nearly representative value for the apparent permeability. For example, an order-of-magnitude estimate of the additional inflow from a 12 m radius crack with a very small aperture yields an apparent permeability of 10^{-20} m^2, a value that is in better agreement with the other permeability values.

E.4 WIPP HORIZON GAS FLOW MEASUREMENT RESULTS SUMMARY THROUGH 1986

This subsection of Appendix E contains information and data on WIPP facility horizon in situ flow tests and measurements conducted through 1986. Flow measurement tests can be grouped into three categories: 1984 tests, N1420 drift tests, and first storage panel tests. The results of these tests are briefly summarized in the following excerpt. More detail on the 1984 and N1420 tests can be found in SEIS Appendix E, SEIS Subsections E.5 and E.6. This subsection is provided to support near-field permeability rates defined in the text.

This subsection is excerpted from Appendices B and C from Stormont et al., 1987, Summary of and Observations About WIPP Facility Horizon Flow Measurements through 1986.

APPENDIX B

TEST RESULTS

APPENDIX B: TEST RESULTS

In-situ gas flow measurements made at the WIPP horizon through 1986 can be grouped into three sets: 1984 tests, N1420 drift tests, and first storage panel tests. In the following sections, results are briefly summarized. Unless otherwise specified, flow rates given are normalized as described in Section A.4.1.

An important aspect of these measurements is the documentation. A test plan and subsequent addenda (Stormont and Peterson, 1984) provide the technical motivation and plans for conducting the tests. Complete test procedures are prepared prior to testing, and are strictly adhered to in the field. Records of completed test procedures, calibrations, notes, data, and data analyses and interpretation are maintained in a controlled notebook system, a copy of which is kept at the WIPP site.

B.1. 1984 Flow Tests

During 1984, eighteen gas flow tests were conducted in two phases at the WIPP disposal horizon. Objectives of the twelve Phase-1 tests were to estimate: permeability and porosity of the halite; permeability variation with distance from the mine surface; influence of the interspersed clay/anhydrite seams on the measured permeability values. Six short-duration, order-of-magnitude flow tests were performed as Phase 2 of this project. Phase-2 tests were used to confirm Phase-1 test results. Both phases are described in detail by Peterson et al. (1985) and summarized below.

B.1.1. Phase 1--All Phase-1 tests were performed during August 1984 from boreholes drilled horizontally upward and downward from Rooms L1 and L2. These rooms are located at the disposal horizon at the north end of the facility (see Figure B.1) and were excavated in April 1984. Tests were performed using the low-pressure test system over intervals from 0.5 to 15 m from the excavation. When multiple tests were conducted in the same borehole, the

borehole was lengthened as required for each subsequent test. The holes used were drilled one to three days before testing. Most tests were shut-in or pressure-decay tests conducted with nitrogen at 0.3 to 0.6 MPa. Typical test durations were on the order of 20 hours. Test results are summarized in Table C.1.

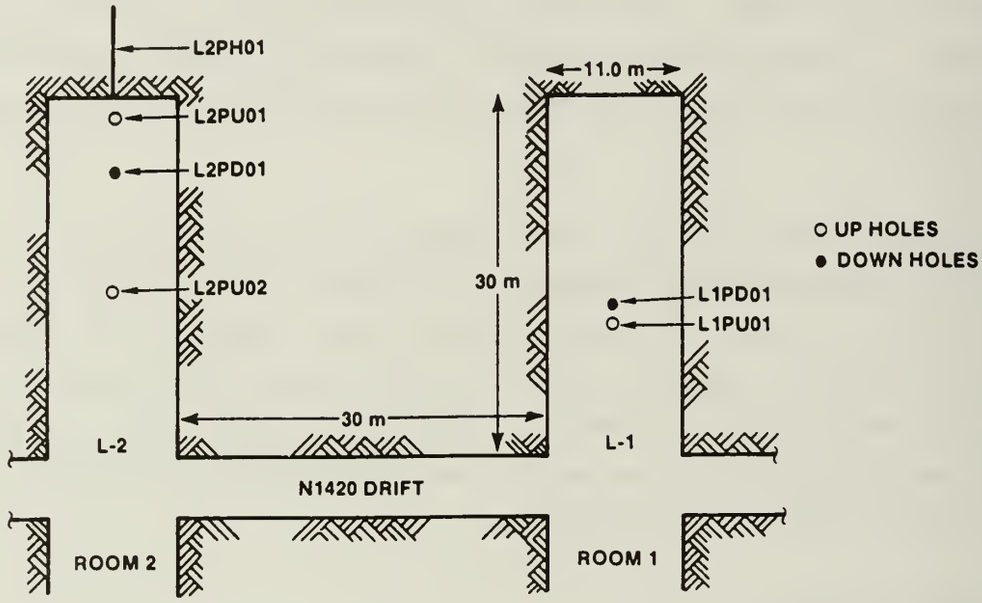

Figure B.1. Location of test holes for Phase-1 tests.

Test intervals composed of predominately halitic rocks and which specifically excluded anhydrite and clay layers accepted gas at flow rates below 1 SCCM; flow rates varied from 0.5 SCCM to less than $4E^{-4}$ SCCM. Note that the three largest flow rates measured in the salt (0.56, 0.52, and 0.26 SCCM) represent an upper limit, because guard zones were not used and packer bypass could not be measured.

Flow rates measured in intervals containing a significant clay or anhydrite seam were much more variable. Flow rates comparable to that of halite intervals (less than 1 SCCM) were measured in three cases. An interval containing a thick clay seam 14 m above the back of Room L-1 accepted gas at less than $4E^{-4}$ SCCM. A clay seam 7 m above Room L-2 was contained in a test

interval which took gas at about $1E^{-2}$ SCCM. Seam B (about 2.1 m above the back of Room L-2) accepted gas at about $5E^{-2}$ SCCM when the measurement was made from borehole L2PU01, located near the heading and midway between the ribs. Seam A (about 4 m above the back of Room L-2) produced a small flow of gas, even when pressurized to 0.65 MPa.

On the other hand, some test intervals containing clay or anhydrite layers had relatively large flow rates. During two tests, Seam B accepted gas at a rate of about 1700 SCCM when the measurements were made from Borehole L2PU02, about 15 m from the heading and midway between the ribs. An interval which contained MB139 accepted gas at a rate of about 500 SCCM; the test borehole (L2PD01) was located approximately 15.2 m from the heading and midway between the ribs.

Permeabilities were calculated for these results by both the transient flow and order-of-magnitude methods. For salt, maximum permeability is less than 1 microdarcy. Calculated porosities were between 0.01 and 0.001. Similar values were found for test intervals which included clay or anhydrite seams that were either well removed from the drift or near the heading or edge of the drift.

Permeability and porosity values were also determined for tests in which relatively large flows were measured. However, the correlation between the measured and calculated test response was poor, suggesting that the formation response was not that of simple Darcy-type flow.

B.1.2. Phase 2--Phase-2 tests were conducted in Room 4, excavated in March 1983 and located at the disposal horizon. Test boreholes are shown in Figure B.2. These order-of-magnitude, constant-flow tests used nitrogen at test pressures less than 0.7 MPa. Test durations ranged from a few minutes to a few hours. Test results are summarized in Table C.2.

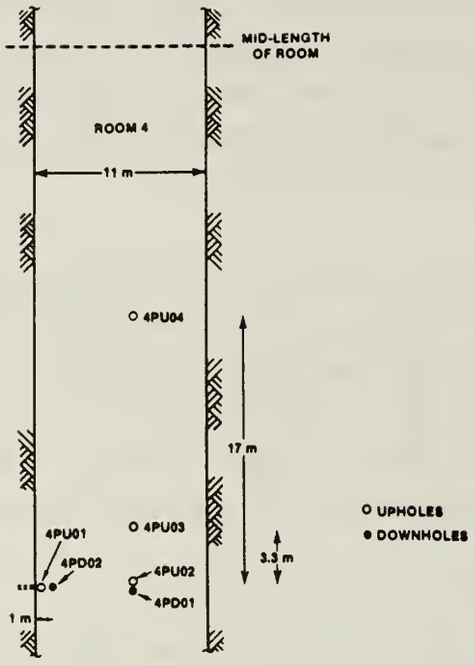

Figure B.2. Test boreholes in Room 4 for Phase-2 tests.

During Phase-2 confirmation tests, MB139 and the clay/anhydrite Seam B accepted gas at rates of $6.4E^5$ and $1.9E^3$ SCCM from boreholes 4PD01 and 4PU04, located along the centerline of Room 4. In contrast, MB139 and Seam B accepted gas at a rate below the approximately 1 SCCM resolution of these particular order-of-magnitude measurements when examined from boreholes near the rib (4PD02 and 4PU01), or from an inclined borehole intersecting MB139 and removed from the boundaries of the excavation. Seam A accepted gas at less than 1 SCCM when tested from Borehole 4PU02 on the centerline of the drift.

B.2 N1420 Tests

A series of tracer-gas/flow tests was conducted in the N1420 drift during January and February 1986. The principal objective was to evaluate flow characteristics of MB139 at different locations relative to nearby excavations. A limited number of tests were conducted to evaluate the first interbed above the storage horizon, Seam B. Follow-up test were conducted during July and August 1986.

Two areas were examined (see Figure B.3). The one located in the N1420 drift between Room 1 and the E0 drift is referred to as the N1420-E0 area. The second, designated L2-N1420-RM2, is located at the N1420 drift intersection with Rooms L2 and 2. Rooms 1 and 2 and the N1420 drift were excavated in March 1983, and the L1 and L2 Rooms in April 1984.

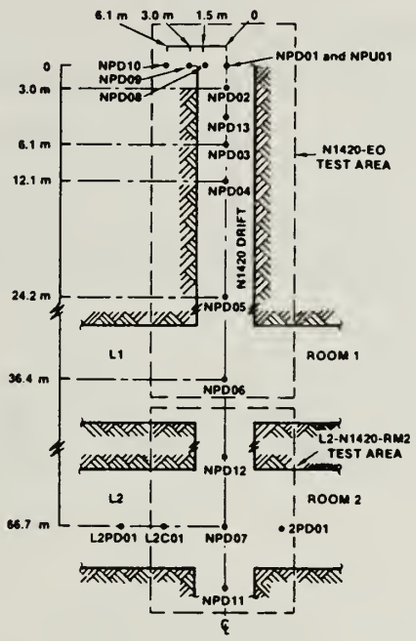

Figure B.3. Test area and boreholes for N1420 tests.

B.2.1. Initial Gas Flow Test--Preliminary order-of-magnitude gas flow tests used to estimate flow rates and gas sampling intervals to be used during the tracer-gas/flow tests are summarized in Table C.3. Initially, a sewer-type single packer was used; however, it was found that as a result of packer bypass flow, this system could only be used to measure flows greater than 1000 SCCM. Consequently, subsequent gas flow measurements were made with a dual packer injection system. Test pressures were limited to less than 0.15 MPa.

The following results were obtained for the test intervals which contained MB139. In the N1420-E0 area, test intervals accepted flows ranging from 10 SCCM to 200 SCCM. In the L2-N1420-RM2 area, test intervals accepted flows ranging from 300 SCCM to 30,000 SCCM. Test intervals in the room L1 and L2

area and those near the room/drift intersection all exhibited flows on the order of 10,000 SCCM.

B.2.2. Tracer Measurements--Tracer gas/flow tests were conducted in the L2-N1420-RM2 area. The first two tests consisted of a source borehole (NPD07) in which N_2 tagged with SF^6 at a $10E^{-8}$ volumetric concentration was injected at a flow rate of $9x10E^3$ SCCM at a downhole pressure of $7x10E^{-6}$ MPag in the interval 1 to 3.1 m beneath the floor containing MB139. During these tests, no tracer arrival was measured in any of the receiving holes located in the N1420 drift, Rooms 2 and L2. A third test using a mixture of N_2 tagged with SF_6 at a volumetric concentration of $10E^{-2}$ was conducted using the flow conditions described above. Prior to this test, tarps were placed on the floor to trap any gas moving up through the floor (see Figure B.4).

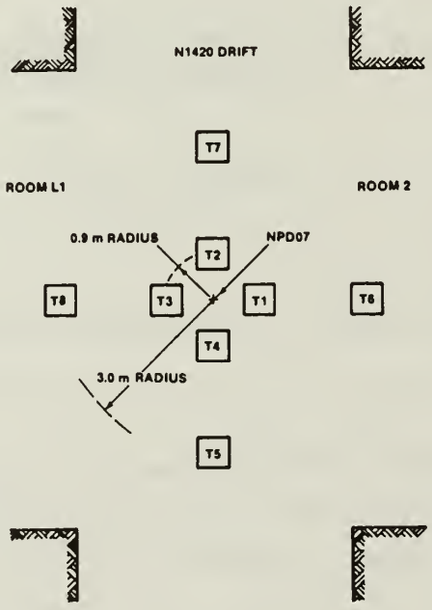

Figure B.4. Location of the tarps in N1420/Room 2/Room L2 intersection.

During the test, gas samples were taken in the boreholes and underneath the tarps. Within 10 minutes after start of the test, tracer was detected below all tarps. Substantial amounts were found below tarps T2, T3, T7 and T8; smaller quantities were found below the remaining tarps. By 13 minutes,

substantial tracer arrived in boreholes in Room L2, and a smaller amount arrived in Borehole L2C01. Small amounts were detected in boreholes in 2PD01 and NPD12 in the 14- to 18-minute interval. Substantial arrivals had occurred at all boreholes by approximately 60 minutes. By 105 minutes, the N1420 drift was saturated with tracer and the test was terminated. Results of these tests suggest that fractures exist which permit rapid communication in both the horizontal and vertical directions. Crude analyses applying Equation (A.5) are consistent with the existence of multiple fractures with a maximum horizontally-oriented fracture aperture about 0.04 cm, and a maximum vertically-oriented fracture aperture about 0.02 cm.

One tracer-gas/flow test performed by injecting N_2 tagged with Freon 13B1 into Borehole NPD04 at a $3.4x10E^{-2}$ MPag downhole pressure resulted in an approximate 5-SCCM flow. The NPD04 borehole was drilled vertically downward and injection occurred between the 1.1- and 3.1-m depths (containing MB139). Prior to the test, tarps were placed on the floor (see Figure B.5). During the test, gas samples were collected for analysis from beneath tarps and from boreholes along the N1420 drift.

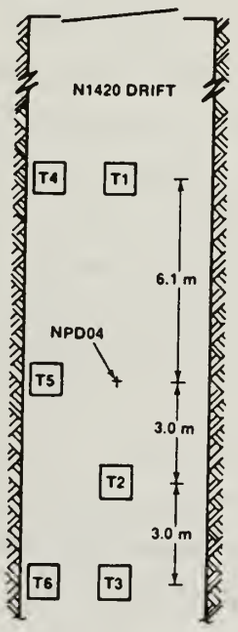

Figure B.5. Location of tarps in N1420 drift.

Within 15 minutes after the test began, tracer was detected in Borehole NPD03. Tracer was found at 30 minutes in Borehole NPD13, and at 105 minutes in NPD02. By the time sampling was terminated (at 300 minutes), tracer had also been found in Borehole NPD08 and beneath Tarp 1. These results suggest the existence of fractures below the floor in the N1420 drift in the region of Borehole NPD03; application of test results to Equation (A.5) infers a maximum horizontal fracture aperture of 0.002 cm.

B.2.3. Follow-Up Flow Tests--Gas flow tests were repeated in existing boreholes with a dual-packer, order-of-magnitude flow measurement system. The objectives were to conduct gas flow tests in intervals containing MB139 from boreholes in the N1420 drift area not previously tested, and to confirm some of the earlier results. Measurements were to be made in the salt between the invert and MB139, which the tracer measurements had revealed were fractured in some locations, and limited tests were to be conducted on the formation immediately above the excavations. Test results are summarized in Table C.4.

In test intervals containing MB139, flow rates from boreholes drilled down from the center of the 6.6-m-wide by 4.0-m-high N1420 drift ranged between 4 and 450 SCCM; measurements made from boreholes located at intersections or in the center of 11.0-m-wide by 4.3-m-high drifts resulted in flow rates greater than $2.5E^5$ SCCM. Measurements made from boreholes near the edge of the drift or outside the bounds of the drift were below 1 SCCM. The salt interval between MB139 and the invert or between Seam B and the back was tested in existing holes by using the straddle zone between the dual packers as the test intervals, and the bottom of the hole as "half" a guard zone. Thus, measured values represent upper limits, because packer bypass could not be measured. Flow rates measured in the salt between MB139 and the invert were quite variable. The highest flow rate ($<7.1E^4$ SCCM) was measured from Borehole NPD08, near the rib in the N1420 drift. Measurements from other boreholes along the center of the N1420 drift varied from less than 0.2 to more than 1000 SCCM. A measurement from Borehole NPD09, which intercepts this salt layer outside the bounds of the N1420 drift, was less than 7 SCCM.

A few similar measurements were made on test intervals above the back. Seam B accepted gas at a rate of about 45 SCCM in a borehole in the N1420

drift (NPU01), and more than $2.5E^5$ from a borehole in Room L-2 (L2CU1). Thus, results were qualitatively comparable to results of tests conducted in MB139; that is, Seam B permitted considerably more flow in the L2-N1420-RM2 area than in the N1420-E0 area. In addition, the salt interval between the back and Seam B was tested in the same holes; flow rates of about 100 and 1700 SCCM were measured in boreholes NPU01 and L2CU1, respectively.

Gas flow and tracer tests indicate that the formation below the floor in both the L2-N1420-RM2 and N1420-E0 test areas is fractured so that flow occurs in the horizontal and vertical directions. The fracturing in the L2-N1420-RM2 area is much more severe than in the N1420-E0 area. For example, a $6.9x10E^{-2}$ MPag downhole pressure in Borehole NPD07 would produce a gas flow rate approximately $5x10E^3$ times larger than would be obtained at the same pressure in Borehole NPD04. Further, the estimated largest fracture in the L2-N1420-RM2 test area has an aperture about 20 times greater than the largest fracture in the N1420-E0 test area.

B.3. First Storage Panel Tests

Flow measurements were conducted in the entryways to the first storage panel during May and June 1986. The objectives were to determine if relatively high flow regions existed in the vicinity of the planned panel seals, and how these regions develop or change with time. These tests were performed in test intervals which contained the first significant interbedding both above and beneath the excavation (Seam B and MB139), and were made near the center of the excavation. These measurements were made as soon as practicable (about one month) after excavation to establish early-time flow characteristics; subsequent measurements will indicate time dependence of the changes in flow.

Measurements were made at three stations in both entryways: the S1600 and S1950 drifts between the E300 and E450 drifts (see Figure B.6). The S1600 entryway is 4.3 m high by 4.6 m wide, and was mined in April 1986. The S1950 entryway is 4.3 m high by 6.7 m wide, and was mined in May 1986. At each station, holes nominally 3.3 m deep in the vertically upward and downward directions were drilled within about 30 days of mining of the drift at that

location. Gas flow measurements with a resolution of 0.1 SCCM, test pressures of about 0.2 MPa, and typical test durations of 4 hours were made within a few days of test borehole drilling. The test intervals into the invert contained MB139 and a portion of salt above and below it. The test intervals into the roof contained Seam B and adjacent salt. All of the test intervals were from 1.3 to 3.3 m from the excavation. Results are summarized in Table C.5.

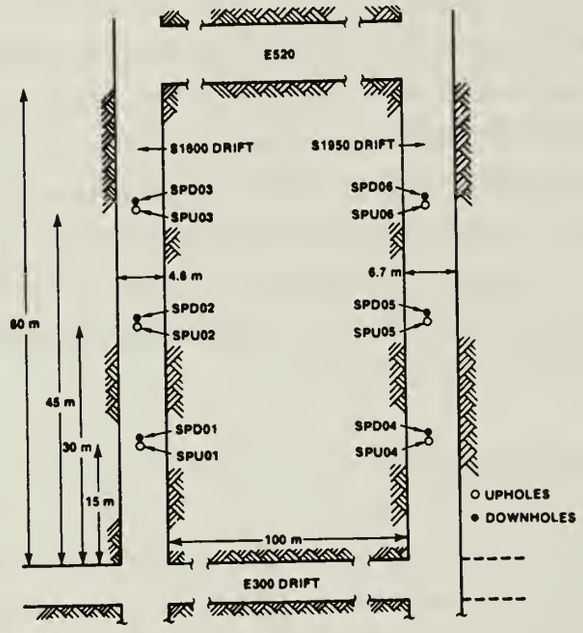

Figure B.6. First storage panel test hole locations.

Flow measured in the downward intervals in the S1600 drift were less than 1 SCCM, whereas in two of the three downward intervals in the S1950 drift the flow was greater than 10 SCCM. In all but one of the six upward intervals, attempts at pressure decay tests once the interval was brought up to about 0.2 MPa were unsuccessful; in fact, the pressure increased while the interval was shut in, indicating gas production from the formation. The only pressure decay test in an upward interval (in the S1950 drift) resulted in an measured flow rate of about 0.1 SCCM.

A set of five upward vertical holes through Seam B in the E300 drift near the first storage panel entries was drilled after testing was complete in the

first panel. The principal objective was to identify gas-producing intervals so they could be cased and fitted with a pressure gage to measure pressure buildup, and perhaps eventually an equilibrium pressure. All these intervals did in fact produce small volumes of gas, and their shut-in pressures are presently being monitored.

APPENDIX C

SUMMARY OF GAS FLOW MEASUREMENT RESULTS

APPENDIX C; SUMMARY OF GAS FLOW MEASUREMENT RESULTS

Appendix C summarizes in-situ gas flow measurement results in tabular form. In these tables results are given both as flow rates and as permeabilities. Flow rates are given for the conditions of a particular test and also normalized to reference conditions. Permeability calculated from a particular test is given as inferred from the transient method (if applicable) and the steady-state method. In this way, results from the two methods can be compared.

Tables C.1 through C.5 provide information about the location of the borehole and test interval with respect to the drift, and identify the primary geologic feature in the test interval. For our purposes, the test interval feature was identified as salt or halite, unless a significant discontinuity was present (MB139, seams A or B). Information is also given about drift dimensions and age at time of the test.

Table C.1. Summary of 1984 Phase 1 Tests

	HOLE			TEST INTERVAL			DRIFT							FLOW RATE	PERMEABILITY ANALYSIS		
NO.	OR	LOCATION W/R/T DRIFT	GEO FEAT	DIST MIN	FROM MAX	DRIFT MEAN	W	SIZE H	(M) AREA	AGE AT TEST (YRS)	TYPE OF TEST		MEASURED FLOW RATE (SCCM)	MEASURED TEST PRESSURE (MPA)	NORMALIZED FLOW RATE (SCCM)	TRANSIENT METHOD K(uD)	POROSITY	STEADY-STATE METHOD K(uD)
1	L2PH01	H	AT HEADING	H	0.5	0.7	0.60	11.0	4.3	47.30	0.250	P.D.	1	< 2.32E-01	0.310	< 2.60E-01	< 2.8E-01	0.01	< 2.9E-01
2	L2PH01	H	AT HEADING	H	0.5	0.7	0.60	11.0	4.3	47.30	0.250	FLOW	2	< 5.02E-01	0.310	< 5.62E-01	< 6.2E-01	0.01	< 3.8E-01
3	L2PU01	U	NEAR HEADING	B	1.7	2.5	2.10	11.0	4.3	47.30	0.250	P.D.	3	1.08E+00	0.640	5.60E-02	4.4E-02	0.001	5.0E-02
4	L2PU02	U	CENTER	B	1.9	2.8	2.35	11.0	4.3	47.30	0.250	FLOW	4	9.00E+03	0.330	1.63E+03	NA	NA	3.7E+03
5	L2PD01	D	CENTER	M	1.5	3.2	2.35	11.0	4.3	47.30	0.250	FLOW	5	8.24E+03	0.410	5.15E+02	8.3E+02	0.01	1.2E+03
6	L2PD01	D	CENTER	H	3.2	4.0	3.60	11.0	4.3	47.30	0.250	P.D.	6	< 7.59E+00	0.570	< 5.21E-01	< 6.3E-01	0.001	< 5.4E-01
7	L2PU01	U	NEAR HEADING	A	4.0	4.9	4.45	11.0	4.3	47.30	0.250	P.D.	7	PRODUCED GAS			PRODUCED GAS		
8	L2PU01	U	NEAR HEADING	H	5.6	6.5	6.05	11.0	4.3	47.30	0.250	P.D.	8	2.27E-01	0.600	1.20E-02	9.3E-03	0.001	1.4E-02
9	L2PH01	H	AT HEADING	H	6.1	7.6	6.85	11.0	4.3	47.30	0.250	P.D.	9	3.00E-02	0.310	4.00E-03	1.0E-03	0.001	4.4E-03
10	L2PU01	U	NEAR HEADING	O	6.8	7.7	7.25	11.0	4.3	47.30	0.250	P.D.	10	2.58E-01	0.600	1.40E-02	9.8E-03	0.005	1.5E-02
11	L1PD01	D	CENTER	H	11.3	13.7	12.50	11.0	4.3	47.30	0.250	P.D.	11	2.53E-01	0.650	4.00E-03	1.0E-03	0.001	4.8E-03
12	L1PU01	U	CENTER	O	13.4	15.2	14.30	11.0	4.3	47.30	0.250	P.D.	12	< 2.50E-02	0.650	< 4.00E-04	< 3.2E-04	0.001	< 4.7E-04
13	L2PU02	U	CENTER	B	1.9	2.8	2.35	11.0	4.3	47.30	0.250	P.D.	13	8.04E+03	0.300	1.84E+03	2.8E+03	0.01	3.3E+03
14	L2PH01	H	AT HEADING	H	1.6	2.0	1.80	11.0	4.3	47.30	0.250	P.D.	14	6.90E-02	0.310	2.90E-02	2.3E-02	0.01	5.0E-02

Table C.2. Summary of 1984 Phase 2 Tests

	HOLE			TEST INTERVAL				DRIFT						FLOW RATE	PERMEABILITY ANALYSIS		
	NO.	OR	LOCATION W/R/T DRIFT	GEO FEAT	DIST MIN	FROM MAX	DRIFT MEAN	W	SIZE H	(M) AREA	AGE AT TEST (YRS)	TYPE OF TEST	MEASURED FLOW RATE (SCCM)	MEASURED TEST PRESSURE (MPA)	NORMALIZED FLOW RATE (SCCM)	TRANSIENT METHOD K(uD)	POROSITY	STEADY-STATE METHOD K(uD)
1	4PDO1	D	CENTER	M	1.2	2.8	2.00	11.0	4.3	47.30	1.667	FLOW	1 1.70E+05	0.110	6.40E+05	NA	NA	> 1.0E+06
2	4PDO2	D	NEAR RIB	M	1.5	2.8	2.15	11.0	4.3	47.30	1.667	FLOW	2 < 5.70E+01	0.650	< 1.87E+00	NA	NA	< 1.0E+01
3	4PU04	U	CENTER	B	1.3	3.4	2.35	11.0	4.3	47.30	1.667	FLOW	3 1.10E+05	0.660	1.90E+03	NA	NA	1.0E+03
4	4PU01	U	NEAR RIB	B	2.8	4.3	3.55	11.0	4.3	47.30	1.667	FLOW	4 < 5.70E+01	0.650	< 1.54E+00	NA	NA	< 1.0E+01
5	4PU02	U	CENTER	A	3.4	5.0	4.20	11.0	4.3	47.30	1.667	FLOW	5 < 5.70E+01	0.650	< 1.54E+00	NA	NA	< 1.0E+01
6	DPDO1	D	REMOVED	M	9.3	12.5	10.90	4.7	4.0	18.80	0.500	FLOW	6 < 5.70E+01	0.650	< 7.70E-01	NA	NA	< 1.0E+01

Table C.3. Summary of N1420 Initial Tests

	NO.	HOLE OR	LOCATION W/R/T DRIFT	TEST INTERVAL GEO FEAT	DIST MIN	FROM MAX	DRIFT MEAN	DRIFT W	SIZE H	(M) AREA	AGE AT TEST (YRS)	TYPE OF TEST		MEASURED FLOW RATE (SCCM)	MEASURED TEST PRESSURE (MPA)	FLOW RATE NORMALIZED FLOW RATE (SCCM)	PERMEABILITY ANALYSIS TRANSIENT METHOD K(uD)	POROSITY	STEADY-STATE METHOD K(uD)
1	NPD02	D	CENTER	M	1.0	2.6	1.80	6.6	4.0	26.40	2.833	FLOW	1	2.00E+02	0.135	2.86E+02	NA	NA	3.0E+02
2	NPD05	D	CENTER	M	1.0	2.8	1.90	6.6	4.0	26.40	2.833	FLOW	2	3.70E+01	0.135	4.90E+01	NA	NA	5.0E+01
3	NPD05	D	CENTER	M	1.0	2.8	1.90	6.6	4.0	26.40	2.833	P.D.	3	6.38E+01	0.135	8.40E+01	NA	NA	8.5E+01
4	NPD04	D	CENTER	M	1.0	2.9	1.95	6.6	4.0	26.40	2.833	FLOW	4	4.00E+01	0.135	4.80E+01	NA	NA	5.2E+01
5	NPD06	D	INTERSECT	M	1.0	2.9	1.95	12.8	4.0	51.20	2.833	FLOW	5	5.60E+03	0.108	3.80E+04	NA	NA	8.4E+04

Table C.4. Summary of N1420 Follow-up Tests

	NO.	HOLE OR	LOCATION W/R/T DRIFT	TEST INTERVAL GEO FEAT	DIST MIN	FROM MAX	DRIFT MEAN	DRIFT SIZE W	SIZE H	(M) AREA	AGE AT TEST (YRS)	TYPE OF TEST	MEASURED FLOW RATE (SCCM)	MEASURED TEST PRESSURE (MPA)	FLOW RATE NORMALIZED FLOW RATE (SCCM)	PERMEABILITY ANALYSIS TRANSIENT METHOD K(uD)	POROSITY	STEADY-STATE METHOD K(uD)
1	L2CU1	U	CENTER	B	1.1	2.8	1.95	11.0	4.3	47.30	3.500	FLOW	1 > 3.10E+04	0.007	> 2.50E+05	NA	NA	> 4.0E+06
2	NPUO1	U	CENTER	H	0.5	0.9	0.65	6.6	4.0	26.40	3.500	P.D.	2 < 4.28E+01	0.239	< 4.27E+01	NA	NA	< 8.7E+01
3	NPDO5	D	CENTER	H	0.4	0.8	0.60	6.6	4.0	26.40	3.500	P.D.	3 < 9.15E-02	0.253	< 7.95E-02	NA	NA	< 8 .E-02
4	NPDO4	D	CENTER	H	0.5	0.9	0.65	6.6	4.0	26.40	3.500	P.D.	4 < 2.95E-01	0.253	< 2.57E-01	NA	NA	< 2.7E-01
5	NPDO3	D	CENTER	H	0.3	0.7	0.50	6.6	4.0	26.40	3.500	FLOW	5 < 4.47E+02	0.135	< 2.56E+03	NA	NA	< 5.2E+03
6	2PD01	D	CENTER	H	0.4	0.8	0.55	11.0	4.3	47.30	3.500	FLOW	6 < 3.42E+02	0.170	< 8.55E+02	NA	NA	< 1.8E+03
7	NPD12	D	CENTER	H	0.4	0.8	0.55	6.6	4.0	26.40	3.500	P.D.	7 < 3.87E+01	0.239	< 3.37E+01	NA	NA	< 6.9E+01
8	NPDO7	D	INTERSECT	H	0.4	0.8	0.55	12.8	4.0	51.20	3.500	P.D.	8 < 1.57E+02	0.237	< 1.60E+02	NA	NA	< 3.3E+02
9	NPDO6	D	INTERSECT	H	0.4	0.8	0.57	12.8	4.0	51.20	3.500	FLOW	9 < 2.75E+02	0.135	< 1.57E+03	NA	NA	< 3.2E+03
10	NPDO9	D	REMOVED	H	0.5	0.9	0.65	6.6	4.0	26.40	3.500	P.D.	10 < 7.50E+00	0.251	< 6.62E+00	NA	NA	< 1.4E+01
11	NPDO8	D	NEAR RIB	H	0.5	0.9	0.65	6.6	4.0	26.40	3.500	FLOW	11 < 1.24E+04	0.135	< 7.10E+04	NA	NA	< 1.5E+05
12	NPDO2	D	CENTER	H	0.5	0.9	0.65	6.6	4.0	26.40	3.500	FLOW	12 < 4.09E+02	0.170	< 1.02E+03	NA	NA	< 5.6E+03
13	NPD01	D	CENTER	H	0.5	0.9	0.65	6.6	4.0	26.40	3.500	P.D.	13 < 7.60E+00	0.239	< 7.50E+00	NA	NA	< 1.6E+00
14	L2CU1	U	CENTER	H	0.5	0.9	0.67	11.0	4.3	47.30	3.500	FLOW	14 < 2.93E+02	0.135	< 1.68E+03	NA	NA	< 3.4E+03
15	NPD02	D	CENTER	M	1.0	2.5	1.75	6.6	4.0	26.40	3.417	FLOW	15 5.72E+02	0.170	4.24E+02	NA	NA	8.7E+02
16	NPD02	D	CENTER	M	1.0	2.5	1.75	6.6	4.0	26.40	3.417	FLOW	16 2.17E+02	0.135	3.68E+02	NA	NA	7.6E+02
17	NPD03	D	CENTER	M	1.0	2.7	1.85	6.6	4.0	26.40	3.417	P.D.	17 1.54E+01	0.239	4.00E+00	NA	NA	4.1E+00
18	NPD05	D	CENTER	M	1.0	2.8	1.90	6.6	4.0	26.40	3.417	FLOW	18 4.49E+02	0.170	2.72E+02	NA	NA	5.6E+02

Table C.4. Summary of N1420 Follow-up Tests (Continued)

	NO.	HOLE OR	LOCATION W/R/T DRIFT	GEO FEAT	TEST INTERVAL DIST MIN	TEST INTERVAL FROM MAX	TEST INTERVAL DRIFT MEAN	DRIFT SIZE (M) W	DRIFT SIZE (M) H	DRIFT AREA	AGE AT TEST (YRS)	TYPE OF TEST	MEASURED FLOW RATE (SCCM)	MEASURED TEST PRESSURE (MPA)	FLOW RATE NORMALIZED FLOW RATE (SCCM)	PERMEABILITY ANALYSIS TRANSIENT METHOD K(uD)	PERMEABILITY ANALYSIS POROSITY	PERMEABILITY ANALYSIS STEADY-STATE METHOD K([illegible])
19	NPD05	D	CENTER	M	1.0	2.8	1.90	6.6	4.0	26.40	3.417	FLOW 19	4.49E+02	0.205	1.61E+02	NA	NA	3.3E+02
20	2PD01	D	CENTER	M	1.0	2.9	1.95	11.0	4.3	47.30	3.500	FLOW 20	> 3.10E+04	0.007	> 2.50E+05	NA	NA	> 4.0E+06
21	NPD12	D	CENTER	M	1.0	2.9	1.95	6.6	4.0	26.40	3.500	P.D. 21	2.62E+01	0.139	6.90E+00	NA	NA	1.4E+01
22	NPD07	D	INTERSECT	M	1.0	2.9	1.95	12.8	4.0	51.20	3.500	FLOW 22	> 3.10E+04	0.007	> 2.50E+05	NA	NA	> 4.0E+06
23	NPD06	D	INTERSECT	M	1.0	2.9	1.95	12.8	4.0	51.20	3.500	FLOW 23	> 3.10E+04	0.007	> 2.50E+05	NA	NA	> 4.0E+06
24	NPD04	D	CENTER	M	1.0	2.9	1.95	6.6	4.0	26.40	3.417	FLOW 24	3.68E+02	0.204	1.30E+02	NA	NA	2.7E+02
25	NPD09	D	REMOVED	M	1.0	3.0	2.00	6.6	4.0	26.40	3.417	P.D 25	1.52E+00	0.239	3.40E-01	NA	NA	3.5E-01
26	NPD08	D	NEAR RIB	M	1.0	3.7	2.35	6.6	4.0	26.40	3.417	P.D 26	< 3.97E-01	0.237	< 1.70E-01	NA	NA	< 6.9E-02
27	NPD01	D	CENTER	M	1.0	3.7	2.35	6.6	4.0	26.40	3.417	FLOW 27	1.15E+02	0.235	2.00E+01	NA	NA	4.2E+01
28	NPU01	U	CENTER	B	1.0	4.3	2.65	6.6	4.0	26.40	3.417	FLOW 28	5.91E+02	0.135	4.51E+02	NA	NA	9.3E+02
29	NPU01	U	CENTER	B	1.0	4.3	2.65	6.6	4.0	26.40	3.417	FLOW 29	3.47E+02	0.170	1.16E+02	NA	NA	2.4E+02
30	NPD10	D	REMOVED	M	1.0	4.7	2.85	6.6	4.0	26.40	3.417	P.D 30	< 7.00E-01	0.239	< 8.00E-02	NA	NA	< 8.7E-02

Table C.5. Summary of First Panel Tests

	NO.	HOLE OR	LOCATION W/R/T DRIFT	GEO FEAT	TEST INTERVAL DIST MIN	FROM MAX	DRIFT MEAN	DRIFT SIZE W	H	(M) AREA	AGE AT TEST (YRS)	TYPE OF TEST	MEASURED FLOW RATE (SCCM)	MEASURED TEST PRESSURE (MPA)	FLOW RATE NORMALIZED FLOW RATE (SCCM)	PERMEABILITY ANALYSIS TRANSIENT METHOD K(uD)	POROSITY	STEADY-STATE METHOD K(uD)
1	SPD06	D	CENTER	M	1.3	3.3	2.30	6.7	4.3	28.81	0.083	P.D. 1	3.30E+01	0.190	1.18E+01	NA	NA	1.3E+01
2	SPU01	U	CENTER	B	1.3	3.3	2.30	4.6	4.3	19.78	0.083	P.D. 2	PRODUCED GAS			PRODUCED GAS		
3	SPU06	U	CENTER	B	1.3	3.3	2.30	6.7	4.3	28.81	0.083	P.D. 3	PRODUCED GAS			PRODUCED GAS		
4	SPU02	U	CENTER	B	1.3	3.3	2.30	4.6	4.3	19.78	0.083	P.D. 4	PRODUCED GAS			PRODUCED GAS		
5	SPU05	U	CENTER	B	1.3	3.3	2.30	6.7	4.3	28.81	0.083	P.D. 5	PRODUCED GAS			PRODUCED GAS		
6	SPD02	D	CENTER	M	1.3	3.3	2.30	4.6	4.3	19.78	0.083	P.D. 6	2.80E-01	0.230	6.00E-02	NA	NA	6.8E-02
7	SPD05	D	CENTER	M	1.3	3.3	2.30	6.7	4.3	28.81	0.083	P.D. 7	1.00E+02	0.220	2.42E+01	NA	NA	2.8E+01
8	SPD01	D	CENTER	M	1.3	3.3	2.30	4.6	4.3	19.78	0.083	P.D. 8	< 1.00E+00	0.230	< 2.30E-01	NA	NA	< 3.0E-01
9	SPU04	U	CENTER	B	1.3	3.3	2.30	6.7	4.3	28.81	0.083	P.D. 9	8.30E-01	0.220	1.90E-01	NA	NA	2.2E-01
10	SPU03	U	CENTER	B	1.3	3.3	2.30	4.6	4.3	19.78	0.083	P.D. 10	PRODUCED GAS			PRODUCED GAS		
11	SPD04	D	CENTER	M	1.3	3.3	2.30	6.7	4.3	28.81	0.083	P.D. 11	2.49E+00	0.230	5.70E-01	NA	NA	6.5E-01
12	SPD03	D	CENTER	M	1.3	3.3	2.30	4.6	4.3	19.78	0.083	P.D. 12	5.30E-01	0.230	1.10E-01	NA	NA	1.3E-01

E.5 1984 GAS FLOW MEASUREMENT TEST RESULTS

This subsection of Appendix E contains Phase I test results of in situ gas flow measurement results collected in 1984. A summary of this test and its results can be found in SEIS Subsection E.4. This subsection is presented to support near-field horizon permeability rates detailed in the text.

This subsection was excerpted from Chapters 4 and 5 of Peterson et al., 1985, WIPP Horizon In-Situ Permeability Measurements.

4. PHASE I TEST RESULTS

A total of twelve tests were performed in six boreholes drilled from Rooms L1 and L2. Each borehole response will be individually discussed in this section. The tests themselves are denoted as No. 1 through No. 12, where the numbers indicate the order in which the tests were conducted. In those cases where multiple tests were conducted in the same borehole, after each test the borehole was lengthened as required for the subsequent test.

The raw data were interpreted as described in Section 3. Permeability and porosity values shown were determined assuming a classical uniform isotropic porous formation. Under those conditions, the measured data is sensitive to the formation permeability, connected porosity, wellbore volume, and geometry. Note here that no attempt was made to consider non-uniform material properties, formation saturation, multiphase flow, or brine movement.

Throughout this discussion, comparisons will be made between the measured and calculated results. Recall that once measured and calculated results matched, the selected material properties (as discussed in Section 3.2) were taken as representative of the formation. In examining these results, note that different portions of the data curves are sensitive to different parameters. For example, the permeability is most sensitive to the slope of the pressure decay curve at late times. The porosity is most sensitive to the amplitude of the pressure decay curve at late times. In addition, the final peak pressure obtained during the initial test interval fill period is very sensitive to both the formation permeability and the assumed wellbore volume.

The sensitivity of the data interpretation technique to the permeability, porosity, and wellbore volume values is illustrated during the following discussion. The sensitivity to both borehole volume and porosity will be shown as part of the Test No. 4 discussion. Porosity

sensitivity will be demonstrated as part of the Test No. 7 results. A demonstration of the permeability sensitivity will be given along with the Test No. 3 and No. 11 results.

Virtually all tests showed evidence of some packer bypass flow. This flow occurs along the packer borehole wall interface and is thought to result from a relatively rough-walled borehole, together with a short packer element. Packer bypass flow is different from the axial flow component illustrated on Figure 4 since flow to the guard zone was coincident with test initiation. In most cases, the packer bypass flow masked axial flow through the formation. Furthermore, bypass flow was insensitive to borehole orientation--thereby indicating it did not result from an asymmetric formation permeability. The flow into the formation was, therefore, taken as $w_F(t)$--as determined by Equation (1)--minus the flow going to the guard interval.

Stratigraphy common to the vertically down boreholes (L1PD01 and L2PD01) is shown on Figure 7. A detailed description of Marker Bed 139 is given on Figure 8. The stratigraphy common to the vertically up boreholes (L1PU01, L2PU01, and L2PU02) is shown on Figure 9. Horizontal borehole (L2PH01) lies in a competent predominately halite layer. The basis of this stratigraphy was developed from core logs of holes in the vicinity of the tests [10]. This stratigraphy was confirmed by examination of drill cuttings and use of borehole cameras.

During the tests, all data were recorded using Hewlett Packard data loggers. These data were then transferred to tapes and subsequently plotted. Computer plots of the raw data are shown in Appendix A.

Six additional permeability tests were performed in the WIPP Facility as the second phase of this project. These short duration confirmation tests were intended to measure "order-of-magnitude" permeability values. Results of these tests are given in Appendix B.

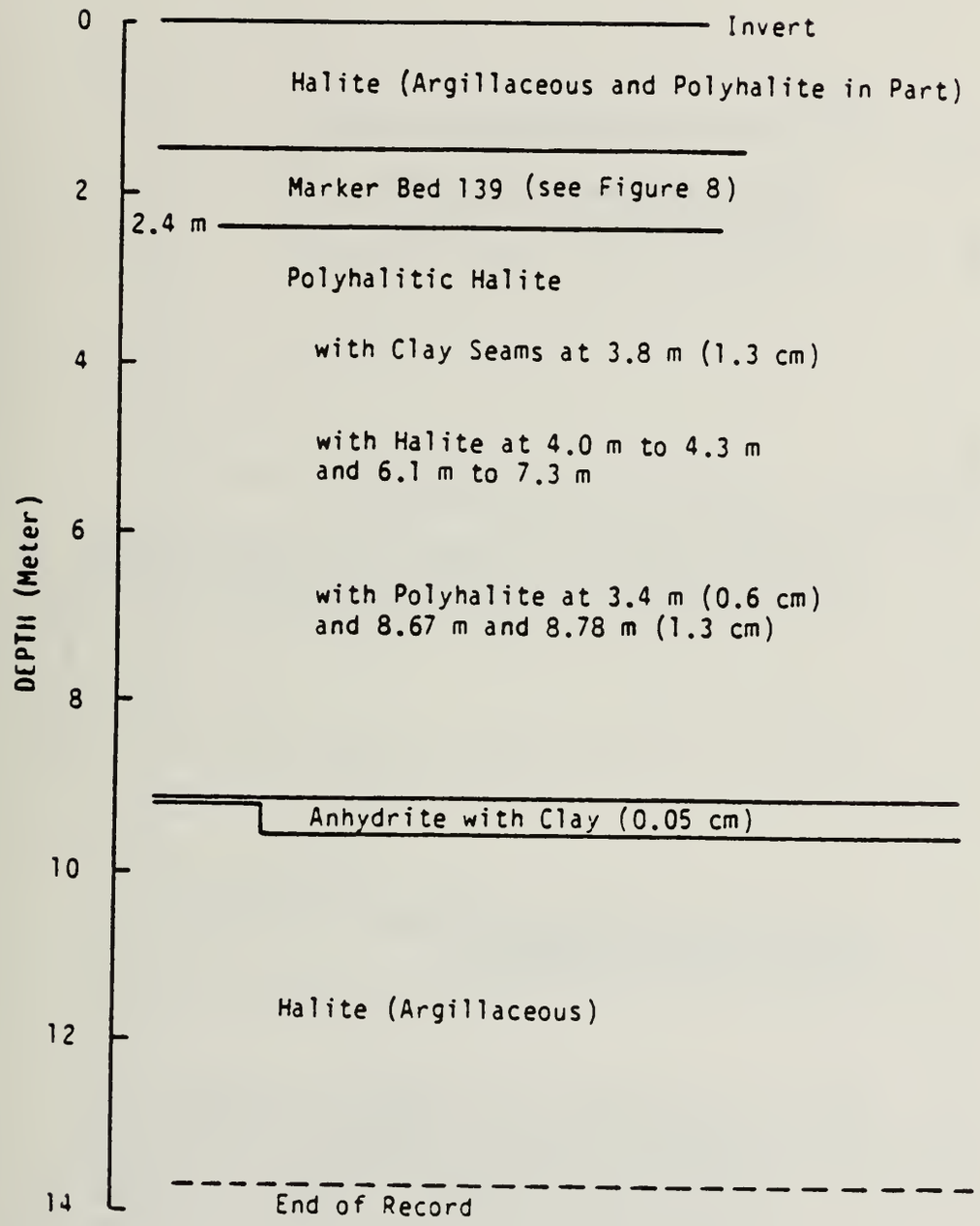

Figure 7. Stratigraphy common to the vertically-down boreholes L1PD01 and L2PD01.

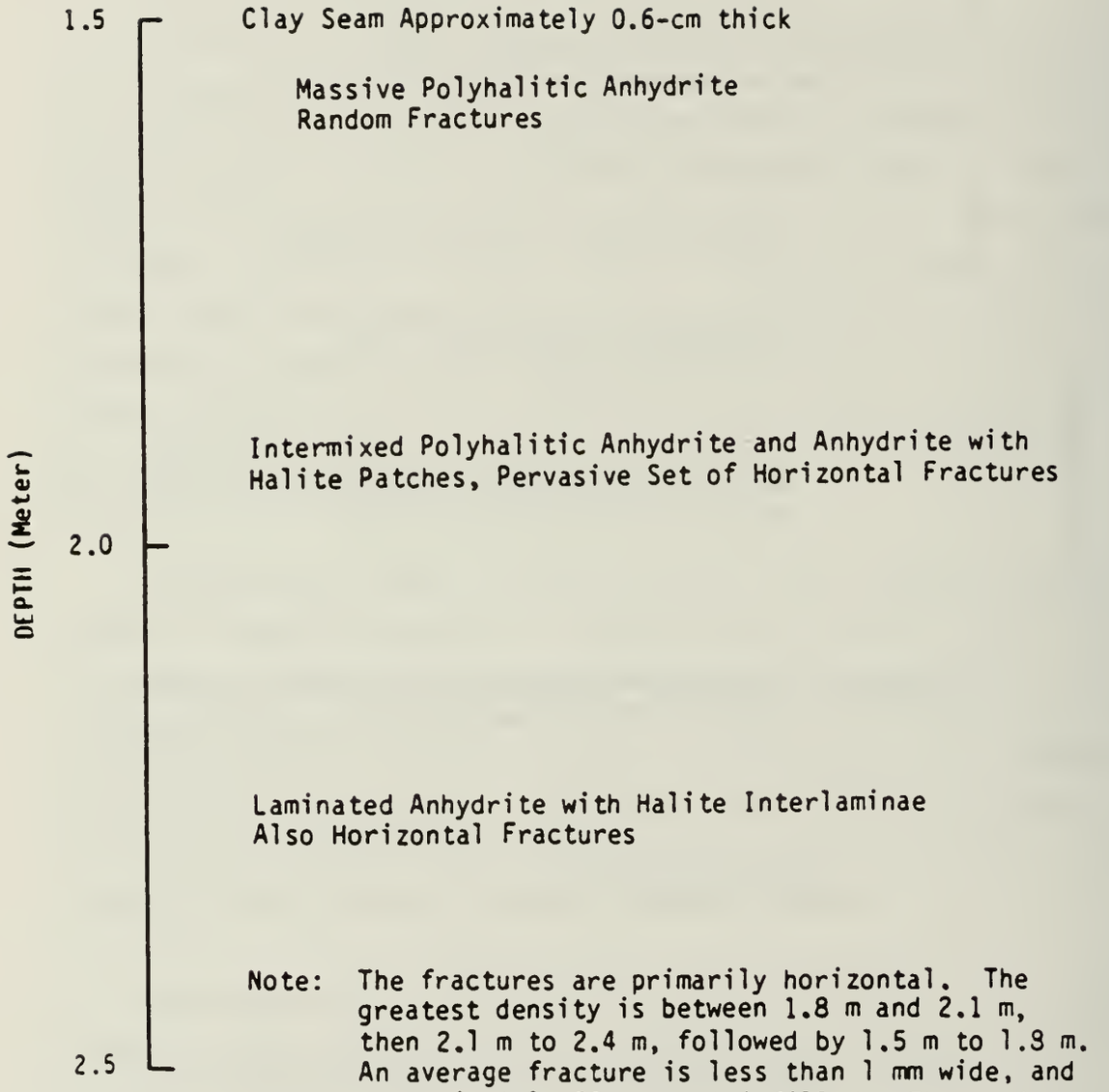

Note: The fractures are primarily horizontal. The greatest density is between 1.8 m and 2.1 m, then 2.1 m to 2.4 m, followed by 1.5 m to 1.8 m. An average fracture is less than 1 mm wide, and approximately 50 percent infilled. The estimated average density is 1 fracture/cm, for a total of 50 to 100 fractures.

Figure 8. Stratigraphy of Marker Bed 139 located 1.5 m to 2.4 m below the invert of Rooms L1 and L2.

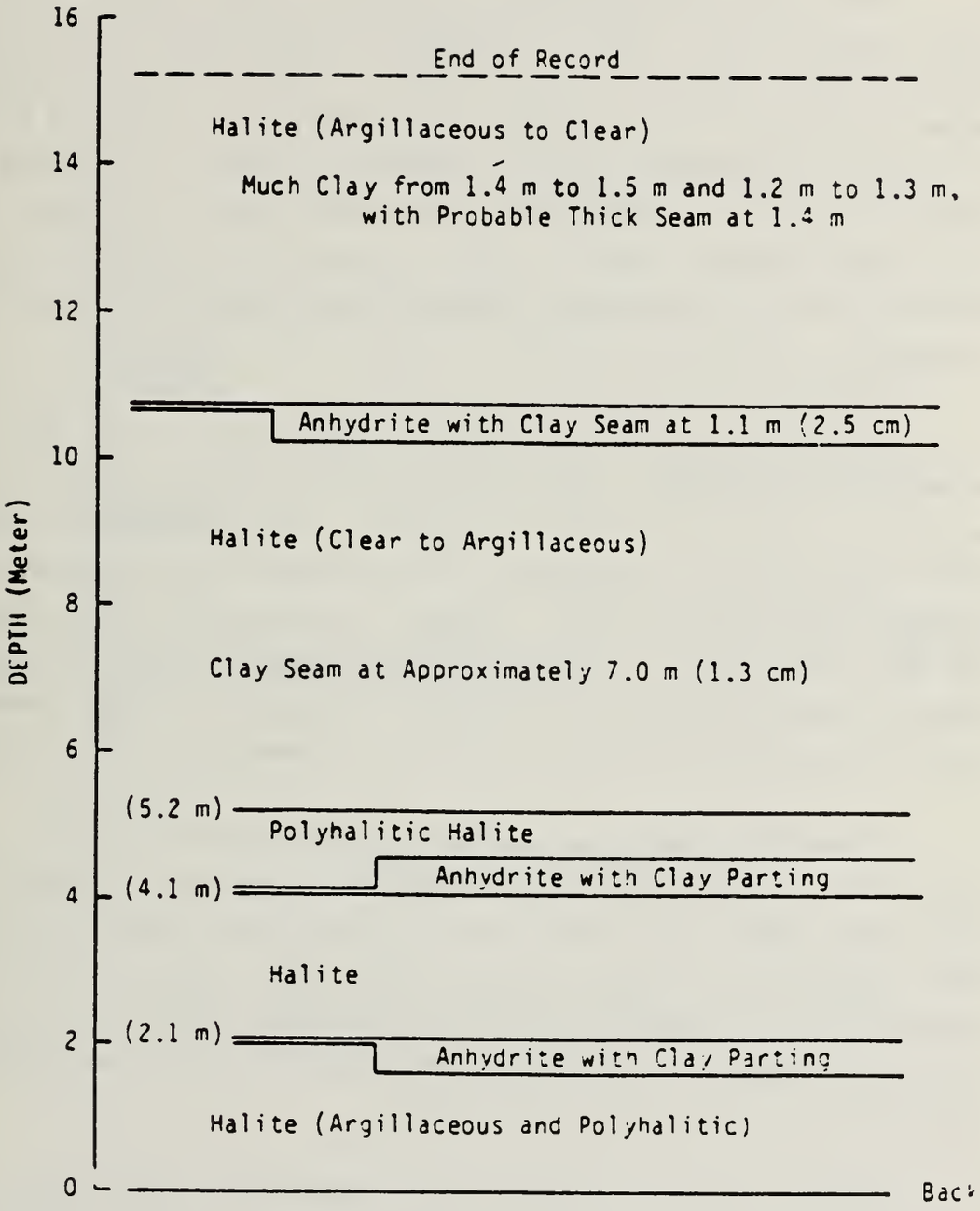

Figure 9. Stratigraphy common to the vertically-up boreholes L1PU01, L2PU01 and L2PU02.

Borehole L2PH01

Three tests were performed in Borehole L2PH01 shown on Figure 10. This borehole which lies in a competent predominately halite bed, was drilled midway between the ribs and at a height of approximately 1.8 meters above the floor of Room L2. In the first test, designed to measure the permeability close to the face, the test interval was located between the 0.5 meter to 0.7 meter depths. The second test was at the 1.6 meter to 2.0 meter depths; and, the third between the 6.1 meter to 7.6 meter depths. Results of Tests No. 1 through 3 are described in the following paragraphs.

In Test No. 1, the test interval was taken as the small region between the two packers. This interval was selected in order to provide a test as close to the face as possible. While performing this test, packer bypass flow to the bottom of the borehole was determined from the pressure rise in that region. However, flow past the smaller packer to the open room could not be measured. As a result, it must be emphasized that the permeability values determined represent a maximum permeability and do not necessarily indicate the actual permeability of this region.

Permeability values were determined by comparing the data with the type curves and tabulated values shown on Figure 5 and in Table I. These comparisons suggest that the flow and pressure decay tests are consistent with permeability values of 6.2×10^{-7} darcy and 2.8×10^{-7} darcy, respectively, provided the formation has a 0.01 porosity. Because the Test No. 1 packer bypass flow could not be determined, additional two-dimensional analyses were not warranted.

Test No. 2 was performed without moving the double packer system. Instead, the end of the hole was used as the test interval. The resulting permeability for this region, again using results shown on Figure 5 and in Table I, indicated a permeability of 2.3×10^{-8} darcy given a porosity of 0.01. This short duration two-hour test was performed to confirm the

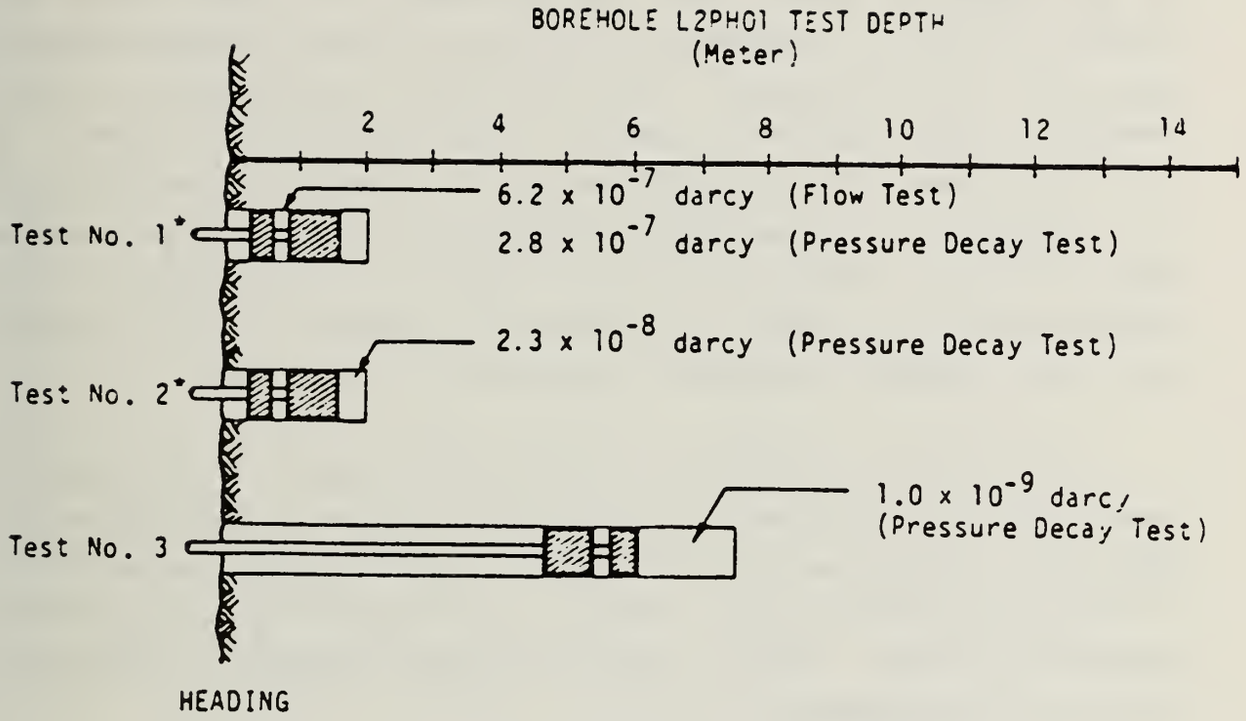

* Packer positions are reversed compared to all other tests.

NOTE: Horizontal borehole L2PH01 was positioned midway between the ribs and a height of approximately 1.9 meters above the floor.

Figure 10. Room L2 horizontal borehole L2PH01 permeability test results.

Test No. 1 results. No attempt was made to perform a detailed analysis of these test data.

In Test No. 3, the packer configuration was reversed to that used throughout the remainder of these tests. Because of the low permeability in this region a shut-in test was performed. The test region was initially filled to a pressure of 0.31 MPa and the resulting pressure decay with time was measured. These data were analyzed using the two-dimensional model described in Section 3 and illustrated on Figure 3. A 10^{-9} darcy permeability and 0.001 porosity provided, as shown on Figure 11, a reasonable comparison between the measured and calculated pressure decay histories. During the 15.3-hour test, a 0.1 MPa increase in pore pressure occurs to a depth of 6 centimeters measured from the borehole wall. This indicates the depth of penetration for this test.

The sensitivity of the data interpretation method to the selected permeability value can be seen by comparing Figure 11 and Figure 12. These later results were obtained using a 3×10^{-9} darcy permeability. It can be seen that the decay history is quite sensitive to the selected permeability values. Clearly, order-of-magnitude permeability differences can be easily evaluated.

The step nature of the measured pressure curve shown on Figures 11 and 12 results because of the sensitivity of the digital recording equipment. This step-type data was obtained during many of the tests reported here, because of the low permeabilities and the associated relatively small pressure changes.

Borehole L2PU01

Four tests were conducted in the vertically up borehole L2PU01 shown on Figure 13. This borehole was positioned midway between the ribs and 1.2 meters from the heading. The associated stratigraphy is shown on Figure 9. These tests were conducted sequentially, as the hole depth was

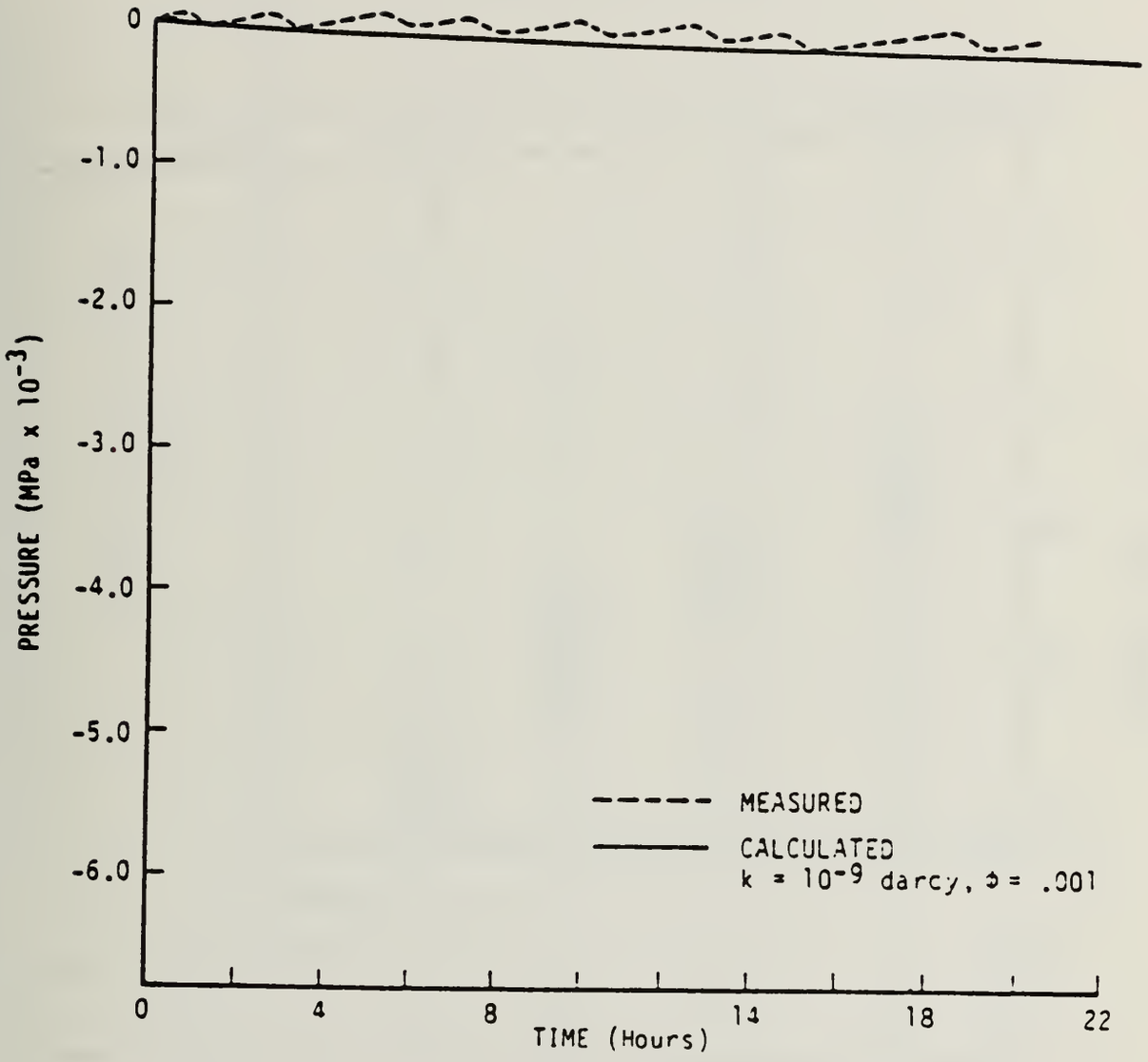

Figure 11. A comparison of the measured Test No. 3 pressure decay with that calculated for permeability and porosity of 10^{-9} darcy and 0.001, respectively.

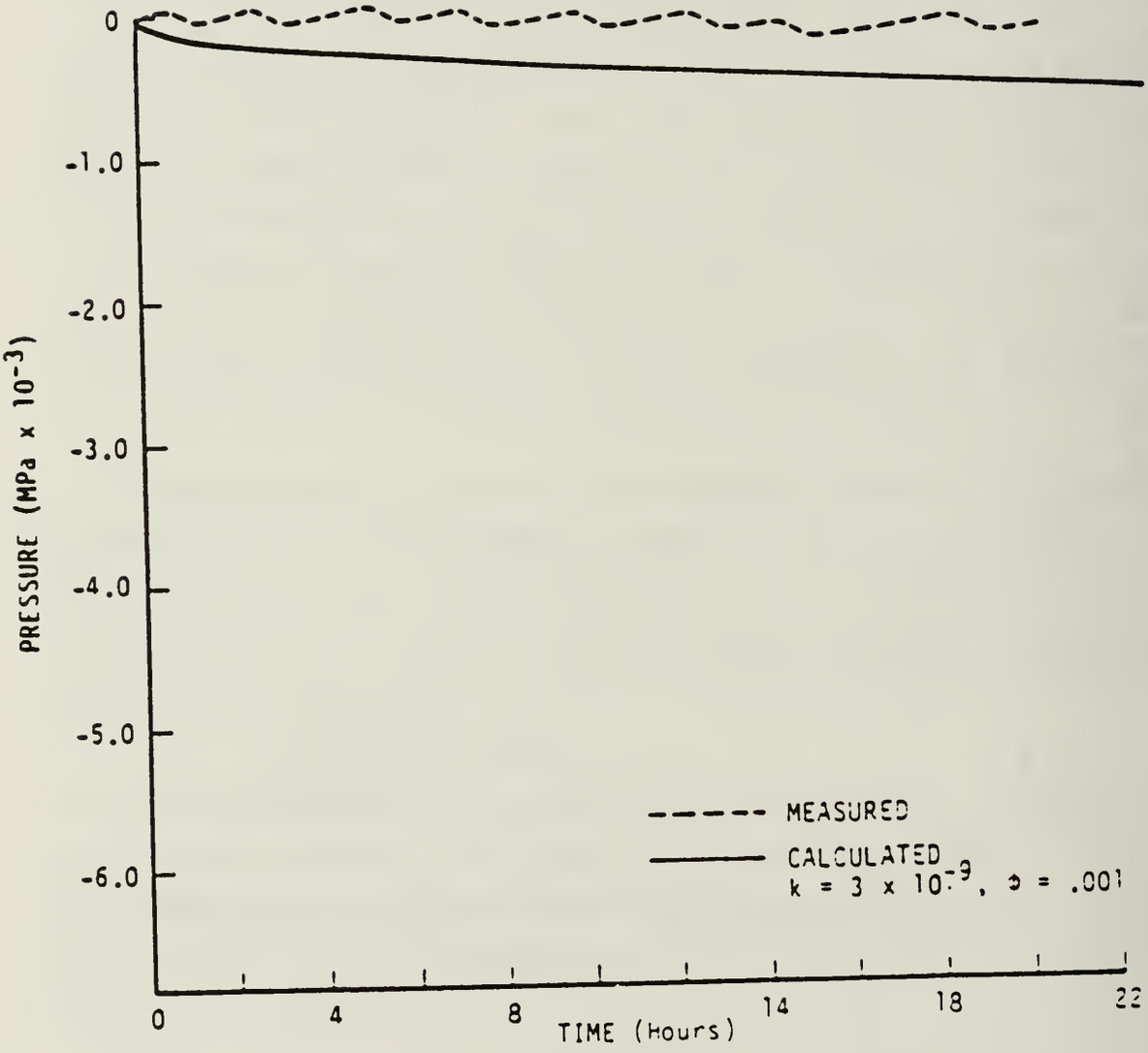

Figure 12. Illustration showing the Test No. 3 calculated pressure decay rate sensitivity to the selected permeability.

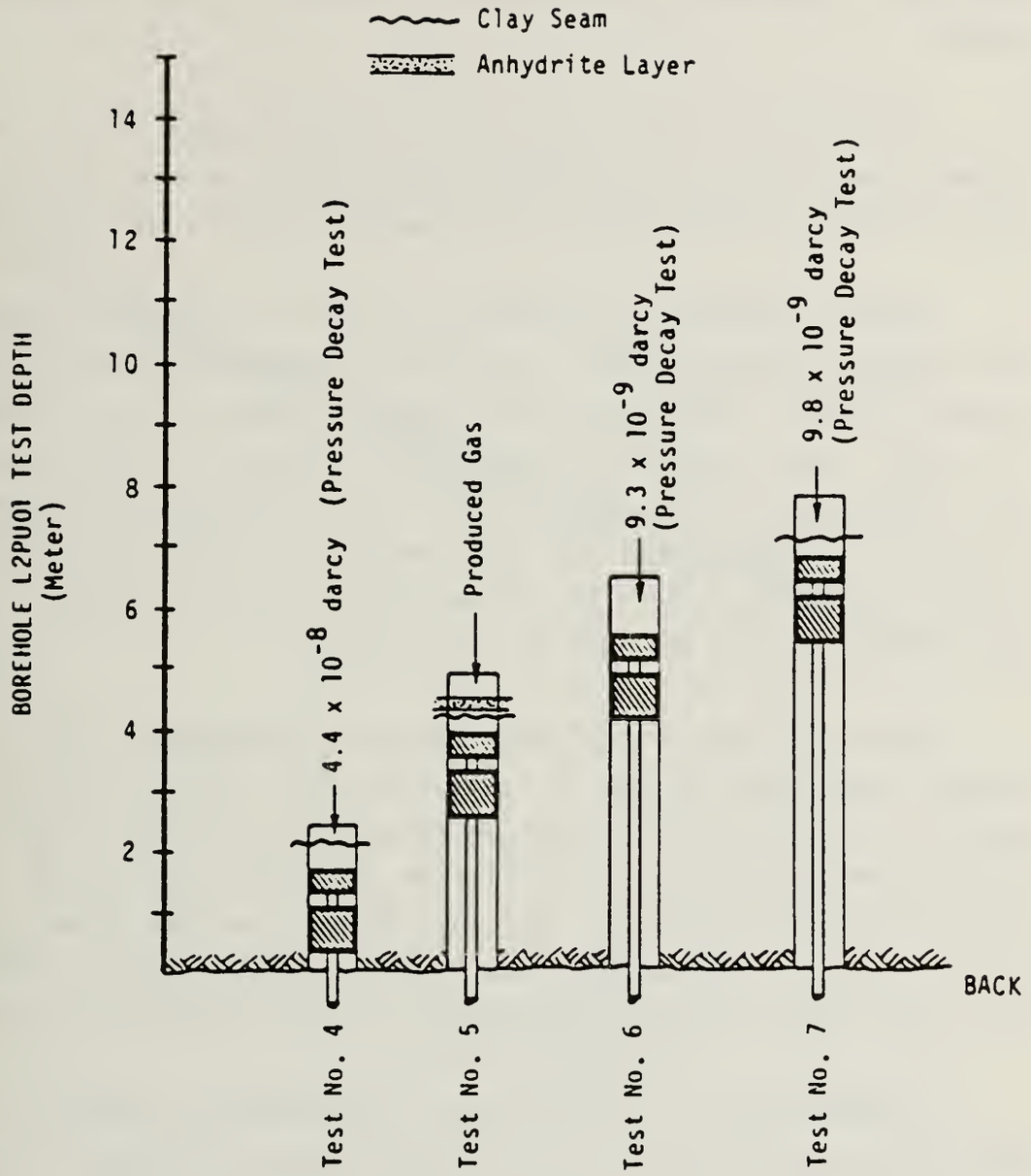

NOTE: Vertical borehole L2PU01 was positioned midway between the ribs and 1.2 meters from the heading.

Figure 13. Room L2 vertical borehole L2PU01 permeability test results.

increased. Results of the tests are discussed in the following paragraphs.

The Test No. 4 test interval was located between the 1.7 meter to 2.5 meter depths and intersected the clay parting shown on Figure 9. Because of the low permeability in this region a shut-in test was performed.

The test interval was initially filled to a 0.64 MPa pressure and the resulting decay measured. As shown on Figure 14, measured and calculated pressure histories were found to agree if one assumes a 4.4×10^{-8} darcy permeability and 0.001 porosity. Calculations show that after 18 hours a 0.1 MPa increase in pore pressure had occurred at a distance of 36 centimeters into the formation. The effective test penetration is, therefore, well beyond any region of wellbore damage or stress relief resulting from drilling of the borehole.

The sensitivity of the data interpretation method to the selected porosity value can be seen by comparing the Figure 14 and Figure 15 results. A porosity of 0.01 is seen to produce a pressure drop of about twice the measured value. Note that the late-time slope of the pressure history calculated using $\phi = 0.01$ is about 20 percent higher than the measured value. This implies that the late time, nearly steady-state flow can be used to predict approximately correct permeability values.

A comparison of the calculated and measured pressure histories during the time required to fill the test interval is shown on Figure 16. The calculated result was obtained using the measured flowrate to the test interval, and the permeability and porosity values shown on Figure 14 as the input condition. The approximate 5 percent deviation in measured and calculated pressure values after one hour simply reflect the uncertainty in the test interval volume.

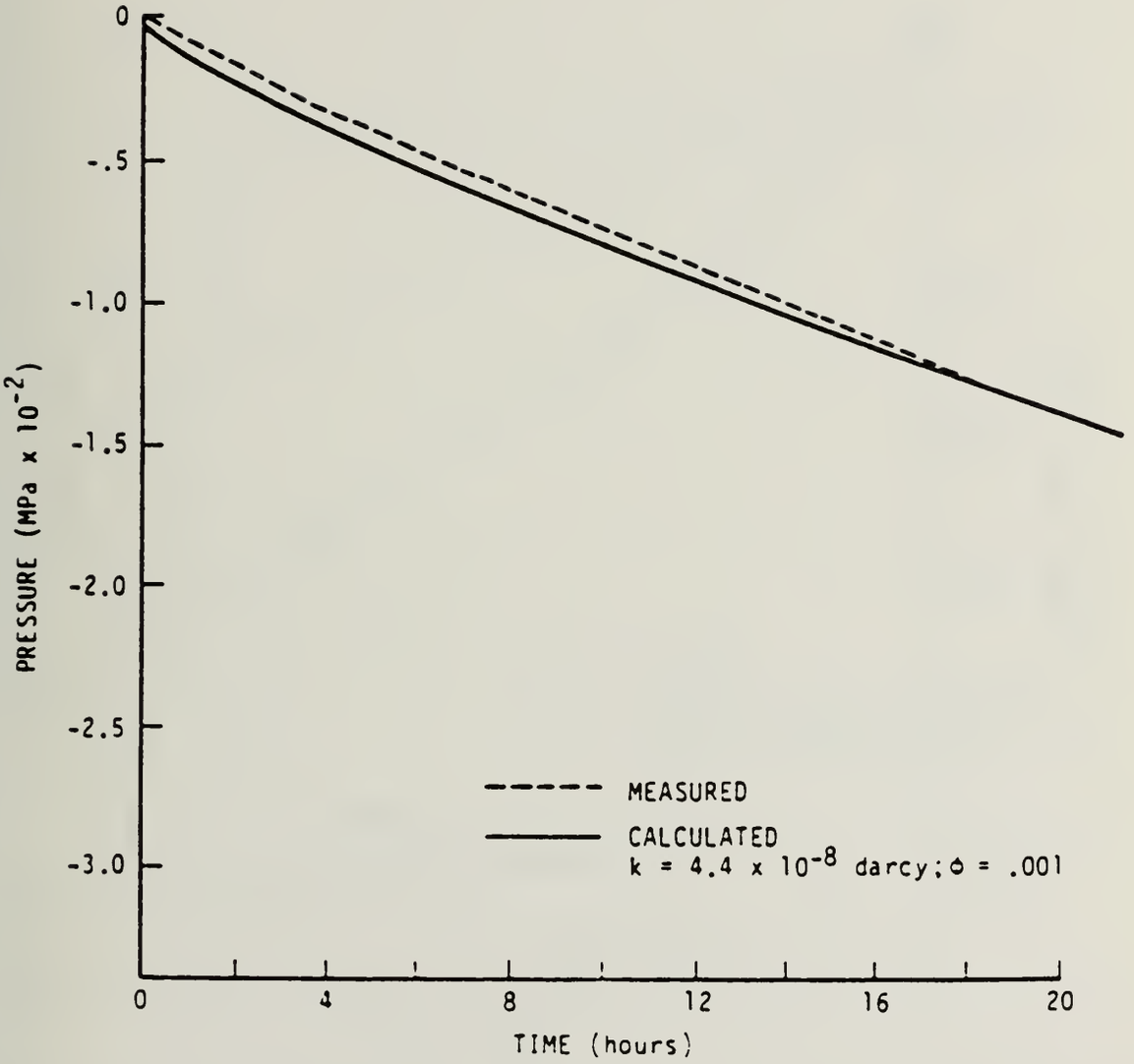

Figure 14. A comparison of the measured Test No. 4 pressure decay with that calculated for permeability and porosity of 4.4 x 10^{-8} darcy and 0.001, respectively.

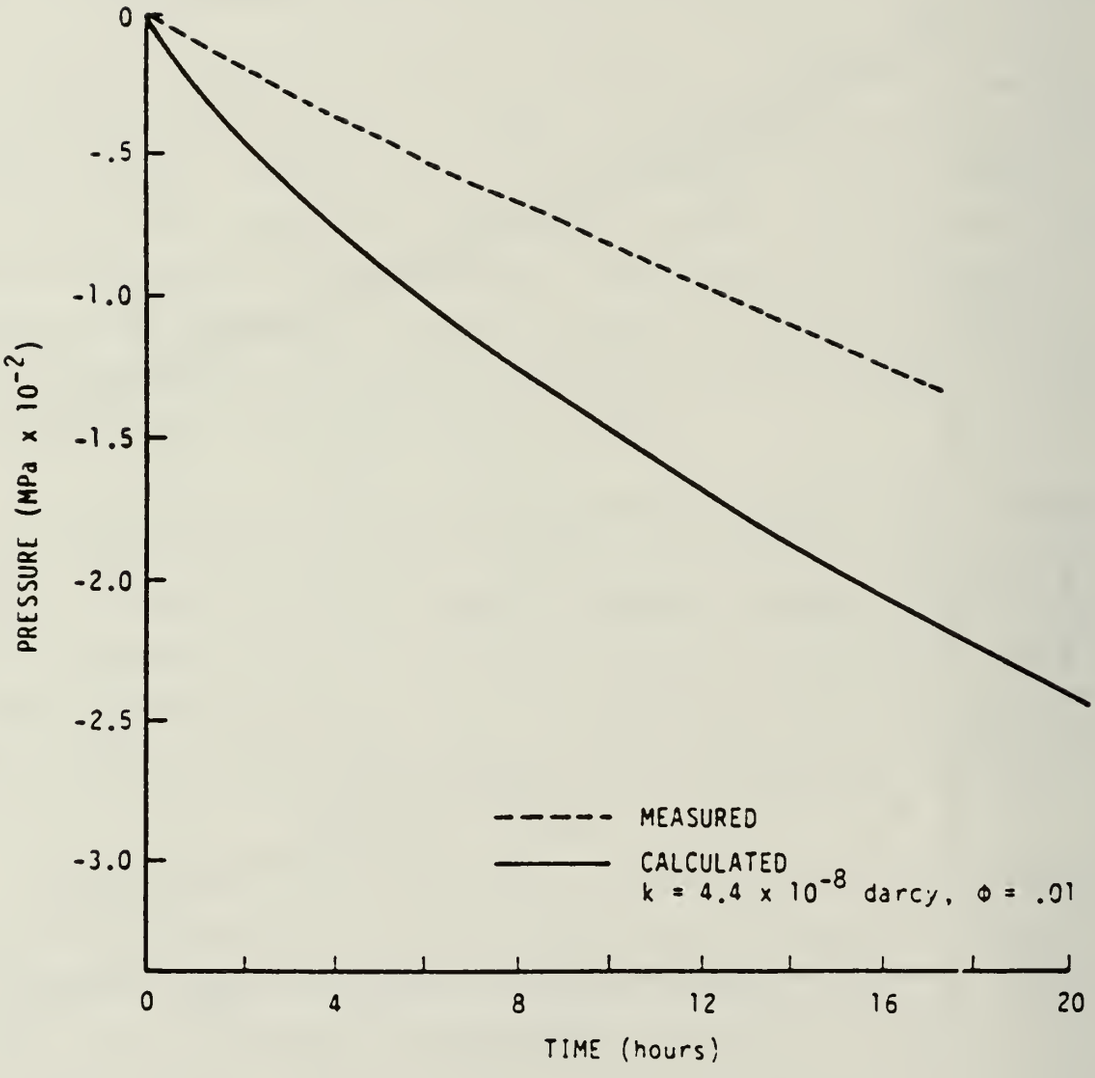

Figure 15. Illustration showing the Test No. 4 calculated pressure decay rate sensitivity to the selected porosity.

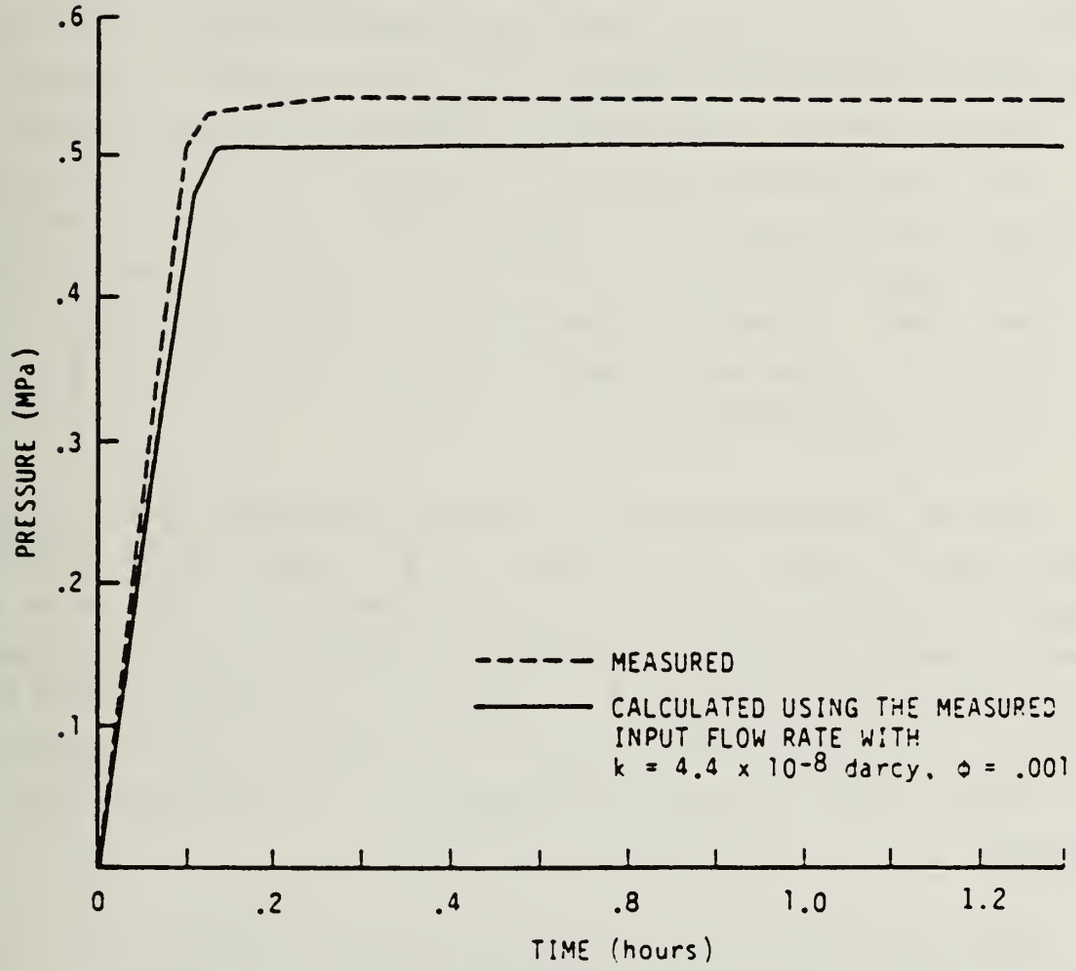

Figure 16. A comparison of the measured Test No. 4 pressure buildup with that calculated using a 1.0×10^4 cubic centimeter test interval volume.

Test No. 5 was conducted between the 4.0 meter to 4.9 meter depths. This interval intersected an approximate 0.2 meter thick anhydrite seam and clay parting.

During Test No. 5, the test interval was filled to an initial 0.65 MPa pressure and the resulting pressure change measured. However, unlike previous tests, the pressure within this interval continued to increase throughout the approximate 20-hour test period as shown in Appendix A. The resulting data are insufficient to determine the characteristics of this very slowly-producing zone. For example, if the drive pressure within the producing zone were 6.9 MPa, then the 0.2 meter thick anhydrite seam would require a permeability of 2×10^{-8} darcy to produce the measured gas flow. In contrast, given the 6.9 MPa drive pressure, a 0.03 meter thick clay seam would require a permeability of about 7×10^{-7} darcy to produce an equivalent flow.

Test No. 6 was performed in a region of competent clear to argillaceous halite between the 5.6 meter and 6.5 meter depths. The test interval was initially filled to a 0.6 MPa pressure and the decay measured. As shown on Figure 17, calculated and measured pressure histories were found to agree given a 9.3×10^{-9} darcy permeability and 0.001 porosity. Calculations show that after 17 hours a 0.1 MPa increase in pore pressure had occurred at a distance of 17 centimeters into the formation.

Test No. 6 results are significant for two reasons. First, this region had essentially the same permeability as that determined in Test No. 3, performed in a different layer. The composition of these layers, while both predominately halite, are somewhat different--suggesting that minor constituents in the halite do not noticeably alter the permeability of these zones. Second, the Test No. 6 and Test No. 3 flows to guard Zone A are comparable. Since boreholes L2PH01 and L2PU01 are oriented at 90° with respect to one another, this suggests that the axial bypass flow

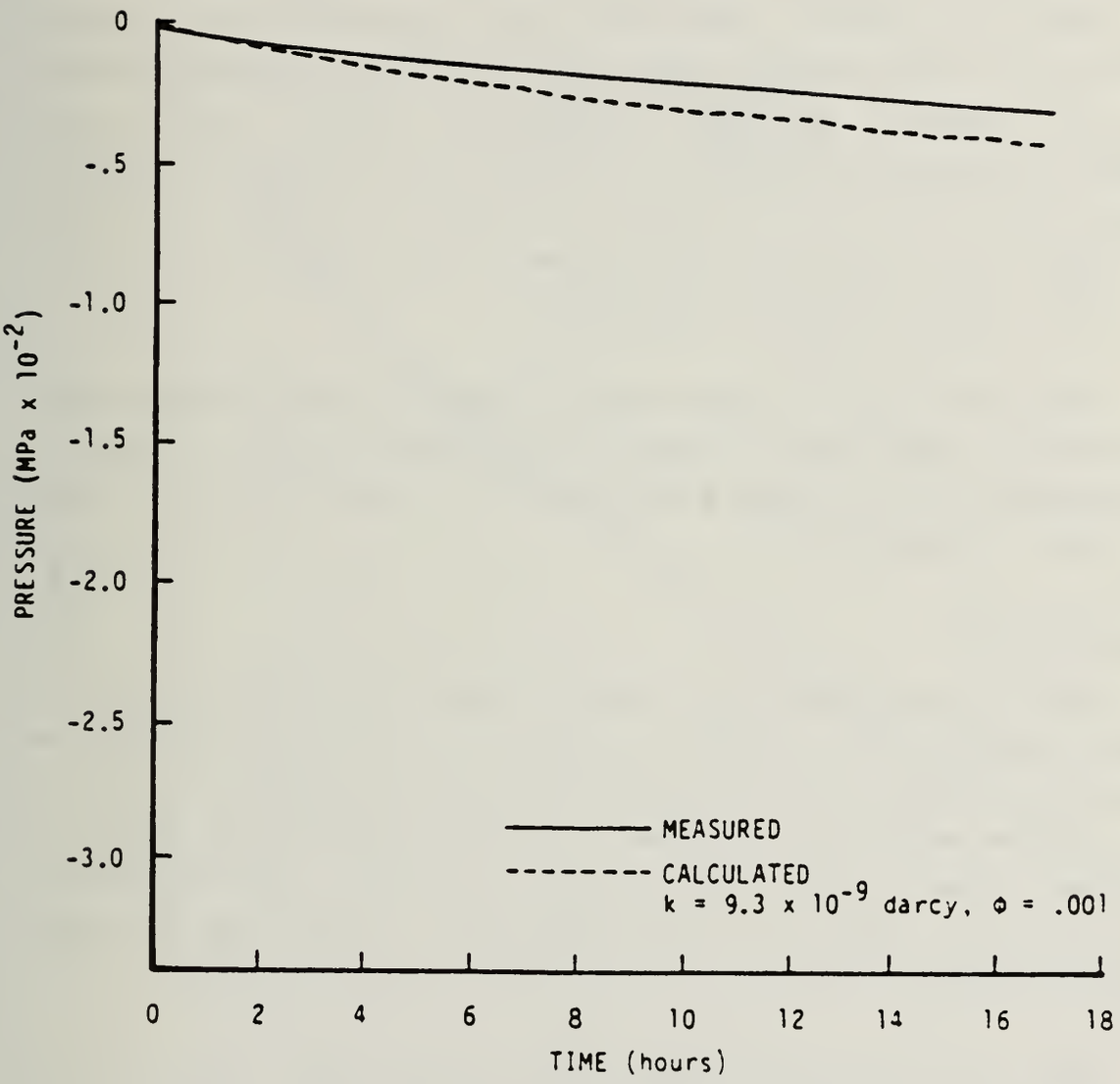

Figure 17. A comparison of the measured Test No. 6 pressure decay with that calculated for permeability and porosity of 9.3 x 10^{-9} darcy and 0.001, respectively.

is not associated with an anisotropic permeability but is instead a result of packer bypass or wellbore damage.

Test No. 7 was conducted over the 6.8 meter to 7.7 meter interval which intersected an approximate 0.2 centimeter thick clay seam positioned at a depth of 7 meters. During this test, the borehole was initially filled to a 0.6 MPa pressure, then shut-in, and the subsequent pressure decay was measured. As shown on Figure 18, measured and calculated pressure decay histories compare favorably if one assumes a formation permeability of 9.8×10^{-9} darcy and porosity of 0.005. Calculations show that after 19 hours a 0.1 MPa increase in pore pressure had occurred at a depth of approximately 10 centimeters.

The sensitivity of the data analysis method to the selected porosity can be seen by comparing the Figure 18 and Figure 19 results. The calculated pressure decay assuming a 0.001 porosity is seen to be significantly less than the measured value.

Borehole L2PU02

Test No. 10 was performed in the 1.9 meter to 2.8 meter interval in Borehole L2PU02 shown on Figure 20. This test interval intersected the clay/anhydrite seam at the 2.1 meter depth shown on Figure 9. This is the same seam evaluated in Test No. 4. Recall that Borehole L2PU07 was positioned midway between the ribs and 15.2 meters from the heading, whereas Borehole L2PU01 was midway between the ribs and just 1.2 meters from the heading.

Both flow and pressure decay tests were performed. Comparisons of the data with the Figure 5 type curves and Table 1 tabulations give permeability values of 2.8×10^{-3} darcy and 3×10^{-3} darcy, respectively. These permeability values are five orders of magnitude larger than obtained in Test No. 4.

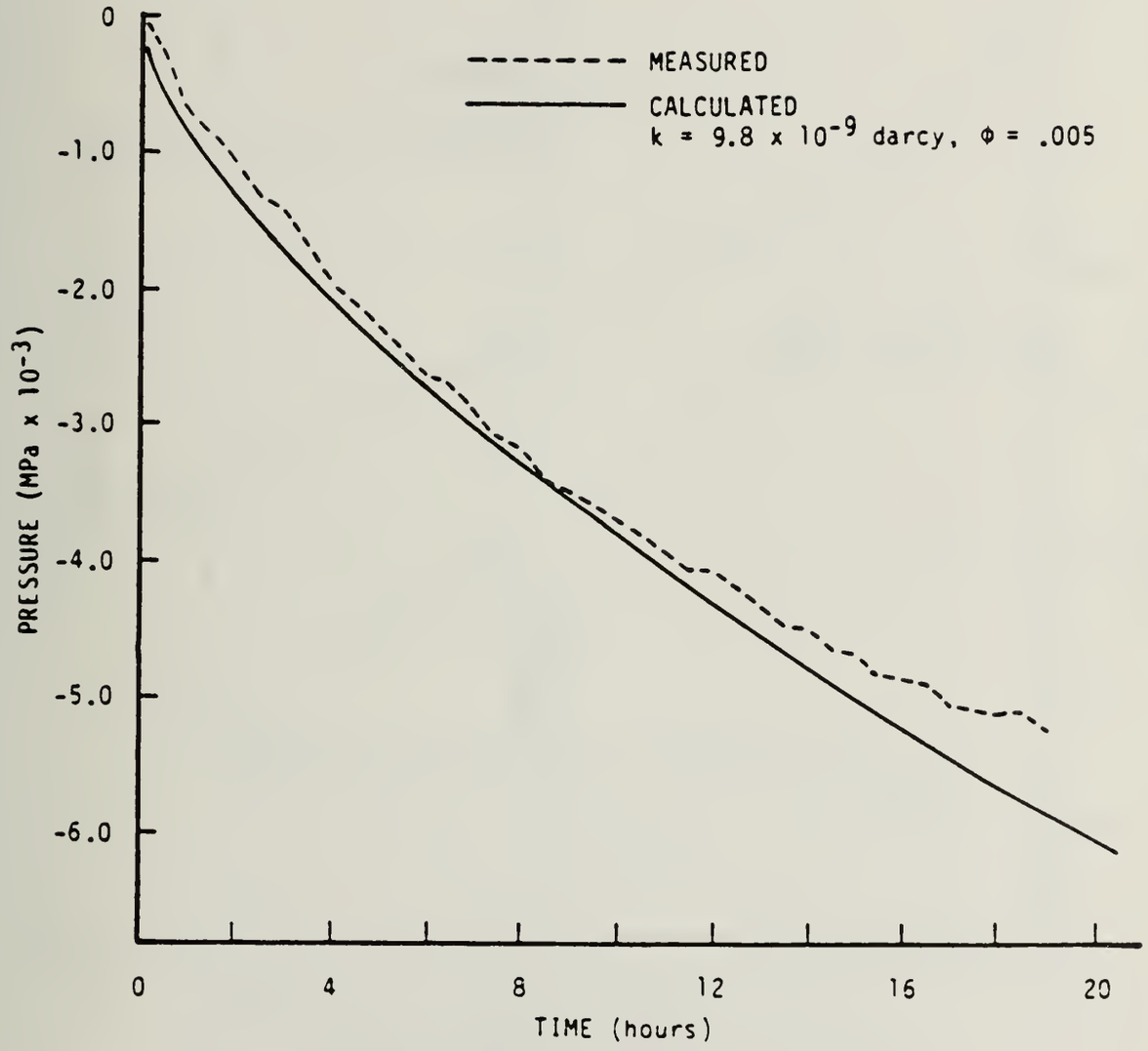

Figure 18. A comparison of the measured Test No. 7 pressure decay with that calculated for permeability and porosity of 9.8×10^{-9} darcy and 0.005, respectively.

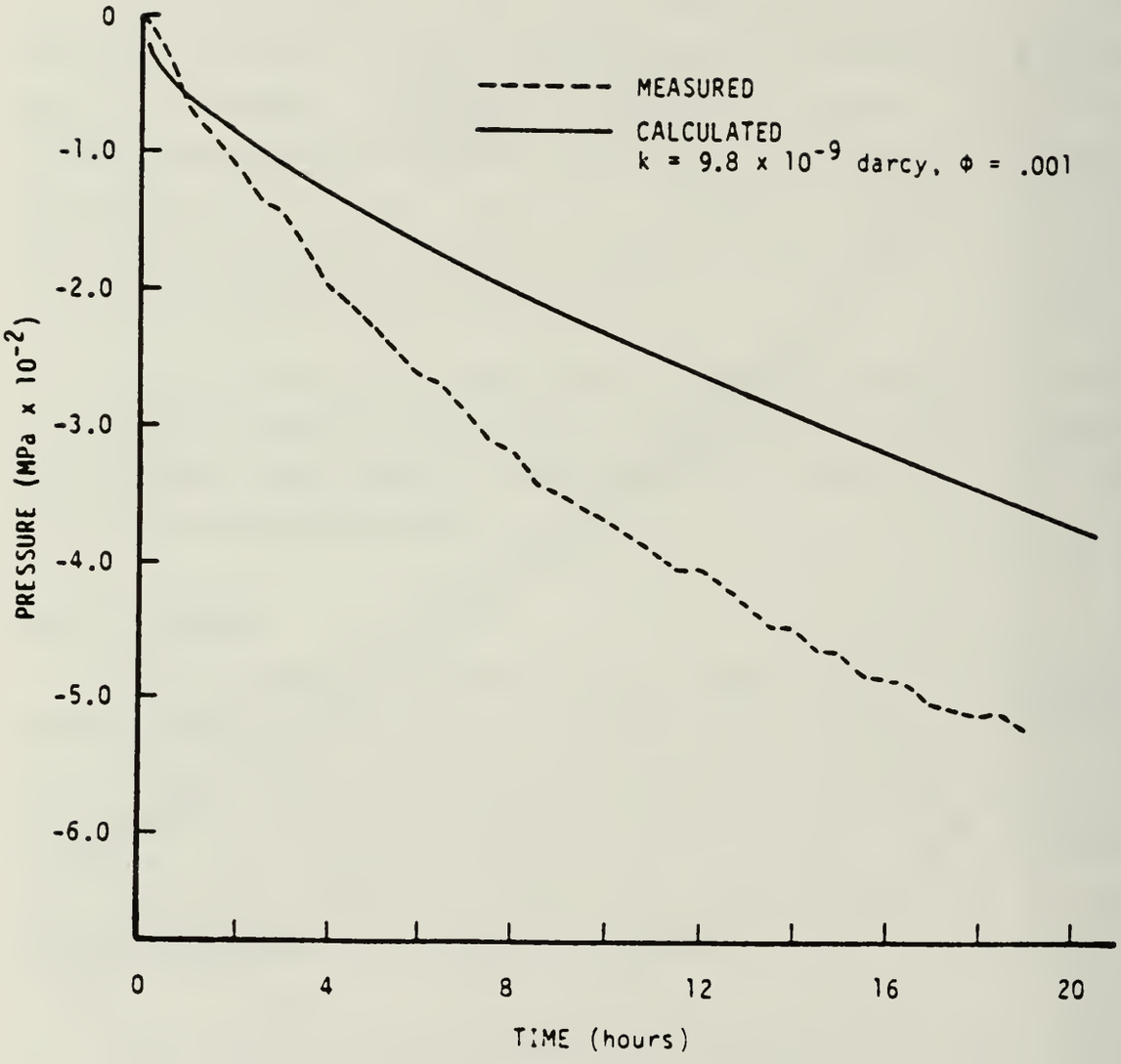

Figure 19. Illustration showing the Test No. 7 calculated pressure decay rate sensitivity to the selected permeability.

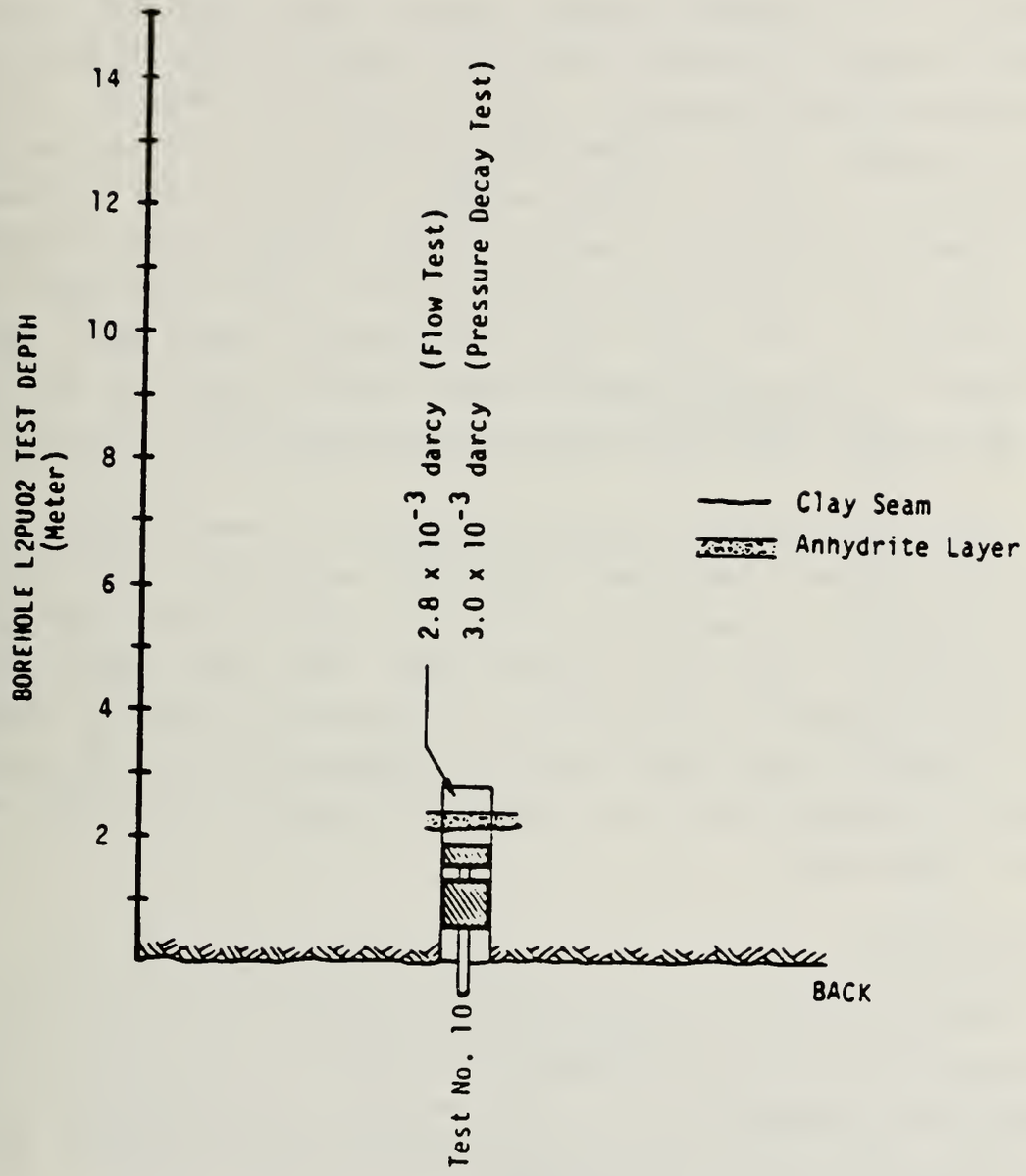

NOTE: Vertical borehole L2PU02 was positioned midway between the ribs and 15.2 meters from the heading.

Figure 20. Room L2 vertical borehole L2PU02 permeability test result.

On Figure 21, the measured test zone pressure history is compared with that calculated using a 2.8×10^{-3} darcy permeability and 0.01 porosity. The comparison between measured and calculated pressure histories is seen to be poor. This is not surprising since the calculated results were obtained assuming a uniform, isotropic formation. Flow in this zone probably occurs predominately through part or all of the clay/anhydrite seam. This, in itself, would not result in the discrepancy shown between calculated and measured values. However, the discrepency does suggest that the response is not that of a simple darcy-type flow. To understand the flow along this clay anhydrite region would require performance of cross-hole flow and tracer tests. Such tests may imply both the fracture extant and, possibly the porosity of the small layer.

Test No. 10 results have been presented in terms of permeability simply to provide a comparison with other test results. This permeability value is an average over the entire test interval, and is not representatiive of the clay anhydrite seam. This test should, therefore, be interpreted in terms of flow. The important information obtained from this test is that a 9000 SCCM flow is obtained at a 0.33 MPa downhole pressure. Additional tests are required to determine the actual permeability of the seam.

Borehole L1PU01

Test No. 12 was conducted in the 13.4 meter to 15.2 meter interval in Borehole L1PU01 shown on Figure 22. As shown on Figure 9, this test interval was surrounded by a region of clear to argillaceous halite containing significant clay from the 13.7 meter to 15.2 meter depths, with a probable thick seam at 14 meters.

During this test, the borehole was initially filled to a 0.65 MPa pressure, then shut-in, and the pressure decay measured. Given a formation permeability of 3.2×10^{-10} darcy and a 0.001 porosity, calculated and measured pressure decay histories compare favorably--as shown on Figure 23. Calculations show that after 16 hours a 0.1 MPa increase in pore pressure had occurred at a depth of only 4.5 centimeters.

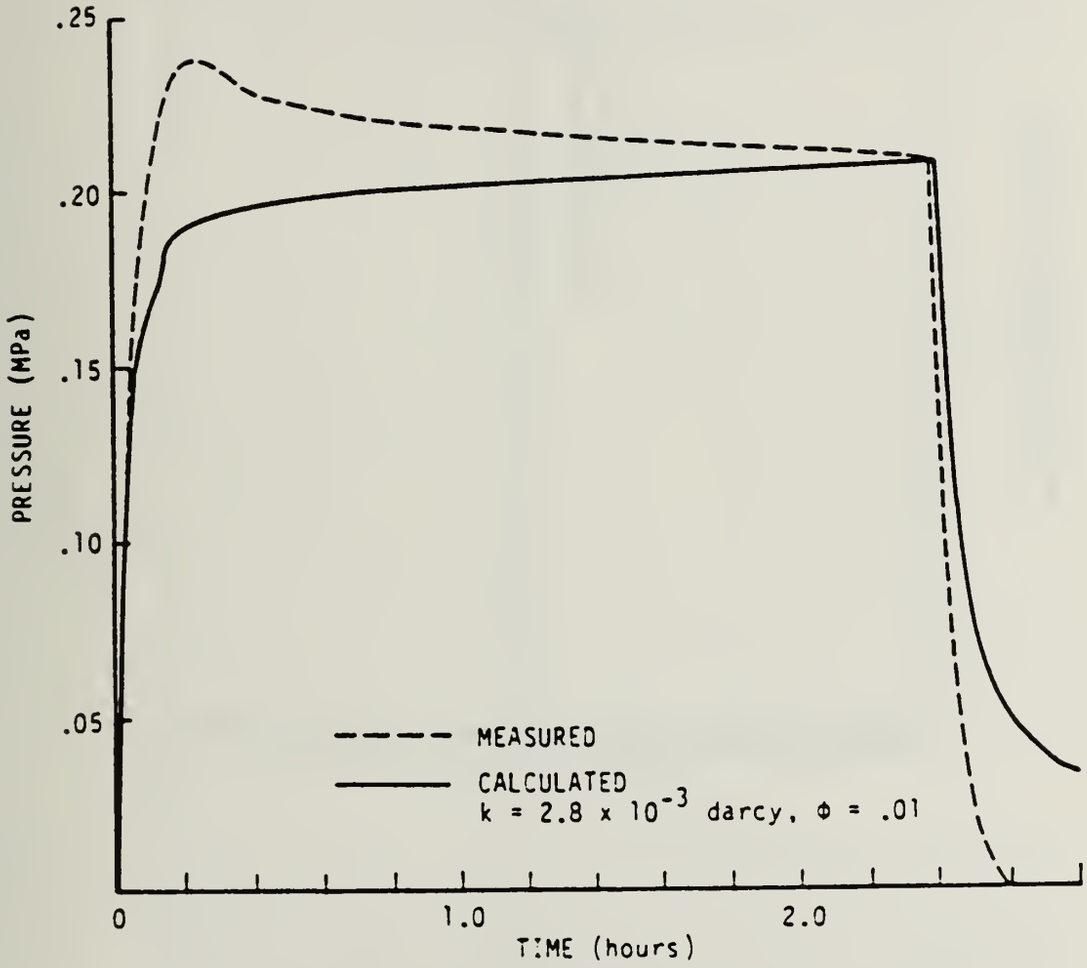

Figure 21. A comparison of the measured Test No. 10 pressure buildup and decay with that calculated using a 1.2×10^4 cubic centimeter test interval volume.

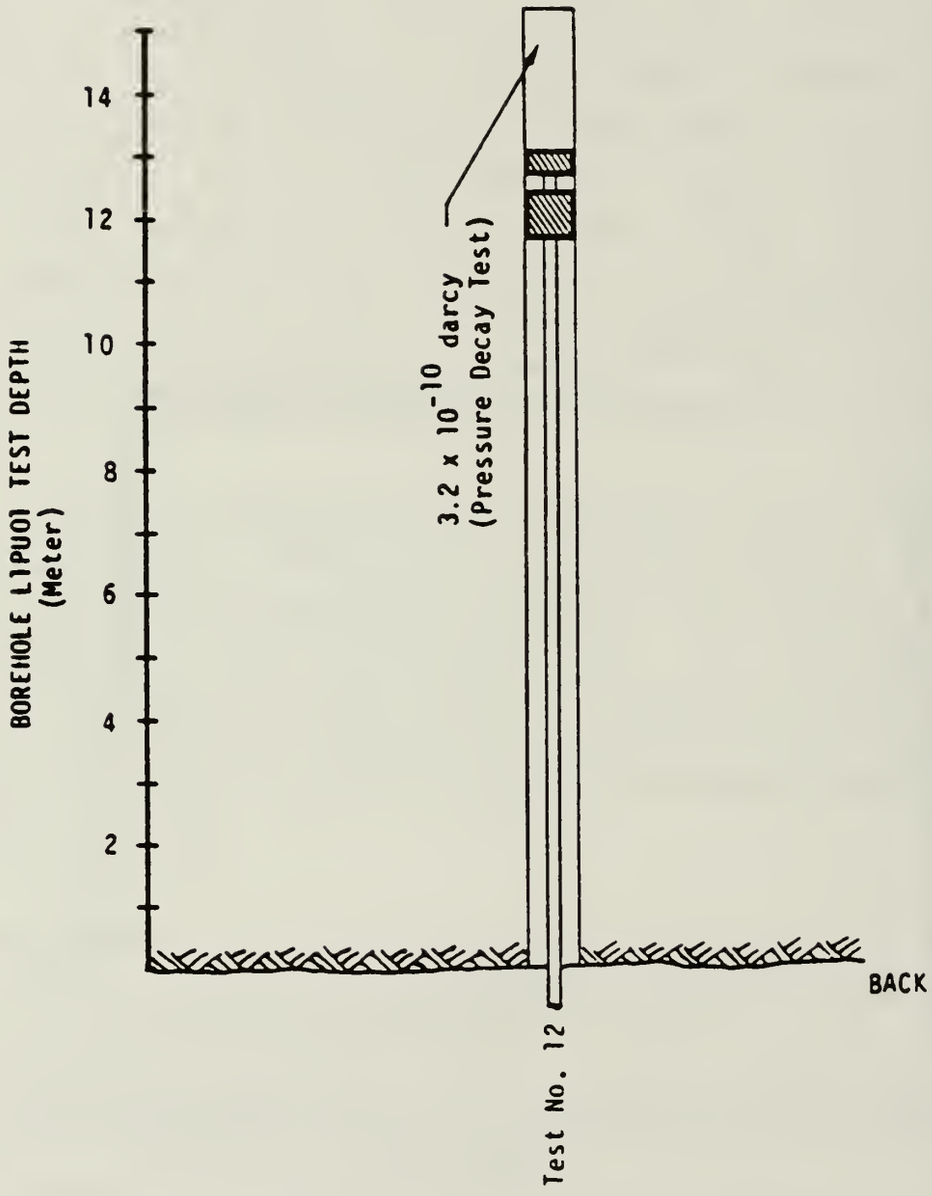

NOTE: Vertical borehole L1PU01 was positioned 6.1 meters from the left rib and 18.3 meters from the heading.

Figure 22. Room L1 vertical borehole L1PU01 permeability test result.

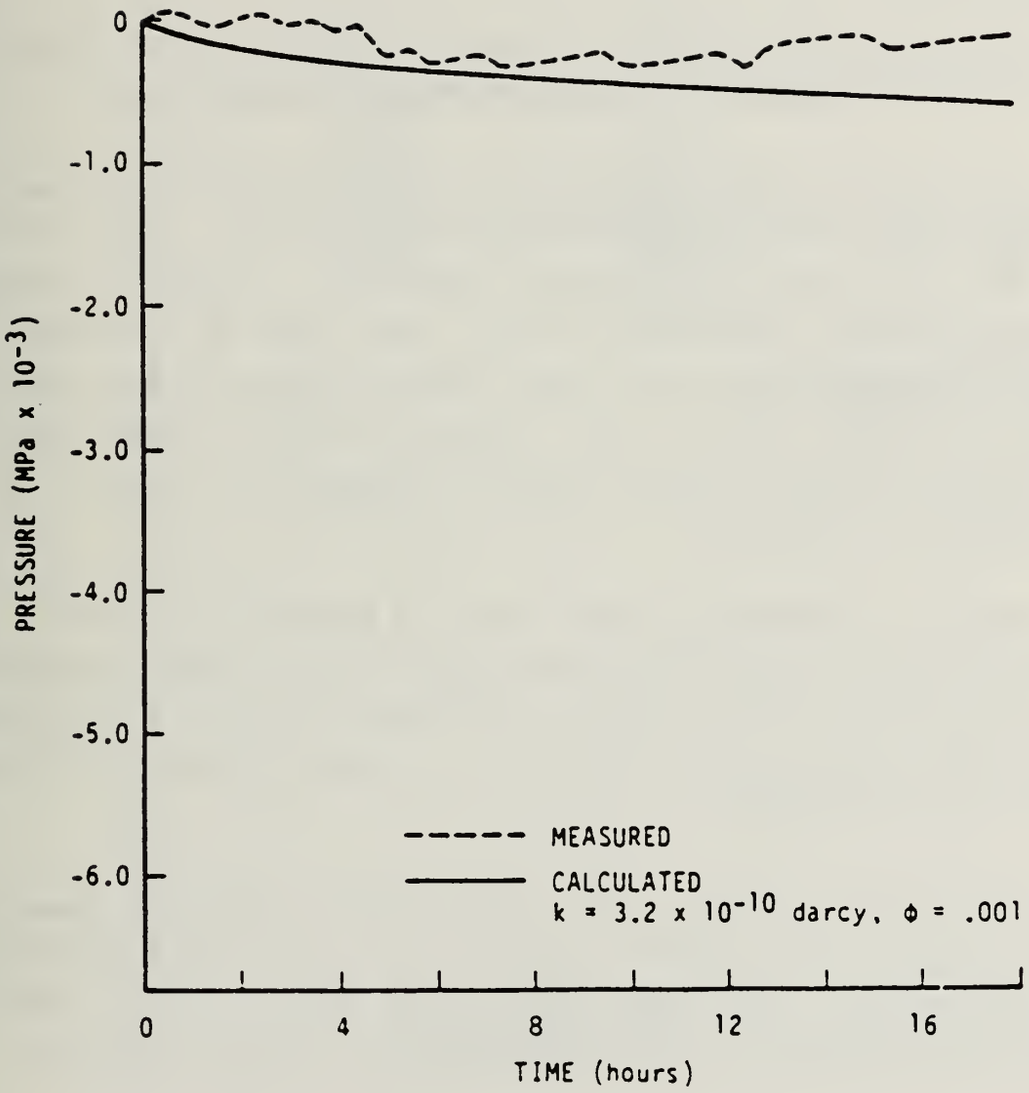

Figure 23. A comparison of the measured Test No. 12 pressure decay with that calculated for permeability and porosity of 3.2 x 10^{-10} darcy and 0.001, respectively.

The results presented on Figure 23 imply that the permeability and, possibly, porosity are even smaller than the values shown. However, this permeability value is clearly below the test sensitivity and cannot be measured during a 20-hour period.

Borehole L2PD01

Two tests were performed in Borehole L2PD01 shown on Figure 24. The associated stratigraphy is shown on Figures 7 and 8.

The Test No. 8 test interval was located between the 6.3 meter to 13.6 meter depths and spanned Marker Bed 139. Test No. 9 was performed over the 13.7 meter to 17.0 meter interval in a region of competent polyhalitic halite. The intent of this later test was to examine the material adjacent to the marker bed. Since the guard interval would be located in Marker Bed 139, the resulting pressure changes would be dominated by backflow from Test No. 8. Consequently, Packer No. 2 was not inflated for Test No. 9.

Test No. 8 consisted of both flow and pressure decay tests. Comparisons of the data with the Figure 5 type curves and Table 1 tabulations give permeability values of 8.3×10^{-4} darcy and 8.4×10^{-5} darcy, respectively, assuming a 0.01 porosity. The reason for the difference in results is not understood.

The measured Test No. 8 test zone pressure history is compared on Figure 25 with that calculated using a 8.3×10^{-4} darcy permeability and 0.01 porosity. The comparison is seen to be poor and does not resemble the response of a classic homogeneous, isotropic formation.

Test No. 8 results indicate that the marker bed at this position will accept a flow of 8300 SCCM with a 0.42 MPa downhole pressure. The actual permeability and flow characteristics of this region can only be

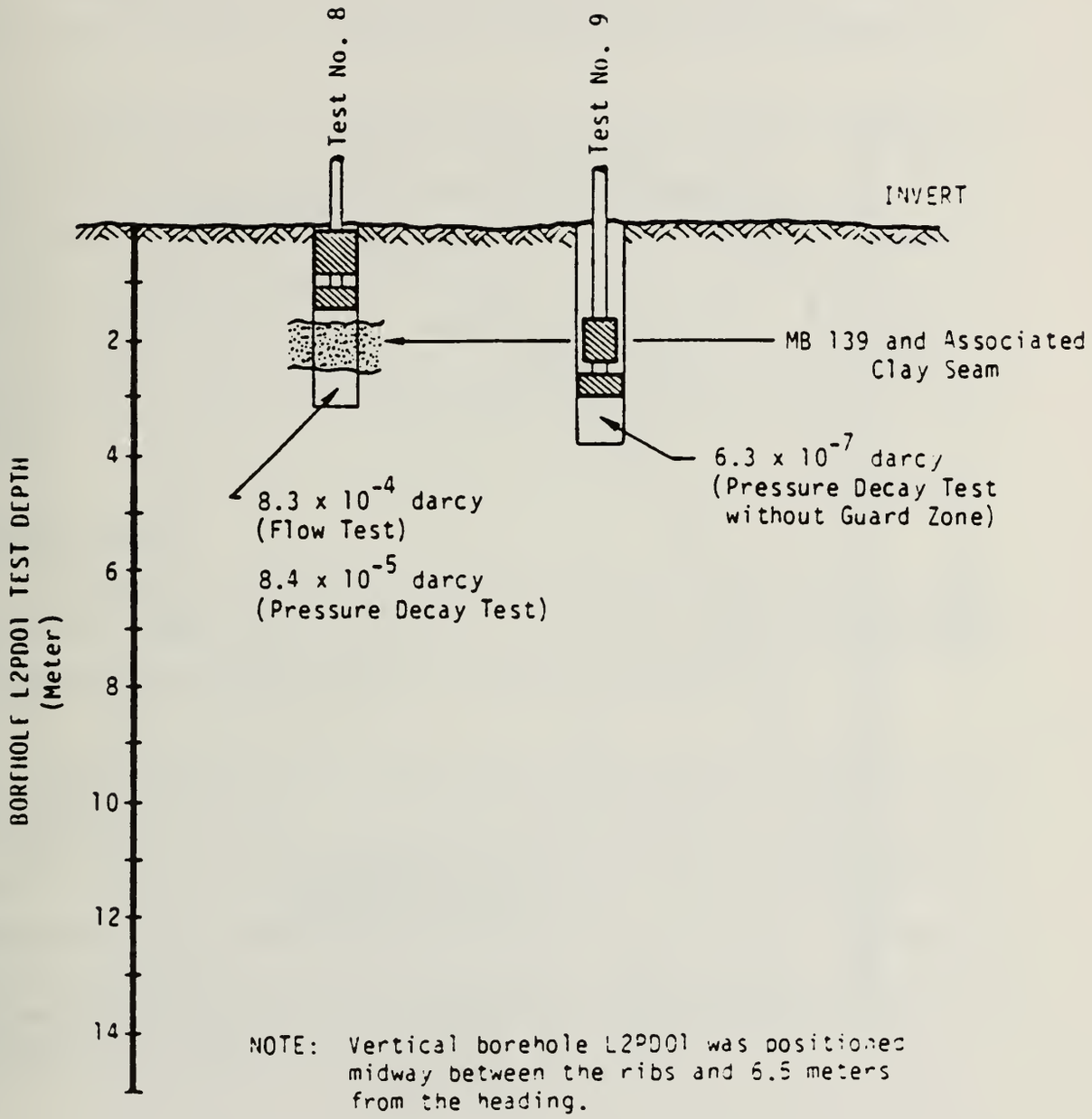

Figure 24. Room L2 vertical borehole L2PD01 permeability test results.

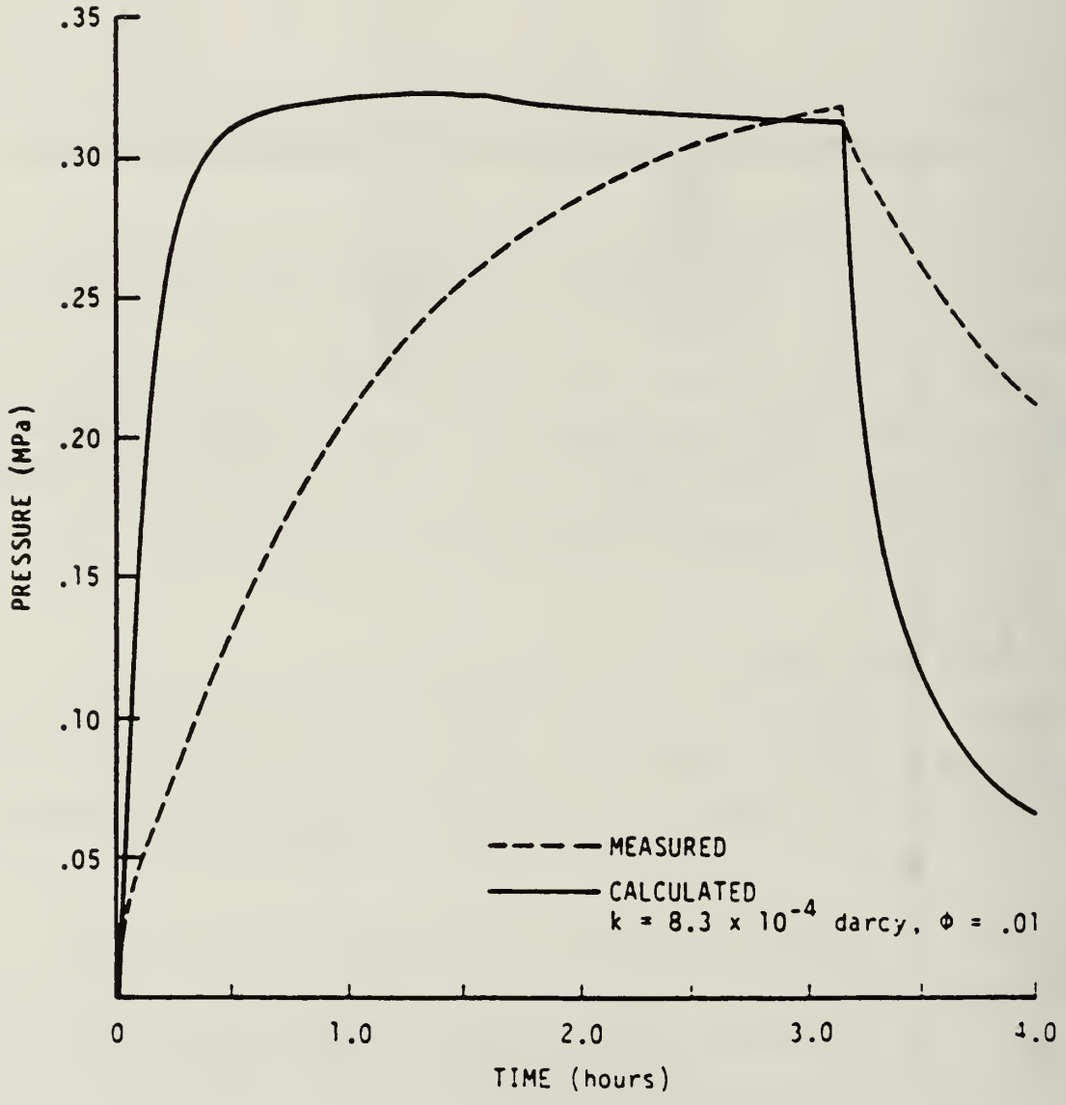

Figure 25. A comparison of the measured Test No. 8 pressure buildup and decay with that calculated using a 2.2×10^4 cubic centimeter test interval volume.

determined through further cross-hole flow and tracer tests. The Test No. 8 permeability values are only provided for comparison purposes and should not be taken as an indication of the Marker Bed 139 permeability.

During Test No. 9, the test interval was pressured to 0.57 MPa, then shut-in, and the subsequent pressure decay measured. As shown on Figure 26, calculated and measured pressure decay histories compare favorably given a formation permeability of 6.3×10^{-7} darcy and a porosity of 0.001, Calculations show that after 14 hours a 0.1 MPa increase in pore pressure had occurred at a depth of 75 centimeters. Since there was no guard zone used for Test No. 9, packer bypass flow could not be measured. As such, the stated permeability value represents an upper limit.

Borehole L1PD01

Test No. 11 was conducted in the 11.3 meter to 13.7 meter interval in Borehole L1PD01 shown on Figure 27. This test interval was surrounded by competent argillaceous halite, as shown on Figure 7.

During this test, the test interval was initially filled to a 0.65 MPa pressure, then shut-in, and the pressure decay monitored. As shown on Figure 28, calculated and measured decay histories compare reasonably given a 10^{-9} darcy formation permeability and a 0.001 porosity. Calculations show that after 18 hours a 0.1 MPa increase in pore pressure had occurred at a depth of only 4.5 centimeters. This minimal pressure front penetration suggests that the permeability at this location can only be accurately measured if test duration is significantly increased.

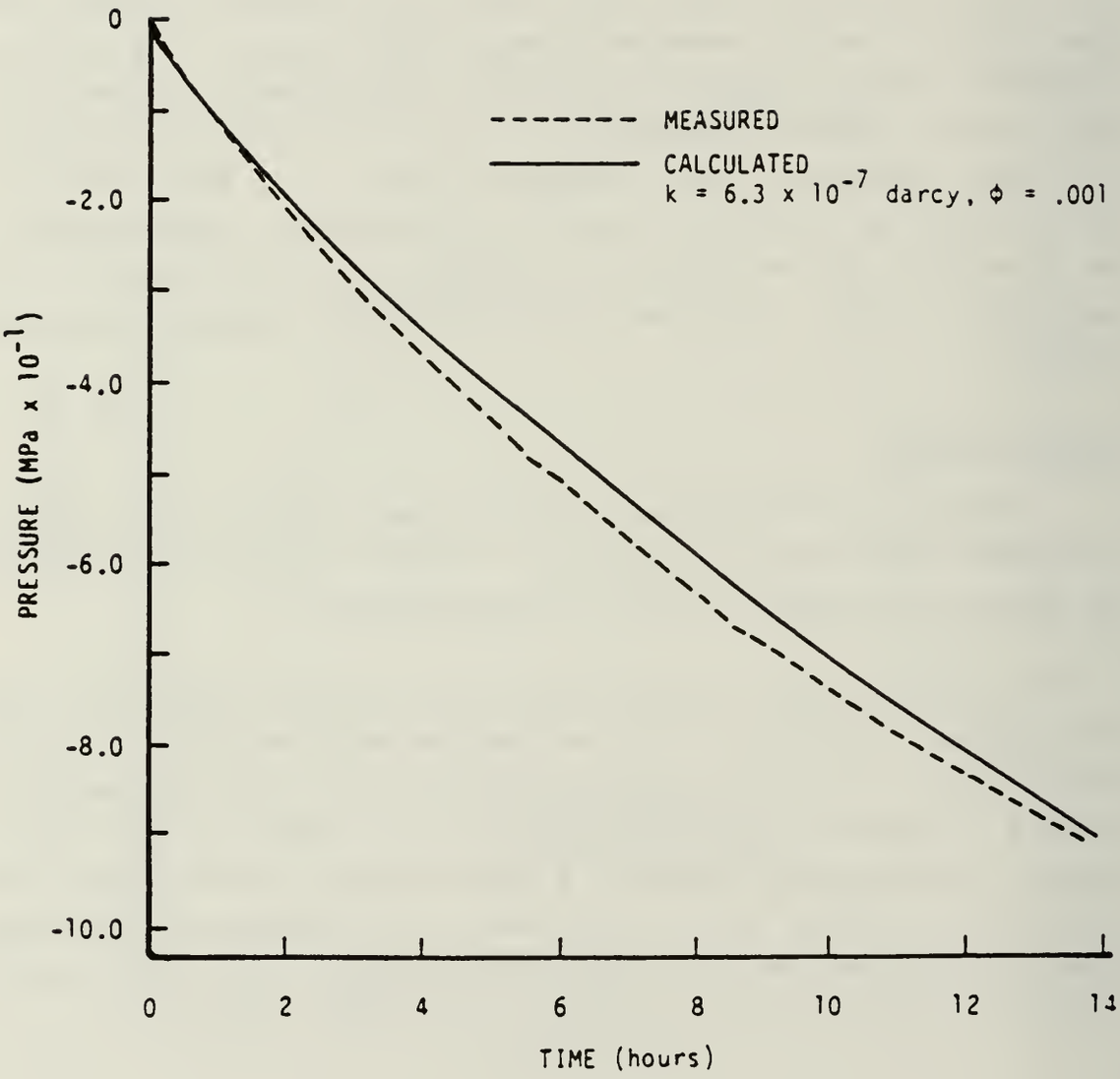

Figure 26. A comparison of the measured Test No. 9 pressure decay with that calculated for permeability and porosity of 6.3×10^{-7} darcy and 0.001, respectively.

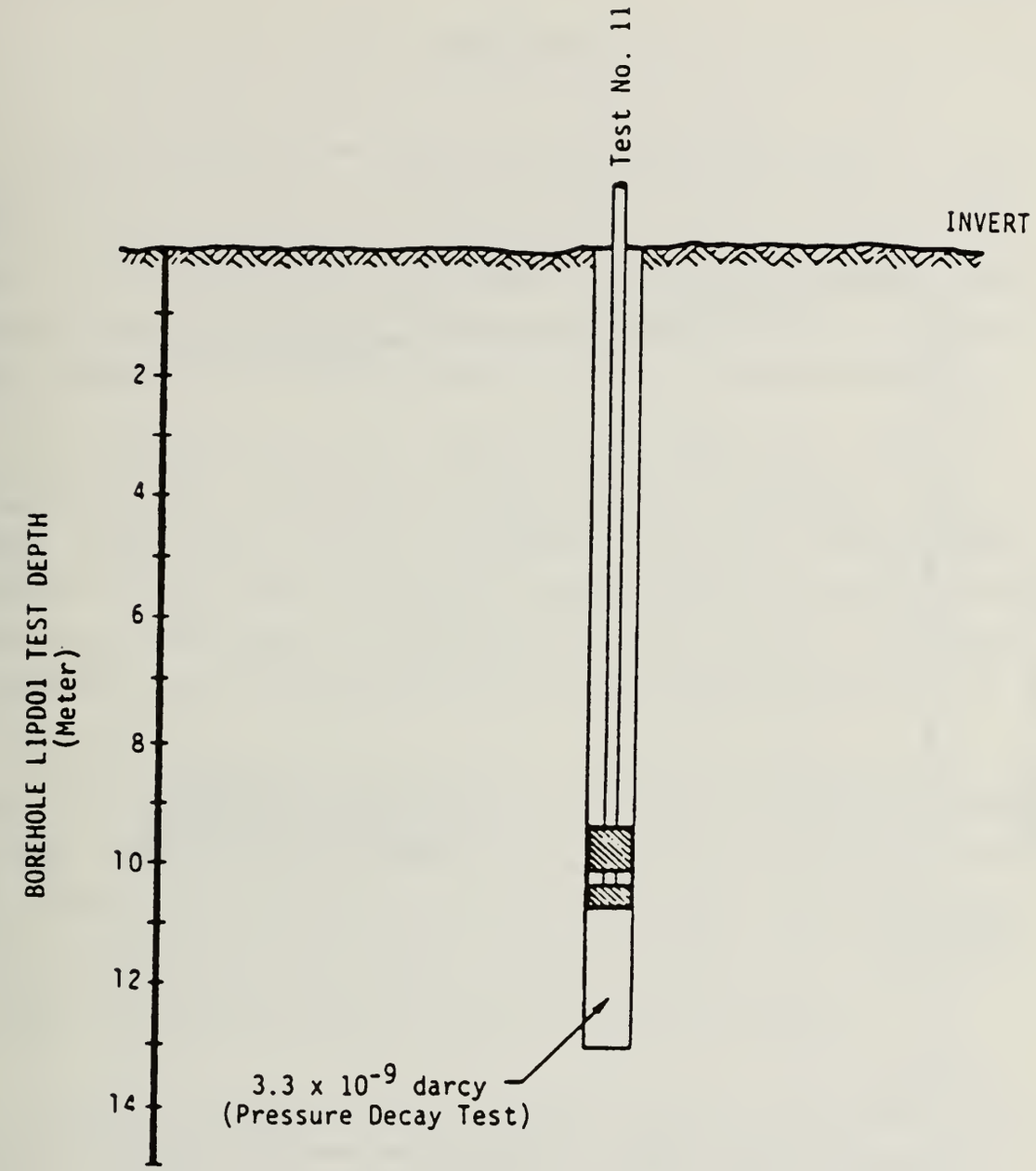

NOTE: Vertical borehole L1PD01 was positioned 6.1 meters from the left rib and 18.3 meters from the heading.

Figure 27. Room L1 vertical borehole L1PD01 permeability test result.

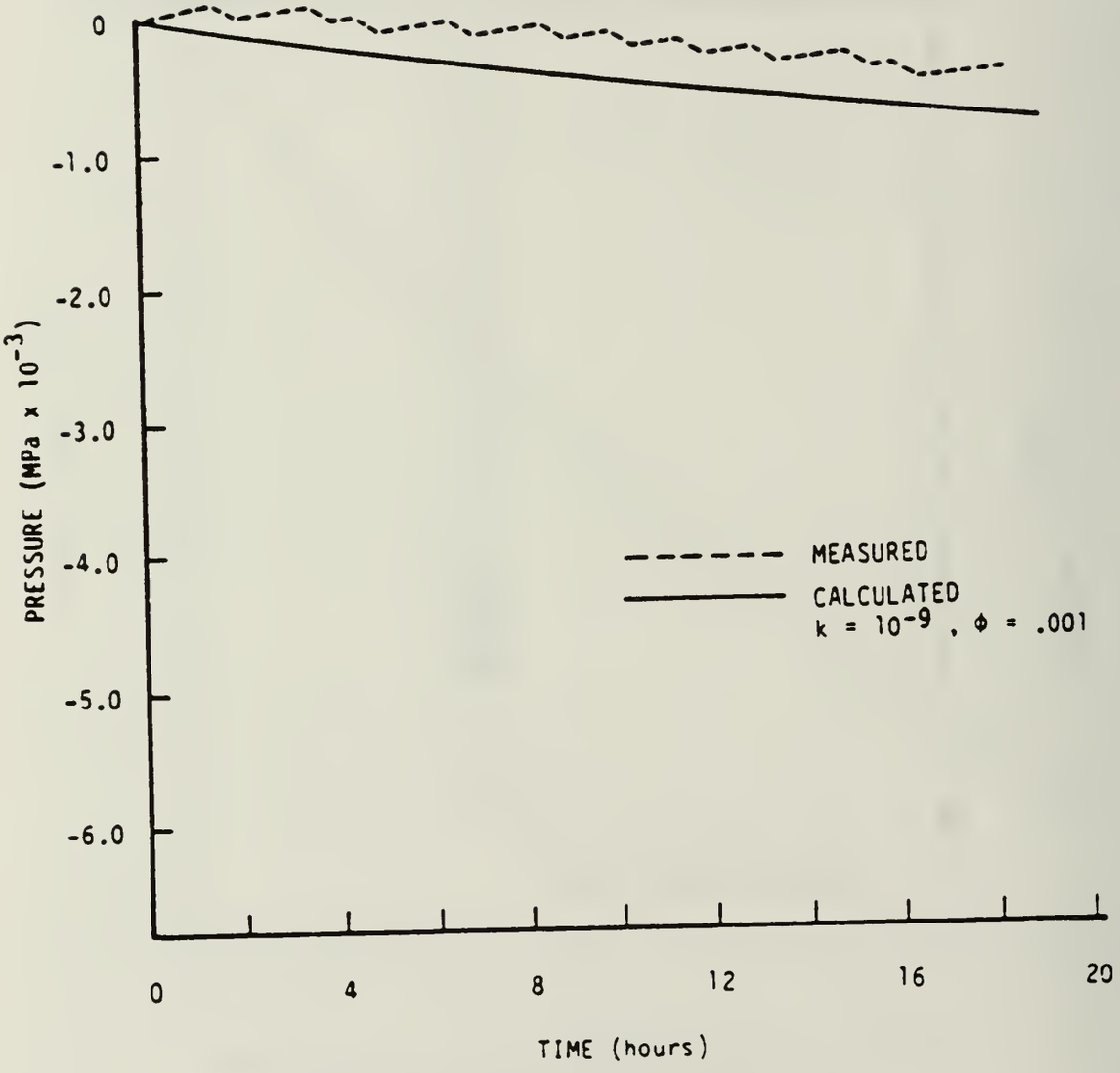

Figure 28. A comparison of the measured Test No. 11 pressure decay with that calculated for permeability and porosity of 10^{-9} darcy and 0.001, respectively.

5. CONCLUSIONS

A total of twelve flow tests were performed during Phase I in boreholes drilled from Rooms L1 and L2. The test objectives were to determine: (1) the permeability and, possibly, the porosity of the competent salt; (2) the permeability variations with distance from the mined surface; and, (3) the permeability of the interspersed clay and anhydrite seams. Results of the tests are summarized in the following paragraphs.

The competent salt was found to have less than a 10^{-8} darcy permeability and an approximate 0.001 porosity. Furthermore, the test results suggest that the salt is isotropic and has no preferred flow direction. Again, salt includes all rock types which are predominately halite--from argillaceous to polyhalitic to clear halite. No variation in permeability was attributable to the different types of halite.

There is some indication that the permeability decreases with increasing distance from the mined surface. This is illustrated on Figure 29, which shows all the low permeability test results. It should be noted that a guard zone was not used in Tests No. 1 and 9; therefore, these results represent an upper limit on the permeability. Even if subsequent testing confirms that permeability values increase as the face is approached, the maximum measured value was less than 10^{-6} darcy.

Generally, those clay and anhydrite regions tested had permeabilities similar to that of the competent salt. There were three exceptions. A clay/anhydrite seam located about 4.0 meters above the back of Room L2 produced a small flow of gas even when pressured to 0.65 MPa. The clay seam located about 2.1 meters above the back in the middle of Room L2 accepted gas at a rate of 9000 SCCM when pressured to 0.33 MPa. This same seam was tight ($k = 4.4 \times 10^{-8}$ darcy) when tested in Borehole L2PU01 located near the heading--thereby indicating the enhanced permeability in Borehole L2PU01 may result from roof sag. A test done in

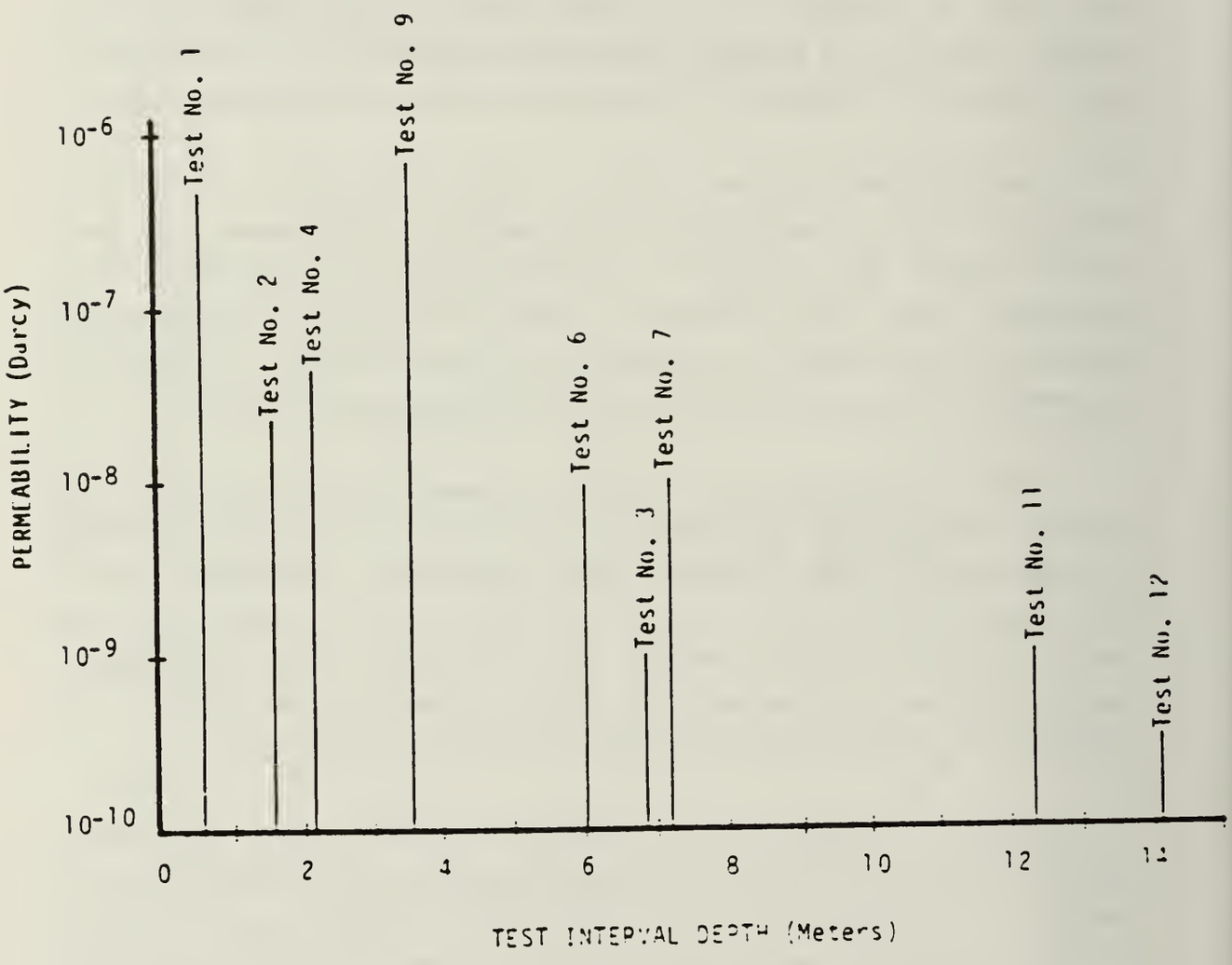

Figure 29. Illustration showing the variation in measured permeability with increasing test interval depth.

Marker Bed 139 in Borehole L2PD01, located approximately 15.2 meters from the heading and midway between the ribs, accepted gas at a rate of 8300 SCCM when pressured to 0.42 MPa.

During the Phase II confirmation tests described in Appendix B, Marker Bed 139 and the clay seam located about 2.1 meters above the back accepted gas at rates of 1.7×10^5 SCCM (greater than 1 darcy permeability) and 1.1×10^5 SCCM (approximate 10^{-3} darcy permeability) when pressured to 0.11 MPa and 0.66 MPa, respectively, from boreholes drilled in the center of Room 4. In contrast, Marker Bed 139 and this clay seam had permeability values below the level of sensitivity (less than 10^{-5} darcy) of the "order-of-magnitude" permeability tests when examined from vertical boreholes positioned near the rib, or from an inclined borehole which intersected Marker Bed 139 in the undisturbed free field. Results of the confirmation tests suggest that the large permeabilities measured in Marker Bed 139 and the clay seam occur as a result of floor heave or roof sag.

All Phase I flow tests were sensitive enough to accurately measure permeabilities down to the 10^{-8} darcy value in a 0.001 porosity formation. Longer duration tests are needed to accurately measure permeability values less than 10^{-8} darcy.

Permeability and porosity values were determined from the data assuming an unsaturated connected pore volume. If this volume were partially or fully saturated, so that fluid migration and/or threshold pressure effects were important, the intrinsic formation permeability would be larger than reported. The influence of pore fluid effects on these <u>in situ</u> tests can only be determined for these low permeability formations through high pressure cross-hole flow and tracer tests. Some indication of these effects could possibly be determined through laboratory tests of properly confined carefully extracted core samples.

Those three regions which either produced gas or accepted large flows could not be adequately characterized by these tests as they did not respond as classical isotropic formations. Cross-hole flow and tracer tests are required to characterize Marker Bed 139 and the clay/anhydrite layers examined in Tests No. 5 and 10. Since the measurement system is very sensitive to the measured four to five order-of-magnitude change in flow found between the competent formation and Marker Bed 139, this type of test can be used to examine the effect of floor heave or roof sag.

E.6 N1420 DRIFT GAS FLOW DATA ANALYSIS AND EVALUATION

This subsection of Appendix E contains a description of gas flow measurement data collected during N1420 drift testing. A summary of this test and its results is presented in SEIS Subsection E.4. This subsection is presented to support near-field horizon permeability rates defined in the text.

This subsection is excerpted from Chapters 4, 5, and 6 of Peterson et al., 1987, WIPP Horizon Free Field Fluid Transport Characteristics.

4. DATA ANALYSIS AND EVALUATION

Data analysis methods are summarized in Section 4.1. Uncertainties inherent in these analyses and interpretations are addressed in the discussion presented in Section 4.2.

4.1 DATA ANALYSIS.

Short duration gas flow tests were performed to obtain order of magnitude permeability estimates for comparison with subsequent brine flow tests and previous gas flow tests. Permeability values were estimated from data obtained from these short duration tests using the simple one-dimensional steady-state radial flow equations described in Reference 5. These estimates assumed an unsaturated formation.

Formation permeability and pore pressure values were determined from the brine test data in an iterative manner using numerical solutions to the appropriate diffusion equations as described in Reference 5. In the analysis, the test region pressure history was calculated as a function of time using selected values for formation permeability, porosity, and pore pressure. When the calculated pressure history corresponded to the measured data, the assumed formation properties were taken as correct.

All brine test analyses assumed radial flow into the borehole from a completely brine saturated formation with a porosity of 0.001. For most calculations, the test region was assumed to be filled with brine having a 3.26×10^3 MPa bulk modulus. Some calculations were performed for the DPD02 tests which assumed a partially gas-filled test region. In those calculations the test region fluid compressibility was taken as that of the brine/gas mixture.

Borehole closure will, in the absence of flow, increase the test region pressure. These pressure changes are generally insignificant for a gas filled test region. However, for a brine flow test it may be necessary to consider closure

effects when estimating formation permeability from the measured test region pressure response.

Borehole closure effects have been considered in some of the analyses presented in this report. Closure rates were determined using the relation between closure, borehole radial stress, and far field stress, which is suggested in References 6 and 7. Results contained in these two references indicate that the change in borehole radius (R) with time may be described by

$$\frac{1}{R}\frac{dR}{dt} \simeq -\alpha \left[\frac{P_o - P_h}{P_o - P_\infty} \right]^5 \qquad (1)$$

where α, P_o, P_h and P_∞ represent the normalized closure rate, far field stress (assumed hydrostatic), internal radial stress applied to the borehole surface, and ambient pressure at the free surface of the drift, respectively. The normalized closure rate was taken as

$$\alpha = 20 \text{ microstrains/day.} \qquad (2)$$

This rate was determined from measurements of drift closure provided in Reference 8. Note that 20 microstrains/day is approximately the same order as that measured by SNL (Reference 9, 10, 11) in 91 cm diameter boreholes.

4.2 DATA EVALUATION

The tests described in this report measured a pressure buildup with time which occurred when the test region shown on Figure 2 was shut-in or isolated. Two parameters were inferred from the resulting data. The asymptotic steady-state pressure value was taken as a measure of the local pore fluid pressure. This pore fluid pressure value was then used together with the time dependent

pressure response to estimate a formation permeability under the assumption that the connected pore space was completely saturated.

The major uncertainties in the interpreted data are not associated with the accuracy of the measurement system as has been discussed in Reference 5. Instead, major uncertainties are introduced by the assumptions which must be used to interpret the data.

The asymptotic steady-state pressure was assumed to represent the pore pressure. This should be correct, independent of formation saturation, provided the measurement system does not leak, and that the predominant pressure response occurred as a result of fluid migration rather than hole closure. If Equations (1) and (2) correctly represent borehole closure, then as will be shown in Section 5, the inferred pore pressure values are independent of these closure effects.

There was no evidence of either packer bypass flow or packer system leakage during the DPD02 test. There was also no evidence of packer system leakage during the DPH01 test. However, as previously discussed in Section 3, it cannot be determined whether there was flow past the DPH01 guard region packer. If such flow did occur, then the actual pore pressure would be higher than the stated value. For example, an approximate 0.5 cc/day leak from the guard region would lower the final measured steady-state asymptotic pressure from about 10 MPa to 8 MPa.

Determination of formation permeability is based upon the inferred pore pressure value and the measured test region time dependent pressure response. Uncertainties in the pore pressure therefore lead to uncertainties in the permeability value.

The various permeability values presented in this report values were determined assuming a fully saturated uniform porous formation and a brine filled or brine/gas filled test region. There is, at this time, no information available concerning the level of saturation or the validity of the uniform porous formation

(i.e. in contrast to a porous/fractured formation) assumption. The effect on the inferred permeability values of a brine/gas filled test region is considered in Section 5.

There are other effects which could influence the estimated permeability values such as threshold pressure effects, Klinkenberg effect on gas tests, and precipitation/dissolution effects. These are discussed in Reference 4.

5. TEST RESULTS

Test results are presented, compared to calculated pressure histories, and discussed in this section. Additional comparisons between measured and calculated results are presented in Appendix B. These additional results demonstrate the sensitivity of the calculated pressure responses to selected values for the formation permeability, the formation porosity, and the test region gas fraction.

It can be seen in Appendix B that the calculated pressure histories are quite insensitive to the low porosity values used for these studies, however they are quite sensitive to changes in the selected permeability and the test region gas fraction.

Zero time for the calculated pressure histories presented in this report is the date of hole completion. The holes were assumed to remain open during the approximate 44 day period prior to initiation of the brine flow tests. The effect of neglecting the open hole period on the calculated pressure histories is illustrated in Appendix B. The local pore pressure distribution changes during the open hole period as a result of flow into the borehole.

5.1 DPH01 TEST RESULTS

A comparison of the calculated and measured DPH01 test region pressure histories is shown on Figure 10. The calculated and measured histories are seen to compare favorably throughout the 199 day shut-in period assuming a formation permeability of 10^{-9} darcy, a porosity of 0.001, and a free field pore pressure of 8.2 MPa. Also shown are calculated pressure histories for assumed permeabilities of 10^{-8} and 10^{-10}. These graphically illustrate the sensitivity of the match between calculated and measured pressure histories.

There was little attempt made to calculationally match the measured pressure increase which occurred following the test region vent at 212 days. As

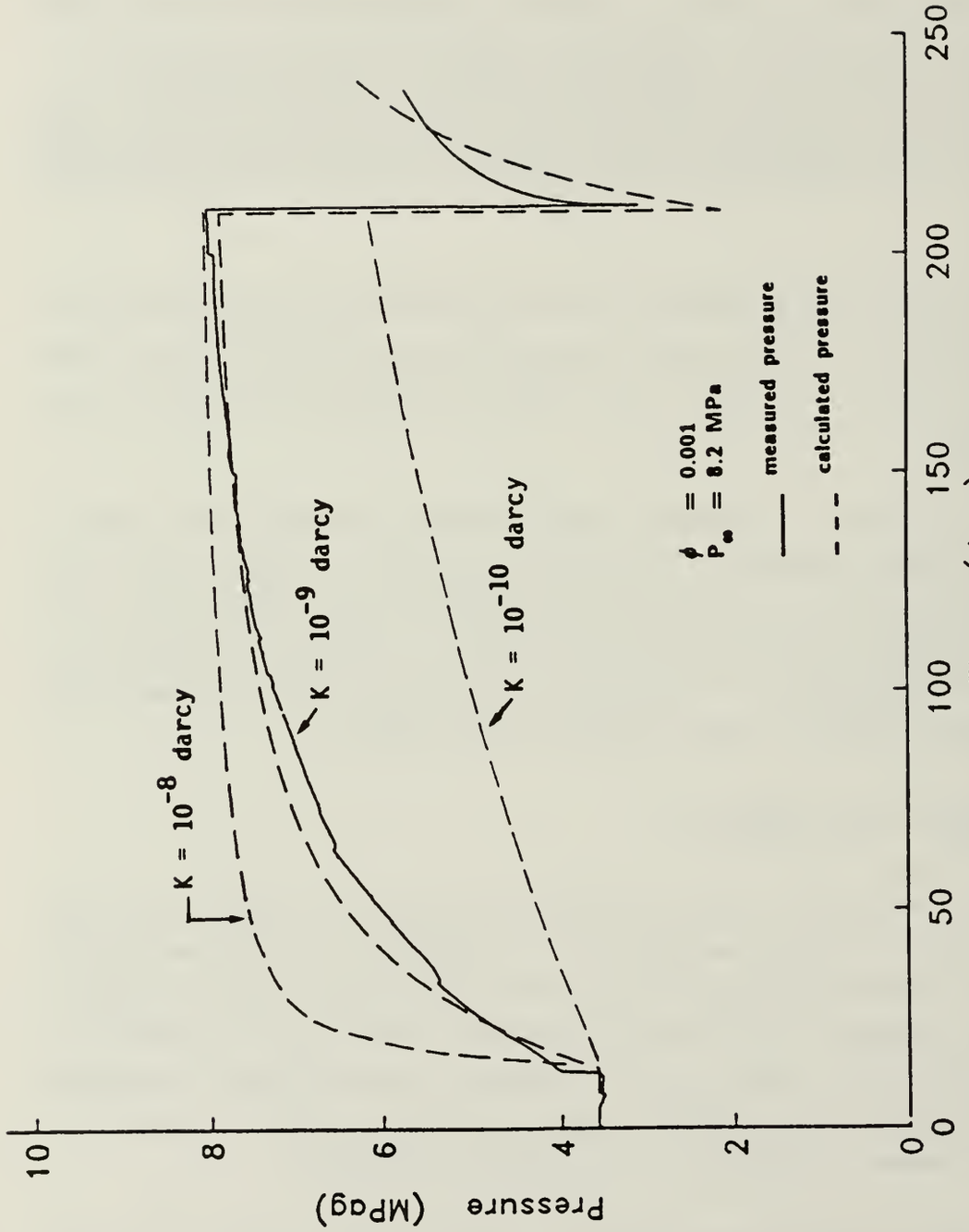

Figure 10. Comparison of the measured DPH01 test region pressure history with that calculated assuming brine inflow but no borehole closure.

shown on Figure 10, the selected formation properties which match the 212 day history give a pressure recovery rate which is more rapid than that measured. This increased rate could be due to the presence of trapped gas within the borehole, or due to system compliance effects. These effects were not investigated during this work.

The test region pressure buildup, calculated to result from hole closure in the absence of flow, is shown on Figure 11. If the Equation (2) ambient pressure closure rate, and the Equation (1) closure rate sensitivity to pressure are correct, then in the absence of flow, borehole closure could force the DPH01 pressure to increase to about 6.1 MPa during the 199-day shut-in period.

A comparison of the measured test region pressure buildup with that calculated to occur as a result of brine inflow plus hole closure is shown on Figure 12. Calculated and measured results are seen to compare favorably assuming the same formation parameters used to obtain the Figure 10 results. In effect, borehole closure, as defined by Equations (1) and (2), does not influence the formation permeability or pore pressure values inferred from the DPH01 test data.

Figure 13 shows the calculated brine flow to an open 10 cm diameter hole assuming the formation properties shown on Figure 10. The flow is allowed to start immediately after hole completion. The inflow approaches an approximate rate of 10^{-2} cc/day per cm of hole length within a few days. This inflow compares favorably to the measured open hole inflow rate of Reference 12, obtained by a humidity monitoring technique, and the inflow rate of Reference 13 determined using a bailing technique.

Fluid was removed from the borehole DPH01 test and guard regions after the 199 day shut-in period. During the process of lowering the test region pressure from 7.9 MPa to 3.0 MPa and the guard region pressure from 7.7 MPa to 3.4 MPa, a total of 57 cc of fluid was removed from the test region while 41 cc of fluid was removed from the guard region. Assuming an absolutely stiff system, and a 3.26×10^{3} MPa brine compressibility, it is estimated that 29 cc

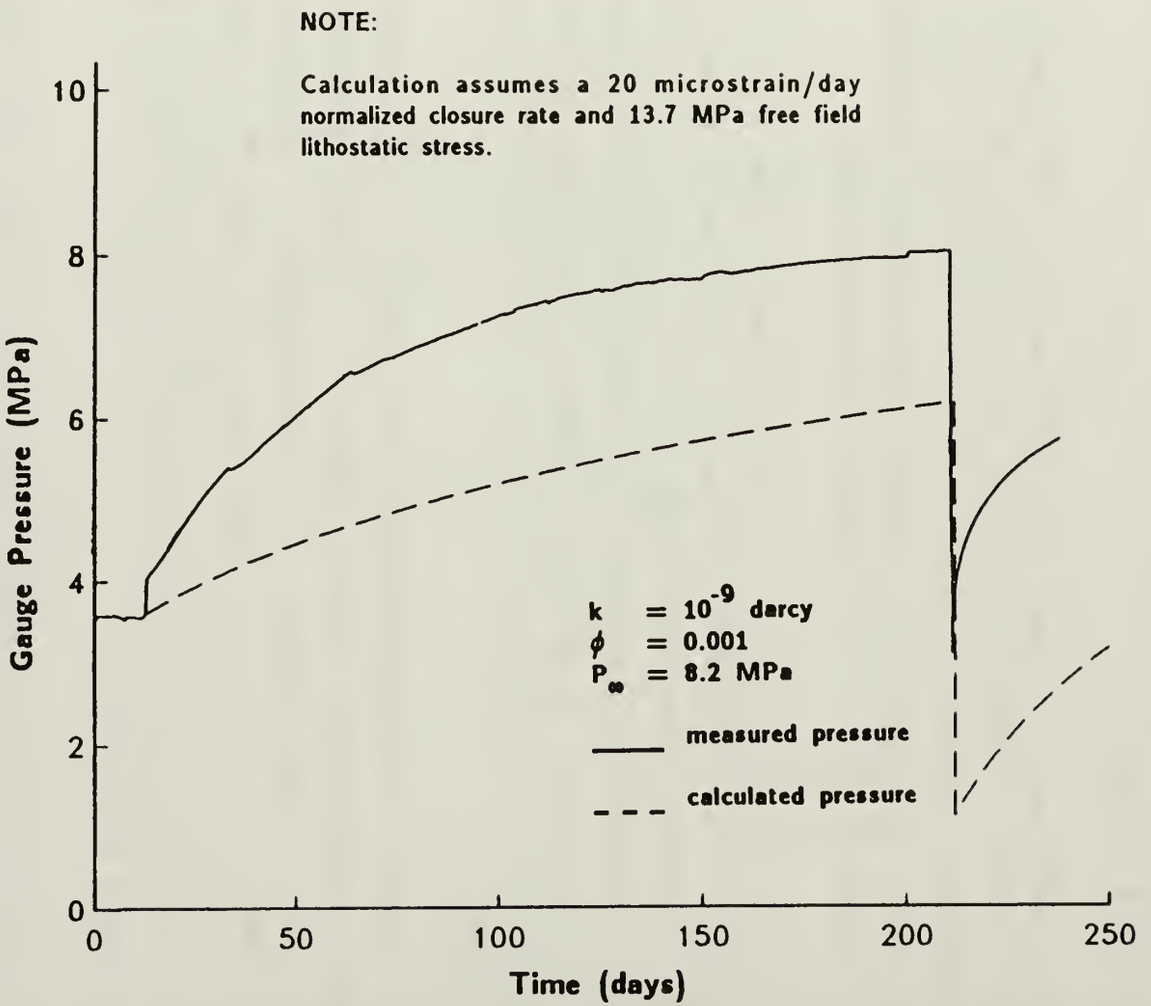

Figure 11. Comparison of the measured DPH01 test region pressure history with that calculated assuming the pressure increase results only from hole closure.

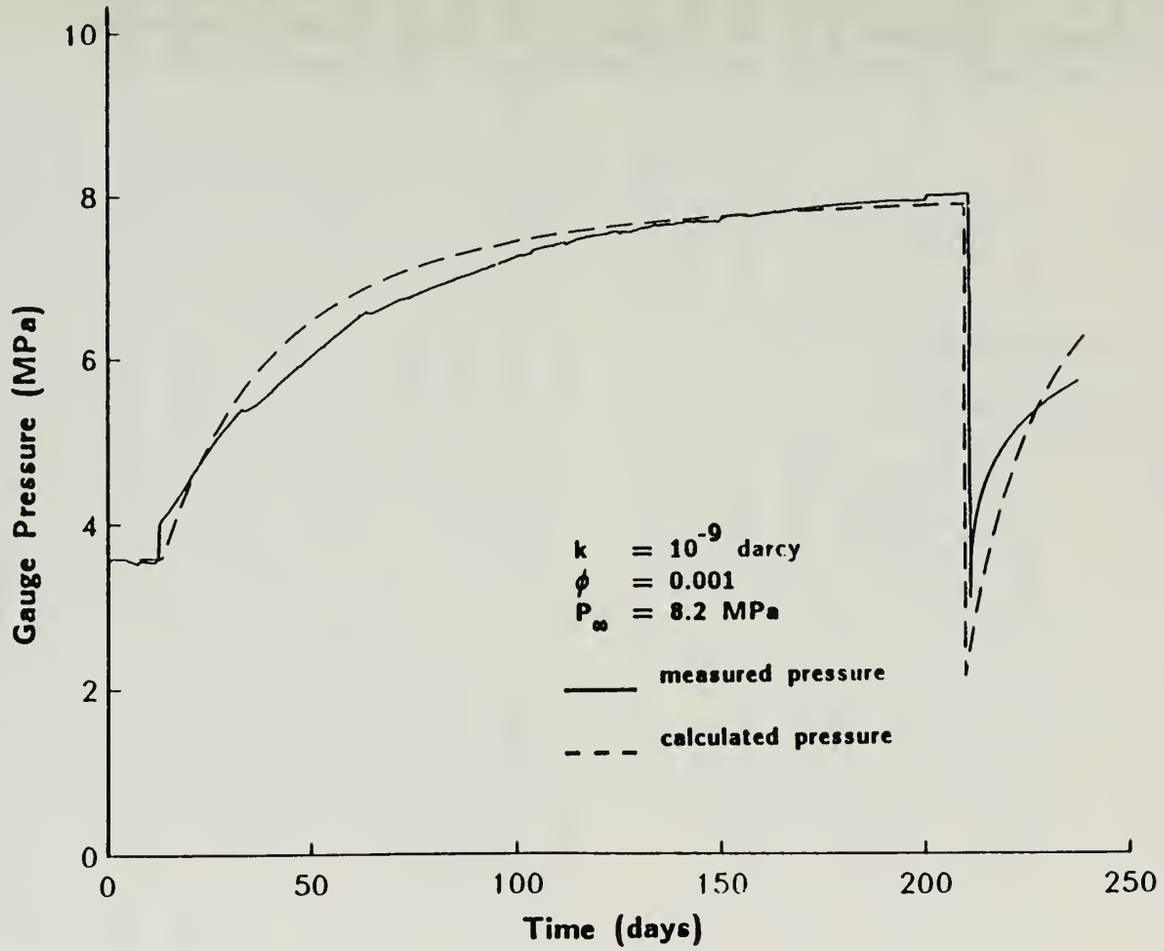

Figure 12. **Comparison of the measured DPH01 test region pressure history with that calculated assuming the pressure increase results from both brine inflow and hole closure effects.**

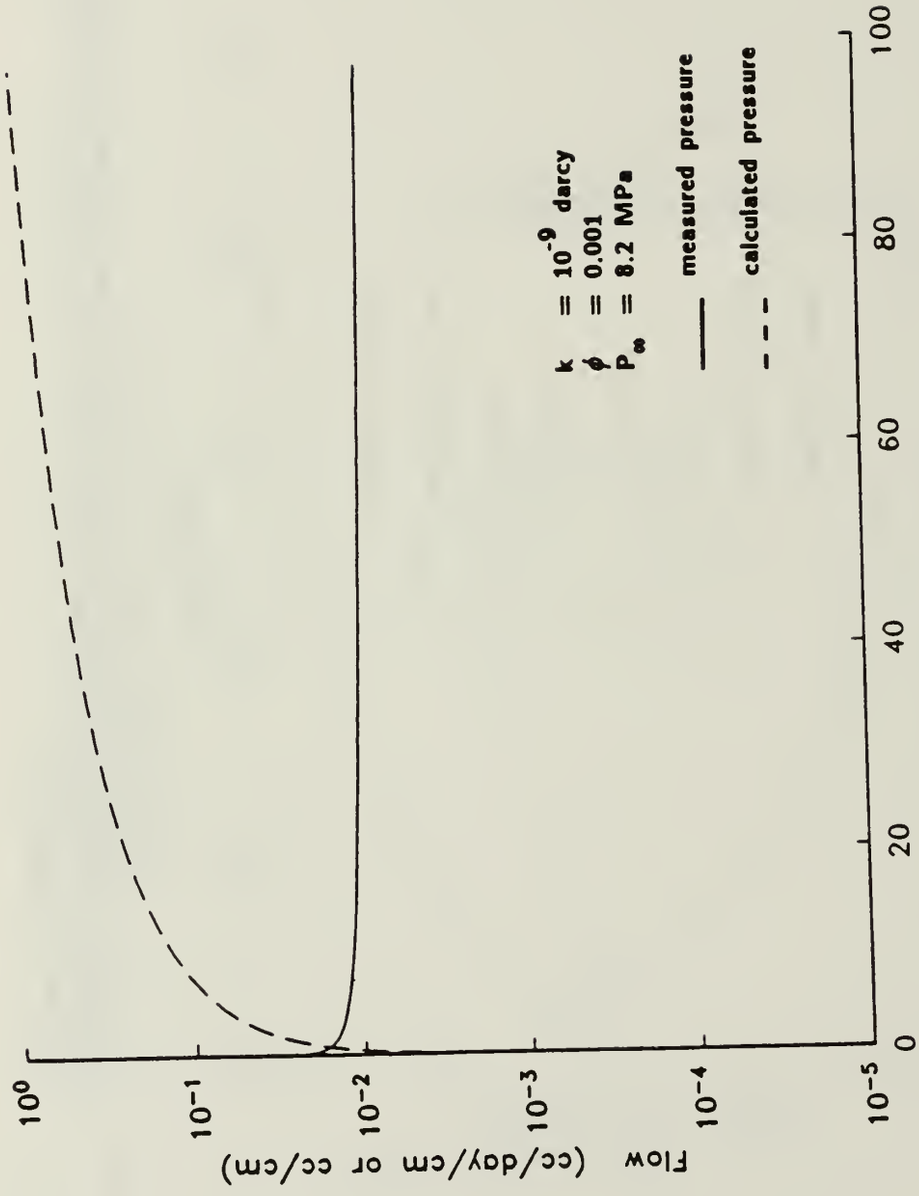

Figure 13. Calculated brine flow to an open 10 cm diameter borehole from a saturated formation having an 8.2 MPag free field pore fluid pressure.

of fluid should be removed from the test region and 3 from the guard region to match the pressure decrease. During this removal procedure, the packer pressure was reduced by 2.0 MPa, hence there would be some associated packer deformation. However, packer deformation cannot account for the excess removed fluid.

One possible explanation for the disparity between the measured and anticipated fluid outflow revolves around the presence of a small amount of gas in the borehole. Recall that DPH01 is a horizontal borehole and that prior to filling the test and guard regions with brine, gas was evacuated from these regions using a vacuum pump. The vacuum pump may not, however, have been able to remove all of the gas contained in the test and guard regions. If, for example, only seven percent of the initial quantity of gas in the borehole remained in the borehole, this amount of air could account for the disparity between the calculated and measured brine removal volumes.

Short-duration, 2.1 MPa pressure, gas flow tests were conducted in borehole DPH01 both before and after performing a brine flow test. Analysis of the May 20, 1986 data shown on Figures 4 and 5 indicate that prior to performing the brine flow tests, gas would flow from the borehole into the surrounding formation at a rate consistent with a permeability of approximately 10^{-8} to 10^{-9} darcy. The January 20, 1987 2.1 MPa pressure gas flow test data shown on Figures 14 and 15 indicate no flow into the formation. This result was to be expected since the formation surrounding the borehole had been subject to a high pressure brine test. Note that the packers were set prior to the May 20, 1986 test and were not deflated until after the January 20, 1987 test.

Initially, the formation would accept gas driven at a 2.1 MPa borehole pressure. However, when the borehole was filled with brine and pressurized to 3.5 MPa, a pressure rise characteristic of potential brine inflow began to occur within 13 days after brine pressurizationn. The reasons for such disparate gas versus brine behavior are unknown at this time. This behavior could result because of threshold pressure effects, precipitation of solids in the flow channels,

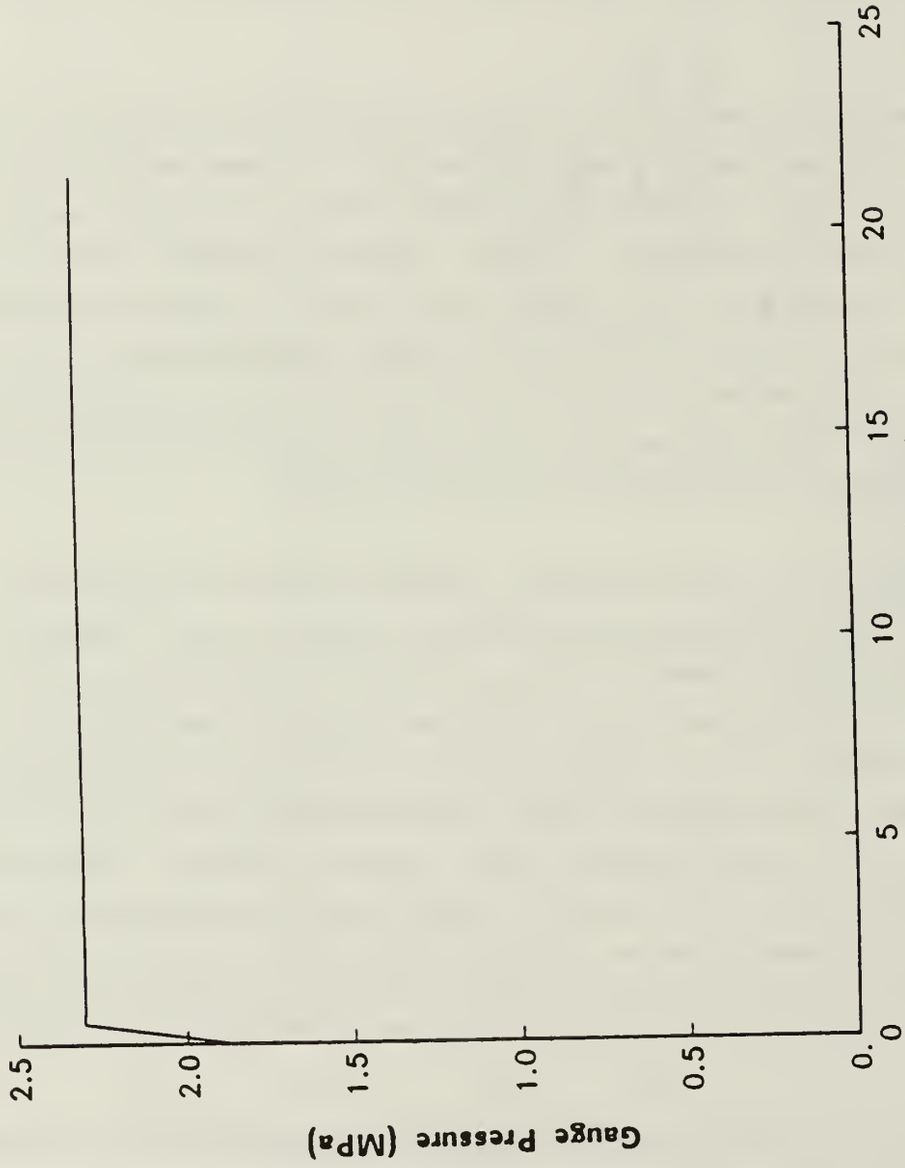

Figure 14. Test region pressure history measured during the January 20, 1987 DPH01 gas flow test.

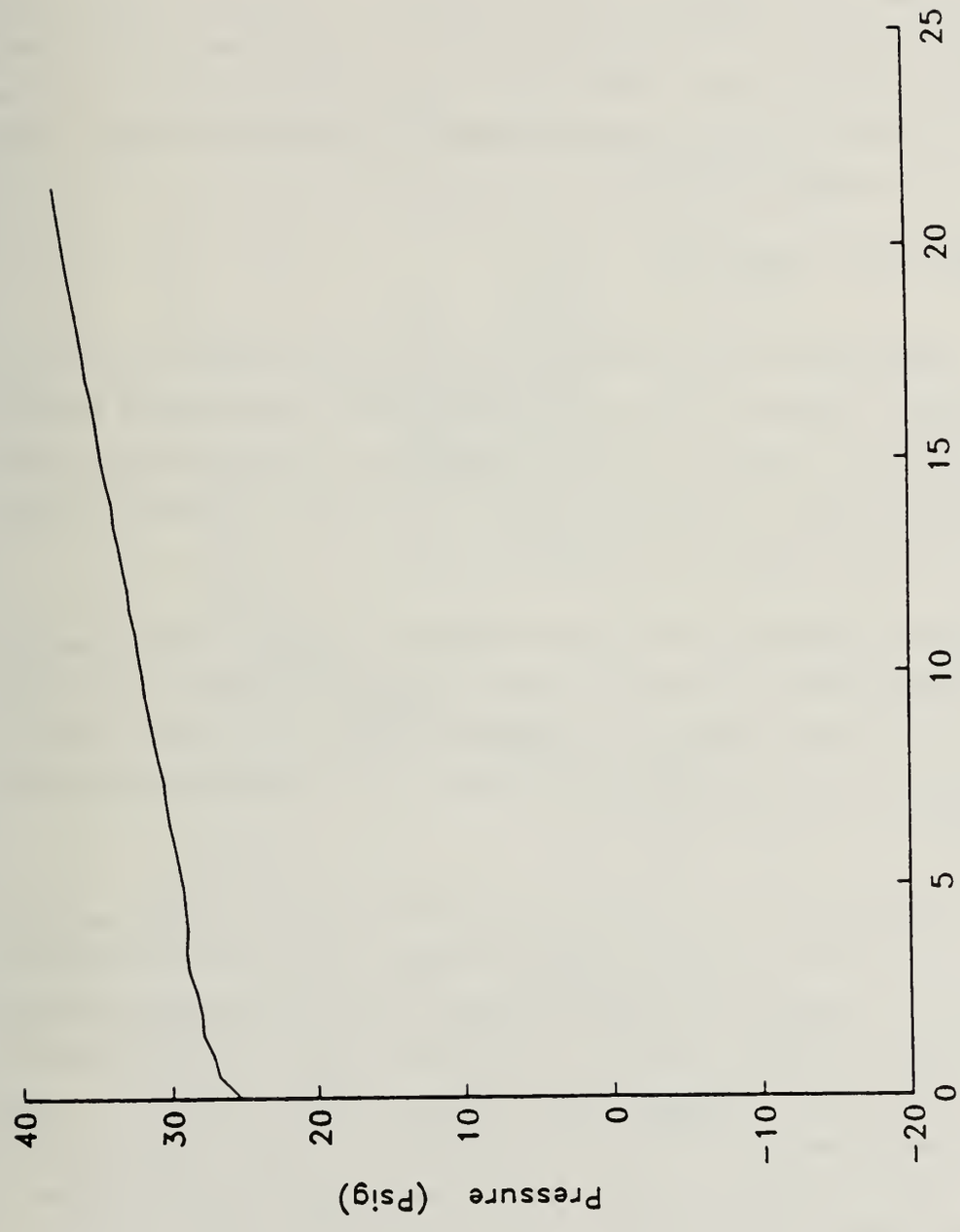

Figure 15. Guard region pressure measured during the January 20, 1987 DPH01 gas flow test.

flow channel plugging by tiny clay particles observed to be suspended in the brine, a locally unsaturated formation, or other means.

Analyses of the Figure 4 and 5 gas flow test results indicate that approximately two-thirds of the gas leaving the test region goes to the guard region due to packer bypass. This flow is rapid enough so that it can be expected that the test and guard region pressures may be similar during the long duration brine flow test.

5.2 DPD02 TEST RESULTS

A comparison of the calculated and measured DPD02 test region pressure histories is shown on Figure 16. The calculated and measured pressure histories are seen to compare favorably throughout the 144 day shut-in period for an assumed formation permeability of 3.0×10^{-9} darcy, a porosity of 0.001, and a free field pore pressure of 10.3 MPa.

The initial shut-in period shown on Figure 16 began six days after the hole was drilled. After the test region was pressurized with brine and shut-in, the test region pressure continued to increase to about 5.5 MPa after which it rapidly decayed as if the formation had fractured. This initial shut-in period was not considered in the calculated results.

At 212 days into the shut-in test, the test zone was vented and then shut-in. The test zone pressure exhibited the pressure rise shown on Figure 16. Little effort was expended to calculationally match the measured pressure increase observed to occur following this test region vent. As can be seen on Figure 16, the materials properties yield a pressure recovery rate which is more rapid than that measured. In order to understand this lack of agreement, an effort was made to consider the influence of a partially gas filled test region on the pressure history after 212 days. These calculational results, which are discussed later, do provide a slightly better fit to the pressure recovery data.

The test region pressure buildup, which is calculated to result from hole closure in the absence of flow is shown on Figure 17. If the Equation (2)

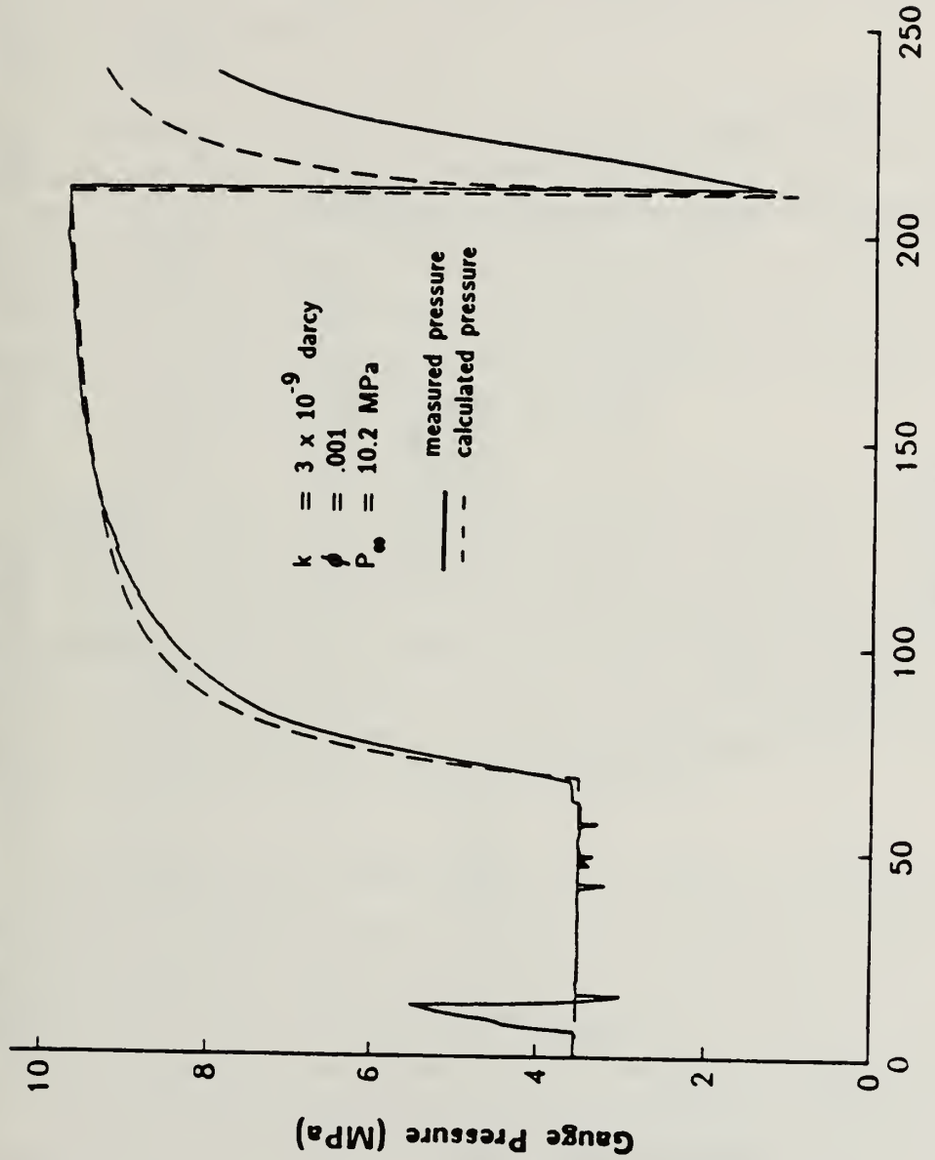

Figure 16. Comparison of the measured DPD02 test region pressure history with that calculated assuming brine inflow but no borehole closure.

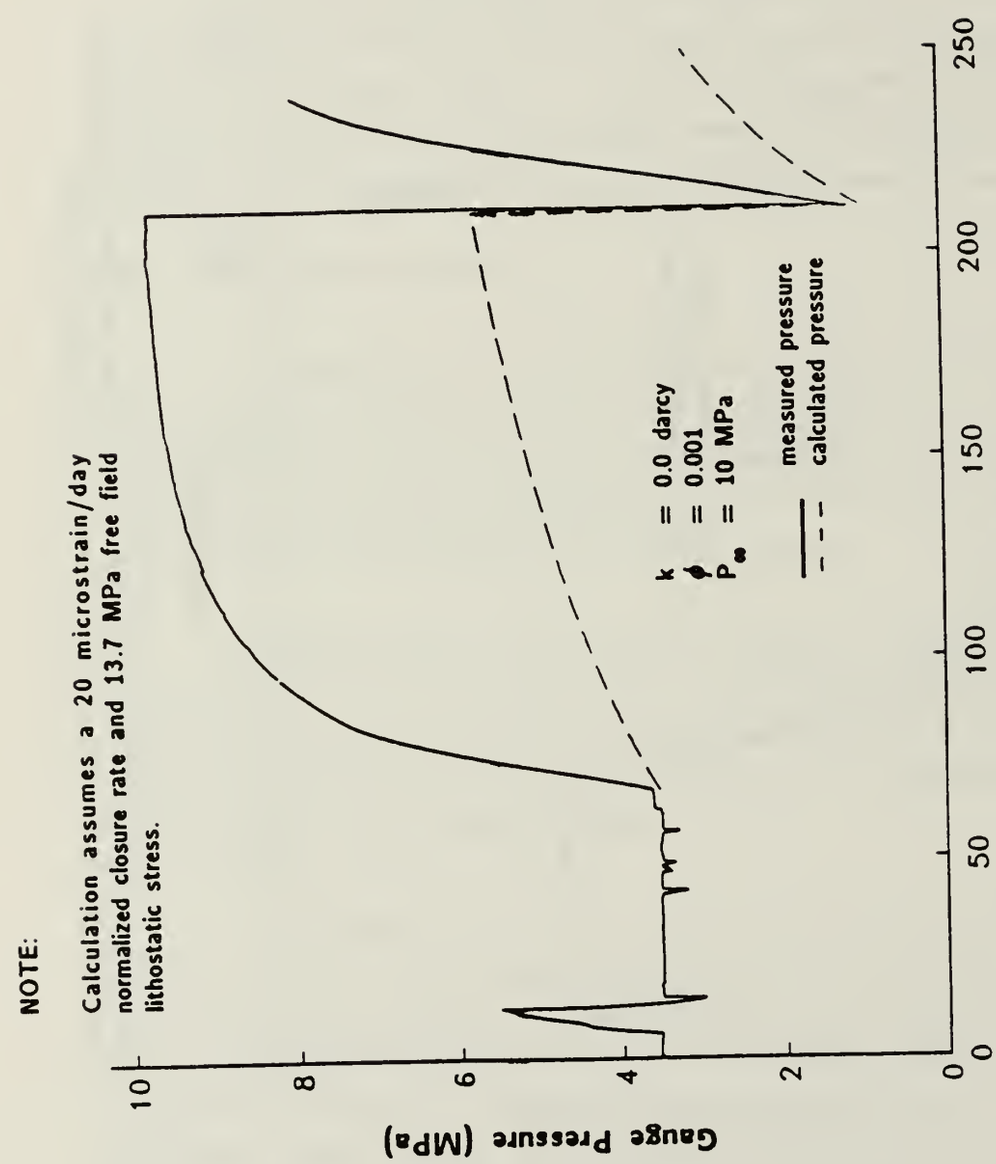

Figure 17. Comparison of the measured DPD02 test region pressure history with that calculated assuming the pressure increase results only from hole closure.

ambient pressure closure rate, and the Equation (1) closure rate sensitivity to pressure are correct, then as can be seen in Figure 17, borehole closure cannot account for the measured time-dependent pressure buildup observed in borehole DPD02. Note also that since this zone is largely anhydrite, borehole closure effects should be nonexistent.

A comparison of the measured test region pressure buildup with that calculated to occur as a result of brine inflow plus hole closure is shown on Figure 18. Calculated and measured results are seen to compare favorably assuming the same formation parameters used to obtain the Figure 16 results. Since these curves agree closely in both cases, borehole closure, as defined by Equations (1) and (2), does not influence the formation permeability or pore pressure values inferred from the DPD02 test data.

Figure 19 shows the calculated brine flow to an open 10 cm diameter hole assuming the same formation properties shown on Figure 16. The flow is allowed to start immediately after hole completion and is seen to approach an approximate rate of 1.2×10^{-2} cc/day per cm of hole length within a few days. This inflow compares favorably to the measured open hole inflow rate of Reference 12 obtained by a humidity monitoring technique and the inflow rate of Reference 13 determined using a bailing technique.

Fluid was removed from the borehole DPD02 test and guard regions after a shut-in period of 144 days. During the process of lowering the test region pressure from 9.7 MPa to 1.3 MPa a total of 870 cc of fluid was removed from the test region while 41 cc was removed from the guard region. It is estimated that 93 cc of fluid should have been removed from the test region assuming a stiff system, and a brine compressibility of 3.26×10^{3} MPa. During this fluid removal procedure the test region packer pressure was dropped by 3.0 MPa. Although there would be some packer deformation associated with this pressure drop it is not sufficient to account for the excess fluid removed from the test region.

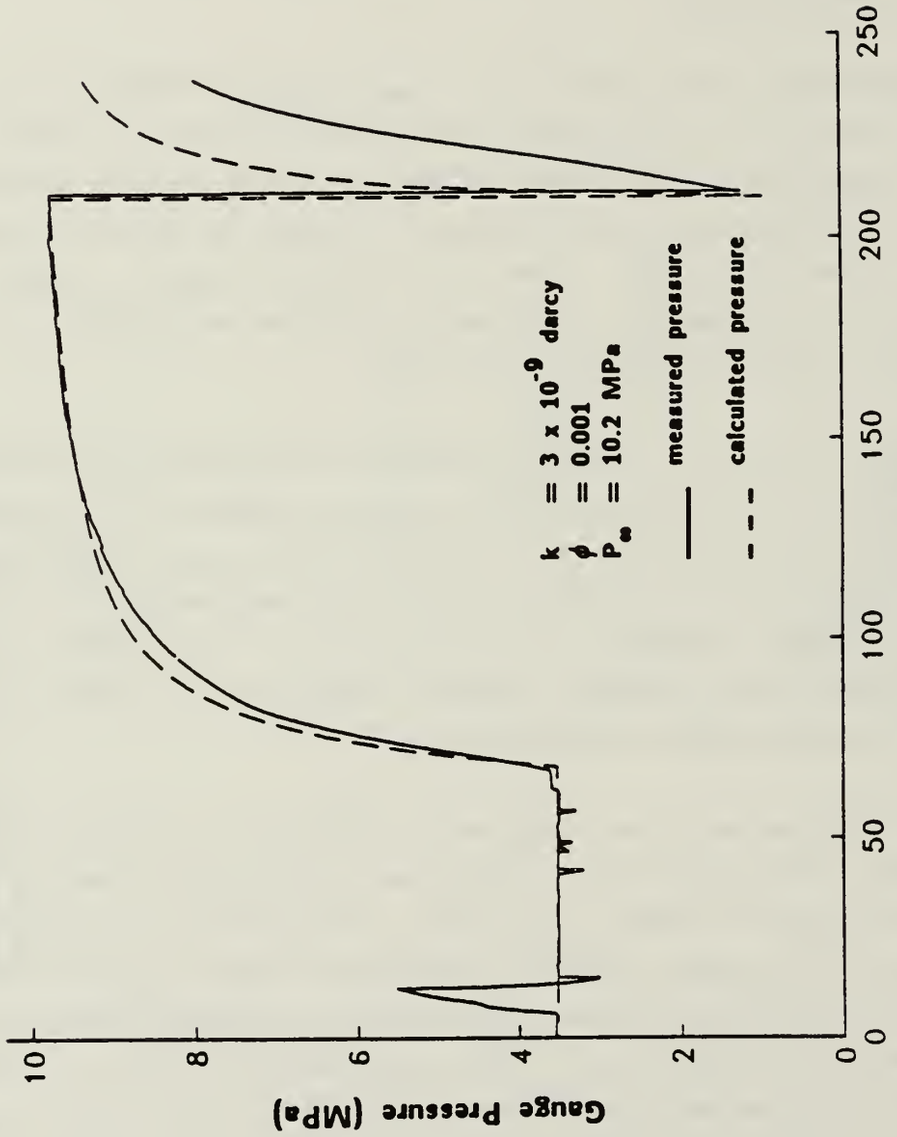

Figure 18. Comparison of the measured DPD02 test region pressure history with that calculated assuming the pressure increase results from both brine inflow and hole closure effects.

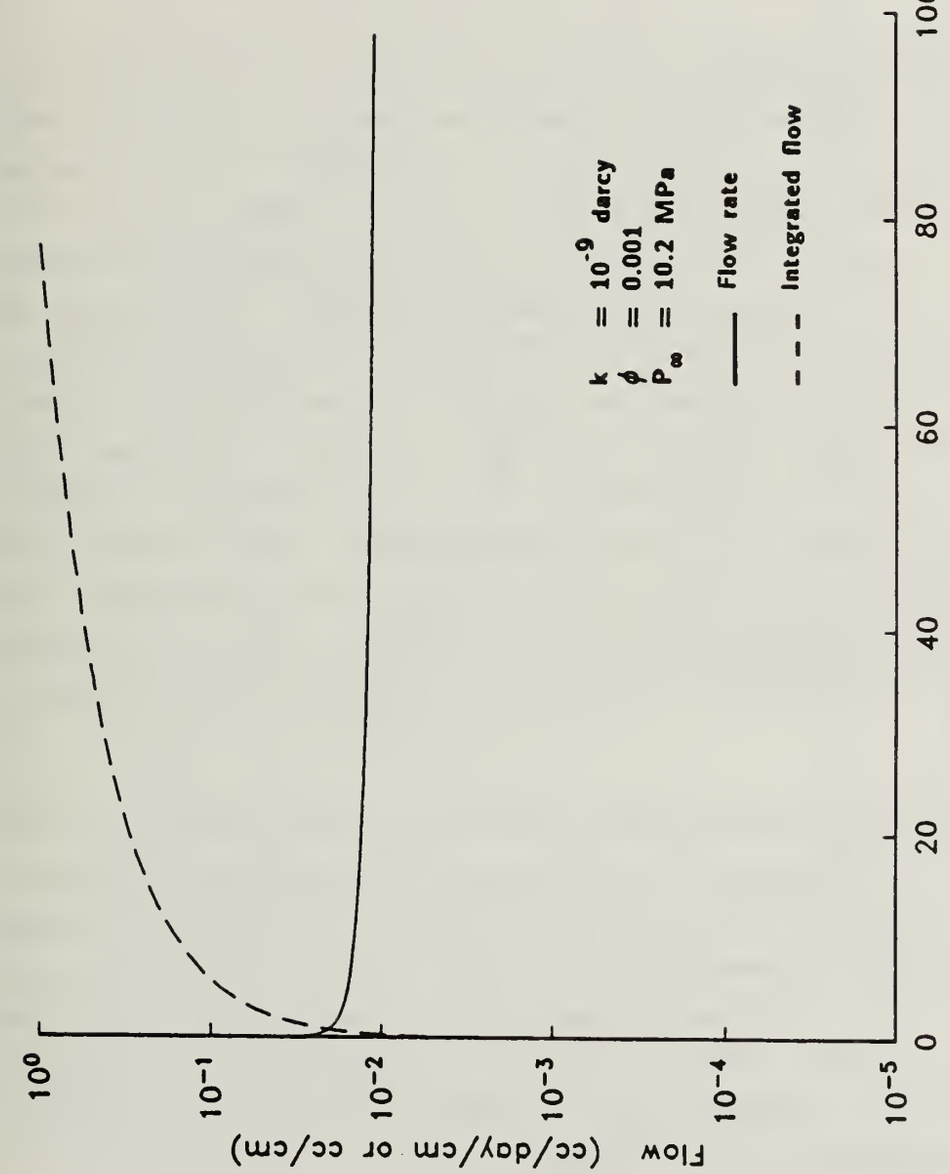

Figure 19. Calculated brine flow to an open 10 cm diameter borehole from a saturated formation having a 10.2 MPag free field pore fluid pressure.

Note that the packers were set prior to the May 20, 1986 test, and were not deflated until after completion of the brine flow test. At that time they were deflated in order to remove brine from the borehole. However, the packer system was not moved prior to the January 20, 1987 test.

A possible explanation for the source of this excess fluid lies in the observation that borehole DPD02 is slanted downward at a 45 degree angle. Prior to filling the test and guard regions of the borehole with brine, gas was evacuated from these regions using a vacuum pump. In addition, once the brine level reached the bottom of the packer, a vent line was opened and brine was circulated in order to attempt to remove any remaining gas. Unfortunately, the small amount of gas which may have remained in the borehole could not account for the disparity between the calculated and measured brine volumes removed. A more likely explanation is that some gas which was injected during the preliminary gas flow test remained in the connected formation void volume surrounding the borehole. The additional compressibility of this brine/gas system could then account for the excess brine removed from the test region. Note that the borehole/formation system would have to contain approximately 10^4 standard cubic centimeters of air or nitrogen to yield the observed volume of fluid removed.

A comparison of the measured test region pressure buildup with that calculated to occur assuming a partially gas filled borehole is shown on Figure 20. Calculated and measured values are seen to compare favorably assuming a formation permeability of 10^{-8} darcy, a porosity of 0.001, a free field pore pressure of 10.3 MPa, and the gas fractions shown on Figure 20. These gas fractions were determined from the brine removal data. For purposes of comparison the best fit obtained with a completely brine filled borehole required a formation permeability of 3×10^{-9} darcy.

Short duration 2.1 MPa pressure, gas flow tests were conducted in borehole DPD02 both before and after performing the brine flow test. Analysis of the May 20, 1986 data shown on Figure 21 indicate that prior to performing the brine flow test, gas would flow from the borehole to the surrounding

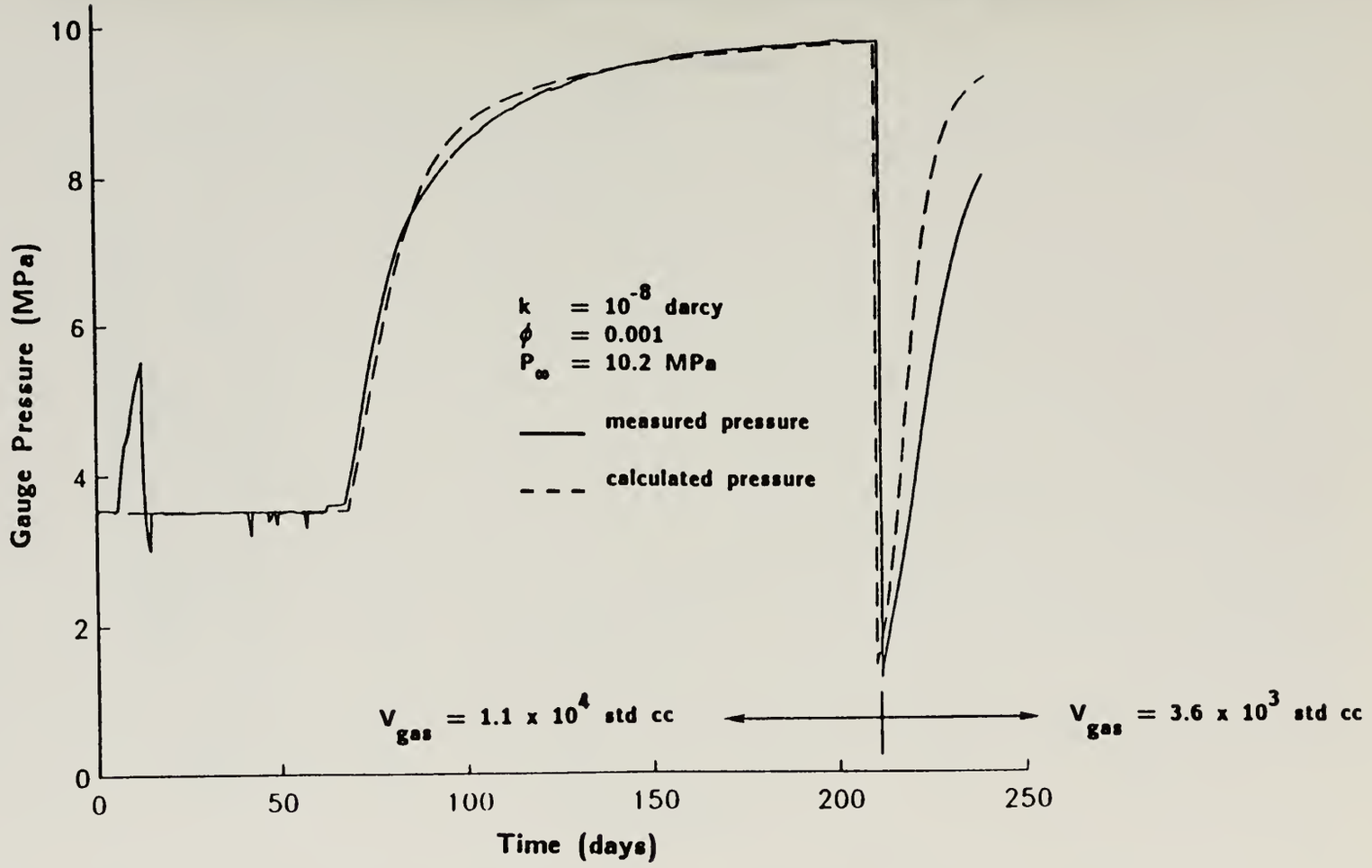

Figure 20. Comparison of the measured DPD02 test region pressure history with that calculated assuming brine inflow to a brine/gas filled borehole.

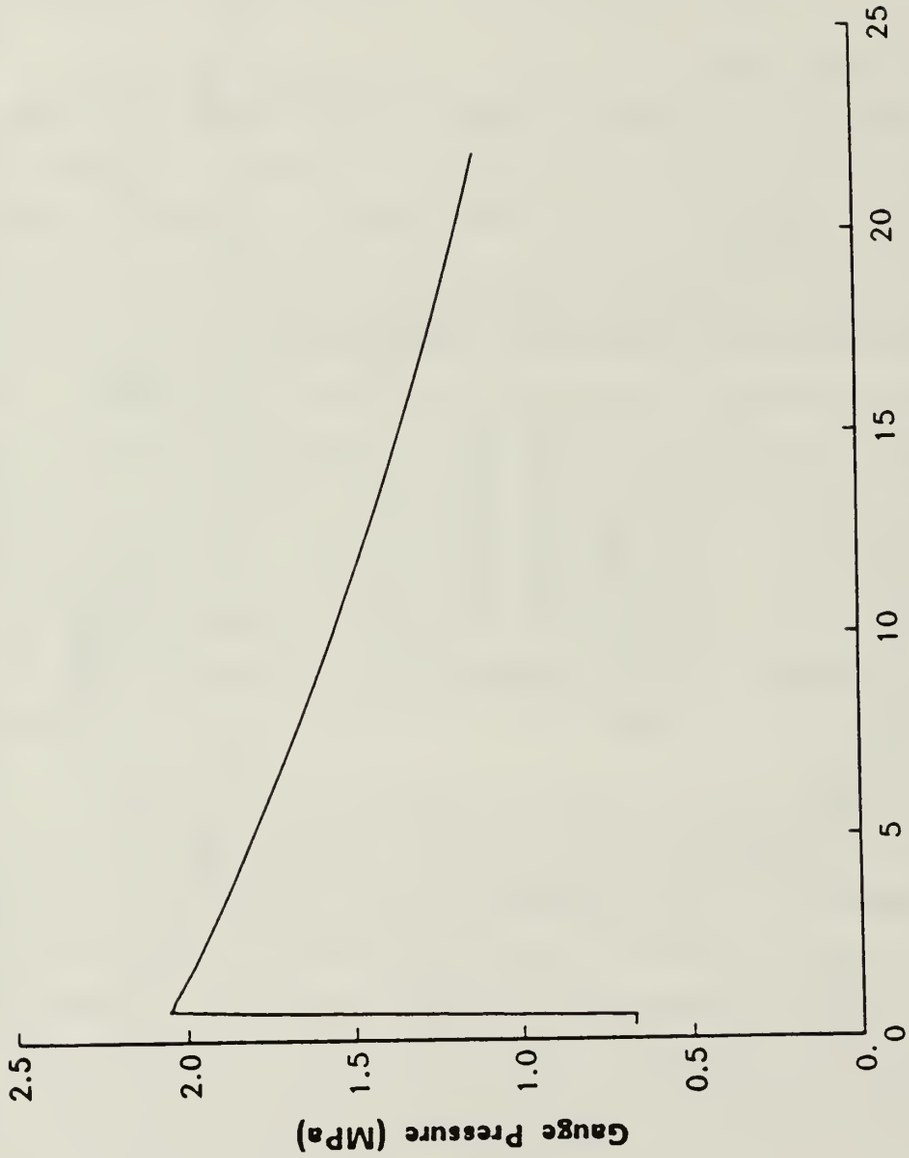

Figure 21. Test region pressure history measured during the June 20, 1986 DPD02 gas flow test.

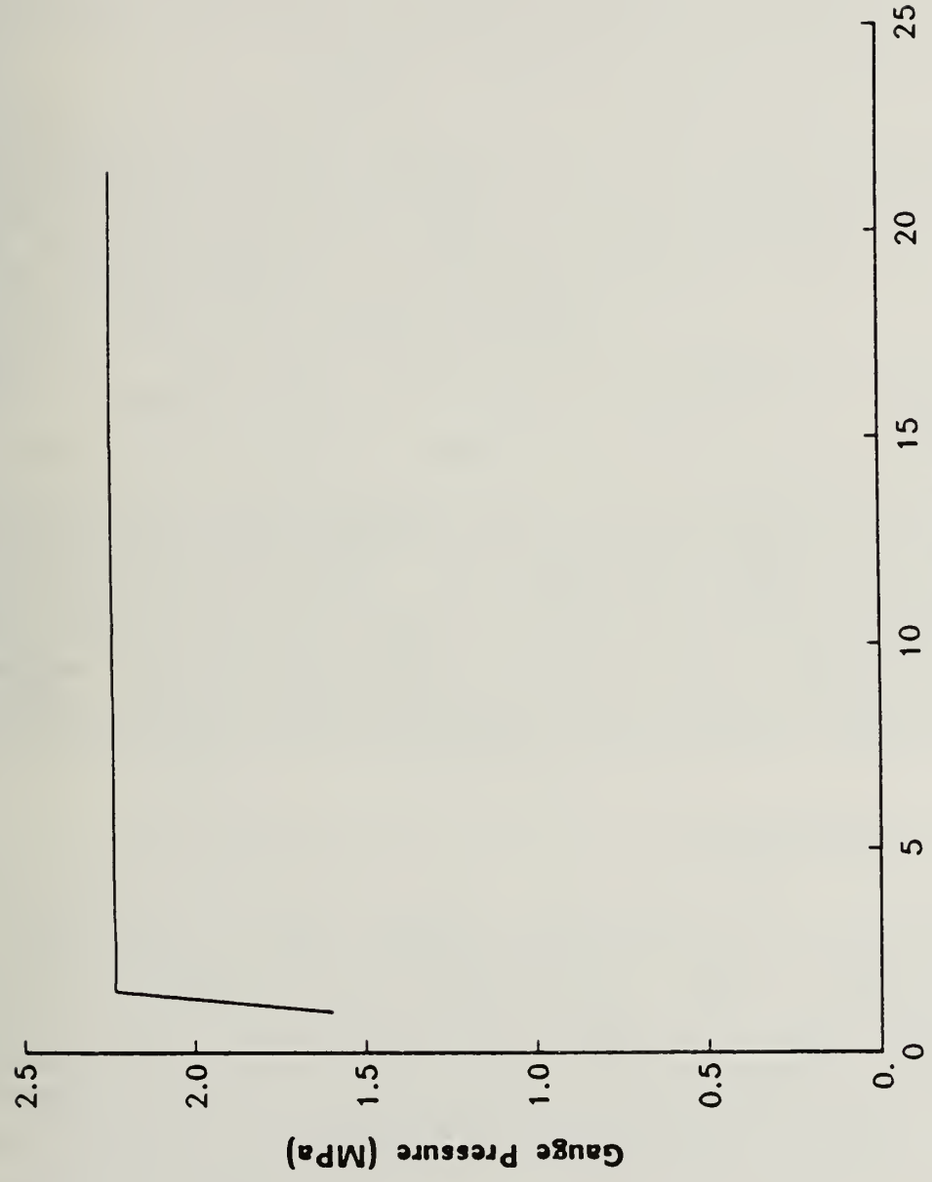

Figure 22. Test region pressure history measured during the January 20, 1987 DPD02 gas flow test.

formation at a rate consistent with an approximate 4 x 10^{-7} darcy permeability. A connected formation void space greater than 2 x 10^{4} cc would be required to accept the measured flow from the borehole. Analysis of the January 20, 1987, 2.1 MPa pressure gas flow test data shown on Figure 22 indicate no flow to the formation. This result was expected since the formation surrounding the borehole had been subject to the high pressure brine test.

Approximately 10^{3} cc of brine were injected into the formation immediately prior to shut-in of the test region at 67 days as shown on Figure 20. This volume of brine is an order of magnitude less than the connected void volume inferred from the May 20, 1986 gas flow test. Unfortunately, the reasons why the formation would initially accept gas at a 2.1 MPa pressure but would not accept a comparable brine volume at 3.5 MPa remain unknown.

As shown in Appendix A there was negligible flow to the borehole DPD02 guard region during the gas flow tests. There was some guard region pressure buildup during the brine flow tests. However, the rate was small compared to either that of the test region or to the rates observed in borehole DPH01. Note that the borehole DPD02 test region intersected Marker Bed 139 while the guard region was located in competent salt.

5.3 DPH02 TEST RESULTS

A brine flow test was conducted in borehole DPH02. Unfortunately a small leak was found to exist in the test region pressure monitoring line at a connection located within the handling sub at an approximate 5 meter borehole depth. This leak was repaired but not retested after the test had progressed 96 days. Data obtained subsequent to this fix indicate the borehole DPH02 test region pressure did increase after shut-in. No attempt was made to determine pore pressure or formation permeability values from the DPH02 test data, since they were neither as extensive nor as unambiguous as those data obtained in DPD02. The data are presented in Appendix A.

6. CONCLUSIONS

Data obtained during the brine flow tests indicate that competent halite within the WIPP horizon exhibits an estimated formation pore pressure of 8.3 MPa. These data further indicate that the Marker Bed 139 region exhibits an estimated pore pressure of 10.3 MPa. Inherent in these estimated pore pressures is the assumption that hole closure does not occur at a rate which is significantly faster than 20 microstrains/day. It was also assumed there was no brine leakage from the test region along the borehole/packer interface or from the measurement system. If leakage did occur the actual pore pressure values would be higher than those presented above.

Formation permeability values were determined from the brine flow test shut-in pressure buildup data based on the above mentioned pore pressure values and the assumption that the host formation is completely brine saturated. Under these assumptions the data are consistent with a competent halite permeability of 10^{-9} darcy and a Marker Bed 139 region permeability of approximately 10^{-8} darcy. All data were consistent with a formation porosity of 0.001. Note, however, that these data are not particularly sensitive to the absolute porosity value and should not therefore be used to infer porosity.

Prior to performing the brine flow tests, short duration 2.1 MPa pressure gas flow tests were performed. During those tests the competent halite accepted flow at a rate consistent with a permeability of approximately 10^{-8} darcy. The Marker Bed 139 region accepted flow at a rate consistent with a permeability of approximately 4×10^{-7} darcy. These permeability values were inferred assuming an unsaturated formation possessing a porosity of 0.001. Subsequent to performing the brine flow tests, gas flow tests were performed. During these tests the formation would not accept gas driven at a test region pressure of 2.1 MPa.

Apparently those flow channels which enabled gas to flow out of the borehole at a 2.1 MPa test region pressure cannot be the same flow channels

through which brine entered the borehole since brine pressures approach free field values of 8.3 or 10.3 MPa. The reasons for the very different gas flow and brine flow test responses remain unknown.

Numerous explanations for the observed results exist. The simplest may be that either as a result of precipitation or possible plugging by fine particulates within the brine. the initial brine flow served to close the gas flow channels. Subsequent pressure buildup resulted from borehole closure and/or brine inflow which occured at so low a rate that it could not be detected during the gas flow tests.

In summary. two brine flow tests were performed. While the data can be interpreted to yield free field pore fluid pressure and formation permeability values. the results are not conclusive. Additional confirmatory testing in other boreholes would be desirable. Specifically. borehole tests in which pressure buildup is measured along with borehole closure rate would provide strong confirmatory evidence for the interpretation of pressure buildup in terms of pore pressure.

E.7 WASTE HANDLING SHAFT PULSE TESTING DATA SUMMARY AND CONCLUSIONS

This subsection of Appendix E contains the test result summary and conclusions from testing in the waste-handling shaft. The results of this test were used to measure the far-field hydraulic conductivities within the Salado Formation. The far-field hydraulic conductivities were converted to permeabilities in the range of 10^{-20} to 10^{-21} m^2. See Table 5.3 for a summary of hydraulic conductivities and calculated permeabilities. This subsection is presented to support far-field permeability estimates.

The text, figures and tables, contained in this subsection are excerpted from Saulnier and Avis, 1988, Interpretation of Hydraulic Tests Conducted in the Waste-Handling Shaft at the Waste Isolation Pilot Plant (WIPP) Site. For a complete reference, please see the Appendix E reference list.

6.0 SUMMARY AND CONCLUSIONS

6.1 Test Results

The permeability-testing program for the WHS was designed to provide the plugging and sealing program with information on the distribution of hydraulic conductivity, the radial variation of formation pressure, and, possibly, the distribution of fractures at various radial distances from the wall of the WHS in parts of the lower Rustler and upper Salado Formations. To accomplish these goals, a series of sub-horizontal boreholes were drilled in the WHS at the 782, 805, 850, and 1320-foot depth levels below ground surface (BGS). Pulse-injection tests were performed in six of these boreholes using a multipacker test tool configured to isolate three test intervals, or zones, in each borehole tested. After installing the multipacker test tool, the packers were inflated with the test zones vented to the atmosphere to dissipate the pressure created in the test zones by the expansion of the packers and the consequent compression of the test-zone fluid. After inflating the packers, the test zones were shut in. The shut-in periods, which were of varying length because of the constraints of other crews' work and shaft-access schedules, were followed by a series of pulse-injection tests in the isolated intervals. The deepest zone in each borehole, or zone #1, was the first zone tested, followed by either zone #2, the center zone, or zone #3, the zone closest to the shaft wall.

Shut-in fluid-pressure responses varied from hole to hole, and from zone to zone within boreholes as shown on the sequence plots for each borehole (Figures 5.2, 5.10, 5.18, 5.26, 5.33, and 5.41). The sequence plots also show that the early parts of the shut-in periods were characterized by relatively large decreases in the packer-inflation pressure. The decreases in packer-inflation pressure were primarily due to packer compliance as the packers expanded during the initial inflation. Temperature may also have had a minor role in the initial packer-

inflation pressure decrease. The fluid-pressure increases during the shut-in periods of the test zones were often accelerated by pulse-injection tests in adjacent zones. This sympathetic response may have been due to a combination of packer compliance and the very low hydraulic conductivities of the rocks being tested. The pressure increases in the test zones in some cases caused pressure increases in the other zones. This effect was probably due to physical movement of the packers as the pressure increased in the test zones. The same effect was noted in some boreholes in response to increases in the packer-inflation pressure. Because of the low hydraulic conductivities of the units tested, these responses to pulse-injection and packer-inflation-pressure increases amounted to low-magnitude pressure pulses on the fluids in the test zones.

The extent and magnitude of these possible effects of packer compliance are unknown at this time. Some preliminary analysis indicates that the effects are important, but do not dominate the observed fluid-pressure responses in the test zones. Without additional testing as recommended in Section 6.2, these effects are not quantifiable.

The pulse-injection tests were analyzed using graph-theoretic-field-modeling (GTFM) techniques. The GTFM model can incorporate the effects of the pretest pressure histories of the test intervals into model simulations of the fluid-pressure response to the pulse injections. The simulations were compared to the observed test data. The analyses were performed in an iterative manner for ranges of hydraulic conductivity and apparent formation pressure to obtain a best-fit match of the model simulations and the observed data.

The GTFM analysis is based on the assumption that the formation pressure is constant over the length of the interval being tested and that no significant head gradient exists in the formation test interval. The decrease in formation pressure caused by the WHS has created a pressure-

drawdown cone that is likely approximately symmetric around the shaft and which extends to a presently unknown distance into the formation. The shape of that drawdown cone is not well defined and it can be assumed to be developed somewhat differently in materials with different hydrologic properties. The results from the pulse-injection tests at the 850-foot depth level indicate that the depressurization at this level extends far enough into the formation so that the formation pressure is apparently the same for all the test-zone responses simulated with GTFM. The depressurization profiles at all test levels, including the 850-foot level, were assumed to be at steady-state during the individual test periods. The assumption of a constant, average formation pressure over the length of the test zones adds additional uncertainty to the modeled results.

The test analyses presented in Section 5 vary from simulations with good matches between observed data and simulated results to those tests in which the observed data were not well matched by the simulations. With the exception of boreholes W782W and W1320E, the zone #1 responses in each borehole were relatively easier to match than the zone #2 and zone #3 tests. The most likely reason for this pattern is that because of the scheduled work activity in the WHS, sufficient time was not available after each pulse-injection test to allow a complete recovery and stabilization period before the next pulse-injection test. Increased elapsed time between tests can often result in data sets which more closely represent true formation responses and are more likely to be better simulated by model solutions.

Table 5.3 lists the magnitude of the pressure pulse injected into each test zone. The magnitude of the pulse indicates the pressure increase above the measured pressure immediately before the start of the pulse-injection sequence. According to Pickens and others (1987), the pressure at the start of a pulse-injection test must be substantially different from both the pretest pressure and the formation pressure to allow a

confident determination of hydraulic conductivity or permeability. In the tests conducted in the WHS boreholes, all the tests except those in borehole W1320E (see Section 5.6) and in the tests in zone #1 in W805SW and W805E achieved that objective.

The sequence plots of the test sequences (Figures 5.2, 5.10, 5.18, 5.26, 5.33 and 5.41) show that, according to the criteria presented in Pickens and others (1987), the pulse tests in zone #1 of W805SW and W805E, and all the tests in W1320E had less-than-adequate pressure pulses. The analyses and observed data for the W805E, W805SW, and W1320E tests indicate that actual formation pressures were not directly measured and the pressures were still building at the end of testing. Because of the slow response to shut in in zone #1 of W805SW, the pressure following the pulse was substantially higher than the pretest pressure, but substantially lower than the apparent formation pressure determined by the test analysis. In zone #1 in W805E, the pressure pulse was greater than the shut-in pressure at the time of testing, but slightly less than the apparent formation pressure. In zones #1 and #2 in W1320E, safety considerations, coupled with the lack of 0- to 2000-psig transducers necessary to monitor the elevated pressures at this depth, prevented raising the pressure to the greater than 500-psig pressure necessary to test these zones more accurately. The apparent formation pressures determined by the analysis for zones #1 and #2 in W1320E are probably lower than actual pressures. The progression in the apparent formation pressures from an underpressurized zone #3 near the shaft wall to increasingly higher pressures in zones #2 and #1 is probably representative of the actual progression in the magnitudes of formation pressures. However, testing limitations related to available time for testing and the pressure range of the pressure transducers prevented collection of a data set representative of actual in situ pressure conditions.

Table 5.3 summarizes the test results for all of the boreholes. Figure 6.1 is a graphic illustration of the formation-pressure profile. The data and the plots show that in each borehole there is a general lowering of pressure near the shaft wall at the test depths. The depressurization extends to about 1-1/2 shaft diameters at the 850 depth level. Apparent pressure communication between zones at the 782 depth level prevents, without further testing, determination of the pattern of depressurization at this level. Because the test-zone pressures were climbing at a significant rate at the end of testing in zone #1 at the 805 and 1320 depth levels, the observed test data appear to indicate that the actual formation pressures may increase to pressures approximating undisturbed, pre-shaft formation pressures at distances greater than one shaft diameter from the shaft. At both levels, however, the actual magnitude of that formation pressure cannot be determined from the available data.

The certainty of the formation-pressure estimates determined by the GTFM analysis of the borehole tests in the WHS is subject to inherent limitations. The tests were of relatively short duration considering the apparently low hydraulic conductivities of the formations tested. Also, many of the zones tested exhibited significant rates of pressure increase near the end of the testing periods after incomplete recovery to the pulse-injection tests. To estimate the reasonableness of the apparent formation pressures determined from the analysis of the WHS borehole tests, the formation-pressure estimates presented in Table 5.3 were compared to recent drill-stem tests of the Rustler Formation in well H-16 by Beauheim (1987; see also Stensrud and others, 1988). These tests indicate a formation pressure at the center of the Culebra, which is at 712.5 feet BGS at H-16 as compared to 718 feet BGS in the WHS, of approximately 160 psig; and a formation pressure at the center of the unnamed lower member of the Rustler, which is at 810 feet BGS in H-16, of approximately 260 psig. These pressures indicate a pressure gradient of

1.08 psi/ft which was used to estimate formation pressure for the upper three test horizons as follows:

Depth Level (feet BGS)	782	805	850
Estimated Pressure (psig)	230	250	300

Borehole tests conducted from holes drilled in the Salado Formation from rooms and drifts at the repository horizon (2130 feet BGS) indicate a formation pressure of 1200 to 1450 psig (Peterson and others, 1987). Comparing these estimated formation pressures to that estimated for the unnamed lower member (260 psig) indicates a pressure gradient of 0.71 to 0.90 psi/ft. Using these gradients, the formation pressure at the 1320 depth level is estimated to be 625 to 730 psig. Given the potential uncertainty of the formation-pressure estimates determined from the GTFM analyses, a comparison of the formation-pressure estimates from H-16 and from the GTFM analysis of the WHS borehole tests (Table 5.3 and Figure 6.1) indicates the following:

- The mudstone of the unnamed lower member at the 782 depth level appears to be depressurized at greater than one shaft diameter from the shaft wall. However, it could also be true that, because of the low hydraulic conductivity indicated for zone #1, a representative estimate of formation pressure was not possible.

- The siltstone of the unnamed lower member at the 805 depth level appears to have an undisturbed formation pressure at greater than one shaft diameter from the shaft wall.

- The formation pressure from zone #1 in borehole W1320E indicates that, at this depth, the Salado Formation may be slightly underpressurized at greater than one shaft diameter from the shaft wall. However, because the pressure was continuing to rise at the end of the zone #1 test period, the formation-pressure estimate of

550 psig probably underestimates the formation pressure of the Salado at this depth and the formation may not be underpressurized.

The source of the apparent underpressure observed in zone #1 at the 782 depth level is unclear. The pressures in zones #2 and #3 are similar and in the range of depressurization within one shaft diameter of the shaft wall as observed in the other boreholes tested. Examination of the sequence plot in Figure 5.2 shows that the pressure in zone #2 increased about 12 psi during the zone #1 pulse injection and the zone #2 pressure continued to rise for the remainder of the test. Zone #1 also increased about 30 psi during the zone #2 pulse injection. While packer compliance cannot be ruled out as the cause of these sympathetic pressure increases, the most likely cause of the apparent depressurization in zone #1 in borehole W782W is pressure communication around the packer, or through the formation. It is also possible that a local fracture near zone #1 intersects either the Culebra or the shaft-liner-to-formation contact where shaft-wall piezometers indicate pressures similar to the zone #1 test results.

At the 850-foot level, water and gas were observed flowing in the borehole. Here, the upper Salado appears to be depressurized to almost 2 shaft diameters from the shaft wall relative to the extrapolated formation pressure of approximately 300 psig. The pretest history period used for the analyses of the pulse-injection tests in W850SW includes the data on the pressure buildup due to water and gas inflow between the drilling and testing of that borehole (see Section 5.4). The amount of pressure buildup indicated by the pressure gage installed on the cap placed on borehole W850W after testing supports the conclusion that the 30- to 70-psig range of apparent formation pressures indicated by the analyses is appropriate for formation conditions at the time of testing. Therefore, the upper Salado appears to have been depressurized relative to the other geologic units tested. If the Rustler-Salado contact zone is relatively transmissive at this location, and if it has been draining

to the key of the shaft liner since its installation in 1984, this drainage could be the source of the depressurization. As indicated on Figure 6.2, pressure-transducer data from the WHS piezometer #211, installed at level 834 just above the Rustler-Salado contact, also appear to show depressurization relative to piezometers in the Culebra and at the 758 depth level in the unnamed lower member of the Rustler Formation. (The piezometer data reported in Bechtel (1986) are data from pressure transducers installed in the concrete liner of the WHS, to monitor any pressure buildup behind the liner. The transducer installations were originally called piezometers by the WIPP-site contractors. For a complete discussion of these pressure-transducer installations see Appendix G in Haug and others (1987).) The WHS-piezometer data support the assumption that depressurization has occurred in the area of the shaft key, although the exact mechanism for this depressurization is unclear.

Figure 6.2 provides a graphic illustration of the fluctuations in pressure and the degree of pressure communication at the shaft-liner-to-formation contact at various depth levels in the WHS. The data show that flutua- tions in pressure are greatest at the Culebra depth level, and that significant fluctuations also occur at level 758 in the unnamed lower member of the Rustler. Figure 6.2 also shows that some pressure fluctuations occur simultaneously at all levels. This pressure communication indicates either direct communication between the geologic units along the shaft-liner-to-formation contact, or pressure communication through fractures or cold joints in the concrete liner. The magnitude of the pressures recorded by the transducers also indicates the degree of depressurization existing at the various depth levels instrumented. As mentioned earlier, these data corroborate the results of the pulse-injection testing that show the most depressurization along the shaft-liner-to-formation contact has occurred near the Rustler-Salado contact zone in the key area of the concrete liner.

Figure 6.3 graphically illustrates the variation of the hydraulic-conductivity values determined by the borehole tests in the WHS both as a function of depth and as a function of distance from the shaft wall. Figure 6.3 shows that all rocks tested have low hydraulic conductivity. Most of the reported values range from 1.0×10^{-14} to 5.0×10^{-14} m/s, with only 4 values falling outside that range. In W850W, the borehole with actively flowing water, the analyses indicated a slightly higher hydraulic conductivity. Considering the test conditions and the uncertainty surrounding the packer-compliance effects of the test tool, the range of one order of magnitude in hydraulic conductivity indicates that, essentially, all the zones and geologic units tested have similar, and low hydraulic conductivities.

The zones tested did not appear to indicate any enhanced permeability near the shaft in test intervals that may have been affected by the excavation of the WHS. In W850W, however, the zone #3 test was unsuccessful because the test interval included either an open fracture or a discontinunity at the concrete liner-formation contact and could not be tested by pulse injection. Therefore, hydraulic conductivity for this zone is significantly higher than found in the other test zones of this and other boreholes. Inspection of the borehole indicated that the liner-formation contact is the most likely channel for the relief of pressure in zone #3 in W850W, and that high permeability is probably not representative of the formation in this portion of W850W.

Because of the design of the test tool, and the space requirements of the WHS conveyance system, the test tool could not be configured to test more of the near-shaft parts of the formation in the boreholes from 0.0 to 5.4 feet from the shaft wall. This situation limited the ability to test the shaft-liner-to-formation contact in many of the boreholes. However, examination of the cores recovered from the boreholes did not reveal any open fractures in the near-shaft-wall parts of the boreholes. The possible pressure communication in zone #1 in borehole W782W is probably,

if it exists in the formation, a local phenomenon at a greater distance from the shaft wall than could be expected from the influence of the excavation techniques. While no fractures attributable to drilling and blasting of the WHS were observed in the mudstones and halites in the tested boreholes, more brittle rocks such as the Magenta and Culebra dolomites could have experienced more construction-induced fracturing. However, the depth levels for testing were specifically chosen because of their significance in the plugging and sealing program, and not as part of a general WHS testing program, thus precluding testing of the Magenta and Culebra.

In summary, the following conclusions may be drawn from the permeability tests conducted in the boreholes drilled in the WHS:

1. The formation pressures determined by GTFM are uncertain because they were derived from relatively short tests in rocks with low hydraulic conductivity. The pressures can, therefore, be referred to as apparent formation pressures. Given the uncertainties as to their magnitudes, the results of all the test analyses nonetheless appear to indicate a pattern in which the formation pressures generally increase moving from the WHS into the formations. The near-shaft parts of the boreholes are probably depressurized because of the presence of atmospheric pressure in the shaft itself.

2. Considering the discussion in (1) concerning the magnitudes of the apparent formation pressures, these apparent formation pressures appear to increase with depth from land surface except where the tested formation has undergone significant depressurization, such as at the 850 depth level, and in the zones within one shaft diameter, as measured radially from the shaft wall.

3. The halite of the upper Salado at the 850 depth level has been depressurized relative to the test zones above it.

4. Water and gas were produced from either discrete fractures or the concrete-liner-to-formation contact in both boreholes at the 850 depth level. A small amount of water was produced from one of the boreholes at the 805 depth level.

5. The hydraulic conductivities of the mudstone, claystone, and evaporite beds are low and range from 6.0×10^{-15} to 1.0×10^{-13} m/s. A potentially important but not well understood factor concerning the uncertainties of the hydraulic-conductivity determinations is the effect of compliance of the multipacker test tool on the fluid-pressure responses measured during testing.

6. No direct evidence of fracturing due to the excavation techniques used in constructing the WHS was observed in the cores of the mudstone and claystone of the lower unnamed member, or in the bedded halite and other evaporite layers of the Salado Formation.

6.2 Recommendations

Two important recommendations are suggested from the results of the permeability-testing program conducted in the WHS at the WIPP site:

1. The design and function of the multipacker test tool should be thoroughly reviewed to determine whether or not design modifications are warranted. In particular, the effect of packer compliance on test results needs to be thoroughly evaluated in order to better understand and interpret the fluid-pressure responses obeserved during testing. In conjunction with the testing of the multipacker test tool, each packer in the inflation system should be configured to allow their pressures to be individually measured. The individual pressure measurements would aid in determining the degree and influence of equipment compliance and any apparent test-zone to test-zone communication.

2. More time should be allowed to conduct each test. This extra time should be used to:

a) allow packer-inflation pressures to stabilize for a longer period before the initial shut in;

b) allow a closer approach to formation pressures during the initial buildup period following initial shut in;

c) allow a longer recovery period for each test so as to more closely approach formation pressure in the test zone, and pressure stabilization in adjacent zones;

d) repeat tests when necessary, especially when pressure communication between test zones is indicated; and

e) shift the position of the multipacker test tool, if necessary, to include areas closer to the shaft wall, or areas where fractures are suspected to cause pressure communication.

If possible, future test programs could also include testing of the Culebra and Magenta dolomites in boreholes drilled from a shaft. By testing formations whose hydraulic properties are already well defined at other nearby locations, more confidence could be placed on both the testing and analysis methodologies.

7.0 REFERENCES

Bechtel National Inc., 1985. Quarterly Geotechnical Field Data Report. U.S. Department of Energy, Waste Isolation Pilot Plant Office, Carlsbad, New Mexico, DOE-WIPP-218.

Bechtel National, Inc. 1986. Interim Geotechnical Field Data Report, Fall 1986. U.S. Department of Energy, Waste Isolation Pilot Plant Project Office, Carlsbad, New Mexico, DOE-WIPP 86-012.

Bredehoeft, J.D. and S.S. Papadopulos, 1980. A Method for Determining the Hydraulic Properties of Tight Formations. Water Resources Research, Vol. 16, No. 1, p. 233-238.

Earlougher, R.C., Jr., 1977. Advances in Well Test Analysis. Soc. Petroleum Engineers of AIME, Monograph Volume of the Henry L. Doherty Series, 264 p.

Haug, A., V.A. Kelley, A.M. LaVenue, and J.F. Pickens, 1987. Modeling of Ground-Water Flow in the Culebra Dolomite at the Waste Isolation Pilot Plant (WIPP) Site: Interim Report. Sandia National Laboratories, Contractor Report SAND86-7167.

Krieg, R.D., 1984. Reference Stratigraphy and Rock Properties for the Waste-Isolation Pilot Plant (WIPP) Project. Sandia Report SAND83-1908, 57 p.

Peterson, E.W., P.L. Lagus, and K. Lie, 1987. WIPP Horizon Free Field Fluid Transport Characteristics. Sandia National Laboratorties, Contractor Report 87-7164.

Pickens, J.F., G.E. Grisak, J.D. Avis, D.W. Belanger, and M. Thury, 1987. Analysis and Interpretation of Borehole Hydraulic Tests in Deep Boreholes: Principles, Model Development, and Applications. Water Resources Research, Vol. 23, No. 7, p. 1341-1375.

Savage, G.J. and H.K. Kesavan, 1979. The Graphic Theoretic Field Model, I, Modelling and Formulations. Journal of the Franklin Institute, Vol. 307, p. 107-147.

Stensrud, W.A., M.A. Bame, T.L. Cauffman, K.D. Lantz, J.B. Palmer, and G.J. Saulnier, Jr., 1988. WIPP Hydrology Program, Waste Isolation Pilot Plant, Southeastern New Mexico, Hydrologic Data Report #6. Sandia National Laboratories, Contractor Report SAND87-7166.

Stormont, J.C., 1984. Plugging and Sealing Program for the Waste Isolation Pilot Plant (WIPP). Sandia National Laboratories, Sandia Report SAND84-1057.

Touloukian, Y.S., W.R. Judd, and R.F. Roy, 1981. Physical Properties of Rocks and Minerals. McGraw-Hill/Cindas Data Series on Material Properties, Y.S. Touloukian and C.Y. Ho, Editors, Volume II-2, 548 p.

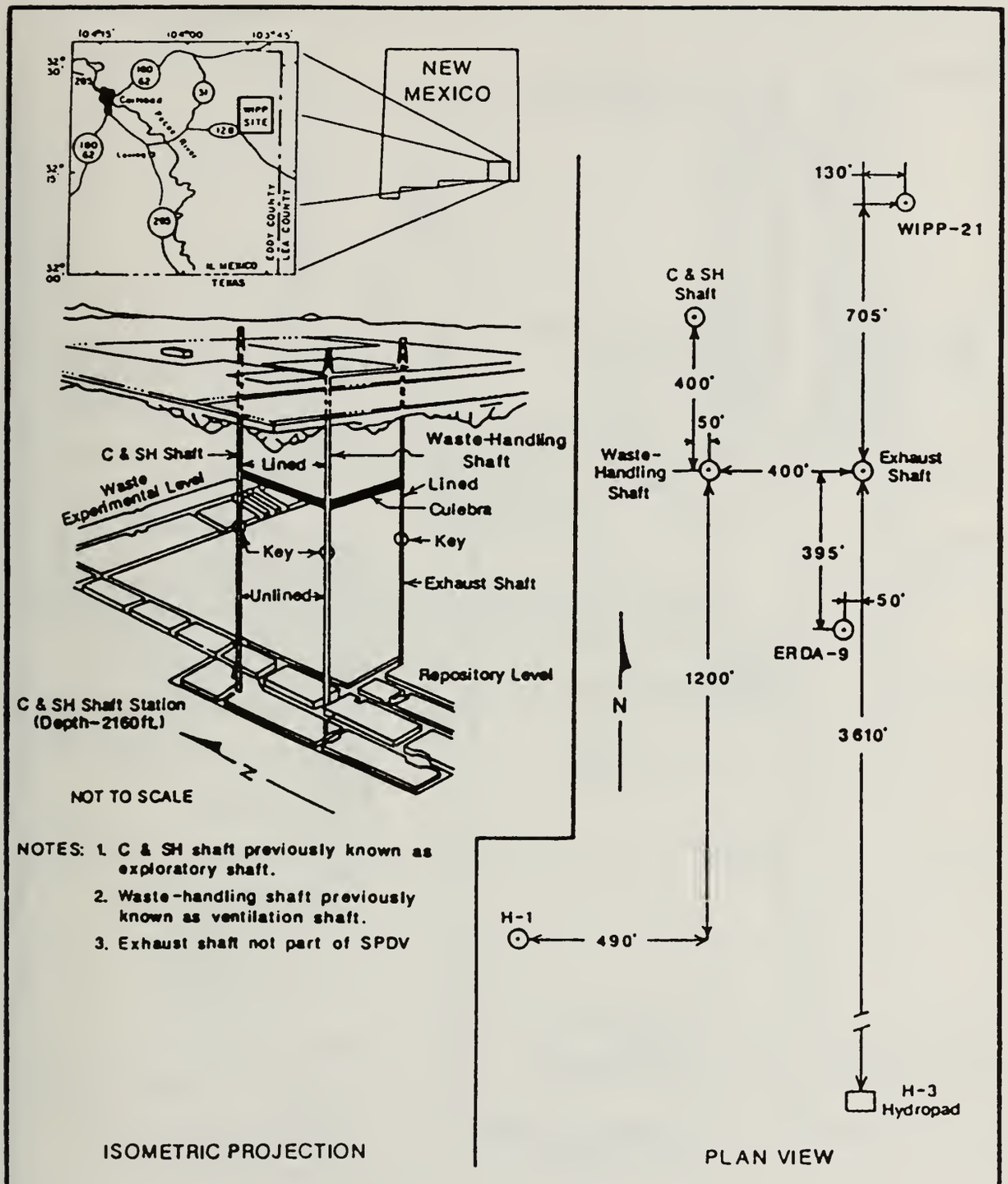

NOTES:
1. C & SH shaft previously known as exploratory shaft.
2. Waste-handling shaft previously known as ventilation shaft.
3. Exhaust shaft not part of SPDV

Drawn by	Date
Checked by	Date
Revisions	Date
H09700K570	

Locations of the Shafts at the WIPP Site
(Modified from Bechtel, 1985)

INTERA Technologies

Figure 1.1

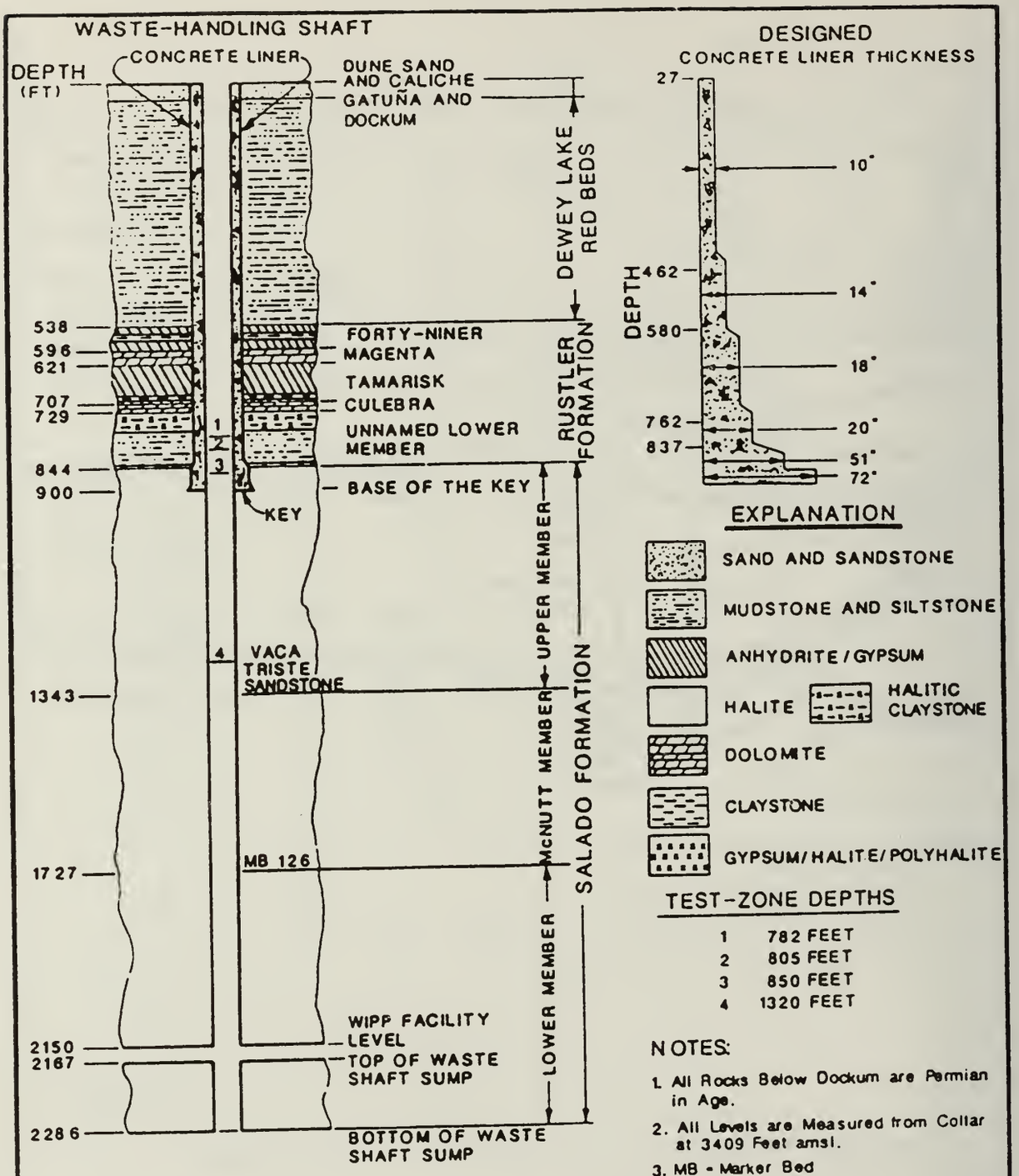

Modified from Bechtel National, Inc. (1985)

Drawn by	Date
Checked by	Date
Revisions	Date
H09700R570	

Generalized Stratigraphy in the Waste-Handling Shaft Showing the Test Zones and the Concrete-Liner Thickness Profile

INTERA Technologies

Figure 1.2

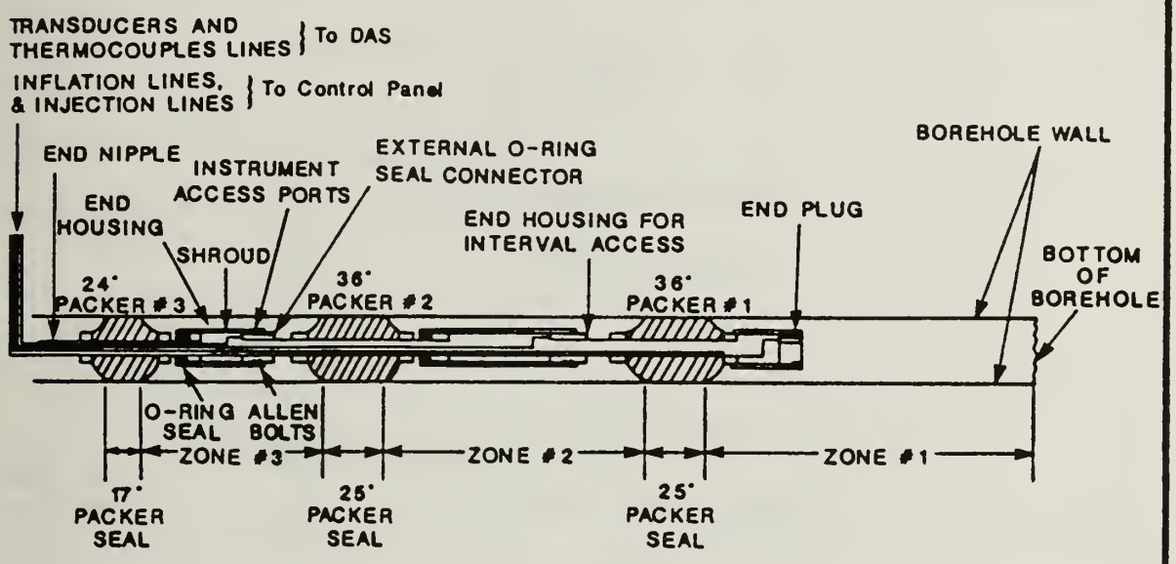

Drawn by	Date
Checked by	Date
Revisions	Date
H09700R570	

Multipacker Test Tool Configured With 3 Packers for Pulse-Injection Testing in the Boreholes Drilled in the Waste-Handling Shaft

INTERA Technologies

Figure 2.1

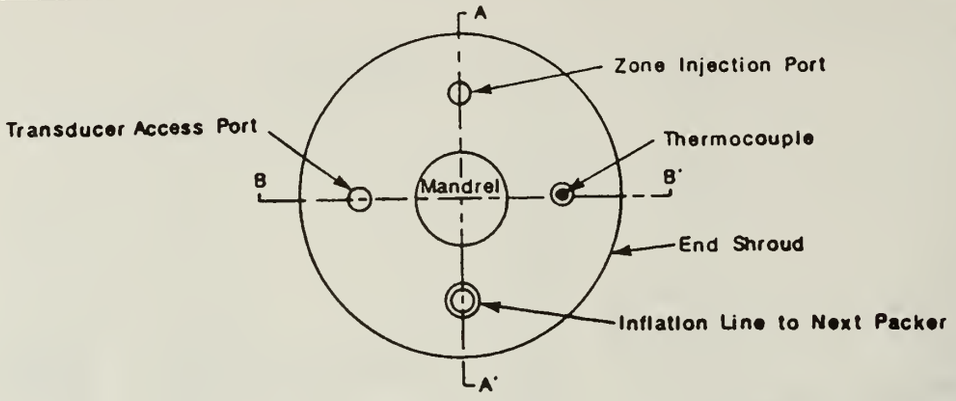

Section A-A'

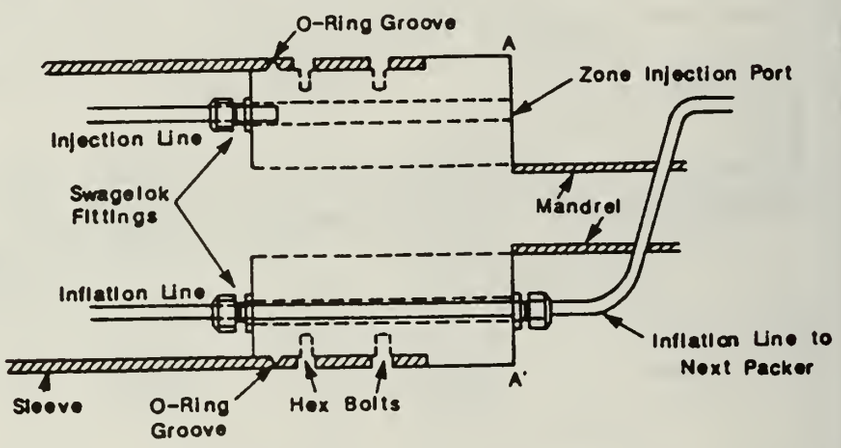

Section B-B'

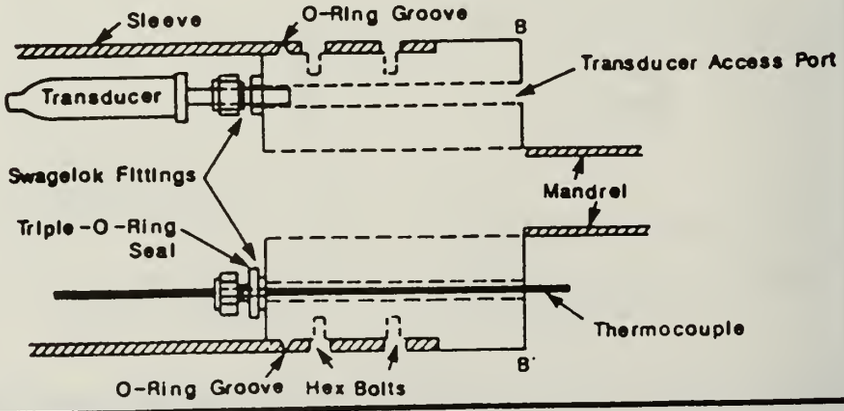

Drawn by	Date
Checked by	Date
Revisions	Date
h09700k570	

Spacer/Shroud End Showing Sensor Access to the Test Zones

INTERA Technologies

Figure 2.2

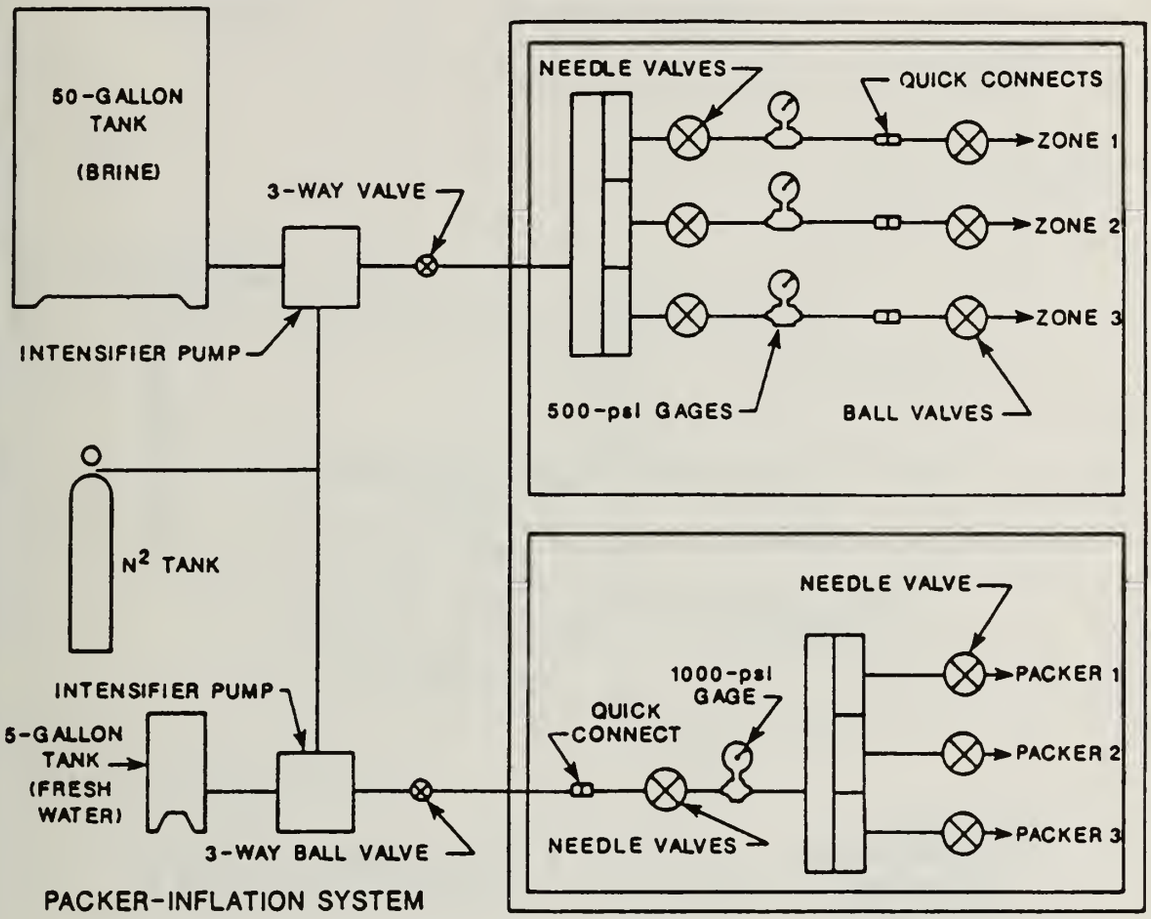

Drawn by	Date	Test Tool Control Panel
Checked by	Date	
Revisions G.S.	Date 6/17/88	
H09700R570		
INTERA Technologies		Figure 2.3

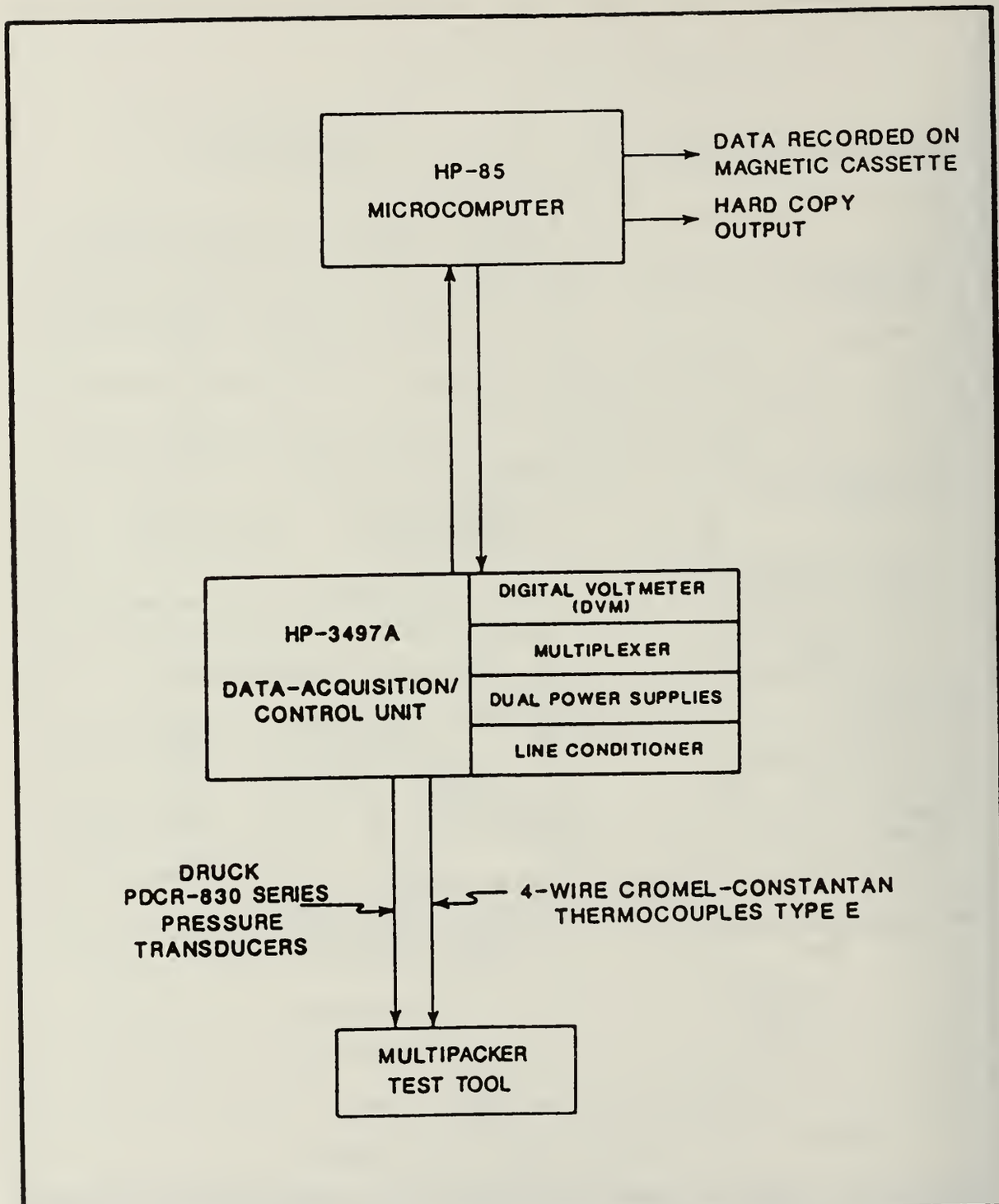

Drawn by	Date
Checked by	Date
Revisions	Date
H09700R570	

Schematic Illustration of the Data-Acquisition System (DAS)

INTERA Technologies

Figure 2.4

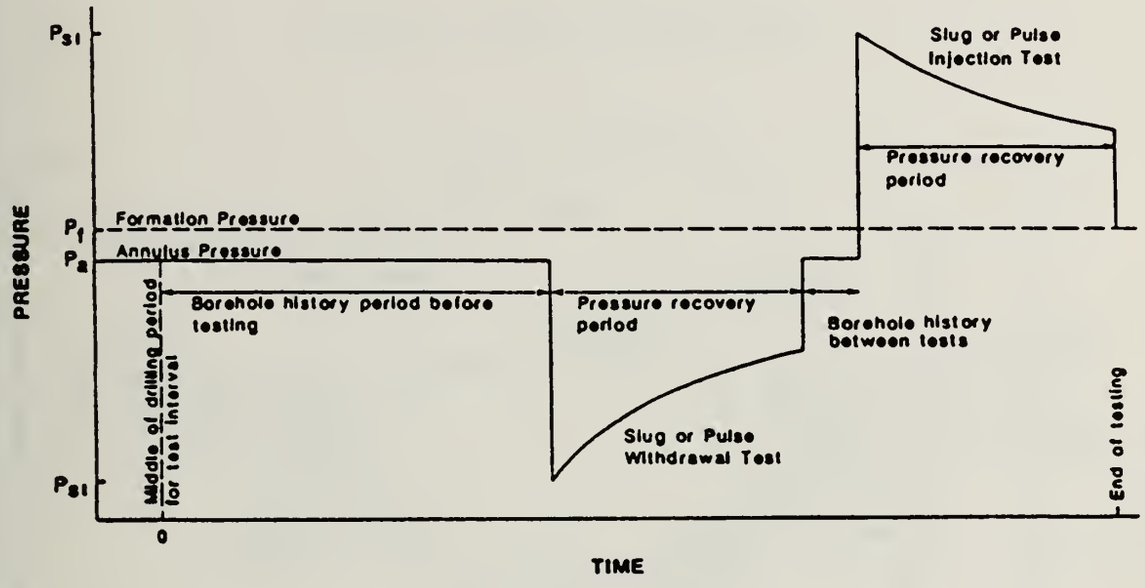

P_f = Formation Pressure

P_{s1} = Pulse or Slug Pressure

Drawn by	Date
Checked by	Date
Revisions	Date
H09700R570	

Schematic Illustration of the Borehole Pressure History that Develops During a Testing Sequence

INTERA Technologies

Figure 3.1

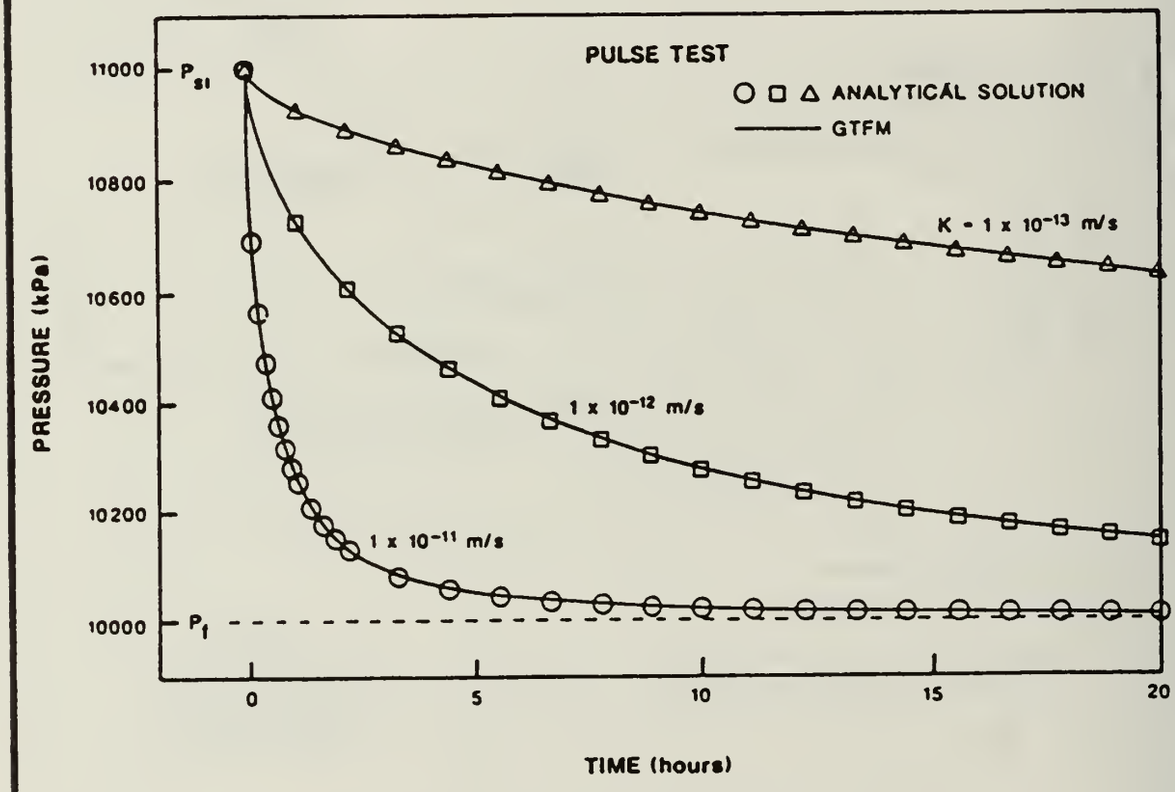

P_f - Formation Pressure

P_{si} - Pulse Pressure

Drawn by	Date
Checked by	Date
Revisions	Date
H09700R570	

Comparison Between GTFM and Bredehoeft and Papadopulos (1980) Analytical Solution Results

INTERA Technologies

Figure 3.2

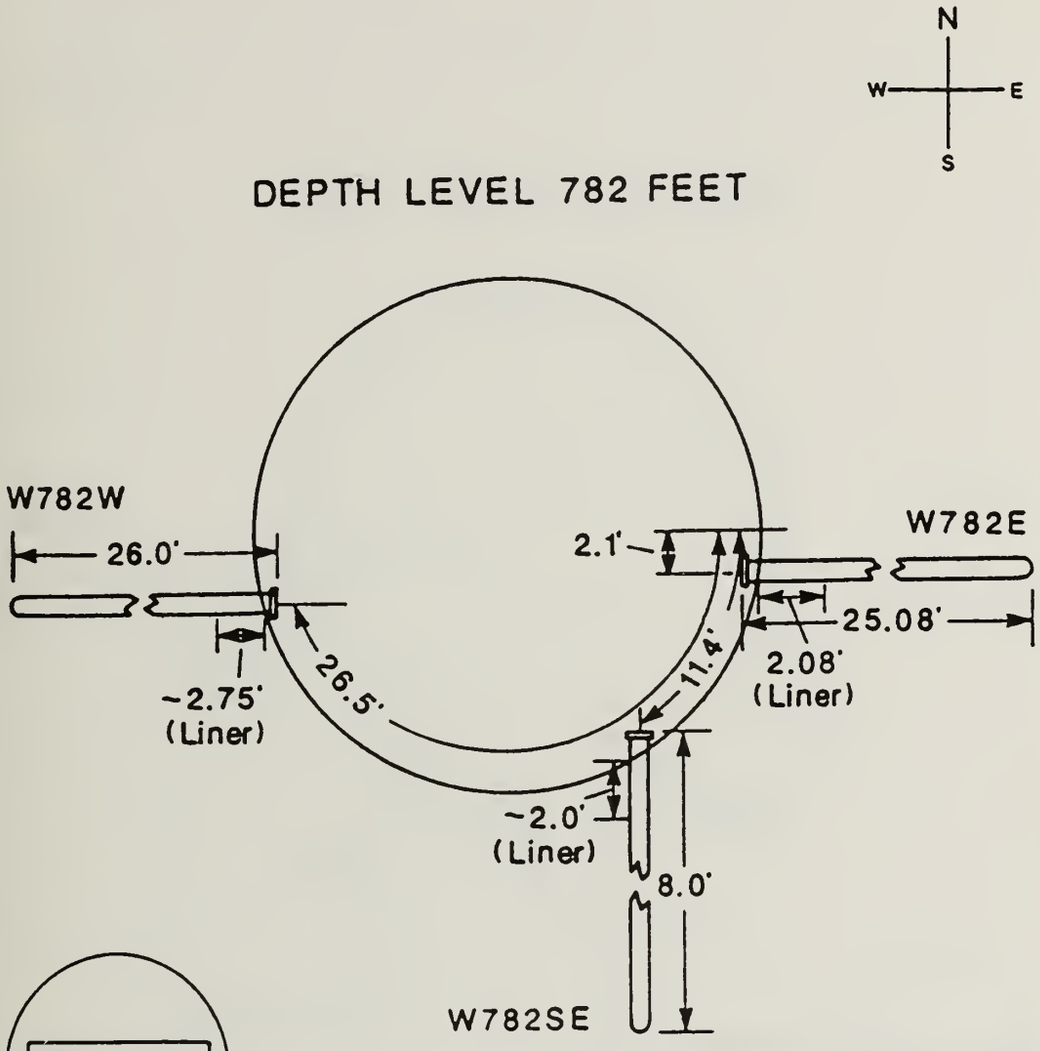

SHAFT ORIENTATION
SHOWING WHS CONVEYANCE-
SYSTEM ELEVATOR

NOTE: Not to Scale

Drawn by	Date	Locations and Orientations of Boreholes Drilled at the 782-Foot Level in the Waste-Handling Shaft
Checked by	Date	
Revisions	Date	
H09700R570		
INTERA Technologies		Figure 4.1

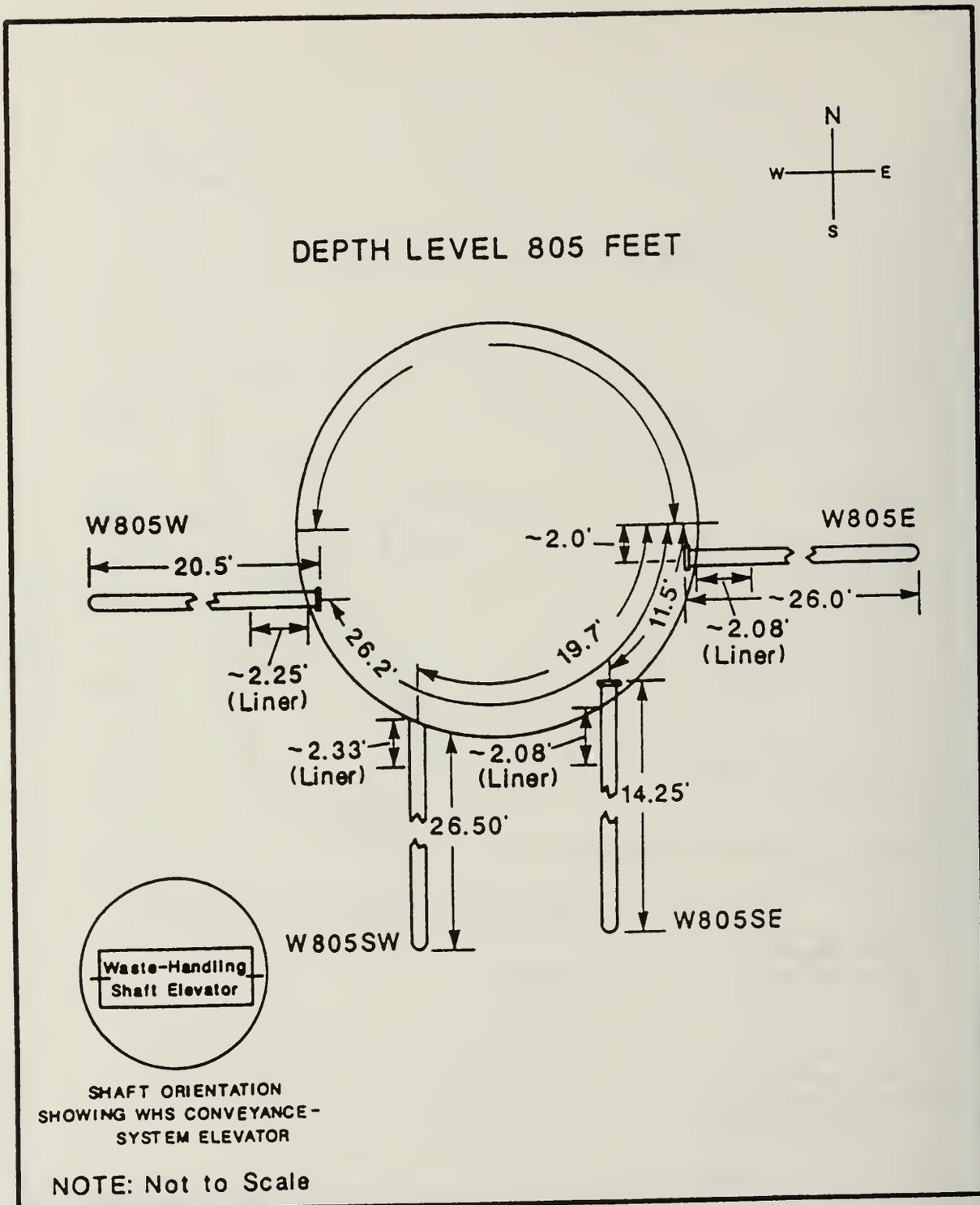

Drawn by	Date
Checked by	Date
Revisions	Date
H09700R570	

Locations and Orientations of Boreholes Drilled at the 805-Foot Level in the Waste-Handling Shaft

INTERA Technologies

Figure 4.2

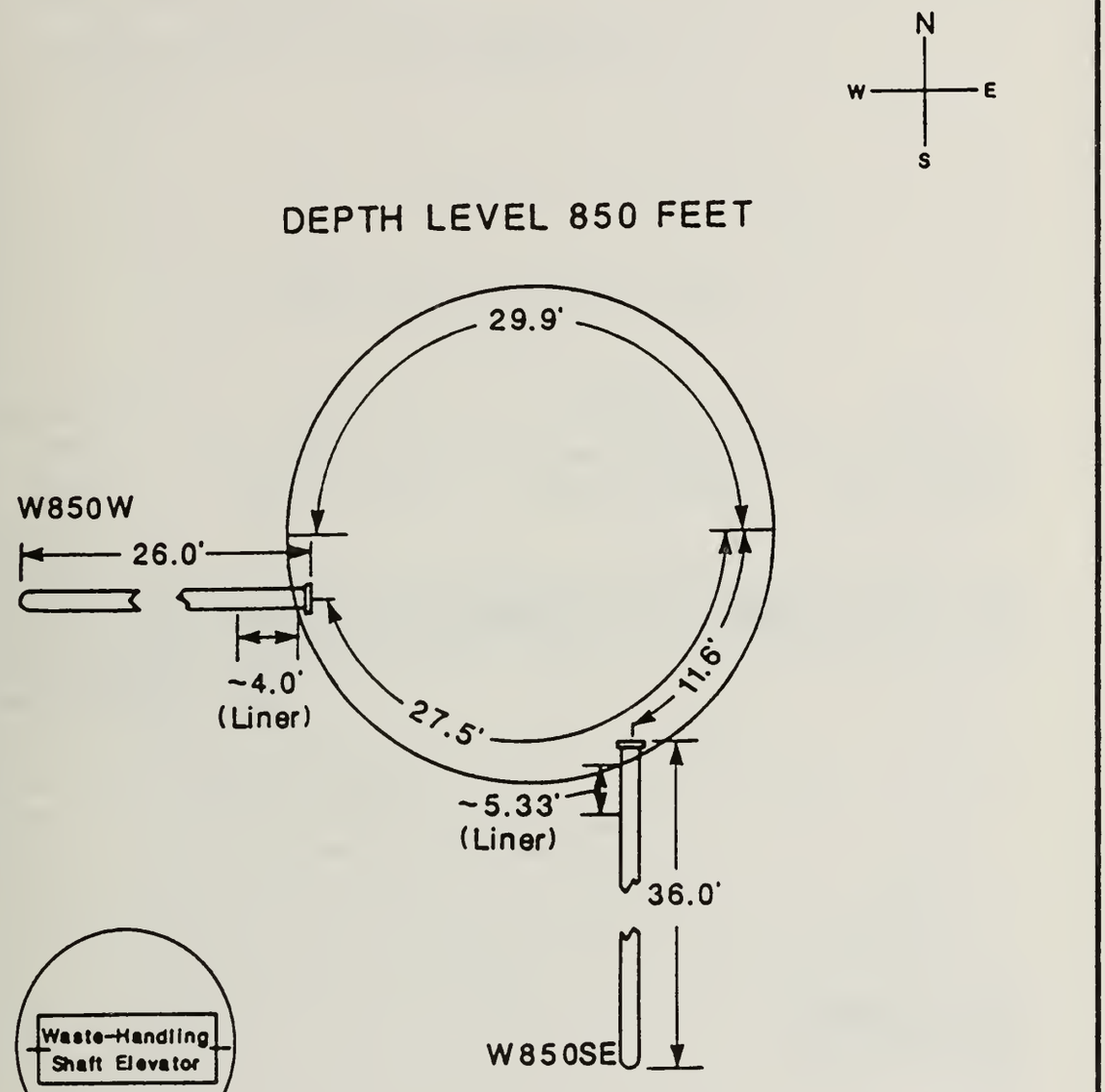

SHAFT ORIENTATION
SHOWING WHS CONVEYANCE-
SYSTEM ELEVATOR

NOTE: Not to Scale

Drawn by	Date
Checked by	Date
Revisions	Date
H09700R570	

Locations and Orientations of Boreholes Drilled at the 850-Foot Level in the Waste-Handling Shaft

INTERA Technologies

Figure 4.3

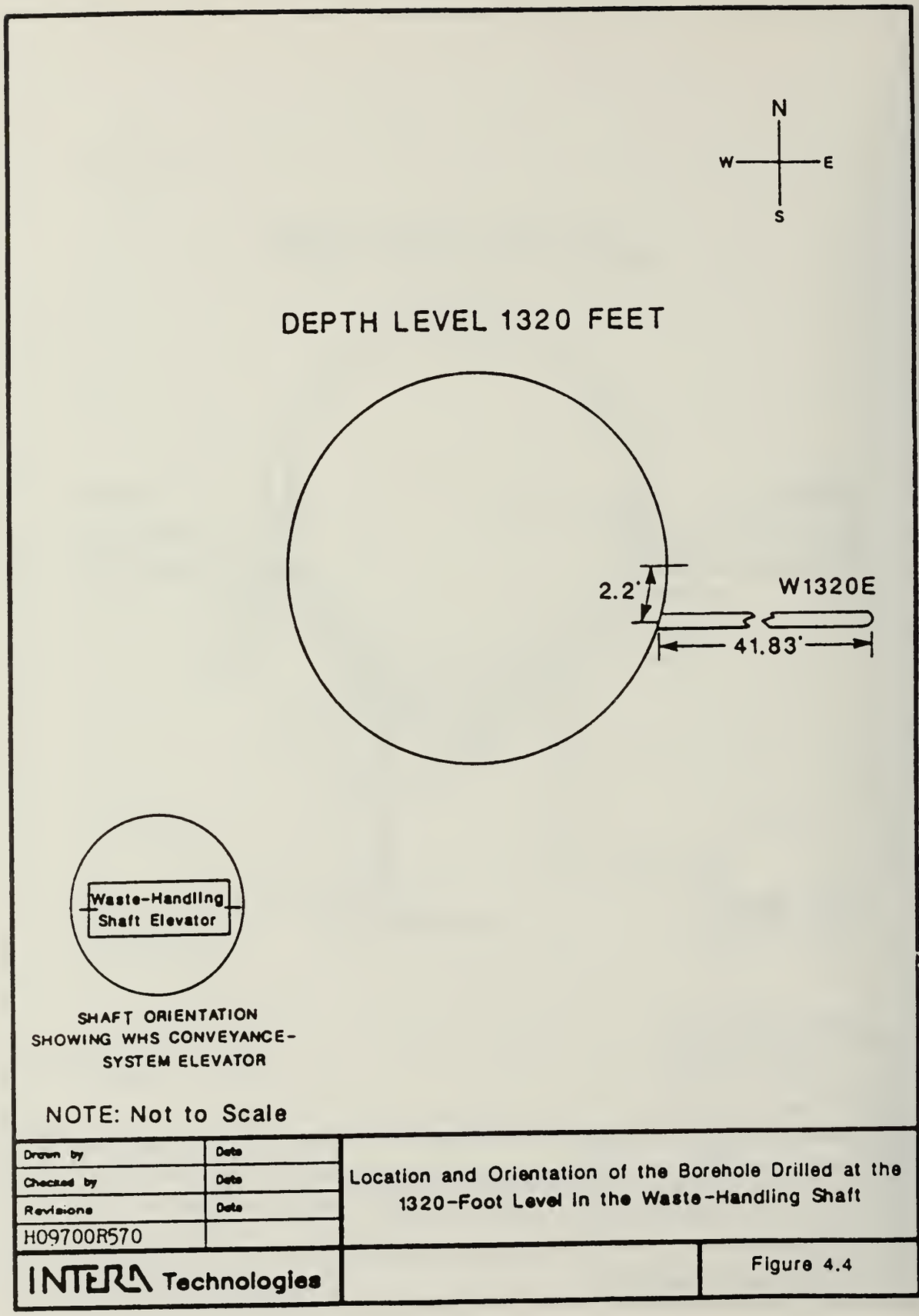

SHAFT ORIENTATION
SHOWING WHS CONVEYANCE-
SYSTEM ELEVATOR

NOTE: Not to Scale

Drawn by	Date
Checked by	Date
Revisions	Date
H09700R570	

Location and Orientation of the Borehole Drilled at the 1320-Foot Level in the Waste-Handling Shaft

INTERA Technologies

Figure 4.4

SHAFT LEVEL: 782 feet BGS

BOREHOLE LOCATION: W782W (West Wall)

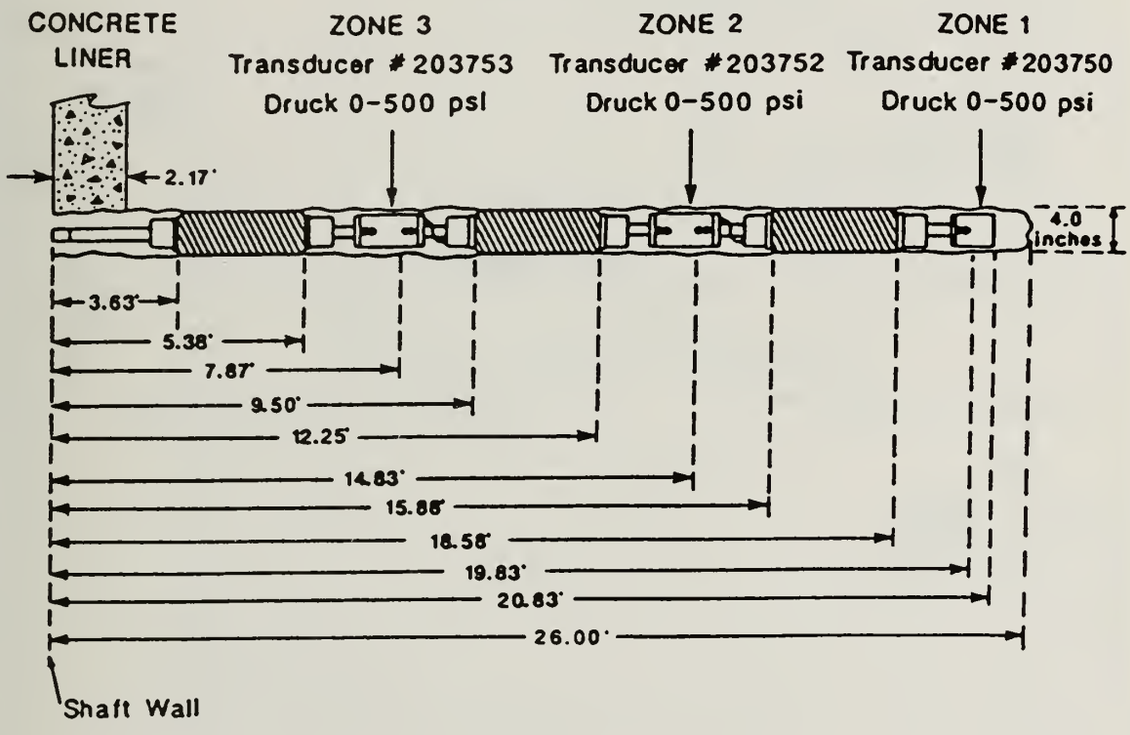

Drawn by	Date	Configuration of the Multipacker Test Tool in Borehole W782W	
Checked by	Date		
Revisions	Date		
H09700R570			
INTERA Technologies			Figure 5.1

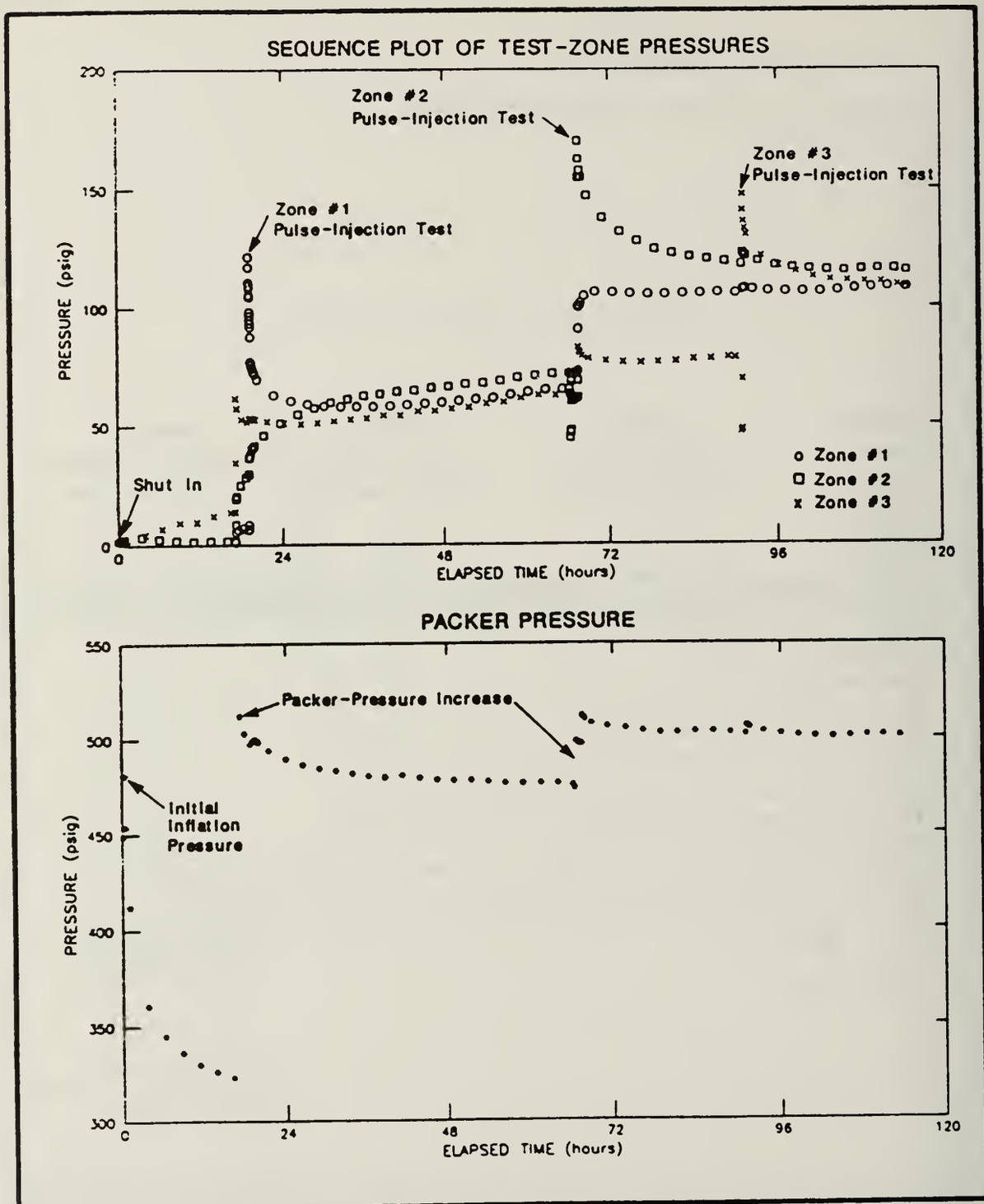

Drawn by	Date
Checked by	Date
Revisions	Date
H09700R570	

Linear-Linear Sequence Plot of the Test-Zone and Packer-Inflation Pressures During Testing in Borehole W782W

INTERA Technologies

Figure 5.2

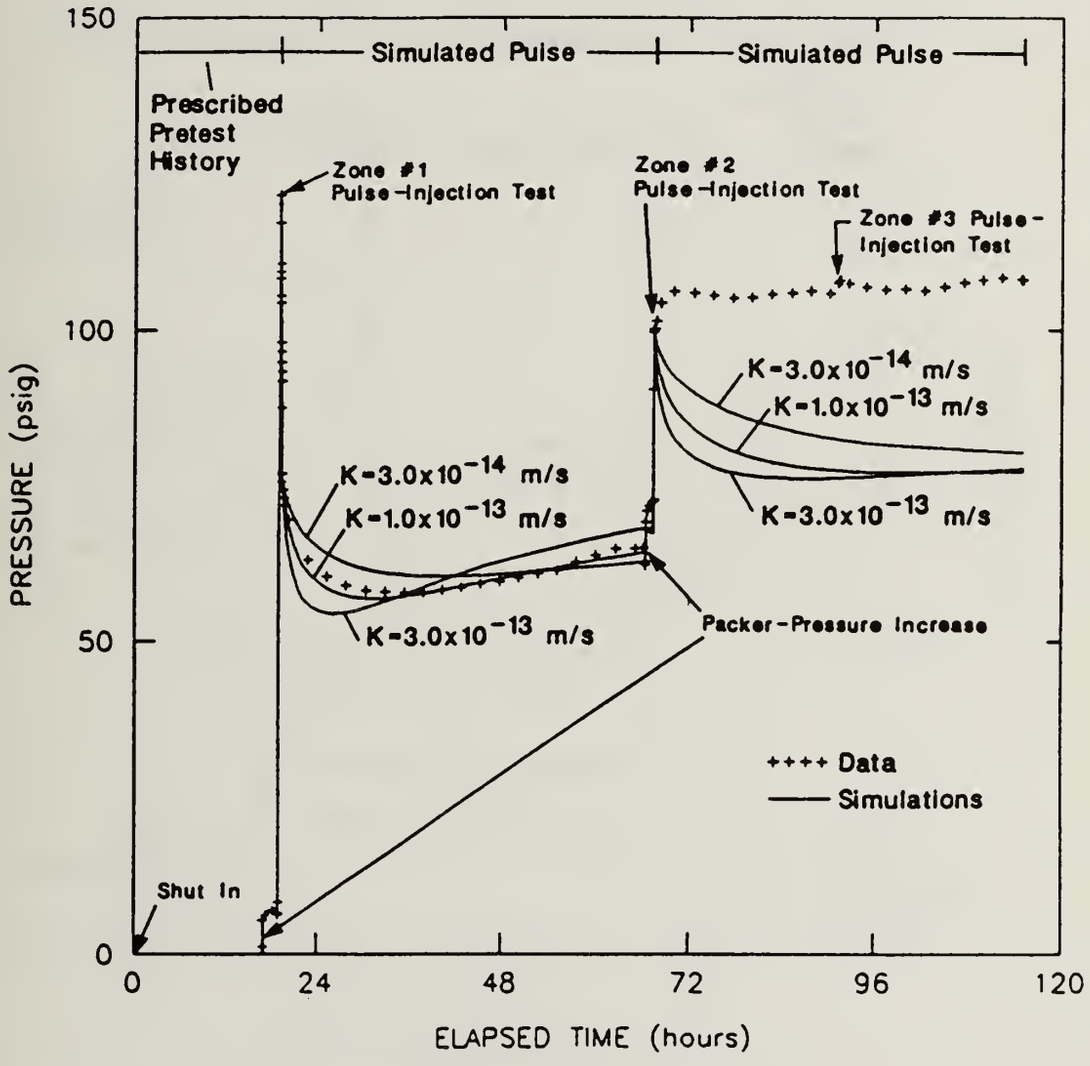

Drawn by	Date	Simulation of the Borehole W782W Zone #1 Pulse-Injection Test; Formation Pressure - 90 psig and Varying Hydraulic Conductivity
Checked by	Date	
Revisions	Date	
H09700R570		
INTERA Technologies		Figure 5.3

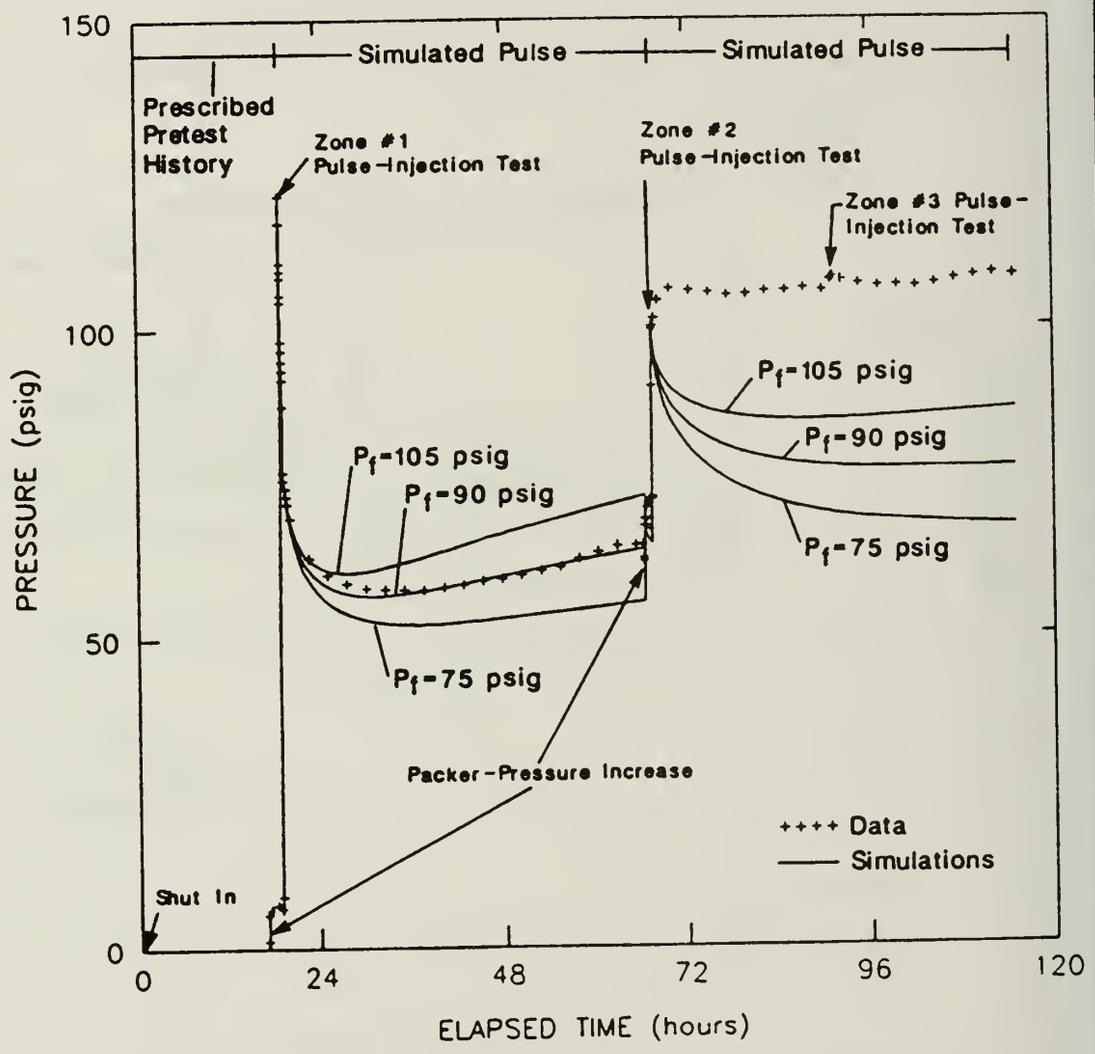

Drawn by	Date
Checked by	Date
Revisions	Date
H:09700R570	

-- Simulation of the Borehole W782W Zone #1 Pulse-Injection Test; Hydraulic Conductivity = 1.0 x 10^{-13} m/s and Varying Formation Pressure

INTERA Technologies

Figure 5.4

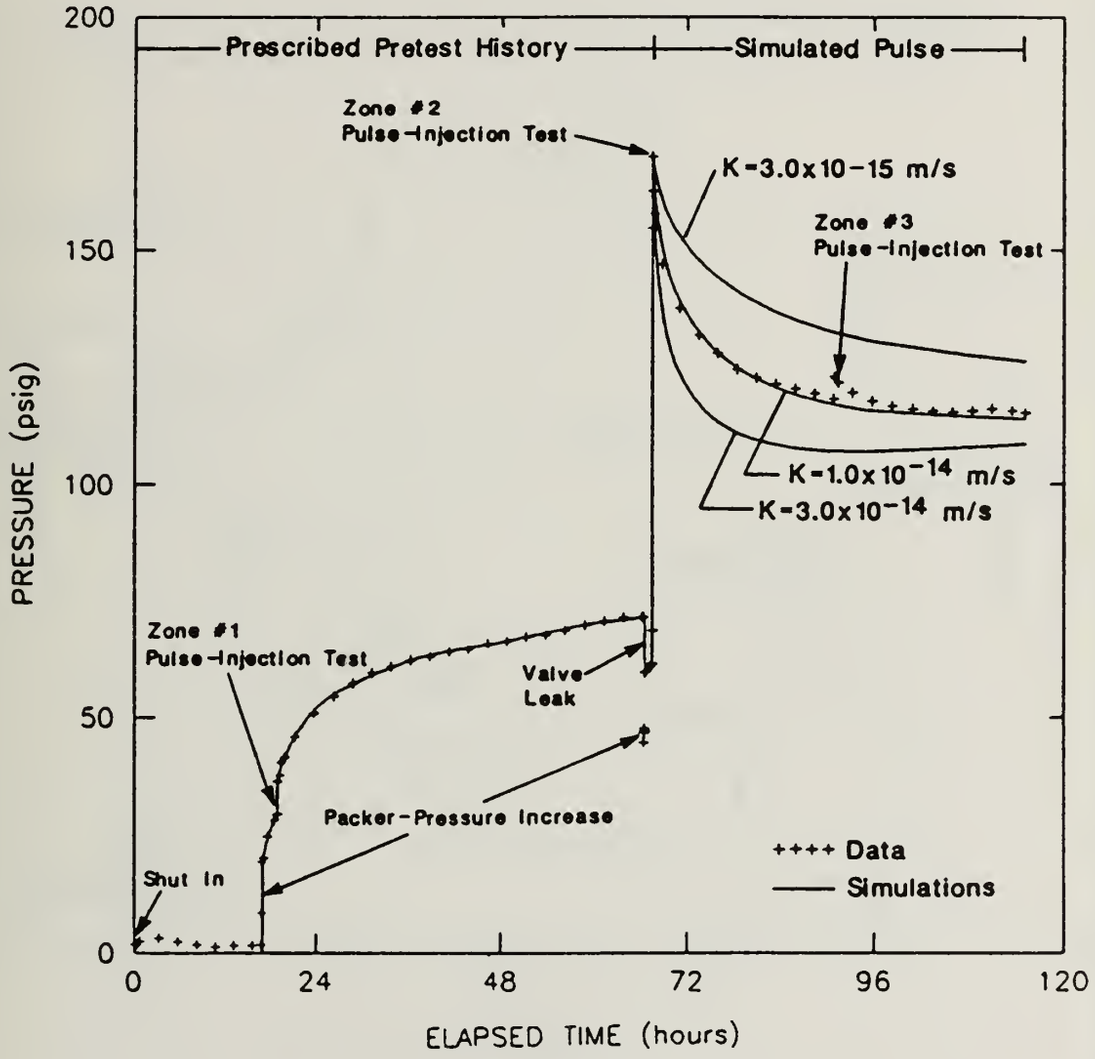

Drawn by	Date	Simulation of the Borehole W782W Zone #2 Pulse-Injection Test; Formation Pressure = 140 psig and Varying Hydraulic Conductivity
Checked by	Date	
Revisions	Date	
H09700K570		
INTERA Technologies		Figure 5.5

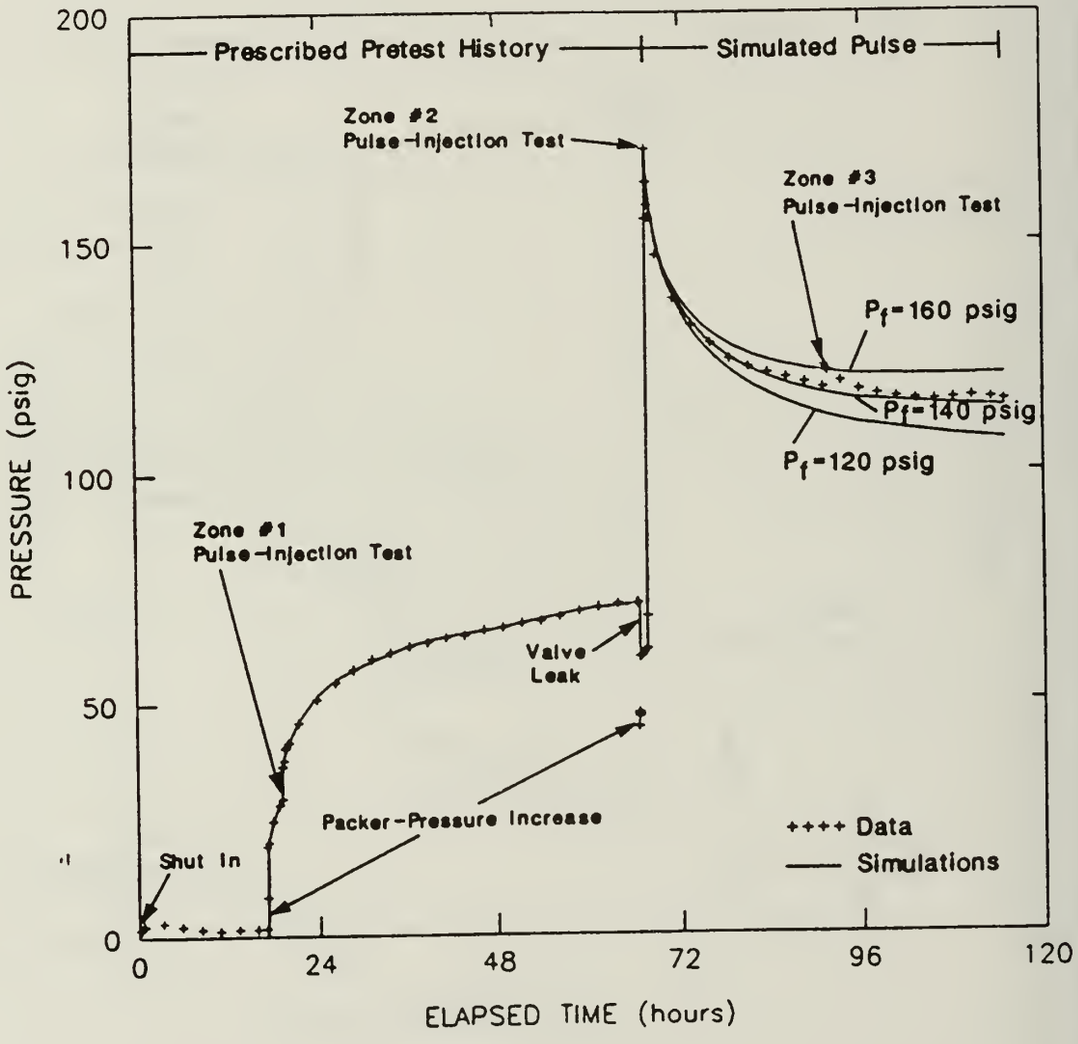

Drawn by	Date
Checked by	Date
Revisions	Date
H09700R570	

Simulation of the Borehole W782W Zone #2 Pulse-Injection Test; Hydraulic Conductivity - 1.0 x 10^{-14} m/s and Varying Formation Pressure

INTERA Technologies

Figure 5.6

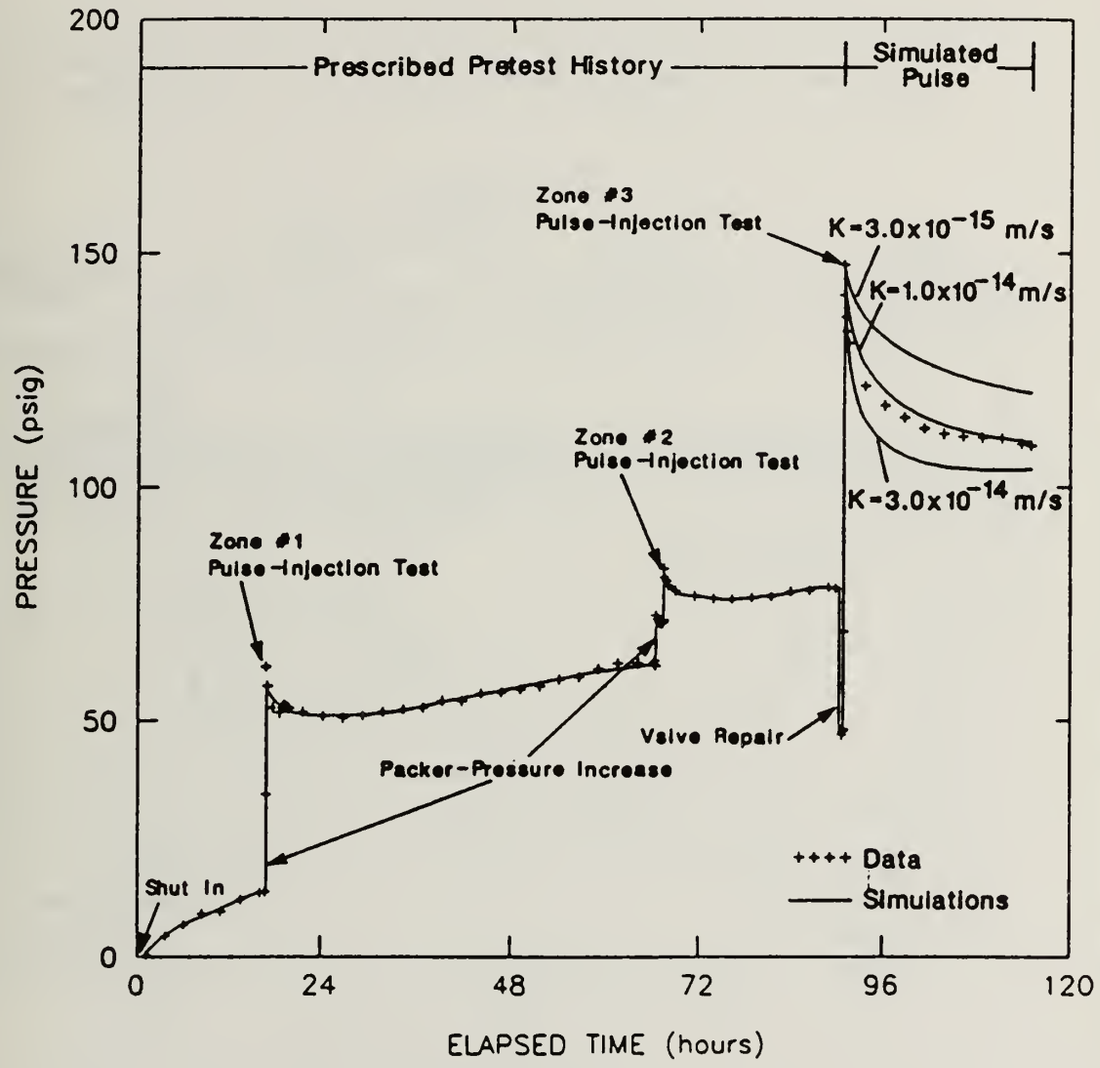

Drawn by	Date	Simulation of the Borehole W782W Zone #3 Pulse-Injection Test; Formation Pressure = 140 psig and Varying Hydraulic Conductivity
Checked by	Date	
Revisions	Date	
H09700R570		
INTERA Technologies		Figure 5.7

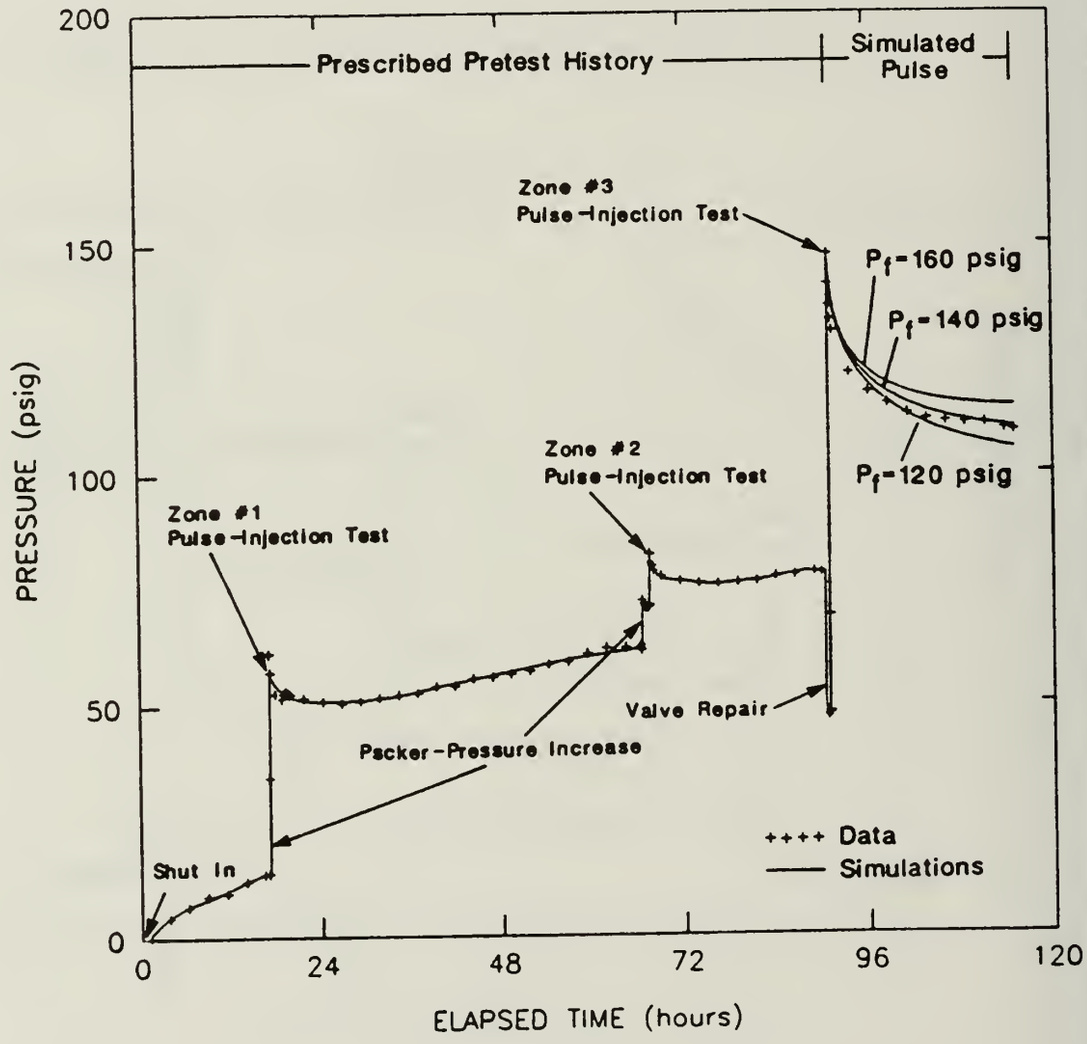

Drawn by	Date	Simulation of the Borehole W782W Zone #3 Pulse-Injection Test; Hydraulic Conductivity = 1.0×10^{-14} m/s and Varying Formation Pressure
Checked by	Date	
Revisions	Date	
H:09700R570		
INTERA Technologies		Figure 5.8

SHAFT LEVEL: 805 feet BGS

BOREHOLE LOCATION: W805E (East Wall)

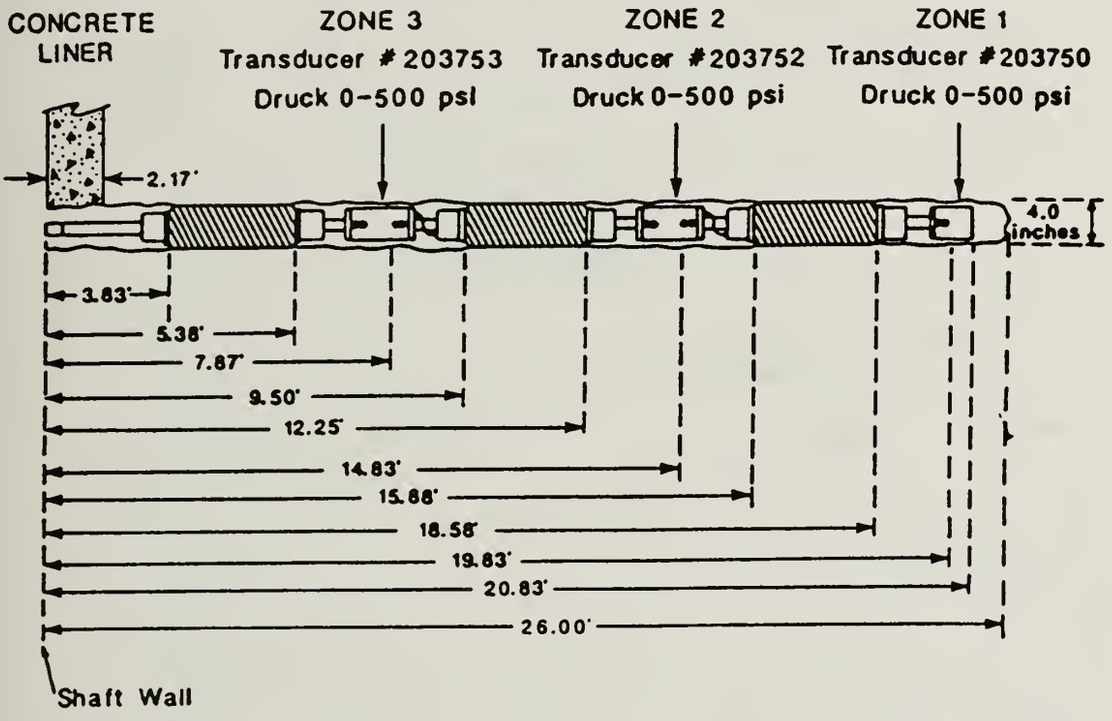

Drawn by	Date	Configuration of the Multipacker Test Tool in Borehole W805E
Checked by	Date	
Revisions	Date	
1109700R570		
INTERA Technologies		Figure 5.9

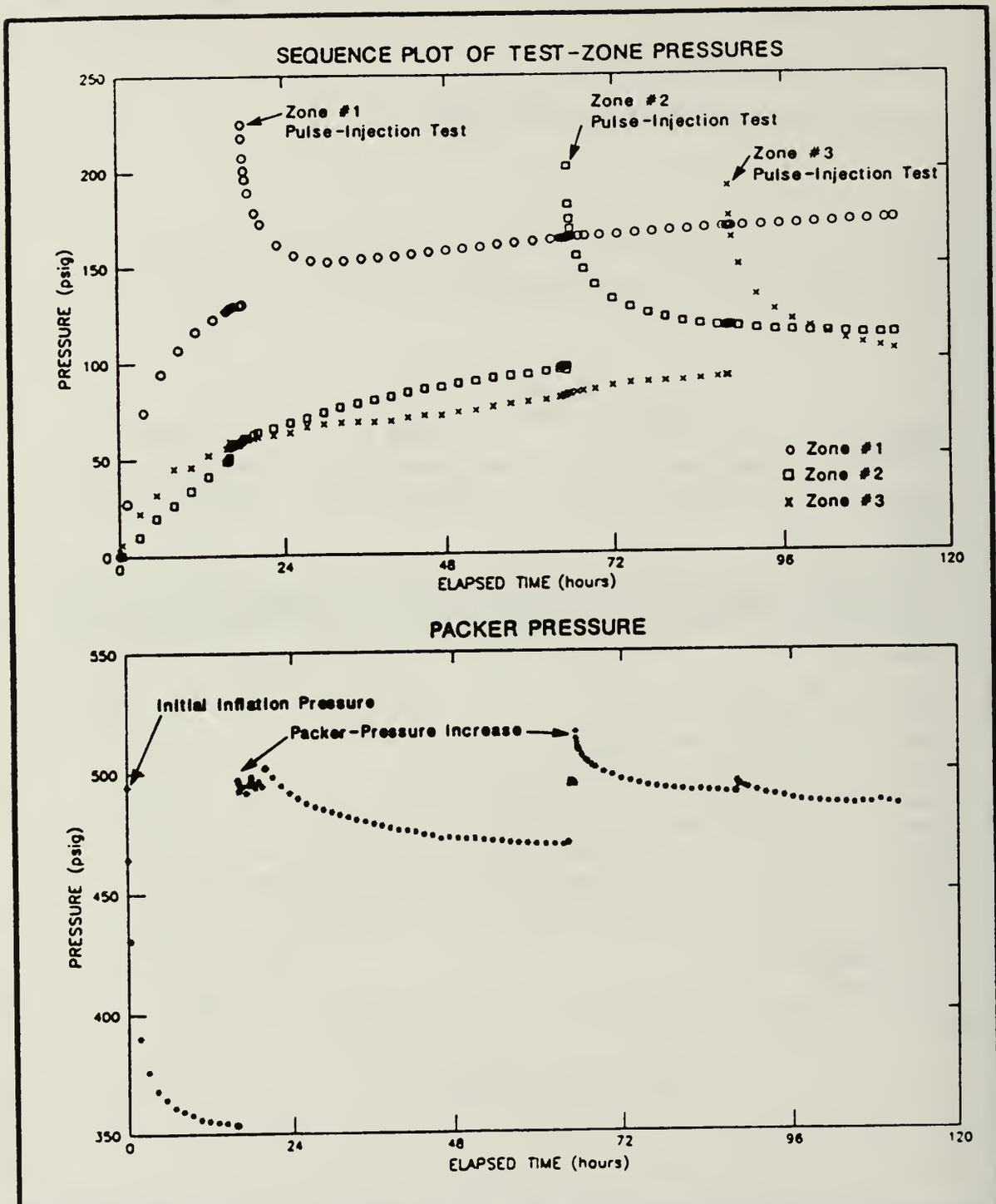

Drawn by	Date
Checked by	Date
Revisions	Date
MC9700K570	

Linear-Linear Sequence Plot of the Test-Zone and Packer-Inflation Pressures During Testing in Borehole W805E

INTERA Technologies

Figure 5.10

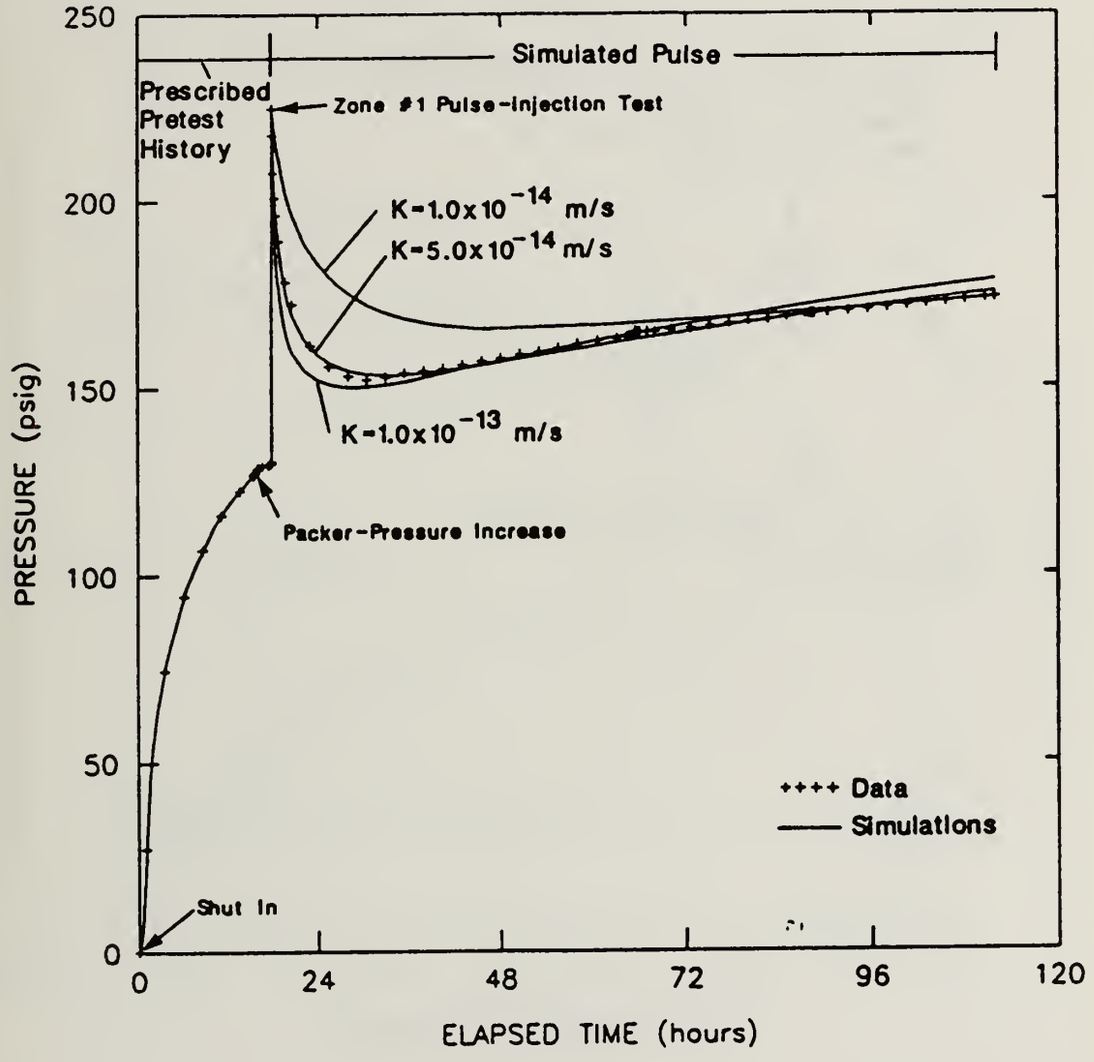

Drawn by	Date
Checked by	Date
Revisions	Date
H09700R570	

Simulation of the Borehole W805E Zone #1 Pulse-Injection Test; Formation Pressure = 225 psig and Varying Hydraulic Conductivity

INTERA Technologies

Figure 5.11

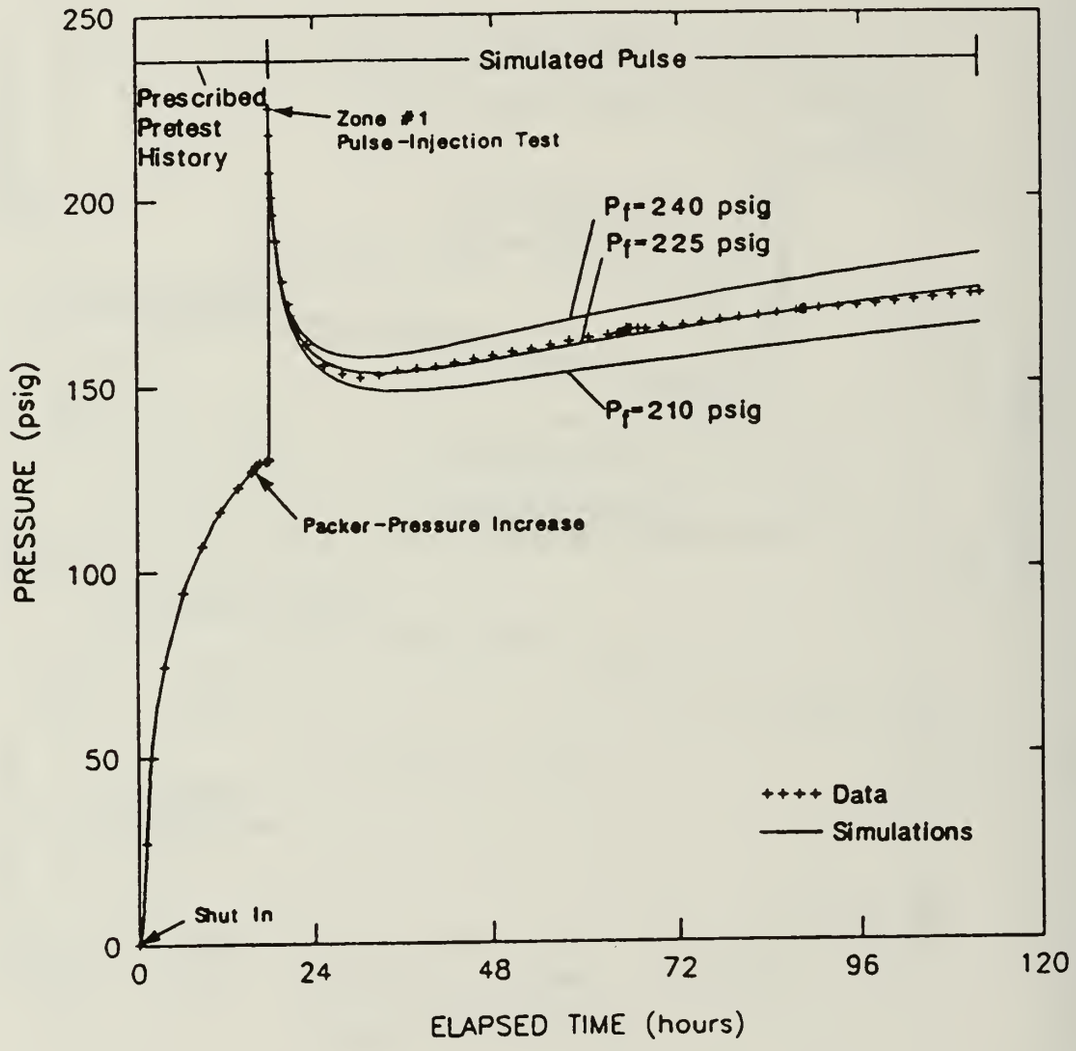

Drawn by	Date	Simulation of the Borehole W805E Zone #1 Pulse-Injection Test; Hydraulic Conductivity = 5.0×10^{-14} m/s and Varying Formation Pressure
Checked by	Date	
Revisions	Date	
H09700R570		
INTERA Technologies		Figure 5.12

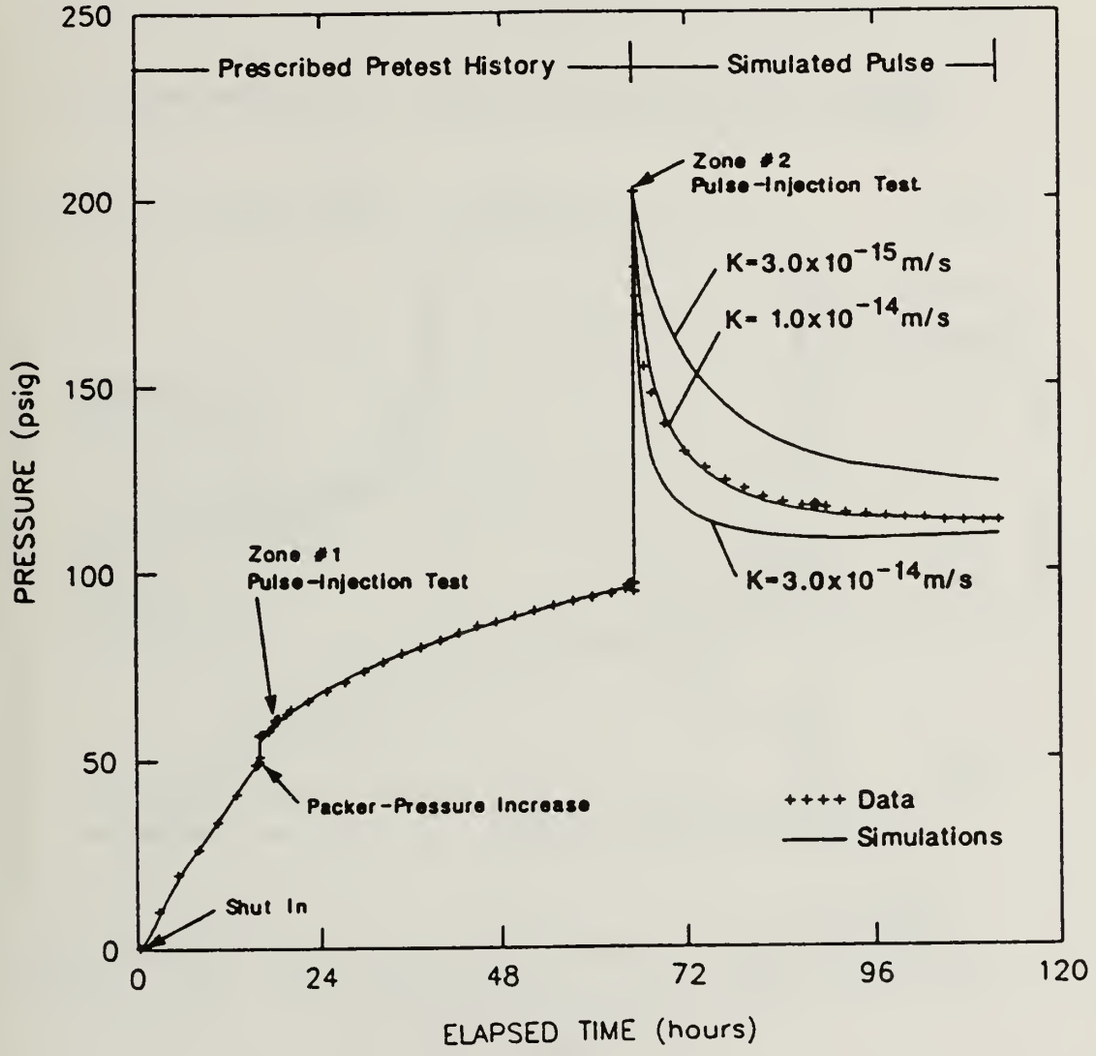

Drawn by	Date
Checked by	Date
Revisions	Date
1109700R570	

Simulation of the Borehole W805E Zone #2 Pulse-Injection Test; Formation Pressure = 140 psig and Varying Hydraulic Conductivity

INTERA Technologies

Figure 5.13

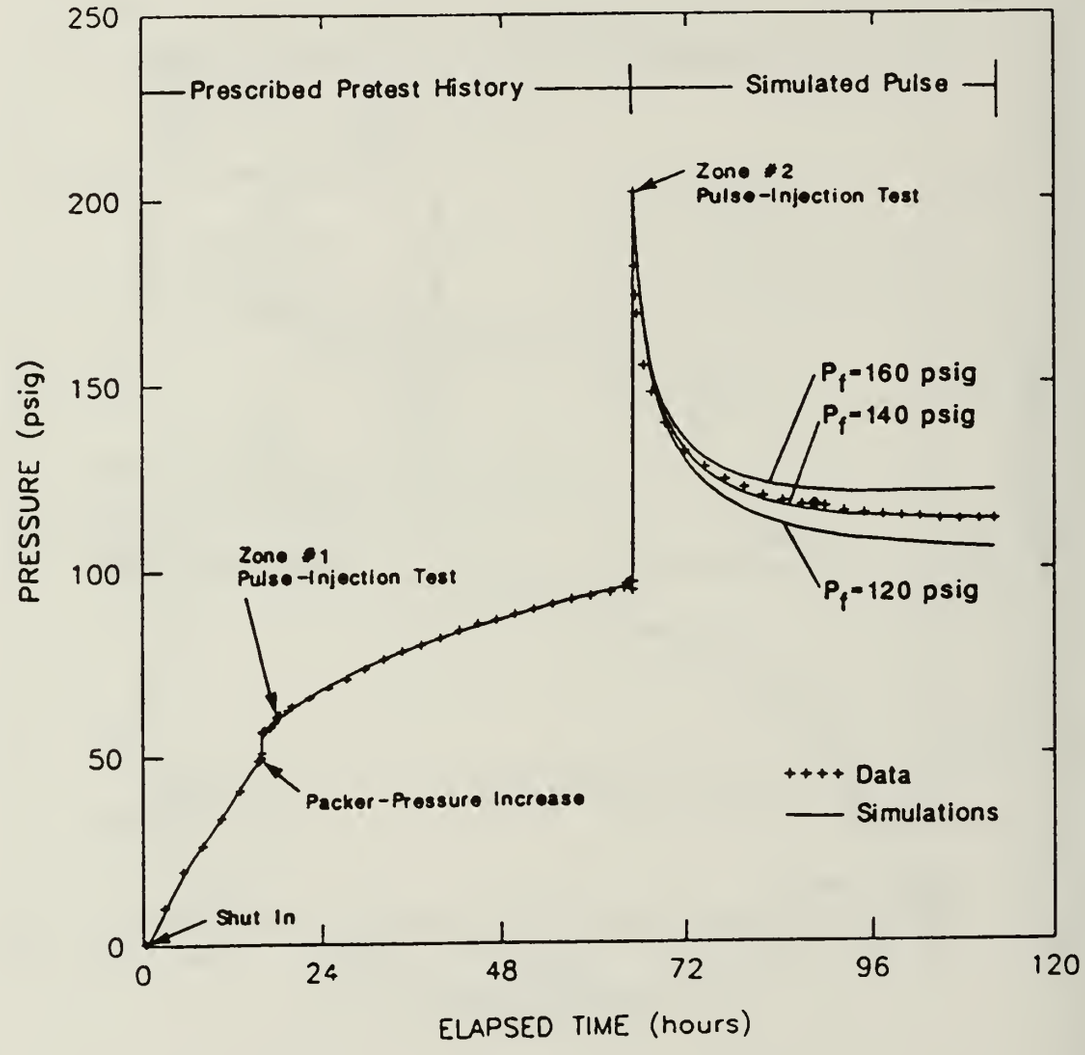

Drawn by	Date	Simulation of the Borehole W805E Zone #2 Pulse-Injection Test; Hydraulic Conductivity = 1.0×10^{-14} m/s and Varying Formation Pressure
Checked by	Date	
Revisions	Date	
H09700R570		
INTERA Technologies		Figure 5.14

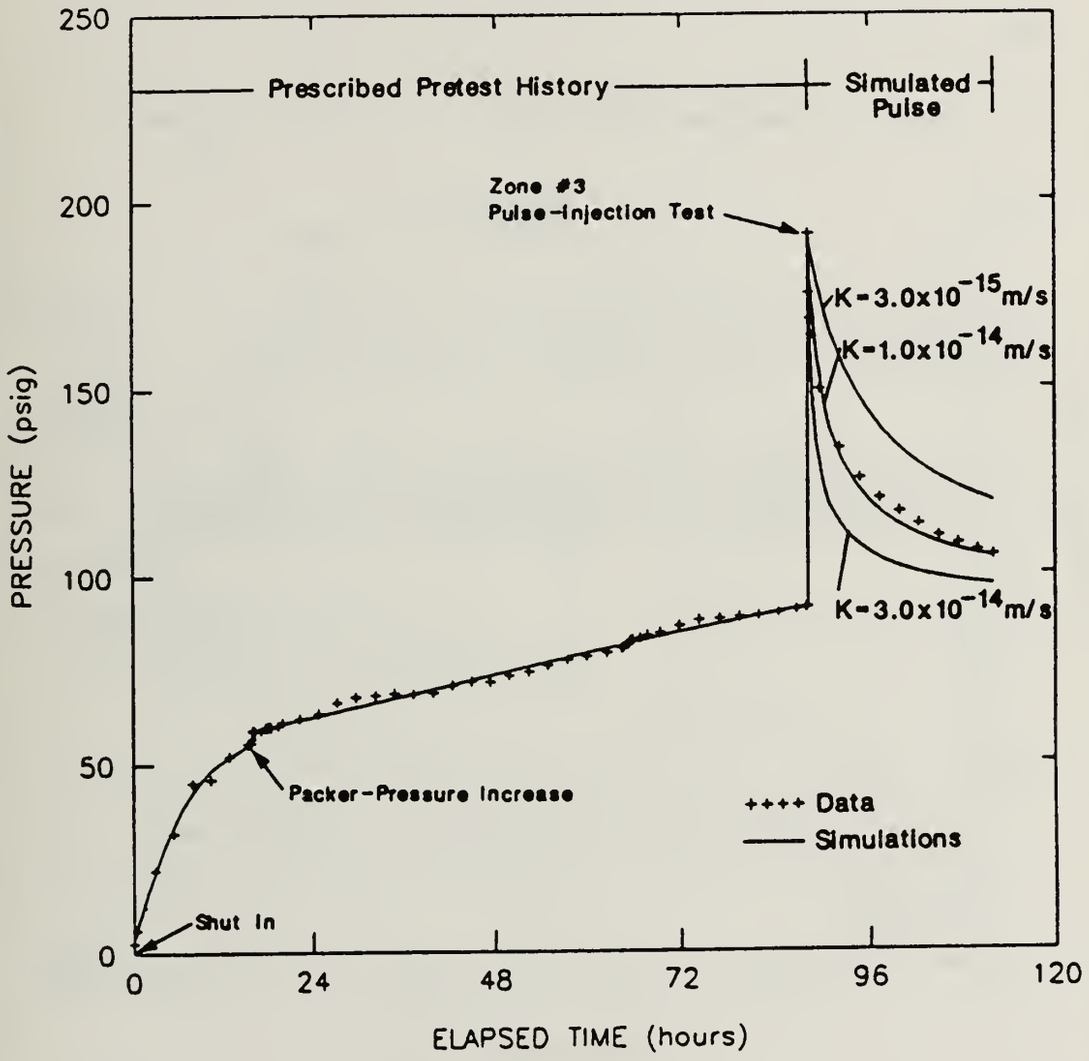

Drawn by	Date
Checked by	Date
Revisions	Date
H09700R570	

Simulation of the Borehole W805E Zone #3 Pulse-Injection Test; Formation Pressure = 110 psig and Varying Hydraulic Conductivity

INTERA Technologies

Figure 5.15

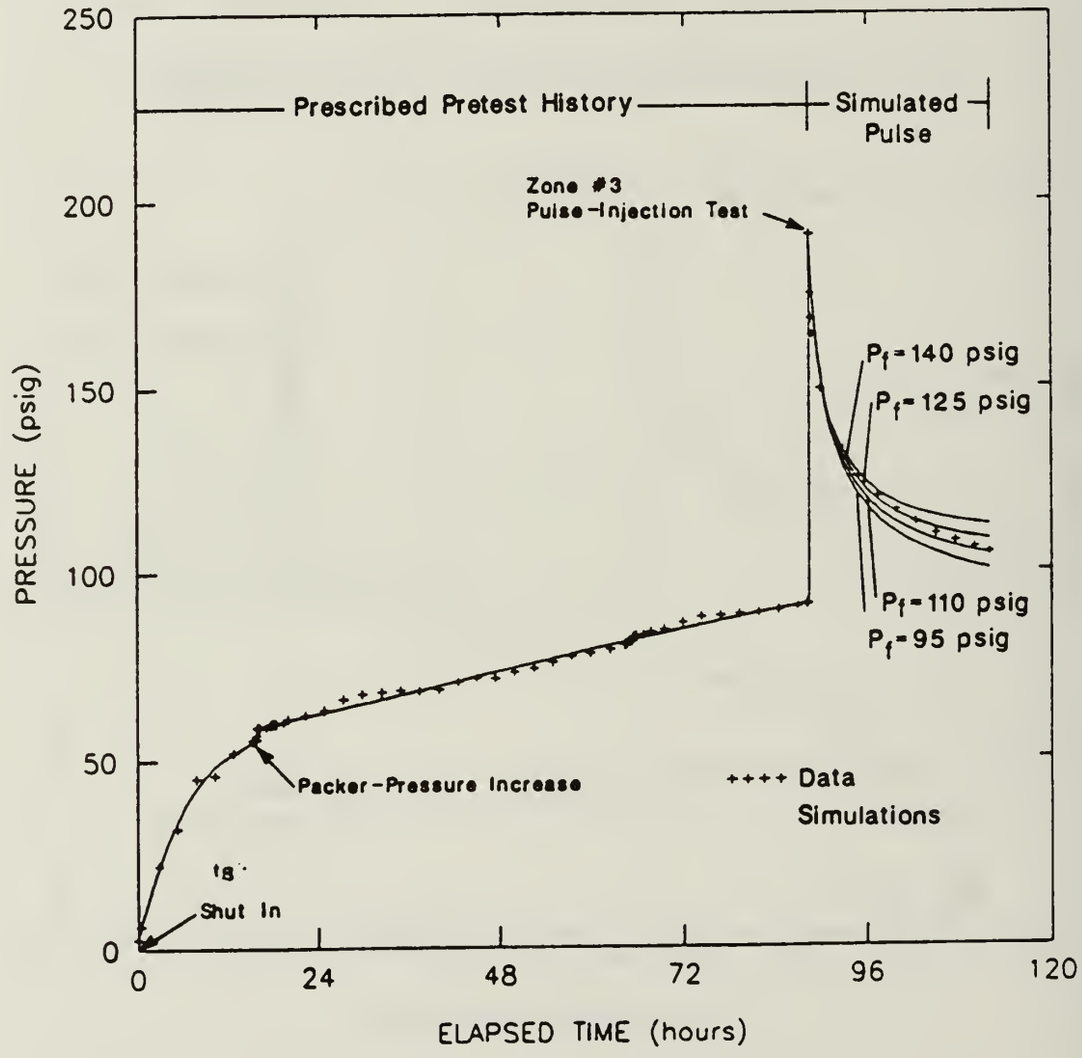

Drawn by	Date
Checked by	Date
Revisions	Date
H09700R570	

Simulation of the Borehole W805E Zone #3 Pulse-Injection Test; Hydraulic Conductivity = 1.0×10^{-14} m/s and Varying Formation Pressure

INTERA Technologies

Figure 5.16

SHAFT LEVEL: 805 feet BGS

BOREHOLE LOCATION: W805SW (Southwest Wall)

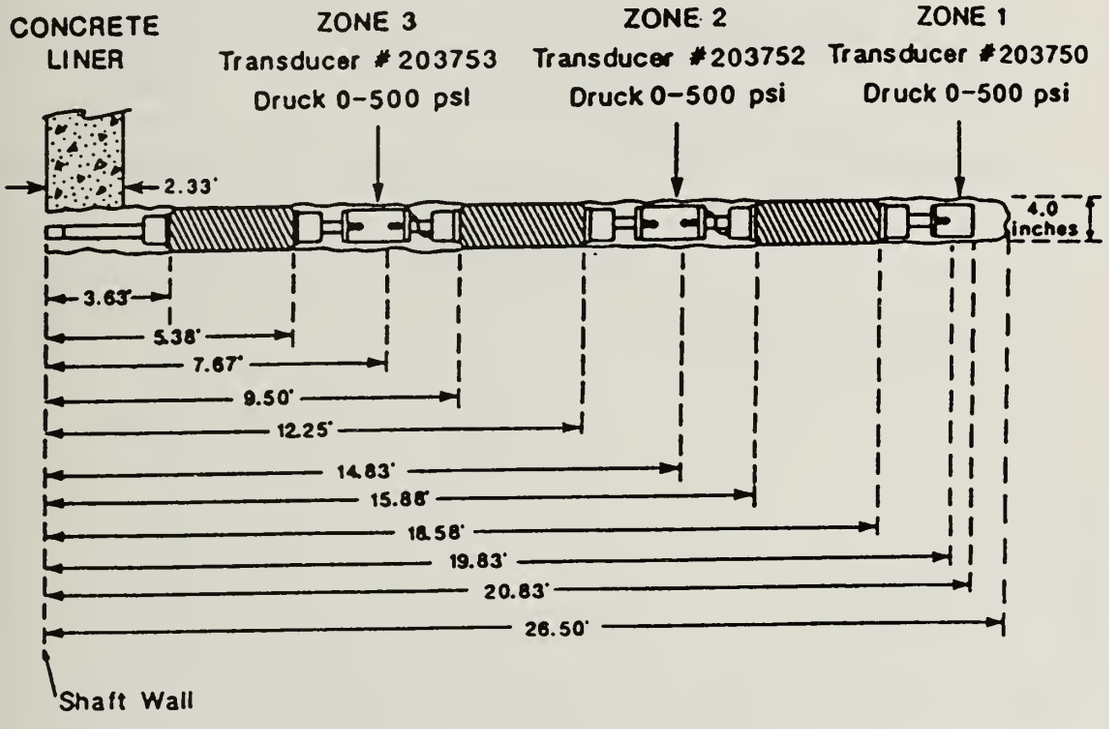

Drawn by	Date	Configuration of the Multipacker Test Tool in Borehole W805SW
Checked by	Date	
Revisions	Date	
H09700R570		
INTERA Technologies		Figure 5.17

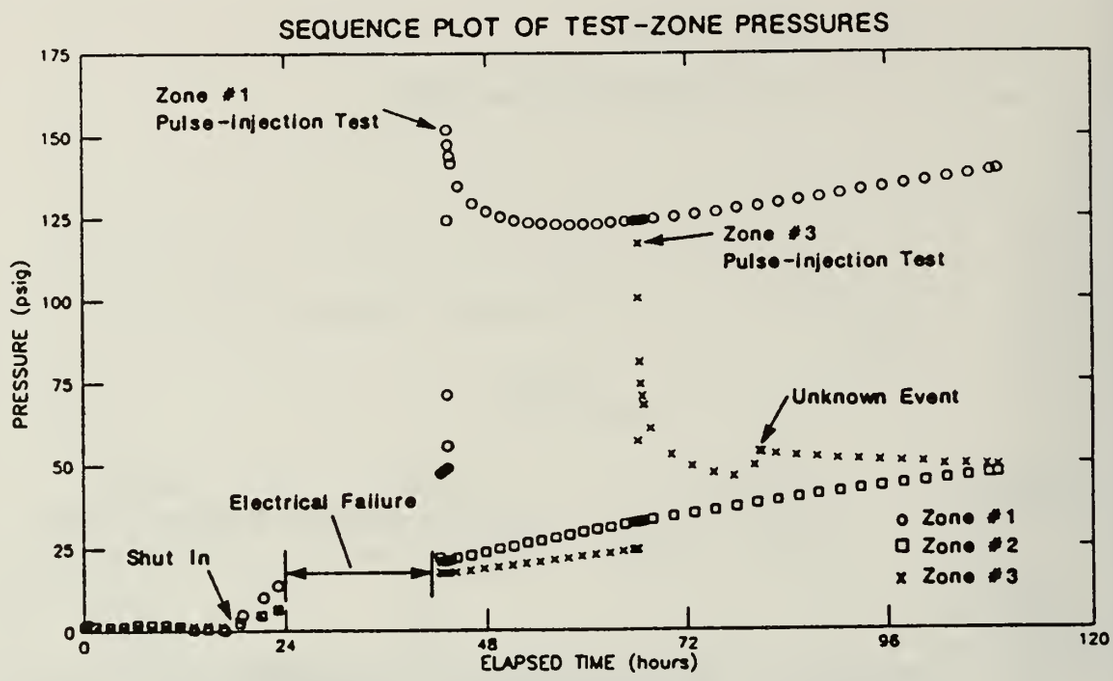

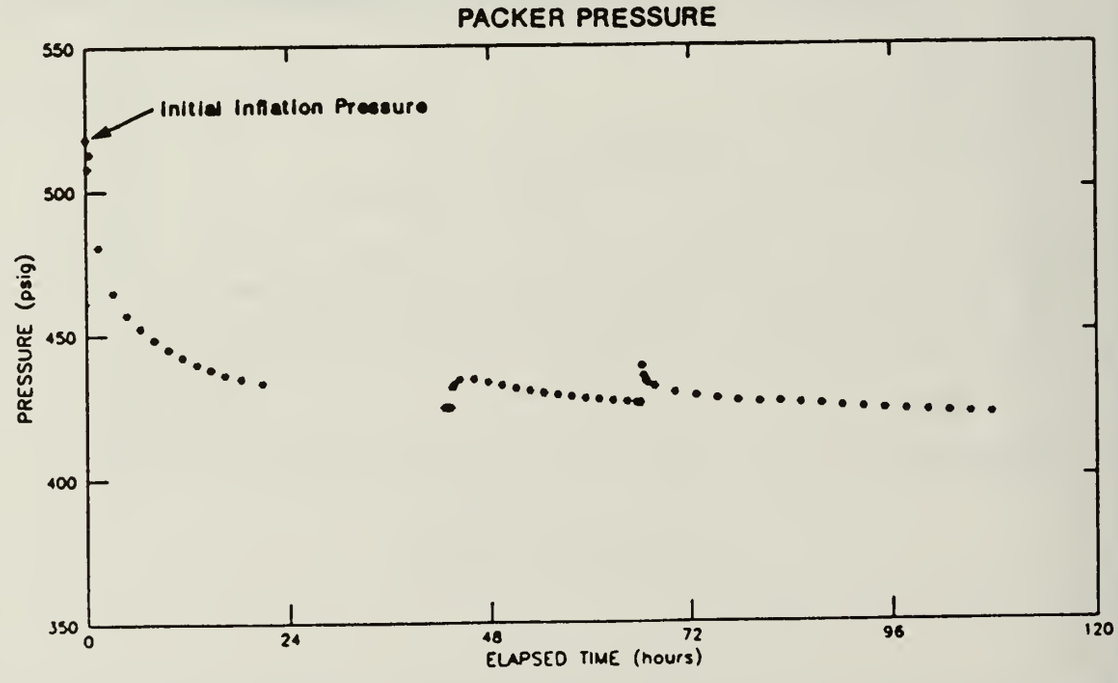

Drawn by	Date
Checked by	Date
Revisions	Date
H09700R570	

Linear-Linear Sequence Plot of the Test-Zone and Packer-Inflation Pressures During Testing in Borehole W805SW

INTERA Technologies

Figure 5.18

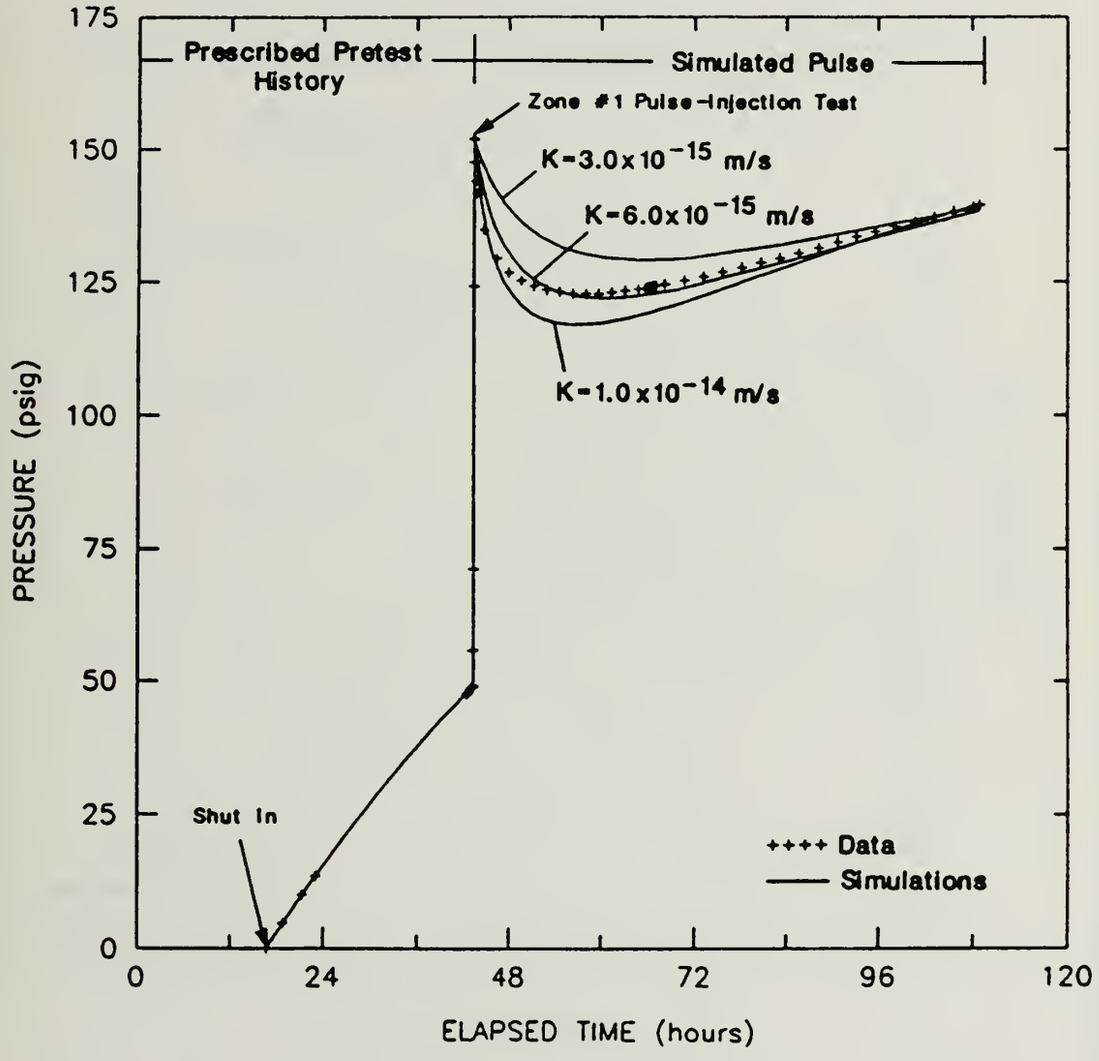

Drawn by	Date	Simulation of the Borehole W805SW Zone #1 Pulse-Injection Test; Formation Pressure = 275 psig and Varying Hydraulic Conductivity
Checked by	Date	
Revisions	Date	
H09700R570		
INTERA Technologies		Figure 5.19

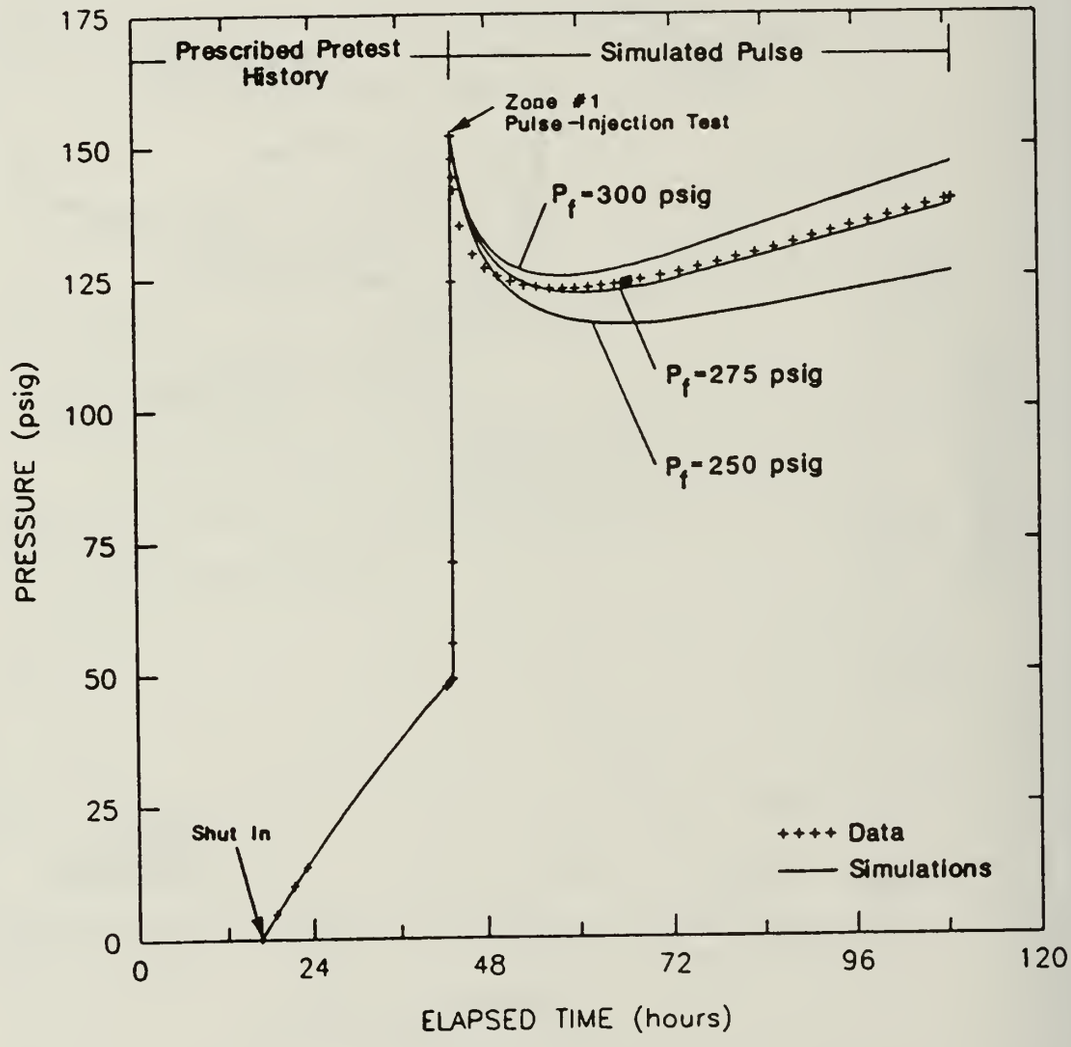

Drawn by	Date
Checked by	Date
Revisions	Date
H09700R570	

Simulation of the Borehole W805SW Zone #1 Pulse-Injection Test; Hydraulic Conductivity = 6.0×10^{-15} m/s and Varying Formation Pressure

INTERA Technologies

Figure 5.20

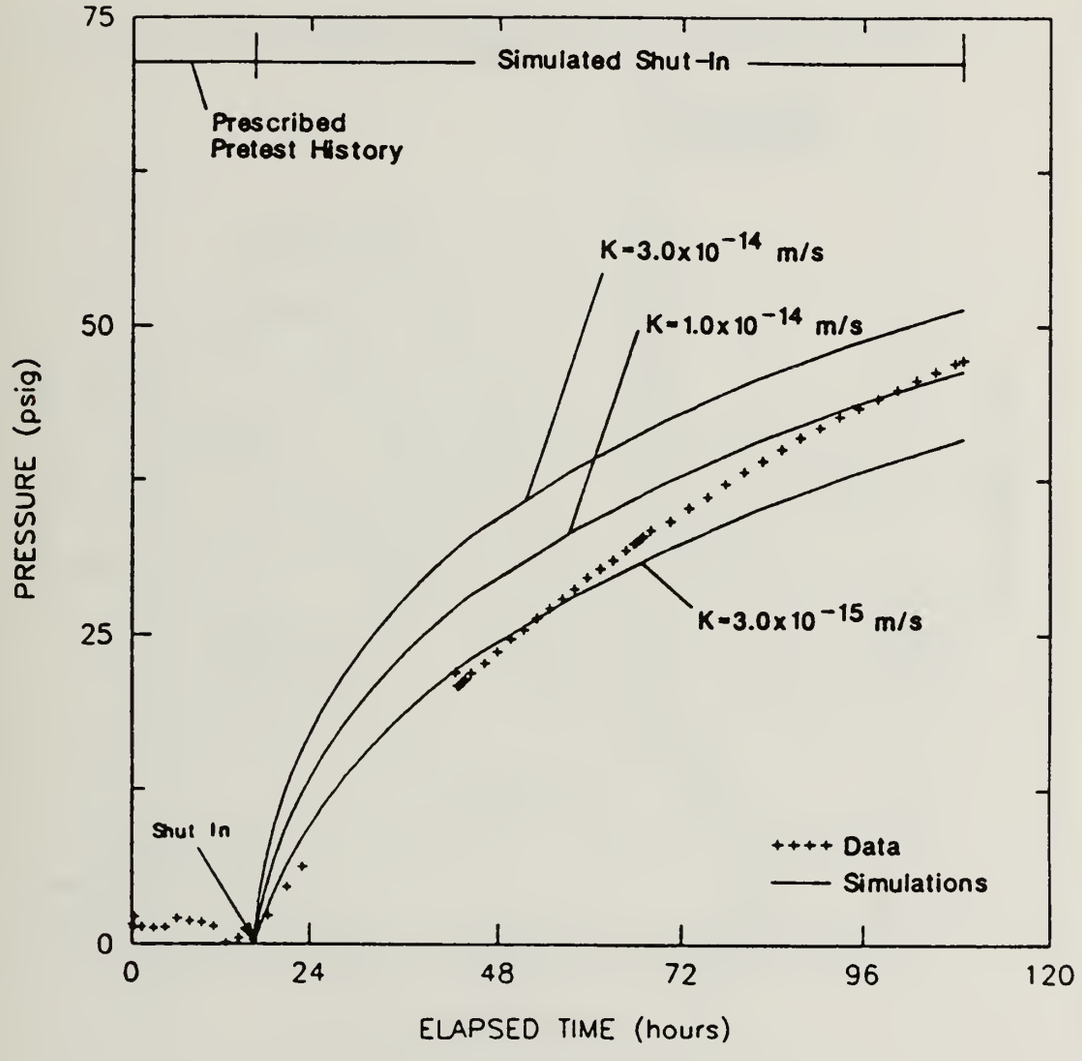

Drawn by	Date
Checked by	Date
Revisions	Date
H09700R570	

Simulation of the Borehole W805SW Zone #2 Shut-In Test; Formation Pressure - 90 psig and Varying Hydraulic Conductivity

INTERA Technologies

Figure 5.21

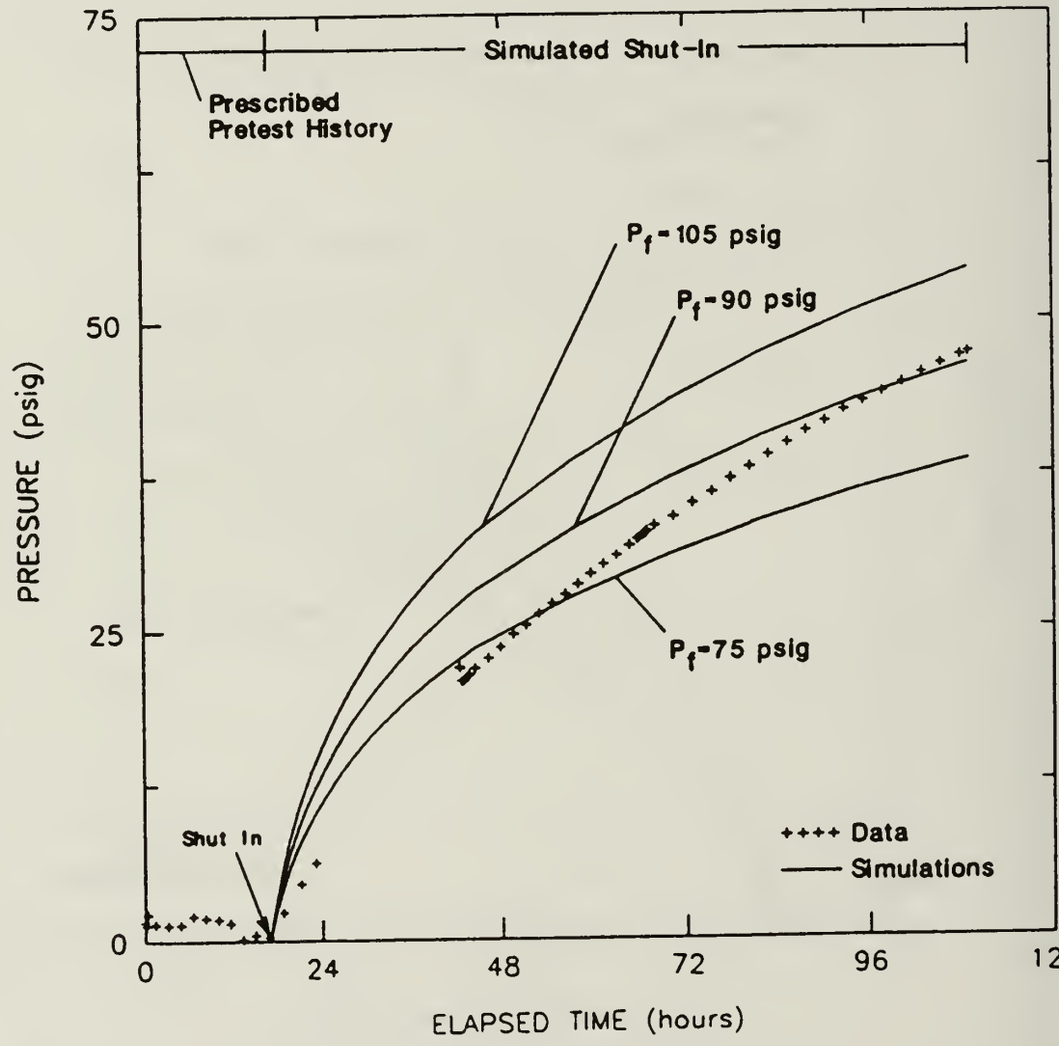

Drawn by	Date	Simulation of the Borehole W805SW Zone #2 Shut-In Test; Hydraulic Conductivity = 1.0×10^{-14} m/s and Varying Formation Pressure
Checked by	Date	
Revisions	Date	
H09700R570		
INTERA Technologies		Figure 5.22

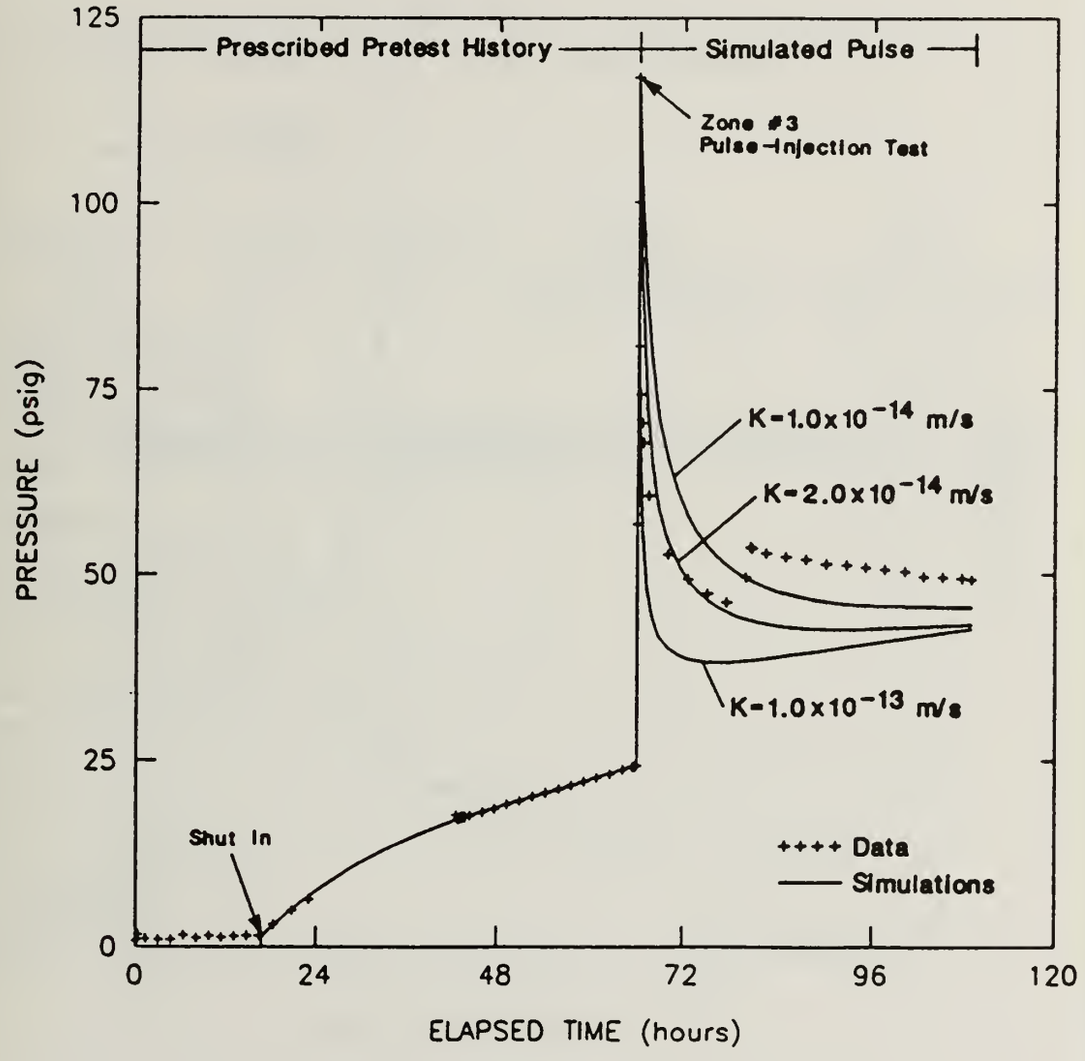

Drawn by	Date
Checked by	Date
Revisions	Date
H09700R570	

Simulation of the Borehole W805SW Zone #3 Pulse-Injection Test; Formation Pressure = 70 psig and Varying Hydraulic Conductivity

INTERA Technologies

Figure 5.23

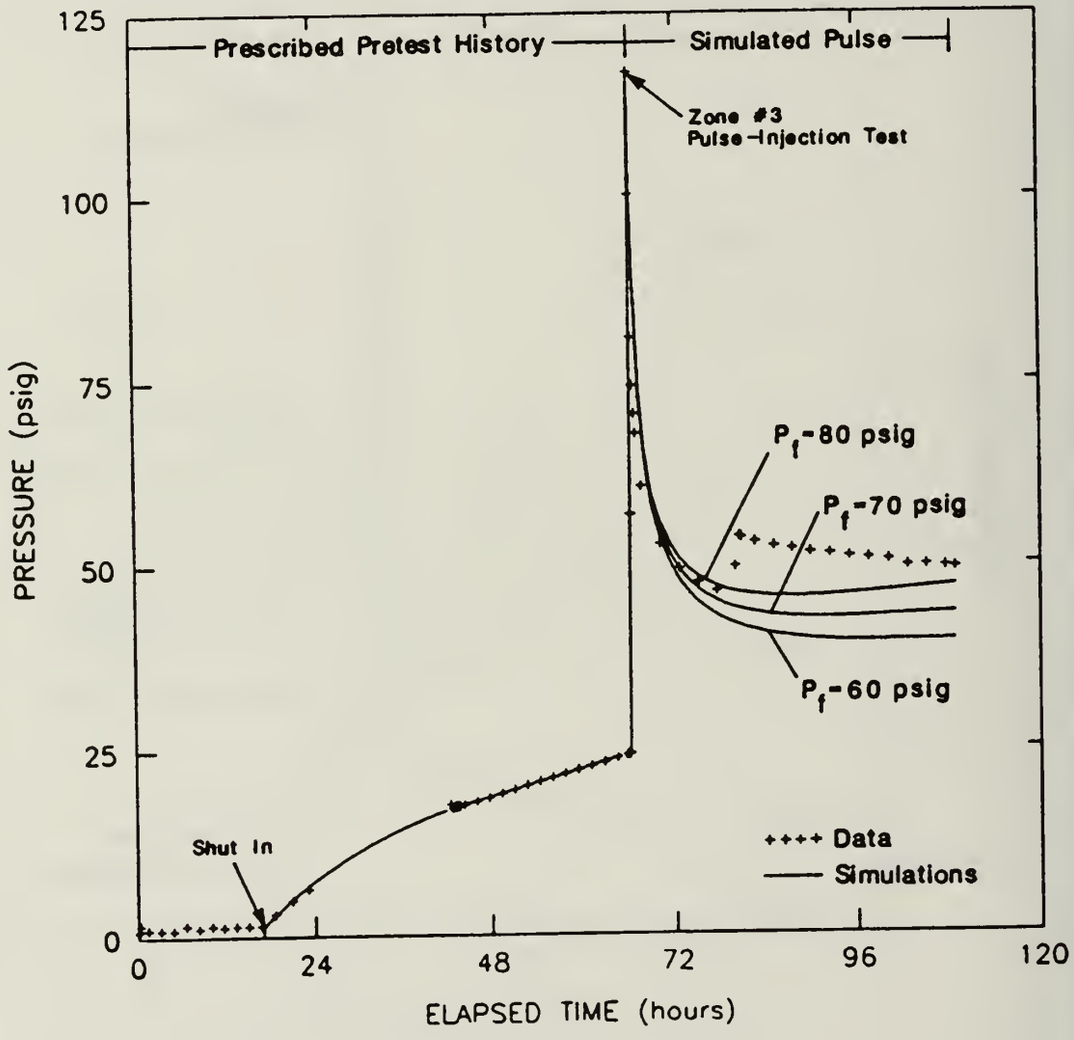

Drawn by	Date
Checked by	Date
Revisions	Date
H09700R570	

Simulation of the Borehole W805SW Zone #3 Pulse-Injection Test; Hydraulic Conductivity = 2.0×10^{-14} m/s and Varying Formation Pressure

INTERA Technologies

Figure 5.24

SHAFT LEVEL: 850 feet BGS

BOREHOLE LOCATION: W850W (West Wall)

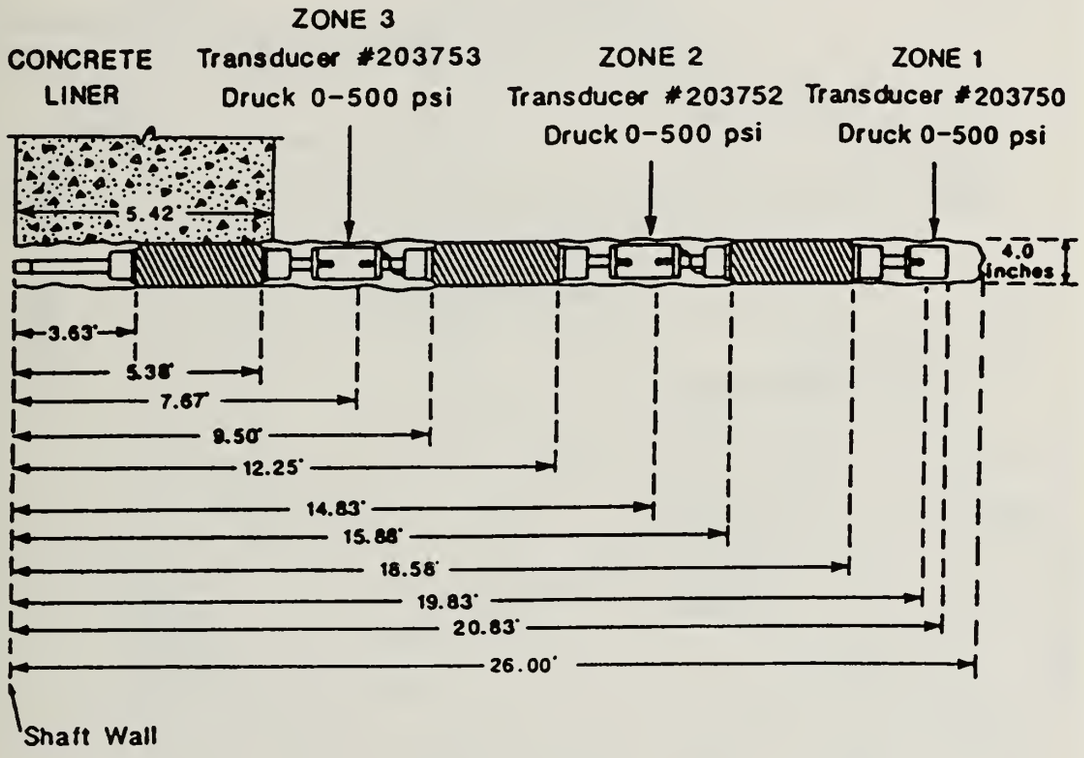

Drawn by	Date
Checked by	Date
Revisions	Date
H09700K570	

Configuration of the Multipacker Test Tool in Borehole W850W

INTERA Technologies

Figure 5.25

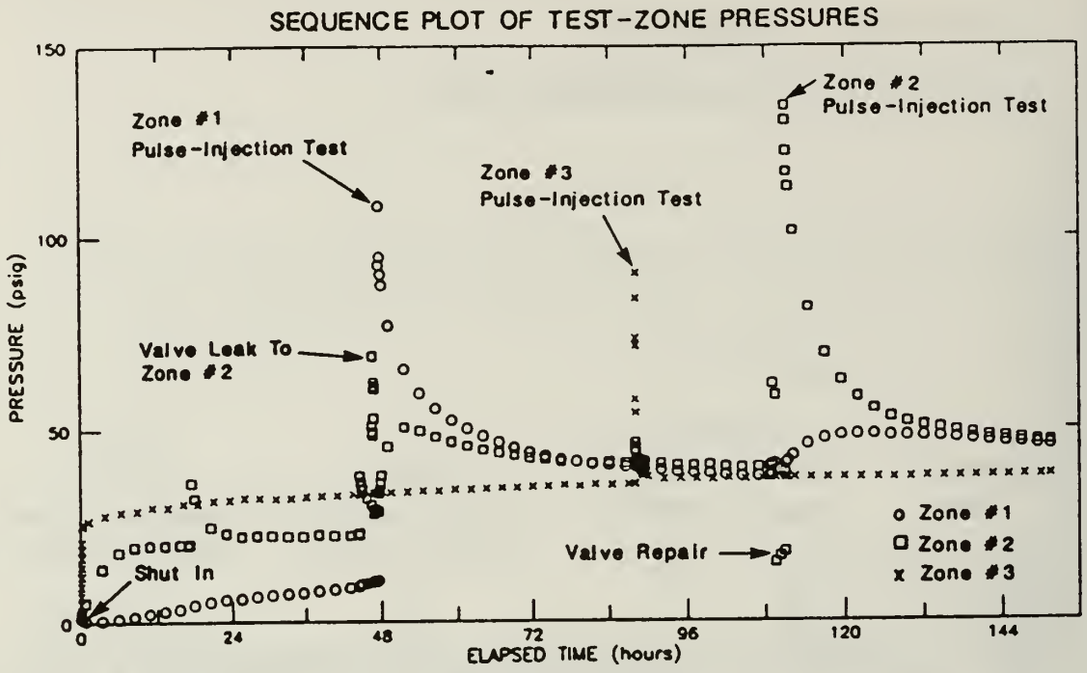

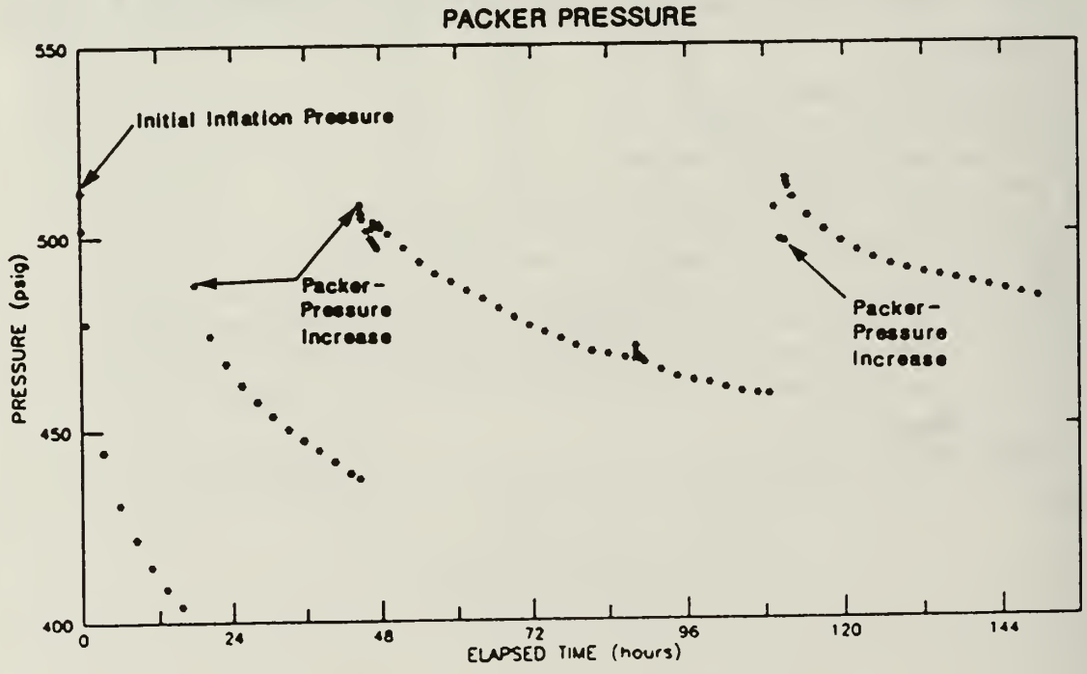

Drawn by	Date
Checked by	Date
Revisions	Date
H09700R570	

Linear-Linear Sequence Plot of the Test-Zone and Packer-Inflation Pressures During Testing in Borehole W850W

INTERA Technologies

Figure 5.26

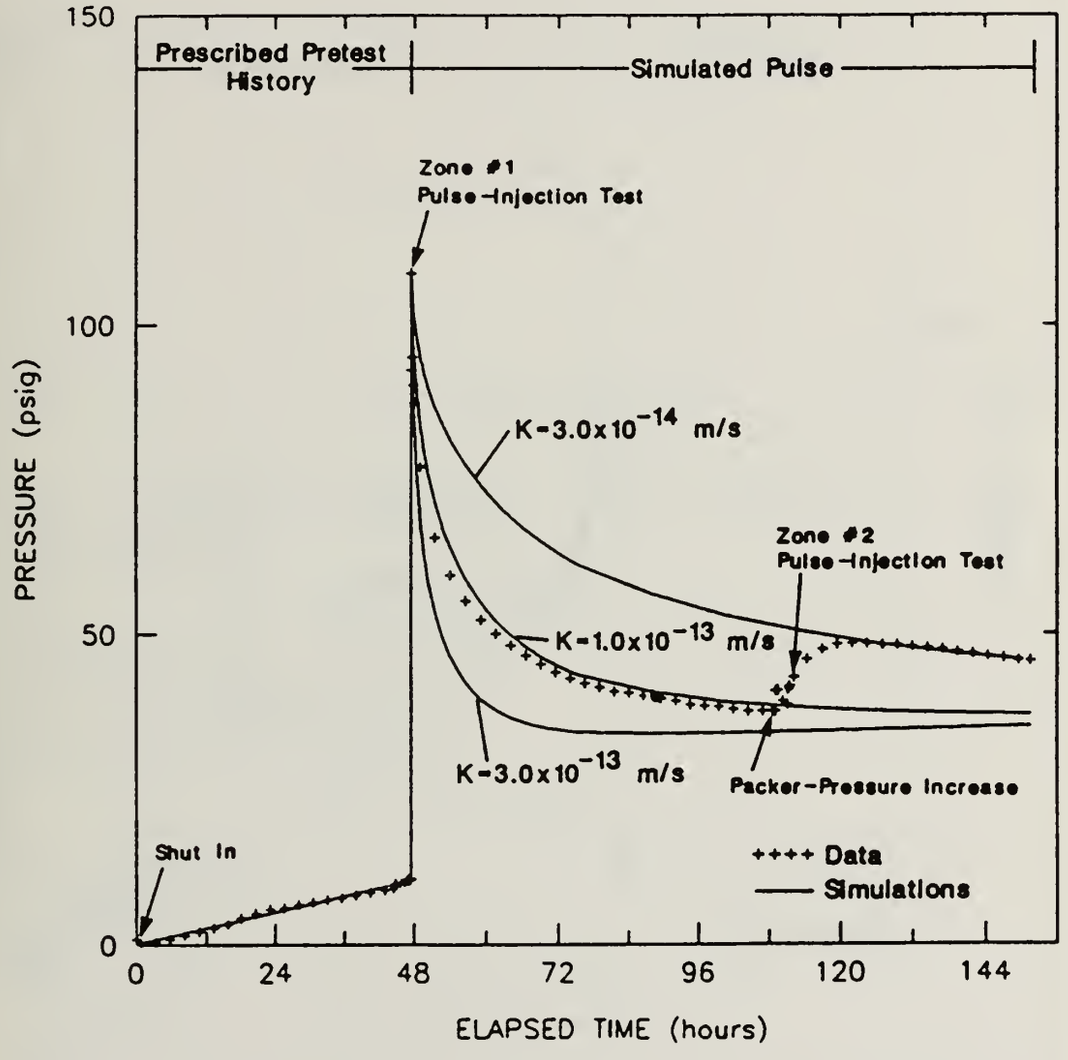

Drawn by	Date	Simulation of the Borehole W850W Zone #1 Pulse-Injection Test; Formation Pressure = 40 psig and Varying Hydraulic Conductivity
Checked by	Date	
Revisions	Date	
H:09700R570		
INTERA Technologies		Figure 5.27

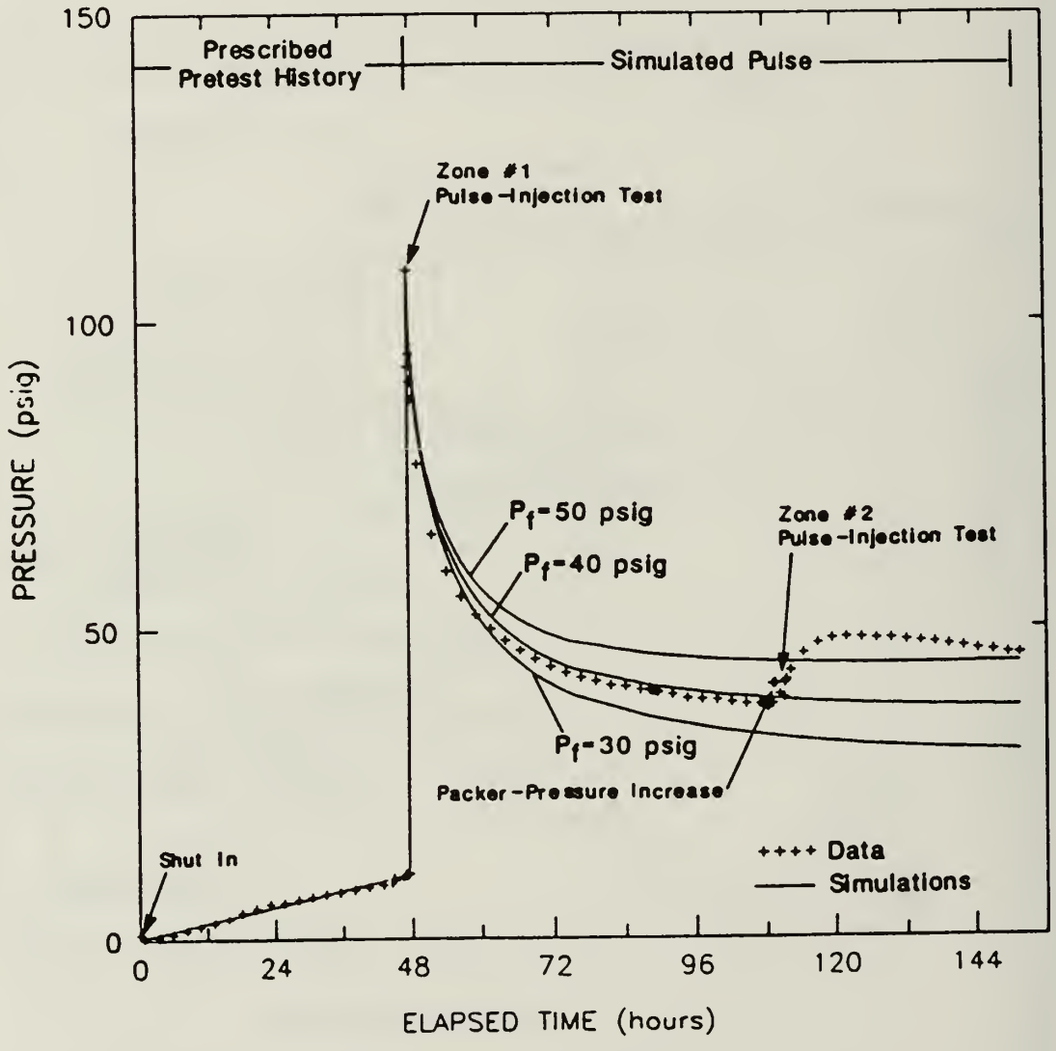

Drawn by	Date
Checked by	Date
Revisions	Date
H09700K570	

Simulation of the Borehole W850W Zone #1 Pulse-Injection Test; Hydraulic Conductivity = 1.0×10^{-13} m/s and Varying Formation Pressure

INTERA Technologies

Figure 5.28

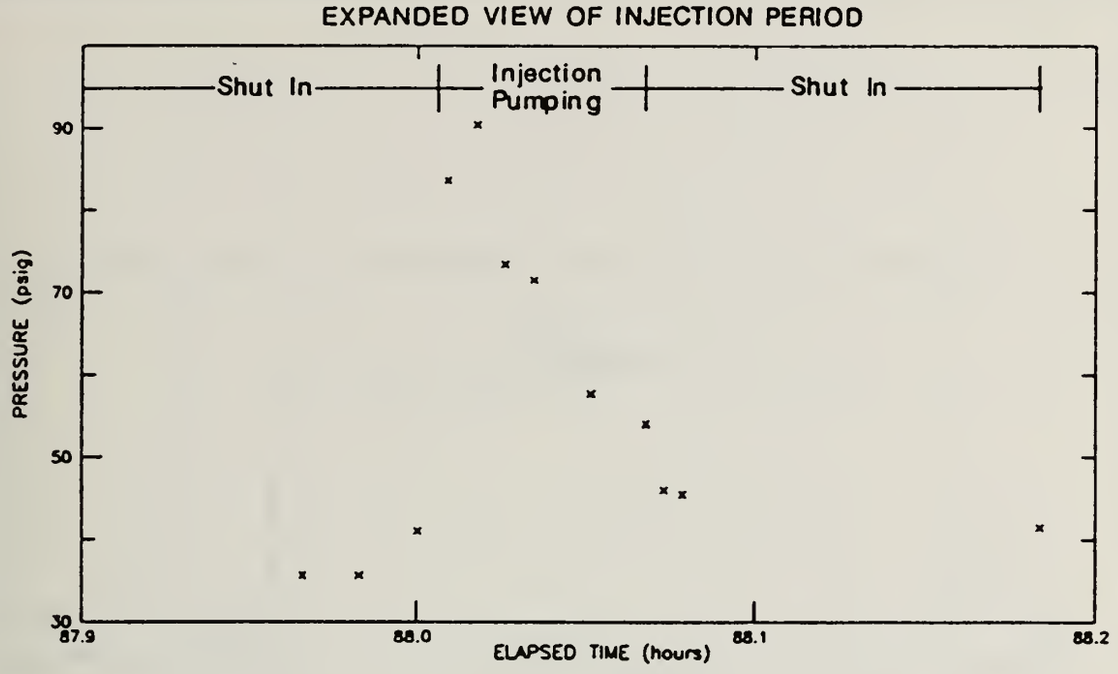

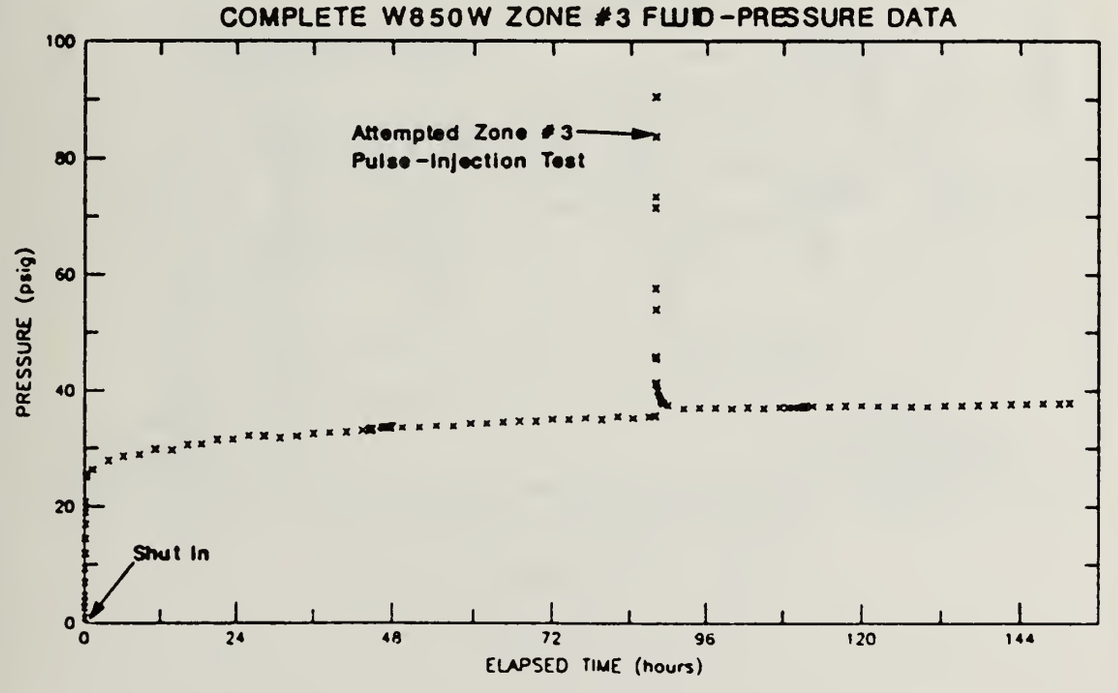

Drawn by	Date
Checked by	Date
Revisions	Date
H09700R570	

Unsuccessful Pulse-Injection in Zone #3, Borehole W850W

INTERA Technologies

Figure 5.29

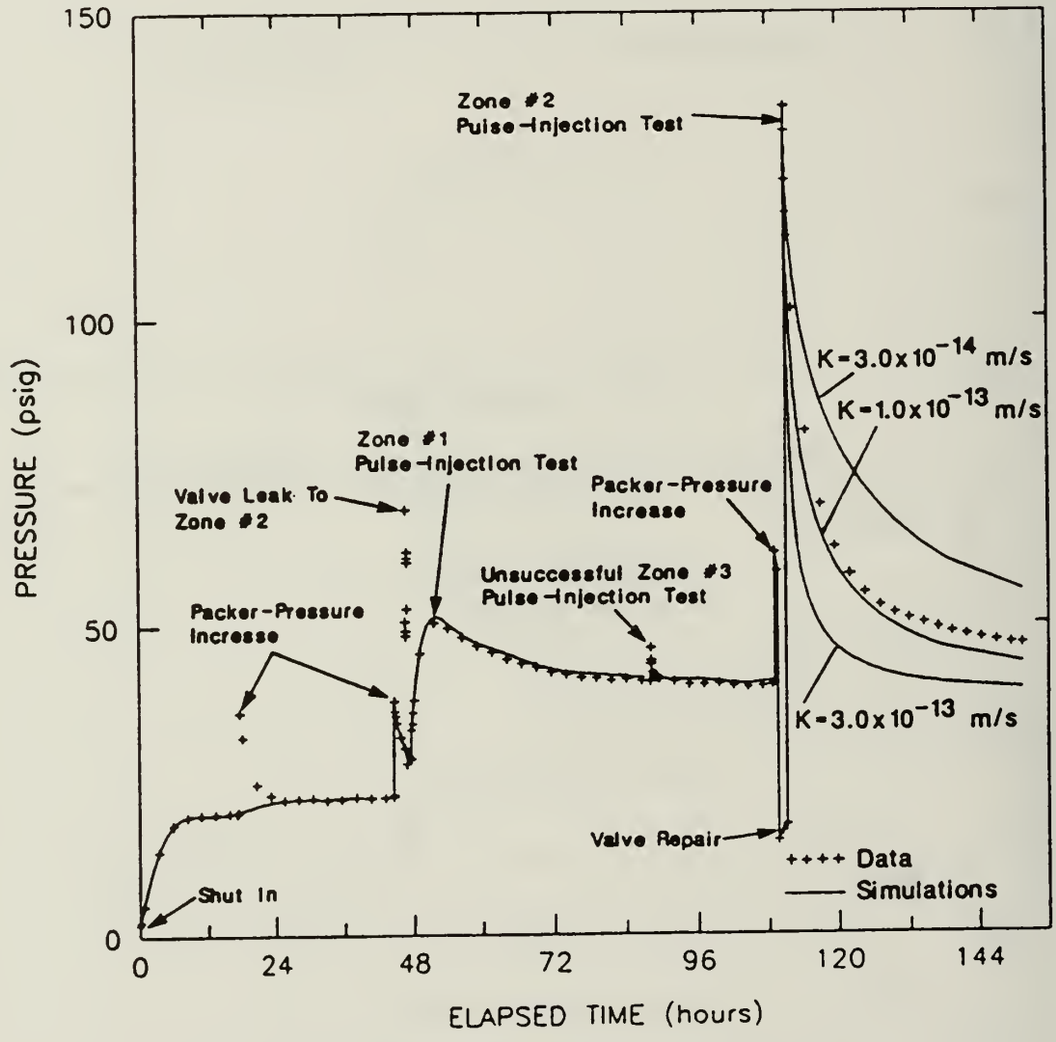

Drawn by	Date
Checked by	Date
Revisions	Date
H09700R570	

Simulation of the Borehole W850W Zone #2 Pulse-Injection Test; Formation Pressure - 40 psig and Varying Hydraulic Conductivity

INTERA Technologies

Figure 5.30

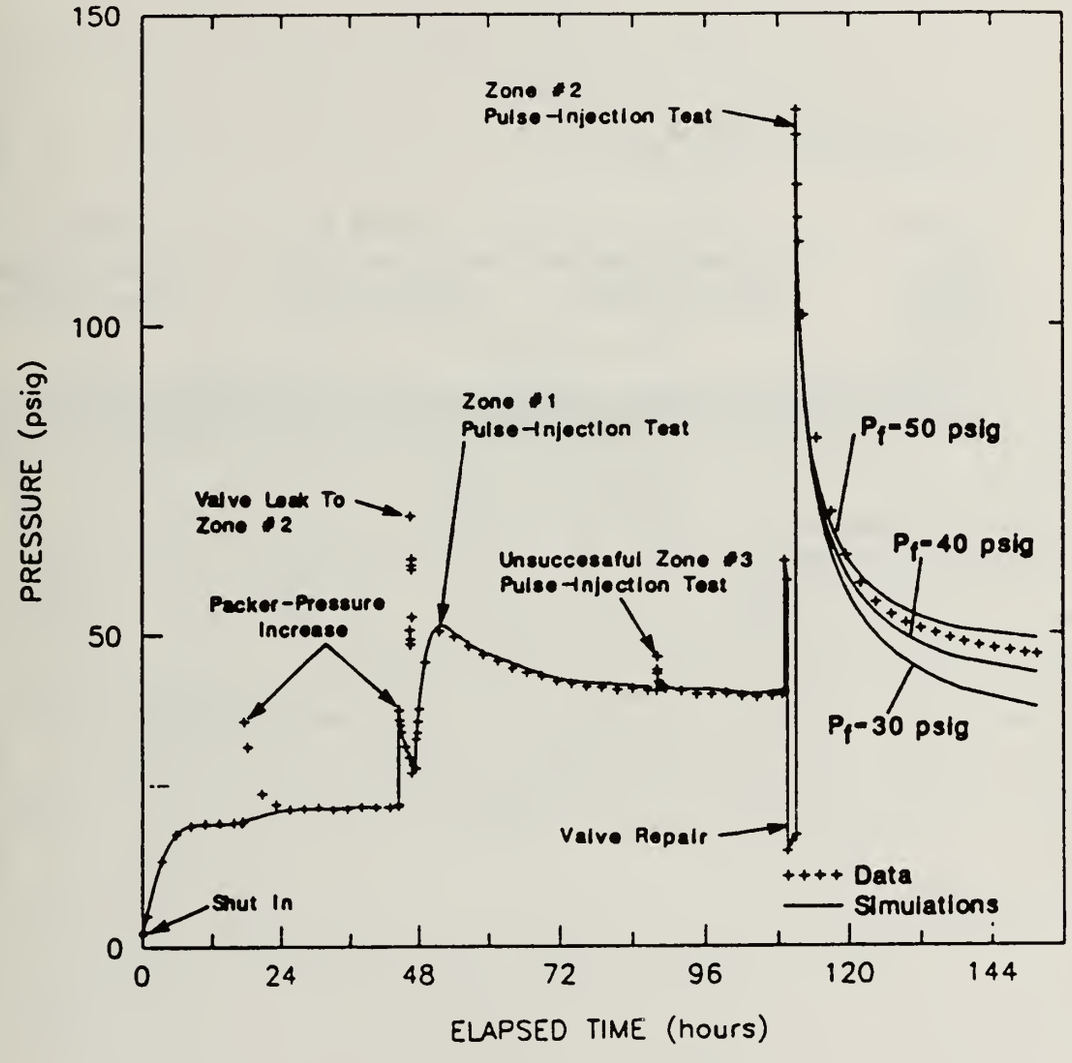

Drawn by	Date
Checked by	Date
Revisions	Date
H09700R570	

Simulation of the Borehole W850W Zone #2 Pulse-Injection Test; Hydraulic Conductivity - 1.0×10^{-13} m/s and Varying Formation Pressure

INTERA Technologies

Figure 5.31

SHAFT LEVEL: 850 feet BGS

BOREHOLE LOCATION: W850SE (Southeast Wall)

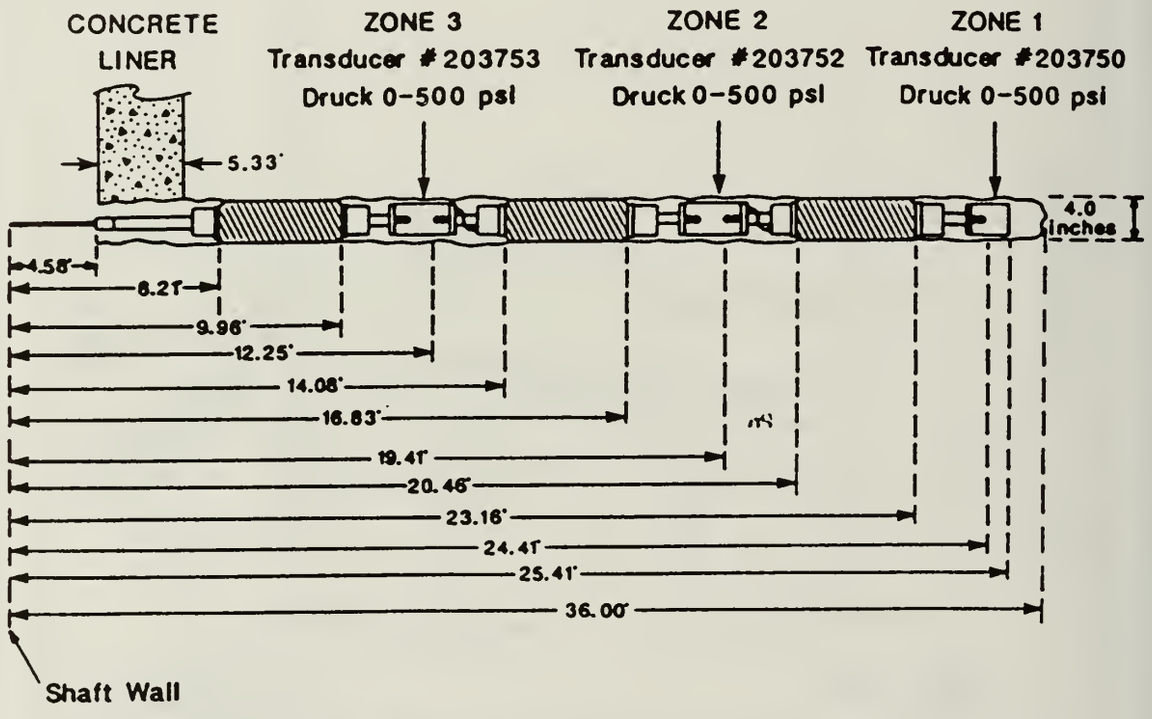

Drawn by	Date	Configuration of the Multipacker Test Tool in Borehole W850SE
Checked by	Date	
Revisions	Date	
H09700R570		
INTERA Technologies		Figure 5.32

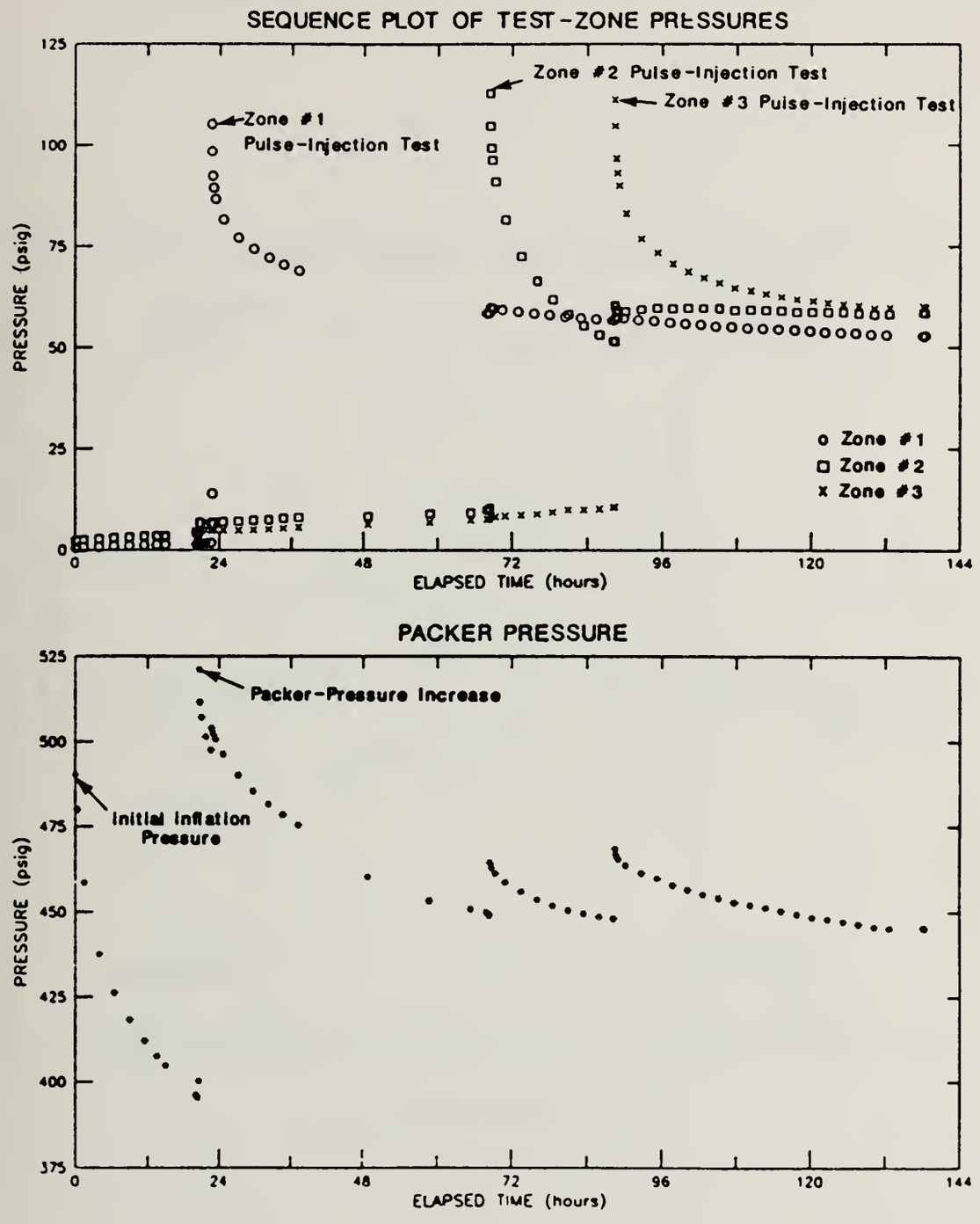

Drawn by	Date
Checked by	Date
Revisions	Date
1:09700R570	

Linear-Linear Sequence Plot of the Test-Zone and Packer-Inflation Pressures During Testing in Borehole W850SE

INTERA Technologies

Figure 5.33

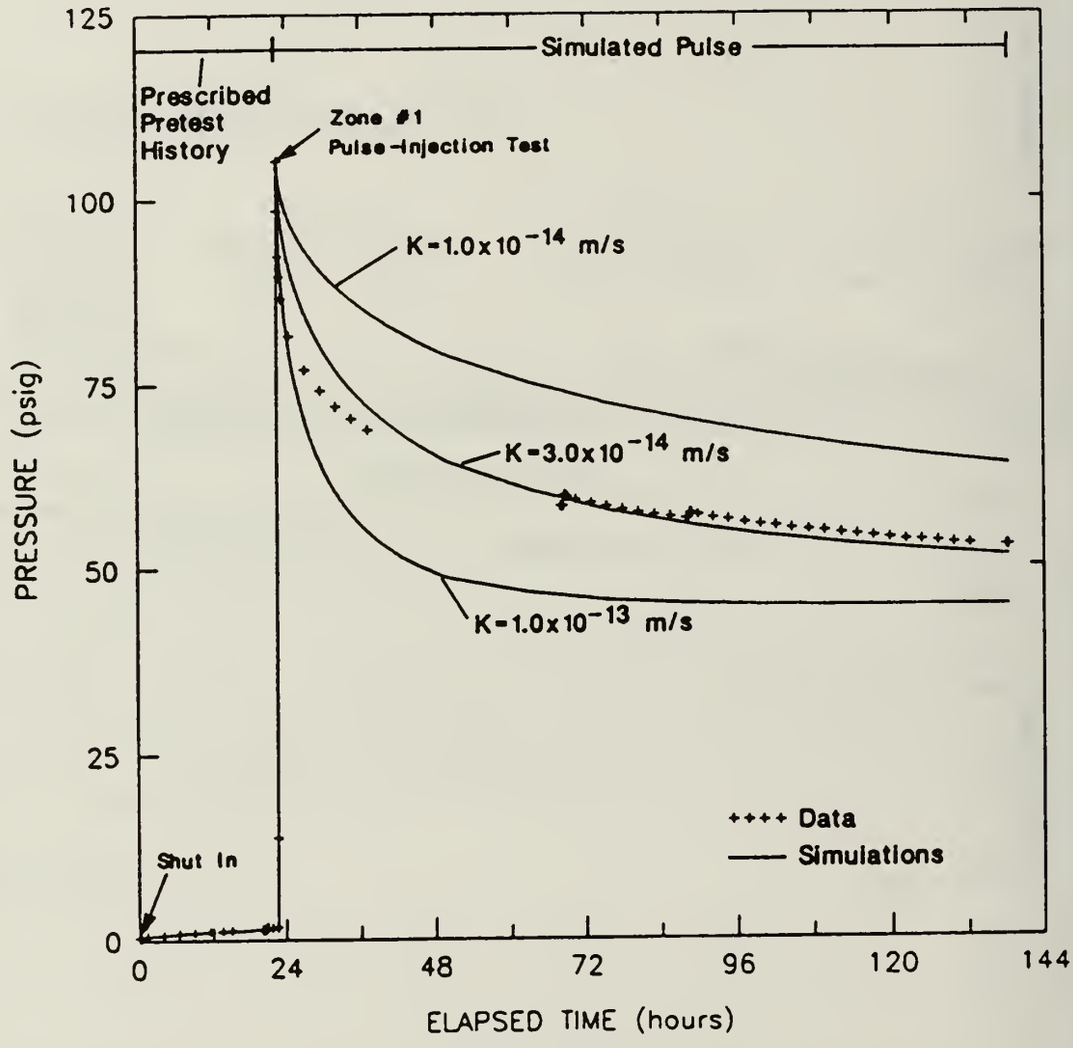

Drawn by	Date
Checked by	Date
Revisions	Date
H09700R570	

Simulation of the Borehole W850SE Zone #1 Pulse-Injection Test; Formation Pressure = 50 psig and Varying Hydraulic Conductivity

INTERA Technologies

Figure 5.34

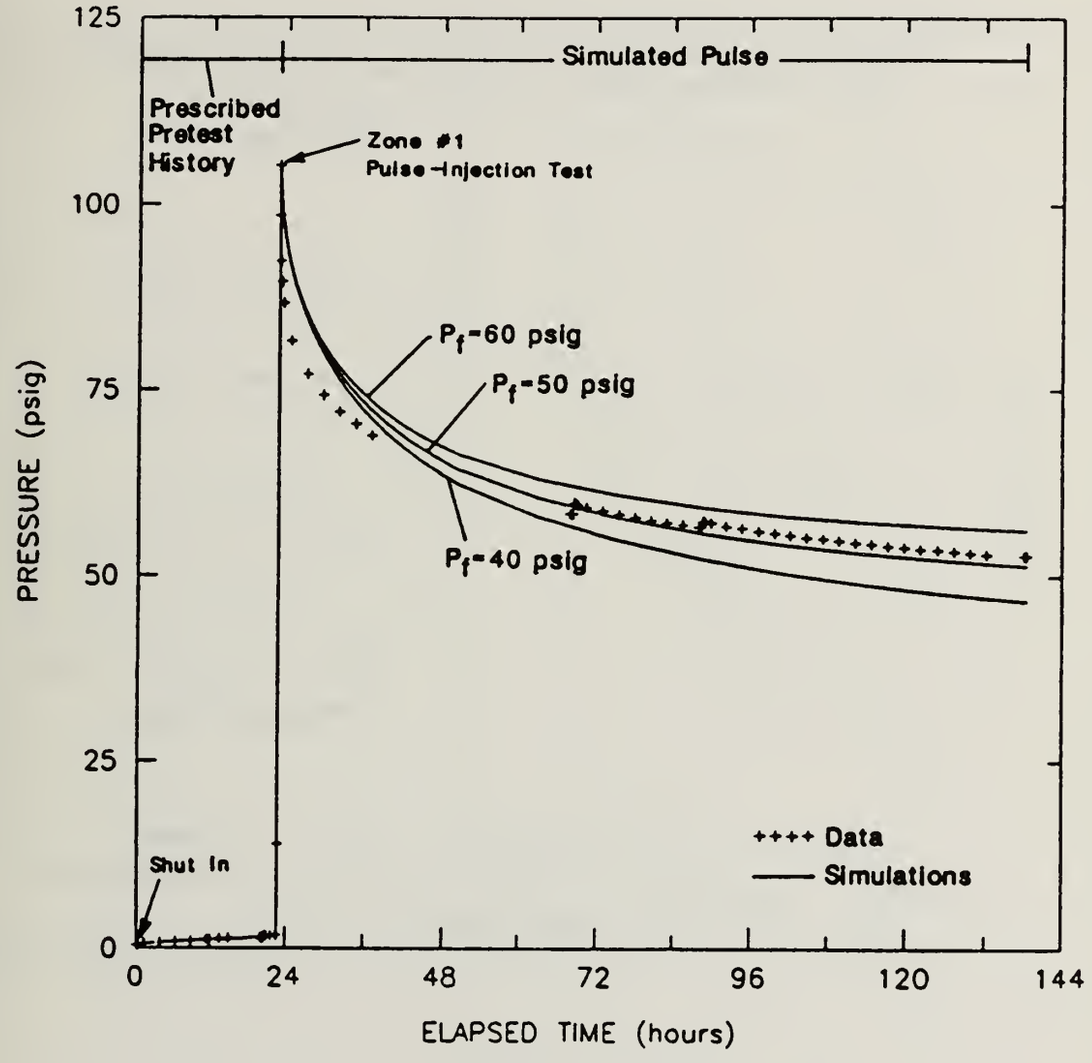

Drawn by	Date
Checked by	Date
Revisions	Date
H09700R570	

Simulation of the Borehole W850SE Zone #1 Pulse-Injection Test; Hydraulic Conductivity = 3.0 x 10^{-14} m/s and Varying Formation Pressure

INTERA Technologies

Figure 5.35

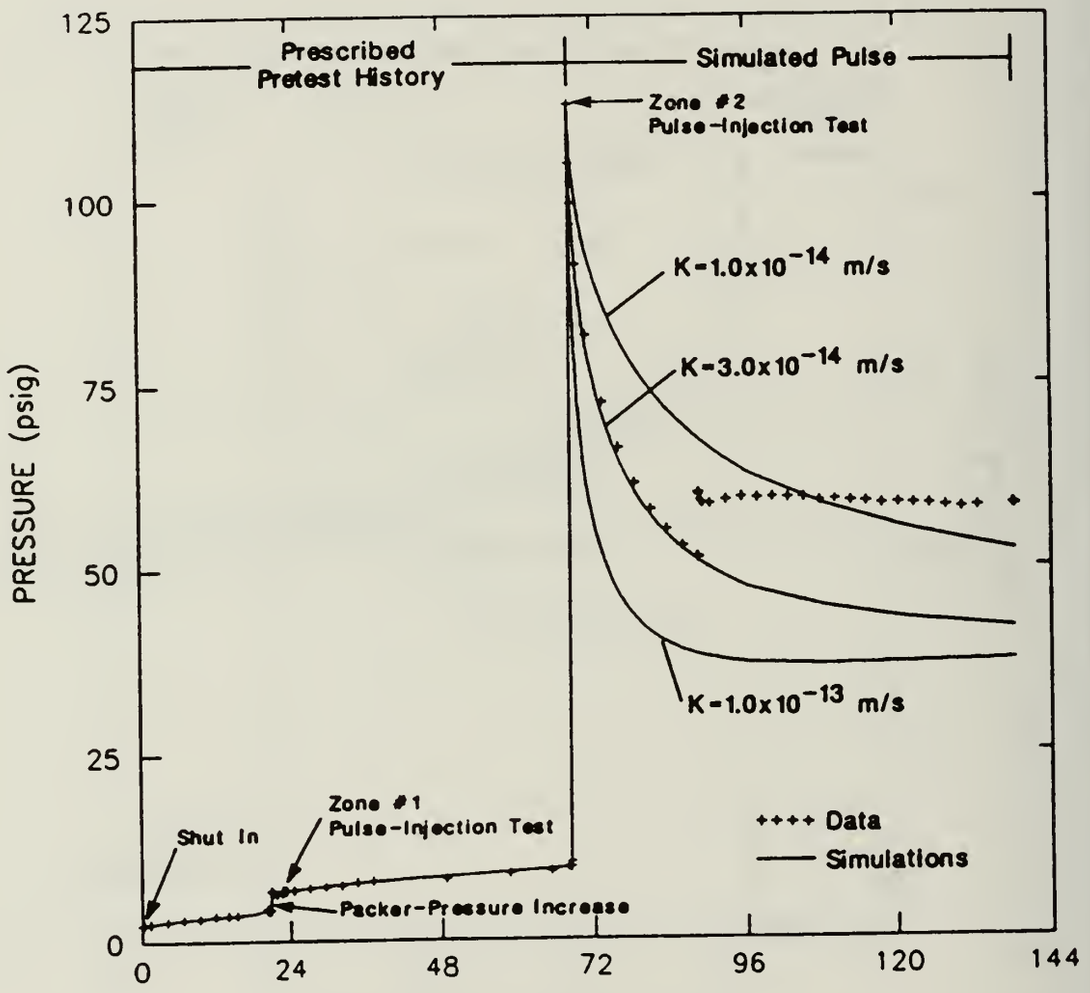

Drawn by	Date
Checked by	Date
Revisions	Date
H09700K570	

Simulation of the Borehole W850SE Zone #2 Pulse-Injection Test; Formation Pressure = 45 psig and Varying Hydraulic Conductivity

INTERA Technologies

Figure 5.36

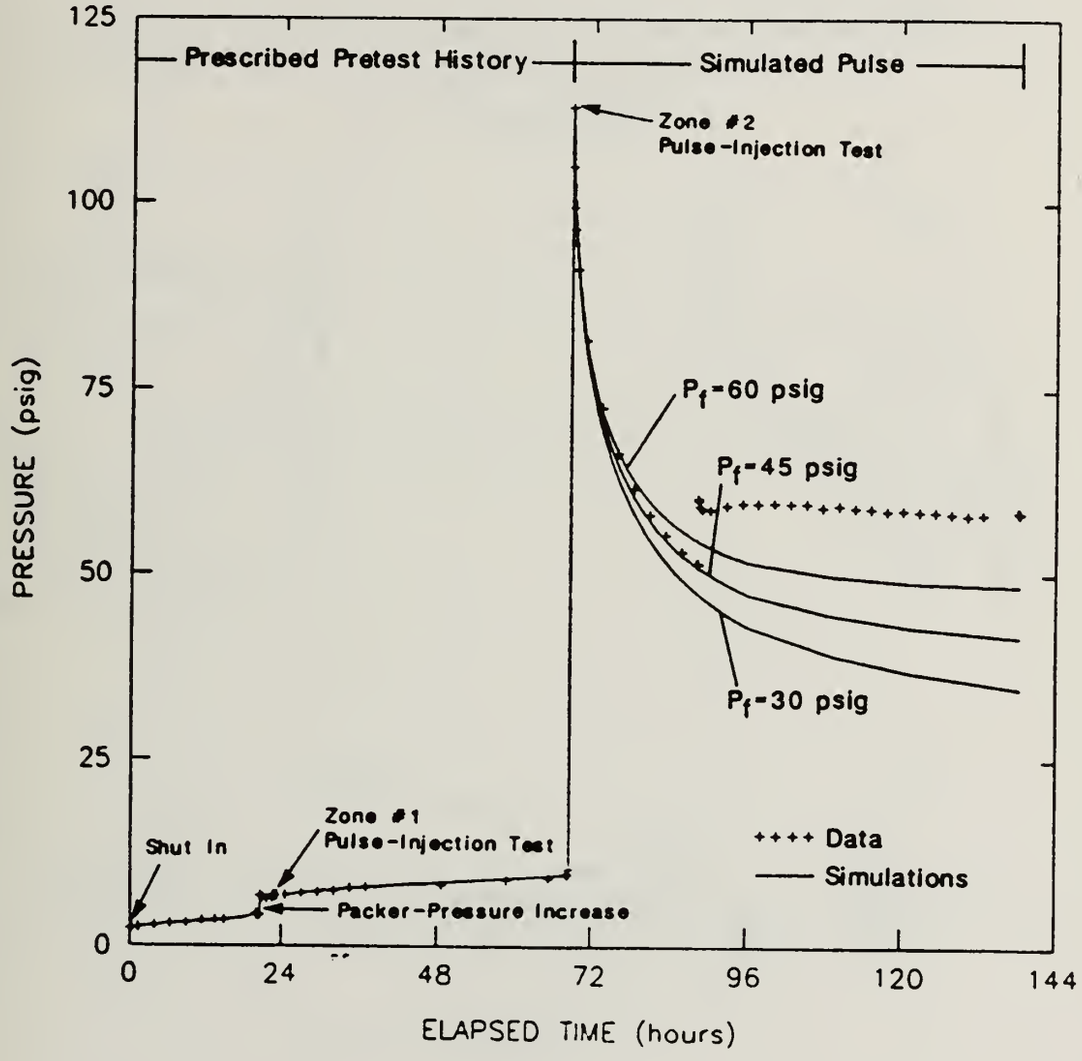

Drawn by	Date	Simulation of the Borehole W850SE Zone #2 Pulse-Injection Test; Hydraulic Conductivity - 3.0×10^{-14} m/s and Varying Formation Pressure
Checked by	Date	
Revisions	Date	
H09700R570		
INTERA Technologies		Figure 5.37

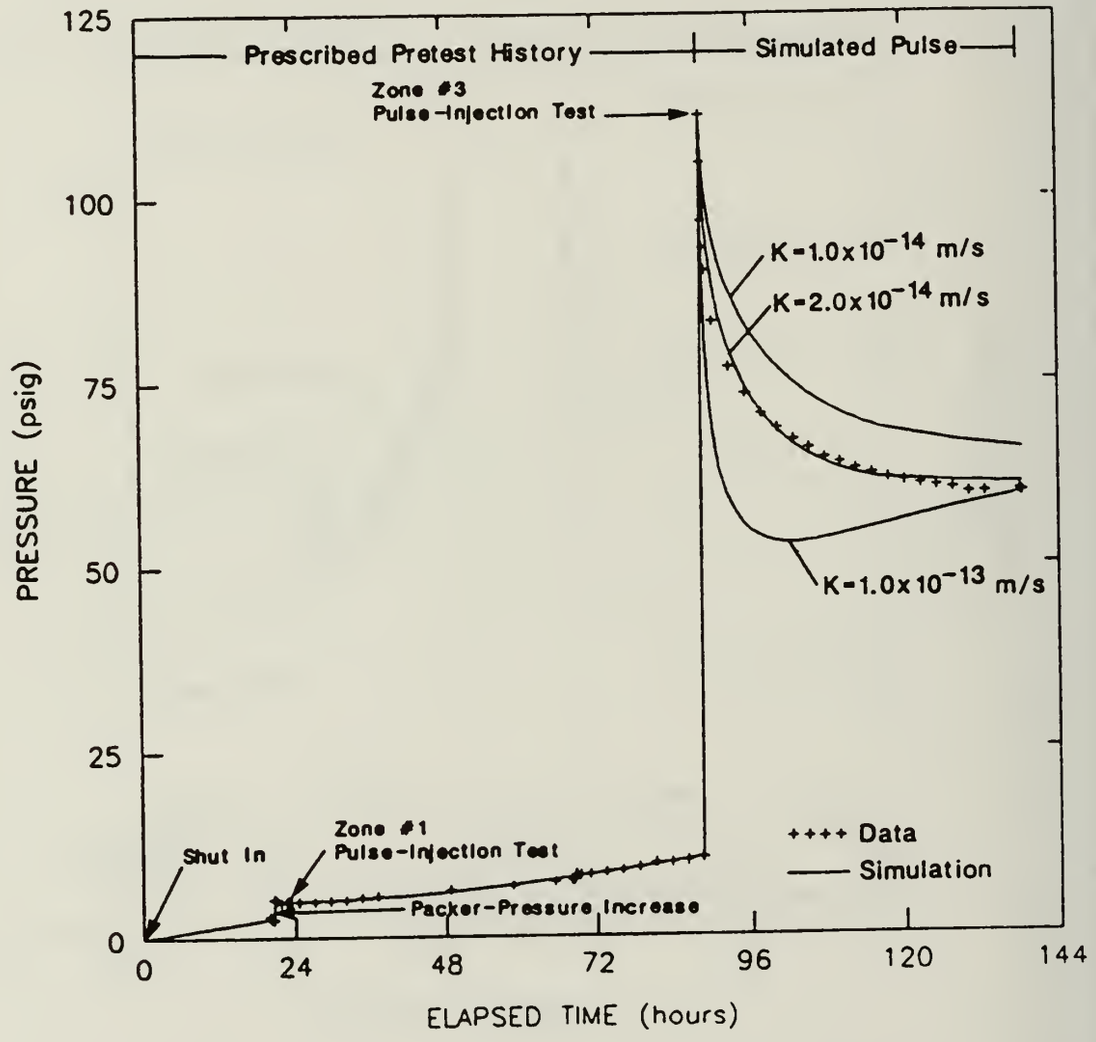

Drawn by	Date	Simulation of the Borehole W850SE Zone #3 Pulse-Injection Test; Formation Pressure - 90 psig and Varying Hydraulic Conductivity
Checked by	Date	
Revisions	Date	
H09700R570		
INTERA Technologies		Figure 5.38

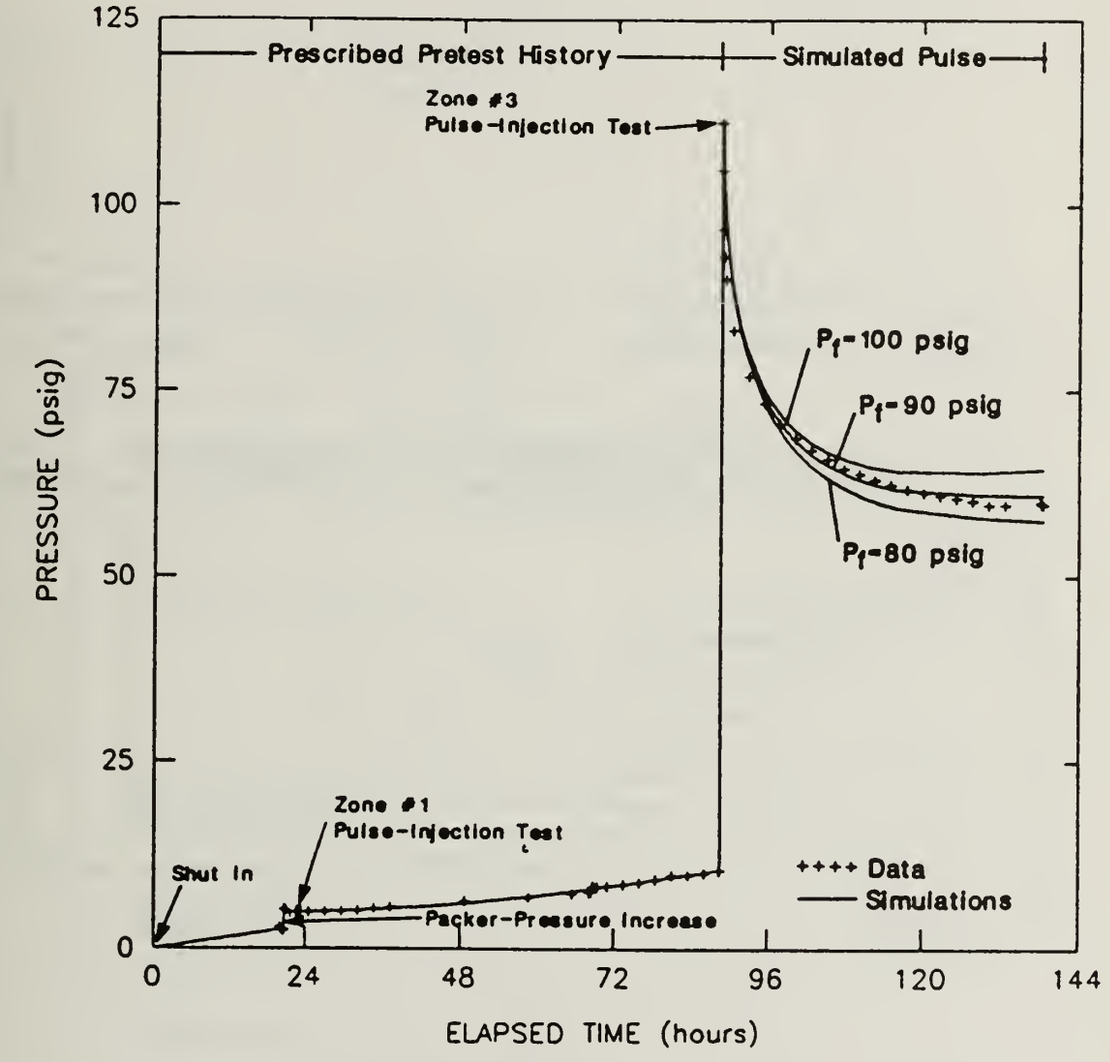

Drawn by	Date
Checked by	Date
Revisions	Date
H09700R570	

Simulation of the Borehole W850SE Zone #3 Pulse-Injection Test; Hydraulic Conductivity = 2.0×10^{-14} m/s and Varying Formation Pressure

INTERA Technologies

Figure 5.39

SHAFT LEVEL: 1320 feet BGS

BOREHOLE LOCATION: W1320E (East Wall)

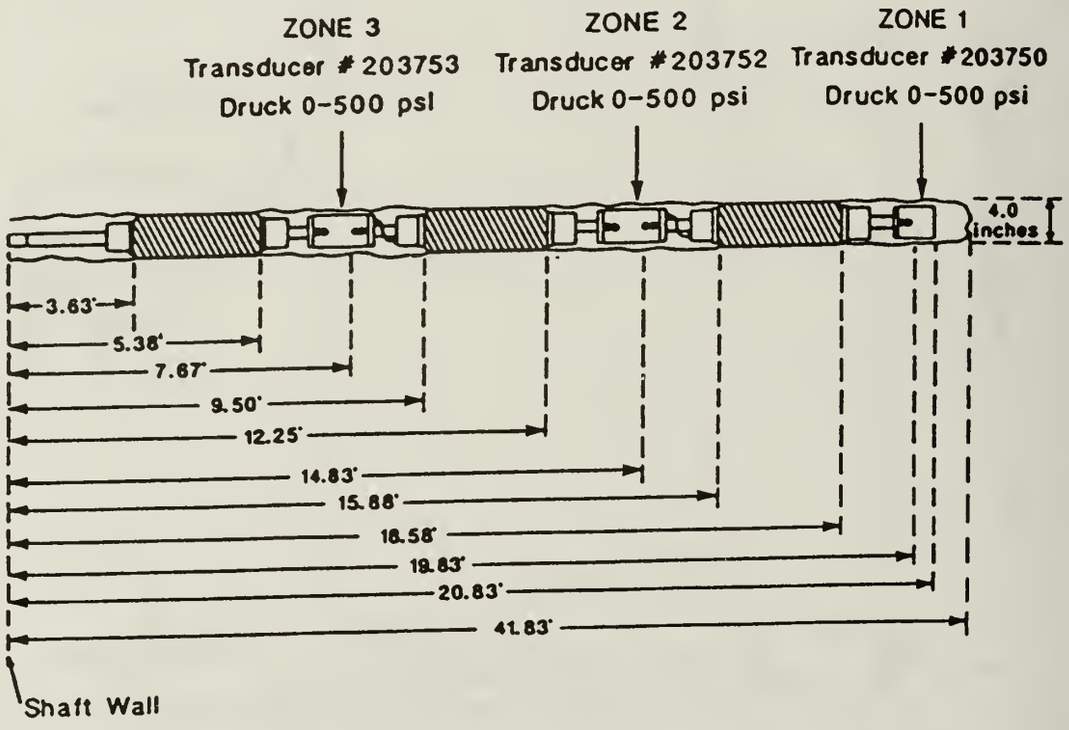

Drawn by	Date
Checked by	Date
Revisions	Date
H09700K570	

Configuration of the Multipacker Test Tool in Borehole W1320E

INTERA Technologies

Figure 5.40

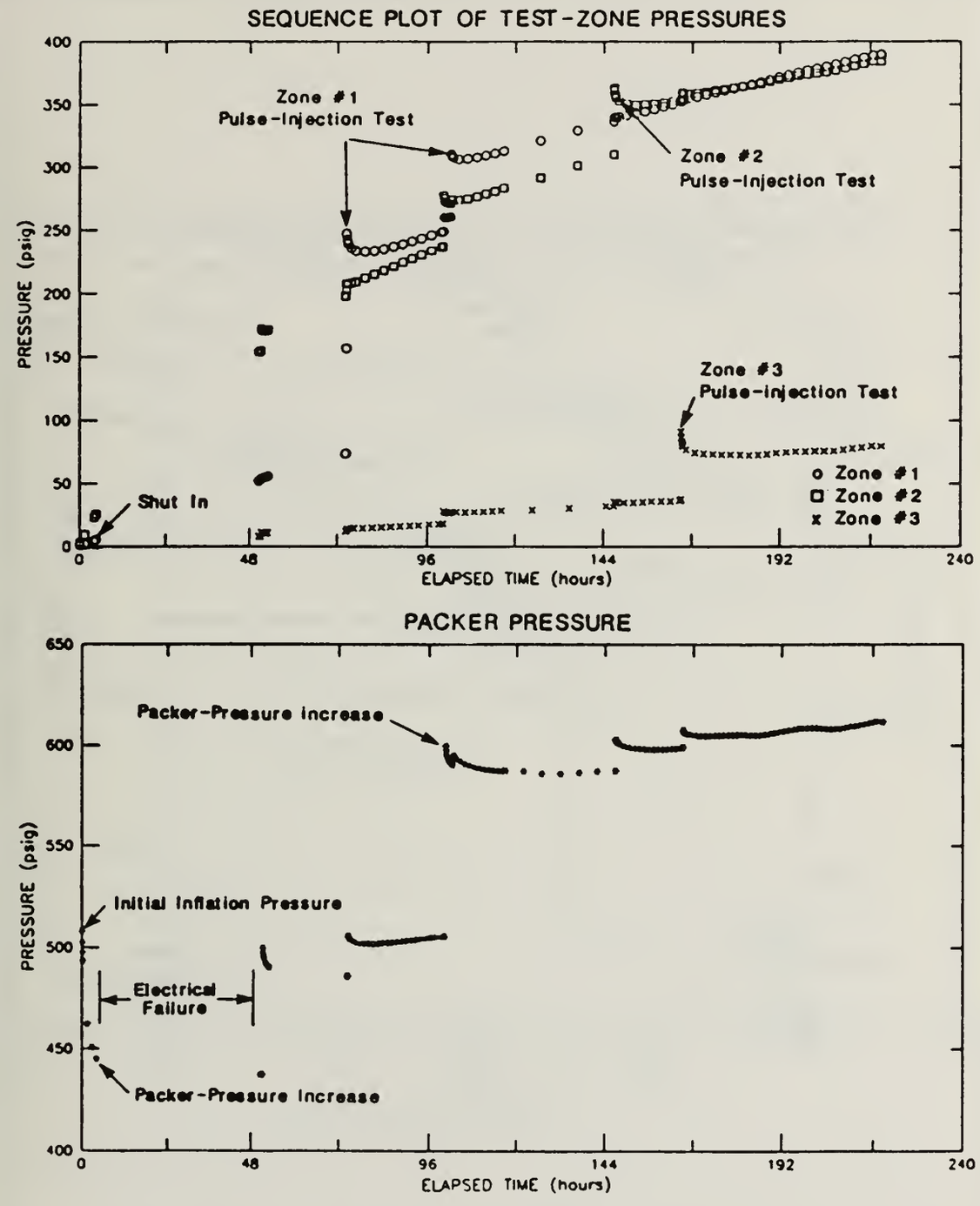

Drawn by	Date
Checked by	Date
Revisions	Date
H09700R570	

Linear-Linear Sequence Plot of the Test-Zone and Packer-Inflation Pressures During Testing in Borehole W1320E

INTERA Technologies

Figure 5.41

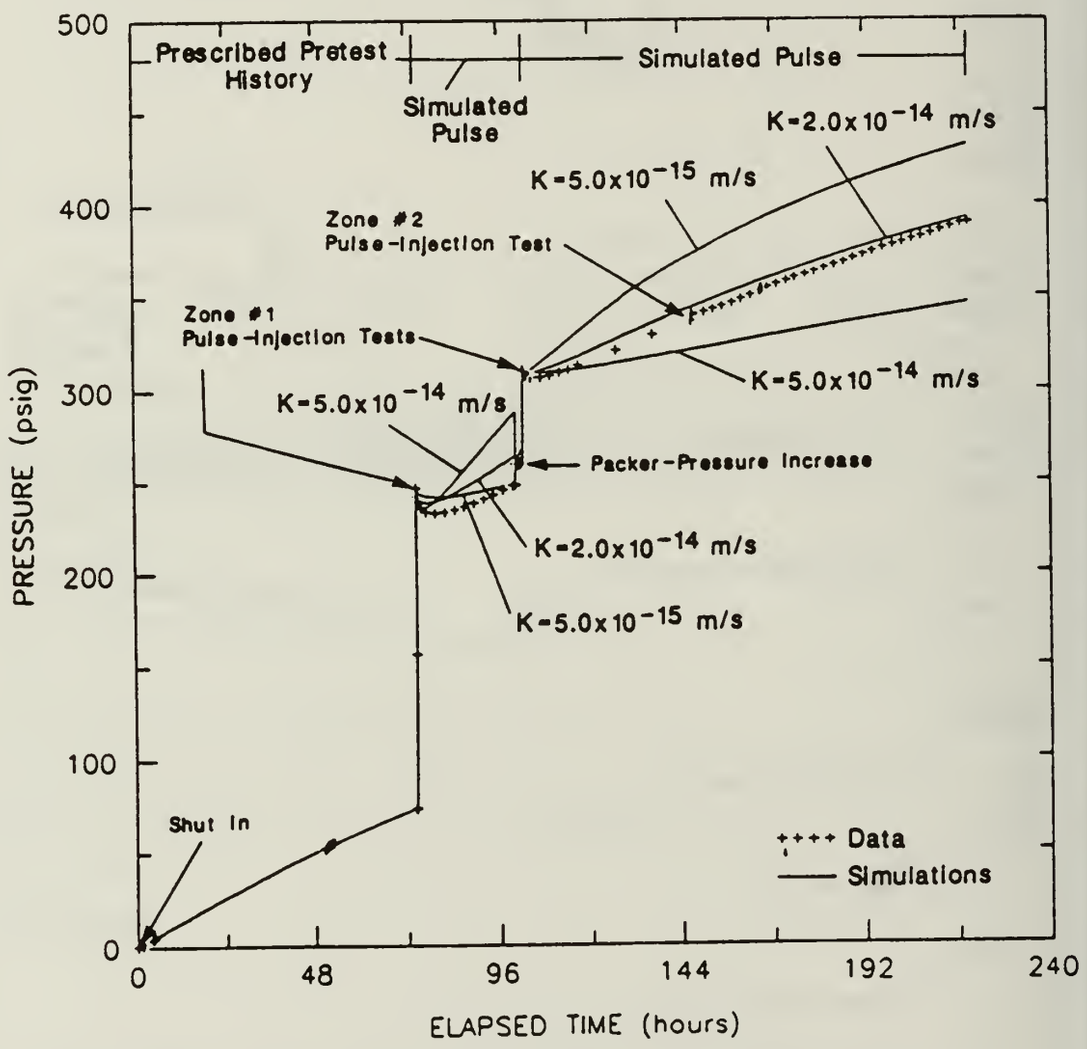

Drawn by	Date
Checked by	Date
Revisions	Date
H09700R570	

Simulation of the Borehole W1320E Zone #1 Pulse-Injection Tests; Formation Pressure = 550 psig and Varying Hydraulic Conductivity

INTERA Technologies

Figure 5.42

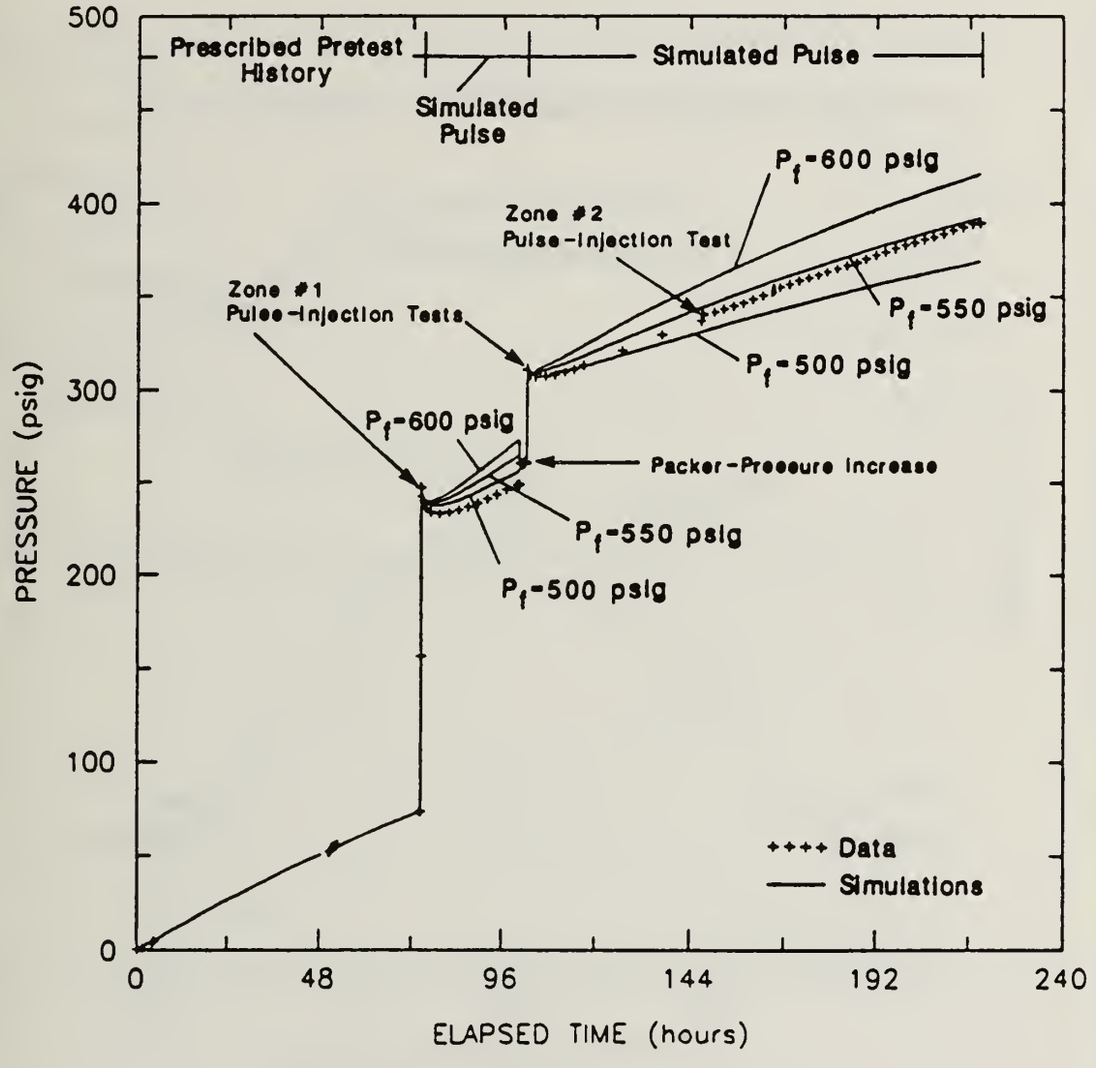

Drawn by	Date
Checked by	Date
Revisions	Date
H09700R570	

Simulation of the Borehole W1320E Zone #1 Pulse-Injection Tests; Hydraulic Conductivity - 2.0 x 10^{-14} m/s and Varying Formation Pressure

INTERA Technologies

Figure 5.43

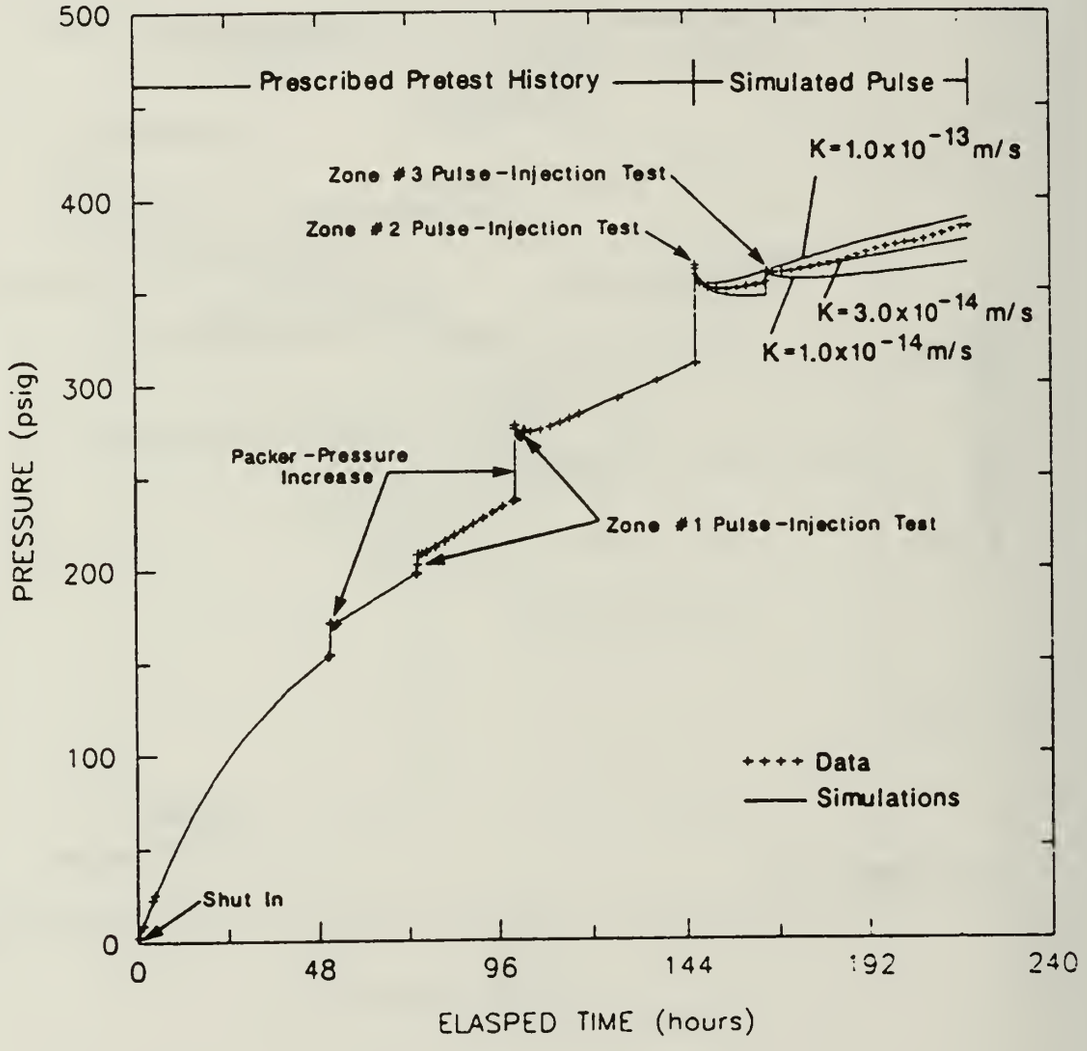

Drawn by	Date
Checked by	Date
Revisions	Date
H09700R570	

Simulation of the Borehole W1320E Zone #2 Pulse-Injection Test; Formation Pressure = 500 psig and Varying Hydraulic Conductivity

INTERA Technologies

Figure 5.44

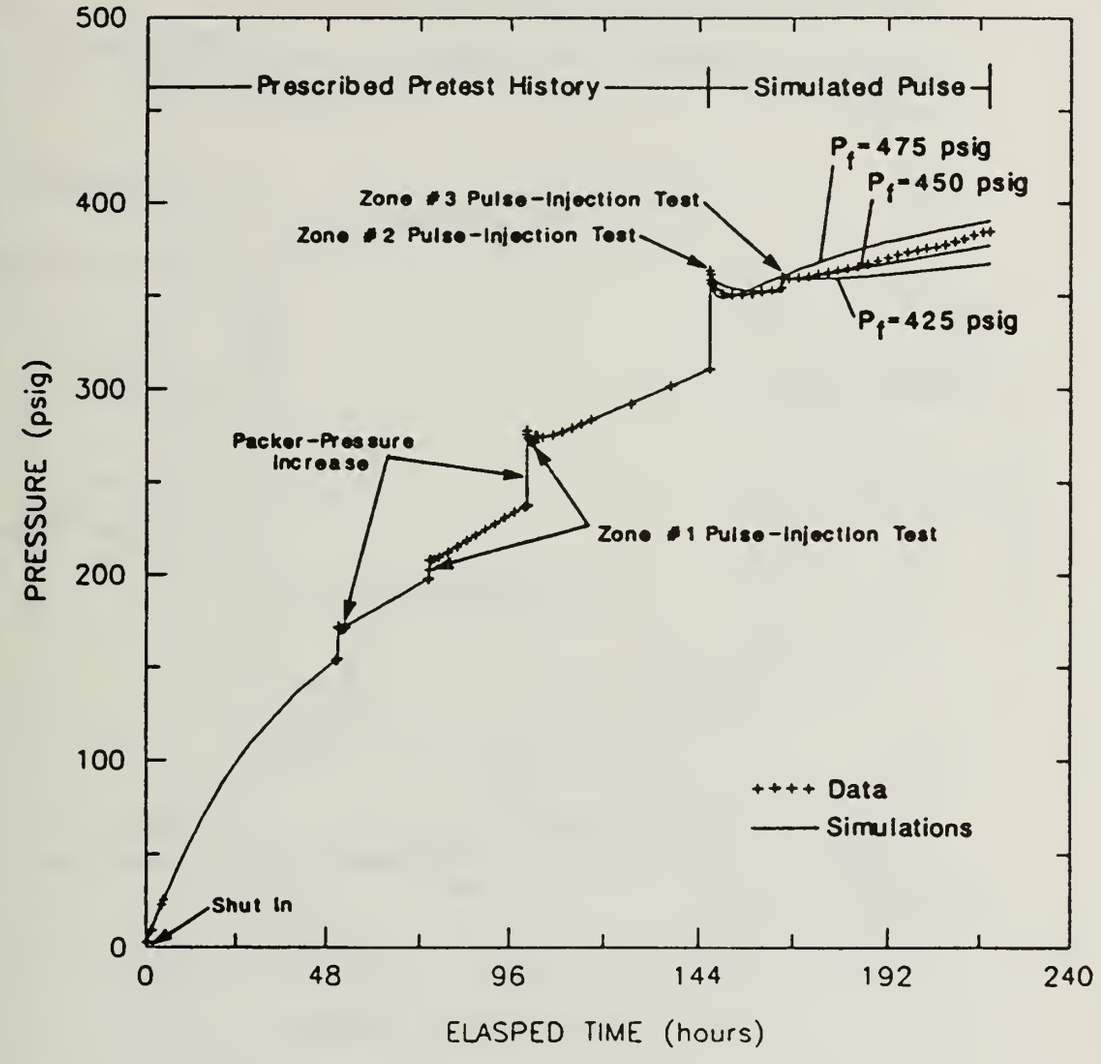

Drawn by	Date
Checked by	Date
Revisions	Date
H09700K570	

Simulation of the Borehole W1320E Zone #2 Pulse-Injection Test; Hydraulic Conductivity = 3.0×10^{-14} m/s and Varying Formation Pressure

INTERA Technologies

Figure 5.45

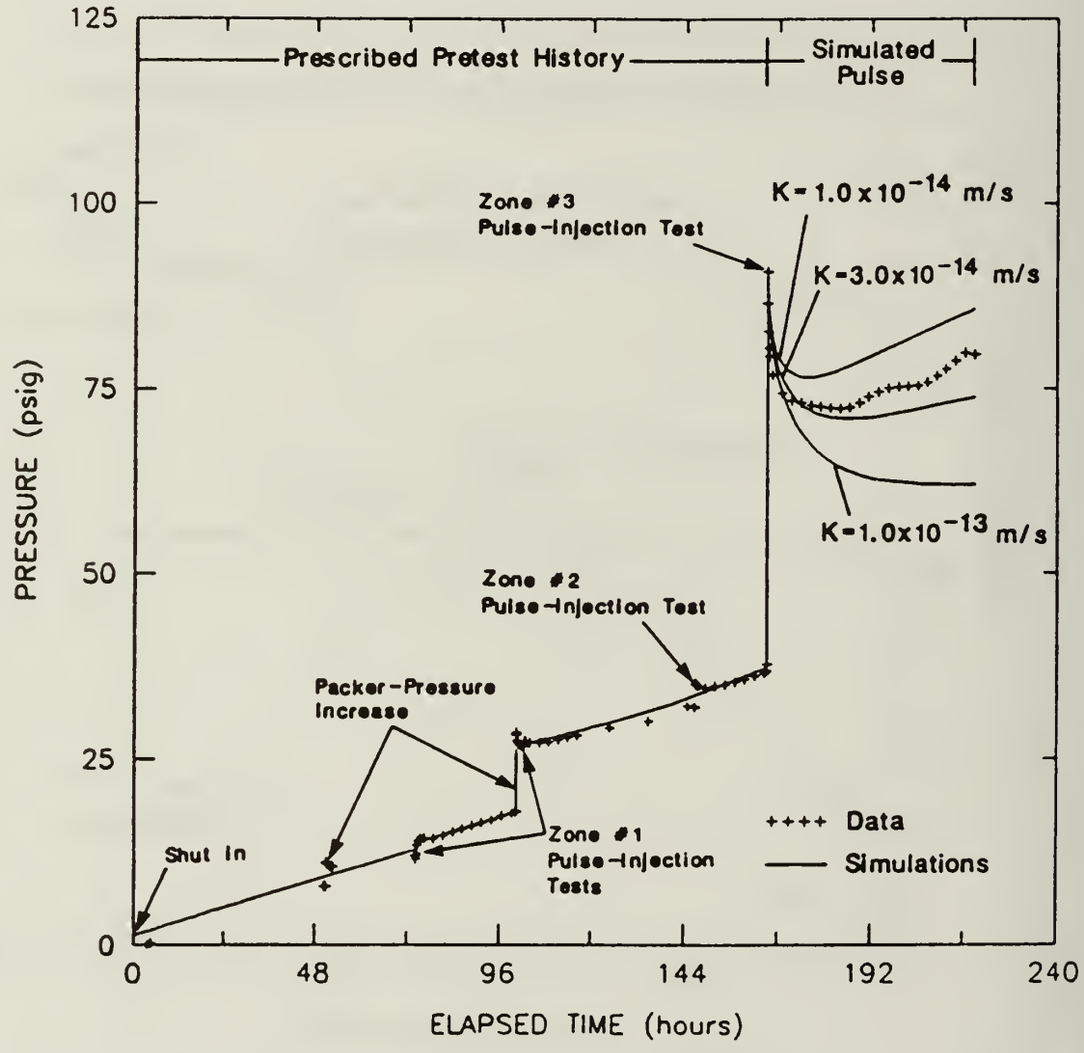

Drawn by	Date	Simulation of the Borehole W1320E Zone #3 Pulse-Injection Test; Formation Pressure = 100 psig and Varying Hydraulic Conductivity
Checked by	Date	
Revisions	Date	
H09700R570		
INTERA Technologies		Figure 5.46

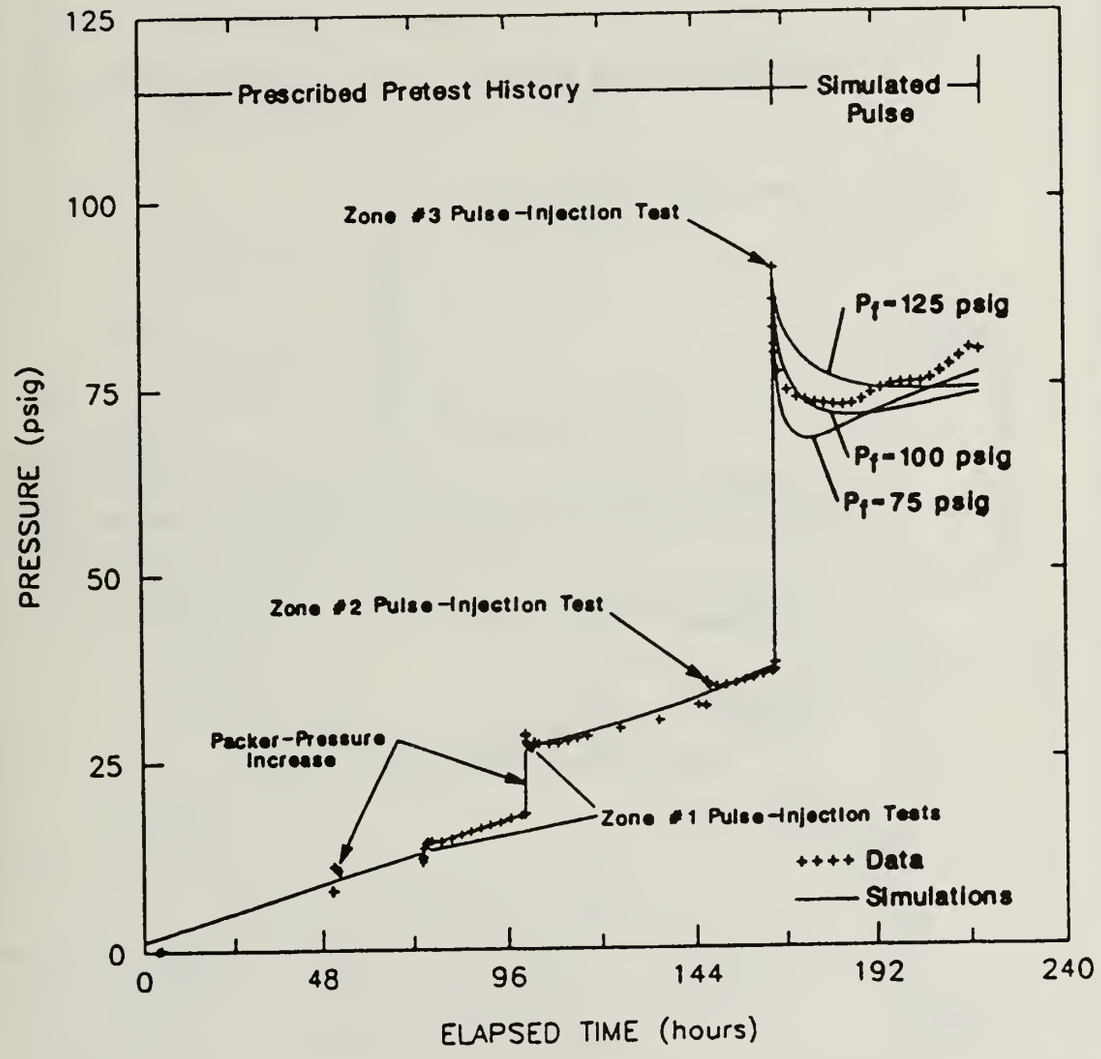

Drawn by	Date
Checked by	Date
Revisions	Date
H09700R570	

Simulation of the Borehole W1320E Zone #3 Pulse-Injection Test; Hydraulic Conductivity = 3.0×10^{-14} m/s and Varying Formation Pressure

INTERA Technologies

Figure 5.47

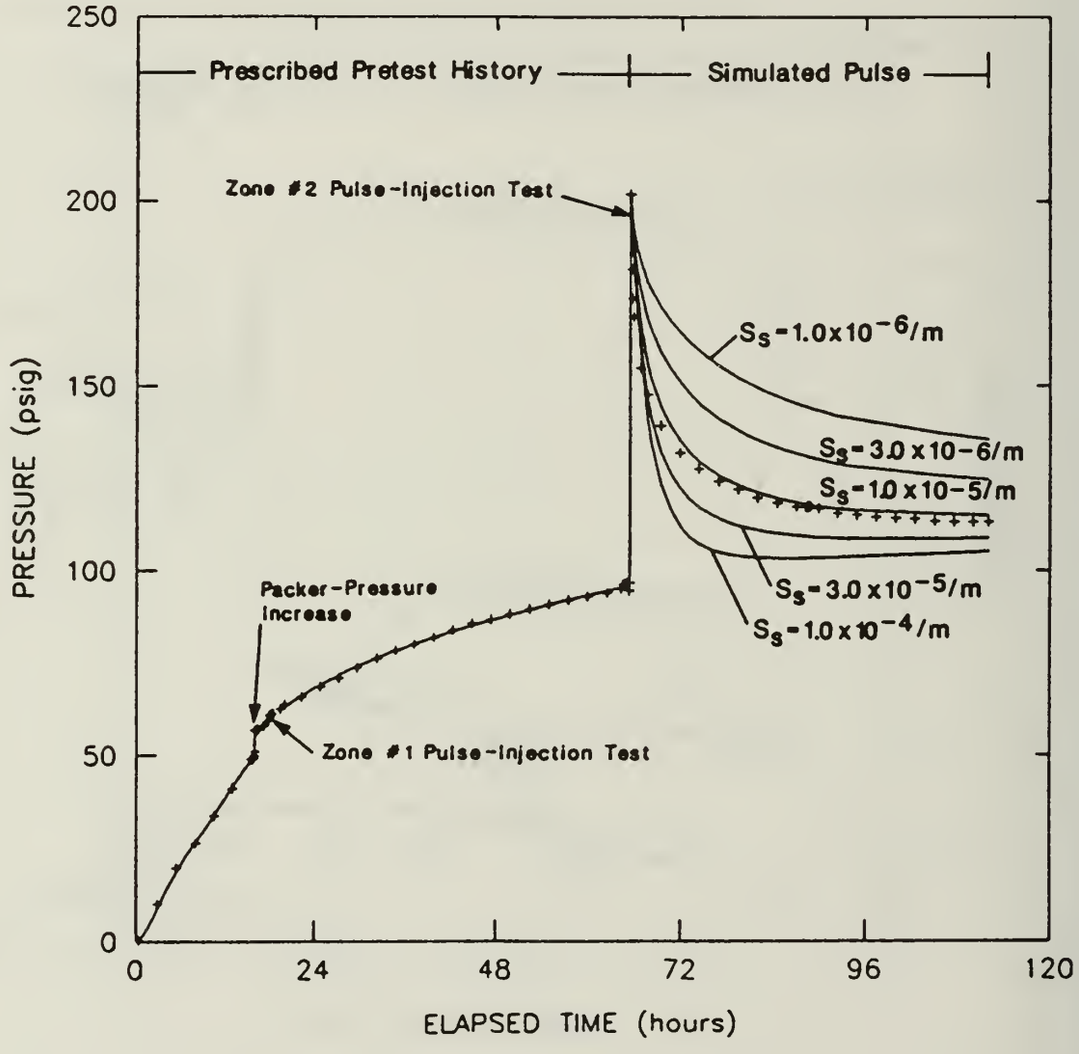

Drawn by	Date	Simulation of the Borehole W805E Zone #2 Pulse-Injection Test; Hydraulic Conductivity = 1.0×10^{-14} m/s, Formation Pressure = 140 psig, and Varying Specific Storage
Checked by	Date	
Revisions	Date	
E:\09700\R570		
INTERA Technologies		Figure 5.48

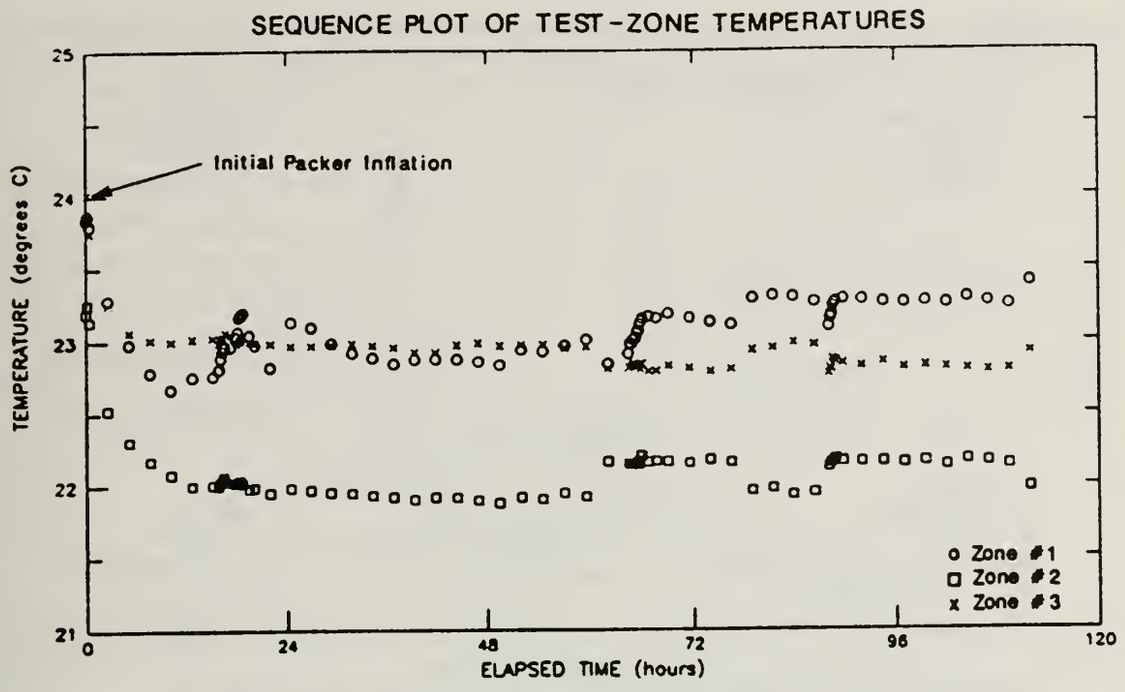

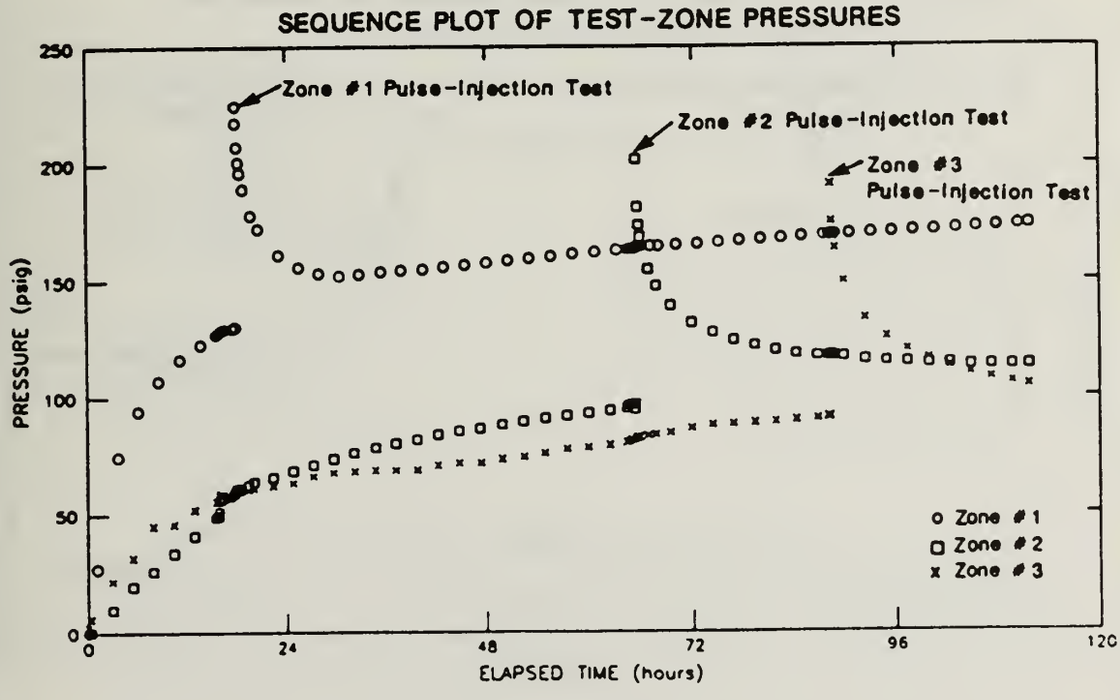

Drawn by	Date
Checked by	Date
Revisions	Date
H09700R570	

Linear-Linear Sequence Plot of the Test-Zone Temperatures and Pressures During Testing in Borehole W805E

INTERA Technologies

Figure 5.50

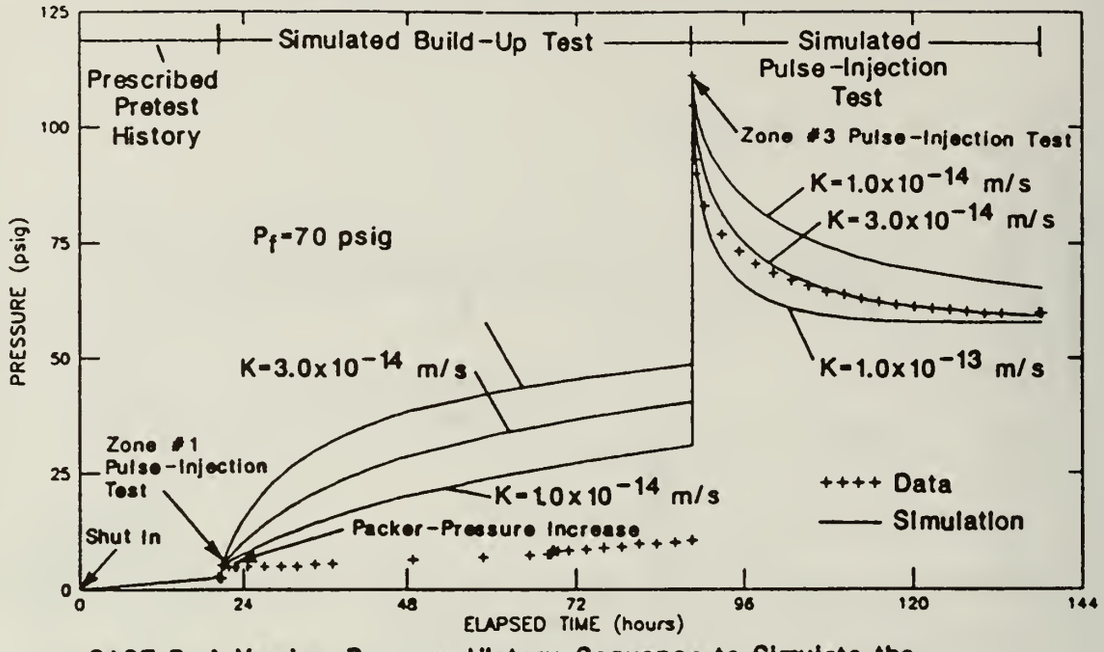

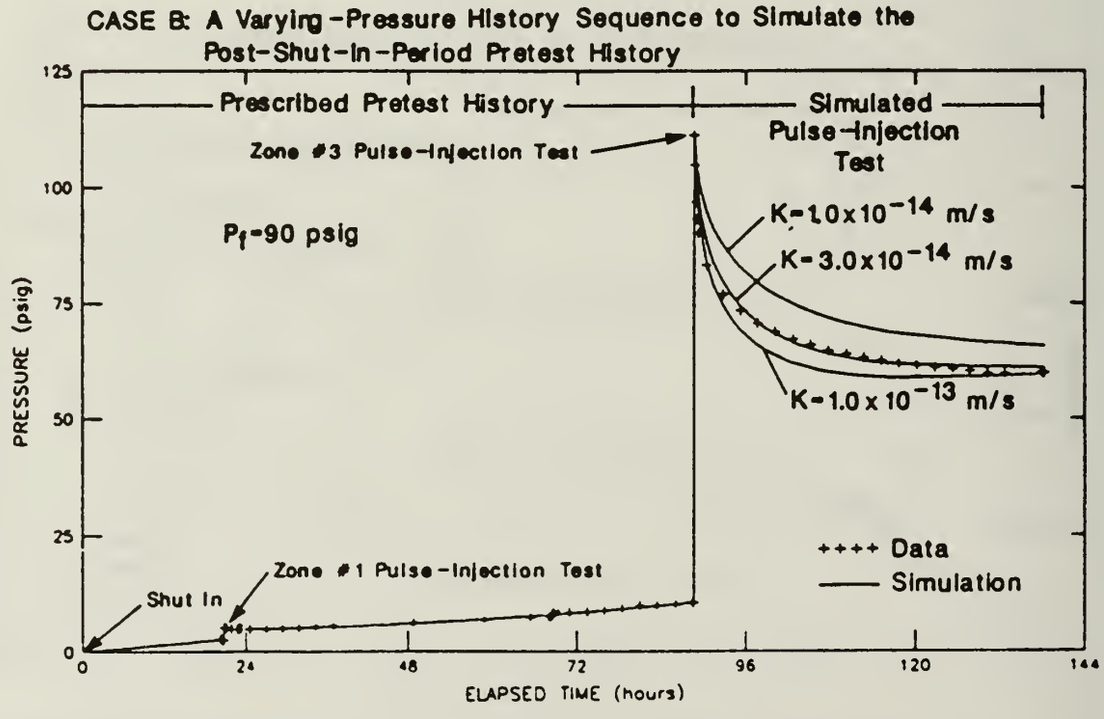

Drawn by	Date
Checked by	Date
Revisions	Date
H09700R570	

Comparison of the Simulations of the Borehole W850SE Zone #2 Pulse-Injection Test Using Case A and Case B

INTERA Technologies

Figure 5.51

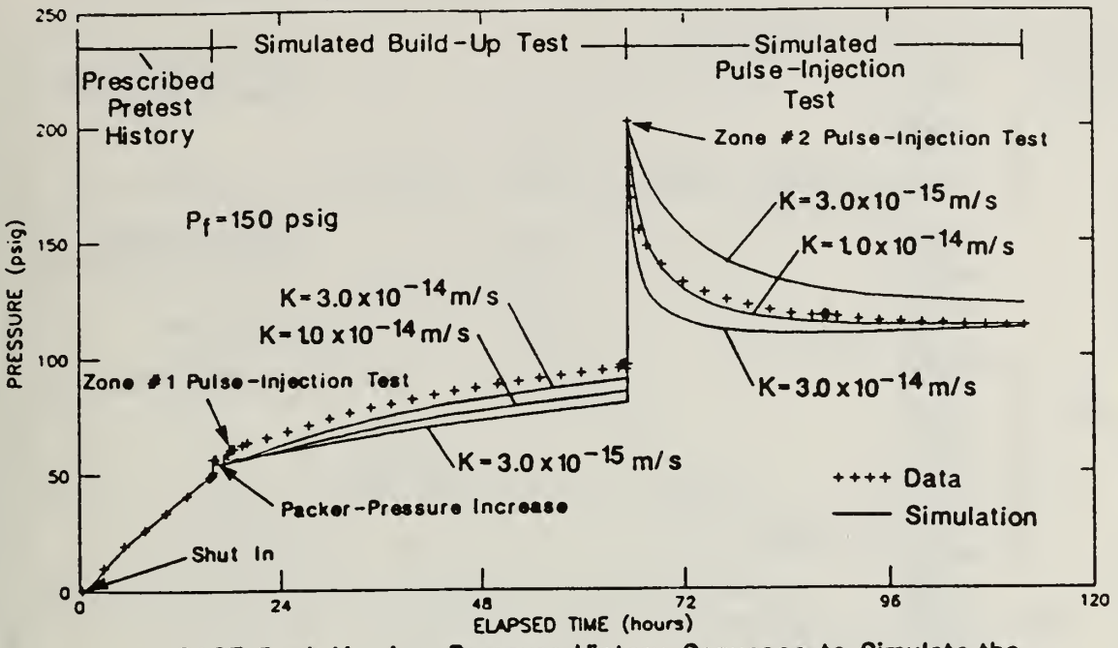

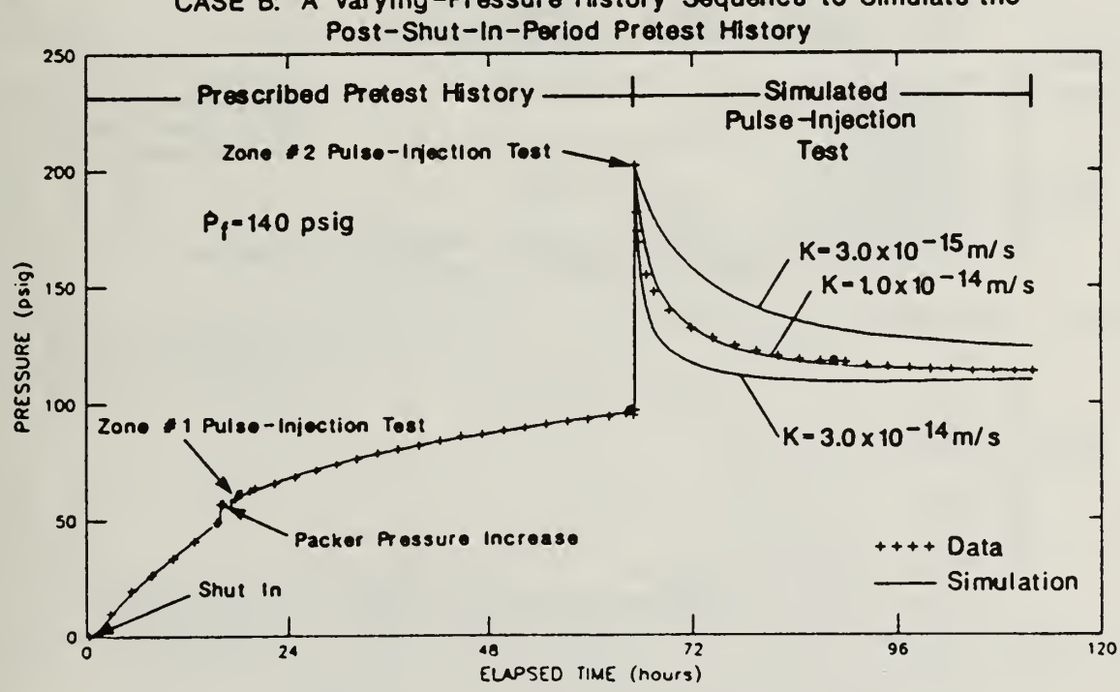

Drawn by	Date
Checked by	Date
Revisions	Date
H0970085670	

Comparison of the Simulations of the Borehole W805E Zone #2 Pulse-Injection Test Using Case A and Case B

INTERA Technologies

Figure 5.52

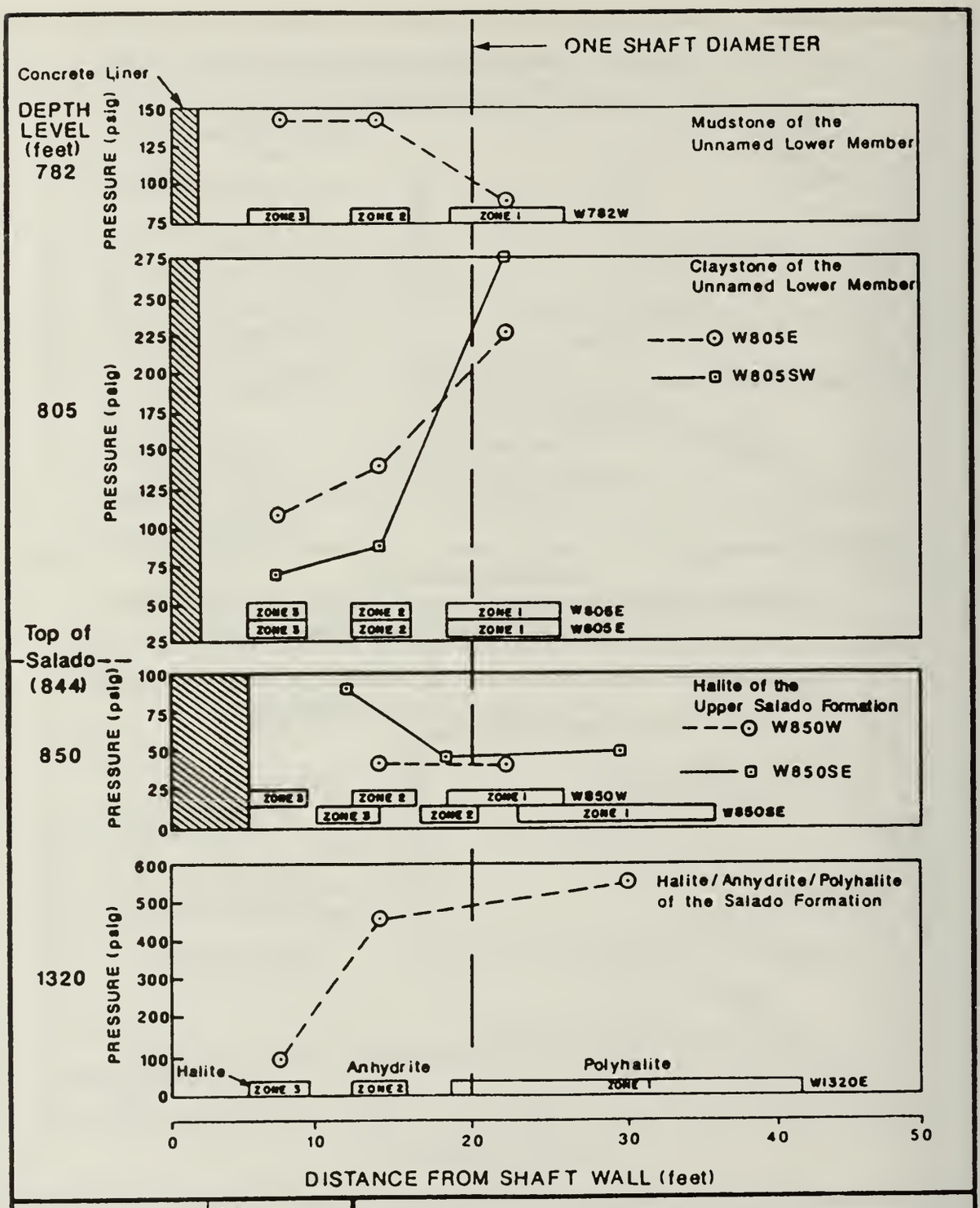

Drawn by	Date
Checked by	Date
Revisions	Date
1104700[illegible]570	

Estimated Formation Pressure vs Distance from the Shaft Wall in the Six Boreholes Tested in the Waste-Handling Shaft

INTERA Technologies

Figure 6.1

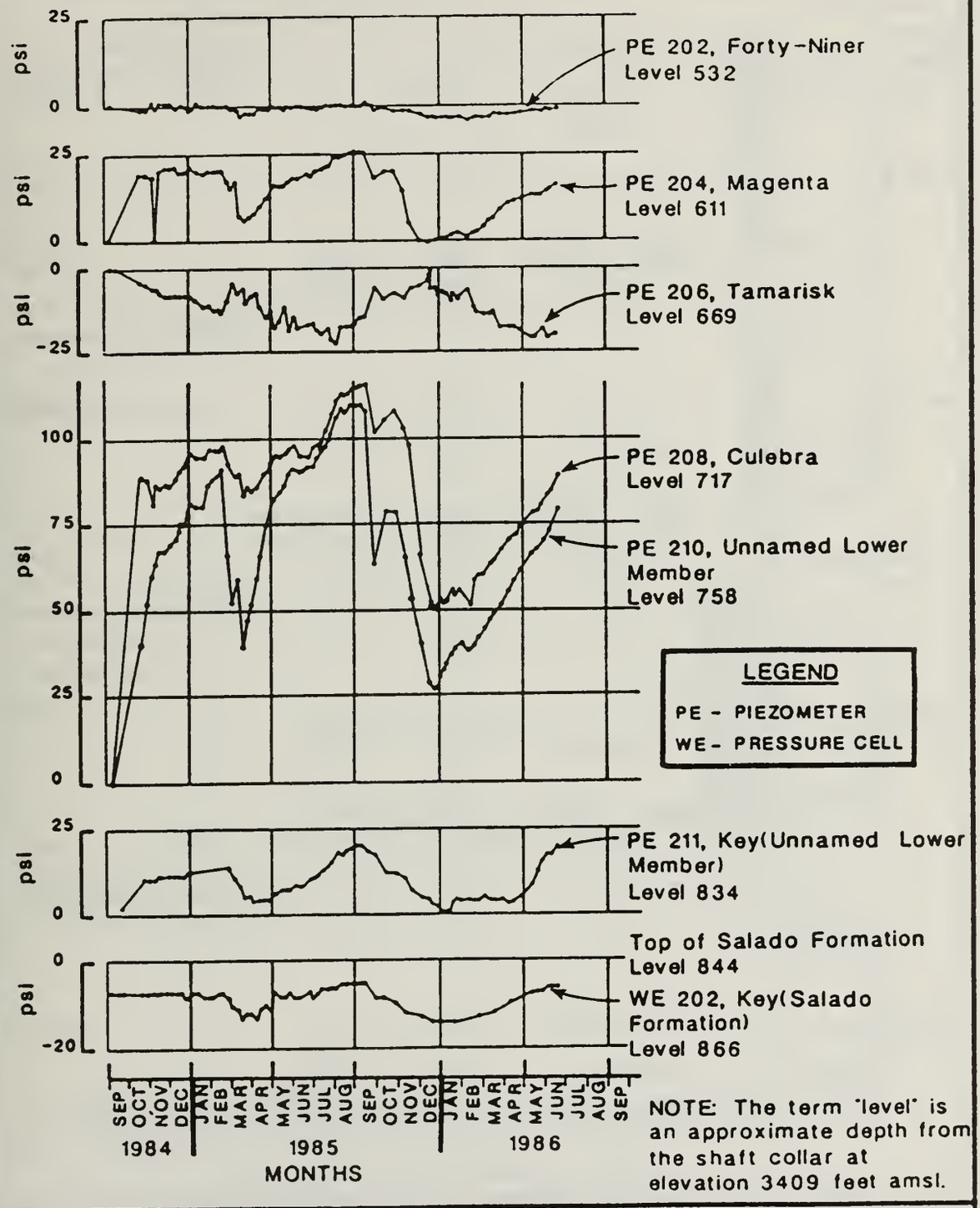

Drawn by	Date
Checked by	Date
Revisions	Date
H09700R570	

Records of Responses of Piezometers and a Pressure Cell in the Waste-Handling Shaft (Data from Bechtel, 1986)

INTERA Technologies

Figure 6.2

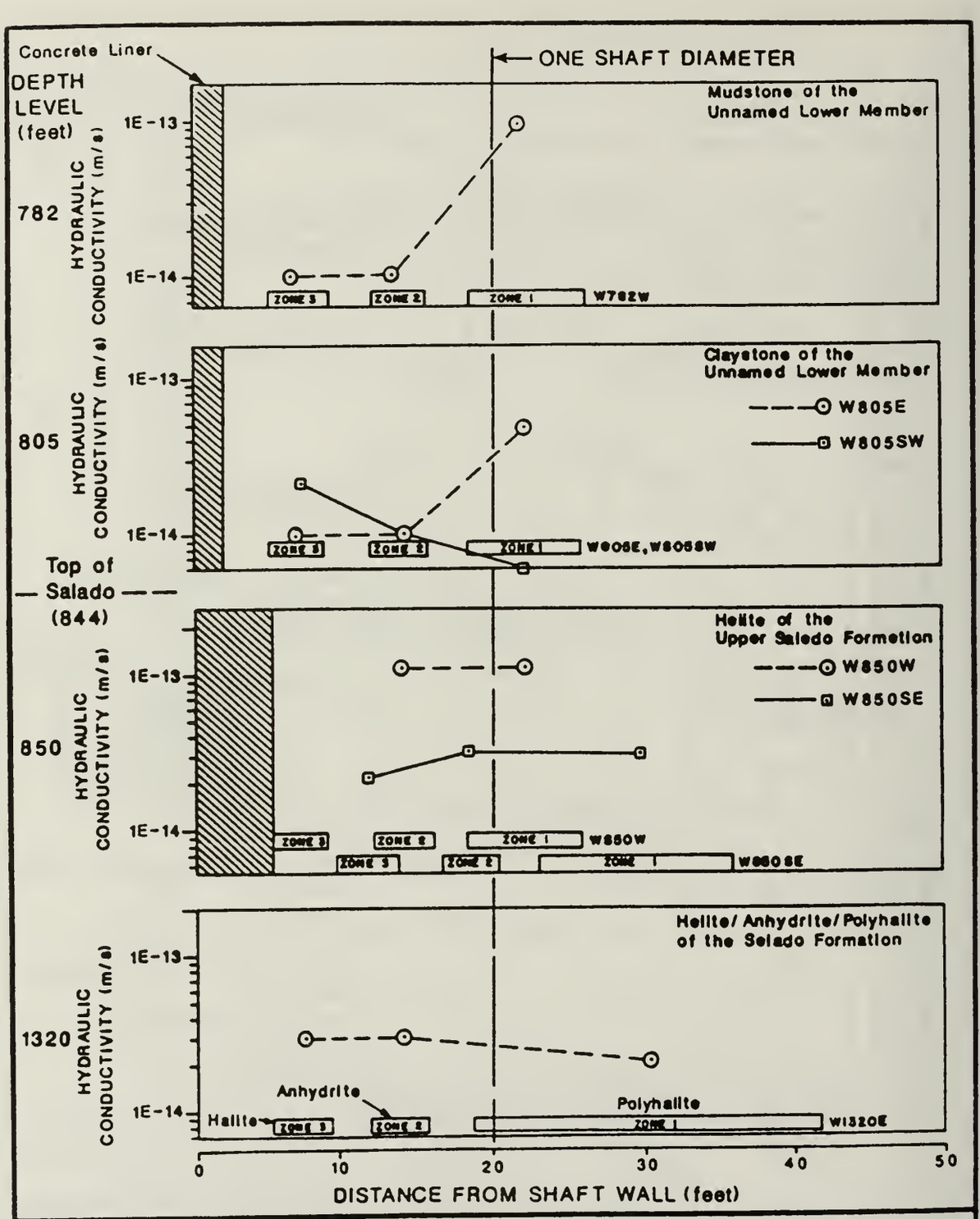

Drawn by	Date
Checked by	Date
Revisions	Date
H09700K570	

Estimated Hydraulic Conductivity vs Distance from the Shaft Wall in the Six Boreholes Tested in the Waste-Handling Shaft

INTERA Technologies

Figure 6.3

BOREHOLE	ZONE #	TEST INTERVAL (feet)	INTERVAL MIDPOINT (feet)	TIME OF DRILLING OF INTERVAL MIDPOINT
W782W	1	18.58 - 26.00	22.29	0150 July 16
	2	12.25 - 15.88	14.07	0030 July 16
	3	5.38 - 9.50	7.44	2350 July 15
W805E	1	18.58 - 26.00	22.29	0030 July 09
	2	12.25 - 15.88	14.07	2315 July 08
	3	5.38 - 9.50	7.44	2220 July 08
W805SW	1	18.58 - 26.50	22.54	2230 August 22
	2	12.25 - 15.88	14.07	2150 August 22
	3	5.38 - 9.50	7.44	2045 August 22
W850W	1	18.58 - 26.00	22.29	2340 July 24
	2	12.25 - 15.88	14.07	2305 July 24
	3	5.38 - 9.50	7.44	2235 July 24
W850SE	1	23.16 - 36.00	29.58	0050 August 05
	2	16.80 - 20.05	18.43	2230 August 04
	3	10.00 - 14.10	12.01	2100 August 04
W1320E	1	18.58 - 41.83	30.21	0030 August 08
	2	12.25 - 15.88	14.07	2150 August 07
	3	5.38 - 9.50	7.44	2045 August 07

NOTE: Distances measured from shaft wall

Drawn by	Date	Estimated Times When the Center of the Test Zones in Each Borehole Were Penetrated by Drilling	
Checked by	Date		
Revisions	Date		
INTERA Technologies			Table 5.1

FLUID PROPERTIES FOR ALL BOREHOLES

Fluid Compressibility	3.1×10^{-10}/Pa (2.1×10^{-6}/psig)
Fluid Density	1200 kg/m^3 (74.8 lb/ft^3)

FORMATION PROPERTIES

BOREHOLE W782W		
	Compressibility	7.0×10^{-11}/Pa (4.8×10^{-7}/psig)
	Porosity	0.25
BOREHOLES W805E and W805SW		
	Compressibility	1.9×10^{-9}/Pa (6.9×10^{-6}/psig)
	Porosity	0.30
BOREHOLES W850W and W850SE		
	Compressibility	4.8×10^{-11}/Pa (3.3×10^{-7}/psig)
	Porosity	0.02
BOREHOLE W1320E		
	Compressibility	2.5×10^{-11}/Pa (1.7×10^{-7}/psig)
	Porosity	0.02

Drawn by	Date	Summary of Model Parameters for the Analysis of Tests in Boreholes in the Waste-Handling Shaft
Checked by	Date	
Revisions	Date	
INTERA Technologies		Table 5.2

BOREHOLE	LITHOLOGY	TEST ZONE	DEPTH INT. (Feet From Shaft Wall)	TEST PERIOD	PRESSURE PULSE (psig)	HYDRAULIC CONDUCTIVITY (m/s)	APPARENT FORMATION PRESSURE (psig)
W782W	Silty Mudstone	1)	18.6-26.0	07/18-22/87	113.3	1.0 E-13	90
		2)	12.3-15.9	07/20-22/87	108.3	1.0 E-14	140
		3)	5.4- 9.5	07/21-22/87	99.4	1.0 E-14	140
W805E	Silty Claystone	1)	18.6-26.0	07/11-15/87	94.7	5.0 E-14	225
		2)	12.3-15.9	07/13-15/87	105.1	1.0 E-14	140
		3)	5.4- 9.5	07/14-15/87	97.8	1.0 E-14	110
W805SW	Silty Claystone	1)	18.6-26.5	08/28-31/87	102.9	6.0 E-15	275
		2)	12.3-15.9	Not Tested		1.0 E-14*	90*
		3)	5.4- 9.5	08/29-31/87	92.6	2.0 E-14	70
W850W	Halite	1)	18.6-26.0	07-30/08-03/87	97.6	1.0 E-13	40
		2)	12.3-15.9	08/2-3/87	116.5	1.0 E-13	40
		3)	5.4- 9.5	07-31/08-3/87	90.4	Not Analyzable	
W850SE	Halite	1)	23.2-36.0	08/19-24/87	103.5	3.0 E-14	50
		2)	16.8-20.5	08/21-24/87	103.1	3.0 E-14	45
		3)	10.0-14.1	08/22-24/87	100.7	2.0 E-14	90
W1320E	Polyhalite/ Anhydrite/ Halite	1)	18.6-41.8	08/11-17/87	173.3	2.0 E-14	550
		2)	12.3-15.9	08/14-17/87	52.6	3.0 E-14	450
		3)	5.4- 9.5	08/15-17/87	53.0	3.0 E-14	100

*Zone #2 analysis from pressure buildup after shut in, August 28 to 31, 1987.

Drawn by	Date
Checked by	Date
Revisions	Date

Summary of Hydraulic Conductivities and Formation Pressures Interpreted from the Testing of the Boreholes in the Waste-Handling Shaft

INTERA Technologies

Table 5.3

E.8 REFERENCES FOR APPENDIX E

Deal, D. E., and J. B. Case, 1987. IT Corporation, Brine Sampling and Evaluation Program, Phase I Report, DOE-WIPP-87-008, prepared by the Engineering and Technology Department of the Management and Operating Contractor, Waste Isolation Pilot Plant Project for the U.S. Department of Energy.

Nowak et al. (Nowak, E. J., D. F. McTigue, and R. Beraun), 1988. Brine Inflow to WIPP Disposal Rooms: Data, Modeling and Assessment, SAND88-0112, Sandia National Laboratories, Albuquerque, New Mexico.

Peterson et al. (E. W. Peterson, P. L. Lagus, and K. Lie), 1987. WIPP Horizon Free Field Fluid Transport Characteristics, SAND87-7164, prepared for Sandia National Laboratories, Albuquerque, New Mexico.

Peterson et al. (E. W. Peterson, P. L. Lagus, J. Brown, and K. Lie), 1985. WIPP Horizon In-Situ Permeability Measurements, SAND85-7166, prepared for Sandia National Laboratories, Albuquerque, New Mexico.

Saulnier, G. J., and J. D. Avis, 1988. Interpretation of Hydraulic Tests Conducted in the Waste-Handling Shaft at the Waste Isolation Pilot Plant (WIPP) Site, SAND88-7001, prepared for Sandia National Laboratories by INTERA Technologies, Inc.

Stormont et al. (J. C. Stormont, E. W. Peterson and P. L. Lagus), 1987. Summary of and Observations about WIPP Facility Horizon Flow Measurements through 1986, SAND87-0176, Sandia National Laboratories, Albuquerque, New Mexico.

APPENDIX F

RADIOLOGICAL RELEASE AND DOSE MODELING FOR PERMANENT DISPOSAL OPERATIONS

Digitized by the Internet Archive
in 2010 with funding from
University of Toronto

TABLE OF CONTENTS

Section		Page
F.1	INTRODUCTION	F-1
F.1.1	Overview of AIRDOS-EPA	F-1
F.1.2	Meteorological Modeling	F-1
F.1.3	Stack Effluent Modeling	F-1
F.1.4	Dispersion Modeling	F-2
F.1.5	Terrestrial Modeling	F-2
F.1.6	Dose Modeling	F-3
F.2	PLUTONIUM-EQUIVALENT CURIE	F-17
F.3	DESCRIPTIONS OF ACCIDENT SCENARIOS ANALYZED IN THE SEIS	F-19
REFERENCES FOR APPENDIX F		F-25

LIST OF TABLES

Table		Page
F.1	Meteorological data: Assessment of routine releases	F-4
F.2	Frequency of atmospheric stability classes for each direction	F-5
F.3	Frequencies of wind directions and true-average wind speeds	F-6
F.4	Frequencies of wind directions and reciprocal-average wind speeds	F-7
F.5	Stack information	F-8
F.6	Terrestrial modeling assumptions	F-9
F.7	Bioaccumulation factors	F-11
F.8	Dose receptor assumptions	F-12
F.9	Dose rate conversion factors	F-13
F.10	Organ dose correction factors	F-14
F.11	Radionuclide specific parameters	F-16
F.12	PE-Ci weighting factors for selected radionuclides	F-18

LIBRARY U. OF I. URBANA-CHAMPAIGN

F.1 INTRODUCTION

This appendix provides information concerning the radiological dose assessment modeling used to evaluate the risks associated with WIPP operations. A discussion of the AIRDOS-EPA computer model and its input parameters for routine and accident conditions is provided, the concept of plutonium equivalent curies is explained, and descriptions of accident scenarios are presented.

F.1.1 OVERVIEW OF AIRDOS-EPA

AIRDOS-EPA (Moore et al., 1979) estimates the radiation dose to either a maximally exposed individual or to an exposed population from the release of a specified quantity of radionuclides to the atmosphere. The code estimates concentrations of radioactivity in air, deposition buildup on ground surface, and ground surface concentrations based on release information, characteristics of the area surrounding the release site (e.g., agricultural productivity and land use), and specified meteorological conditions. These estimates, combined with intake rates for man, were used to estimate the radiation dose to an adult human receptor from potential exposure pathways for routine and accidental releases.

F.1.2 METEOROLOGICAL MODELING

The WIPP site area was modeled as a 50-mile-radius circular grid system with the site located at the center. Site-specific meteorological data, typical of annual average conditions, were specified for the assessment of routine annual releases. The annual frequency of wind direction was first determined for each of the 16 principal compass directions. The frequency of each Pasquill stability category, ranging from category A (very unstable) to category G (extremely stable), was then determined for each of the 16 directions. The average wind speed was entered for each wind direction and Pasquill category. The average depth of the atmospheric mixing layer (lid) for the area was specified to limit the vertical dispersion of the plume after it travels some distance downwind of the source. The value used applies to routine and accidental releases. For the assessment of accidental releases from the WIPP, stable meteorological conditions that allow minimal dispersion were assumed: a wind speed of 2m/s under stability class F (very stable) conditions.

F.1.3 STACK EFFLUENT MODELING

The Waste Handling Building stack and/or the storage exhaust shaft are the two possible release points for routine and accidental releases (release points are referred to as "stacks" for modeling purposes). AIRDOS-EPA requires input describing each area or point of release.

Because the air will be discharged from the "stacks" at a relatively high velocity, the release will effectively take place at a height above the physical stack. Models for

momentum-dominated plumes (Rupp, 1948) were used to estimate effective stack heights for releases associated with routine operations and projected accidents. This method employed an effective "stack velocity" in determining the effective height of the release. For releases associated with postulated accidents, the effective stack heights were estimated using Rupp's equation and reflected actual stack velocity measured during the postulated accidental release.

F.1.4 DISPERSION MODELING

The Gaussian plume model of Pasquill (1961), as modified by Gifford (1961), estimates plume dispersion in the downwind direction. The values recommended by Briggs (1969) for the horizontal and vertical dispersion coefficients were used for dispersion and depletion calculations. The code permits consideration of dry deposition and scavenging for determining deposition of radionuclides on ground surfaces. Dry deposition is the process by which particles are deposited on grass, leaves, and other surfaces by impingement, electrostatic deposition, chemical reactions, or chemical reactions with surface components. The rate of deposition on earth surfaces is proportional to the ground-level concentrations of the radionuclides in air (Slade, 1968).

Scavenging is primarily due to the washout of particles from a plume by rain or snow and is, therefore, a function of the precipitation rate. The scavenging coefficient was averaged over an entire year, including periods during which rain or snow would not fall. Scavenging can thus be described as a continuous removal of a fraction of the plume per second over the entire year.

The value for the total ground deposition rate used in assessing routine releases was the sum of the dry deposition and the scavenging rates. For the accidental release assessment, scavenging due to precipitation was conservatively ignored. The code removes the deposited fraction and maintains a mass balance along the plume as the concentration of the plume decreases.

F.1.5 TERRESTRIAL MODELING

As previously stated, the area surrounding the WIPP site was modeled as a 50-mile-radius circular grid system with the WIPP facilities located at the center. Within the grid, 20 distances were specified in each of the 16 compass directions. Each distance represented the midpoint of a sector. Eleven distances were specified within a 5-mile radius of the WIPP. The remaining nine distances were specified at about 5-mile incremental distances from the center of the site. Within each sector formed by the grid system, WIPP-specific data were used for population, agricultural area, surface-water area, and numbers of beef and dairy cattle. These data are summarized in Section 2.1 of the draft Final Safety Analysis Report (DOE, 1988).

Other factors used in modeling terrestrial and food crop transport are provided in U.S. Nuclear Regulatory Commission (NRC) Regulatory Guide 1.109 (NRC, 1977). One-half of the anticipated operational life of the facility, 12.5 years, was specified as the period of time allowed for long-term buildup of radioactivity on surface soils.

F.1.6 DOSE MODELING

The AIRDOS-EPA computer model estimates radiological intake rates at specified environmental locations. Resultant doses are then calculated through various exposure modes, using the ground-level concentrations in air and ground deposition rates computed from the meteorological input. To estimate the collective population dose, average values in the crosswind direction over each sector were used for the air concentrations and ground deposition rates. The average individual dose was determined by dividing the population dose by the number of individuals in the exposed population. The dose to an individual receiving a maximum dose (maximally exposed) was determined directly by the code. It was assumed that the individual was located on the center line of the discharge plume at the point of highest off-site ground-level concentration or at a designated location. The dose to maximally exposed existing residents at Mills Ranch and to a hypothetical individual residing at the site boundary at the point of maximum air concentration of radionuclides routinely released was also calculated.

Exposure pathways, primarily the air pathway, are discussed in Subsection 5.0. The model calculates doses to total body, lungs, red bone marrow, lower large intestine wall, stomach wall, kidneys, liver, endosteal cells, thyroid, testes, and ovaries. The doses calculated are 50-year dose commitments resulting from a one-year exposure for routine releases or one-time exposure for accidental releases.

The internal dose conversion factors used in the calculation were those reported in Dunning (1986). The inhalation factors were based on the ICRP Task Group Lung Model, which simulates the behavior of particulate matter in the respiratory tract. The inhalation factors used correspond to a median aerodynamic diameter of 0.3 micron. The ingestion factors were based on a four-segment catenary model with exponential transfer of radioactivity from one segment to the next. Retention of nuclides in other organs was represented by linear combinations of decaying exponential functions. In the inhalation and ingestion models, cross-irradiation (irradiation of one organ by nuclides contained in another) is included.

The Dunning dose factors are based on the ICRP and NCRP models endorsed by the DOE in its August 5, 1985, Vaughan memorandum (DOE, 1985). The DOE dose conversion factors are calculated for particles with an activity median aerodynamic diameter (AMAD) of 1 μm. Using DOE recommended methods, Dunning (1986) calculated dose factors for 0.3-μm AMAD particles. Further, Dunning calculated dose factors using the same organ uptake fractions for daughter products as for the parent, as recommended in more recent ICRP guidance. Comparison of the Dunning dose factors with those recommended by the DOE indicates that Dunning's approach is slightly more conservative. External dose rate conversion factors developed by Kocher (1981) are used.

Where the chemical form and solubility of nuclides in the source term was not known, the solubility class which yielded the highest effective dose commitment was used in the model. For the alpha emitters, a quality factor of 20 was used in the calculation as recommended in ICRP Publication 26 (ICRP, 1977).

Input parameters to the AIRDOS EPA model specific to the WIPP site are documented in Tables F.1 through F.11.

TABLE F.1 Meteorological data: Assessment of routine releases

Parameter	Value (units)
Lid Height	1,435 (m)
Average Temperature	288.8 (°K)
Average Rainfall	24.13 (cm/yr)
Frequency of Atmospheric Stability classes for Each Direction	Table F-2
Frequencies of Wind Directions and True-Average Wind Speeds	Table F-3
Frequencies of Wind Directions and Reciprocal-Average Wind Speeds	Table F-4
Pasquill Category Temperature Gradients[a]	
E	0.0055 (°K/m)
F	0.0280 (°K/m)
G	0.0400 (°K/m)

[a] Categories A-D are not utilized in the AIRDOS-EPA Code

TABLE F.2 Frequency of atmospheric stability classes for each direction

SECTOR[a]	Fraction of time in each stability class						
	A	B	C	D	E	F	G
1	0.3701	0.0168	0.0037	0.0299	0.1252	0.1121	0.3422
2	0.4469	0.0163	0.0042	0.0265	0.0898	0.0714	0.3449
3	0.5295	0.0153	0.0088	0.0306	0.0722	0.0482	0.2954
4	0.4420	0.0122	0.0021	0.0326	0.0570	0.0855	0.3686
5	0.5465	0.0178	0.0076	0.0293	0.0561	0.0726	0.2701
6	0.5657	0.0046	0.0062	0.0428	0.0413	0.0428	0.2966
7	0.5331	0.0134	0.0134	0.0404	0.0538	0.0336	0.2723
8	0.6558	0.0061	0.0048	0.0400	0.0461	0.0218	0.2254
9	0.5740	0.0084	0.0042	0.0391	0.0705	0.0517	0.2521
10	0.3376	0.0084	0.0038	0.0287	0.0738	0.1937	0.3540
11	0.1871	0.0100	0.0047	0.0535	0.1212	0.1796	0.4439
12	0.2813	0.0246	0.0086	0.1044	0.1597	0.1413	0.2801
13	0.2030	0.0070	0.0034	0.0240	0.0907	0.1979	0.4740
14	0.2627	0.0208	0.0091	0.1053	0.1756	0.1144	0.3121
15	0.2320	0.0044	0.0132	0.0485	0.1497	0.1174	0.4347
16	0.2981	0.0154	0.0154	0.0615	0.1231	0.0712	0.4153

[a] Wind directions are numbered counterclockwise beginning with 1 for due north.

TABLE F.3 Frequencies of wind directions and true-average wind speeds

Wind Toward[a]	Frequency	Wind Speeds for Each Stability Class (meters/sec)						
		A	B	C	D	E	F	G
1	0.091	3.91	2.62	2.62	3.69	3.29	3.58	2.40
2	0.127	4.37	3.92	3.25	3.94	4.80	5.54	2.71
3	0.188	3.95	3.78	3.85	3.86	4.18	4.56	2.94
4	0.085	3.28	4.01	3.87	3.95	3.92	3.32	2.95
5	0.052	4.47	5.34	6.61	5.32	5.39	4.80	3.01
6	0.049	4.74	5.10	6.25	5.64	6.18	5.16	2.93
7	0.043	4.42	2.98	3.05	4.17	4.91	4.04	2.65
8	0.033	4.08	3.39	4.36	4.23	4.28	3.57	2.65
9	0.034	4.26	4.29	3.15	3.87	4.40	3.79	2.70
10	0.031	4.03	2.27	2.25	3.16	3.52	3.97	2.94
11	0.029	3.57	2.27	2.86	3.31	3.41	4.54	2.79
12	0.031	4.28	3.18	0.85	3.08	4.88	5.21	2.11
13	0.050	5.66	3.37	5.11	4.74	5.09	6.01	3.57
14	0.042	4.85	0.85	4.10	3.73	3.40	5.39	3.00
15	0.038	3.75	3.61	4.08	2.73	3.58	5.81	2.63
16	0.052	3.54	2.28	3.15	2.73	2.45	2.11	2.23

[a] Wind directions are numbered counterclockwise starting at 1 for due north.

TABLE F.4 Frequencies of wind directions and reciprocal-average wind speeds

Wind Toward[a]	Frequency	Wind Speeds for Each Stability Class (meters/sec)						
		A	B	C	D	E	F	G
1	0.091	3.11	2.00	2.00	2.71	2.58	2.78	1.83
2	0.127	3.46	2.74	2.99	2.76	3.48	4.45	2.29
3	0.188	3.04	2.46	3.21	3.09	3.04	3.55	2.12
4	0.085	2.51	3.20	3.33	2.84	2.93	2.50	1.68
5	0.052	3.31	4.09	5.99	4.08	3.68	3.64	1.90
6	0.049	3.11	3.59	5.54	3.81	4.16	3.69	1.96
7	0.043	3.12	1.80	2.80	2.85	3.46	2.57	1.86
8	0.033	2.84	2.28	2.84	2.75	3.21	2.34	1.89
9	0.034	3.00	2.12	2.89	1.99	2.70	2.08	1.91
10	0.031	2.75	1.47	2.25	1.71	2.04	2.51	2.02
11	0.029	2.52	1.40	3.10	1.99	2.30	2.76	2.00
12	0.031	2.68	1.96	0.85	1.47	1.94	2.55	2.11
13	0.050	3.57	1.76	2.64	2.39	2.71	4.35	2.15
14	0.042	3.14	0.85	2.02	1.99	1.71	4.23	2.11
15	0.038	2.50	2.42	2.05	1.62	2.19	1.76	1.83
16	0.052	2.70	1.21	2.89	2.04	1.83	1.17	1.63

[a] Wind directions are numbered counterclockwise starting at 1 for due north.

TABLE F.5 Stack information

Parameter	Waste Handling Building	Storage Exhaust Filter Building
Number of Stacks	1	2
Stack Height	32.0 (m)	7.3 (m)
Stack Diameter	2.4 (m)[a]	3.1 (m)
Velocity of Stack Gas	9.5 (m/s)	13.6 (m/s)

[a] Equivalent diameter.

TABLE F.6 Terrestrial modeling assumptions

Parameters	Value (Units)	Basis
Buildup Time for Surface Deposition	4,562.5 (day)	
Fraction of Locally Grown Produce	1.0	Conservatism
Fraction of Radioactivity Retained on Leafy Vegetables After Washing	0.5	NRC, 1977
Time Delay for Ingestion:		
Pasture Grass by Animals	0 (hr)	NRC, 1977
Stored Feed by Animals	2160 (hr)	
Leafy Vegetables by Man	24 (hr)	
Produce by Man	24 (hr)	
Removal Rate Constant for Physical Loss by Weathering	2.1×10^{-3} (hr^{-1})	NRC, 1977
Pasture Grass	720 (hr)	
Crops and Leafy Vegetables	1440 (hr)	
Agricultural Productivity per Unit Area:		Baes and Orton, 1979
Grass-Cow-Milk Pathway	0.28 (kg/m^2)	
Produce and Leafy Vegetable	1.9 (kg/m^2)	
Effective Surface Density of Soil	240 (kg/m^2)	Moore et al., 1979
Fraction of Yearly and Daily Feed from Pasture	1.0	Conservatism
Consumption Rate of Contaminated Feed or Forage by Animals	15.6 (kg/day)	Baes and Orton, 1979
Transport Time from Animal Feed-Milk-Man	2.0 (day)	NRC, 1977
Average Time from Slaughter of Meat to Consumption	20.0 (day)	NRC, 1977

Appendix F F-9 Table F.6 Sixth Parameter, Value (Units) column: NRC, 1977 should appear in the Basis column.

TABLE F.6 Concluded

Parameters	Value (Units)	Basis
Fraction of Meat-Producing Herd Slaughtered Each Day	2.74×10^{-3}	Conservatism
Muscle Mass of Meat-Producing Animal	200 (kg)	Site-specific evaluation
Milk Production of Cow	11 (l/day)	Site-specific evaluation
Fallout Interception Fraction:		
Pasture	0.57	Miller, 1979
Vegetables	0.20	NRC, 1977
Fraction of Food Grown in Local Gardens:		Conservatism
Produce	0.76	
Leafy Vegetables	1.00	

TABLE F.7 Bioaccumulation factors[a]

Element	Uptake fraction		Concentration factor	
	Milk (days/kg)	Meat (days/kg)	Pasture	Crops
Cobalt	2.0×10^{-3}	2.0×10^{-2}	2.0×10^{-2}	3.1×10^{-3}
Nickel	1.0×10^{-3}	6.0×10^{-3}	6.0×10^{-2}	2.6×10^{-2}
Strontium	1.5×10^{-3}	3.0×10^{-4}	2.5×10^{0}	1.1×10^{-1}
Yttrium	2.0×10^{-5}	3.0×10^{-4}	1.5×10^{-2}	2.6×10^{-3}
Ruthenium	6.0×10^{-7}	2.0×10^{-3}	7.5×10^{-2}	8.7×10^{-3}
Rhodium	1.0×10^{-2}	2.0×10^{-3}	1.5×10^{-1}	1.7×10^{-2}
Antimony	1.0×10^{-4}	1.0×10^{-3}	2.0×10^{-1}	1.3×10^{-2}
Tellurium	2.0×10^{-4}	1.5×10^{-2}	2.5×10^{-2}	1.7×10^{-3}
Cesium	7.0×10^{-3}	2.0×10^{-2}	8.0×10^{-2}	1.3×10^{-2}
Barium	3.5×10^{-4}	1.5×10^{-4}	1.5×10^{-1}	6.5×10^{-3}
Cerium	2.0×10^{-5}	7.5×10^{-4}	1.0×10^{-2}	1.7×10^{-3}
Praseodymium	2.0×10^{-5}	3.0×10^{-4}	1.0×10^{-2}	1.7×10^{-3}
Samarium	2.0×10^{-5}	5.0×10^{-3}	1.0×10^{-2}	1.7×10^{-3}
Europium	2.0×10^{-5}	5.0×10^{-3}	1.0×10^{-2}	1.7×10^{-3}
Thorium	5.0×10^{-6}	6.0×10^{-6}	8.5×10^{-4}	3.7×10^{-5}
Uranium	6.0×10^{-4}	2.0×10^{-4}	8.5×10^{-3}	1.7×10^{-3}
Plutonium	1.0×10^{-7}	5.0×10^{-7}	4.5×10^{-4}	2.0×10^{-5}
Neptunium	5.0×10^{-6}	5.5×10^{-5}	1.0×10^{-1}	4.4×10^{-3}
Americium	4.0×10^{-7}	3.5×10^{-6}	5.5×10^{-3}	1.1×10^{-4}
Curium	2.0×10^{-5}	3.5×10^{-6}	8.5×10^{-4}	6.5×10^{-6}

[a] From Baes et al., 1984.

TABLE F.8 Dose receptor assumptions

Parameter	Value (units)	Basis
Breathing rate of man	9.47×10^5 (cm^3/min)	Conservatism
Depth of water for immersion dose	244 (cm)	Conservatism
Fraction of time spent swimming	0.01	Conservatism
Rate of human ingestion		NRC, 1977
Average individual:		
Produce	190 (kg/yr)	
Milk	110 (l/yr)	
Meat	95 (kg/yr)	
Leafy vegetables	18 (kg/yr)	
Maximum individual:		
Produce	520 (kg/yr)	
Milk	310 (l/yr	
Meat	110 (kg/yr)	
Leafy vegetables	64 (kg/yr)	

TABLE F.9 Dose rate conversion factors[a]

Isotope	Photon Dose Rate Conversion Factors			
	Decay Constant (day^{-1})	Immersion in Air (rem-cm^3/μCi-hr)	Immersion in Water (rem-cm^3/μCi-hr)	Surface (rem-cm^2/μCi-hr)
Co-60	4.96×10^{-4}	2.465×10^{3}	5.360×10^{0}	4.305×10^{-1}
Ni-63	1.98×10^{-5}	0	0	0
Sr-90	8.98×10^{-5}	0	0	0
Y-90	2.60×10^{-1}	0	0	0
Ru-106	1.88×10^{-3}	0	0	0
Rh-106	2.00×10^{3}	2.030×10^{2}	4.390×10^{-1}	4.052×10^{-2}
Sb-125	2.50×10^{-1}	4.204×10^{2}	9.159×10^{-1}	8.948×10^{-2}
Te-125m	1.20×10^{-2}	3.018×10	7.766×10^{-2}	1.359×10^{-2}
Cs-134	9.21×10^{-4}	1.524×10^{3}	3.288×10^{0}	3.001×10^{-1}
Cs-137	8.72×10^{-5}	0	0	0
Ba-137m	3.91×10^{2}	5.867×10^{2}	1.262×10^{0}	1.173×10^{-1}
Ce-144	2.44×10^{-3}	1.785×10	4.124×10^{-2}	4.558×10^{-3}
Pr-144	5.78×10	3.140×10	6.753×10^{-2}	5.276×10^{-3}
Sm-151	2.11×10^{-5}	1.081×10^{-2}	2.748×10^{-5}	1.595×10^{-5}
Eu-152	1.96×10^{-4}	1.126×10^{3}	2.457×10^{0}	2.161×10^{-1}
Eu-154	2.97×10^{-4}	1.228×10^{3}	2.668×10^{0}	2.296×10^{-1}
Th-232	1.35×10^{-13}	1.034×10^{0}	2.612×10^{-3}	2.363×10^{-3}
U-233	1.17×10^{-8}	6.288×10^{-1}	1.561×10^{-3}	1.156×10^{-3}
U-235	2.67×10^{-12}	1.443×10^{2}	3.233×10^{-1}	3.988×10^{-2}
U-238	4.22×10^{-13}	1.038×10^{0}	2.654×10^{-3}	2.519×10^{-3}
Np-237	8.88×10^{-10}	2.967×10	7.132×10^{-2}	2.338×10^{-2}
Pu-238	2.20×10^{-5}	1.372×10^{0}	3.511×10^{-3}	3.304×10^{-3}
Pu-239	7.78×10^{-8}	5.655×10^{-1}	1.431×10^{-3}	1.27×10^{-3}
Pu-240	2.89×10^{-7}	1.304×10^{0}	3.351×10^{-3}	3.144×10^{-3}
Pu-241	1.44×10^{-4}	0	0	0
Pu-242	5.01×10^{-9}	1.085×10^{0}	2.781×10^{-3}	2.608×10^{-3}
Am-241	4.14×10^{-6}	2.486×10	6.161×10^{-2}	1.781×10^{-2}
Cm-244	1.08×10^{-4}	1.274×10^{0}	3.275×10^{-3}	2.895×10^{-3}
Cf-252	7.18×10^{-4}	9.495×10^{-1}	2.443×10^{-3}	1.967×10^{-3}

From Kocher (1981).

TABLE F.10 Organ dose correction factors[a]

Isotope	T.Body	R.Mar.	Lungs	Endost.	S.Wall	Lli Wall	Thyroid	Liver	Kidneys	Testes	Ovaries
Co-60	.570	.540	.530	.560	.490	.490	.660	.500	.530	.700	.480
Ni-63	0	0	0	0	0	0	0	0	0	0	0
Sr-90	0	0	0	0	0	0	0	0	0	0	0
Y-90	0	0	0	0	0	0	0	0	0	0	0
Ru-106	0	0	0	0	0	0	0	0	0	0	0
Rh-106	.553	.528	.518	.582	.478	.468	.647	.484	.507	.692	.466
Sb-125	.539	.511	.502	.582	.461	.451	.631	.467	.489	.678	.447
Te-125m	.170	.032	.083	.137	.060	.052	.170	.061	.138	.260	.059
Cs-134	.560	.540	.530	.580	.490	.480	.662	.490	.520	.700	.480
Cs-137	0	0	0	0	0	0	0	0	0	0	0
Ba-137m	.558	.532	.522	.581	.482	.047	.655	.488	.512	.696	.473
Ce-144	.515	.388	.459	.721	.407	.390	.655	.414	.440	.674	.355
Pr-144	.612	.587	.579	.608	.538	.534	.700	.548	.582	.755	.507
Sm-151	.046	.005	.013	.019	.008	.008	026	.005	.015	.063	.009
Eu-152	.560	.520	.520	.580	.480	.480	.660	.490	.520	.700	.470
Eu-154	.570	.530	.530	.580	.490	.490	.670	.500	.530	.710	.480
Th-232	.096	.043	.066	.111	.055	.051	.098	.058	.062	.114	.049
U-233	.191	.135	.161	.258	.142	.138	.228	.144	.146	.241	.125
U-235	.541	.480	.500	.722	.450	.442	.673	.456	.468	.690	.398
U-238	.050	.016	.028	.047	.022	.020	.042	.023	.024	.059	.020
Np-237	.391	.257	.339	.559	.294	.279	.496	.304	.321	.515	.259
Pu-238	.033	.004	.010	.015	.007	.007	.014	.006	.007	.035	.007

TABLE F.10 Concluded

Isotope	Organ Dose Correction Factors[a]										
	T.Body	R.Mar.	Lungs	Endost.	S.Wall	Lli Wall	Thyroid	Liver	Kidneys	Testes	Ovaries
Pu-239	.074	.039	.049	.077	.042	.041	.068	.041	.042	.087	.037
Pu-240	.034	.005	.011	.016	.007	.007	.016	.007	.008	.037	.007
Pu-241	0	0	0	0	0	0	0	0	0	0	0
Pu-242	.035	.005	.011	.018	.008	.008	.017	.007	.008	.038	.008
Am-241	.385	.171	.317	.570	.261	.231	.504	.285	.317	.528	.221
Cm-244	.034	.004	.009	.012	.005	.006	.012	.004	.005	.037	.006
Cf-252	.042	.007	.013	.020	.009	.009	.019	.008	.008	.047	.009

[a] From Kocher (1981).

TABLE F.11 Radionuclide specific parameters

50-Year Committed Dose Factors - Dunning (1986)

Sol[a]	Isotope	Effective	Red Marrow	Lungs	Endosteal	Stomach Wall	Lli Wall	Thyroid	Liver	Kidneys	Testes	Ovaries
Y[b]	Co-60	2.2×10^{-1}	6.4×10^{-2}	1.3	5.0×10^{-2}	1.0×10^{-1}	3.0×10^{-2}	6.0×10^{-2}	1.2×10^{-1}	5.8×10^{-2}	9.9×10^{-3}	1.8×10^{-2}
D	Ni-63	3.1×10^{-3}	3.0×10^{-3}	1.1×10^{-2}	3.0×10^{-3}	3.1×10^{-3}	3.5×10^{-3}	3.0×10^{-3}	3.0×10^{-3}	3.0×10^{-3}	3.0×10^{-3}	3.0×10^{-3}
Y	Sr-90	1.3	1.1	1.1×10	2.5	8.6×10^{-3}	7.6×10^{-2}	8.5×10^{-3}	8.8×10^{-3}	8.5×10^{-3}	8.5×10^{-3}	8.5×10^{-3}
Y	Y-90	8.4×10^{-3}	1.0×10^{-3}	3.4×10^{-2}	1.0×10^{-3}	1.6×10^{-3}	4.7×10^{-2}	3.5×10^{-5}	1.0×10^{-3}	3.5×10^{-5}	3.5×10^{-5}	3.5×10^{-5}
Y	Ru-106	4.8×10^{-1}	5.1×10^{-2}	3.8	5.1×10^{-2}	5.3×10^{-2}	1.4×10^{-1}	5.1×10^{-2}	5.2×10^{-2}	5.2×10^{-2}	5.2×10^{-2}	5.2×10^{-2}
D	Rh-106	1.5×10^{-6}	1.1×10^{-8}	1.2×10^{-5}	1.0×10^{-8}	3.8×10^{-7}	4.8×10^{-9}	1.1×10^{-8}	1.8×10^{-8}	1.0×10^{-8}	4.4×10^{-9}	5.2×10^{-9}
W	Sb-125	1.2×10^{-2}	2.2×10^{-3}	8.0×10^{-2}	1.2×10^{-2}	2.3×10^{-3}	1.2×10^{-2}	1.2×10^{-3}	3.9×10^{-3}	1.2×10^{-3}	9.0×10^{-4}	1.3×10^{-3}
W	Te-125m	7.3×10^{-3}	1.1×10^{-2}	3.8×10^{-2}	1.2×10^{-1}	4.6×10^{-4}	8.1×10^{-3}	3.7×10^{-4}	3.8×10^{-4}	3.7×10^{-4}	3.4×10^{-4}	4.6×10^{-4}
D	Cs-134	4.6×10^{-2}	4.4×10^{-2}	4.3×10^{-2}	4.0×10^{-2}	4.6×10^{-2}	5.1×10^{-2}	4.1×10^{-2}	4.7×10^{-2}	4.7×10^{-2}	4.8×10^{-2}	4.2×10^{-2}
D	Cs-137	3.2×10^{-2}	3.1×10^{-2}	3.2×10^{-2}	3.0×10^{-2}	3.2×10^{-2}	3.3×10^{-2}	2.9×10^{-2}	3.2×10^{-2}	3.2×10^{-2}	3.2×10^{-2}	3.0×10^{-2}
D	Ba-137m	6.5×10^{-7}	1.3×10^{-7}	4.0×10^{-6}	1.1×10^{-7}	8.3×10^{-7}	3.9×10^{-8}	1.2×10^{-7}	2.3×10^{-7}	1.3×10^{-7}	2.4×10^{-8}	4.0×10^{-8}
Y	Ce-144	3.8×10^{-1}	9.5×10^{-2}	2.9	1.7×10^{-1}	1.0×10^{-2}	1.3×10^{-1}	6.9×10^{-3}	9.4×10^{-1}	8.2×10^{-3}	6.9×10^{-3}	7.1×10^{-3}
Y	Pr-144	4.3×10^{-5}	6.7×10^{-7}	3.5×10^{-4}	6.7×10^{-7}	2.0×10^{-5}	6.0×10^{-7}	5.9×10^{-7}	1.2×10^{-6}	8.9×10^{-7}	5.6×10^{-7}	5.7×10^{-7}
W	Sm-151	3.0×10^{-2}	4.1×10^{-2}	1.2×10^{-2}	5.1×10^{-1}	4.4×10^{-5}	1.9×10^{-3}	6.8×10^{-7}	1.4×10^{-1}	1.2×10^{-6}	6.4×10^{-7}	7.8×10^{-7}
W	Eu-152	2.2×10^{-1}	2.9×10^{-1}	2.1×10^{-1}	8.9×10^{-1}	7.4×10^{-2}	5.6×10^{-2}	3.1×10^{-2}	1.3	1.4×10^{-1}	2.4×10^{-2}	4.8×10^{-2}
W	Eu-154	2.9×10^{-1}	3.9×10^{-1}	2.9×10^{-1}	1.9	6.6×10^{-2}	6.6×10^{-2}	2.6×10^{-2}	1.6	1.2×10^{-1}	2.2×10^{-2}	4.3×10^{-2}
W	Th-232	1.6×10^{-3}	3.3×10^{3}	3.5×10^{3}	4.1×10^{4}	2.8	2.9	2.8	2.3×10	2.9	2.8	2.8
Y	U-233	1.3×10^{2}	2.5	1.1×10^{3}	4.0×10	9.1×10^{-2}	1.2×10^{-1}	9.0×10^{-2}	9.0×10^{-2}	1.6×10	9.0×10^{-2}	9.0×10^{-2}
Y	U-235	1.2×10^{2}	2.5	1.0×10^{3}	3.8×10	8.7×10^{-2}	1.3×10^{-1}	8.7×10^{-2}	8.7×10^{-2}	1.5×10	8.6×10^{-2}	8.6×10^{-2}
Y	U-238	1.2×10^{2}	2.4	9.8×10^{2}	3.5×10	8.0×10^{-2}	1.2×10^{-1}	7.9×10^{-2}	8.2×10^{-2}	1.4×10	8.0×10^{-2}	7.9×10^{-2}
W	Np-237	5.0×10^{2}	7.1×10^{2}	6.0×10	8.8×10^{3}	8.0×10^{-2}	1.5×10^{-1}	4.1×10^{-2}	1.9×10^{3}	1.5×10^{-1}	1.1×10^{2}	1.1×10^{2}
W	Pu-238	4.6×10^{2}	6.5×10^{2}	1.2×10^{3}	8.1×10^{3}	6.0×10^{-3}	1.2×10^{-1}	3.5×10^{-3}	1.8×10^{3}	3.7×10^{-3}	1.0×10^{2}	1.0×10^{-2}
W	Pu-239	5.2×10^{2}	7.3×10^{2}	1.2×10^{3}	9.1×10^{3}	5.6×10^{-3}	1.1×10^{-1}	3.3×10^{-3}	2.0×10^{3}	3.4×10^{-3}	1.2×10^{2}	1.2×10^{2}
W	Pu-240	5.2×10^{2}	7.3×10^{2}	1.2×10^{3}	9.1×10^{3}	5.6×10^{-3}	1.1×10^{-1}	3.3×10^{-3}	2.0×10^{3}	3.5×10^{-3}	1.2×10^{2}	1.2×10^{2}
W	Pu-241	1.0×10	1.5×10	1.2×10	1.9×10^{2}	1.6×10^{-4}	6.7×10^{-4}	5.6×10^{-5}	3.8×10	3.2×10^{-4}	2.5	2.5
W	Pu-242	4.9×10^{2}	6.9×10^{2}	1.1×10^{3}	8.7×10^{3}	5.7×10^{-3}	1.1×10^{-1}	3.3×10^{-3}	1.9×10^{3}	4.1×10^{-3}	1.1×10^{2}	1.1×10^{2}
W	Am-241	5.3×10^{2}	7.5×10^{2}	6.8×10	9.4×10^{3}	1.4×10^{-2}	1.2×10^{-1}	6.3×10^{-3}	2.0×10^{3}	2.1×10^{-2}	1.2×10^{2}	1.2×10^{2}
W	Cm-244	2.8×10^{2}	3.9×10^{2}	7.1×10	4.8×10^{3}	6.3×10^{-3}	1.2×10^{-1}	3.8×10^{-3}	1.1×10^{3}	3.9×10^{-3}	5.9 x 10	5.9 x 10
Y	Cf-252	1.5×10^{2}	1.4×10^{2}	1.1×10^{3}	1.8×10^{3}	6.1×10^{-1}	5.0×10^{-1}	2.2×10^{-1}	4.7×10^{2}	8.5×10^{-1}	2.0 x 10	2.0 x 10

[a] Solubility class yielding highest effective dose for particle size of 1 micron. All other organ dose factors are those yielding highest dose irrespective of solubility class.

[b] D, W, and Y refer to lung clearance rate in days, weeks, or years.

F.2 PLUTONIUM-EQUIVALENT CURIE

The PE-Ci is intended to eliminate the dependency of radiological analyses on the specific radionuclide composition of a TRU waste stream. A unique radionuclide composition and/or distribution is associated with each TRU waste generator and storage facility. By normalizing all radionuclides to a common radiotoxic hazard index, radiological analyses can be conducted for the WIPP which are independent of these variations. Plutonium-239, as a common component of defense TRU wastes, was selected as the radionuclide to which the radiotoxic hazard of other TRU radionuclides could be indexed. Since TRU radionuclides primarily represent inhalation hazards, a valid relationship can be established which normalizes the inhalation hazard of a TRU radionuclide to that of Pu-239.

To obtain this correlation, the 50-year effective committed dose equivalent or dose conversion factor (DCF) for a unit intake of each radionuclide is used. These DCFs have been determined by the method described in International Commission on Radiological Protection (ICRP) Publications 26 and 30 (ICRP-26, 1977; ICRP-30, 1979).

For a known quantity of radioactivity and radionuclide distribution, the Pu-239 equivalent activity is determined using radionuclide-specific weighing factors. The Pu-239 equivalent activity (AM) can be characterized by:

$$AM = \sum_{i=1}^{K} \frac{A_i}{WF_i}$$

where:

K = the number of TRU radionuclides
A_i = the activity of radionuclide i
WF_i = the PE-Ci weighting factor of radionuclide i.

WF_i is further defined as the ratio:

$$WF_i = \frac{E_o}{E_i}$$

where:

E_o (rem/Ci) = the 50-year effective whole-body dose commitment due to the inhalation of Pu-239 particulates with a 1.0-μm AMAD (activity median aerodynamic diameter) and a W pulmonary clearance class.

E_i (rem/Ci) = the 50-year effective whole-body dose commitment due to the inhalation of radionuclide i particulates with a 1.0-μm AMAD and the pulmonary clearance class resulting in the highest 50-year effective committed dose equivalent.

The values of E_o and E_i can be obtained from Dunning (1986, Appendix I). Weighting factors calculated in this manner are presented in Table F-12 for selected radionuclides of interest.

TABLE F.12 PE-Ci weighting factors for selected radionuclides

Radionuclide	Pulmonary Clearance Class[a]	Weighting Factor
Uranium-233	Y	4.0
Neptunium-237	W	1.0
Plutonium-236	W	3.1
Plutonium-238	W	1.1
Plutonium-239	W	1.0
Plutonium-240	W	1.0
Plutonium-241	W	52.0
Plutonium-242	W	1.1
Americium-241	W	1.0
Americium-243	W	1.0
Curium-242	W	29.0
Curium-244	W	1.9
Californium-252	Y	3.5

[a] W = Weekly; Y = Yearly

F.3 DESCRIPTIONS OF ACCIDENT SCENARIOS ANALYZED IN THE SEIS

Operations at the WIPP and accident scenarios postulated in the FEIS have been re-evaluated. This SEIS, consistent with the draft FSAR (DOE, 1988), discusses eleven potential accidents involving CH waste (accidents C0 through C10) and six involving RH waste (accidents R1 through R6). Additional information concerning the accident scenarios described below appears in Section 7.3 of the draft FSAR. The potential extent of damage to the waste container involved and the amount of activity released as a result of the accident are provided.

C0: Forklift Tine Strikes TRUPACT-II in Radiological Control Area. The new TRUPACT-II design necessitates the removal of the TRUPACT-II from the transport trailer in the Radiological Control Area prior to moving the TRUPACT-II into the Waste Handling Building. It is postulated that the forklift may be misaligned and that the forklift tine may strike the TRUPACT-II and cause it to fall off the transporter. Such a fall is not postulated to cause any release because the test conditions for the TRUPACT-II are more severe than this accident.

C1: Vehicle Collision with a Shipping Container in Off-Loading Area. Vehicles transporting waste from offsite will travel at a very low speed (5 to 10 miles/hour) in the off-loading area. A vehicle collision accident would cause less damage to shipping containers on the vehicle than if the containers fell 30 feet, since a 30-foot free fall would result in an impact velocity of 30 miles/hour. DOT regulations specify that a Type B package must be capable of withstanding a 30-foot drop without releasing radioactive material. Since the shipping container is a Type B package, no activity is postulated to be released in this vehicle collision accident.

C2: Drum Drop from a Forklift in the Inventory and Preparation Area. It is postulated that during the handling process a bundle of CH TRU waste drums is dropped from a forklift in the inventory and preparation area. Since the waste drums are Type A packages (per 49 CFR), they are designed and tested to withstand a 4-foot drop onto an unyielding surface without being damaged enough to release any activity. However, since the vertical lift exceeds the rated design, it is conservatively assumed that the drop causes the lids of the drums to be knocked off and the inner plastic liners to tear.

Because of the short distance of the drop, it is assumed that 25 percent of the drum contents is spilled. Of the spilled fraction, 0.1 percent is assumed to be resuspended in the room air. It is conservatively assumed that 5 percent of the total radioactivity contained in the drum is contained in the allowed fraction (1 weight percent) that is less than 10 microns in diameter. Consistent with the assumed frequency of this event, the drum is assumed to contain the average drum content of 12.9 PE-Ci of radioactivity. Since depletion of activity in the room air was considered to be equivalent to resuspension, the total amount of suspended radioactivity in the room air is 1.6×10^{-4} PE-Ci. Credit was taken for the permanently installed on-line high-efficiency particulate air (HEPA) filters,

which reduce the total source term to the environment by a factor of 10^6. Thus, the total activity released to the environment is 1.6×10^{-10} PE-Ci.

To assess the adequacy of facility design and operating procedures with respect to worker safety, the dose consequences to workers have been estimated. Workers in the immediate vicinity of the postulated accident were assumed to respond as trained and immediately exit the work area. Due to the expected slow rate of contamination spread, internal deposition was therefore not estimated for these workers. Although it is unlikely that other workers in the inventory and preparation area would not be made aware of the accident, it was assumed that a worker remains. The total activity inhaled by this worker is therefore related to how long he/she remains in the area before becoming aware of the incident and exits, and how rapidly the release spreads. For the purpose of this analysis, the spread of activity was modeled as half a hemisphere expanding at a rate estimated to be equivalent to the ventilation flow rate for the inventory and preparation area (about 25 cm/s). This expanding "cloud" was assumed to spread to a worker in the neighboring work area, conservatively estimated to be about 20 feet away. An example of this calculation is contained in Section 7.3 of the draft FSAR. The total activity calculated to be inhaled by the worker is 1.0×10^{-8} PE-Ci. Because workers are trained to leave the work area in the event of an accident that could damage a waste container, this estimate is considered to be conservative.

C3: Drum(s) Punctured by a Forklift in the Inventory and Preparation Area. An operator error may result in a forklift hitting a stack of CH TRU waste drums. It was conservatively assumed that two drums were punctured by the forks and that the lid of a third drum was knocked off as it falls from the stack. Operating procedures caution the operator not to back the forks out of a puncture, but it was assumed that the drums become disengaged from the forks. Since not all of the waste fall out of the damaged drums, it was assumed that 25 percent of the radioactive content was released from the drum that lost a lid and 10 percent was released from each punctured drum. As for accident C2, of the spilled fraction that is less than 10 microns in diameter, 0.1 percent was assumed to be resuspended in the room air. Consistent with previous analyses, it was assumed that 5 percent of the total radioactivity contained in the drums was contained in the allowed fraction (1 weight percent) that is less than 10 microns in diameter. Consistent with the frequency of the event, it was further assumed that the drums contain an average loading of 12.9 PE-Ci each. Therefore, 2.9×10^{-4} PE-Ci of radioactivity was suspended in the room air. Credit was taken for the continuously operating on-line HEPA filters, which reduced the total release to the environment by a factor of 10^6. This postulated accident would result in a discharge to the environment of 2.9×10^{-10} PE-Ci.

A worker in an adjacent area could inhale 1.5×10^{-8} PE-Ci based on the exposure model described in C2. Again, the worker's dose commitment is expected to be much smaller than that projected in the SEIS because workers will be trained to evacuate the work area immediately after any accident that could damage a waste container.

C4: Transporter Hits a Pallet in the Underground Storage Area. Operator error may result in the transporter striking a pallet of CH TRU waste drums in the underground storage area and causing the drums to fall. Although it is unlikely that such an incident would cause sufficient damage to the drums to result in an activity release, it was conservatively assumed that the lid of one the drums is knocked off because of the fall and the inner liner tears.

This accident scenario results in a release from the drum identical with the release for accident C2 with the exception that it occurs within the underground storage area. Because of the long distance from the location of the accident to the release point, particle deposition and resuspension were considered. The net result is a conservative estimate of depletion of the released activity by only 20 percent prior to reaching the outside environment. Although they are designed to be activated in case of an accidental release of radioactivity underground, no credit was taken for HEPA filters because they are not continuously on-line and require activation by radiation detection instruments. For the purpose of this analysis, the detection instruments were not assumed to activate the HEPA filters. Occurrence of this postulated accident resulted in a release of 1.3×10^{-4} PE-Ci from the exhaust shaft stack.

Due to the longer distance of travel between the point of release and the worker and the higher rate of airflow within the mine, the release and subsequent exposure were modeled somewhat differently than a release in the Waste Handling Building. For this accident, the release to the drift was assumed to be homogeneously distributed within a segment of the mine volume equivalent to a 4.0 x 3.4 x 6.1 meter cloud volume (8.3×10^{7} cm^3). The worker was subject to exposure during the cloud passage time, approximately 15 seconds based upon a linear ventilation flow rate of 300 cm per second. As a result of this postulated accident, this worker could inhale 1.0×10^{-8} PE-Ci. No credit was taken for respirator protection due to the short duration of exposure. Again, this was considered conservative since the area downstream of the active waste storage room would normally be unoccupied.

C5: Drum(s) Drop from a Forklift in the Underground Storage Area. This accident and its consequences are bounded by the accident described in C4.

C6: Drums Are Punctured by a Forklift or Other Machine in the Underground Storage Area. The conditions for this accident, including drum inventories and releases, were the same as described in C3 except that no credit was taken for HEPA filters. However, since the environmental release actually occurs at some distance from the location of the accident, depletion of the released activity in the underground was considered. As discussed for accident C4, depletion accounts for removal of 20 percent of the activity released from the drums.

The release to the environment from this accident was 2.3×10^{-4} PE-Ci. Worker exposure is modeled as for accident C4. The worker was calculated to inhale 1.8×10^{-8} PE-Ci.

C7: Spontaneous Ignition in a Drum (Waste Handling Building). Although the WIPP WAC controls the types/quantities of pyrophoric materials that could be

shipped to the WIPP, and therefore reduce the likelihood of fire in a waste container, the annual probability of a spontaneous ignition occurring during the processing of a container through the Waste Handling Building was estimated based on past operational experience. The operational database indicated that for roughly 1.8 million container-years of operation with TRU-type wastes similar to that to be handled at the WIPP, there has been only one recorded instance of a container fire. Contributing circumstances to this occurrence included the drum being painted black, exposure to direct sunlight, and improper packaging material. At the WIPP the containers are painted white, not exposed to direct sunlight, and would be certified WAC requirements. Due to these reasons and the low historic probability of a spontaneous ignition, this accident was not considered to be a reasonably foreseeable event in the Waste Handling Building.

C8: Hoist Cage Drop. The design features of the waste hoist and cage are discussed in Section 4.3 of the draft FSAR. The hoist cage is equipped with multiple cables, providing a safety factor that makes its failure a very unlikely event. In the absence of a detailed assessment of the probability of a hoisting system failure, the WIPP Final Environmental Impact Statement and previous draft versions of the WIPP Safety Analysis Report have postulated and evaluated the consequences of a hoist drop accident. Recently, a survey and review of Mine Safety and Health Administration reports on hoisting accidents and a detailed failure modes analysis of the WIPP waste hoisting system have been conducted. Results indicate that hoisting system failure resulting in dropping waste down the shaft has an annual probability of 1.7×10^{-8} or about one catastrophic hoist accident in 60 million years of operation and is therefore not considered a reasonably foreseeable event.

C9: Diesel Fuel Fire in CH TRU Waste Storage Array Underground. In the interest of improved safety, engineering changes have been incorporated that render the underground diesel-fuel fire scenario in the CH TRU Waste Storage Array an unreasonably foreseeable scenario. These design changes can be summarized as follows:

1. All underground diesel vehicles will have a governor that limits speed to 20 mph. This effectively limits the impact energy associated with a vehicle accident.

2. All diesel fuel tanks will comply with specification SAE J703a. This specification requires that the fuel tank survive a 30-foot drop test onto a flat nonyielding surface. (The 30-foot drop is equivalent to a 30-mph impact.) Further, all fuel tanks will be located within the vehicle structure so that they are protected from puncture.

3. All non-steel fuel lines will have braided steel armor and be mounted such that they are protected from abrasion, impact, and operating damage.

4. The fuel tank size will be limited to 60 gallons.

C10: Fire Within a Drum Underground. This postulated accident was similar to C7, previously described. However, due to the length of time the drums would

be present in the underground relative to the time spent in the Waste Handling Building, spontaneous ignition within a drum was more conceivable following emplacement within the storage area. Should a fire occur within a drum within a storage array, it was not expected to propagate to adjacent waste containers.

Since waste containers will spend essentially all of their time in the storage area, the probability of a drum fire will be highest in this area and will subsequently be evaluated. For the purpose of bounding all reasonable foreseeable accident consequences, the drum involved was assumed to contain 1000 PE-Ci of radioactivity. Since only a small fraction of drums in the existing stored waste inventory have a radioactivity content that exceeds 100 PE-Ci, the probability that a 1000 PE-Ci drum would be involved is very small. The spontaneous ignition was assumed to aerosolize 0.25 percent of the radioactivity content and this entire aerosolized fraction was released to the underground drift. This release was subject to a high amount of deposition due to the heated aerosol reacting with the relatively cool surfaces within the facility. This deposition was estimated to result in a depletion fraction of approximately 80 percent. As modeled in accident C4, although the HEPA filtration system is designed to be activated in response to an accidental release of radioactive materials underground, no credit for filtration was assumed in this assessment. The environmental release from the storage exhaust shaft assuming the absence of HEPA filtration was 0.5 PE-Ci. Waste was emplaced and stored downstream of workers and, therefore, no dose consequence to an underground worker is postulated for this event.

R1: Crane Impacts on a Shipping Cask in the Receiving Area. Since the crane velocity and travel distance are limited, and the distance available for shipping cask drop is less than 30 feet, a postulated accident involving a crane hitting a shipping cask is less severe than that of a cask free falling 30 feet to an unyielding surface. A Type B package must withstand a 30-foot free fall without significant damage. Since the shipping cask is a Type B package, no significant activity was considered to be released as a result of this postulated accident.

R2: Shipping Cask Drops in the Receiving Area. A cask dropped in the receiving area will fall less than 30 feet. Since the shipping cask is a Type B package, no activity was considered to be released for this postulated accident.

R3: Shipping Cask Drops in the Cask Preparation Area. A cask dropped in the cask preparation area will drop less than 30 feet. Since the shipping cask is a Type B package, no significant activity is considered to be released for this postulated accident.

R4: RH TRU Waste Canister Drops from Hot Cell into the Transfer Cell. It is possible that a canister containing RH TRU waste could be dropped into the transfer cell from the hot cell (a distance of about 36 feet) in the event that a grapple fails. Even with a drop over this distance, it is unlikely that a canister would be damaged enough to result in any release of radioactivity. However, for this SEIS analysis, it is assumed that the canister does breach and one percent of its total radioactive contents is released. Five percent of the radioactivity released is assumed to be less than 10 microns in diameter and a resuspension factor of $1 \times 10^{-5}/m$ is assumed to apply. Depletion and

resuspension are traded off equally, and the total amount of radioactivity that becomes airborne is assumed to be reduced by the HEPA filters, which provide a 10^{-6} reduction in the source term. The canister is assumed to contain a total of 2.5×10^{3} Ci of radioactivity, including 1000 PE-Ci of transuranics. Based on these assumptions, 3.4×10^{-10} Ci of fission and activation products, and 5.0×10^{-10} PE-Ci of transuranics would be released to the environment. Since the transfer cell and hot cell are not occupied during canister transfer operations, doses to workers inside the facility are not calculated.

R5: Hoist drop with a Canister of RH TRU Waste. As discussed in accident C9, failure of the hoisting system is not a reasonably foreseeable scenario.

R6: Fire Involving RH TRU Waste. RH TRU waste is transferred from the waste shaft to an appropriate storage area by the diesel-powered RH waste transporter. The waste is contained within a steel canister and the canister is transported inside a shielded cask. The storage operation consists of horizontally emplacing an RH TRU waste canister into a borehole and then plugging the borehole with a shield plug; experimental waste canisters are emplaced in vertical boreholes, which are subsequently backfilled. One canister is handled at a time, and after emplacement is complete, the contents are isolated from all reasonably foreseeable accidents. Prior to emplacement, the canister is contained within the facility cask and the combination of this cask and the steel canister prevents the waste from becoming involved in any credible fire during a handling accident. Therefore, a fire involving RH TRU waste would not result in any significant release of radioactivity to the environment or exposure to operating personnel.

REFERENCES FOR APPENDIX F

Baes, C. F., and T. H. Orton, 1979. "Productivity of Agricultural Crops and Forage," in Hoffman, F. O., and C. F. Baes ed., 1979, A Statistical Analysis of Selected Parameters for Predicting Food Chain Transportation and Internal Dose of Radionuclides, ORNL/NUREG/TM-282.

Baes et al. (Baes, C. F., R. D. Sharp, A. L. Sjoreen, and R. W. Shor), 1984. A Review and Analysis of Parameters for Assessing Transport of Environmentally Released Radionuclides Through Agriculture, ORNL-5786, Oak Ridge National Laboratory, Oak Ridge, Tennessee.

Briggs, G. A., 1969. "Plume Rise," AEC Critical Review Series, TID-25075.

Davies, 1966. Aerosol Science. Academic Press, New York.

DOE (Department of Energy), 1985. "Radiation Standards for the Protection of the Public in the Vicinity of DOE Facilities," Memorandum from William A. Vaughan, Assistant Secretary for Environment, Safety, and Health, U.S. Department of Energy (August 5, 1985), Washington, D.C.

DOE (U.S. Department of Energy), 1988. Final Safety Analysis Report, Waste Isolation Pilot Plant (Draft), DOE/WIPP 88-XXX, Carlsbad, New Mexico.

Dunning, D. E., 1986. Estimates of Internal Dose Equivalent From Inhalation and Ingestion of Selected Radionuclides, WIPP-DOE-176, Rev. 1, Westinghouse Electric Corporation - Advanced Energy Systems Division, Albuquerque, New Mexico.

Gifford, F. A., 1961. "Use of Routine Meteorological Observations for Estimating Atmospheric Dispersion," Nuclear Safety 2 (4):47-57.

ICRP (International Commission on Radiological Protection), 1977. Recommendations of the International Commission on Radiological Protection, ICRP Publication 26 (ICRP 77), Pergammon Press, Elmsford, New York.

ICRP (International Commission on Radiological Protection), 1979. Limits for Intakes of Radionuclides by Workers, ICRP Publication 30 (ICRP 79a) Pergammon Press, Elmsford, New York.

Kocher, D. C., 1981. Dose Rate Conversion Factors for External Exposure to Photons and Electrons, NUREG/CR-1918, ORNL/NUREG-79.

Miller, C. W., 1979. "The Interception Fraction," in Hoffman, F. O., and C. F. Baes ed., A Statistical Analysis of Selected Parameters for Predicting Food Chain Transport and Internal Dose of Radionuclides, Final Report, ORNL/NUREG/TM-282.

Moore et al. (Moore, R. E., C. F. Baes III, L. M. McDowell-Boyer, A. P. Watson, F. O. Hoffman, J. C. Pleasant, and C. W. Miller), 1979. AIRDOS-EPA: A Computerized Methodology for Estimating Environmental Concentrations and Dose to Man for Airborne Release of Radionuclides, Oak Ridge National Laboratory, Oak Ridge, Tennessee.

NRC (U.S. Nuclear Regulatory Commission), 1977. Regulatory Guide 1.109, Calculation of Annual Doses of Man from Routine Releases of Reactor Effluents for the Purpose of Evaluating Compliance with 10 CFR Part 50, Appendix I (Revision I), Office of Standards Development.

Pasquill, F., 1961. "The Estimation of the Dispersion of Windborne Material," Metereological Mag., Vol. 90, pg. 33.

Rupp, A. F., 1948. Dilution of Stack Gases in Cross Winds, USAEC Report AECD-1811 (CE-1620) Clinton Laboratories.

Slade, D. H., ed., 1968. Meteorology and Atomic Energy - 1968, U.S. AEC/Division of Technical Information.

APPENDIX G

TOXICITY PROFILES, RISK ASSESSMENT METHODOLOGY, AND MODELS FOR CHEMICAL HAZARDS

LIBRARY U. OF I. URBANA-CHAMPAIGN

TABLE OF CONTENTS

Section		Page
G.1	INTRODUCTION	G-1
G.2	1,1,2-TRICHLORO-1,2,2-TRIFLUOROETHANE	G-2
G.3	METHYLENE CHLORIDE	G-4
G.4	1,1,1-TRICHLOROETHANE	G-7
G.5	CARBON TETRACHLORIDE	G-10
G.6	LEAD	G-13
G.7	TRICHLOROETHYLENE	G-16
G.8	AIR DISPERSION MODEL	G-19
G.9	EXPOSURE ASSESSMENT	G-21
G.10	RISK ESTIMATION	G-23
REFERENCES FOR APPENDIX G		G-26

LIBRARY U. OF I. URBANA-CHAMPAIGN

G.1 INTRODUCTION

Toxicity profiles are provided to give the reader a brief introduction and understanding of the chemical components and their potential health effects. It is important to remember that any chemical can cause health effects if individuals are exposed to high enough doses.

The profiles are intended to provide information on:

- Physical/Chemical Properties: A description of properties that aid in predicting how the chemical will behave in the environment.
- Fate and Transport: Indicates, where possible, what happens to the chemical within the environment.
- Health Effect: Background information on potential health effects in humans or animals from acute or chronic exposures. In addition, information is provided on various exposure routes (i.e., inhalation, oral or dermal).
- Effects on Wildlife: Includes a discussion of the toxic effects of the chemicals on aquatic and terrestrial organisms.
- Regulatory Standards and Guidelines: A description of various parameters that have been developed to protect human health and the environment.

The toxicology profiles are intended to be brief overviews of individual chemicals and not extensive reviews. They are, however, intended to include the major health effects (i.e., toxicity) and other aspects of the chemical in question.

Subsection G.8 includes a description of the air dispersion models used to estimate concentrations of hazardous chemicals released during routine operations and accidents. The various input parameters and assumptions used in the models are provided.

The exposure parameters and methods used to estimate the daily intakes of hazardous chemicals are provided in Subsection G.9. The methodology and calculations for determining the long-term or short-term risks associated with exposure to carcinogenic and noncarcinogenic chemicals are given in Subsection G.10.

G.2 1,1,2-TRICHLORO-1,2,2-TRIFLUOROETHANE

SUMMARY

1,1,2-Trichloro-1,2,2-trifluoroethane (Freon 113) is a chlorine containing, non-hydrogenated fluorocarbon. Exposure to high doses can affect the central nervous system, heart, and liver. 1,1,2-Trichloro-1,2,2-trifluoroethane is mainly of environmental concern due to its ability to destroy atmospheric ozone.

IDENTIFICATION

CAS Number: 76-13-1

Synonyms:
Halocarbon 113
Refrigerant 113
TTE
Freon 113
FC-113
Fluorocarbon 113

CHEMICAL AND PHYSICAL PROPERTIES

Molecular Weight	197.5
Boiling Point	47.6° C
Melting Point	-35° C
Specific Gravity	1.5635 at 25° C
Vapor Pressure	284 torr at 20° C
Solubility	Insoluble in water, soluble in alcohol, ether, and benzene

FATE AND TRANSPORT

1,1,2-Trichloro-1,2,2-trifluoroethane is highly volatile. It is more likely to reach the stratosphere than hydrogenated fluorocarbons (Clayton and Clayton, 1981). There it photodissociates, producing chlorine atoms which destroy the ozone layer (National Research Council, 1976; Council on Environmental Quality, 1975; National Science Foundation, 1975).

HEALTH EFFECTS

1,1,2-Trichloro-1,2,2-trifluoroethane is a weak narcotic. Impairment of psychomotor abilities (e.g., loss of ability to concentrate, mild lethargy) have been observed in human volunteers (ACGIH, 1986; Stopps and McLaughlin, 1967). The threshold for impairment is approximately 2500 ppm (Stopps and McLaughlin, 1967). Exposure to massive doses also produces irritation of the respiratory tract and liver cell enlargement (ACGIH, 1986). Slight diffuse degenerative fatty infiltration of the liver has been observed in rats after seven, 19-hour exposures to 5000 ppm (Kniskern and Pittsman, 1952).

1,1,2-Trichloro-1,2,2-trifluoroethane may cause degreasing of the skin. Since it has a low boiling point, if the liquid is splashed into the eyes or on the skin, freezing may result. Frostbite can occur which if not properly attended to, can result in gangrene (Clayton and Clayton, 1981).

1,1,2-Trichloro-1,2,2-trifluoroethane has cardiac sensitization potential (ACGIH, 1986; Gosselin, 1984; Clayton and Clayton, 1981). At concentrations greater than 25,000 ppm, dogs, monkeys, and rats (exposed under various conditions) experienced tachycardia, hypotension or myocardial depression (Aviado, 1975). Abuse of fluorocarbon-containing aerosol products has led to death due to cardiac sensitization to endogenous catecholamines, resulting in ventricular fibrillation (Gosselin, 1984). Doses below maternal toxicity produced no changes in the offspring of pregnant rabbits (both oral and inhalation exposures) (Busey, 1967).

The Ames test shows 1,1,2-Trichloro-1,2,2-trifluoroethane to be nonmutagenic. Carcinogenic studies have not been reported (ACGIH, 1986).

REGULATIONS, STANDARDS, AND GUIDELINES

Human Health

OSHA PEL	1000 ppm	(NIOSH, 1985)
ACGIH TLV-TWA	1000 ppm	
TLV-STEL	1250 ppm	

(The ACGIH guidelines should provide a margin of safety in preventing systemic effects and cardiac sensitization) (ACGIH, 1986).

Reference Dose (RfD) 30mg/kg/day (based on an oral NOAEL of 273 mg/kg/day in humans with psychomotor impairment as the most sensitive end point) (IRIS, 1989)

Aquatic Organisms

No regulations, standards, or guidelines are presently available governing the exposure of aquatic organisms to 1,1,2-Trichloro-1,2,2-trifluoroethane.

G.3 METHYLENE CHLORIDE

SUMMARY

Methylene chloride is irritating to the skin, eyes, and mucous membranes. Short term inhalation produces narcosis, and long term exposure produces symptoms of neurotoxicity. Methylene chloride causes liver, lung and mammary gland tumors in mice and rats. Hepatotoxicity in experimental animals has been demonstrated.

IDENTIFICATION

CAS Number:	75-09-2
Chemical Formula:	Ch_2Cl_2
Synonyms:	Dichloromethane Methane dichloride Methylene bichloride

CHEMICAL AND PHYSICAL PROPERTIES

Molecular Weight	84.93	
Specific Gravity	1.3255 at 20° C	
Melting Point	-96.7° C	
Boiling Point	39.75° C at 76 torr	
Vapor Pressure	440 torr at 25° C	(ACGIH, 1986)
Refractive Index	1.4237 (20° C)	
Solubility	2 g/100 ml water at 20° C; soluble in ethanol, ethyl ether, acetone	
Flash Point	none	
Log Octanol/Water Partition Coefficient	1.25	(Clayton and Clayton, 1981)

FATE AND TRANSPORT

Because of its high vapor pressure, methylene chloride is easily volatilized. However, atmospheric accumulation is not of great concern due to scavenging from the troposphere by hydroxyl radicals (EPA, 1985). This reaction produces carbon dioxide, and small amounts of carbon monoxide and phosgene. Phosgene is hydrolyzed to hydrochloric acid and carbon dioxide (EPA, 1979). Methylene chloride has moderate

water solubility; therefore rain washout from the atmosphere may be important in the fate process (ATSDR, 1987). Absorption to soil is unlikely (Dilling et al., 1975). Biodegradation occurs aerobically and anaerobically. Bioaccumulation and bioconcentration are not important fate processes (Hansch and Leo, 1979).

HEALTH EFFECTS

Methylene chloride is a skin, eye, and mucous membrane irritant (ACGIH, 1986). Upper respiratory tract irritation occurs at levels of approximately 100 ppm in humans (Welch, 1987). Short term inhalation (300-800 ppm) leads to decreases in auditory functions and impairment of various psychomotor tasks (Stewart et al., 1972). Longer term inhalation causes neurotoxicity, including headache, dizziness, nausea, memory loss, paresthesia, tingling in the hands and feet, and narcosis (loss of consciousness) (Welch, 1987). These central nervous system effects could be partially due to the metabolism of methylene chloride producing carboxyhemoglobin (Cherry et al., 1983). Burns may result if methylene chloride liquid is placed on the skin (Welch, 1987).

Animal studies have shown methylene chloride to be hepatotoxic (toxic to the liver). Fatty infiltration of the liver was evident in guinea pigs exposed to 5200 ppm for six hours (Morris et al., 1979). Weinstein and Diamond (1972) observed transient fatty changes in the livers of mice exposed to 5000 ppm for seven days. A significant increase in liver cytochrome p-450 was induced in rats exposed by inhalation to 500 ppm (Norpoth et al., 1974). Longer term exposures by inhalation cause centrilobular fat accumulation in livers of mice (Weinstein and Diamond, 1972). Haun et al. (1972) showed cytoplasmic vacuolation and the presence of fat droplets in the livers of rats and dogs. An increased incidence of hemosiderosis, cytomegaly, and cytoplasmic vacuolization has been reported in livers of rats and mice exposed to methylene chloride by inhalation (NTP, 1986). Only very high exposure concentrations will cause serious liver effects in humans (ATSDR, 1987). Cardiac sensitization is seen in animals, but only when given epinephrine (Clark and Tinston, 1973).

Methylene chloride causes cancer in laboratory animals. Increases in liver tumors (NTP, 1986), lung tumors (NTP, 1986) and mammary gland tumors (Burek et al., 1980; 1984; Nitschke et al., 1982; NTP, 1986) have been reported in rats and mice. There have been no statistically different tumor occurrences between exposed and non-exposed humans (ATSDR, 1987). It has been concluded that methylene chloride is weakly mutagenic in mammalian systems (EPA, 1987a, b). There is no evidence that methylene chloride is a teratogen (an agent causing fetal malformities) (Clayton and Clayton, 1981).

EFFECTS ON WILDLIFE

In the flow-through and static method tests, fathead minnows (*Pimephales promelas*) exposed to methylene chloride experienced loss of equilibrium, melanization, narcosis, and swollen, hemorrhaging gills. These effects are reversible is caused by short exposures of sublethal levels (Alexander et al., 1978). At concentrations of 100 μg/L, developmental stages of some amphibian species may be affected. Concentrations of

1 mg/L and above may cause substantial reproductive impairment in amphibians (Black et al., 1982). High concentrations (approximately 21 percent) of methylene chloride reduces photosynthesis in alfalfa seedlings by 82 percent (Lehmann and Paech, 1972).

REGULATIONS, STANDARDS, AND GUIDELINES

Human Health

OSHA	TLV-TWA	500 ppm 1000 ppm ceiling
ACGIH	TLV-TWA	100 ppm
	TLV-STEL	500 ppm
NIOSH	TLV-TWA	75 ppm 500 ppm 15 min. ceiling

IARC Group 3 - indefinite animal carcinogen

EPA Group B - probable human carcinogen

Reference Dose (RfD)	0.05 mg/kg/day (ATSDR, 1987) [based on a NOAEL in rats of 5 mg/kg/day with hepatic histological changes as the most sensitive endpoint]
Drinking Water Equivalent Level (DWEL)	1.75 mg/L (IRIS, 1989)

Aquatic Organisms

No regulations, standards, or guidelines presently exist governing the exposure of aquatic organisms to methylene chloride.

G.4 1,1,1-TRICHLOROETHANE

SUMMARY

Exposure to 1,1,1-trichloroethane can cause central nervous system depression, as well as damage to the cardiovascular system, lungs, liver, and kidneys. It is an irritant to the eyes, skin, and mucous membranes. The primary process of elimination of 1,1,1-trichloroethane from the environment is through photo-oxidation in the atmosphere. Neither IARC nor the EPA classify 1,1,1-trichloroethane as a carcinogen. However, some of the animal studies are inconclusive.

IDENTIFICATION

CAS Number:	71-55-6
Chemical Formula:	$C_2H_3Cl_3$
IUPAC Name:	1,1,1-trichloroethane
Synonyms:	Methyl chloroform 1,1,1-TCA Chlorothene
Appearance:	colorless liquid

CHEMICAL AND PHYSICAL PROPERTIES

Molecular Weight	133.40
Specific Gravity	1.3376 at 20° C (Sax, 1984)
Melting Point	-32.5° C
Boiling Point	74.1° C
Vapor Pressure	100 mm at 20° C, 155 mm at 30° C
Vapor Density	4.63 (Verschueren, 1983)
Solubility	44 mg/L in water at 25° C; soluble in acetone, benzene, carbon tetrachloride, ether, methanol (Sax, 1984)

FATE AND TRANSPORT

The most important route of elimination of 1,1-1-trichloroethane (1,1,1-TCA) from the environment is by reaction with hydroxyl radicals in the atmosphere (photo-oxidation). 1,1,1-TCA is eliminated from surface water primarily through volatilization. It is able to

adsorb onto organic matter in the sediment; however, this is probably not a major route of elimination from surface water. 1,1,1-TCA readily migrates from soil to groundwater, the rate of transport through soil depending on its composition (EPA, 1987).

HEALTH EFFECTS

A number of toxic effects of 1,1,1-TCA have been observed. The most common of these is central nervous system depression manifested by dizziness, incoordination, and impaired judgment at low concentrations, and anesthesia and death at high concentrations. Cardiovascular effects such as cardiac arrest ventricular fibrillation, and sensitization to inephrine-induced arrhythmias have been observed, as well as damage to the lungs, liver, and kidneys. 1,1,1-TCA is moderately irritating to the skin and mucous membranes and is a severe eye irritant in rabbits (Sax, 1984). The oral LD_{50} value for 1,1,1-TCA in rats in approximately 11,300 mg/kg (IRIS, 1989), and the inhalation LC_{50} in rats is approximately 14,000 mg/kg for a seven hour exposure (Verschueren, 1983).

1,1,1-TCA has been found to be mutagenic in *Salmonella typhimurium* (Farber, 1977) and to cause transformation in rat embryo cells (Price, 1978). Although several carcinogenic studies have been performed, the doses administered resulted in direct mortality or no significant increase in tumor formation (IRIS, 1989).

EFFECTS ON WILDLIFE

1,1,1-Trichloroethane has a relatively low acute toxicity in aquatic species, with LC_{50} values ranging from 52.8 ppm for the most sensitive species to 113.0 ppm for the least sensitive species reported (Verschueren, 1983). In aquatic species, 1,1,1-TCA has an elimination half-life of two days and a bioconcentration factor of nine, and therefore has only a slight bioaccumulation potential (EPA, 1984).

At this time, there are no data available on the chronic toxicity of 1,1,1-TCA in aquatic species, or on the effects of 1,1,1-TCA on other species of wildlife.

REGULATIONS, STANDARDS, AND GUIDELINES

Human Health

OSHA	TLV-TWA	350 ppm (NIOSH, 1985)
ACGIH	TLV-TWA	350 ppm
	TLV-STEL	450 ppm (ACGIH, 1986)
NIOSH		350 ppm-15 minute ceiling (NIOSH, 1985) 500 ppm 15 min. ceiling
IARC	Group 3	indefinite animal carcinogen (IARC, 1987)

EPA Group D	not classifiable as to human carcinogenicity (IRIS, 1989)	
Reference Dose (RfD)	0.09 mg/kg/day (based on a NOAEL in guinea pigs of 90 mg/kg/day with hepatic histological changes as the most sensitive endpoint (Torkelson et al., 1958)	
MCL	200 μg/L	
Ambient Water Quality Criterion	water and fish consumption	218.4 mg/liter
	fish consumption only	1,030 mg/liter
	(IRIS, 1989)	

Aquatic Organisms

The U.S. EPA has reported the following lowest effect levels (LECs) for 1,1,1-trichloroethane on aquatic organisms:

Freshwater:

- Acute Toxicity 18.0 mg/L
- Chronic Toxicity No data

Saltwater:

- Acute Toxicity 31.2 mg/L
- Chronic Toxicity No data

These data, however are not adequate for establishing water quality criteria.

G.5 CARBON TETRACHLORIDE

SUMMARY

Carbon tetrachloride is a suspect human carcinogen and is known to produce liver tumors in laboratory animals. Carbon tetrachloride causes liver damage, as well as damage to the kidneys, skin, and eyes. Carbon tetrachloride may be readily absorbed through the skin. Acute exposure to carbon tetrachloride by inhalation, ingestion, or skin absorption may cause central nervous system depression.

IDENTIFICATION

CAS Number:	56-23-5
Chemical Formula:	CCl_4
IUPAC Name:	Tetrachloromethane
Synonyms:	Tetrachloromethane Perchloromethane

CHEMICAL AND PHYSICAL PROPERTIES

Molecular Weight	153.84
Specific Gravity	1.589
Melting Point	-23° C
Boiling Point	76.7° C
Vapor Pressure	90 mm at 20° C
Vapor Density	5.32
Solubility	800 mg/L liter H_2O at 20° C; miscible in alcohol, benzene, chloroform, ether, carbon disulfide (Merck, 1983; Sax, 1984; Verschueren, 1983)

FATE AND TRANSPORT

Volatilization is the major transport process for the removal of carbon tetrachloride from aquatic systems (EPA, 1979). Carbon tetrachloride in the troposphere degrades very slowly by reaction with hydroxyl radicals (EPA, 1979; EPA, 1987). It can diffuse to the stratosphere where it is degraded by exposure to higher energy ultraviolet light to form CCl_3 radicals, chlorine atoms, and phosgene. This photolysis reaction is thought to be the predominant environmental fate process for carbon tetrachloride. There is no clear

evidence of selective concentration (adsorption) of carbon tetrachloride in soils or sediments (EPA, 1979). Carbon tetrachloride migrates readily to groundwater and may be expected to remain there for months to years (EPA, 1987).

HEALTH EFFECTS

Carbon tetrachloride is a suspect human carcinogen and is known to be carcinogenic in rats, mice, and hamsters (IARC, 1979). Liver tumors are most commonly seen, but adrenal tumors have also been observed (Weisburger, 1977). Data on mutagenicity, teratogenicity, and reproductive effects have been inconclusive (Verschueren, 1983).

Carbon tetrachloride has been shown to produce nonmalignant liver damage as well as kidney damage in animals and humans (ACGIH, 1986). Symptoms of liver dysfunction may include nausea, anorexia, vomiting, stomach-ache, and jaundice, but dysfunction may also be asymptomatic (ACGIH, 1986).

Central nervous system depression has been experienced in cases of acute and chronic exposure to carbon tetrachloride. Atmospheric levels of 45-97 ppm have reportedly produced dizziness and headaches (Kazantzis, 1960).

Substances such as barbiturates and chlorinated biphenyls have been shown to enhance the effects of carbon tetrachloride. Consumption of alcoholic beverages is known to markedly increase the toxicity of carbon tetrachloride (Maling, 1975; Cornish, 1973; Carlson, 1975).

Carbon tetrachloride is a skin and eye irritant due to its defatting action and appreciable blood levels of carbon tetrachloride have been reported due to skin absorption.

EFFECTS ON WILDLIFE

Carbon tetrachloride has been shown to be toxic to freshwater aquatic life at acute exposure concentrations as low as 35,200 ug/liter, and as low as 50,000 ug/liter in saltwater aquatic species (EPA, 1980). LC_{50} values ranging from 67 ppm to 150 ppm have been reported for subacute exposures to carbon tetrachloride in aquatic species (Verschueren, 1983). A bioconcentration factor of 19 has been reported for carbon tetrachloride in fish (EPA, 1986).

REGULATIONS, STANDARDS, AND GUIDELINES

Human Health

OSHA TWA	10 ppm 25 ppm ceiling	(OSHA, 1987)
ACGIH TLV-TWA	5ppm	(ACGIH, 1986)

NIOSH TWA	10 ppm 25 ppm ceiling	(NIOSH, 1985)

IARC Group 2B Sufficient evidence of animal carcinogenicity

EPA Group B2 Probable human carcinogen

Reference Dose (RfD) 0.0007 mg/kg/day

Drinking Water Equivalent Level (DWEL) 25 μg/liter

10^{-6} Cancer Risk 0.3 μg/liter

Aquatic Organisms

There are inadequate data for establishing ambient water quality criteria for aquatic organisms (EPA, 1980).

G.6 **LEAD**

SUMMARY

Lead is found in the earth's crust at about 15 ppm. Lead isotopes are the stable products of decay of three natural radioactive elements: from the uranium series-^{206}Pb, from the thorium series-^{208}Pb, and from the actinium series-^{207}Pb. Lead forms two series of compounds corresponding to the oxidation states of +2 and +4, the most common being +2 (Kirk-Othmer, 1985).

Lead and its compounds are persistent in the environment and are cumulative poisons. High doses of lead result in damage to the central nervous system and loss of kidney function (Sittig, 1979).

IDENTIFICATION

CAS Number: 7439921

Chemical Symbol: Pb

Synonyms: C.I. 77575
Lead Flake
Lead s2

CHEMICAL AND PHYSICAL PROPERTIES

Molecular Weight:	207.19
Boiling point:	1740° C
Melting point:	327.5° C
Specific gravity:	11.35
Vapor pressure:	1 mm @ 973° C
Solubility:	Slightly soluble in H_2O in presence of nitrates, ammonium salts, and CO_2

FATE AND TRANSPORT

Lead exhibits the +2 oxidation state in aqueous systems. Natural compounds of lead are not usually mobile in ground or surface water since it tends to combine with carbonate or sulfate ions to form insoluble compounds under oxidizing conditions and forms extremely insoluble lead sulfide under reducing conditions.

Sorption processes are effective in reducing the concentration of soluble lead in natural waters and result in enrichment of bed sediments near the source. The tendency for lead to form complexes with naturally occurring organic material increases its adsorptive affinity for clays and other mineral surfaces. Removal of lead by sorption and precipitation occurs more rapidly in alkaline waters; therefore, lead is considerably more mobile in acidic waters.

Benthic microbes can methylate lead to form tetramethyl lead which is volatile and more toxic than inorganic lead. Biomethylation may provide a mechanism for remobilization of lead in the bed sediments. Bioaccumulation of weakly sorbed lead phases also may result in remobilization (EPA, 1979).

HEALTH EFFECTS

Lead enters the body through inhalation and ingestion, is absorbed into the circulatory system from the lungs and digestive tract, and is excreted via the urine and feces. About 90 percent of the ingested lead passes through the gastrointestinal tract unabsorbed. About 10 percent of the ingested lead is excreted in urine with lesser amount in sweat, hair, and nails. Under conditions of approximately steady state, more than 90 percent of absorbed lead in the body is in the skeleton, where it remains in a relatively inert state (Lee, 1972).

Particle size and chemical composition affect the readiness with which lead is absorbed from the lungs and digestive tract. Small particles and highly soluble compounds are more readily absorbed, hence more hazardous, than larger particles and compounds with lower solubility.

Lead and its compounds are cumulative poisons. The most common signs of lead exposure are gastrointestinal: anorexia, nausea, vomiting, diarrhea, and constipation followed by colic. Lead can also affect hemoglobin synthesis and red blood cell survival as well as the central and peripheral nervous systems (Kirk-Othmer, 1985).

An early effect of lead on the kidney is the development of intranuclear inclusion bodies in the renal tubular lining. With continued exposure, swelling and mitochondrial changes occur in proximal tubular lining cells (Ratcliffe, 1981).

Epidemiological investigations on exposed population groups and experiments on rats have shown that the placenta does not represent an important barrier to lead. Experiments on female mice have shown that ingested lead may cause, depending on the dose, a reduction of pregnancies, a decrease in embryo weight, or abortion. At high doses of lead and low calcium diet chromosomal abnormalities were found in primates (DiFerrante, 1979).

REGULATIONS, STANDARDS, AND GUIDELINES

Human Health

OSHA PEL	0.05 mg/m^3
ACGIH TLV-TWA	0.15 mg/m^3
EPA Acceptable Intake	1.4OE-03 mg/kg/day (Oral Route) 4.30E-04 mg/kg/day (Inhalation Route)
Safe Drinking Water Act (ARAAR)	0.05 mg/l (MCL) 0.02 mg/l (Proposed MCLG)
EPA Ambient Water Criteria	50 ug/l (Aquatic Organisms & Drinking Water)
Clean Air Act (ARAAR)	1.5 (90-day) ($\mu g/m^3$)

Aquatic Organisms

Bioconcentration factors for aquatic organisms range from 60 in marine and freshwater fish to 200 in marine and freshwater plants and invertebrates (EPA, 1979). Decreasing pH increases the availability of divalent lead, the principal form accumulated by aquatic animals.

G.7 TRICHLOROETHYLENE

SUMMARY

Trichloroethylene is an industrial solvent that induces central nervous system depression, adversely affects the liver, kidneys, and hematological systems, and sensitizes the heart to endogenous catecholamines. Lung, liver, and kidney tumors are increased significantly in exposed rats and mice.

IDENTIFICATION

CAS Number: 79-01-6

Chemical Formula: C_2HCl_3

Synonyms: Trichloroethene
TCE
Ethylene trichloride

CHEMICAL AND PHYSICAL PROPERTIES

Molecular Weight	131.4
Specific Gravity	1.45560 at 25/4° C
Melting Point	-86.8° C
Boiling Point	87.0° C
Vapor Pressure	77 torr at 25° C
Refractive Index	1.4777 at 20° C
Solubility	0.1 g/100 ml water at 20° C; soluble in ethanol and ethyl ether (Clayton and Clayton, 1981)

FATE AND TRANSPORT

Trichloroethylene vaporizes easily. However, accumulation in the atmosphere is not of critical importance. Hydroxyl radicals react with trichloroethylene to form hydrochloric acid, carbon monoxide, carbon dioxide, and carboxylic acid (EPA, 1979). The atmospheric half-life of trichloroethylene is approximately seven days (ATSDR, 1988b). It is highly mobile in the soil, and subject to significant leaching (HSDB, 1987; EPA, 1979). Since biodegradation under aerobic conditions is slow, trichloroethylene is relatively persistent in subsurface soils and groundwater (Barrio-Lage et al., 1987; Hallen et al., 1986; Wilson et al., 1986; Fogel et al., 1986; Vogel and McCarthy, 1985).

HEALTH EFFECTS

Inhalation of trichloroethylene causes irritation of the eyes and upper respiratory tract, as well as central nervous system (CNS) depression (Hazline, 1989; Sittig, 1985; Gosselin, 1984; Clayton and Clayton, 1981, Nomiyama and Nomiyama, 1977). CNS effects experienced include visual disturbances, mental confusion, fatigue (Clayton and Clayton, 1981), and at sufficiently high concentrations, euphoria, analgesia, and anesthesia (ACGIH, 1986).

Sensitization of the heart has occurred in humans at anesthetic levels (Clayton and Clayton, 1981). This has also been observed in dogs (Reinhardt et al., 1973) and rabbits (White and Carlson, 1979, 1981). If trichloroethylene is left in contact with the skin, defatting and fissuring, followed by erythema (redness) may result (Clayton and Clayton, 1981).

Trichloroethylene is hepatotoxic and nephrotoxic in experimental animals. Mice exposed to 37 ppm for 30 days had increased liver weights and vacuolated hepatocytes (Kjellstrand et al., 1983, 1981). Rats also showed an increase in liver weights when subjected to 55 ppm, 8 hr/day, 5 days/week for 14 weeks (Kimmerle and Eben, 1973) and >50 ppm continuously for 12 weeks (Nomiyama et al., 1986). Other unspecified treatment-related hepatic effects were also noted by Nomiyama et al. (1986).

Renal effects include increased kidney weights and dysfunction in rats exposed to >150 ppm for 12 weeks (Nomiyama et al., 1986) and renal tubular meganucleocytosis in rats exposed to >300 ppm for 7 hr/day, 5 days/week for 104 weeks (Maltoni et al., 1986).

Hematological system alterations have been experienced by experimental animals subjected to trichloroethylene. Rats treated for ten days with >50 ppm had concentration-dependent inhibition of delta-aminolevulinate (ALA) dehydrogenase activity in the liver and bone marrow cells, increased ALA synthetase, decreased heme saturation of tryptophan pyrrolase, and decreased cytochrome p-450 in the liver (Fujita et al., 1984). Nomiyama et al. (1986) exposed rats to >50 ppm for 12 weeks and observed dose-related changes in hemoglobin, hematocrit, and erythroblast count. Myleotoxic anemia has been shown in rabbits (Mazza and Brancaccio, 1967).

Teratogenicity data for trichloroethylene in humans are inconclusive. In rat pups, skeletal ossification anomalies were produced by dams subjected to >100 ppm for 4 hr/day on days 8 and 21 of gestation (Healy et al., 1982).

Trichloroethylene is weakly mutagenic in some microbial test systems (Clayton and Clayton, 1981). These data are inadequate to assess human carcinogenicity caused by trichloroethylene (ATSDR, 1988b). However, trichloroethylene has been proven to be carcinogenic in rats and mice, causing renal adenomas and carcinomas, lung adenomas, and hepatomas (Maltoni et al., 1986; NTP, 1986, 1982; Fukuda et al., 1983; Bell et al., 1978).

EFFECTS ON WILDLIFE

The availability of data pertaining to the toxic effects of trichloroethylene on wildlife is limited. Chlorophyll-containing algae and plants exposed to trichloroethylene lose their color at 600 mg/l (Verschueren, 1983). LC_{50} values of approximately 50 mg/l were noted for three freshwater species tested.

The EPA has reported lowest effect levels (LECs) for acute exposure to trichloroethylene of 45 mg/l, and 2 mg/l for freshwater and saltwater organisms, respectively. No LECs for chronic exposures have been reported.

REGULATIONS, STANDARDS, AND GUIDELINES

Human Health

OSHA	PEL	100 ppm 200 ppm ceiling
ACGIH	TLV-TWA	50 ppm
	TLV-STEL	200 ppm (ACGIH, 1986)
NIOSH	TWA	25 ppm (10 hr) (Hazline, 1989)
EPA	Group B2	probable human carcinogen (IRIS, 1989)
IARC	Group 3	indefinite animal carcinogen (IARC, 1987)

Aquatic Organisms

There are inadequate data for establishing ambient water quality criteria for aquatic organisms.

G.8 AIR DISPERSION MODEL

The "Users Network for Applied Modeling of Air Pollution" (UNAMAP) 6 version of the Industrial Source Complex Model (ISC)was used to estimate ambient concentrations of materials released from emission sources ("stacks") at the WIPP site. Releases resulting from routine operations and postulated on-site accident events, aboveground and underground, were modeled.

LONG-TERM MODEL

The long-term version of the model (ISCLT) projected the annual average aboveground concentrations, based on the annual average of meteorological data recorded at Carlsbad during the five-year period 1950 to 1954. Input mixing heights and ambient temperatures were obtained from Holzworth (1972) and National Weather Service records, respectively. The model was run in the "regulatory default" mode. For convenience, the emission rate was assumed to be 10 grams per second (5 gms/sec from each stack). To determine the ambient concentrations resulting from a different emission rate, a ratio of the actual and assumed emission rates was taken and applied to the predicted ambient concentrations.

The receptor field consisted of a rectangular grid extending 50,000 meters north, east, south, and west from the originating point of the emission. The physical location of the point of origin was the centerline of the vertical ventilation exhaust duct.

Ambient concentrations for underground workers were estimated manually using the following assumptions:

- Storage chamber dimensions are 33 feet x 300 feet x 13 feet
- Air velocity is 300 cm/sec
- Air flow is parallel to the long axis of the chamber
- Hazardous chemicals are uniformly mixed in the air stream.

Using these assumptions, ambient concentration ($\mu g/m^3$) is the quotient of the release rate (μg/sec) and the ventilation volumetric flow rate (m^3/sec).

SHORT-TERM MODEL

Short-term concentrations were estimated by the ISC model (ISCST) running in the short-term mode. Short-term releases were assumed to be discharged from the emergency filtration system with a flow rate of 60,000 cfm to a single stack. Generic

meteorological data (48 combinations of wind speed and stability customarily used in UNAMAP screening models) were used in the ISCST model. For each of the 48 combinations, a one-hour duration was arbitrarily assigned. In all instances, wind was assumed to be blowing from the south. Hypothetical receptors were located due north of the stack at distances from 50 to 50,000 meters. As in the ISCLT modeling, the emission rate for ISCST modeling was assumed to be 10 grams per second. For different emission rates, the predicted ambient concentrations shown were multiplied by the emission rate ratio.

The assumptions inherent in generic meteorological data are:

- The 48 combinations cover the entire spectrum of meteorological conditions that could be obtained.

- Each of the 48 combinations can occur at some time or other.

Thus, the highest potential short-term exposure can be identified as well as the distance at which this exposure occurs. This is a health-protective approach, since there is a low probability of all the necessary conditions occurring simultaneously. The emission rate was again assumed to be 10 grams per second. To determine the ambient concentrations resulting from a different emission rate, a ratio of the actual and assumed emission rates was taken and applied to the predicted ambient concentrations.

Manual calculations were used to estimate ambient concentrations of hazardous chemicals potentially released during postulated on-site accident events. Some accident-specific assumptions are described in Appendix F. For each accident event, it was assumed that the total release was equal to the total concentration of volatile organics in the void volume of breached containers. Concentrations in the air in the vicinity of each accident were estimated using these assumptions.

For the aboveground accident events, the release was assumed to disperse into a hemisphere which expands at a given rate for a given time. Concentrations of organics within the volume of the hemisphere were assumed to be uniform. For underground accidents, a similar procedure was followed. However, the underground release was assumed to disperse into an underground mined out area which was 4.0 meters x 3.4 meters x 6.0 meters in dimension. Again, concentration within this volume was assumed to be uniform. Estimations of particle releases of lead during a single drum fire underground were made based on the vapor pressure of elemental lead. The ISCST model was used to predict the resulting aboveground concentration at the off-site receptor location.

G.9 EXPOSURE ASSESSMENT

Consistent with the health-protective approach to risk assessment, potential exposures to releases of hazardous chemicals resulting from routine operations are estimated for hypothetical workers located at the points of maximum on-site concentrations above and below ground identified by the air dispersion modeling. Estimates of potential exposures were also made for a hypothetical resident located at the point of maximum concentration at the WIPP site boundary.

EXPOSURE PARAMETERS

The potential receptor was assumed in each case modeled to weigh 70 kilograms (kgs). Adults are used as the model residential receptor since no actual receptor exists at the site boundary. In fact, the nearest actual resident to the facility is more than three miles from the boundary. The increased sensitivity of the elderly or very young receptor from considerations such as body weight is mitigated by the additional dilution of the already very low predicted concentrations at the site boundary (see Section 5.0).

The daily respiratory volume was assumed to be 20 cubic meters (m^3) for a 24-hour period (residential exposures) (EPA, 1986) and 12 m^3 for an eight-hour period (occupational exposures) (EPA, 1985). Due to a lack of chemical-specific data for volatile organics, a transfer coefficient of 1.00 was used to model uptake and absorption via the lungs for these chemicals.

The rate of lead deposition in the lungs was assumed to range from approximately 30 to 50 percent of particulates inhaled, while up to 70 percent of deposited lead was assumed to be absorbed within ten hours of exposure (ATSDR, 1988a). To maintain a health-protective approach,a transfer coefficient of 0.35 (i.e., 70 percent x 50 percent) was used to represent deposition and absorption in the exposure estimates for lead.

Potential exposures to hazardous chemicals during routine operations were estimated for each exposure scenario (SEIS Section 5.0). For each receptor location, five-year and 20-year annualized average concentrations were calculated for each chemical. This average was derived from the following formula:

$$C_r = [C_1u_1 + C_2u_2 + \ldots C_iu_i \ldots + C_nu_n] / n \,, \quad n = 1,\ldots,5 \text{ or } n = 1,\ldots,20, \quad \text{(G-1)}$$

where:

C_r = annualized average concentration for a given chemical at the specific receptor location ($\mu g/m^3$),

C_i = average annual concentration ($\mu g/m^3$) for a given chemical, i = 1,...,n,

u_i = number of drum units, i = 1,...,n.

The u_i values are based on the chemical-specific emission periods,which are related to the minimum and maximum concentrations for each chemical. The u_i for each year represents the number of drum-units available to produce emissions in that year. For potential underground releases to aboveground receptors (occupational and residential), the chemical-specific u_i ranges from 1.00 to 5.00 22,000-drum units for the Test Phase and is 6,000-drum units for the subsequent 20 years for disposal operations. For example, the minimum emission period for methylene chloride is 2.45 years. Based on the assumptions for drum emplacement in the first five-year period, u_1 = 1.00, u_2 = 2.00, and $u_3 = u_4 = u_5$ = 2.45. For years 5 through 20, each u_i = 1.00. For potential underground releases to underground receptors, the yearly chemical-specific u_i is 1.00 for the entire permanent disposal phase. Similarly, the yearly chemical-specific u_i is 1.00 for releases from aboveground operations for the entire 20-year period.

ESTIMATION OF DAILY INTAKES OF HAZARDOUS CHEMICALS

For routine operation, the annualized averages for each chemical for both the Test Phase and the permanent disposal phase were used to estimate the chemical-specific daily intakes for the residential, aboveground occupational, and underground occupational receptors. The daily intake was estimated by

$$I_{ri} = (C_r V A_i) / fW , \; i = 1,...6, \qquad \text{(G-2)}$$

where:

I_{ri} = estimated daily intake of the ith chemical (mg/kg-day), i = 1,...6,

V = scenario-specific respiratory volume (m^3/day),

A_i = transfer coefficient for the ith chemical, i = 1,...6,

f = conversion factor (1000 μg/mg),

W = body weight (kg).

Concentrations available to receptors potentially exposed as a result of accident events were based on the total void volume gas concentrations and short-term modeling employing the specific dispersion characteristics of a given accident area.

G.10 RISK ESTIMATION

While the estimation of human health risks for this assessment employed a quantitative evaluation of the data available on waste characterization, these estimates are more meaningful when viewed in a relative, and therefore more qualitative, sense (see Section 9.0). The precision of these estimates was limited by the uncertainties associated with the size and quality of the data base. In this assessment, these limitations were partially mitigated by defining a range of extremes. However, overriding uncertainties still persist. An analysis of these uncertainties is given in Section 5.0.

LONG-TERM RISK ESTIMATION FOR CARCINOGENS: ROUTINE OPERATIONS

For any Class A or B carcinogen (by the classification of the EPA's Carcinogenic Advisory Group) that is projected to average greater than one percent by weight of the waste, predicted air pathway exposures that may result from emissions associated with routine facility operations are compared to unit cancer risks (EPA, 1986). Excess incremental lifetime cancer risks resulting from inhalation of vapors will be estimated for the receptors associated with each scenario. These estimates are based on guidance provided by the SPHEM and the Air Toxics Assessment Manual (California Air Pollution Control Officers Association [CAPCOA], 1987).

Of the representative chemicals for the waste, there are three volatile organics that are Class A or B carcinogens: carbon tetrachloride, methylene chloride (dichloromethane) and trichloroethylene (TCE). The estimated daily intakes for these chemicals were used to estimate the risk of the occurrence of one excess case of cancer as a result of the estimated exposures to these chemicals. This lifetime incremental excess cancer risk is given by

$$R_i = q_1^* I_{ri} LC \ , \ i = 1,...,3, \qquad \text{(G-3)}$$

where:

R_i = excess incremental lifetime cancer risk for the ith chemical, i = 1,...,3,

q_1^* = chemical-specific cancer potency factor $(mg/kg\text{-}day)^{-1}$,

I_{ri} = estimated daily intake of the ith chemical for a given receptor (mg/kg-day), i =1,...,3,

LC = lifetime correction factor.

The lifetime correction factor was used to adjust the risk estimates to the specific length of the exposure period. The resulting estimate was interpreted as the lifetime risk of

a single excess cancer occurrence based on the specific exposure period. An average lifetime is defined as 70 years (EPA, 1986). For the WIPP, four LCs were required. These are:

- Residential: 5/70 and 20/70, because residential exposures are assumed to be for 24 hours per day, 365 days per year for the two exposure periods.

- Occupational: (8/24)(240/365)(5/70) and (8/24)(240/365)(20/70), since occupational exposures are assumed to be 8 hours per day, 240 days per year for the entire 5-year and 20-year period.

LONG-TERM RISK ESTIMATION FOR NONCARCINOGENS: ROUTINE OPERATIONS

Potential risks were estimated for noncarcinogens projected to average greater than one percent by weight of the waste (Rockwell, 1988). Estimates of daily intakes for each chemical were compared with acceptable daily levels for chronic intake (AIC) according to procedures for deriving "hazard indices" described in the SPHEM (EPA, 1986).

The hazard index (HI) for a given chemical may be defined as the ratio between the daily intake of that chemical and an acceptable reference level. Clearly, an HI less than unity implies that the exposure to the given chemical is acceptable.

Hazard indices were calculated for each of these based on the estimated daily intakes in Tables 5.7 through 5.11. The chemical-specific hazard index was estimated as follows:

$$HI_i = I_{ri} / RL_i, \quad i = 1,...,3, \qquad \text{(G-4)}$$

where:

HI_i = hazard index for the ith chemical, i = 1,...,3,

I_{ri} = estimated daily intake of the ith chemical for a given receptor (mg/kg-day), i = 1,...,3,

R_i = reference level for the ith chemical (mg/kg-day), i = 1,...,3.

Here the reference level is the AIC, since exposures for the routine operations scenario are assumed to be over periods of 5 continuous years and 20 continuous years.

RISKS ASSOCIATED WITH ACCIDENT SCENARIOS

Accident events as defined in Appendix F are short-term events with respect to potential exposures and associated risks. To estimate these risks, hazard indices were calculated as described previously. The accident scenarios are assumed to involve potential exposures to the only occupational population because all hypothetical

accidents occur either in the waste handling building or underground. No significant residential exposures are assumed to occur due to the restricted access to the facility, the filtration system design, operational protocols for accident control and cleanup, and the concentration dilution as a function of distance.

Estimates of intake per exposure were compared with appropriate, short-term occupational standards. These include the time-weighted average Threshold Limit Values (TLVs) (ACGIH, 1986) and Immediate Danger to Life and Health (IDLH) criteria (CHEMTOX, 1988). In the case of lead, an IDLH has not been established. Therefore, lead exposures were compared to the TLV only. As before, an HI less than unity (one) implies that the exposure to the given chemical is acceptable.

REFERENCES FOR APPENDIX G

ACGIH (American Conference of Governmental Industrial Hygienists), 1986. Documentation of the Threshold Limit Values and Biological Exposure Indices, fifth edition, Cincinnati, Ohio.

ACGIH (American Conference of Governmental Industrial Hygienists), 1984. Documentation for the Threshold Limit Values, fourth edition. (1980) and updates (1981, 1982, 1983, 1984), ACGIH, Cincinnati, Ohio.

ATSDR (Agency for Toxic Substances and Disease Registry), 1988a. Toxicology Profile for Lead, Oak Ridge National Laboratory, Oak Ridge, Tennessee, draft.

ATSDR (Agency for Toxic Substances and Disease Registry), 1988b. Toxicological Profile for Trichloroethylene, draft, prepared by Technical Resources, Inc. under contract, No. 68-03-23618.

ATSDR (Agency for Toxic Substances and Disease Registry), 1987. Toxicological Profile for Methylene Chloride, draft, prepared by Life Systems Inc.

Alexander H. C., W. M. McCarty, and E. A. Bartlett, 1978. Toxicity of perchlorethylene, trichloroethylene, 1,1,1-trichloroethane, and methylene chloride to fathead minnows. Bull. Environ. Contam. Toxicol, 20:344-352, (cited in U. S. EPA, 1985).

Aviado, D. M., 1975. Toxicology 3:321.

Barrio-Lage G., F. Z. Parsons, and R. S. Nassar, 1987. "Kinetics of the depletion of trichloroethylene," Environ. Sci. Technol. 21:366-370.

Bell, Z. G., K. H. Oson, and T. J. Benya, 1978. "Final report of audit findings of the Manufacturing Chemists Association," administered trichloroethylene chronic inhalation study at Industrial Biotest Laboratories, Inc., Decatur, Illinois, unpublished, (cited in ATSDR, 1988b).

Black, J. A., W. J. Birge, W. E. McDonnell, A. G. Westerman, B. A. Ramey and D. M. Bruser, 1982. "The Aquatic Toxicity of Organic Compounds to Embryo-Larval Stages of Fist and Amphibians," Res. Report No. 133, Water Resource Institute, University of Kentucky, (cited in U. S. EPA, 1985).

Burek, J. D., K. D. Nitschke, T. Bell, D. L. Wackerle, A. C. Childs, J. Beyer, D. A. Dittenber, L. W. Rampy, and M. J. McKenna, 1984. Methylene chloride: a two year inhalation toxicity and oncogenicity study in rats and hamsters, Fund. Appl. Toxicology 4 (1): 30-47, (cited in ATSDR, 1987).

Burek, J. D., K. D. Nitschke, T. Bell, D. L. Wackerle, A. C. Childs, J. Beyer, D. A. Dittenber, L. W. Rampy, and M. J. McKenna, 1980. "Methylene chloride: a two year inhalation toxicity and oncogenicity study in rats and hamsters," Toxicology Research Laboratory, Health and Environmental Sciences, Dow Chemical Company, Midland, Michigan, (cited in ATSDR, 1987).

Busey, W. M., 1967. Unpublished data, Hazelton Labs., Falls Church, Virginia, sponsored by Haskill Lab., DuPont Co., Wilmington, Delaware (February 1967), (cited in ACGIH, 1986).

CAPCOA (California Air Pollution Control Officer Association), 1987. Air Toxics Assessment Manual, August.

CHEMTOX Database, 1988. Resource Consultants, Brentwood, Tennessee.

Carlson, G. P., 1975. Toxicol. 5:69, (cited in ACGIH, 1986).

Cherry, N., H. Venable, and H. Woldron, 1983. "The Acute Behavioral Effects of Solvent Exposure," J. Soc. Occup. Med. 33:13-18, (cited i ATSDR, 1987).

Clark, D. G. and D. J. Tinston, 1973. Br. F. Pharm. 49:355, (cited in Clayton and Clayton, 1981).

Clayton, G. D., and F. E. Clayton, eds., 1981. Patty's Industrial Hygiene and Toxicology, third edition, John Wiley and Sons, New York.

Cornish, H. H. et al., 1973. Am. Ind. Hyg. Assoc. J. 34:487.

Council on Environmental Quality, 1975. Fluorocarbons and the Environment, (cited in Clayton and Clayton, 1981).

DiFerrante, E., 1979. Trace Metals: Exposure and Health Effects, Pergamon Press.

Dilling, W. L., N. B. Tefertiller and G. J. Kallos, 1975. Evaporation rates of methylene chloride, chloroform, 1,1,1-trichloroethane, trichloroethylene, tetrachloroethylene, and other chlorinated compounds in dilute aqueous solutions, Environ. Sci. Technol. 9 (a): 833-838, (cited in ATSDR, 1987).

Doull, J., Klaasen, C. D., and M. O. Amour, 1979. Casarett and Doull's Toxicology: The Basic Science of Poisons, second edition, MacMillan Publishing Co., Inc., New York.

EPA (Environmental Protection Agency), 1988. "Solid Waste Disposal Facility Criteria," 53 Federal Register, 33421-2.

EPA (Environmental Protection Agency), 1988b. Update to health assessment document and addendum for dichloromethane (methylene chloride): Pharmaco-kinetics, mechanism of actions, and epidemiology, draft report, EPA 600/8-87/1030A.

EPA (Environmental Protection Agency), 1986. Superfund Public Health Evaluation Manual. Office of Emergency and Remedial Response, Office of Solid Waste and Emergency Response, U.S. Environmental Protection Agency.

EPA (Environmental Protection Agency), 1985. "Development of Statistical Distribution or Ranges of Standard Factors Used in Exposure Assessments," Office of Research and Development, Washington, D.C.

EPA (Environmental Protection Agency), 1985. Health Assessment Document for Dichloromethane (methylene chloride), final report, Environmental Protection Agency, Research Triangle Park, North Carolina.

EPA (Environmental Protection Agency), 1984. Health Effects Assessment for 1,1,1-Trichloroethane, Environmental Criteria and Assessment Office, Cincinnati, Ohio, ECAO-CIN-HOO5.

EPA (Environmental Protection Agency), 1980. Ambient Water Quality Criteria for Carbon Tetrachloride. Office of Water Regulations and Standards, Criteria and Standards Division, Washington, D. C., EPA 440/5-80-026.

EPA (Environmental Protection Agency), 1979. Water-Related Environmental Fate of 129 Priority Pollutants, Vol. I and II, 440/4-79-029, Office of Planning and Water Standards, Washington, D.C.

Farber, H., 1977. Manager of Environmental Affairs, Dow Chemical, Letter to James Price, Chief of Air Quality Data Analysis, Texas Air Control Board, Austin, Texas, (cited in IRIS, 1989).

Fogel, M. M., A. R. Taddio, and S. Fogel, 1986. "Biodegradation of chlorinated ethenes by a methane-utilizing mixed culture," App. Environ. Micro. 51:720-4, (cited in ATSDR, 1988).

Fujita, H., A. Koizumi, M. Yamamoto, M. Kumai, T. Gadamoto, and M. Skeda, 1984. "Inhibition of delta-azminoleuvliante dehydratase in trichloroethylene-exposed rats, and the effects on heme regulation," Biochem. Biophysi. Acta 800:1-10, (cited in ATSDR, 1988).

Fukuda, K., K. Takemota, and H. Tsuruta, 1983. "Inhalation carcinogenicity of trichloroethylene in mice and rats," Ind. Health 21:243-254, (cited in ATSDR, 1988).

Gosselin, R. E., 1984. Clinical Toxicology of Commercial Products, fifth edition, Williams and Wilson, Baltimore, Maryland.

Hallen, R. T., J. W. Pyne, Jr., and P. M. Malton, 1986. "Transformation of chlorinated ethenes and ethanes by anaerobic microorganisms," in ACS Div. Environ. Chem., 192nd National Mt. 25: 344-6, (cited in ATSDR, 1988).

Hansch, C. and A. J. Leo, 1979. Substituent Constraints for Correlation Analysis in Chemistry and Biology. John Wiley and Sons, New York, New York, p. 173, (cited in ATSDR, 1987).

Haun, C. C., E. H. Vernot, K. I. Darmer, and S. S. Diamond, 1972. Continuous animal exposure to low levels of dichloromethane, AMRL-TR-72-130, Paper No. 12, In: Proceedings of the Third Annual Conference on Environmental Toxicology, Wright-Patterson Air Force Base, Ohio, Aerospace Medical Research Laboratory, pp. 199-208, (cited in ATSDR, 1987).

Hazline (Hazard Line), January 1989. On line.

Healy, T. E., T. R. Poole, and A. Hooper, 1982. "Rat fetal development and maternal exposure to trichloroethylene at 100 development and maternal exposures to trichloroethylene at 100 ppm," Dr. J. Anaesth: 54:337-341, (cited in ATSDR, 1988).

Holzworth, G. C., 1972. "Mixing Heights, Wind Speeds, and Potential for Urban Air Pollution Throughout The Contiguous United States," EPA.

HSDB (Hazardous Substances Data Bank), 1987. September 1987, on line.

IARC (International Agency for Research on Cancer), 1987a. "IARC Monographs on the Evaluation of Carcinogenesis Risks to Humans," Overall Evaluations of Carcinogenicity: An updating of IARC Monographs, Volumes 1-42. (Supplement 7) International Agency for Research on Cancer.

IARC (International Agency for Research on Cancer), 1987b. "IARC Monographs on the evaluation of Carcinogenic Risks to Humans," (Supplement 7).

IARC (International Agency for Research on Cancer), 1979. "IARC Monographs on the Evaluation of Carcinogenic Risk of Chemicals to Humans," vol. 20: Some Halogenated Hydrocarbons, World Health Organization, Lyon, France, pp. 371-399.

IRIS (Integrated Risk Information System), 1989. U.S. EPA., January.

Kazantzis, G. and R. R. Bomford, 1960. Lancet 1:360, (cited in ACGIH, 1986).

Kimmerle, G., and A. Eban, 1973. "Metabolism, excretion: 1. Experimental exposures on rats," Arch. Toxicol. 30:1215-126, (cited in ATSDR, 1988).

Kirk-Othmer ed., 1985. Concise Encyclopedia of Chemical Technology, Wiley-Interscience.

Kjellstrand P., B. Holmquist, A. Alma, M. Kanje, S. Romare, I. Jonsson, L. Mannson, and M. Bjerkamo, 1983. "Trichloroethylene: Further studies of the effect on body and organ weights and plasma butyryl cholinesterase activity in mice," Acta. Pharmacl. Toxicology. 53:375-384, (cited in ATSDR, 1988).

Kjellstrand P., M. Kanje, L. Mannson, M. Bjerkamo, S. Mortenson, J. Lanke, and B. Holmquist, 1983. "Trichloroethylene: Effects on body and organ weights in mice, rats, and gerbils," Toxicology, 21:105-115.

Kniskern, L. A. and W. E. Pittsman, 1952. Industrial Test Lab., No. 2335, Progress Report NS-041001, Philadelphia Naval Shipyard, Pennsylvania, (February 1952), (cited by ACGIH, 1986).

Lee, D. H. K. ed., 1972. Metallic Contaminants and Human Health, Academic Press.

Lehmann, J., and D. Paech, 1972. "Effects of Some Vaporized Lipophilic Solvents on Carbon Dioxide Fixation, Experentia 28:1415-1416, (cited in ATSDR, 1987).

Lewis, R. J. ed., 1979. Registry of Toxic Effects of Chemical Substances, ninth edition, U.S. Department of Health and Human Services, National Institute for Occupational Safety and Health, Cincinnati, Ohio.

Maling, H. H. et al, 1975. Tox. Appl. Pharm. 33:291, (cited in ACGIH, 1986).

Maltoni C., G. Lefemine, and G. Cotti, 1986. "Experimental Research on Trichloroethylene Carcinogenesis," Archir. Res. Industrial Carcinogenesis Series, ed C. Maltoni, and M. A. Mehlman, Vol. V, Princeton Scientific Publishing Co., Inc., Princeton, New Jersey, (cited in ATSDR, 1988).

Mazza, V., and A. Brancaccio, 1967. "Characteristics of the formed elements of the blood and bone marrow in experimental trichloroethylene intoxication," Folia Med., 501381-324, (cited in ATSDR, 1988).

Merck, (The Merck Index), 1983. 10th ed. Merck and Company, Rahway, New Jersey.

Morris, J. B., F. A. Smith, and R. H. Garman, 1979. "Studies on Methylene Chloride-induced Fatty Liver," Exp. Molec. Path. 30:386-393, (cited in ATSDR, 1987).

NCRP (National Council on Radiation Protection and Measurements), 1984a. Exposures from the Uranium Series with Emphasis on Radon and its Daughters, Report No. 77.

NCRP (National Council on Radiation Protection and Measurements), 1984b. Radiological Assessment: Predicting the Transport, Bioaccumulation, and Uptake by Man of Radionuclides Released to the Environment, Report No. 76.

NIOSH (National Institute for Occupational Safety and Health), 1985. NIOSH Pocket Guide to Chemical Hazards, U.S. Department of Health and Human Services, Public Health Service Centers for Disease Control.

NTP (National Toxicology Program), 1986. "Toxicology and carcinogenesis studies of dichloromethane (methylene chloride) (CAS No. 75-09-2) in F344/N rats and B6C3F1 mice (inhalation studies)," Tech. Rep. Ser. 306, (cited in ATSDR, 1987).

NTP (National Toxicology Program), 1986. "Toxicology and carcinogenesis studies of Trichloroethylene in F344/N rats and B6C3F1/mice," NTP TR 243, U. S. Department of Health and Human Services, National Institutes of Health, Bethesda, Maryland.

NTP (National Toxicology Program), 1982. "Carcinogenesis bioassay of trichloroethylene in F344 rats and B6C3F1 mice", CAS No. 70-01-06, NTP 81-94, NIH Publication No. 82-1799, (cited in ATSDR, 1988).

National Research Council, 1976. Halocarbons, Environmental Effects of Chlorofluoromethane Release, (cited in Clayton and Clayton, 1981).

National Science Foundation, 1975. The Possible Impact of Fluorocarbons and Halocarbons on Ozone, (cited in Clayton and Clayton, 1981).

Nitschke, K. D., J. D. Burek, T. Bell, L. W. Rampy, and M. G. McKenna, 1982. "Methylene chloride: a two year inhalation toxicity and oncogenicity study," Toxicology Research Laboratory, Health and Environmental Sciences, Dow Chemical Company, Final Report, (cited in ATSDR, 1987).

Nomiyama, E., H. Nomiyama, and H. Arai, 1986. "Re-evaluation of subchronic toxicity of trichloroethylene," Toxicol. Lett. 31 (Suppl.), 225 (Abstract), (cited in ATSDR, 1988).

Nomiyama, E., and H. Nomiyama, 1977. "Dose-responses relationship for trichloroethylene in man," Int. Arch. Occup. Environ. Health, 30:237-248, (cited in ATSDR, 1988).

Norpoth, K., V. Witting, M. Springorans, and C. Wittig, 1974. "Induction of microsomal enzymes in the rate liver by inhalation of hydrocarbon solvents," Int. Arch. Aberted, 33:315-321, (cited in ATSDR, 1987).

Oehme, F. W., 1979. Toxicity of Heavy Metals in the Environment, Part 2, Macel Dekker, Inc.

OSHA (Occupational Safety and Health Administration), 1987. Occupational Safety and Health Reporter, The Bureau of National Affairs, Inc., Washington, D. C.

Price, P. J., C. M. Hassett, and J. J. Mansfield, 1978. "Transforming activities of trichloroethylene and proposed industrial alternatives," In vitro 14:290-293.

Ratcliffe, J. M., 1981. Lead in Man and the Environment, Ellis Horwood Ltd.

Reinhardt, C. F., L. S. Mullen, and M. E. Maxfield, 1973. "Epinephrine-induced cardiac arrhythmia potential of some common industrial solvents," J. Occup. Med. 15:953, (cited in ATSDR, 1988).

Rockwell International Corp., 1988. "Hazardous Constituents of Rocky Flats Transuranic Waste," Internal letter for distribution from J. K. Paynter, May 24, 1988, WCPO 2-31, Golden, Colorado.

Sax, N. I., 1989. Dangerous Properties of Industrial Materials, seventh edition, New Van Nostrand Reinhold Company.

Sax, N. I., 1984. Dangerous Properties of Industrial Materials, sixth edition, New Van Nostrand Reinhold Company.

Sittig, M., 1985. Handbook of Toxic and Hazardous Chemicals and Carcinogens, second edition, Noyes Publications, New Jersey.

Sittig, M., 1979. Hazardous and Toxic Effects of Industrial Chemicals, Moyes Data Corp.

Stewart, R. D., T. N. Fischer, M. J. Hosko, J. L. Peterson, E. D. Baretta, and H. C. Dodd, 1972. "Experimental human exposure to methylene chloride," Arch. Environ. Health, 25:342-348.

Stopps, G. J. and M. McLaughlin, 1967. American Ind. Hyg. Assoc. J. 23:43, (cited by ACGIH, 1986).

Thomson, B. M., and R. J. Heggen, 1983. "Uranium and Water: Managing Common Resources," Chemtech, May, 1983.

Torkelson, T. R., F. Oyen, D. D. McCollister, and V. K. Rowe, 1958. "Toxicity of 1,1,1-trichloroethane as determined on laboratory animals and human subjects," Am. Ind. Hyg. Assoc. J. 19:353-362, (cited in IRIS, 1989).

USDHHS (U.S. Department of Health and Human Services), 1985. Fourth Annual Report on Carcinogens, NTP 85-002, USDHHS, National Toxicology Program, Research Triangle Park, North Carolina.

USDHHS (U.S. Department of Health and Human Services), 1978. Occupational Health Guidelines, USDHHS, Cincinnati, Ohio.

Verschueren, K., 1983. Handbook of Environmental Data on Organic Chemicals, second edition, Van Nostrand Reinhold Co., New York.

Vogel, T. M., and P. L. McCarthy, 1985. "Biotransformation of tetrachloroethylene to trichloroethylene, dichloroethylene, vinyl chloride, and carbon dioxide under methanogenic conditions," Appl. Environ. Microbiol. 49:1030-1083, (cited in ATSDR, 1988).

Weinstein, R. S. and S. S. Diamond, 1972. "Hepatotoxicity of dichloromethane (methylene chloride) with continuous inhalation exposure at a low dose level," In: Proceedings of the Third Annual Conference on Environmental Toxicology, Wright-Patterson Air Force Base, Ohio, Aerospace Medical Research Laboratory, pp. 209-220.

Weisburger, E. K., 1977. "Carcinogenicity studies in halogenated hydrocarbons," Environ.Health Perspec. 21:7-16.

Welch, L., 1987. "Reports of clinical disease secondary to methylene chloride exposure -- a collection of 141 cases," ONTS/EPA 3/31.

White, J. F., and G. P. Carlson, 1981. "Epinephrine-induced cardiac arrhythmias in rabbits exposed to trichloroethylene potentiation by ethanol," Toxico. Appl. Pharmacol., 60:466-471, (cited in ATSDR, 1988).

White, J. F., and G. P. Carlson, 1979. "Influence of alternations in drug metabolism in spontaneous and epinephrine-induced cardiac arrhythmias in animals exposed to trichloroethylene," Toxico. Appl. Pharmacol., 47:515-527, (cited in ATSDR, 1988).

Wilson, B. H., G. G. Smith, and J. F. Rees, 1986. "Biotransformation of selected alkylbenzenes and halogenated aliphatic hydrocarbons in methanogenic aquifer material: A microcosm study." Environ. Sc. Technology, 20:997-1002, (cited in ATSDR, 1988).

Digitized by the Internet Archive in 2010 with funding from Boston Public Library

APPENDIX H

PUBLIC INFORMATION AND INTERGOVERNMENTAL AFFAIRS

Digitized by the Internet Archive in 2010 with funding from Boston Public Library

TABLE OF CONTENTS

Section		Page
H.1	PUBLIC INFORMATION	H-1
H.1.1	ESTABLISHMENT OF THE WIPP VISITOR PROGRAM AND CENTER	H-1
H.1.2	IMPLEMENTATION OF PUBLIC INFORMATION PROGRAM	H-1
H.2	INTERGOVERNMENTAL AFFAIRS	H-6
H.3	INTERGOVERNMENTAL AFFAIRS AND PUBLIC INFORMATION PLAN FOR THE WIPP SEIS	H-9

LIBRARY U. OF I. URBANA-CHAMPAIGN

H.1 PUBLIC INFORMATION

Public information and participation activities undertaken during the preparation of the FEIS are described in Subsection 14.4 of the FEIS. This subsection lists the public hearings that were held and describes the notices of availability that were published. A 141-day public comment period was held on the draft SEIS.

Since the completion of the FEIS, the DOE has undertaken a range of intergovernmental affairs and public information activities to inform the public of the development of the WIPP, provide opportunities for interested parties to express concerns and comments to the DOE, and keep key government agencies and interest groups informed of issues and progress related to the WIPP project. These intergovernmental and public information activities are described in detail below.

H.1.1 ESTABLISHMENT OF THE WIPP VISITOR PROGRAM AND CENTER

The WIPP Visitor Center was established in 1988 to provide information to area residents regarding the history, design, and plans for the WIPP. The center includes a multi-room exhibit that demonstrates the need for the WIPP, plant design, plans for waste handling, and projections for the life of the WIPP. The WIPP Visitor Center is managed by the WIPP Project Office of Public Affairs in Carlsbad, New Mexico, and staff members are available to discuss visitors' questions about the project. The center is an extension of the WIPP project tour program so that those who are unable to go to the site may receive similar information.

Interested groups may take tours of the WIPP as part of the visitor program. Between 1981 and 1984, only visits by foreign nationals were recorded as part of the tour program; there were 23 visits from 169 foreign visitors during that period. Between 1984 and 1988, all visits were recorded; 648 tours were conducted for 7,520 visitors. The visitors have included the Governors of New Mexico, Colorado, and Idaho and members of Congress from New Mexico, Colorado, Idaho, Oklahoma, and Louisiana.

H.1.2 IMPLEMENTATION OF PUBLIC INFORMATION PROGRAM

In implementing its public information program, the DOE has conducted public hearings; held public awareness tours; sponsored a speakers' bureau; participated in dedications; attended professional and scientific meetings; held community update meetings; participated in community days and fairs; responded to media inquiries; sponsored media events; and prepared numerous publications addressing WIPP-related issues. These activities are described below.

Public Hearings. Since the FEIS was published in 1980, the DOE has participated in two sets of public hearings that have addressed environmental issues related to the WIPP. The issues these hearings have addressed include:

- Site and Preliminary Design Validation (SPDV) Program. The DOE held hearings on the results of the SPDV in Santa Fe and Albuquerque, New Mexico, April 19 and May 16, 1983, respectively. Following the hearings, a notice was published in the Federal Register that reaffirmed the 1981 Record of Decision and the decision to proceed to full construction.

- The BLM held administrative land withdrawal hearings for the WIPP at Albuquerque and Carlsbad, New Mexico in May, 1983.

- Land Withdrawal Bill. In 1987, Congress considered legislation that would permanently withdraw the land to be used for the WIPP from the public domain and assign administrative responsibility to the DOE. WIPP staff members testified at hearings for the bill in Washington, D.C., and Carlsbad, New Mexico. Congress did not act on this bill prior to adjournment.

Public Awareness Tours. The DOE conducted public awareness tours in three cities in Utah, two cities in Idaho, 14 cities in New Mexico, five cities in Colorado, and five cities in Wyoming. These tours informed residents and leaders along waste transportation routes about the WIPP and transportation issues. The DOE issued press releases in each of the 29 cities, and the tours received extensive media coverage. Almost 2,500 people attended the exhibits and discussed issues with WIPP staff members and thousands more were reached through press coverage.

Speakers' Bureau. Since the DOE established a speakers' bureau in 1987, 183 presentations have been made to 7,671 persons in civic clubs, professional organizations, schools, and other groups. These presentations have covered issues such as transportation of waste to the WIPP, waste handling operations, safety at the WIPP, the WIPP environmental programs, and overviews of the WIPP for elementary and secondary students.

Dedications. The DOE has held official dedications for the WIPP and associated facilities and has invited the public to these events. These dedications have included the following:

- The ground breaking for the Waste Handling Building was held in 1984, and the facility was dedicated in 1987. The Waste Handling Building is the largest surface facility at the WIPP, and some 560 persons attended the two functions.

- The WIPP Visitor Center was dedicated in 1988. This facility is located at the WIPP Project Office in Carlsbad, New Mexico and about 175 persons attended its dedication.

- The Alternative Emergency Operations Center (AEOC) was dedicated in 1988. The AEOC was developed to provide another location for emergency personnel to conduct emergency response activities if the primary Emergency

Operations Center (EOC) at the WIPP site is inaccessible during an emergency. The DOE negotiated an agreement for joint DOE, state, county, and city use of the AEOC, and about 30 persons attended its dedication.

- The DOE developed and installed a display on the WIPP project at DOE's National Atomic Museum at Kirtland Air Force Base in Albuquerque, New Mexico. About 50 persons attended the 1988 opening of the display.

- The DOE provided a regularly updated display on the WIPP project for the Carlsbad Centennial Museum which attracted hundreds of visitors in 1988.

Professional Conferences. The DOE has provided the scientific community with information about the WIPP project through professional conferences as follows:

- At the DOE Model Conference in Oak Ridge, Tennessee in 1988, the DOE's exhibit presented WIPP information to 700 radioactive and hazardous waste management professionals.

- At the 1987, 1988, and 1989 Waste Management Conferences in Tucson, Arizona, WIPP information was presented to 1,300 national and international radioactive waste management professionals.

- At Carlsbad, New Mexico in May 1988 and Odessa, Texas in November 1988, the WIPP Institutional Program gave status updates on institutional activities within the western and southern states to Defense Transuranic Waste Program participants.

- In November 1987, a presentation was made on the WIPP project and institutional and public affairs outreach to the American Society for Public Administration at El Paso, Texas.

Community Activities. The DOE has held both regularly and specially scheduled community update meetings with community leaders in New Mexico. Updates on the WIPP project have been held in Carlsbad, Artesia, Roswell, and Hobbs, New Mexico. Seminars explaining how to participate in the Federal government procurement system have also been held in these locations for local businesses and contractors.

In the informal context of "community days," the DOE has provided the community with opportunities to meet with WIPP staff members and tour its facilities. These events included the following:

- WIPP Family Day at the WIPP site in 1987. The DOE invited families of WIPP employees to an informal picnic and tour of the site; this event provided WIPP employees' family members with a general overview of the facility, a demonstration and overview on transportation, an environmental overview, and tours of the Waste Handling Building and the underground areas.

- Southeast New Mexico Community Leaders Day in 1988. The WIPP Public Affairs Office organized this event for elected officials and community leaders

in southern New Mexico. The event included surface and underground tours and overviews of the WIPP project.

- Southeastern New Mexico Community Days in 1988. Organized by the WIPP Public Affairs Office, this event drew about 1,450 persons; the DOE provided overviews and surface and underground tours.

- Northern New Mexico Community Day in 1988. The WIPP Public Affairs Office organized this event, which included a general overview, transportation overview and demonstration, environmental overview, and tours of the Waste Handling Building and the underground areas. The event drew about 785 persons.

- Water Fair. The DOE assisted the State of New Mexico in gathering water samples from the Carlsbad area by co-sponsoring a Water Fair with the Environmental Improvement Division. More than 70 samples were brought to the fair by residents who desired to receive free water analyses.

- Eddy County Fair, 1985 through 1988. The DOE provided an information booth and exhibit at this fair in Carlsbad, New Mexico. About 2,000 people visited the booth.

- Eastern New Mexico State Fair in 1986, 1987, and 1988. The DOE provided an information booth and exhibit at this fair in Roswell, New Mexico; about 2,000 persons visited the booth.

- New Mexico State Fair in September 1988. The DOE sponsored an information booth and exhibit at this fair in Albuquerque, New Mexico. About 6,000 persons stopped at the booth.

Media. The DOE, through its Office of Intergovernmental and External Affairs and the WIPP Public Affairs Office, is committed to responding to press inquiries with accurate and timely information. In addition to requests for information from southeastern New Mexico, information has been provided to regional media including The Albuquerque Journal and Tribune, Albuquerque television stations, Albuquerque radios stations (KOB and KGGM), the Boise Statesman in Idaho, and the Denver Post and Rocky Mountain News in Colorado. National requests have included inquiries from The Chicago Tribune, USA-Today News, Newsweek and Time magazines, the New York Times, Cable News Network, and The MacNeil/Lehrer Report.

Media events sponsored by the DOE were designed to provide the media with in-depth information about key issues of public interest. For example:

- The DOE exhibited the TRUPACT-II testing in Albuquerque, New Mexico. Local and national media and public officials were invited to this event. The TRUPACT-II containers were dropped from 30 feet onto an unyielding surface, dropped onto a blunted spike, and burned.

- The DOE sponsored a tour to demonstrate the TRUPACT-II full-scale model in Carlsbad, New Mexico; Idaho Falls, Idaho; and Portland, Oregon. The

purpose of this tour was to answer questions from interested media about the proposed transportation routes for waste materials and about the proposed contents of the TRUPACT II containers.

Publications. In addition to the public information activities described above, the DOE has prepared numerous publications addressing different WIPP issues. The titles of these publications are:

"Waste Isolation Pilot Plant -- WIPP"
"In-Situ Testing at the Waste Isolation Pilot Plant"
"Visitor Information"
"Certification Requirements"
"Transuranic Waste"
"Environmental Protection"
"Participants/Lines of Communication"
"Why Salt? Why Southeastern New Mexico?"
"Raptor Studies and the WIPP Environment"
"Waste Handling Procedures at WIPP"
"Commonly Asked Questions"
"Transportation: A Satellite Tracking System"
"Transportation: TRUPACT-II"
"Safety Through the Project"
"Waste Handling Building"
"Highway Route Selection"
"States Training and Education Program"
"Public Law 96-164"
WIPP Project Speakers' Bureau Presentations.

H.2 INTERGOVERNMENTAL AFFAIRS

An important function related to the WIPP Project Office of Public Affairs is to keep interested government officials informed of key issues and progress related to the WIPP project. In the process, the DOE has worked closely with numerous Federal, state, and local government agencies. In some cases, the DOE has regularly attended meetings of key governmental agencies, and WIPP project staff members have participated in the on-going meetings of governmental groups as follows:

- The Environmental Evaluation Group (EEG) provides New Mexico's independent oversight of the WIPP project. The group has a professional staff and is responsible to the president of New Mexico Institute of Mining and Technology. WIPP staff members have conducted 28 quarterly reviews of the WIPP project for the EEG.

- The Radioactive and Hazardous Materials Committee (RHMC) oversees WIPP project activities for the New Mexico legislature. Since 1979, WIPP staff members have attended about 50 meetings of the RHMC.

- The Radioactive Waste Consultation Task Force (RWCTF) is an executive task force that oversees the WIPP project for the Governor of New Mexico. In 1985, the DOE was invited to the meetings of the RWCTF and has attended eight meetings since then.

- The National Academy of Sciences (NAS) WIPP Panel is composed of 11 prominent scientists and has met approximately three times a year since 1979. WIPP project staff members were available for the 30 meetings.

- The Pacific States Alliance (PSA) is a three-state committee established to study and recommend measures to transport radioactive material safely through Washington, Oregon, and Idaho. The DOE participated in four meetings in 1988 and 1989 with the PSA and attends all PSA meetings to identify concerns, address questions, and provide project updates.

- The Western Governors' Association (WGA) is an alliance of governors from 11 western states dedicated to uniformly representing the western governors in intergovernmental affairs. The DOE regularly attends WGA meetings to identify concerns, address questions, and provide project updates.

- Congressional support. The WIPP Project Office has responded on numerous occasions to requests for information from different members of Congress, and has conducted briefings and tours for interested members who have visited the facility.

In addition to regular involvement with these governmental groups, the WIPP Project Office of Public Affairs has met on request and initiated meetings with other governmental groups interested in the project. These meetings have included the following:

- Santa Fe Interested Citizens. Approximately 20 elected and appointed Santa Fe, New Mexico leaders toured the WIPP site and received briefings.

- National Congress of American Indians (NCAI). The WIPP Project Office met with NCAI members on two different occasions. In December 1987, WIPP staff members met with the leaders of New Mexico Indian Tribes and Pueblos. In February 1988, WIPP staff members also met with officials of Indian Tribes and Pueblos from outside of New Mexico. At these meetings, WIPP staff members discussed Indian concerns, provided WIPP project information, and conducted site tours.

- All Indian Pueblo Council (AIPC). After AIPC publicly expressed opposition to the WIPP project, the DOE met with the AIPC in 1988 to hear concerns and respond to questions and comments. The AIPC represents New Mexico's 19 Indian pueblos on matters for which unity and numbers enhance the pueblos' interests.

- Interstate Route 84 Task Force. In July 1988, WIPP staff members conducted a public information tour in Oregon along the route of proposed Interstate Route 84 to provide information on the transport of TRU wastes through Oregon and to identify and address concerns. WIPP project staff members responded to media questions, provided technical expertise, and displayed the full-scale TRUPACT-II model.

- Hanford Waste Board and Advisory Committee (Oregon). This group sponsored four public information meetings along the proposed Interstate Highway 84 corridor in Oregon. The DOE attended these meetings to provide the public with information on the transport of TRU wastes through Oregon and to identify and address concerns. WIPP project staff members responded to media questions, provided technical expertise, and displayed the full-scale TRUPACT-II model.

- Western Interstate Energy Board (WIEB). WIPP project staff members attended three meetings held by the WIEB on the WIPP during 1987 and 1988. The WIEB is an interstate compact group representing 16 western states in many environmental and intergovernmental affairs.

- Southern States Energy Board (SSEB). The SSEB held a meeting on the WIPP in 1987 and WIPP project staff members attended. The SSEB is a non-profit interstate compact serving as the regional representative of 16 southern states in energy and environmental matters. The SSEB also held a meeting in Carlsbad, New Mexico and toured the WIPP site in September 1988.

- DOE Field Offices. Personnel associated with or supporting the WIPP Project Office meet with the DOE's Idaho, Oak Ridge, and Savannah River Operations Offices to plan, coordinate, and interface with the states within their regions.

- Office of Civilian Radioactive Waste Management (OCRWM). The WIPP Project Office met and worked with DOE OCRWM four times in 1987 and

1988. During these meetings, the DOE attended OCRWM's Transportation Coordination Group meetings to exchange information about transportation policy, hosted the OCRWM Transportation Institution Support Manager on a visit to the WIPP site, and participated in the OCRWM Institution Planning for Transportation Activities meeting.

- Mine Safety and Health Administration (MSHA). Pursuant to a Memorandum of Understanding between MSHA and DOE, the MSHA conducts safety inspections of the underground WIPP facility.

- Other State of New Mexico Agencies. The DOE met with the State Highway Commission to discuss highway upgrading and with the Radiation Technical Advisory Council to discuss TRU waste transportation and other agenda items. The State Highway Commission has responsibility for maintenance of state roads and shipments of hazardous materials over those roads. The Radiation Technical Advisory Council is responsible for radiation protection in New Mexico.

- Local government agencies. The DOE met with the Raton, New Mexico City Council in 1988 to address concerns about waste transportation. After the meeting, the City Council defeated a resolution to restrict the transportation of radioactive waste through city limits. Instead, the council voted to support the New Mexico Municipal Leagues resolution. The DOE has addressed the Santa Fe City Council on the constituents in and the handling of radioactive mixed wastes and has participated in public forums sponsored by the League of Women Voters, City of Santa Fe, and Santa Fe County.

- Commercial Vehicle Safety Alliance (CVSA). The DOE met with the CVSA in 1988 to keep informed on CVSA's pilot study for the inspection of radioactive shipments. The CVSA is an alliance of states that is trying to establish uniform inspection procedures for all hazardous materials shipments.

- Confederated Tribes of the Umatilla Indian Reservation (CTUIR). The DOE attended a workshop on transportation of radioactive materials in 1988. The CTUIR is composed of the Umatilla, Cayuse, and Walla Walla Indian Tribes in northeastern Oregon.

- Eight Northeast Tribes of Oklahoma. The DOE met with this group in 1988 to inform the tribes about WIPP issues. This group is a state-chartered forum that represents the Eastern Shawnee, Seneca-Cayuga, Quapaw, Peoria, Wyandot, Miami, Modoc, and Ottawa Indian Tribes on issues of common concern.

H.3 INTERGOVERNMENTAL AFFAIRS AND PUBLIC INFORMATION PLAN FOR THE WIPP SEIS

In conjunction with the preparation of this WIPP SEIS, the DOE Albuquerque Operations Office has established an Office of Intergovernmental Affairs and Public Information (IAPI). The objective of the IAPI Office is to ensure that public information and public participation activities for this SEIS are in compliance with the CEQ's regulations implementing the NEPA and DOE's NEPA guidelines. To ensure the public has adequate opportunities for involvement in this SEIS, the DOE implemented the following activities:

- Intergovernmental Affairs. The DOE has met with 1) representatives of the States of New Mexico, Colorado, Utah, Idaho, Washington, Oregon, and Wyoming; 2) the Western Governors' Association; 3) the Southern States Energy Board; 4) the National Congress of American Indians and Council of Energy Resource Tribes; 5) EPA and BLM; 6) key environmental groups; 7) New Mexico's Environmental Evaluation Group; and 8) Congressional representatives from the host and corridor states and from oversight committees. The purposes of these meetings were to discuss the planned content of the SEIS, to receive any input regarding environmental issues, and to review the schedule for completion of the NEPA process.

  These meetings provided important input into the development of the SEIS, particularly in the focusing of transportation issues and collection of relevant data. The meetings helped the SEIS Office of Intergovernmental Affairs and Public Information identify information needs that government officials and the interested public may have.

- Federal Register Notice. A Notice of Preparation of the SEIS appeared in the Federal Register on February 17, 1989.

- Mailing List. The DOE developed a comprehensive mailing list for distribution of this SEIS and other materials. The mailing list is a compendium of interested public; Federal, state, and local agencies; elected officials; tribal officials; public interest groups; and others. Sources for this mailing list were responses to the February 17, 1989 Federal Register notice, the 10 waste generator facilities, the FEIS distribution list, the DOE Office of Intergovernmental and External Affairs, and others. In response to informational materials prepared by the SEIS Project Office during the early public information efforts on the SEIS, numerous interested parties asked to be added to the mailing list.

- Others. A variety of press releases and public service announcements have been prepared and distributed to the media and to others on the mailing list.

Digitized by the Internet Archive in 2011 with funding from
University of Illinois Urbana-Champaign

APPENDIX I

METHODS AND DATA USED IN LONG-TERM CONSEQUENCE ANALYSES

LIBRARY U. OF I. URBANA-CHAMPAIGN

TABLE OF CONTENTS

Section			Page
I.0	INTRODUCTION		I-1
I.1	METHODS		I-2
	I.1.1	The NEFTRAN Code	I-2
	I.1.2	The Swift II Groundwater Transport Code	I-5
		I.1.2.1 Implementation of Brine-Reservoir and Borehole Submodels	I-5
		I.1.2.2 Generalized Brine-Reservoir Response	I-8
		I.1.2.3 Reservoir-Borehole-Aquifer Coupling	I-9
	I.1.3	Calculations for Radiation Exposure Pathways	I-11
		I.1.3.1 Philosophy of Dose Limitations in ICRP	I-11
		I.1.3.2 Release at the Head of the Intruding Well	I-12
		I.1.3.3 Geologist Exposure	I-12
		I.1.3.4 Doses Received by Indirect Pathways	I-13
		I.1.3.5 Exposure from Stock Well Water	I-18
	I.1.4	Calculations for Chemical Exposure Pathways	I-22
		I.1.4.1 Lead Solubility in WIPP Composite Brine	I-22
		I.1.4.2 Modeling Assumptions for Calculating Lead Solubility in Culebra Groundwater	I-23
		I.1.4.3 Lead Solubility in Culebra Groundwaters	I-25
		I.1.4.4 Health Effects Associated with Stable Lead from Wind Dispersion	I-25
		I.1.4.5 Health Effects from Exposure to Stable Lead in Beef	I-33
I.2	DATA		I-34
	I.2.1	Final Waste Porosity	I-34
	I.2.2	Radionuclide sorption	I-37
		I.2.2.1 Rationale for Extrapolation of K_d Values	I-41
		I.2.2.2 Rationale for Choices of Recommended K_d Values	I-45
	I.2.3	Brine reservoir Parameters	I-46
		I.2.3.1 Initial Reservoir Pressure	I-46
		I.2.3.2 Reservoir Thickness	I-49
		I.2.3.3 Reservoir Transmissivity	I-50
		I.2.3.4 Reservoir Fluid Density	I-50
		I.2.3.5 Reservoir Boundary	I-50
		I.2.3.6 Reservoir Porosity	I-52
		I.2.3.7 Reservoir Compressibility	I-53
	I.2.4	Borehole Parameters	I-53
	I.2.5	Repository Source-Term Parameters	I-56
	I.2.6	Culebra Parameters	I-59
REFERENCES FOR APPENDIX I			I-67

LIST OF FIGURES

Figure		Page
I.1.1	Conceptualization of the high pressure release scenario	I-6
I.2.1	Generalized distribution of Castile Formation brine occurrences and approximate extent of the Castile "Disturbed Zone" in the Northern Delaware Basin	I-47
I.2.2	Representative plan for plugging a borehole through the repository to a Castile Formation brine reservoir	I-55

LIST OF TABLES

Table		Page
I.1.3.1	Maximum dose received by a member of the drilling crew	I-13
I.1.3.2	Radionuclide concentrations in the dry mud pit	I-14
I.1.3.3	Air concentration and deposition flux values	I-15
I.1.3.4	Steady-state soil concentrations	I-16
I.1.3.5	Soil-to-plant and forage-to-food-product transfer factors (Case II)	I-17
I.1.3.6	50-year committed dose equivalent (CDE) and committed effective dose equivalent (CEDE) factors	I-18
I.1.3.7	Maximum doses received by a person through indirect pathways	I-19
I.1.3.8	Steps in the calculation of human exposure: From radionuclide concentrations in the stock well water to their concentrations in beef	I-20
I.1.3.9	Steps in the calculation of human exposure: From radionuclide concentrations in beef to committed dose to humans	I-21
I.1.4.1	Element concentration entered into the EQ3NR code: Brine solubility calculations	I-24
I.1.4.2	Ionic species and total lead solubility in WIPP composite brine	I-24
I.1.4.3	Element concentrations entered into the EQ3NR code and Pb solubility for the dominant aqueous species: Culebra solubility calculations	I-26
I.1.4.4	Calculation of inhalation of Pb-containing particulates	I-28
I.1.4.5	Calculation of the ambient lead concentration at receptor site	I-29
I.2.1.1	Final void volumes in waste	I-35
I.2.2.1	K_d values for radionuclide transport in the matrix of the Culebra dolomite	I-38
I.2.2.2	K_d values for radionuclide transport in the fracture clays of the Culebra dolomite	I-38
I.2.2.3	K_a values for radionuclide transport in the fracture clays of the Culebra dolomite	I-39
I.2.2.4	K_d and K_a values for radionuclide transport in tunnels, seals, and MB 139	I-39
I.2.2.5	Sources of K_d data used to estimate values for repository (Case I) and Culebra (Case II) transport (saline water ± organic ligands)	I-42
I.2.3.1	Base-case and range of values of parameters describing the brine reservoir	I-48
I.2.4.1	Specifications for intrusion borehole for Case II simulations	I-54
I.2.5.1	Specification of waste radionuclide species and their initial mass inventory (including stable lead) in the repository for the Case II simulations	I-57
I.2.5.2	Specifications for repository parameters used in Case II simulations	I-58
I.2.6.1	Parameter base-case and range values selected for the Culebra dolomite	I-60
I.2.6.2	Summary of porosities measured in Culebra core samples	I-61
I.2.6.3	Summary of formation factors and calculated tortuosities from Culebra core samples	I-66

Digitized by the Internet Archive in 2011 with funding from University of Illinois Urbana-Champaign

I.0 **INTRODUCTION**

This appendix describes the analytical methods, codes, and exposure calculations used to calculate the impacts from the postulated long-term release scenarios discussed in Subsection 5.4. It also presents the basis for selecting the input data values used in the codes.

I.1 METHODS

I.1.1 THE NEFTRAN CODE

The NEFTRAN code (Network Flow and Transport) (Longsine et al., 1987) is used to calculate radionuclide releases from an undisturbed repository in Cases IA and IB. It is a ground-water flow and radionuclide transport code developed by Sandia National Laboratories for the U.S. Nuclear Regulatory Commission. Codes that preceded NEFTRAN are NWFT (Campbell et al., 1979) and NWFT/DVM (Campbell et al., 1981). It was designed with the assumption that all significant flow and radionuclide transport progresses along discrete one-dimensional legs or paths. A flow field is represented by the assemblage of these legs forming a network. The solution of the flow equations in NEFTRAN requires pressure boundary conditions and it is required that these conditions be specified as part of the input data.

NEFTRAN first solves the flow equations for the network using Darcy's Law. From this, the average interstitial fluid and radionuclide velocities for each leg are calculated. The code then uses a Distributed Velocity Method (DVM) applied over the entire length of the migration path using an average velocity for each isotope calculated from the isotopic velocities in all legs. The DVM technique treats convective-dispersive transport by simulating the movement of an ensemble of representative particles. Dispersion is treated by assigning a velocity distribution to these particle ensembles (Campbell et al., 1986).

The user can set up and input any network in the generalized network scheme through a specification of the number of legs, the number of junctions, the junctions bounding each leg, and the junctions where boundary conditions are specified. The hydraulic head gradient provides the driving force for fluid flow through the leg. Conservation of mass at each junction is the assumption that allows the flow network to represent a flow system. This conservation law is given by

$$\sum_j M_j = 0 \qquad \text{(I-1)}$$

where j is the index of summation over all legs that are connected at the given junction, and M_j is the mass flow rate for the jth leg in units of mass per unit time. For the case when the jth leg is bounded by junctions j1 and j2, the mass flow rate in the leg is represented by the equation

$$M_j = \rho_j K_j A_j \left(\frac{(P_{j1} - P_{j2})}{Z_j \rho_j g} + \frac{(E_{j1} - E_{j2})}{Z_j} \right) \qquad \text{(I-2)}$$

where A_j is the cross-sectional area, K_j is the hydraulic conductivity, E_{ji} is the elevation of the ith junction, g is the acceleration due to gravity, P_{ji} is the pressure at the ith junction, Z_j is the length of the leg, and ρ_j is the fluid density.

To account for the effects of brine concentration on the flow, the hydraulic conductivity is weighted as

$$K_j = K'_j \left[\frac{\mu_f}{\mu_j} \right] \left[\frac{\rho_j}{\rho_f} \right] \qquad \text{(I-3)}$$

K_j is the fresh-water hydraulic conductivity for the jth leg, μ_f and ρ_f are the respective viscosity and density of fresh water at approximately 20 degrees C, μ_j and ρ_j are the respective actual viscosity and density in the jth leg.

A matrix equation is developed by applying Equation (I-1) to a boundary junction, substituting Equation (1-2) for M_j with $\Theta_j = A_j K_j / Z_j g$, and repeating this procedure for each junction in the network. The resulting matrix equation is

$$\underline{\underline{\Theta}}\, \underline{p} = \underline{e} \qquad \text{(I-4)}$$

where $\underline{\underline{\Theta}}$ is a matrix of coefficients containing function of $\Theta_j = A_j K_j / Z_j g$, $\underline{p}$ is a vector of unknown pressures, and $\underline{e}$ is a vector of junction elevations and boundary pressures.

NEFTRAN calculates the mass flow rate in each leg using Equation (I-2) and divides it by the corresponding density to determine the volumetric flow rate. This flow rate is then used to calculate the fluid velocity for the jth leg

$$v_{fj} = \frac{Q_j}{A_j \cdot \phi_j} \qquad \text{(I-5)}$$

where ϕ_j is the porosity of the leg and Q_j is the volumetric flow rate.

If j=1,2,...,n is the number of legs along a given radionuclide migration path, NEFTRAN uses the weighted average fluid velocity v_f over the migration path given by

$$\bar{v}_f = \sum_{j=1}^{n} Z_j \Big/ \left[\sum_{j=1}^{n} \frac{Z_j}{v_{fj}} \right] \qquad \text{(I-6)}$$

for the transport simulation such that it preserves total migration time. This approach results in a combination of all legs into a single one-dimensional segment having average properties. This approach has been shown to be sufficient provided the legs in the migration path represent either porous media or transport through fractures with no diffusion into the adjacent matrix blocks.

The Distributed Velocity Method (DVM) is the direct simulation technique used in NEFTRAN to treat the convective-dispersive transport of chains of radionuclides. The DVM approach can treat radionuclide chains of arbitrary length and distribution coefficients. Some numerical dispersion can result from the DVM technique. This dispersion, however, can be controlled while still retaining the efficiency required for risk analysis (Campbell et al., 1981).

The DVM technique is based on the concept that, due to heterogeneity of the flow field, several alternative paths exist for migration of particles from position x' to x where x is the receiver point and donor points are located at coordinates x'. If the density of an ensemble of particles at time t' is given by $\rho(x',t')$, and the density $\rho(x,t)$ at x for $t > t'$ can be determined by introducing a velocity distribution P(v). The equation describing the density of particle at point x is obtained by summing over all possible donor points in the following manner

$$\rho_o(x, t) = \int_{-\infty}^{\infty} dvP(v)\rho(x - v\Delta t, t - \Delta t) \qquad (I\text{-}7)$$

where

$$\Delta t = t - t'$$

The propagation of the initial conditions from time t' to time t is given by Equation (I-7). An integration over "injection" time must be performed in addition to that over velocity, if a source $S(x,\tau)$ is included. Sources could result from either transport of wastes from the repository or decay of a radioactive parent. The propagation of the density function from time t' to t (Equation I-7) is implemented numerically in DVM by discretizing time and space. Also, the velocity-space domain is discretized by dividing the velocity dimension into a few intervals based on equal probability. The propagation of particles is then implemented by simulating the migration of particles in each velocity interval. For the latter, the location of the source is time dependent.

NEFTRAN provides for every species to have a different retardation factor in each leg of the migration path. The average species velocity for each leg is treated separately. The mean species velocity caused by dispersion in the leg for the kth species in the jth leg is given by

$$\bar{v}_{kj} = v_{fj}/R_{kj} \qquad (I\text{-}8)$$

NEFTRAN maintains a mean velocity for each species while calculating distributed velocities about the mean in each leg. When particles begin a time step as a parent species and end the time step as a daughter, NEFTRAN calculates the average velocity by weighting species velocities with the average time as each species

$$v_m(1,. . . \rho) = \frac{1}{(\Delta t)_j} \sum_{j=1}^{p} TS_j \, v_j \qquad (I\text{-}9)$$

The output of NEFTRAN consists of the following:

1. Pressure at each junction of the flow network
2. Volumetric flow rate at each leg of the flow network

3. Discharge rate (in curies/day) of each radionuclide as a function of time at the end of the transport path specified by the user.

In the calculation of Cases IA and IB, the arrival times of radionuclides at the top of shaft or any other point of interest were determined by the times at which the discharge rates rose to 10^{-18} Ci/day.

I.1.2 THE SWIFT II GROUNDWATER TRANSPORT CODE

The SWIFT II (Sandia Waste Isolation Flow and Transport) Code is used to calculate releases from a disturbed repository (Cases IIA through IID). This code requires specification of the time-varying flow out of a brine reservoir and up the borehole to the Culebra. This flow rate is calculated by analytical models described in this section. SWIFT II is a fully transient, three-dimensional code that has been under development and maintenance since 1975. The program has been comprehensively documented and extensively tested. Calculational comparisons to experimental data have resulted in a program that is both accurate and versatile.

SWIFT II solves the coupled equations for transport in geologic media. This code considers the following processes:

- fluid flow
- dominant-species miscible displacement (brine)
- trace-species miscible displacement (radionuclide chains).

The first three processes indicated above are coupled by means of the fluid density and viscosity. This coupling results in a determination of the velocity field that is needed for a calculation of the third and fourth processes.

I.1.2.1 Implementation of Brine-Reservoir and Borehole Submodels

Figure I.1.1 is a drawing of a brine-reservoir breach. It represents a borehole that passes through the repository and connects a brine reservoir to the Culebra. LaVenue et al. (1988) have detailed the most recent model of the Culebra, having calibrated the steady-state flow field to the field data using SWIFT II. The analysis described in this section uses the Culebra model of LaVenue et al., with the pressurized brine reservoir considered analytically as a source term.

In terms of its initial and hydraulic properties, the brine-reservoir submodel is represented by the form

$$Q = A_Q + B_Q \delta p \qquad \text{(I-10)}$$

where δp is the change in pressure within the Culebra source block m during time-step δt. Quantity Q is the volumetric rate of water injection into block m during time-step δt. Q, as well as the flow-rate parameters A_Q and B_Q, are assumed constant during δt. Q varies as a function of time step to reflect depletion of the brine reservoir.

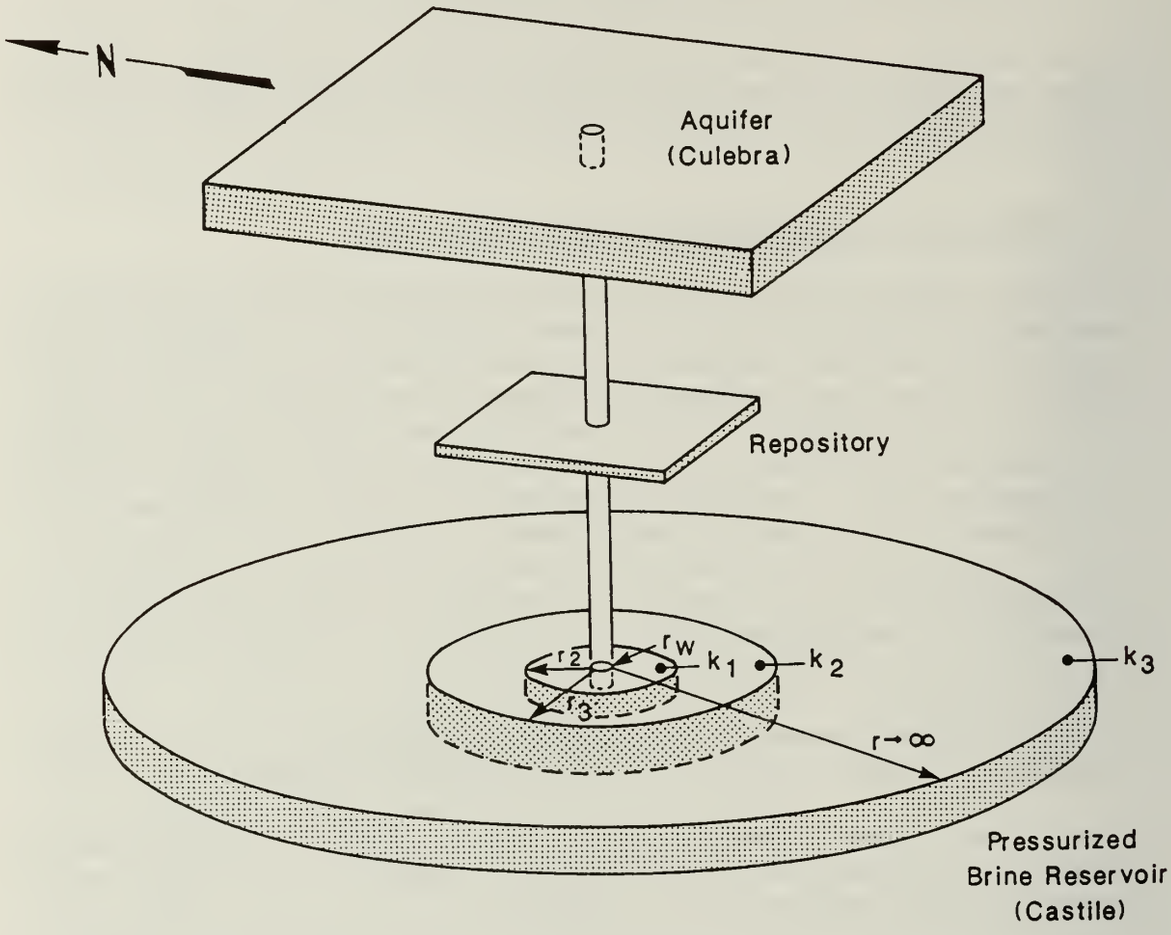

NOT TO SCALE

REF: LAPPIN et al., 1989.

LEGEND

k_1 - HIGH PERMEABILITY AREA
k_2 - LOWER PERMEABILITY AREA
k_3 - VERY LOW PERMEABILITY AREA
r_w - WELL RADIUS
r_2 - RADIUS OF HIGH PERMEABILITY AREA
r_3 - RADIUS OF LOWER PERMEABILITY AREA
$r \rightarrow \infty$ - RADIUS OF VERY LOW PERMEABILITY AREA

FIGURE I.1.1
CONCEPTUALIZATION OF THE HIGH-PRESSURE RELEASE SCENARIO

The brine-reservoir submodel is discussed in the following three subsections. The first subsection describes the influence functions P_I and W_I used to characterize pressure and flow rate, respectively, at the borehole-reservoir interface. The second subsection specifies brine-reservoir response in terms of P_I and its time derivative P'_I. The third and final subsection couples the Culebra and the reservoir to determine a Culebra source term of the form specified in Equation (I-10).

Influence Functions. Van Everdingen and Hurst (1949) consider two basic influence functions useful in determining pressure drawdown and flow rate at the borehole-reservoir interface. W_I represents a constant-pressure condition at $r = r_w$ (Figure I.1.2.1). This term is called the terminal-pressure influence function. The second influence function P_I represents a constant-rate condition at $r = r_w$. This term is the terminal-rate influence function. These functions provide basic functions that, through superposition, result in a general solution.

P_I and W_I are derived from a dimensionless flow equation assumed to have cylindrically symmetric form

$$\frac{1}{r_D}\frac{\partial}{\partial r_D}\left[k_D\, r_D \frac{\partial \Delta p}{\partial r_D}\right] = \frac{\partial \Delta p}{\partial t_D} \qquad \text{(I-11)}$$

where Δp is the pressure drawdown.

For well radius r_w, porosity ϕ, total compressibility c, viscosity μ, and reference permeability k_o, the dimensionless quantities in Equation (I-11) are defined as follows

$$r_D = r/r_w, \quad t_D = t/t_w, \quad t_w = \phi c r_w \mu / k_o, \text{ and } k_d = k/k_o \qquad \text{(I-12)}$$

The reference permeability k_o is set equal to k for an homogeneous system. The result is $k_d = 1$, which is the form of the flow equation given in Van Everdingen and Hurst (1949).

Initial conditions assuming a state of equilibrium in the borehole and reservoir result in the equation

$$\Delta p(r_D, t_D=0) = 0 \qquad \text{(I-13)}$$

At the wellbore-reservoir interface, boundary conditions distinguish two influence functions. For P_I

$$\frac{\partial \Delta p}{\partial r_D}(r_D = 1, t_D) = -1 \,. \qquad \text{(I-14)}$$

For W_I the equation is

$$\Delta p(r_D=1, t_D) = 1 \qquad \text{(I-15)}$$

The constant-rate influence function is obtained as a solution of Equation (I-11) evaluated at the wellbore interface

$$P_I = \Delta p(r_D=1, t_D) \tag{I-16}$$

The dimensionless flow rate at the wellbore interface is given by $\partial \Delta p_D / \partial r_D (r_D=1, t_D)$. Integration over dimensionless time yields the constant-pressure influence function

$$W_I = \int_0^{t_D} \left[\frac{\partial \Delta p}{\partial r_D} \right]_{r_D=1} dt_D \tag{I-17}$$

Van Everdingen and Hurst (1949) assumed homogeneity and derived analytic expressions for P_I and W_I. Frick and Taylor (1962) tabulated these functions. Observations indicate that brine reservoirs at the WIPP site have heterogeneous hydraulic properties. The brine reservoir properties are based on WIPP-12 data. These data indicate that a relatively high-permeability region k_1 located near the well serves as a collection area for a larger region having a lower permeability k_2 (Figure I.1.2.1).

Lappin et al. (1989, Section 3.4.3) present interpretations of the WIPP-12 brine-reservoir test data that result in two permeability regions k_1 and k_2 surrounding the borehole. The assumption is made that yet a third low-permeability zone k_3 provides an effectively infinite source of pressurized brine. Its distance $r > r_3$ is sufficiently great, however, and its permeability k_3 (equal to the permeability of the intact rock) is so small that it does not participate within the time scale of observations from the WIPP-12 field testing. For the three-zone characterization of the brine reservoir, the dimensionless permeability function assumes the form

$$k_D(r_D) = \begin{cases} k_1/k_o & 1 \le r_D \le r_{D2} \\ k_2/k_o & r_{D2} < r_D \le r_{D3} \\ k_3/k_o & r_D > r_{D3} \end{cases} \tag{I-18}$$

The radii r_w, r_2, and r_3 are specified in Figure I.1.2.1. For this heterogeneous system, the reference permeability has been arbitrarily set to $k_o = k_1$. Assuming heterogeneous properties makes an analytic solution difficult. As a result, the study uses the numerical algorithms of the GTFM model (Pickens et al., 1987) to generate the desired influence functions. A tabulation of these functions provides input for SWIFT II.

I.1.2.2 Generalized Brine-Reservoir Response

The influence function W_I represents the total flow that occurs in response to a pressure drop of unity. If the pressure drop at the wellbore $\Delta p_w = \Delta p_w(r_D=1)$ is constant, but differs from unity, then the flow rate is $\Delta p_w W_I$. If, further, Δp_w varies as a function of time, then the principle of superposition (Carslaw and Jaeger, 1959) yields the cumulative fluid flow

$$W_D(t_D) = \int_0^{t_D} \Delta p_w'(\lambda) W_I(t_D - \lambda) d\lambda \tag{I-19}$$

where Δp_w denotes the pressure drop at the wellbore-reservoir interface and the prime denotes differentiation with respect to the argument. Carter and Tracy (1960) approximate Equation (I-19) with a form more suitable for numerical computations by assuming a linear variation within a given time step $t_D^n \leq t_D \leq t_D^{n+1}$

$$W_D^{n+1} = W_D^n + Q_D (t_D - t_D^n) \tag{I-20}$$

where a superscript denotes the time level and Q_D represents an average rate of flow during the time step.

Carter and Tracy (1960) evaluate the flow rate Q_D by equating the right-hand sides of Equations (I-19) and (I-20). Through the use of a step-function Laplace transforms with respect to t_D the equation becomes

$$s\overline{\Delta p}_w \overline{W}_1 = [(W_D^n - Q_D t_D^n)/s] + [Q_D/s^2] \tag{I-21}$$

Here is the Laplace-transform variable, and the bars denote transformed quantities. The analysis of Carter and Tracy becomes approximate with Equation (I-21). Performing an inverse Laplace transform and solving the resulting equation for Q_D gives

$$Q_D = (\Delta p_w^{n+1} - W_D^n P'_I{}^{n+1})/(P_I^{n+1} - t_D^n P'_I{}^{n+1}) \tag{I-22}$$

This equation gives the flow rate as a function of the pressure drop Δp_w at the wellbore. The injection volume W can be accumulated numerically as a function of time, and P_I and P'_I can be evaluated from tables. However, Equation (I-22) applies only to the brine reservoir. The hydraulic coupling to the Culebra is presented below.

I.1.2.3 Reservoir-Borehole-Aquifer Coupling

The following equations characterize the pressure response of the brine reservoir.

$$Q = A_I + B_I \Delta p_{bw} \tag{I-23}$$

where the subscript $_b$ is used to distinguish brine-reservoir quantities, and

$$A_I = -(Q_w/W_w) W^n P_I'^{n+1}/(P_I^{n+1} - t_D^n P_I'^{n+1}) \tag{I-24}$$

and

$$B_I = Q_w/(P_I^{n+1} - t_D^n P_I'^{n+1}) \tag{I-25}$$

Equations (I-23) to (I-25) represent the pressure response of the brine reservoir. In order to characterize the borehole, the analysis assumes a finite transmissibility T_w in the plugs and rubble. The borehole flow is governed by the equilibrium condition

$$Q = T_w (p_{bw} - p_w - \rho_s g \Delta h) \tag{I-26}$$

The saturated brine of density ρ_s is assumed to occupy the wellbore with a vertical distance Δh separating the centroids of the Culebra and the brine reservoir.

The static pressure difference $\Delta p_o = P_{bo} - \rho_s g\Delta h - p_o$ can be substituted into Equation (I-26), giving the equation

$$Q = T_w (\Delta p_w - \Delta p_{bw} - \Delta p_o) \tag{I-27}$$

where Δp_{bw} and Δp_w represent pressure drops of the brine reservoir and the aquifer, respectively.

Hydraulic coupling to the Culebra requires that the analysis focus on the grid-block m that was penetrated by the wellbore. The coupling is influenced by several factors. These include the pore value of the block, its transmissive connections to neighboring blocks, and the hydraulic connection between the wellbore and the grid block. To characterize the latter, the following relation between the borehole flow and pressure differences is assumed

$$Q = M (p_w - p) \tag{I-28}$$

which indicates a proportionality between flow rate and pressure drop between the wellbore and the grid-block center.

M, the mobility, is given by

$$M = 2\pi(\mu_o/\mu)(K/\rho_o g)\Delta z/\ln(r_1/r_w) \tag{I-29}$$

where K is the hydraulic conductivity of the grid block, Δz is the thickness of the Culebra, and ρ_o and μ_o are reference values of density and viscosity, respectively. These parameters are used to convert hydraulic conductivity to permeability. The quantities ρ and μ vary as functions of the average salinity of the fluid in the grid block.

Equation (I-28) along with Equation (I-29) and the equation

$$\ln(r_1/r_w) = r_w(1+\Delta r/r_w) [\ln(\Delta r/r_w)-1]/(\Delta r - r_w) \tag{I-30}$$

provide a definition of the mobility as the hydraulic conductance from the wellbore radius to the radius of the average pressure. Equation (I-28) can be written in the form

$$Q = M(\Delta p - \Delta p_w) \tag{I-31}$$

The flow rate injected into the Culebra can be represented as

$$Q = [A_I + B_I (\Delta p_o + \Delta p)] T/(T + B_I) \tag{I-32}$$

The net transmissibility due to borehole-aquifer coupling is

$$T^{-1} = T_w^{-1} + M^{-1} \tag{I-33}$$

The assumption has been made that the wellskin of the brine reservoir is sufficiently high in permeability relative to T_w and M that it may be neglected in Equation (I-33).

Expressions for A_Q and B_Q in Equation (I-1) are

$$A_Q = [A_I + B_I (\Delta p_o + \Delta p^n)] T/(T + B_I) \quad \text{(I-34)}$$

and

$$B_Q = - TB_I/(T + B_I) \quad \text{(I-35)}$$

Equations (I-34) and (I-35) are the equations necessary for a determination of the flow rate.

I.1.3 CALCULATIONS FOR RADIATION EXPOSURE PATHWAYS

This section describes the conversion from amounts of released radionuclides to human radiation exposures (Cases IIA through IID). The 1980 FEIS analyzed the effects of radioactivity release from the WIPP through consideration of the consequences of five different hypothetical scenarios that would result in the movement of radionuclides to the biosphere. The analysis of these scenarios followed a pathway that led from radionuclide movement through the geosphere to transport through the biosphere after discharge into the Pecos River at Malaga Bend and ultimately predicted radiation doses to the people living in the area. Direct-access releases to the surface from an intrusion borehole were also included. Human dose estimates in the FEIS used information from the International Commission on Radiological Protection.

The SEIS concentrates on the effects of release of radioactivity from the WIPP through an estimate of the consequences of two different hypothetical cases. Human dose estimates are based on the new International Commission on Radiation Protection (ICRP) philosophy in ICRP 26 and 30 (ICRP, 1977; and ICRP, 1979, respectively). Indications are that analyses with the new ICRP philosophy for internal dose assessment are less restrictive than the previous methods (ICRP, 1959) for about 25 percent of the radionuclides considered, more restrictive for about 25 percent, and about the same for the remaining 50 percent (Poston, 1985).

With the exception of this somewhat changed philosophy, the pathways calculations in the SEIS repeat the FEIS pathways calculations with a minimum of change. This approach responds to changes in repository design and improved understanding of local geohydrology rather than to changes in biological pathway parameters.

I.1.3.1 Philosophy of Dose Limitations in ICRP

The International Commission on Radiological Protection recommends (ICRP, 1977) a system of dose limitations based on three principles. The first of these is that no practice shall be adopted unless it results in a net positive benefit. The second is that all exposures shall be kept as low as reasonably achievable (ALARA). The third principle is that the dose equivalent to an individual shall not exceed the ICRP recommended limits.

In addition, the ICRP also suggests two other methods of controlling exposure. It recommends controlling exposure on an annual basis through an annual dose equivalent limit and also with a "committed effective dose equivalent." This is the dose equivalent received from internally deposited material integrated over a 50-year working life. The "committed effective dose equivalent" is the concept that is used for calculating internal doses in this SEIS.

A discussion of the possible pathways for Cases I and II (A and B) now follows. The pathway begins as a release to the surface at the top of the intruding borehole.

I.1.3.2 Release at the Head of the Intruding Well

The release at the top of the intrusion well consists of two elements. A repository panel is breached by a borehole, and cuttings are removed directly from the panel. Then later the drillhole penetrates a brine reservoir in the Castile Formation and more material is brought to the surface. The time required to drill from the repository level down to the brine reservoir is about 15 hours. During this time radioactive material continues to be eroded from the consolidated waste by the swirl of the drilling fluid.

Penetration of the Castile brine pocket results in pressurized brine mixing with the drilling fluid in the borehole and flowing with it up to the wellhead. About 1000 barrels of brine-pocket fluid are assumed to mix with the drilling fluid and recirculate through the panel to the surface. The equivalent of three drums of consolidated wastes is assumed removed in the form of cuttings and eroded material. The drilling operation ends and the borehole is plugged and capped, and the immediate supply of radioactive material to the surface ceases.

I.1.3.3 Geologist Exposure

The approach used to calculate the highest individual external dose received by a member of the drilling crew is the same as that used in the FEIS Section 9.7.1.5. The highest individual external dose is received by a geologist who examines cuttings for a period of one hour at a distance of one meter (about one yard). The samples are treated as point sources with no self-shielding effects. Elements considered are plutonium-238, plutonium-239, plutonium-240, uranium-233, uranium-235, americium-241, and neptunium-237.

The calculation uses the equation (USPS, 1970)

$$Exp = 0.5 \cdot n \cdot E \cdot C \qquad \text{(I-36)}$$

where Exp is the exposure rate at one-meter distance from the source (mR/hr), E is the gamma ray energy (MeV), n is the number of gamma quanta per disintegration, and C is the activity of the sample (mCi). As indicated above, the geologist examines a sample for one hour. The sample is assumed to have a volume of 526 cm^3. After the disposal room is fully compacted, a single consolidated drum will occupy a volume of about 21.5 gal (81 l). The ratio of volumes implies that the sample occupies 1/155 of the consolidated drum; the radioactivity in a single sample is obtained by dividing the

inventory-per-drum values by 155. The dose to the geologist on a per sample basis is presented in Table I.1.3.1.

TABLE I.1.3.1 Maximum dose received by a member of the drilling crew

Nuclide Nuclide	C (mCi/sample)	E (MeV)	n (γ-q/dis)	Exp (mR/hr-sample)
Plutonium-239	35.0	0.099	8.0×10^{-5}	1.4×10^{-4}
Plutonium-239	4.0	0.0		
Plutonium-240	1.0	0.65	2.0×10^{-7}	6.5×10^{-8}
Uranium-233	0.06	0.029	1.7×10^{-4}	1.5×10^{-7}
Uranium-235	3.2×10^{-6}	0.143	0.11	
		0.185	0.54	
		0.204	0.05	3.0×10^{-7}
Americium-241	7.1	0.06	0.36	0.077
Neptunium-237	7.3×10^{-5}	0.0		
Total				0.077

I.1.3.4 Doses Received by Indirect Pathways

The inventory in the analysis described above involves the equivalent of three drums of consolidated waste material brought to the surface during the drilling operation. The material (cuttings and particles eroded from the room contents by drilling fluid) are deposited into a settling pond at the top of the drillhole. After the drilling operations end, the radioactive material present in the settling pond is available for transport through airborne or surface-water pathways.

A ranch family hypothetically resides at a distance of 500 meters (550 yd) downwind from this settling pond. Exposure to the family is through two pathways:

- Inhalation of contaminated air
- Ingestion of foods (meat, milk, and above- and below-surface food crops) produced on the ranch.

The settling pond is assumed to be 14 ft wide, 35 ft long, and 12 ft deep. The pond contains 44,000 gal of mud and has a surface area of 500 ft^2. There is also a second pit called the suction pit downstream of the settling pit. The volume of these two pits

totals about three times the volume of the borehole. It is assumed that all waste materials are discharged into the settling pit. Radionuclide concentrations in the dry mud pit are shown in Table I.1.3.2.

TABLE I.1.3.2 Radionuclide concentrations in the dry mud pit

Nuclide	Concentration (Ci/g)
Americium-241	2.83×10^{-8}
Neptunium-237	2.91×10^{-13}
Plutonium-238	1.42×10^{-7}
Plutonium-239	1.54×10^{-8}
Plutonium-240	3.86×10^{-9}
Uranium-233	2.57×10^{-10}
Uranium-235	1.29×10^{-14}

A procedure called the squared Gaussian plume model (FEIS, Section K.3.1) was used to calculate the downwind surface air concentration at a distance of 500 m (550 yd) and the resulting dry-deposition flux. Provided the area of the mud pit is small [less than 100 square meters (120 yd^2)], the suspended material transported to distances greater than about 100 meters (110 yd) from the pit may be assumed to come from a point source. The Gaussian plume model for air concentration downwind is given by the expression

$$\chi = \frac{2Q}{\sqrt{2\pi}\ 3\sigma_y\ \sigma_z\ u} \qquad \text{(I-37)}$$

where

χ = ground-level air concentration (Ci/m^3)
Q = source strength (Ci/sec)
$3\sigma_y$ = lateral width of assumed uniform distribution (m)
σ_z = vertical standard deviation (m)
u = average wind speed (m/sec).

These air concentrations and deposition fluxes are shown in Table I.1.3.3.

TABLE I.1.3.3 Air concentration and deposition flux values

Nuclide	Concentration (Ci/m^3)	Flux (Ci/m^2-s)	Deposition (Ci/m^2-yr)
Americium-241	3.07×10^{-18}	3.07×10^{-20}	9.70×10^{-13}
Neptunium-237	3.16×10^{-23}	3.16×10^{-25}	9.96×10^{-18}
Plutonium-238	1.54×10^{-17}	1.54×10^{-19}	4.85×10^{-12}
Plutonium-239	1.68×10^{-18}	1.68×10^{-20}	5.29×10^{-13}
Plutonium-240	4.19×10^{-19}	4.19×10^{-21}	1.32×10^{-13}
Uranium-233	2.79×10^{-20}	2.79×10^{-22}	8.82×10^{-15}
Uranium-235	1.40×10^{-24}	1.40×10^{-26}	4.41×10^{-19}

Parameters involved in this calculation include the following:

1. resuspension rate
2. wind velocity
3. density of dry drilling mud
4. mud pit surface area
5. depth available for resuspension
6. deposition velocity
7. particle size.

The source area is approximated by choosing a vertical standard deviation and lateral width of the assumed Gaussian distribution and identifying a virtual point source 20.6 m (22.5 yd) upwind of the leeward side of the pit. Steady-state soil concentrations at 100 years (within 2 percent of steady state) appear in Table I.1.3.4.

Transfer factors used in the dose calculations are given in Table I.1.3.5.

Data on human food consumption per capita are required for the four pathways. Data for the United States were taken from Till and Meyer (1983, Table 6.8). They are 508 g/day for milk, 206 g/day for meat products, 103 g/day for below-surface crops, and 202 g/day for above surface crops. Each steer eats 15 kg of fresh forage per day.

TABLE I.1.3.4 Steady-state soil concentrations

Nuclide	Concentration (Ci/kg(soil))
Americium-241	9.48×10^{-18}
Neptunium-237	9.74×10^{-23}
Plutonium-238	4.74×10^{-17}
Plutonium-239	5.17×10^{-18}
Plutonium-240	1.29×10^{-18}
Uranium-233	8.62×10^{-20}
Uranium-235	4.31×10^{-24}

The analysis used various computer codes to tabulate the committed effective dose equivalent for various body organs per unit activity inhaled or ingested. The organs included in these tabulations are those explicitly considered by the ICRP to be at risk. The committed dose equivalent is the total dose equivalent that an organ or tissue of the body is expected to receive over the 50-year period following exposure. It is recognized that in most environmental applications, more rigorous evaluation requires information on the time variation in the dose equivalent rates for the various tissues at risk. This information provides the time dependence of environmental conditions, and therefore that of the intake could be assessed with consideration of the years of remaining life. It is also recognized that overestimates by factors of 2 to 3 in the risk are possible by not using the time-dependent nature of the organ dose equivalent rates and the years of life remaining.

Committed dose equivalent (CDE) and committed effective dose equivalent (CEDE) factors used in the analysis are shown in Table I.1.3.6.

TABLE I.1.3.5 Soil-to-plant and forage-to-food-product transfer factors (Case II)

Nuclide	Soil-to-Plant (kg-soil/kg-plant)	Forage-to-Food Product (day/kg-food or day/kg-milk)
Beef:		
Americium-241	4.2×10^{-2}	3.6×10^{-6}
Neptunium-237	9.2×10^{-2}	5.0×10^{-6}
Plutonium-238	1.4×10^{-2}	1.0×10^{-6}
Plutonium-239	1.4×10^{-2}	1.0×10^{-6}
Plutonium-240	1.4×10^{-2}	1.0×10^{-6}
Uranium-233	1.7×10^{-2}	3.4×10^{-4}
Uranium-235	1.7×10^{-2}	3.4×10^{-4}
Milk:		
Americium-241	4.2×10^{-2}	2.0×10^{-6}
Neptunium-237	9.2×10^{-2}	5.0×10^{-6}
Plutonium-238	1.4×10^{-2}	2.7×10^{-6}
Plutonium-239	1.4×10^{-2}	2.7×10^{-6}
Plutonium-240	1.4×10^{-2}	2.7×10^{-6}
Uranium-233	1.7×10^{-2}	6.1×10^{-4}
Uranium-235	1.7×10^{-2}	6.1×10^{-4}
Dried edible below surface crops:		
Americium-241	6.4×10^{-5}	
Neptunium-237		
Plutonium-238	1.4×10^{-3}	
Plutonium-239	1.4×10^{-3}	
Plutonium-240	1.4×10^{-3}	
Uranium-233	9.0×10^{-4}	
Uranium-235	9.0×10^{-4}	
Dried edible above surface crops:		
Americium-241	2.8×10^{-5}	
Neptunium-237	1.5×10^{-2}	
Plutonium-238	1.7×10^{-4}	
Plutonium-239	1.7×10^{-4}	
Plutonium-240	1.7×10^{-4}	
Uranium-233	1.0×10^{-3}	
Uranium-235	1.0×10^{-3}	

Note. All data are from Till and Meyer (1983), Tables 5.16, 5.18, 5.36, and 5.37. The data from Table 5.16 were divided by 10 or 4.5 for dry-to-wet conversion. Transfer factors were selected assuming that vegetables would be washed before being eaten.

TABLE I.1.3.6 50-year committed dose equivalent (CDE) and committed effective dose equivalent (CEDE) factors (rem/μCi)

Nuclide	Ingestion CEDE (rem/μCi)	Inhalation CDE (rem/μCl)
Americium-241	4.5	10,000
Neptunium-237	3.9	9,600
Plutonium-239	0.054	3,300
Plutonium-239	0.058	3,800
Plutonium-240	0.058	3,800
Uranium-233	0.025	1,100
Uranium-235	0.025	1,000

Note. All data are from DOE (1988). The CEDE values are for the whole body; the CDE values are for critical organs. Lungs are the critical organ for uranium inhalation. Bone is the critical organ in all other cases.

The doses to the other tissues in the body are generally no more than a tenth of the doses to the body from radionuclides ingested and inhaled.

Table I.1.3.7 lists the maximum doses received by a person through indirect pathways for each nuclide of importance. These pathways include ingestion of foods provided by animals feeding on the land as well as crops grown below and aboveground (root and leafy vegetables). The inhalation pathway assumes a breathing rate of 2.7×10^{-4} m^3/s. This table summarizes the exposure calculated for a person living on the hypothetical farm described in the section below for a 50-year committed effective dose equivalent.

I.1.3.5 Exposure from Stock Well Water

In addition to radiation exposure at the top of the intrusion borehole at the WIPP site itself, there is a possible exposure pathway through a stock well down-gradient about 5 km (3 mi). The starting point for these calculations is where the stock well draws water from the Culebra aquifer. The salinity of the water at this well is low enough for the cattle to drink. Concentrations of the radionuclides within the stock well are given in Table 5.7. The SEIS calculation selects concentrations at 10,000 years, since at that time the concentrations are still rising. The human exposure calculated here is the exposure of a person who eats beef from those cattle.

The calculation assumes that eight cattle graze in the square mile (2.6 km^2) around the well. Each animal requires 13 gal/day (49 l/day) of water to drink. Therefore, allowing for rainfall at the rate of 20 cm/yr and evaporation at the rate of 200 cm/yr and a stock pond whose area is 139 ft^2 (0.0013 hectares), this well is pumped at the rate of 120 gal/day (460 l/day).

TABLE I.1.3.7 Maximum doses received by a person through indirect pathways

Committed Effective Dose Equivalents After a 1-Year Exposure (mrem/50 yr)					
Nuclide	Beef	Milk	Vegetables	Root Crops	Inhalation
Americium-241	3.04×10^{-12}	9.97×10^{-11}	8.81×10^{-11}	1.03×10^{-10}	2.62×10^{-1}
Neptunium-237	8.23×10^{-17}	4.86×10^{-16}	4.20×10^{-13}		2.58×10^{-6}
Plutonium-238	1.69×10^{-14}	2.69×10^{-16}	3.30×10^{-11}	1.35×10^{-10}	4.37×10^{-1}
Plutonium-239	1.98×10^{-15}	3.15×10^{-17}	3.87×10^{-12}	1.58×10^{-11}	5.40×10^{-2}
Plutonium-240	4.94×10^{-16}	7.89×10^{-18}	9.68×10^{-13}	3.95×10^{-12}	1.35×10^{-2}
Uranium-233	5.87×10^{-15}	6.22×10^{-14}	1.59×10^{-13}	7.29×10^{-14}	2.62×10^{-4}
Uranium-235	2.93×10^{-19}	3.11×10^{-18}	7.95×10^{-18}	3.65×10^{-18}	1.19×10^{-8}
Total ingested dose:			4.87×10^{-10}		
Total inhaled dose:					7.66×10^{-1}

The maximally exposed individual is assumed to eat beef from the cattle at the rate of 86 g/day (NCRP, 1984, Table 5.3).

Table I.1.3.8 shows the chain of logic leading from the concentrations of the various radionuclides in the well water to the concentrations of those radionuclides in the beef. Table I.1.3.9 continues from the concentration in beef to the dose to humans, expressed as the 50-year committed dose from a one year's consumption of that beef.

TABLE I.1.3.8 Steps in the calculation of human exposure: From radionuclide concentrations in the stock well water to their concentrations in beef.

Nuclide	A Concentration in well kg (nuclide)/ kg (brine)	B Specific activity (Ci/g)	C Concentration in pond (Ci/l)	D Conversion factor (d/kg)	E Concentration in beef (Ci/kg)
			Case IIA		
Pb-210	7.61×10^{-19}	$7.63 \times 10^{+1}$	7.43×10^{-14}	3.0×10^{-4}	1.11×10^{-15}
Ra-226	5.46×10^{-17}	1.0	6.99×10^{-14}	2.5×10^{-4}	8.73×10^{-15}
Th-230	8.21×10^{-23}	2.02×10^{-2}	2.12×10^{-21}	6.0×10^{-6}	6.37×10^{-25}
U-234	1.68×10^{-18}	6.25×10^{-3}	1.34×10^{-17}	2.0×10^{-4}	1.34×10^{-19}
			Case IIB		
Np-237	8.73×10^{-9}	7.05×10^{-4}	7.55×10^{-9}	5.5×10^{-5}	2.08×10^{-11}
Pb-210	1.20×10^{-13}	$7.63 \times 10^{+1}$	1.17×10^{-8}	3.0×10^{-4}	1.76×10^{-10}
Pu-239	8.36×10^{-10}	6.22×10^{-2}	6.66×10^{-8}	5.0×10^{-7}	1.66×10^{-12}
Pu-240	1.07×10^{-10}	2.28×10^{-1}	3.13×10^{-8}	5.0×10^{-7}	7.83×10^{-13}
Ra-226	8.63×10^{-12}	1.0	1.10×10^{-8}	2.5×10^{-4}	1.38×10^{-10}
Th-229	3.65×10^{-11}	2.13×10^{-1}	9.95×10^{-9}	6.0×10^{-6}	2.99×10^{-12}
Th-230	9.01×10^{-12}	2.02×10^{-2}	2.33×10^{-10}	6.0×10^{-6}	6.99×10^{-14}
U-233	2.92×10^{-7}	9.68×10^{-3}	3.61×10^{-7}	2.0×10^{-4}	3.61×10^{-9}
U-234	7.94×10^{-9}	6.25×10^{-3}	6.35×10^{-8}	2.0×10^{-4}	6.35×10^{-10}
U-236	7.71×10^{-9}	6.47×10^{-5}	6.39×10^{-9}	2.0×10^{-4}	6.39×10^{-12}
			Case IIC		
Np-237	2.98×10^{-8}	7.05×10^{-4}	2.69×10^{-8}	5.5×10^{-5}	7.40×10^{-11}
Pb-210	4.15×10^{-14}	$7.63 \times 10^{+1}$	4.05×10^{-9}	3.0×10^{-4}	6.07×10^{-11}
Pu-239	4.14×10^{-14}	6.22×10^{-2}	3.29×10^{-12}	5.0×10^{-7}	8.24×10^{-17}
Pu-240	2.32×10^{-14}	2.28×10^{-1}	6.77×10^{-12}	5.0×10^{-7}	1.69×10^{-16}
Ra-226	2.98×10^{-12}	1.0	3.81×10^{-9}	2.5×10^{-4}	4.76×10^{-11}
Th-229	1.58×10^{-11}	2.13×10^{-1}	4.30×10^{-9}	6.0×10^{-6}	1.29×10^{-12}
Th-230	3.57×10^{-12}	2.02×10^{-2}	9.22×10^{-11}	6.0×10^{-6}	2.77×10^{-14}
U-233	8.59×10^{-8}	9.68×10^{-3}	1.06×10^{-6}	2.0×10^{-4}	1.06×10^{-8}
U-234	2.86×10^{-8}	6.25×10^{-3}	2.29×10^{-7}	2.0×10^{-4}	2.29×10^{-9}
U-236	8.84×10^{-9}	6.47×10^{-5}	7.32×10^{-10}	2.0×10^{-4}	7.32×10^{-12}
			Case IID		
Np-237	2.57×10^{-10}	7.05×10^{-4}	2.32×10^{-10}	5.5×10^{-5}	6.38×10^{-13}
Pb-210	1.46×10^{-15}	$7.63 \times 10^{+1}$	1.43×10^{-10}	3.0×10^{-4}	2.14×10^{-12}
Pu-239	6.58×10^{-13}	6.22×10^{-2}	5.24×10^{-11}	5.0×10^{-7}	1.31×10^{-15}
Pu-240	3.83×10^{-13}	2.28×10^{-1}	1.12×10^{-10}	5.0×10^{-7}	2.80×10^{-15}
Ra-226	1.05×10^{-13}	1.0	1.34×10^{-10}	2.5×10^{-4}	1.68×10^{-12}
Th-229	1.52×10^{-13}	2.13×10^{-1}	4.13×10^{-11}	6.0×10^{-6}	1.24×10^{-14}
Th-230	1.20×10^{-13}	2.02×10^{-2}	3.10×10^{-12}	6.0×10^{-6}	9.31×10^{-16}
U-233	2.55×10^{-10}	9.68×10^{-3}	3.16×10^{-9}	2.0×10^{-4}	3.16×10^{-11}
U-234	2.56×10^{-10}	6.25×10^{-3}	2.04×10^{-9}	2.0×10^{-4}	2.04×10^{-11}
U-236	7.40×10^{-11}	6.47×10^{-5}	6.12×10^{-12}	2.0×10^{-4}	6.12×10^{-14}

Column C = A x B x 1100(g/l) x 1.1635
Column E = C x D x 50(l/d)

TABLE I.1.3.9 Steps in the calculation of human exposure: From radionuclide concentrations in beef to committed dose to humans.

Nuclide	E Concentration in beef (Ci/kg)	F Ingestion rate (Ci/d)	G CEDE (rem/μCi)	H Committed dose (mrem)
Case IA (Total = 2.09×10^{-4})				
Pb-210	1.11×10^{-15}	9.58×10^{-17}	5.1	1.78×10^{-4}
Ra-226	8.73×10^{-16}	7.51×10^{-17}	1.1	3.02×10^{-5}
Th-230	6.37×10^{-25}	5.48×10^{-26}	5.3×10^{-1}	1.06×10^{-14}
U-234	1.34×10^{-19}	1.15×10^{-20}	2.6×10^{-1}	1.1×10^{-9}
Case IIB (Total = $7.2\times10^{+1}$)				
Np-237	2.08×10^{-11}	1.79×10^{-12}	3.9	2.54×10^{-5}
Pb-210	1.76×10^{-10}	1.52×10^{-11}	5.1	2.82×10^{-4}
Pu-239	1.66×10^{-12}	1.43×10^{-13}	4.3	2.25×10^{-7}
Pu-240	7.83×10^{-13}	6.74×10^{-14}	4.3	1.06×10^{-7}
Ra-226	1.38×10^{-10}	1.19×10^{-11}	1.1	4.77
Th-229	2.99×10^{-12}	2.57×10^{-13}	3.5	3.28×10^{-1}
Th-230	6.99×10^{-14}	6.01×10^{-15}	5.3×10^{-1}	1.16×10^{-3}
U-233	3.61×10^{-9}	3.11×10^{-10}	2.7×10^{-1}	$3.06\times10^{+1}$
U-234	6.35×10^{-10}	5.46×10^{-11}	2.6×10^{-1}	5.18
U-236	6.39×10^{-12}	5.49×10^{-13}	2.5×10^{-1}	5.01×10^{-2}
Case IIC (Total = $1.29\times10^{+2}$)				
Np-237	7.40×10^{-11}	6.37×10^{-12}	3.9	9.06
Pb-210	6.07×10^{-11}	5.22×10^{-12}	5.1	9.72
Pu-239	8.24×10^{-17}	7.08×10^{-18}	4.3	1.11×10^{-5}
Pu-240	1.69×10^{-16}	1.46×10^{-17}	4.3	2.28×10^{-5}
Ra-226	4.76×10^{-11}	4.09×10^{-12}	1.1	1.64
Th-229	1.29×10^{-12}	1.11×10^{-13}	3.5	1.42×10^{-1}
Th-230	2.77×10^{-14}	2.38×10^{-15}	5.3×10^{-1}	4.60×10^{-4}
U-233	1.06×10^{-8}	9.15×10^{-10}	2.7×10^{-1}	$9.02\times10^{+1}$
U-234	2.29×10^{-9}	1.97×10^{-10}	2.6×10^{-1}	$1.87\times10^{+1}$
U-236	7.32×10^{-12}	6.30×10^{-13}	2.5×10^{-1}	5.75×10^{-2}
Case IID (Total = 9.15×10^{-1})				
Np-237	6.38×10^{-13}	5.49×10^{-14}	3.9	7.81×10^{-2}
Pb-210	2.14×10^{-12}	1.84×10^{-13}	5.1	3.43×10^{-1}
Pu-239	1.31×10^{-15}	1.13×10^{-16}	4.3	1.77×10^{-4}
Pu-240	2.80×10^{-15}	2.40×10^{-16}	4.3	3.77×10^{-4}
Ra-226	1.68×10^{-12}	1.44×10^{-13}	1.1	5.79×10^{-2}
Th-229	1.24×10^{-14}	1.07×10^{-15}	3.5	1.36×10^{-3}
Th-230	9.31×10^{-16}	8.00×10^{-17}	5.3×10^{-1}	1.55×10^{-5}
U-233	3.16×10^{-11}	2.71×10^{-12}	2.7×10^{-1}	2.67×10^{-1}
U-234	2.04×10^{-11}	1.76×10^{-12}	2.6×10^{-1}	1.67×10^{-1}
U-236	6.12×10^{-14}	5.27×10^{-15}	2.5×10^{-1}	4.81×10^{-4}

Column F = E x 0.086(kg/d)
Column H = F x G x 365(day) x 1000(mrem/rem)

Column A is from the flow calculations reported by Lappin et al. (1989, Chapter 7 and Appendix E) and reviewed in SEIS Section 5.7.2.6. The factor of 1.165 used in going from Column A to Column C is the factor by which the water in the stock pond is enriched by evaporation. The factor in Column D that converts from the amount of water the steer drinks to the concentration of a radionuclide in his flesh is from Till and Meyer (1983, Table 5.37). The factors given by these authors are actually for the forage-to-beef pathway, used here because of the lack of any similar table for the water-to-beef pathways, and as recommended in NRC Regulatory Guide 1.109 (NRC, 1976). The conversion factors of Column G are from tables for individual radionuclides in DOE/EH-0071 (DOE, 1988). These last factors allow for all the steps from the ingestion of beef to the resultant committed effective dose equivalent, including the amount of the nuclide not excreted.

By way of example, the 129 mrem total dose calculated in Case IIC for a person eating the contaminated beef watering at the stock well for one year is a 50-year committed effective dose equivalent. If the individual used this beef for only one year, he would receive an average annual exposure of 2.6 mrem, which is approximately 1/40 the 100-mrem average annual background present in the United States. However, this individual will continue to eat beef. It is standard procedure to calculate the total dose equivalent for radionuclides deposited in the body that will occur over a 50-year period. This is reported in the year that the radionuclide is ingested. On this basis, a committed effective dose equivalent of 129 mrem is about 30 percent higher than background.

I.1.4 CALCULATIONS FOR CHEMICAL EXPOSURE PATHWAYS

Lead is used as an indicator chemical parameter for the purpose of evaluating potential risks associated with the hazardous chemical component of TRU waste during the long-term (i.e., 10,000 year) performance of the WIPP. Unlike organic compounds that will degrade with time, metals will be perpetually present in the waste. The initial concentration of metals in the waste will remain constant with time, although the prevalent chemical species may be altered with time due to changes in the repository environment. Lead is the most prevalent metal present in the waste, and the potential for exposure to lead through releases is expected to bound any potential for exposure through releases associated with any other hazardous chemicals in the long term.

I.1.4.1 Lead Solubility in WIPP Composite Brine

The concentration of heavy metals in solution is controlled by the solubility of various oxides, carbonates, sulfates, and sulfides. The solid and aqueous species present in aqueous systems is dependent on oxidation-reduction reactions (measured in terms of Eh) and acid-base reactions (measured in terms of pH). A system has reached equilibrium when the forward reaction just balances the reverse reaction. When substances are mixed, such as when brine comes in contact with the TRU waste in the repository, they undergo chemical changes. In natural systems, a final equilibrium is probably never attained because chemical reactions occur at different rates and the environment may be changed by a process that alters the chemistry of the system. Regardless of the rate at which equilibrium is attained, equilibrium relationships are useful for predicting chemical changes that can or cannot occur.

The concentration of lead in WIPP composite brine (Abitz et al., 1989) was calculated using the Pitzer equations employed in the EQ3NR solubility/speciation computer code (Wolery, 1983; Jackson, 1988) by equilibrating the native brine with the mineral anglesite (PbSO4) at pH = 6.1, Eh = 411 mV, T = 27°C. Eh was constrained by the NH4+/NO3 redox couple. For a system defined by these parameters, and equal concentrations of CO_3^{-} and SO_4^{-}, cerussite ($PbCO_3$) is the predicted stable phase (Brookins, 1988). However, anglesite ($PbSO_4$) was utilized in the solubility model because both Pb^{++} and CO_3^{-} are not mutually present in any one of the thermodynamic data bases accessed by the EQ3NR code. This presents no critical problem when evaluating solubility models for WIPP composite brine because the total inorganic carbon (estimate of CO_3^{-}) rarely exceeds 5 mg/l, whereas SO_4^{-} averages 17,000 mg/l. Therefore, it is assumed that the activity of CO_3^{-} in the brine is negligible.

Table I.1.4.1 contains the element concentrations entered into the EQ3NR code for the brine solubility simulation. The calculated lead concentration, with mean ionic values for log a(±), are shown in Table I.1.4.2. The solubility for lead is 116 mg/l. When using the solubility values, it should be kept in mind that they represent the maximum concentrations which can exist in solution. Actual concentrations are influenced by several factors, including dissolution rates and available surface area. The log a(±) values indicate which species complexes are likely to be present in the brine, with the most dominant complexes having the number closest to zero (e.g., PbCl species for Pb). Unfortunately, Pitzer's equations cannot evaluate the relative concentrations among species of an ion pair (e.g., $PbCl^{+}$ versus $PbCl_2$), so the charge on the dominant species cannot be predicted. For the purposes of further calculations, the charge on the dominant species is assumed to be zero.

I.1.4.2 Modeling Assumptions for Calculating Lead Solubility in Culebra Groundwater

Aqueous speciation/solubility calculations with the EQ3NR code (Wolery, 1983) were performed to estimate the lead solubility in Culebra groundwaters (using representative samples from wells H-2a, H-3b and H-14 in Randall et al., 1988). In addition to lead, the elements active in this problem were boron, carbon, calcium, chlorine, fluorine, iron, hydrogen, potassium, magnesium, manganese, sodium, oxygen, sulfur, silicon, and strontium. The number of aqueous species (178-194) and minerals (208-225) that are active in a given problem is unique for each groundwater composition. However, the number of gas species was seven in all three cases. The solubility model is based on the following assumptions:

1. Cerussite is the stable solid phase for lead under the indicated temperature, pressure, Eh (oxidation-reduction state), and pH of the system.

2. The system oxidation-reduction reactions are considered in equilibrium with the entered Eh value based on platinum electrode measurements.

3. Thermodynamic equilibrium is evaluated with the B-dot equations of Helgeson (1969), which are applicable to solutions with ionic strengths no greater than about one molal (moles/kg H_2O).

4. No reaction-rate or biological kinetics are considered.

TABLE I.1.4.1 Element concentrations entered into the EQ3NR code: Brine solubility calculations

Element or complex	Concentration (mg/l)
Br^-	1,380
Cl^-	194,000
F^-	6.4
I^-	11
NO_3^-	11
SO_4^{--}	17,000
B	1,480
Ca^{++}	328
K^+	18,100
Mg^{++}	18,200
Mn^{++}	1.21
Na^+	83,400
NH_4^+	136
Sr^{++}	1.7

TABLE I.1.4.2 Ionic species and total lead solubility in WIPP composite brine

Ionic Species	Log a(±)
Pb^{++} Cl^-	-1.20
Pb^{++} Br^-	-2.78
Pb^{++} SO_4^{--}	-3.90
Pb^{++} I^-	-4.21
Pb^{++} F^-	-4.40
Total Pb = 116.2 mg/l	

Assumptions 2 and 4 are necessary because of limitations in the available data. The first assumption is based on theoretical calculations of stable phases in an aqueous solution containing equal concentrations of sulfate, carbonate and the cation of interest (lead) at a temperature of 25°C and a pressure of 1 atmosphere (Brookins, 1988).

Culebra groundwaters used in these models have ionic strengths of about 0.9 molal, which is near the indicated upper limit for valid use in the thermodynamic equilibrium equations. Solubility values reported here represent the maximum concentrations that can exist in a solution equilibrated with the indicated pure solid phases. It should be noted, however, that natural ground waters rarely equilibrate with pure solid phases (e.g., $PbCO_3$). This is especially true for sulfate and carbonate minerals, which show extensive solid solution with calcium, magnesium, manganese, iron, zinc, and barium. If mineral solid solutions were equilibrated with the aqueous fluid, slightly lower solubilities would probably be calculated for lead. EQ3NR has the capability to model this type of scenario for carbonate solid solutions containing calcium, magnesium, manganese, iron, zinc, but not lead. Therefore, the solubility values derived from pure mineral phases are the maximum concentrations that can exist in the solution, but not necessarily the actual concentrations.

I.1.4.3 Lead Solubility in Culebra Groundwaters

Groundwater in the Culebra has been sampled from several wells located within the 16-square-mile WIPP boundary and analyses from three of these (wells H-2a, H-3c, and H-14) are used in this evaluation. These wells were selected because they are in the general direction of the hypothetical well location. The maximum concentration of lead that can occur in the Culebra groundwater obtained from each well was calculated using the EQ3NR code with the Debye-Huckel B-Dot equations (Wolery, 1983) by equilibrating the groundwater with anglesite ($PbSO_4$). Anglesite is the predicted stable phase at 25 °C and 1 atmosphere (Brookins, 1988) for the values of Eh and pH listed in Table I.1.4.3. Table I.1.4.3 also contains the element concentrations entered into the EQ3NR code and the total element and aqueous species concentrations. The solubility range of lead is 52.8 to 54.4 mg/l. These solubility values represent the maximum concentrations that can exist in solution. Actual concentrations, as previously noted, are influenced by several factors, including dissolution and precipitation rates.

The model results indicate that lead solubility in Culebra groundwater is not increased to a large degree with increasing chloride concentration (e.g., well H-2a versus well H-3b). The dominant lead species in the Culebra groundwater was calculated to be uncharged $PbCO_3$.

I.1.4.4 Health Effects Associated with Stable Lead from Wind Dispersion

As described in Cases IIA and IIB (Section 5.7.2.6), drilling mud containing TRU waste constituents is brought to the surface in the scenario involving oil and gas exploration. These drilling fluids and associated cuttings are assumed to be disposed of in a mud pond located at the site. The abandoned mud pond eventually dries and its contents are subject to wind erosion.

TABLE I.1.4.3 Element concentrations entered into the EQ3NR code and Pb solubility for the dominant aqueous species: Culebra solubility calculations

	Code Inputs		
Parameter	Well H-2a	Well H-3b	Well H-14
T (°C)	22.4	22.4	22.0
Eh (mv)	60	199	70
pH	7.8	7.3	7.7
	Concentration (mg/l)		
Element or Complex	Well H-2a	Well H-3b	Well H-14
Cl^-	4800	27800	8200
Br^-	bdl[a]	27.5	14
F^-	2.1	1.6	0.8
HCO_3^-	54	47	40
SO_4^{--}	2900	4800	1500
$B(OH)_3$	57	137	63
Ca^{++}	670	1300	1800
Fe^{++}	0.42	0.14	0.4
K^+	100	450	250
Mg^{++}	160	830	530
Mn^{++}	0.07	0.14	bdl*
Na^+	2600	17000	3300
$SiO_2(aq)$	13.5	13	14
Sr^{++}	9.8	31.5	31

	Resultant Output					
	Well H-2a		Well H-3b		Well H-14	
Solid Phase	Aqueous Species	Concentration (mg/l)	Aqueous Species	Concentration (mg/l)	Aqueous Species	Concentration (mg/l)
$PbCO_3$	Total Pb	53.3	Total Pb	54.4	Total Pb	52.7
	$PbCO_3$	57.1	$PbCO_3$	59.4	$PbCO_3$	6.8
			$PbCl^+$	1.0		
			$PbCl_2$	0.5		

[a] bdl = below detection limit of analytical method

No exposure to humans from stable lead contained in the mud is expected prior to the mud drying. The dried mud, however, is subject to wind erosion and dispersion of lead particulates. Human exposure to the lead occurs through inhalation of airborne particulates.

The methodology used to calculate the dispersion of particulates in air is the same as that described in the FEIS, Appendix K. Additional assumptions used in calculating the air transport of particulates containing stable lead in this scenario are:

- The surface area of the mud pond is 500 ft^2 (46.45 m^2).
- The mud pond contains 22,000 gallons of dried mud, including 6 kg of stable lead (i.e., the equivalent of 3 drums of waste with an average lead content of 2 kg each).
- The resuspension rate of one-micron particulates from the mud pond is 5.06×10^{-12}.
- The receptor is 570 yd downwind from the center of the mud pond.

The particulate deposition velocity is 0.01 m/sec, resulting in a calculated ground deposition rate of 5.16×10^{-17} g/m^2-s.

Using these assumptions, the calculated ambient air concentration of stable lead at the downwind receptor location is 5.16×10^{-9} g/m^3. The amount of ground surface deposition at the same location over a one-year time period is 1.63×10^{-9} g/m^2.

The potential human receptor was assumed to weigh 70 kg, and a daily respiratory volume of 20 m^3/day was assumed (EPA, 1986). The rate of lead deposition in the lungs was assumed to be 50 percent of the particles inhaled, while up to 70 percent of this deposited lead was assumed to be absorbed (ATSDR, 1988), resulting in a transfer coefficient of 0.35 (i.e., 70 percent x 50 percent). The calculated daily intake of lead by a receptor is compared to the acceptable daily intake levels for chronic exposure (AIC). The calculated AIC-based hazard index as described in EPA (1986) is used for determination of potential risk to human health. The equations used to calculate lead uptake by humans are provided in Tables I.1.4.4 and I.1.4.5.

The daily intake of lead by humans in this scenario, using the calculated air concentration of 5.16×10^{-9} g/m^3, is 5.16×10^{-13} mg/kg-day. The daily intake can be compared to the acceptable level for chronic intake (AIC) (EPA, 1986). This acceptable level is 4.3×10^{-4} mg/kg-day. The calculated AIC-based hazard for lead is therefore $5.16 \times 10^{-13}/4.3 \times 10^{-4} = 1.2 \times 10^{-9}$. This value is considerably less than unity, indicating that the intake of stable lead is well below the acceptable reference level. The dose calculated for ingestion represents the most direct and, therefore, the highest intake of lead by a human receptor. Because of the small quantity of lead deposited on the ground surface (i.e., 1.63×10^{-9} g/m^2) and the even smaller amounts potentially taken up by animals and plants, it can be assumed that all other potential exposure pathways

in this scenario (e.g., ingestion of vegetables, milk and meat) will be orders of magnitude below health-based levels.

TABLE I.1.4.4 Calculation of inhalation of Pb-containing particulates

Equation: $I_r = (C_{Ai}(RV)(T_{A1})/A(W_A)$

I_r = daily Pb intake (mg/kg/day)

C_{Ai} = Pb in air (g/m^3)

RV = daily respirator volume (mg/m^3/day)

T_{A1} = transfer coefficient across lungs

A = conversion factor ($\mu g/mg$)

W_A = average adult body weight (kg)

Assumptions:

RV = 20 m^3/day (EPA, 1986)

T_{A1} = (50% deposited in lungs)(70% absorbed) = 0.35 (ATSDR, 1988)

A = 1000

W_A = 70 kg

C_{Ai} = 5.16×10^{-9} g/m^3

Calculations:

I_r = $\{(5.16 \times 10^{-9})(20)(.35)\}/(1000)(70)$

= 5.16×10^{-13} mg/kg-day

AIC = 4.3×10^{-4} mg/kg-day

Hazard Index (HI)

HI = I_r/AIC

= 1.20×10^{-9}

TABLE I.1.4.5 Calculation of the ambient lead concentration at receptor site

---

Equation:

$$X = \frac{2C\ d_o\ A\ K\ \Omega\ (10^4)}{2\pi\ 3\ \Gamma_y\ \Gamma_z\ u}$$

Where:

C = mud density (2.0 g/cm^3)

d_o = depth available for resuspension (1 cm)

A = area of mud pit (46.45 m^2)

K = resuspension rate ($5.065 \times 10^{-12}\ S^{-1}$)

(10^4) = conversion cm^2/m^2

Ω = 3.6×10^{-5} g/g (concentration of Pb in dried mud pit)

Γ_y = 57.68 m

Γ_z = 40.92 m

u = average wind speed (3.7 m/s)

Calculations:

$$X = \frac{2 \times 2 \times 1 \times 46.45 \times 5.065 \times 10^{-12} \times 3.6 \times 10^{-5} \times 10^4}{2\pi \times 3(57.68) \times 40.92 \times 3.7}$$

$X = 5.16 \times 10^{-15}\ g/m^3$ or $5.16 \times 10^{-9}\ \mu g/m^3$

TABLE I.1.4.5 Continued

Equation 1:

$$C_{w_{im}} = C_{w_i} F_{m_i} f_w Q_w \exp[-\beta_{w_i} th_m]$$ (Whelan et al., 1984)

Where:

$C_{w_{im}}$ = [Pb] in meat (mg/kg)

C_{w_i} = [Pb] in water (mg/L)

F_{m_i} = water-to-meat transfer coefficient $(kg/day)^{-1}$

f_w = fraction of total water intake that is water containing Pb

Q_w = daily water intake of beef cattle (L/day)

β_{w_i} = decay constant for Pb in water $(day)^{-1}$

th_m = holdup time from slaughter to consumption (days)

Assumptions:

A steer produces 200 kg (441 lb) of beef (Baes et al., 1984)

$F_{m_i} = 3 \times 10^{-4}$ (Baes et al., 1984)

f_w = 1 (i.e., all water consumed is assumed to contain lead)

Q_w = 49 L/day

β_{w_i} = 0 (Pb is environmentally persistent (EPA, 1986))

- th_m = 20 days (Whelan et al., 1984)

Calculations:

$$C_{w_{im}} = C_{w_i} (3 \times 10^{-4}) (1) (49) (e^{-0}) = 0.0148\ C_{w_i}$$

$$= (0.0148) \times (2.31)$$
$$= 0.034 \text{ mg (lead)/kg (beef)}$$

TABLE I.1.4.5 Continued

Equation 2:

$$I_r = C_{w_{im}} (IR)_m (GPF)/(W_A)$$ (Modified from Envirosphere, 1987)

Where:

I_r = daily intake of Pb by consumer (mg/kg-day)

$(IR)_m$ = meat ingestion rate (kg/day)

(GPF) = gut partition factor

W_A = average adult body weight (kg)

Assumptions:

$(IR)_m$ = 0.20 kg/day (adult males 19-50)

GPF = 0.15 (ATSDR, 1988)

W_A = 70 kg (EPA, 1986)

Calculations:

$I_r = C_{w_{im}} (0.20)(0.15)/70 = 4.29 \times 10^{-4} C_{w_{im}}$

$= (4.29 \times 10^{-4})(.034)$

$= 1.46 \times 10^{-5}$ mg/kg-day

HEALTH INDEX FOR PB CONSUMPTION

Equation 3:

HI = I_r/AIC (EPA, 1986)

AIC = 4.30×10^{-4} mg/kg-day (EPA, 1986)

HI = $1.46 \times 10^{-5}/4.30 \times 10^{-4} = 0.034$

TABLE I.1.4.5 Concluded

INTAKE BY BEEF CATTLE

Equation 4:

$$I_c = (C_w)_i (GPF)(Q_w)/(W_c)$$ (modified from Whelan et al., 1984)

Where:

I_c = intake per day per steer (mg/kg-day)

W_c = steer average body weight (kg)

Assumptions:

GPF = 0.15 (ATSDR, 1988)

W_c = 400 kg (Merck, 1979)

Calculations:

$I_c = C_{w_i} (0.15)(49.21)/400$

$= 1.85 \times 10^{-2} C_{w_i}$

$= (1.85 \times 10^{-2})(2.31) = 0.043$ mg/kg-day

Assume:

C_{w_i} = 2.31 mg/L

I_c = 0.043 mg/kg-day

= Adult cattle will tolerate 6 mg/kg-day for 2-3 years (Botts, 1977)

$C_{w_{im}}$ = 0.034 mg/kg

$I_r = 1.46 \times 10^{-5}$ mg/kg-day

AIC $= 4.3 \times 10^{-4}$ mg/kg-day

HI = 0.034

I.1.4.5 Health Effects from Exposure to Stable Lead in Beef

This section examines the potential human health impacts associated with the release of stable lead to the biosphere. The release scenario examined involves a breaching of the repository by a single borehole that penetrates both a waste panel and the pressurized brine of the Castile Formation below the host formation (Case IIB). The scenario and the assumptions used to model the subsequent release of stable lead to the Culebra are described in Section 5.4.2.6. The concentrations of stable lead calculated to reach a stock well at various time periods throughout 10,000 years are included in this appendix. This assessment assumes that beef cattle consume water from a hypothetical stock well that contains the maximum concentration of lead (2.31 mg/l) and that this concentration is maintained in the stock pond throughout the lifetime of the cattle. The equations used to calculate lead uptake by humans are provided in the following pages.

The methodology for this assessment involves calculating the amount of lead uptake per unit body weight of the cattle, the concentration of lead retained in beef, and the concentration of lead ingested by humans consuming this beef.

To calculate lead intake by cattle, it is assumed that 49 liters per day of water containing 2.31 mg/l lead is consumed. An average steer weighs 400 kg (882 lb) (Merck & Co., 1979). A gut partitioning factor of 0.15 is used to account for the fact that not all of the lead ingested by cattle is retained in the beef (e.g., a portion of the lead will be excreted). Thus, the cattle may uptake and retain lead at the rate of 0.043 mg/kg-day. It has been estimated that a mature steer will tolerate 6 mg/kg-day lead for two to three years (Botts, 1977). Assuming the concentration of lead in the stock water remains constant throughout the lifetime of the steer, it is estimated that 0.034 mg of lead per kg of beef will be available for human consumption.

For the purposes of these calculations, it is estimated that an adult male (age 19 to 50) consumes 0.20 kg of beef daily. Adult male body weight averages 70 kg (154 lb). The daily human retention of lead, assuming 0.034 mg/kg of lead in the beef consumed, is 1.45×10^{-5} mg/kg-day.

The estimate of the daily intake of lead by humans calculated in this manner can be compared to the acceptable daily level for chronic intake (AIC) according to procedures described in the Superfund Public Health Evaluation Manual (EPA, 1986) (see SEIS Section 5.2.3.1.6). The acceptable daily level for chronic intake (AIC) is 4.30×10^{-4} mg/kg-day (EPA, 1986). The calculated AIC-based hazard index for lead is 0.034. This value is considerably less than unity, indicating that the estimated intake of lead is well below the acceptable reference level. In other words, the ingestion of this concentration of lead every day throughout the life of the consumer will not result in adverse health effects.

I.2 DATA

I.2.1 FINAL WASTE POROSITY

If it is assumed, for purposes of calculation, that structural changes do not take place after mechanical compaction, the void volume remaining within a room after waste compaction determines the maximum amount of brine that may eventually enter the room. This value is difficult to estimate, however, because the mechanical and physical properties of the waste are highly variable and poorly characterized.

The compressive stress exerted by the surrounding salt is not sufficient to completely eliminate all voids in the waste. As the waste is compacted, its resistance to additional densification increases, and it becomes rigid enough to prevent further void reduction. A near-term limiting void volume within the repository, associated with purely mechanical densification and expected to be attained in about 60 years, is used for this analysis and is assumed to represent a "steady state."

Even after 60 years, the state of the repository will continue to change, as biological decomposition and chemical corrosion alter the chemical and structural nature of the waste. This longer-term evolution of the physical state of the repository is expected to be complex, to occur over a long period of time, and to include interactions between compaction processes and possible repository expansion as a result of gas generation. Its quantitative characterization may never be possible. At least for metal wastes, densification may continue beyond that produced by early room closure, and consequently the near-term limiting void volume is considered the greatest void volume that will exist within the waste. The final room porosity enters the calculations in this report in three ways. First, the estimated porosity is used to estimate the final permeability of the repository. This value does not enter directly into the calculations except for gas storage. Permeability is used indirectly in the calculations to determine whether Castile brine-reservoir fluids effectively mix with the waste in the repository. Second, the final porosity estimate is used to estimate the volumes available within the repository for gas storage or saturation with brine. Finally, the porosity estimate is used to determine the volume of brine available to dissolve radionuclides. Dissolution is limited either by the mass required to reach the solubility limit of individual radionuclides or by the total mass of the radionuclides present, whichever is less.

The final void volume used here is based on the distribution of waste types in storage (Table I.2.1.1) (Oak Ridge National Laboratory, 1988). A total of 6804 drums are assumed to be stored in seven-pack configurations within a disposal room, each with an internal volume of 0.21 m^3. In assigning final porosities to each component, combustible waste (low-strength plastics, paper, and rags) is assumed to have such low strength that the near-term interconnected void porosity will be 0.1 or less after compaction to lithostatic pressure (approximately 14 MPa). Because combustible waste will collapse to a dense, interlocking structure, its hydraulic response is considered to be similar to that of silt, with a hydraulic conductivity of 10^{-8} m/s. (The porosity is

TABLE I.2.1.1 Final void volumes in waste

	Waste Form				
	Combustible	Sludge	Metal/Glass	Other	Total
Emplaced					
Percent of total volume by weight in storage	30	17	33	20	100
Initial volume in disposal room	429	243	472	286	1430 m^3
Percent of solids per drum	24.8	66.5	21.9	---	
Final					
Solids volume (m^3)	106	162	103	93	464 m^3
Void volume (m^3)	12	18	68	25	123 m^3
Waste volume					587 m^3

Sources. Oak Ridge National Laboratory, 1988; Clements and Kudera, 1988; Butcher, 1989.

$n = V_v/V$, where V is the compacted volume, and V_v is the void volume. $V = V_v + V_s$, where V_s is the solid volume that the waste would occupy if no voids were present. Later, the void ratio, e, will be used, which is defined as $e = V_v/Vr_s$, or $e = n/1 - n$).

The mechanical properties of sludge are not well defined, but this category of waste represents only 17 percent of the total waste inventory. Sludge is much more difficult to compact than combustible waste, and therefore its total void content after compaction is likely to be greater. The same interconnected porosity, 0.1, is assumed for it in the compacted state, however, because many sludges may have a high cement content and are expected to form hydration products that decrease void interconnectivity. In the absence of any data about the hydraulic conductivity of sludge, a value two orders of magnitude greater than for grout has been assumed. The hydraulic

conductivity of grout is 1×10^{-11} m/s (Coons et al., 1987), implying a final-state conductivity of 1×10^{-9} m/s for sludges.

The strengths of metallic and glass wastes make them much less compactible than combustible and sludge wastes. Most of the waste is metallic in content. The final porosity assumed for metal and glass waste is 0.4, based on powder-metallurgy literature (Hausner and Kumar, 1982) and on data on supercompaction (Scientific Ecology Group, Inc., private communication), which suggests that compaction of metal waste to much greater than 0.6 of theoretical solid density is not likely. A lower final porosity for the metal waste can be expected, however, if the crushed-salt and bentonite backfill intrudes into the open spaces between the pieces of metal, a process that could reduce porosity by as much as 50 percent. Thus, a lower bound to metal-waste porosity is taken to be 0.20.

The properties of the waste category referred to as "other" remain undefined. In the absence of further information about the composition of this waste, its compacted porosity is assumed to be the average porosity of the combined combustible, sludge, and metal and glass waste categories, weighted according to the portion of the inventory that each represents.

Final void volumes for combustible, sludge, and metal and glass waste categories are given in Table I.2.1.1. The volume of solid waste per drum is computed using the average initial void fraction of each waste category (Clements and Kudera, 1988; Butcher, 1989). Adding in the void volume of the unspecified "other" category of waste (20 percent of the inventory), the total void volume per room is 123 m^3, corresponding to a solids volume of 464 m^3. This yields a porosity of 0.212 of the final total waste volume of 587 m^3. If the void volume per room is assumed to be reduced 50 percent by self intrusion, the void volume per room is approximately 123 m^3 – 34 m^3 = 89 m^3, but the total solid volume increases by 34 m^3, from 464 to 498 m^3. This corresponds to a porosity of 0.152. The "expected" final void volume for the consolidated waste is the average of the estimated void volumes, or 106 m^3 per room, corresponding to an interconnected void porosity of 0.182.

The estimates above apply only to the waste and do not include any final-state porosity of backfill in the room, because the compacted salt-bentonite backfill is expected to be relatively impermeable. The void-volume calculations take no credit for the fact that the metal and glass waste may contain minor amounts of easily compacted materials such as combustibles or sorbents. The only study that has quantitatively inventoried the contents of TRU waste in detail (Clements and Kudera, 1985) showed that metals represent only about 80 percent by weight of the INEL metal waste (Butcher, 1989). The remainder of the metal category contents is combustible material (12 percent) and cement (5 percent), which would reduce its compacted porosity. A major uncertainty in this analysis is introduced by the absence of any information about the compactibility of the various waste types, although tests to determine compactibility are in progress.

An estimate was made of how rapidly the limiting void volume within a disposal room is approached (Figure 5.2). The calculated rate of closure of an empty disposal room (Munson et al., 1989) was used to determine the void volume at a given time. The void

volume was obtained by subtracting the volumes of the solids in the waste and backfill and the volume of brine flowing into the room as a function of time (Nowak et al., 1988) from its current volume. Figure 5.2 is not completely consistent with values listed in Table I.2.1.1 because, in the absence of experimental results, equal rates of consolidation of waste and backfill were assumed.

An assumption in using closure data for an empty room for this estimate is that any backstress by the room contents is insufficient to retard void reduction. This appears to be warranted for room porosity greater than approximately 0.3: finite-element calculations show that backstress is significant only during the latest stages of closure. The no-backstress assumption is also consistent with the current model for compaction of the waste, which assumes that the final void volume depends only on the stress applied to the waste, and not on the stress history; that is, the only effect of backstress is to prolong the time required to achieve the final compacted state. This assumption, however, is another source of uncertainty. Estimates using these assumptions show that the limiting void volume could be achieved in 40 to 60 years; 60 years is assumed in Section 5.4.2.4, Brine Inflow. The amount of brine blowing into the room during the 60 years is estimated to be between 6 and 37 m^3, a factor of 4 less than would be required to saturate the 123 m^3 of void volume at final state. In fact, all this brine can be sorbed by the bentonite in the backfill (Subsection 5.4.2.4). In addition, the pressure of decomposition gases within the room, even assuming none leak out, would not reach lithostatic pressure in 60 years (Lappin et al., 1989, Section 4.10.2).

I.2.2 RADIONUCLIDE SORPTION

The K_d values used in the SEIS analyses are summarized in Tables I.2.2.1 through I.2.2.4. Table I.2.2.1 contains K_d values that are used to calculate radionuclide retardation in the matrix of the Culebra dolomite. Tables I.2.2.2 and I.2.2.3 contain sorption ratios for the clays that line the fractures in the aquifer. Table I.2.2.4 contains K_d values for use in radionuclide transport in the tunnels, seals, and Marker Bed 139 at the repository level. If the volume of the clays within the fractures is known, then the K_d's in Table I.2.2.2 can be used to calculate retardation within the fractures using the following expression

$$R = 1 + \rho_c K_{dc} (K_c / K), \qquad \text{(I-38)}$$

where K_{dc} is the distribution coefficient for the clay given in Table I.2.2.2; ρ_c is the density of the clay (2.5 g/cm^3); K_c is the thickness of the clay coating the fracture; and K is the fracture width (Neretnielka and Rasmuson, 1984).

Table I.2.2.1 K_d values for radionuclide transport in the matrix of the Culebra dolomite (ml/g)

Case	Pu	Am	Cm	U	Np	Pb, Ra	Th
Case I	100	200	(200)	1	(1)	(1)	(100)
Case IIA	50	200	(200)	1	(1)	(0.1)	(50)
Case IIB	25	100	(100)	1	(1)	(0.05)	(25)

Values in parentheses are poorly known; estimated by assumption of behavior similar to a homolog element.

Source. Lappin et al., 1989, Table E-10.

TABLE I.2.2.2 K_d values for radionuclide transport in the fracture clays of the Culebra dolomite (ml/g)

Case	Pu	Am	Cm	U	Np	Pb, Ra	Th
Case I	300	500	(500)	10	(10)	(100)	300
Case IIA	200	(300)	(300)	10	(10)	(10)	(200)
Case IIB	(100)	(100)	(100)	(1)	(1)	(5)	(100)

Values in parentheses are poorly known; estimated by assumption of behavior similar to a homolog element.

Source. Lappin et al., 1989, Table E-11.

TABLE I.2.2.3 K_a values for radionuclide transport in the fracture clays of the Culebra dolomite (ml/m^2)

Case	Pu	Am	Cm	U	Np	Pb, Ra	Th
Case I	6	10	(10)	0.2	(0.2)	2	6
Case IIA	6	(6)	(6)	0.2	(0.2)	(0.2)	(6)
Case IIB	(2)	(2)	(2)	(0.02)	(0.02)	(0.1)	(2)

Values in parentheses are poorly known; estimated by assumption of behavior similar to a homolog element.

Source. Lappin et al., 1989, Table E-12.

TABLE I.2.2.4 K_d and K_a values for radionuclide transport in tunnels, seals, and MB 139

	Pu	Am	Cm	U	Np	Pb, Ra	Th
Clay in crushed Salado salt, K_d (ml/g)	100	100	100	1	(10)	(1)	(100)
Anhydrite in MB 139, K_d (ml/g)	100	25	25	(1)	(1)	(1)	(100)
Anhydrite in MB 139, K_a (ml/m^2)	3700	925	(925)	(37)	(37)	(37)	(3700)

Values in parentheses are poorly known; estimated by assumption of behavior similar to a homolog element.

Source. Lappin et al., 1989, Table D-5.

Surface area-based distribution coefficients K_a (ml/m^2) for the clay are listed in Table I.2.2.3. These were calculated from the K_d's assuming a surface area of 50 m^2/g. This is similar to the surface area of 32 m^2/g measured by Nowak (1980) on a reference montmorillonite used in europium sorption studies and within the range of 15 to 88 m^2/g measured by Soudek (1984) on montmorillonite used in ion exchange studies.

A retardation factor for use in a transport equation for fracture-dominated flow where sorption occurs on the surface of the fracture fill clay can be calculated as

$$R = 1 + aK_a/\phi \qquad \text{(I-39)}$$

where K_a is the sorption ratio in Table I.2.2.3, a is the specific surface of the fracture (fracture surface area per unit volume of fracture), and ϕ is the porosity.

Similarly a retardation factor for use in transport through the porosity-controlled flow in the tunnels and seals can be calculated as

$$R = 1 + \rho K_d (1 - \phi)/\phi \qquad \text{(I-40)}$$

where K_d is the distribution coefficient given in Table I.2.2.4, ρ is the grain density, and ϕ is the porosity.

The following procedure was used to obtain the recommended K_d values listed above. First, initial ranges of values were obtained from studies carried out under chemical conditions that were similar in some way to those expected under a variety of mixing ratios in the various media. Second, K_d values obtained under conditions closest to those expected in the WIPP were extrapolated to reference conditions consistent with the descriptions of Cases I and II. Data from parametric studies or theoretical calculations for simple, well-constrained systems were used to estimate the magnitude of the change in the K_d that might be related to differences between the actual experimental conditions and the range of conditions possible for the cases. Finally, uncertainties in the future physicochemical conditions in the repository and along the flow path in the Culebra dolomite were considered. Possible deviations of K_d values from those estimated in the previous step were evaluated, and a set of conservative, realistic K_d values was selected.

In the waste panels, solution chemistry will be dominated by the composition of Salado brines, leachates from the waste, concrete and steel drums, and the products of microbial degradation. In the SEIS analyses, it was assumed that the important sorbing substrates will be iron oxide corrosion products and bentonite backfill. Radionuclide transport within the waste panel has not been considered in the report. Available sorption data were used to estimate the partitioning of radionuclides between solution and suspended solids.

The amount of radionuclide sorbed to the particulates will be related to the solution composition and to the total number of sorption sites of the substrate. Consideration was first given to sorption capacity independent of the effects of solution composition. For an oxide or oxyhydroxide, the total sorption capacity is related to the number of surface hydroxyl groups. For a clay such as bentonite, the sorption capacity will be

determined by both the number of exchangeable (fixed-charge) sites and the number of hydroxyl groups (Kent et al., 1988).

The total sorption capacities of iron oxyhydroxide and bentonite were estimated from experimental data obtained under conditions very different from those assumed for the waste panel. Under conditions of low total dissolved solids, low concentration of cations such a Mg^{+2} and Ca^{+2} and low organic concentration, sorption capacities of bentonite could range from 10 to 100 milliequivalents (meq) per 100 grams (Dever, 1982; Tsunashima et al., 1981). Under similar conditions, the sorption capacity of iron oxyhydroxides could range from 60 to 300 meq per 100 grams (estimated from data in Hayes et al. (1988, Table 1). The actual sorption capacities will depend on the crystallinity and stoichiometry of the clays and iron oxides present in the repository.

Moderate concentrations of carbonate, organic-sequestering agents, Mg^{+2}, and Ca^{+2}, however, will keep some of the sorption sites from being occupied by actinide ions. The effects of the solution composition on sorption are discussed in more detail in Lappin et al. (1989, Section 3.3.4.2).

I.2.2.1 Rationale for Extrapolation of K_d Values

Table I.2.2.5 summarizes a variety of data on experimental measurements of K_d's in brine. The values for K_d used in this SEIS are lower than those listed in Table I.2.2.5. Many of the K_ds for the actinides reported in the literature are in the range 10,000 to 100,000 ml/g. The K_d's were calculated solely from the loss of radioactivity from solution, and therefore small errors in the measurement of a trace amount of radionuclide remaining in solution could lead to large errors in the calculated K_d. Review of experimental procedures used to obtain the values suggests that the results could be compromised by unrecognized precipitation; this error would lead to high K_ds that would overestimate the extent of sorption. This kind of error could be especially important for data from WIPP Brine A and B. Saturation index calculations by Melfi (1985) indicated that Brine A is supersaturated with respect to calcite ($CaCO_3$) and that Brine B is supersaturated with respect to gypsum ($CaSO_4 \cdot 2H_2O$). The extent to which the actinides or fission products can be incorporated into the crystal structure of either of these minerals has not been determined.

The uncertainties in the course of the future chemical evolution of the repository and aquifer require consideration of large ranges of pH, Eh, organic content, and carbonate content of the groundwaters. These possible variation in solution chemistry could result in order-of-magnitude changes of the K_ds from the values obtained in the experimental studies listed in Table I.2.2.5. Evaluation of the magnitude of these changes requires several assumptions about the nature of sorption reactions occurring on the substrates.

TABLE I.2.2.5 Sources of K_d data used to estimate values for repository (Case I) and Culebra (Case II) transport (saline water ± organic ligands). (See Lappin et al. (1989), Table 3-4 for compositions of WIPP brines A and B)

				Reported K_d range					
Reference	Water	Rock	Organics	Pu	Am	Cm	U	Np	Eu
Nowak (1980)	Brine A	Bentonite	None	$2.3x10^3$ to $3.4x10^3$					350
	Brine B	Bentonite	None	$2x10^4$ to $4x10^4$	$4.1x10^3$ to $1.4x10^4$				$1.4x10^3$ to $1.7x10^3$
Dosch (1978)	Brine A	Clay	None						$>1x10^3$
	Brine B	Clay	None	$4x10^4$ to $7.2x10^4$	310 to 1100	$2.7x10^3$ to $1.9x10^4$			$>1x10^4$
	Dissolution	Halite	None	17 to 59	11 to 306	56 to 354			
	Brine	(as clay)	None	($1x10^4$ to $2x10^4$)	($3.8x10^3$ to $1.8x10^5$)	$2x10^4$ $2.1x10^5$			
	Brine A	Rustler Dolomite							$>5x10^3$
	Brine B	Rustler Dolomite	None	$2.1x10^3$ to $5.4x10^3$	$3.2x10^2$ to $2.6x10^3$	$1.3x10^3$ $1.2x10^4$			$>5x10^3$
	Brine B	Anhydrite	None	$6.7x10^3$	$2.9x10^2$	$4.2x10^3$			$>1x10^3$
Dosch (1981)	Brine A	Culebra Dolomite	None				0 to 2		
	Brine B	Culebra Dolomite					1.5 to 608		
Serne (1977)	Brine A	Rustler Dolomite					29 to 52		
	Brine B	Culebra Dolomite	None	50 to 200	340 to 1160	0.0 to $1.2x10^4$	0 to10 to 7.1	28	22 to 40

TABLE I.2.2.5 Continued

Reference	Water	Rock	Organics	Reported K_d range					
				Pu	Am	Cm	U	Np	Eu
Paine (1977)	Brine B	Culebra Dolomite	EDTA, etc.	25 to 6000	100 to 2.8×10^4				
	Brine B	Rustler Dolomite	Waste	560 to 1.8×10^4	5.7×10^4 to 1.7×10^5				70 to 660
	Brine B	Anhydrite	Waste						400
	Brine B	Clay	Waste						2.8×10^4
Tien (1983)	Salt brine	Claystone	None	3×10^2 to 1×10^4 Ra = 3	90 to 1000	3×10^2 to 1×10^4	50	5 to 2000	
	(TDS: > 3×10^{-4})	Carbonate	None	50 to 6×10^3	3×10^2 to 2×10^4	3×10^2 to 1×10^4	0 to 3	15 to 30	
		Salts	None	20 to 1×10^4	3×10^2 to 2×10^5	3.5×10^2 to 2×10^5			

TABLE I.2.2.5 Concluded

Additional References	Water	Rock	Reported K_d range Pu	Am	Cm	U	Np	Eu
Dosch (1978)	Solution C	Rustler Dolomite	$2.4x10^3$ to $7.3x10^3$	$2.4x10^3$ to $2.2x10^4$	$4.2x10^4$ to $1.1x10^5$			$>1x10^4$
	Solution C	Clay	$4x10^4$ to $1.8x10^5$	$2.3x10^3$ to $3.5x10^3$	$1.6x10^5$ to $4.2x10^5$			$>1x10^4$
	Solution C	Anhydrite	$7.7x10^5$	$2.2x10^3$	$1.8x10^5$			$>1x10^3$
Dosch (1981)	Solution C H2 (B,C)	Rustler Dolomite Culebra Dolomite					13 to 175 0.6 to 7.4	
Lynch & Dosch (1980)	H2 (B,C)	Rustler Dolomite	83 to 1055	119 to 383				
Serne (1977)	Solution C	Culebra Dolomite	42 to 2206	2500 to 3000	$1.6x10^3$ to $4.3x10^4$	0 to 16	5 to 35	
Tien et al (1983)	Saline H_2O	Claystone	300	200 to	1000	20	1 to 75	
	(TDS: $5x10^3$ to $3x10^4$	Carbonate	Ra = 30 500 Th = $2.7x10^3$ to $1x10^4$	3000	3000	3	21	
Tien (1983)	Fresh H_2O	Claystone	30 to $1x10^4$700 to Ra = 300	700 to $1x10^4$	1.270 $1x10^5$	2 to 400		
	(TDS: < $5x10^3$	Carbonate	100-7000 Th = $1x10^3$ to $1x10^5$	500 to $1x10^5$ $1x10^5$	$6x10^3$ to $4x10^4$	0 to 15	15 to 30	

For the purpose of the SEIS, it is assumed that only the clay, anhydrite, and salt components of the Salado will come into contact with the radionuclides during transport. It is assumed that none of the elements sorb onto halite (K_d = 0). The sorption of trace metals onto salt-like minerals such as anhydrite is poorly understood; the paucity of relevant data precludes extrapolation of sorption behavior to physicochemical conditions that differ from those specifically examined in the experimental studies listed in Table I.2.2.5. Some qualitative extrapolations are made; they are based solely on the predicted aqueous speciation of the radionuclides.

I.2.2.2 Rationale for Choices of Recommended K_d Values

The data for the simple systems discussed above suggest that the amount of sorption of actinides onto either clays or sulfates present in the repository could be several orders of magnitude less than that suggested by the K_d data listed in Table I.2.2.5. Although it is possible that under the worst case conditions, the K_ds will be close to zero, there is evidence that some sorption will occur; therefore in the SEIS the K_ds are not assumed to be zero. The rationales behind the K_d values chosen for each element are given below.

Plutonium. K_d values are decreased by 2 to 3 orders of magnitude from the values in Table I.2.2.5 to account for the potential effect of carbonate complexation.

Americium. K_d values are decreased by factors of 3 to 1000 from values listed in the table to account for the potential effects of organic complexation. For example, Swanson (1986) found that EDTA significantly decreased Am sorption onto kaolinite and montmorillonite. The magnitude of this effect was a function of the pH and concentrations of EDTA, Ca, Mg, and Fe in solution.

Curium. K_d values were decreased by factors of 3 to 100 from the values listed in Table I.2.2.5 based on the assumption of similar behavior to Am and Eu.

Uranium and Neptunium. Generally, low K_d's have been measured in waters relevant to the WIPP. The K_d of uranium is very dependent on the pH and the extent of complexation by carbonate and organic ligands. A low value (K_d = 1) has been assumed in the SEIS to account for the possible effects of complexation and competition. Theoretical calculations (Siegel et al., 1989) and arguments based on similarities in speciation, ionic radii, and valence (Chapman and Smellie, 1986) suggest that the behavior of neptunium will be similar to that of uranium.

Thorium. There are few data for thorium under conditions relevant to the WIPP. Thorium K_d values were estimated from data for plutonium, a reasonable homolog element (Krauskopf, 1986). Data describing sorption of Th onto kaolinite (Riese, 1982) suggest that a high concentration of Ca and Mg will prevent significant amounts of sorption onto clays in the repository. Stability constants for organo-thorium complexes suggest that

organic complexation could be important in the repository and may inhibit sorption (Langmuir and Herman, 1980).

Radium. There are very few sorption data for radium under conditions relevant to the WIPP. K_d values in Table I.2.2.5 were estimated from assumption of homologous Ra-Pb behavior in Tien et al. (1983). Data from Riese (1982) suggest that Ra will sorb onto clays but that high concentrations of Ca and Mg will inhibit sorption. Langmuir and Riese ((1985) present theoretical empirical arguments that suggest that Ra will coprecipitated in calcite and gypsum/anhydrite in solutions close to saturation with respect to these minerals.

I.2.3 BRINE RESERVOIR PARAMETERS

In order to model the hydraulic connection between the Culebra member and a brine reservoir in the underlying Castile Formation, it is necessary to realistically define the hydrologic parameters that govern the transient hydraulic response of the brine reservoir. These parameters include

- o P_i initial reservoir pressure
- o b reservoir thickness
- o T reservoir transmissivity
- o ρ reservoir fluid density
- o r_b effective distance to the reservoir boundary
- o ϕ reservoir porosity
- o α reservoir compressibility

Interpretation of flow and buildup data from the WIPP-12 brine reservoir indicates that the reservoir is heterogeneous (Popielak et al., 1983). As a result, the hypothetical WIPP brine reservoir is being modeled as consisting of three separate media. Base-case values for each of the parameters listed above are derived from the available data on WIPP-12 (D'Appolonia, 1982 and 1983; Popielak et al., 1983). Uncertainty ranges about these base-case values are derived from the limited data base from twelve other wells that have penetrated brine reservoirs in the Castile Formation in the vicinity of the WIPP site. Because data on eleven of these brine occurrences are limited, the parameter range is derived in most cases from the WIPP-12 and ERDA-6 data. For well locations and distributions of Castile brine occurrence, see Figure I.2.1. The following sections define the base case and ranges of the appropriate parameters. The selections are summarized in Table I.2.3.1.

I.2.3.1 Initial Reservoir Pressure

Two types of data were considered to be best suited for determining initial reservoir pressure. The first is the data on the earliest buildup recorded after encountering the brine reservoir, and the second is the data on the longest buildup recorded.

After the brine reservoir was encountered, WIPP-12 was shut in for 1.43 days. The buildup observed after shut-in was near instantaneous, because only a very limited volume of reservoir fluid had been produced. The maximum pressure observed during

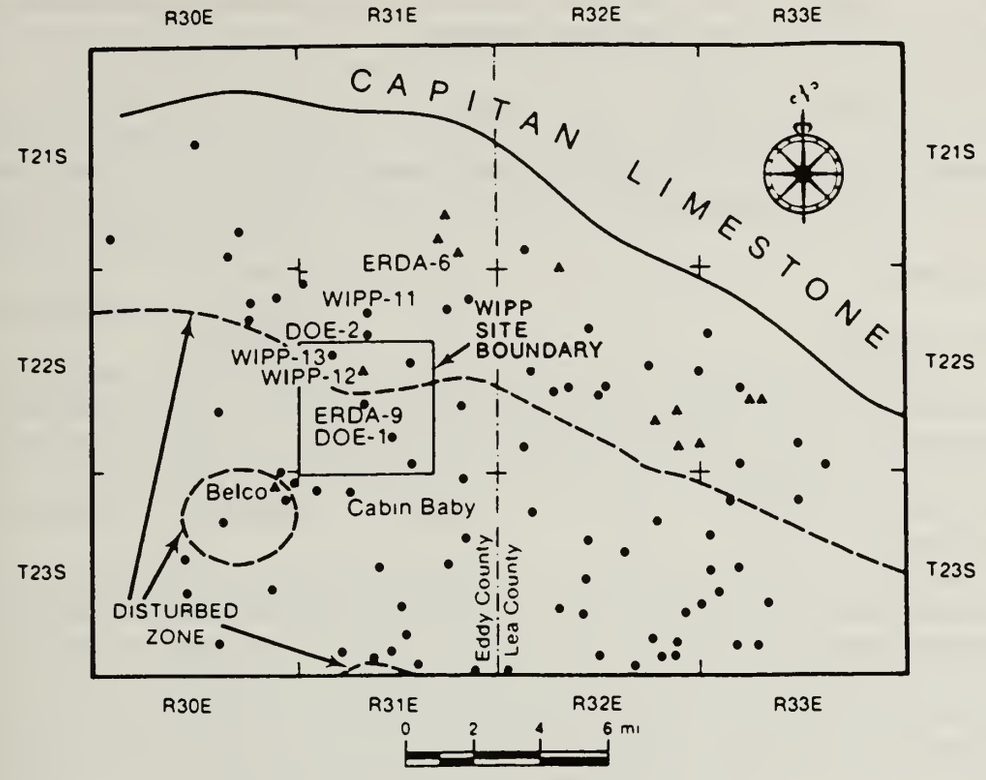

LEGEND

REF: LAPPIN, 1988.

▲ BOREHOLE IN WHICH CASTILE FORMATION BRINE WAS ENCOUNTERED

● BOREHOLE THAT PENETRATED THE CASTILE FORMATION BUT DID NOT ENCOUNTER BRINE (ERDA-9 IS INCLUDED FOR REFERENCE ONLY)

FIGURE 1.2.1
GENERALIZED DISTRIBUTION OF CASTILE FORMATION BRINE OCCURENCES AND APPROXIMATE EXTENT OF THE CASTILE "DISTURBED ZONE" IN THE NORTHERN DELAWARE BASIN

TABLE I.2.3.1 Base-case and range of values of parameters describing the brine reservoir

Parameter	Symbol	Base case	Range	Units
Initial pressure	P_i	12.7	7.0 to 17.4	MPa
Effective thickness	b	7.0	7.0 to 24.0	m
Transmissivity of inner zone	T_i	$7x10^{-4}$	$7x10^{-6}$ to $7x10^{-2}$	m^2/s
Distance to intermediate zone contact	r_2	300	100 to 900	m
Transmissivity of intermediate zone	T_o	$7x10^{-6}$	$7x10^{-8}$ to $7x10^{-4}m^2$	m^2/s
Distance to outer zone contact	r_3	2000	30 to 8600	m
Transmissivity of outer zone	T_m	$1x10^{-11}$	Constant	m^2/s
Fluid density	ρ_f	1240	Constant	kg/m^3
Porosity	ϕ	0.005	0.001-0.01	
Compressibility	α	$1x10^{-9}$	$1x10^{-10}$ to $1x10^{-8}$	1/Pa

this buildup was 1.5 MPa at the surface, a good choice for static reservoir pressure. This pressure corresponds to a reservoir pressure of 12.7 MPa when extrapolated to the center of the brine reservoir at WIPP-12 (918.8 m below the ground surface (BGS)).

The longest buildup period followed Flow Test 3. The flow sequence was 7.0 days in length, followed by a buildup period lasting 278.4 days. For this test, the Horner method (Lee, 1982) was appropriate. By extrapolating to a Horner time of one, an undisturbed reservoir pressure of 1.4 MPa was obtained. This corresponds to an initial pressure of 12.6 MPa at the reservoir center depth of 918.8 m BGS.

For this modeling study, the base-case reservoir pressure is taken from the highest pressure monitored during the testing of the brine reservoir at WIPP-12, which is equivalent to a pressure of 12.7 MPa at the reservoir center. Of the 13 wells in the northern Delaware Basin that have encountered brine reservoirs, only four, including

WIPP-12, have been tested adequately enough to estimate the formation pressure. These pressures range from 12.6 to 14.3 MPa at formation depth (Popielak et al., 1983). Minimum pressures for nine other wells have been estimated from the minimum pressure needed to allow flow at the surface. From these nine estimates, minimum formation pressures range from 7.0 to 17.4 MPa. The range of initial reservoir pressures for this study is therefore taken to be 7.0 to 17.4 MPa. The base-case value is representative of the WIPP-12 reservoir (for which the best data are available) and is 12.7 MPa at reservoir depth.

I.2.3.2 Reservoir Thickness

In most cases, the brine reservoirs encountered in the Castile Formation are in the lower portion of the uppermost anhydrite unit present at that location. The uppermost anhydrite unit at WIPP-12 is Anhydrite III, which is locally 96.6 m thick (Popielak et al., 1983). The WIPP-12 brine reservoir was at the base of Anhydrite III and appears to have been limited to a small fractured zone.

Anhydrite III at WIPP-12 was mapped by coring, caliper logs, acoustic televiewer logs, neutron logs, and spinner logs (Popielak et al., 1983). A review of these observations identified seven megascopic fractures in Anhydrite III. All these fractures were high-angle fractures with dips ranging from 70 degrees to vertical. Only two showed any evidence of brine production, as identified by the spinner log conducted by the USGS (D'Appolonia, 1982). The uppermost brine-producing fracture (fracture C) extended from 916.2 to 917.1 m; the lowermost (fracture D) extended from 919.0 to 921.1 m BGS. These depths were taken from the acoustic televiewer log. The spinner log defined the interval from which nearly 100 percent of the flow was coming as that between 916.2 to 921.4 m BGS, which correlates well with both the caliper log and the acoustic televiewer log (Popielak et al., 1983; D'Appolonia, 1982).

Because the reservoir is heterogeneous and composed of high-angle fractures, its thickness is difficult to define from borehole reconnaissance at a single location. The base-case effective thickness of the reservoir is estimated to be 7 m and to occur between 915.3 and 922.3 m BGS. The center of the reservoir is taken to be at a depth of 918.8 m BGS, which is the center of the interval that produced nearly all of the inflow at WIPP-12 (D'Appolonia 1982). All downhole pressures are referenced from a depth of 918.8 m BGS. The base-case effective thickness of 7 m shown in Table I.2.3.1 can be considered a minimum thickness. From the center of the reservoir to the base of Anhydrite III is approximately 12.0 m. The maximum effective thickness will be considered 24 m centered at 918.8 m BGS. Because the product of hydraulic conductivity and thickness (transmissivity) cannot be determined in the reservoir characterization analyses, sensitivity calculations will be performed upon transmissivity. The variation in transmissivity caused by thickness uncertainty will be less than the variation in transmissivity caused by uncertainty in hydraulic conductivity. As a result, the total variation in formation transmissivity will be driven largely by hydraulic conductivity variation, as described in the following section.

I.2.3.3 Reservoir Transmissivity

For modeling, the WIPP-12 reservoir is conceptualized as being composed of two separate, concentric, fractured media with different transmissivities. Because this modeling study will allow very long flow periods in the brine reservoir, the far-field matrix is also expected to contribute to the reservoir response. This matrix is modeled by attaching an infinite low-transmissivity zone to the outside edge of the intermediate zone through the application of a Carter-Tracy boundary condition (Carter and Tracy, 1960; Reeves et al., 1986). This outermost zone represents the intact Castile Anhydrite III. Popielak et al. (1983) determined that the intact formation matrix had a permeability of less than 2×10^{-19} m^2. Assuming a thickness of 7 m, the transmissivity of the outer zone is equal to approximately 1×10^{-11} m^2/s. The transmissivity of the outer zone is at least six to eight orders of magnitude smaller than the base-case transmissivity of the inner and intermediate zones. For this modeling study, outer zone represented by the Carter-Tracy boundary condition is assigned a constant transmissivity of 1×10^{-11} m^2/s.

From hydraulic interpretations, it was determined that the inner region of the reservoir can be modeled as a cylindrical zone having a transmissivity of 7×10^{-4} m^2/s and extending out from the well to an effective radius of 300 m. The remainder of the reservoir was interpreted as having a smaller mean transmissivity. This intermediate zone is assigned a lower transmissivity equal to 7×10^{-6} m^2/s out to a radius of 2000 m. These values are interpreted from WIPP-12 testing and are considered base-case values listed in Table I.2.3.1 for the hypothetical brine reservoir. The transmissivities of these two zones are estimated to range, somewhat arbitrarily, by two orders of magnitude from the base-case values. The only Castile brine reservoir transmissivity data available for comparison to these base-case values and ranges are presented by Popielak et al. (1983), who determined transmissivities from as low as 1.6×10^{-9} m^2/s at ERDA-6 to as high as 8×10^{-4} m^2/s at WIPP-12.

I.2.3.4 Reservoir Fluid Density

The brine from the WIPP-12 brine reservoir has an average level of total dissolved solids of 328,000 mg/l, as determined from laboratory analyses of 13 water samples (Popielak et al., 1983). The average specific gravity, based on 59 field analyses, is 1.215. In addition to these traditional analyses, four borehole-pressure-gradient surveys were performed in 1982 and 1983 at WIPP-12 as part of the hydraulic testing program. These surveys showed pressure gradients ranging from 0.0121 to 0.0123 MPa/m, with an average of 0.0122 MPa/m. This average gradient corresponds to an average fluid density of 1240.6 kg/m^3. For this study, the base-case brine-reservoir fluid density is taken to be 1241 kg/m^3. This parameter will not be varied, and a representative range is not defined.

I.2.3.5 Reservoir Boundary

Because of the isolated distribution of brine-reservoir encounters in the Castile Formation, the reservoirs must be considered limited, with some outer boundary beyond which hydraulic communication is minimal. Methods used to infer the limits of brine reservoirs in the Castile Formation are varied. One method is to look at a map of wells penetrating the Castile Formation and identify which wells did, and which did not,

encounter a brine reservoir. When a well that encountered a brine reservoir is surrounded by wells that did not, the distance of the latter wells from the brine-reservoir well represents a maximum radius for the boundary of that reservoir. For example, WIPP-12 is surrounded by four nearby wells that did not encounter brine in the Castile Formation. These four wells range in distance from 2 to 3 km from WIPP-12. Therefore, if it is conservatively assumed that WIPP-12 is located at the center of the reservoir and the reservoir is circular, the WIPP-12 reservoir has at most a 2000 m radius. Most brine reservoirs in the Castile in the northern Delaware Basin are found to have radii varying from approximately 800 to 3200 m. Other shapes than circular are possible, but they have not been included in the analysis.

A recent investigation of a different kind that may be used to delineate the extent of the WIPP-12 brine reservoir is a time-domain electromagnetic survey (TDEM) performed at land surface over the waste-emplacement panels (Earth Technology, 1988). This study suggests that there is a low-resistivity body, interpreted as a brine reservoir, within the Castile Formation under portions of the waste-emplacement panels. If one assumes that this brine is connected to the WIPP-12 brine reservoir, then one reservoir boundary is at least 1600 to 2000 m from WIPP-12.

Another method of inferring the reservoir extent at WIPP-12 is to estimate the total bulk volume of the reservoir using the concept of the storage coefficient of an elastic aquifer. The storage coefficient is defined as the volume of water removed from a vertical column of aquifer of height m and unit basal area when the head declines by one unit (Domenico, 1972). The equation for the storage coefficient can be written as

$$S = b \rho g (\alpha + \phi \beta) \tag{I-41}$$

where b is the aquifer thickness, ρ is fluid density, g is the acceleration due to gravity, α is the compressibility of solids, ϕ is the porosity, and β is the compressibility of the fluid. Domenico (1972) showed that the amount of water released from storage for a given head decline over an area A is equal to

$$\Delta V = S A \Delta h \tag{I-42}$$

where h is the given head decline. Equation (I-42) can be expanded to

$$\Delta V = \rho g (\alpha + \phi \beta) (bA) \Delta h \tag{I-43}$$

where the product (bA) is equal to the bulk volume of the aquifer (V_b) over which the unit decline in head has occurred and from which water has subsequently been released. Knowing that pressure decline is equal to the product ($g\Delta h$), and solving for the bulk volume of the aquifer, Equation (I-43) can be expressed as

$$V_b = V / (\alpha + \phi \beta) \Delta P \tag{I-44}$$

Therefore, if the total compressibility of an aquifer and the total pressure change ΔP that has occurred as a result of known fluid volume release (ΔV) are known, an estimate of the total bulk volume of the aquifer can be made. This calculation assumes that the pressure change has been uniform over the total bulk volume and that no

mass has been transferred across the aquifer boundaries. Assuming a total thickness and a reservoir geometry, one can estimate the distance to the reservoir boundary.

From the time of initial penetration of the brine reservoir at WIPP-12 to the end of Flow Test 3, a volume of 36,935 m^3 was produced from the reservoir. The residual pressure drop measured at the wellbore at the end of a 278.4 day shut in was 0.23 MPa. For the range of total compressibilities, adopted Equation (I-44) gives a range in aquifer bulk volume of 1.66×10^7 to 1.66×10^9 m^3. Then, if the brine reservoir is a right-circular cylinder with a range in effective thickness from 7 to 24 m, the estimated reservoir boundary radius is between 460 and 8600 m. Popielak et al. (1983) reported that at the ERDA-6 reservoir the production of 262.3 m^3 of reservoir fluid resulted in a change in pressure in the aquifer of 0.36 MPa. Using the same ranges of compressibility and effective thickness as above, the range in aquifer bulk volume at ERDA-6 is estimated to be 7.32×10^4 to 7.32×10^6 m^3. This corresponds to a range in estimated reservoir radius from 30 to 560 m.

The final method considered here for identifying boundaries or large-scale heterogeneities is hydraulic-test interpretation. The hydraulic data do not provide evidence to accurately define the outer boundary location for the WIPP-12 brine reservoir. However, the fact that the reservoir did not recover to static pressure during 278 days of buildup following Flow Test 3 suggests that a boundary may have been encountered in the volume of rock stressed during the testing activities at WIPP-12.

The potential range of reservoir radii based on the minimum and maximum estimates calculated using the various methods is from 30 to 8600 m. The minimum and maximum estimates, and therefore the range, for reservoir radii come from the calculation based upon estimating the total reservoir bulk volume. The large variation in these estimates comes from the two-order-of-magnitude range in the uncertainty of total aquifer compressibility. Although it is not probable that any of these brine reservoirs have radii as great as 8600 m, this value will be used to represent a maximum case (i.e., greatest volume). The base-case reservoir radius, taken from the hydraulic interpretations presented in an earlier section, is 2000 m. Because for long flow periods the hydraulic response of the reservoir is a product of the coupled matrix-fracture diffusivities, a Carter-Tracy boundary condition is attached to the peripheral edge of the modeled region. This boundary condition represents the low-permeability far-field anhydrite matrix, which is considered homogeneous and infinite.

I.2.3.6 Reservoir Porosity

Porosity determinations were made on the reservoir anhydrite through geophysical logging and laboratory tests. A neutron-porosity log, a gamma-density log, and an acoustic log were used to estimate total porosity within Anhydrite III of the Castile Formation. Estimates of porosity from these logs ranged from 0 to 5 percent (Popielak et al., 1983). Laboratory porosity determinations were also performed on two intact pieces of core from Anhydrite III. The first piece of core (from 858 m BGS) had a porosity of 0.8 percent, and the second piece (from 916.5 m BGS) had a porosity of 0.2 percent (Popielak et al., 1983).

The brine occurrence appears to be associated with a zone of secondary porosity resulting from the deformation fracturing of the brittle anhydrites. A medium like this is often characterized by very low secondary porosities and high transmissivities. Because we have no accurate means of estimating secondary porosity for this medium, this modeling will adopt the same range of secondary porosity of 0.1 to 1.0 percent that was used by Popielak et al. (1983). The base-case value of porosity is chosen to be 0.5 percent.

I.2.3.7 Reservoir Compressibility

In this study, the specific storage is calculated in the classical hydrogeologic representation where the medium compressibility is normalized with respect to the bulk volume (Narasimhan and Kanehiro, 1980). The medium compressibility (α) for a triaxial system can be defined as the inverse of the bulk modulus (B) of the rock

$$\alpha = (1/B) \qquad \text{(I-45)}$$

The bulk compressibility of Anhydrite III was estimated from values of the bulk modulus determined from acoustic logs that were run in WIPP-12. Popielak et al. (1983) reported that the values of bulk modulus for Anhydrite III range from 3.45×10^{10} to 6.89×10^{9} Pa. This represents a compressibility range from 2.9×10^{-11} to 1.45×10^{-10} Pa^{-1}. These values are considered representative of the intact anhydrite. The compressibility of a fractured or jointed rock is generally an order of magnitude higher than that of a non-fractured rock (Freeze and Cherry, 1976). Freeze and Cherry give a range for medium compressibility for a fractured or jointed rock of from 1×10^{-8} to 1×10^{-10} Pa^{-1}. This study adopts this range of compressibility and takes 1×10^{-9} Pa^{-1} to be the base-case value.

I.2.4 BOREHOLE PARAMETERS

In Cases I and II, a borehole is assumed to be drilled through the repository and to encounter a brine reservoir within the Castile Formation. In this section, the borehole location and properties used in the simulations are discussed. The respective parameters are summarized in Table I.2.4.1.

The borehole is assumed to pass through the center of the southwestern waste panel. This is conservative in that travel times in the Culebra aquifer calculated using the ground-water flow model are shortest between the southwestern corner of the waste-storage area and off-site locations such as that of the hypothetical stock well.

Elevations of the ground surface and the Rustler units are based on the H-3 hydropad because of its nearness. The elevation for the center of the facility is taken from Bechtel (1985). Interpolation between WIPP-12 and Cabin Baby-1 was used to determine the elevation of the Salado-Castile contact at the breach-borehole location. The elevation for the center of the brine reservoir is based on interpolation between the Anhydrite III elevation at WIPP-12 and Cabin Baby-1 and the relative position of the brine reservoir in Anhydrite III at WIPP-12. A schematic representation of the borehole showing elevations and thicknesses of the various units of interest and the locations of the 60-m long borehole plays are shown in Figure I.2.2.

TABLE I.2.4.1 Specifications for intrusion borehole for Case II simulations

Parameter	Value	Units
Borehole UTM location at center of southwestern waste panel	613324 3581146	m E m N
Elevations		
Ground surface	1033	m
Center of Culebra	825	m
Rustler-Salado contract	783	m
Center of waste panel	381	m
Salado-Castile contact	181	m
Center of brine reservoir	109	m
Drilled diameter		
In Rustler (oil well)	0.413	m
In Rustler (gas well)	0.457	m
In Salado and Castile (oil well)	0.311	m
In Salado and Castile (gas well)	0.356	m
Hole diameters used in numerical analysis		
Cased inside diameter of average hole in Rustler	0.326	m
Diameter of average borehole in Salado and Castile	0.334	m
Borehole plugs		
Lengths	60	m
Locations (above brine reservoir, below potash zone, and below Rustler)		
Effective borehole permeability		
Open borehole period	infinite	
Plug in Castile	10^{-15}	m^2
Plugs in Salado	10^{18}	m^2
For times greater than 150 years		
Case IIA	10^{12}	m^2
Cases IIB and IIC	10^{-11}	m^2

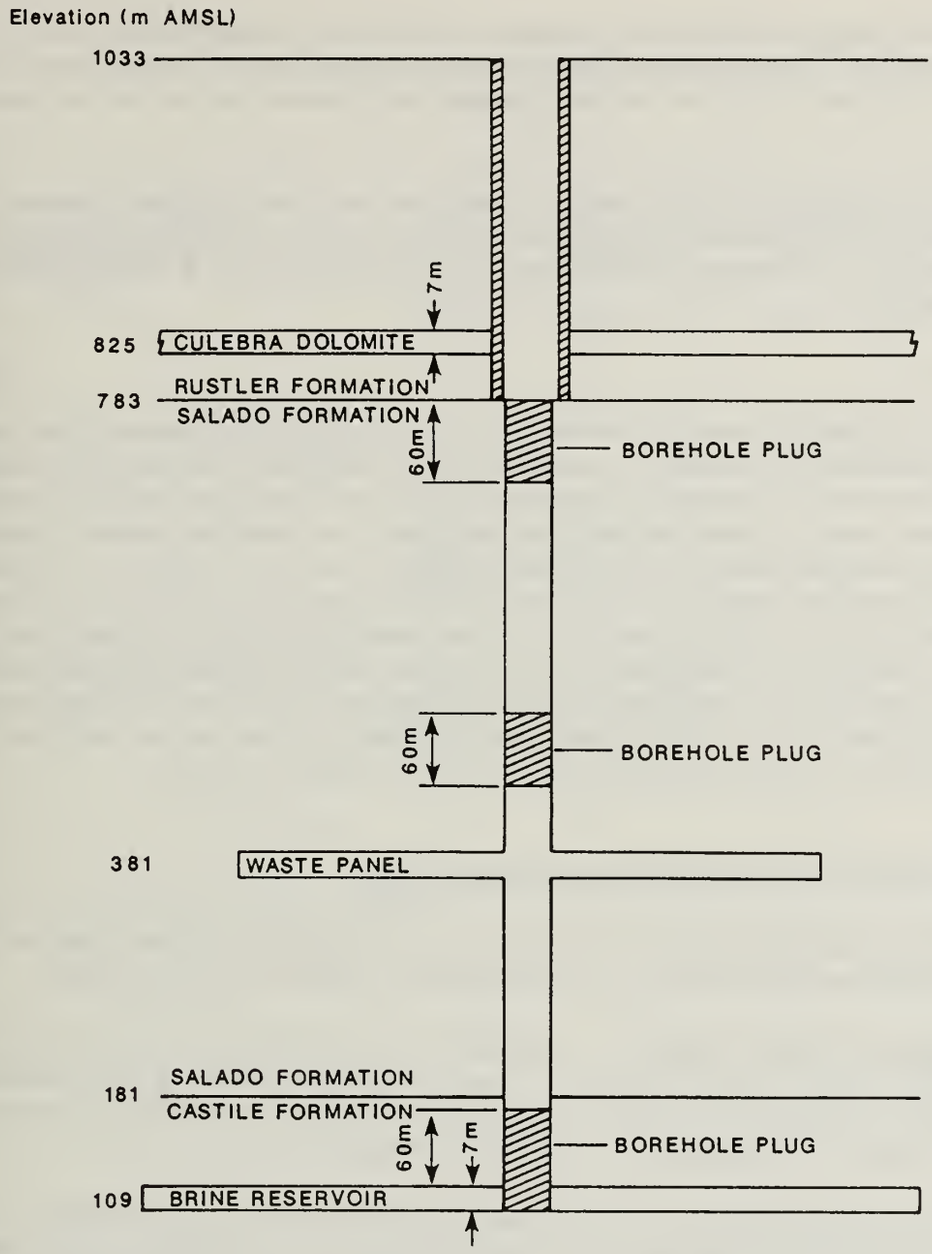

REF: LAPPIN et al., 1989.

FIGURE I.2.2

REPRESENTATIVE PLAN FOR PLUGGING A BOREHOLE THROUGH THE REPOSITORY TO A CASTILE FORMATION BRINE RESERVOIR

Borehole diameters for oil and gas wells are 0.413 m (16-1/4 inch) and 0.457 m (18 inch), respectively, from ground surface to the top of the Salado Formation and 0.311 m (12-1/4 inch) and 0.356 m (14 inch), respectively, below the top of the Salado Formation.

In the SWIFT II simulations, the hydraulic conductance of the borehole between the brine reservoir and the Culebra is used as input for modeling the hydraulic coupling of the two aquifers. The hydraulic conductance is defined in terms of a transmissibility T_w by the relation

$$T_w = kA/L \qquad \text{(I-46)}$$

where k is the effective borehole permeability, A is the borehole cross-sectional area, and L is the length of the plugs or "rubbleized" borehole zones. Since two potential borehole diameters are possible in exploratory drilling of oil and gas wells, an average cross-sectional area for these two well types was used. An effective borehole hydraulic conductance was calculated as a harmonic average (i.e., $K_{ave} = [(1/K_1 + 1/K_2)/2]^{-1}$) using the appropriate borehole or plug lengths with specific permeabilities and cross-sectional areas. For modeling purposes, it is assumed that the plugs remain intact for the first 75 years after emplacement, and then their transmissibilities increase linearly until 150 years, when the effective borehole permeability is 10^{-12} m^2 for Case IIA and 10^{-11} m^2 for Case IIB. This time-varying transmissibility is implemented stepwise with equal increments to the transmissibility at 75, 100, 125, and 150 years.

I.2.5 REPOSITORY SOURCE-TERM PARAMETERS

The parameters necessary for quantifying the source term to the Culebra aquifer for the Case II simulations using SWIFT II are summarized in Tables I.2.5.1 and I.2.5.2.

Waste Species and Mass Inventory. Calculations were performed for four radioactive decay chains (^{240}Pu, ^{239}Pu, ^{238}Pu, and ^{241}Am) and stable lead for a time period of 10,000 years. The initial total waste inventory for the decay-chain members of interest and stable lead in the repository is presented in Table I.2.5.1.

Source Term in the Repository. For the Case II simulations, the mass of waste in one panel was assumed to be exposed to circulating fluids. The concentration of the waste species in these fluids is constrained by their solubilities. For the radionuclides, the solubilities were set equal to 10^{-6} and 10^{-4} molar for Cases IIA and IIB, respectively. The solubility for stable Pb was set at 116 mg/l in the repository fluids. All fluids entering the borehole from the waste panel had concentrations at these values except as modified by radioactive decay and the total mass available in one panel. The solubility of stable lead in the Culebra groundwaters was specified at 54 mg/l.

TABLE I.2.5.1 Specification of waste radionuclide species and their initial mass inventory (including stable lead) in the repository for the Case II simulations

Decay Chain or Waste Species	Nuclide	Half Life (years)	Initial Waste Inventory (Ci)	(g)
$^{240}Pu \rightarrow {}^{236}U$	^{240}Pu	6.54×10^3	1.05×10^5	4.76×10^5
	^{236}U	2.34×10^7	0	0
^{239}Pu	^{239}Pu	2.41×10^4	4.25×10^5	6.93×10^6
$^{238}Pu \rightarrow {}^{234}U \rightarrow {}^{230}Th \rightarrow {}^{226}Ra \rightarrow {}^{210}Pb$	^{238}Pu	87.7	3.90×10^6	2.31×10^5
	^{234}U	2.44×10^5	0	0
	^{230}Th	7.7×10^4	0	0
	^{226}Ra	1.6×10^3	0	0
	^{210}Pb	22.3	0	0
$^{241}Am \rightarrow {}^{237}Np \rightarrow {}^{233}U \rightarrow {}^{229}Th$	^{241}Am	4.32×10^2	7.75×10^5	2.26×10^5
	^{237}Np	2.14×10^6	8.02	1.14×10^4
	^{233}U	1.59×10^5	7.72×10^3	8.15×10^5
	^{229}Th	7.43×10^3	0	0
Stable Pb	n.a.	n.a.	n.a.	1.33×10^9

Note: n.a. means not applicable

TABLE I.2.5.2 Specifications for repository parameters used in Case II simulations

Parameter	Symbol	Base Case	Units
Soluble radionuclide concentration for each decay-chain member i			
Case IIA	C_s	1×10^{-6}	molar
	C_s	2.4×10^{-7}	kg/kg
Cases IIB and IIC	C_s	1×10^{-4}	molar
	C_s	2.4×10^{-5}	kg/kg
Soluble stable-Pb concentration			
in repository	C_s	1.16×10^{2}	mg/L
	C_s	1.16×10^{-4}	kg/kg
in Culebra	C_s	5.4×10^{1}	mg/L
	C_s	5.4×10^{-5}	kg/kg
Mass in initial waste inventory	M_i	Reported in Table I.2.5.1	g
Mass of waste in contact with circulating fluids after borehole is plugged	---	$M_i/8$	g
Fluid loading from repository to the borehole (q)	---	1.3	m^3/yr

Note. Based on the specified radionuclide solubilities expressed as molarity, solubility values expressed as kg/kg have about a 6 percent range. Because of the large uncertainty in molarity values, a single solubility value for all radionuclides was used in numerical simulations.

Calculations of brine inflow indicate an average value of 1.3 m^3/yr for one panel of seven rooms plus accessways. In the Case II simulations, this flux is added to the flux from the brine reservoir to the Culebra. As a consequence of the different specified hydrologic properties of the rooms for Case IIA and IIB, the mass loading to the borehole is different for the two situations. For Cases IIA and IIC, all fluid flowing from the brine reservoir is assumed to have access to the waste mass in one panel, whereas in Cases IIB and IID, the fluid from the brine reservoir does not come in contact with the waste. In the first three cases, 1.3 m^3/yr of Salado brine inflow that has contacted the waste mass is specified to enter the borehole and flow to the Culebra aquifer. In Case IID, 0.1m^3/yr, from one room only, passes through the waste mass to the borehole.

I.2.6 CULEBRA PARAMETERS

A fractured porous medium is assumed to exist along the travel path between the breach borehole and the stock well. The definition of the flow path, the stock-well location, and the solute-transport properties within the Culebra are discussed below. Additional discussion on fracturing in the Culebra and its effect on hydraulic and tracer tests is presented in Reeves et al. (1987). The base-case and range of values for the Culebra parameters are summarized in Table I.2.6.1. The range of values is presented for discussion purposes only. They are not used in the Case IIA simulations. For Cases IIB, IIC, and IID, lower or higher end values of the range were selected, whichever would result in more rapid or longer distance solute transport.

A double-porosity flow is assumed along the travel path. The double-porosity data base is limited; base-case and ranges of parameter values are documented using available data, but must be considered as uncertain.

Regional Flow Field. A review of the hydrologic modeling for the Culebra in the vicinity of the WIPP site is discussed in Lappin et al. (1989, Section 3.3.5). The Culebra groundwater flow model by LaVenue et al. (1988) is the most recent model available for estimating the Darcy-velocity distribution in the regional flow field and for determining the travel path from the borehole to the stock well. Calibration of the model included hydrologic data available up to about October 1987. The model was calibrated to undisturbed head conditions only and did not include data from the large-scale multipad pumping tests that have been performed at the WIPP site. Full details on the calibrated Culebra transmissivity distribution and steady-state head distribution are presented in LaVenue et al. (1988).

As discussed above in Section I.2.4, the borehole is assumed to be drilled through the center of the southwestern waste panel. A particle-tracking code was used to determine the flow path for transport from this release location to a hypothetical stock well. The location of the stock well was based on two constraints: the well is assumed to lie on a flow path from the breach borehole, and the well must be located in an area where the water is potentially fresh enough to support stock.

TABLE I.2.6.1 Parameter base-case and range values selected for the Culebra dolomite

Parameter	Symbol	Base Case	Range	Units
Free-water diffusivity	D'	$5x10^{-6}$	$5x10^{-7}$ to $9x10^{-5}$	cm^2/s
Radionuclides: Case IIAD'	$1x10^{-6}$	n.a.	cm^2/s	
Cases IIB, IIC, IID	D'	$5x10^{-7}$	n.a.	cm^2/s
Stable Pb: Case IIA	D'	$4x10^{-6}$	n.a.	cm^2/s
Cases IIB, IIC, IID	D'	$1x10^{-6}$	n.a.	cm^2/s
Matrix tortuosity		0.15	0.03-0.5	
Case IIA		0.15	n.a.	
Cases IIB, IIC, IID		0.03	n.a.	
Fracture spacing	2L'	2.0	0.25-7.0	m
Case IIA	2L'	2.0	n.a.	m
Cases IIB, IIC, IID	2L'	7.0	n.a.	m
Porosity	ϕ	0.16	0.07-0.30	
Case IIA	ϕ	0.16	n.a.	
Cases IIB, IIC, IIC	ϕ	0.07	n.a.	
Fracture porosity	ϕ	$1.5x10^{-3}$	$1.5x10^{-4}$ to $1.5x10^{-2}$	
Matrix distribution coefficient				
Case IIA: Plutonium	k_d	50	-	ml/g
Americium	k_d	200	-	ml/g
Uranium	k_d	1	-	ml/g
Neptunium	k_d	1	-	ml/g
Thorium	k_d	50	-	ml/g
Radium	k_d	0.1	-	ml/g
Lead	k_d	0.1	-	ml/g
Cases IIB, IIC, IID				
Plutonium	k_d	25	-	ml/g
Americium	k_d	100	-	ml/g
Uranium	k_d	1	-	ml/g
Neptunium	k_d	1	-	ml/g
Thorium	k_d	25	-	ml/g
Radium	k_d	0.05	-	ml/g
Lead	k_d	0.05	-	ml/g

Note: The Culebra groundwater flow model presented in LaVenue et al. (1988) was used for calculating fluxes and determining flow paths. The transient fracture flux along the flow path from the release point in the Culebra aquifer to the off-site stock well is calculated through hydraulic coupling of the brine reservoir, borehole region, and Culebra aquifer.

Table I.2.6.2 Summary of porosities measured in Culebra core samples

Well	Sample Identification Number	Porosity Determination (%) Helium or Air	Water Resaturation
H-2a	-1	11.6	11.3
H-2a	-2	12.2	
H-2b	1-1	14.1	
H-2b	2-1, 3-1	15.4	
H-2b	1-2	11.8	
H-2b	2-2, 3-2	10.3	
H-2b1	-1F	10.5	
H-2b1	-1	8.2	8.8
H-2b1	-2	14.2	
H-2b1	-3	15.3	15.8
H-3b2	1-3	18.8	
H-3b2	1-4	16.8	
H-3b3	2-3, 3-3	18.0	
H-3b3	2-4, 3-4V	20.2	
H-3b3	1-6	24.4	
H-3b3	2-5, 3-5	20.5	
H-4b	1-9	29.7	
H-4b	2-6, 3-6V	20.8	
H-5b	-1	12.5	
H-5b1	-1A	13.0	
H-5b1	-1B	15.6	
H-5b1	-2	22.8	23.7
H-5b1	-2F	24.8	
H-5b1	-3	13.3	12.8
H-6b	2-7	10.8	
H-6b	2-8	11.6	
H-6b	1-7	10.7	
H-6b	1-8	25.5	
H-7b1	-1	17.7	18.1
H-7b1	-1F	14.9	
H-7b1	-2A	20.6	
H-7b1	-2B	27.8	
H-7b2	-1	15.9	14.8
H-7b2	-2	11.8	12.9
H-7c	-1A	12.5	12.9
H-7c	-1B	16.5	
H-7c	-1C	13.4	
H-7c	-1F	13.8	
H-10b	-1	8.9	
H-10b	-2	11.5	11.7
H-10b	-2F	6.6	
H-10b	-3	11.2	10.6

TABLE I.2.6.2 Concluded

Well	Sample Identification Number	Porosity Determination (%) Helium or Air	Water Resaturation
H-11	-1	15.5	15.3
H-11	-2	10.5	11.3
H-11	-2F	10.4	
H-11b3	-1	30.3	27.5
H-11b3	-1F	22.3	
H-11b3	-2	9.9	10.3
H-11b3	-2F	12.3	
H-11b3	-3	13.0	12.6
H-11b3	-4	15.2	
H-11b3	-4F	22.4	
W-12	-1A	2.8	
W-12	-1B	11.4	
W-12	-2	11.6	11.9
W-12	-2B	12.6	
W-12	-2F	13.5	
W-12	-3	13.4	13.0
W-13	-1	14.3	15.2
W-13	-2	21.9	22.6
W-13	-2F	26.0	
W-13	-3A	17.9	
W-13	-3B	9.7	
W-25	-1	11.5	12.0
W-26	-1	12.4	12.2
W-26	-1F	11.2	
W-26	-2	12.6	12.6
W-26	-3	12.7	
W-28	-1A	14.2	
W-28	-1B	13.0	
W-28	-2	18.7	18.8
W-28	-3	17.0	16.9
W-28	-3F	17.9	
W-30	-1	12.8	12.4
W-30	-2	15.0	15.2
W-30	-3A	17.6	
W-30	-3B	14.9	13.9
W-30	-3F	14.9	
W-30	-4	23.9	
AEC-8	-1	7.9	8.6
AEC-8	-1F	12.2	
AEC-8	-2	10.9	10.6

Number of Samples - 82
Average - 15.2%
Standard Deviation - 5.3%
Range - 2.8 to 30.3%

Free-Water Diffusivity. Base-case and range values for free-water diffusion coefficients for the radionuclides of interest and stable lead are presented in Lappin et al. (1989; Subsection E.2.4.2). A single value is necessary for all members of a decay chain because of the numerical formulation of the SWIFT II model. For Case IIA, values of $1x10^{-6}$ cm^2/s and $4x10^{-6}$ cm^2/s are selected for the radionuclides and stable lead, respectively. Values a factor of 2 smaller were used for the Case IIB simulation.

The base-case and range of values selected for this study are substantially lower than those in Reeves et al. (1987) for two reasons: 1) the previous study did not specifically address the radioactive decay-chain members identified in the present study, and 2) the much higher salinities that are a result of flow from the Salado and Castile can cause a reduction in the free-water diffusivity by as much as a factor of 2.

Matrix Porosity. Porosities have been measured in the laboratory for 82 core samples of Culebra dolomite from 15 borehole or hydropad locations at and surrounding the WIPP site. The results are summarized in Table I.2.6.2. Porosities were measured by the Boyle's Law technique using helium or air on all samples and by the water-resaturation technique on 30 samples. An excellent correlation was obtained between porosity values from the two techniques. From the 82 samples with porosity measurements using the Boyle's Law technique, an average porosity of 15.2 percent was obtained with a range from about 3 to 30 percent. For comparison, core samples from the H-3 and H-11 hydropads, which are the two hydropads closest to the offsite pathway, had average porosities of 19.8 percent (6 samples) and 16.2 percent (10 samples), respectively. Porosities ranged from about 17 to 24 percent for the H-3 hydropad and about 10 to 30 percent for the H-11 hydropad.

Matrix-porosities of Culebra dolomite measured by Sandia National Laboratories using the ^{22}Na diffusion technique range from 1.1 to 8.7 percent. Corresponding tortuosities range from 0.09 to 0.1. The porosities calculated from the diffusion experiments are termed diffusion-porosity values and are lower than those measured by Boyle's Law or mercury-porosimetry techniques. These values lie at the lower end of the range of values shown in Table I.2.6.2. Possible explanations for the differences between values measured by these different techniques include sample heterogeneity, incomplete resaturation of previously dried samples, and deviations of actual pore geometry from the idealized model assumed in simple versions of Fick's First Law of Diffusion for solute migration in a porous rock. In general, the samples used in the diffusion measurements are fine-grain dolomites free from large cracks and are chosen for mineral homogeneity and structural competence. No claim has been made that these samples are representative of the Culebra dolomite in general or that these results are transferable to field-scale transport.

For transport along the off-site pathway in the Culebra, a base-case matrix porosity of 16 percent is chosen for the Case IIA simulation. For Case IIB, a matrix porosity of 7 percent is selected as a lower end value. Although lower values have been measured or derived, an average lower value of 7 percent along the flow path is considered most representative.

Matrix Tortuosity. Tortuosity values for dolomite are not available, although a review of the literature does permit an estimation of a potential range. Bear (1972), in his review of unconsolidated media, presents values ranging form 0.3 to 0.7. De Marsily (1986) reports tortuosities varying from 0.1 for clay to 0.7 for sand. Barker and Foster (1981) report diffusion coefficients for Cl^- in chalk samples that indicate tortuosities of 0.02 to 0.17. Katsube et al. (1986) calculate tortuosity values from 0.02 to 0.19 from diffusion experiments on crystalline-rock samples. As noted earlier, diffusion experiments performed by Sandia National Laboratories on a limited number of core samples have yielded tortuosities in the range of 0.09 to 0.1.

Matrix-tortuosity estimates for the Culebra were calculated based on formation-factor and matrix-porosity determinations on 15 core samples. The values, ranging from 0.03 to 0.33 with an average value of 0.14, are summarized in Table I.2.6.3.

For the Case IIA simulations, a base-case matrix tortuosity of 0.15 was selected as representative. This value is the same as that used in the regional-scale transport simulations presented in Reeves et al. (1987). A lower-end estimate of 0.03 for matrix tortuosity was selected for the Case IIB simulations.

Rock Density. Rock-density determinations were performed on 73 Culebra core samples from 15 borehole or hydropad locations. The values range from 2.78 to 2.84 g/cm^3 with an average and standard deviation of 2.82 and 0.02, respectively. A value of 2.82 g/cm^3 was chosen as the base-case value for all simulations.

Fracture Porosity. Estimates of the fracture porosity can be obtained by interpretation of tracer tests conducted at sites exhibiting double-porosity transport behavior. Tracer tests have been performed at five locations (H-2, H-3, H-4, H-6, and H-11 hydropads) at the WIPP site. Of these, the tests conducted at the H-3, H-6, and H-11 hydropads appear to demonstrate fracture-transport behavior as evidenced by the very rapid tracer breakthrough between wells on at least one flow path at each hydropad site. Detailed test interpretations have been reported for only the H-3 hydropad (Kelley and Pickens, 1986).

A first estimate of the fracture porosity can be calculated from the convergent-flow tracer tests by the relation

$$\phi_f = Q\, t_p / \pi\, r_t^2\, b \qquad \text{(I-47)}$$

where ϕ_f is the fracture porosity, Q is the discharge rate at the pumping well, t_p is the time to reach the peak concentration, r_t is the distance between the tracer-addition and pumping wells, and b is the aquifer thickness.

The time to reach the peak concentration is used in this estimation procedure because it is assumed that this time is representative of the average transport rate between the tracer-addition and pumping wells. Although the time to reach the peak concentration is also dependent on longitudinal dispersivity and diffusive losses to the matrix, this approach provides a first estimate of fracture porosity for calibration of the tracer-breakthrough curves.

The calculated fracture porosities for the flow paths exhibiting the strongest fracture control are 2×10^{-3} and 1×10^{-3} for the H-3 and H-11 hydropads, respectively. Since these two hydropads are closest to the off-site transport pathway, an average value of 1.5×10^{-3} was selected as the base-case fracture porosity.

Matrix-Block Length. The fractured Culebra dolomite is conceptualized in this study as consisting of three orthogonal fracture sets that define rectilinear matrix units. Both horizonal and vertical (or near vertical) fracture sets have been observed in core samples, shaft excavations, and in outcrop areas (Kelley and Pickens, 1986). The matrix-block sizes are expected to vary spatially across the WIPP site. However, since the matrix-block-size data base is so limited at the present time, the effects of this variability cannot be assessed. Therefore, this study analyzes double-porosity effects in terms of an "equivalent" block size assumed to be applicable over the entire length of the travel path.

Block sizes have been interpreted for the H-3 hydropad in the range of 0.25 to 1.2 m for the two travel paths at the hydropad (Kelley and Pickens, 1986). While detailed interpretations have not been completed for the H-11 hydropad tracer test, a preliminary evaluation of the breakthrough curves suggests matrix-block sizes in the range of 0.8 to 3 m. A base-case value of 2 m is selected for matrix-block length, with a range of values of 0.25 to 7 m. There is no physical significance to the value of 7 m chosen as the upper limit for fracture spacing. It simply corresponds to a representative measured thickness for the Culebra dolomite. Base-case and upper end matrix-block sizes of 2 and 7 m were selected for the Case IIA and Case IIB simulations, respectively.

Longitudinal Dispersivity. A review of the literature for various tracer-test scales and contaminant-plume sizes (e.g., Lalleman-Barres and Peaudecerf, 1978; Pickens and Grisak, 1981) suggests that, up to moderate travel distances of 500 to 1000 m, longitudinal dispersivity can be expressed as a function of the mean travel distance of the solute. Longitudinal dispersivity, as indicated by these authors, ranges from several to 10 percent of the travel-path length. Although it is assumed that longitudinal dispersivity is directly related to the mean travel distance of the solute, one would not expect the longitudinal dispersivity to increase beyond some maximum or asymptotic value. This study adopts a range of 50 m to 300 m, i.e., approximately 1.5 to 9 percent of the average path length (3280 m), with a base-case value equal to 100 m.

Matrix Distribution Coefficients. Estimates of the distribution coefficients (k_d) for the radionuclides and stable Pb, describing their interaction with the Culebra under Case II conditions, are presented and discussed in Lappin et al. (1989, Appendix E). There is a considerable uncertainty in defining representative k_d values for the waste species of interest; however, estimates were based on the limited data available. The values used in the Case IIA through Case IID simulations are summarized in Table I.2.6.1.

TABLE I.2.6.3 Summary of formation factors and calculated tortuosities from Culebra core samples

Well	Identification Number	Helium Porosity (%)	Formation Factor	Calculated Tortuosity
H-2b1	-1F	10.5	326.77	0.03
H-5b1	-2F	24.8	12.20	0.33
H-7b1	-1F	14.9	73.49	0.09
H-7c	-1F	13.8	79.61	0.09
H-10b	-2F	6.6	406.78	0.04
H-11	-2F	10.4	94.82	0.10
H-11b3	-1F	22.3	36.35	0.12
H-11b3	-2F	12.3	101.93	0.08
H-11b3	-4F	22.4	32.74	0.14
W-12	-2F	13.5	47.30	0.16
W-13	-2F	26.0	13.26	0.29
W-26	-1F	11.2	68.77	0.13
W-28	-3F	17.9	26.30	0.21
W-30	-3F	14.9	31.49	0.21
AEC-8	-1F	12.2	90.09	0.09
AVERAGE		15.6%	96.13	0.14
RANGE		6.6 - 26.0%		0.03 - 0.33

REFERENCES FOR APPENDIX I

Abitz, R. J., J. Myers, and P. Drez, 1989. "Composition of Salado Formation Brines from the WIPP Repository Horizon," DOE-WIPP Publication, in review.

ATSDR (Agency for Toxic Substances and Disease Registry), 1988. "Toxicological Profile for Lead," Oak Ridge National Laboratory, Oak Ridge, Tennessee, draft.

Baes et al. (C. F. Baes, III, R. D. Sharp, A. L. Sjorean, and R. W. Shor), 1984. A Review and Analysis of Parameters for Assessing Transport of Environmentally Released Radionuclides Through Agriculture, ORNL-5786, Oak Ridge National Laboratory, Oak Ridge, Tennessee.

Barker, J.A., and S.S.D. Foster, 1981. "A Diffusion Exchange Model for Solute Movement in Fissured Porous Rock." Quarterly Journal of Engineering Geology, London. V.14, p.17-26.

Bear, J., 1972. Dynamics of Fluids in Porous Media, American Elsevier Publishing Company, New York, New York, p. 764.

Beauheim, R. L., 1987. "Interpretations of Single-Well Hydraulic tests Conducted At and Near the Waste Isolation Pilot Plant (WIPP) Site, 1983-1987," SAND87-0039, Sandia National Laboratories, Albuquerque, New Mexico, for the U.S. Department of Energy.

Bechtel National Inc., 1985. Quarterly Geotechnical Data Report, DOE-WIPP 221, prepared for U.S. Department of Energy,

Botts, R. P., 1977. The Short-Term Effects of Lead on Domestic and Wild Animals, EPA-600/3-77-009, Corvallis Environmental Research Laboratory, Corvallis, Oregon.

Brookins, D. B., 1988. Eh-pH Diagrams for Geochemistry, Springer-Verlag, Berlin-Heidelberg-New York.

Butcher, B. M., 1989, January. "Simulated Waste Compositions and Properties," unpublished.

Campbell, J. E., D. E. Longsine, and M. Reeves, 1986. Risk Methodology for Geologic Disposal of Radioactive Waste: The Distributed Velocity Method of Solving the Convective-Dispersion Equation, SAND80-0717, NUREG/CR-1376, Sandia National Laboratories, Albuquerque, New Mexico.

Campbell, J. E., D. E. Longsine, and R. M. Cranwell, 1981. Risk Methodology for Geologic Disposal of Radioactive Waste: The NWFT/DVM Computer Code User's

Manual, SAND81-0886, NUREG/CR-2081, Sandia National Laboratories, Albuquerque, New Mexico.

Campbell, J. E., P. C. Kaestner, B. S. Langkopf, and R. B. Lantz, 1979. Risk Methodology for Geologic Disposal of Radioactive Waste: The Network Flow and Transport (NWFT) Model, SAND79-1920, NUREG/CR-1190, Sandia National Laboratories, Albuquerque, New Mexico.

Carslaw, H. S. and J. C. Jaeger, 1959. Conduction of Heat in Solids, 2nd ed., Oxford University Press, New York, New York, pp. 30-32.

Carter, R. D. and C. W. Tracy, 1960. "An Improved Method for Calculating Water Influx," Transactions of the Society of Petroleum Engineers, Vol. 219, pp. 515-517, American Institute of MIning Engineers.

Chapman, N. A., and J. A. T. Smellie, 1986, June. "Natural Analogues to the Conditions around a Final Repository for High-Level Radioactive Waste," Chemical Geology, Vol. 55, No. 3/4.

Clements, T. L. Jr., and Kudera, D. E., 1985, September. TRU Waste Sampling Program: Volume 1 -- Waste Characterization, EGG-WM-6503, Vol. 1, EG&G, Idaho Falls, Idaho.

Coons et al. (W. Coons, A. Bertgstrom, P. Gnirk, M. Gray, B. Knecht, R. Pusch, J. Steadman, B. Stillborg, M. Tokonami, and M. Vaajasaari), June 1987. State-of the Art Report on Potentially Useful Materials for Sealing Nuclear Waste Repositories, Stripa Project Report 87-12, Swedish Nuclear Fuel and Waste Management Co., Stockholm, Sweden.

D'Appolonia Consulting Engineers, Inc., 1982. Data File Report: ERDA-6 and WIPP-12 Testing, prepared for Westinghouse Electric Corporation and the U.S. Department of Energy, Albuquerque, New Mexico, 7 volumes.

D'Appolonia Consulting Engineers, Inc., 1983. Data File Report: ERDA-6 and WIPP-12 Testing, Addendum 2, prepared for Westinghouse Electric Corporation and the U.S. Department of Energy, Albuquerque, New Mexico.

De Marsily, G., 1986. Quantitative Hydrogeology. Academic Press, New York, New York, p. 440.

Appendix I I-68 References Tenth citation author, Dever, should read Drever.] Cliffs,

DOE (U.S. Department of Energy), 1988. Internal Dose Conversion Factors for Calculation of Dose to the Public, DOE/EH-0071, Washington, D.C.

DOE (U.S. Department of Energy), 1985. Committed Dose Equivalent Tables for U.S. D.O.E. Population Dose Calculations, ed. J. P. Corley. Pacific Northwest Laboratory. U.S. DOE, Office of Operational Safety, Washington, D.C.

Domenico, P. A., 1972. Concepts and Models in Groundwater Hydrology, McGraw-Hill Book Company, New York, New York.

Dosch, R. G., 1981. Solubility and Sorption Characteristics of Uranium (VI) Associated with Rock Samples and Brines/Groundwaters from WIPP and NTS, SAND80-1595, Sandia National Laboratories, Albuquerque, New Mexico.

Dosch, R. G., and A. W. Lynch, 1978. Interaction of Radonuclides with Geomedia Associated with the Waste Isolation Pilot Plant (WIPP) in New Mexico, SAND78-0297, Sandia National Laboratories, Albuquerque, New Mexico.

EPA (U.S. Environmental Protection Agency), 1986. Superfund Public Health Evaluation Manual, Office of Solid Waste and Emergency Response, OSWER Directive 9285.4-1, EPA 540/1-86/060, USEPA, Washington, D.C.

Earth Technology Corporation, 1988. Final Report for Time Domain Electromagnetic (TDEM) Surveys at the WIPP Site. SAND87-7144, Sandia National Laboratories, Albuquerque, New Mexico, for the U.S. Department of Energy. Sandia National Laboratories, Albuquerque, New Mexico.

Envirosphere Company, 1987. EPUS-Environmental Pathways Uncertainty and Screening Model User Guide. Prepared for California Energy Commission.

Freeze, R. A. and J. A. Cherry, 1976. Groundwater. Prentice-Hall, Englewood Cliffs, New Jersey.

Frick, T. C., and R. W. Taylor, eds., 1962. Petroleum Production Handbook, Vol. II, Society of Petroleum Engineers of AIME, Dallas, Texas.

Hausner, H. H., and M. Kumar Mal, 1982. Handbook of Powder Metallurgy, Chemical Publishing Co., p. 123.

Hayes, K. F., C. Papelis, and J. O. Leckie, 1988, October. "Modeling Ionic Strength Effects on Anion Adsorption at Hydrous Oxide/Solution Interfaces," Journal of Colloid and Interface Science, Vol. 125, No. 2.

Helgeson, H. C., 1969. "Thermodynamics of Hydrothermal Systems at Elevated Temperatures and Pressures," American Journal of Science, Vol. 267, pp. 729-804.

ICRP (International Commission on Radiological Protection), 1959. Report of the ICRP Committee II on Permissible Dose for Internal Radiation, International Commission on Radiological Protection, ICRP Publication 2, Pergamon Press, New York, New York.

Appendix I	I-69	References	Thirteenth citation publication number, ICRP Publication, should read ICRP Publication 23.	ask olic

Manual, SAND81-0886, NUREG/CR-2081, Sandia National Laboratories, Albuquerque, New Mexico.

Campbell, J. E., P. C. Kaestner, B. S. Langkopf, and R. B. Lantz, 1979. Risk Methodology for Geologic Disposal of Radioactive Waste: The Network Flow and Transport (NWFT) Model, SAND79-1920, NUREG/CR-1190, Sandia National Laboratories, Albuquerque, New Mexico.

Carslaw, H. S. and J. C. Jaeger, 1959. Conduction of Heat in Solids, 2nd ed., Oxford University Press, New York, New York, pp. 30-32.

Carter, R. D. and C. W. Tracy, 1960. "An Improved Method for Calculating Water Influx," Transactions of the Society of Petroleum Engineers, Vol. 219, pp. 515-517, American Institute of Mlning Engineers.

Chapman, N. A., and J. A. T. Smellie, 1986, June. "Natural Analogues to the Conditions around a Final Repository for High-Level Radioactive Waste," Chemical Geology, Vol. 55, No. 3/4.

Clements, T. L. Jr., and Kudera, D. E., 1985, September. TRU Waste Sampling Program: Volume 1 -- Waste Characterization, EGG-WM-6503, Vol. 1, EG&G, Idaho Falls, Idaho.

Coons et al. (W. Coons, A. Bertgstrom, P. Gnirk, M. Gray, B. Knecht, R. Pusch, J. Steadman, B. Stillborg, M. Tokonami, and M. Vaajasaari), June 1987. State-of the Art Report on Potentially Useful Materials for Sealing Nuclear Waste Repositories, Stripa Project Report 87-12, Swedish Nuclear Fuel and Waste Management Co., Stockholm, Sweden.

D'Appolonia Consulting Engineers, Inc., 1982. Data File Report: ERDA-6 and WIPP-12 Testing, prepared for Westinghouse Electric Corporation and the U.S. Department of Energy, Albuquerque, New Mexico, 7 volumes.

D'Appolonia Consulting Engineers, Inc., 1983. Data File Report: ERDA-6 and WIPP-12 Testing, Addendum 2, prepared for Westinghouse Electric Corporation and the U.S. Department of Energy, Albuquerque, New Mexico.

De Marsily, G., 1986. Quantitative Hydrogeology. Academic Press, New York, New York, p. 440.

Dever, J. I., 1982. The Geochemistry of Natural Waters, Prentice Hall, Englewood Cliffs, New Jersey, pp. 78-79.

DOE (U.S. Department of Energy), 1988. Internal Dose Conversion Factors for Calculation of Dose to the Public, DOE/EH-0071, Washington, D.C.

DOE (U.S. Department of Energy), 1985. Committed Dose Equivalent Tab
D.O.E. Population Dos
Laboratory. U.S. DOE,

Domenico, P. A., 1972. Concepts and Models in Groundwater Hydrology, McGraw-Hill Book Company, New York, New York.

Dosch, R. G., 1981. Solubility and Sorption Characteristics of Uranium (VI) Associated with Rock Samples and Brines/Groundwaters from WIPP and NTS, SAND80-1595, Sandia National Laboratories, Albuquerque, New Mexico.

Dosch, R. G., and A. W. Lynch, 1978. Interaction of Radonuclides with Geomedia Associated with the Waste Isolation Pilot Plant (WIPP) in New Mexico, SAND78-0297, Sandia National Laboratories, Albuquerque, New Mexico.

EPA (U.S. Environmental Protection Agency), 1986. Superfund Public Health Evaluation Manual, Office of Solid Waste and Emergency Response, OSWER Directive 9285.4-1, EPA 540/1-86/060, USEPA, Washington, D.C.

Earth Technology Corporation, 1988. Final Report for Time Domain Electromagnetic (TDEM) Surveys at the WIPP Site. SAND87-7144, Sandia National Laboratories, Albuquerque, New Mexico, for the U.S. Department of Energy. Sandia National Laboratories, Albuquerque, New Mexico.

Envirosphere Company, 1987. EPUS-Environmental Pathways Uncertainty and Screening Model User Guide. Prepared for California Energy Commission.

Freeze, R. A. and J. A. Cherry, 1976. Groundwater. Prentice-Hall, Englewood Cliffs, New Jersey.

Frick, T. C., and R. W. Taylor, eds., 1962. Petroleum Production Handbook, Vol. II, Society of Petroleum Engineers of AIME, Dallas, Texas.

Hausner, H. H., and M. Kumar Mal, 1982. Handbook of Powder Metallurgy, Chemical Publishing Co., p. 123.

Hayes, K. F., C. Papelis, and J. O. Leckie, 1988, October. "Modeling Ionic Strength Effects on Anion Adsorption at Hydrous Oxide/Solution Interfaces," Journal of Colloid and Interface Science, Vol. 125, No. 2.

Helgeson, H. C., 1969. "Thermodynamics of Hydrothermal Systems at Elevated Temperatures and Pressures," American Journal of Science, Vol. 267, pp. 729-804.

ICRP (International Commission on Radiological Protection), 1959. Report of the ICRP Committee II on Permissible Dose for Internal Radiation, International Commission on Radiological Protection, ICRP Publication 2, Pergamon Press, New York, New York.

ICRP (International Commission on Radiological Protection), 1975. "Report of the Task Group on Reference Man: Anatomical, Physiological, and Metabolic Characteristics," ICRP Publication, Pergamon Press, New York, New York.

ICRP (International Commission on Radiological Protection), 1977. Recommendations of the International Commission on Radiological Protection, ICRP Publication 26, Pergamon, New York.

ICRP (International Commission on Radiological Protection), 1979. Annals of the ICRP, ICRP Publication 30, "Limits for Intake of Radionuclides by Workers," Pergamon Press, New York, New York.

Jackson, K. J., 1988, Verification and Validation Studies of the Addition of Pitzers' Equations to the EQ3/6 Brine Model, UCRL-53841, Lawrence Livermore National Laboratory, Livermore, California, .

Katsube, T. J., T. W. Melnyk, and J. P. Hume, 1986. Pore Structure from Diffusion in Granitic Rocks. Atomic Energy of Canada Ltd., Technical Record 381, p.28.

Kelley, V. A, and J. F. Pickens, 1986. Interpretation of the Convergent-Flow Tracer Tests Conducted in the Culebra Dolomite at the H-3 and H-4 Hydropads at the Waste Isolation Pilot Plant (WIPP) Site. SAND86-7161, Sandia National Laboratories, Albuquerque, New Mexico.

Kent, D. B., V. S. Tripathi, N. B. Ball, and J. O. Leckie, 1988, March. Surface-Complexion Modeling of Radionuclide Adsorption in Subsurface Environments, NUREG/CR-4807, SAND86-7175, Sandia National Laboratories, Albuquerque, New Mexico.

Krauskopf, K. B., 1986. "Thorium and Rare-Earth Metals as Analogs for Actinide Elements," Chemical Geology, Vol. 55.

Lallemand-Barres and P. Peaudecerf, 1978. "Recherche des Relations Entre les Valeurs Mesurées de la Dispersivité Macroscropique d'un Milieu Aquifère, ses Autres Charactéristiques et les Conditions de Mesure." Rech. Bull. Bur. Geo. Min., Ser. 2, Sec.III, 4-1978, pp. 277-284.

Langmuir, D., and A. C. Riese, 1985. "The Thermodynamic Properties of Radium," Geochimica et Cosmochimica Acta, Vol. 49, pp. 1593-1601.

Langmuir, D., and J. S. Herman, 1980. "The Mobility of Thorium in Natural Waters at Low Temperatures," Geochimica et Cosmochimica Acta, Vol. 44, pp. 1753-1766.

Lappin, A. R., R. L. Hunter, and D. Garber, eds., 1989. Systems Analysis, Long-Term Radionuclide Transport, and Dose Assessment, Waste Isolation Pilot Plant (WIPP), Southeastern New Mexico, SAND89-0462, Sandia National Laboratories, Albuquerque, New Mexico.

LaVenue et al. (A. M. LaVenue, A. Haug, and V. A. Kelley), 1988. Numerical Simulation of Ground-Water Flow in the Culebra Dolomite at the Waste Isolation Pilot Plant (WIPP) Site: Second Interim Report. SAND88-7002, Sandia National Laboratories.

Lee, W. J., 1982. Well Testing, SPE Textbook Series Vol. I, Society of Petroleum Engineers of AIME, Dallas, Texas.

Longsine, D. E., J. Bonano, and C. P. Harlan, 1987. User's Manual for the NEFTRAN Computer Code, NUREG/CR-4766, SAND86-2405, Sandia National Laboratories, Albuquerque, New Mexico.

Lynch, A. W., and R. G. Dosch, 1980. Sorption Coefficients for Radionuclides on Samples from the Water-Bearing Magenta and Culebra Members of the Rustler Formation. SAND80-1064, Sandia National Laboratories, Albuquerque, New Mexico.

Melfi, J. R., 1985, September. A Geochemical Model for Radionuclide Speciation in High Ionic Strength Solutions, Abstract of Thesis, University of New Mexico, Albuquerque, New Mexico.

Appendix I	I-71	References	Fifth citation title, The Merck Manual, New should read The Merck Veterinary Manual.

Munson, D. E., A. F. Fossum, and P. E. Senseny, 1989. "Approach to First Principles Model Prediction of Measured WIPP In Situ Room Closure in Salt," Proceedings of the 30th U.S. Rock Mechanics Symposium, at the University of West Virginia, June 19-22, 1988. A. A. Balkema, Rotterdam, Netherlands, to be published.

Narasimhan, T. N. and B. Y. Kanehiro, 1980. "A Note on the Meaning of Storage Coefficient." Water Resources Research, Vol.16, No.2, pp.423-429.

NCRP (National Council on Radiation Protection and Measurements), 1984. "Radiological Assessment: Predicting the Transport, Bioaccumulation, and Uptake by man of Radionuclides Released to the Environment." NCRP Report 76, Bethesda, Maryland.

Neretnieka, I., and A. Rasmuson, 1984. "An Approach to Modeling Radionuclide Migration in a Medium with Strongly Varying Velocity and Block Sizes Along the Flow Path," Water Resources Research, Vol. 20, No. 12, pp. 1823-1836.

Nowak, E.J., 1980. Radonuclide Sorption and Migration Studies of Getters for Backfill Barriers, SAND79-1110, Sandia National Laboratories, Albuquerque, New Mexico.

NRC (U.S. Nuclear Regulatory Commission), 1976. NRC, "Calculation of Annual Doses to Man from Routine Releases of Reactor Effluents for the Purpose of Evaluating Compliance with 10 CFR Part 50, Appendix I." Regulatory Guide 1.10911, NRC, Washington, D.C.

ORNL (Oak Ridge National Laboratory), 1988. Integrated Data Base for 1988: Spent Fuel and Radioactive Waste Inventories, Projections, and Characteristics. DOE/RW-0006, Rev. 4, Oak Ridge National Laboratory, Oak Ridge, Tennessee.

ICRP (International Commission on Radiological Protection), 1977. Recommendations of the International Commission on Radiological Protection, ICRP Publication 26, Pergamon, New York.

ICRP (International Commission on Radiological Protection), 1979. Annals of the ICRP, ICRP Publication 30, "Limits for Intake of Radionuclides by Workers," Pergamon Press, New York, New York.

Jackson, K. J., 1988, Verification and Validation Studies of the Addition of Pitzers' Equations to the EQ3/6 Brine Model, UCRL-53841, Lawrence Livermore National Laboratory, Livermore, California, .

Katsube, T. J., T. W. Melnyk, and J. P. Hume, 1986. Pore Structure from Diffusion in Granitic Rocks. Atomic Energy of Canada Ltd., Technical Record 381, p.28.

Kelley, V. A, and J. F. Pickens, 1986. Interpretation of the Convergent-Flow Tracer Tests Conducted in the Culebra Dolomite at the H-3 and H-4 [illegible] Waste Isolation Pilot Plant (WIPP), [illegible] Laboratories, Albuqu[illegible]

Kent, D. B., V. S. Tripathi, [illegible]. O. Leckie, 1988, March. Surface-Complexion Modeling of Radionuclide Adsorption in Subsurface Environments, NUREG/CR-4807, SAND86-7175, Sandia National Laboratories, Albuquerque, New Mexico.

Krauskopf, K. B., 1986. "Thorium and Rare-Earth Metals as Analogs for Actinide Elements," Chemical Geology, Vol. 55.

Lallemand-Barres and P. Peaudecerf, 1978. "Recherche des Relations Entre les Valeurs Mesurées de la Dispersivité Macroscropique d'un Milieu Aquifère, ses Autres Charactéristiques et les Conditions de Mesure." Rech. Bull. Bur. Geo. Min., Ser. 2, Sec.III, 4-1978, pp. 277-284.

Langmuir, D., and A. C. Riese, 1985. "The Thermodynamic Properties of Radium," Geochimica et Cosmochimica Acta, Vol. 49, pp. 1593-1601.

Langmuir, D., and J. S. Herman, 1980. "The Mobility of Thorium in Natural Waters at Low Temperatures," Geochimica et Cosmochimica Acta, Vol. 44, pp. 1753-1766.

Lappin, A. R., R. L. Hunter, and D. Garber, eds., 1989. Systems Analysis, Long-Term Radionuclide Transport, and Dose Assessment, Waste Isolation Pilot Plant (WIPP), Southeastern New Mexico, SAND89-0462, Sandia National Laboratories, Albuquerque, New Mexico.

LaVenue et al. (A. M. LaVenue, A. Haug, and V. A. Kelley), 1988. Numerical Simulation of Ground-Water Flow in the Culebra Dolomite at the Waste Isolation Pilot Plant (WIPP) Site: Second Interim Report. SAND88-7002, Sandia National Laboratories.

Lee, W. J., 1982. Well Testing, SPE Textbook Series Vol. I, Society of Petroleum Engineers of AIME, Dallas, Texas.

Longsine, D. E., J. Bonano, and C. P. Harlan, 1987. User's Manual for the NEFTRAN Computer Code, NUREG/CR-4766, SAND86-2405, Sandia National Laboratories, Albuquerque, New Mexico.

Lynch, A. W., and R. G. Dosch, 1980. Sorption Coefficients for Radionuclides on Samples from the Water-Bearing Magenta and Culebra Members of the Rustler Formation. SAND80-1064, Sandia National Laboratories, Albuquerque, New Mexico.

Melfi, J. R., 1985, September. A Geochemical Model for Radionuclide Speciation in High Ionic Strength Solutions, Abstract of Thesis, University of New Mexico, Albuquerque, New Mexico.

Merck & Co., Inc., 1979. The Merck Manual, e.d. O. H. Siegmund, Rahway, New Jersey.

Munson, D. E., A. F. Fossum, and P. E. Senseny, 1989. "Approach to First Principles Model Prediction of Measured WIPP In Situ Room Closure in Salt," Proceedings of the 30th U.S. Rock Mechanics Symposium, at the University of West Virginia, June 19-22, 1988. A. A. Balkema, Rotterdam, Netherlands, to be published.

Narasimhan, T. N. and B. Y. Kanehiro, 1980. "A Note on the Meaning of Storage Coefficient." Water Resources Research, Vol.16, No.2, pp.423-429.

NCRP (National Council on Radiation Protection and Measurements), 1984. "Radiological Assessment: Predicting the Transport, Bioaccumulation, and Uptake by man of Radionuclides Released to the Environment." NCRP Report 76, Bethesda, Maryland.

Neretnieka, I., and A. Rasmuson, 1984. "An Approach to Modeling Radionuclide Migration in a Medium with Strongly Varying Velocity and Block Sizes Along the Flow Path," Water Resources Research, Vol. 20, No. 12, pp. 1823-1836.

Nowak, E.J., 1980. Radonuclide Sorption and Migration Studies of Getters for Backfill Barriers, SAND79-1110, Sandia National Laboratories, Albuquerque, New Mexico.

NRC (U.S. Nuclear Regulatory Commission), 1976. NRC, "Calculation of Annual Doses to Man from Routine Releases of Reactor Effluents for the Purpose of Evaluating Compliance with 10 CFR Part 50, Appendix I." Regulatory Guide 1.10911, NRC, Washington, D.C.

ORNL (Oak Ridge National Laboratory), 1988. Integrated Data Base for 1988: Spent Fuel and Radioactive Waste Inventories, Projections, and Characteristics. DOE/RW-0006, Rev. 4, Oak Ridge National Laboratory, Oak Ridge, Tennessee.

Paine, R. T., 1977. Chemistry Related to the WIPP Site, Draft Final Report, Sandia Contract GTK/07-1488, Chemistry Department, University of New Mexico, Albuquerque, New Mexico.

Pickens, J. F., and G. E. Grisak, 1981. "Scale-Dependent Dispersion in a Stratified Granular Aquifer," Water Resources Research, Vol. 17, No.4, pp. 1191-1211.

Pickens et al. (J. F. Pickens, G. E. Grisak, J. D. Avis, D. W. Belanger, and M. Thury), 1987. "Analysis and Interpretation of Borehole Hydraulic Tests in Deep Boreholes: Principles, Model Development, and Applications," Water Resources Research, Vol. 23, No. 7, 1341-1375.

Popielak, R. S., R. L. Beauheim, S. R. Black, W. E. Coons, C. T. Ellingson, and R. L. Olsen, 1983. Brine Reservoirs in the Castile Formation Waste Isolation Pilot Plant (WIPP) Project Southeastern New Mexico. Prepared by D'Appolonia Consulting Engineers, TME 3153, Inc., for the U.S. Department of Energy.

Poston, J. W., 1985. Internal Dose Assessment, Technical Management Services, New Hartford, Connecticut.

Randall, W. S., M. E. Crawley, and M. L. Lyon, 1988. 1988 Annual Water Quality Data Report for the Waste Isolation Pilot Plant. DOE-WIPP 88-006, U.S. Department of Energy.

Reeves, M., D. S. Ward, N. D. Johns, and R. M. Cranwell, 1986. Theory and Implementation for SWIFT II. The Sandia Waste-Isolation Flow and Transport Model for Fractured Media Release 4.84. NUREG/CR-3328. SAND83-1159. Sandia National Laboratories, Albuquerque, New Mexico, for the U.S. Nuclear Regulatory Commission.

Reeves, Mark, V. A. Kelley, and J. F. Pickens, 1987. Regional Double-Porosity Solute Transport in the Culebra Dolomite: An Analysis of Parameter Sensitivity and Importance at the Waste Isolation Pilot Plant (WIPP) Site. SAND87-7105, Sandia National Laboratories, Albuquerque, N.M.

Riese, A. C., 1982. Adsorption of Radium and Thorium onto Quartz and Kaolinite: A Comparison of Solution/Surface Equilibria Models, Ph.D. Thesis, Colorado School of Mines, Golden, Colorado.

Serne, R.J., D. Rai, M.J. Mason, and M. Molecke, 1977. Batch K_d Measurements of Nuclides to Estimate Migration Potential at the Proposed Waste Isolation Pilot Plant in New Mexico, PNL-2448, Pacific Northwest Laboratories, Richland, Washington.

Siegel, M. D., S. J. Lambert, and K. L. Robinson, eds., 1989. Hydrogeochemical Studies of the Rustler Formation and Related Rocks in the WIPP Area, Southeastern New Mexico, SAND88-0196, Sandia National Laboratories, Albuquerque, New Mexico.

Soudek, A., 1984. Binary and Ternary Ion Exchange on Sodium Montmorillonite for Application to Backfill in Nuclear Water Disposal," Master's Thesis, Chemical Engineering, University of California, Berkeley, California.

Swanson, J. L., 1986. Organic Complexant-Enhanced Mobility of Toxic Elements in Low-Level Wastes: Final Report, NUREG/CR-4660, PNL-4965-10, Pacific Northwest Laboratory, Richland, Washington.

Tien, P. L., F. B. Nimick, A. B. Muller, P. A. Davis, R. V. Guzowski, L. E. Dida, and R. L. Hunter, 1983. Repository Site Data and Information in Bedded Salt; Palo Duro Basis, Texas, NUREG/CR-3129, SAND82-2223, Sandia National Laboratories, Albuquerque, New Mexico.

Tsunashima, A., G. W. Brindley, and M. Bastovanov, 1981. "Adsorption of Uranium from Solutions by Montmorillonite; Compositions and Properties of Uranyl Monmorillonites," Clays and Clay Minerals, Vol. 29, No. 1.

Till, J. E. and H. R. Meyer, 1983. Radiological Assessment: A Textbook on Environmental Dose Analysis, NUREG/CR-3332, U.S. Nuclear Regulatory Commission, Washington D.C.

USPHS (U.S. Public Health Service), 1970. Radiological Health Handbook, Rockville, Maryland.

Van Everdingen, A. F. and W. Hurst, 1949. "Application of the Laplace Transformation to Flow Problems in Reservoirs," Transactions of the Society of Petroleum Engineers, American Institute of Mining Engineers, Dallas, Texas, Vol. 186, p. 305-324.

Whelan, G., D. L. Strenge, J. G. Droppe, Jr., B. L. Steelman, and J. W. Burk, 1987, The Remedial Action Priority System (RAPS): Mathematical Formulation, DOE/RL/87-09, PNL-6200, UC-11, Pacific Northwest Laboratory.

Wolery, T. J., 1983. EQ3NR - A Computer Program for Geochemical Aqueous Speciation-Solubility Calculations: User's Guide and Documentation, UCRL-53414, Lawrence Livermore National Laboratory, Livermore, California.

APPENDIX J

BIBLIOGRAPHY

TABLE OF CONTENTS

Section		Page
J.1	INTRODUCTION	J-1
J.2	DESIGN DEVELOPMENT	J-2
J.3	ENVIRONMENTAL	J-5
J.4	GEOCHEMISTRY	J-12
J.5	GEOLOGY	J-18
J.6	HYDROLOGY	J-38
J.7	REPOSITORY TECHNOLOGY	J-53
J.8	RESOURCES	J-106

J.1 INTRODUCTION

This appendix contains the most current bibliography related to the WIPP. The list contains most writings about the WIPP, not merely those referenced in this document. The citations are organized into seven subject areas:

1. Design Development
2. Environmental
3. Geochemistry
4. Geology
5. Hydrology
6. Repository
7. Resources

J.2 DESIGN DEVELOPMENT

Bechtel National, Inc., 1979. Geology Laboratory Results of Rock Testing, Document No. 22-4-510-04, Rev. 2, San Francisco, California.

Bechtel National, Inc., 1979 & 1980. WIPP Title I Design Report, and supplements.

Bechtel National, Inc., 1980. Waste Isolation Pilot Plant, Design Basis, Exploratory Shaft, D-31-R-03, Rev. 2.

Bechtel National, Inc., 1980. Waste Isolation Pilot Plant, Design Basis, Exploratory Shaft Geomechanical Instrumentation, D-32-X-01, Rev. 2.

Bechtel National, Inc., 1980. Waste Isolation Pilot Plant, Design Basis, Exploratory Shaft Furnishings and Station, D-37-S-02, Rev. 2.

Bechtel National, Inc., 1980. Waste Isolation Pilot Plant, Design Basis, SPDV Underground Excavations, D-51-W-02.

Bechtel National, Inc., 1981. Stability Analysis of Underground Openings, RMC-II, Study Report No. 51-R-510-04, Rev. 0.

Bechtel National, Inc., 1982. Waste Isolation Pilot Plant, Design Bases, Underground Experimental Areas, D-52-K-04, Rev 2.

Bechtel National, Inc., 1983. Primary Creep of Rock Salt, 76-D-540AD-01, San Francisco, California.

Bechtel National, Inc., 1983. Waste Isolation Pilot Plant, Design Basis, Exhaust Shaft, D-35-R-01, Rev. 1.

Bechtel National,Inc., 1983. Waste Isolation Pilot Plant, Design Basis, Design Classification, D-76-K-03, Rev. 9.

Bechtel National, Inc., 1983. Waste Isolation Pilot Plant, Design Basis, Geomechanical Instrumentation, D-76-X-01, Rev. 6.

Bechtel National, Inc., 1983. Waste Isolation Pilot Plant, Design Basis, WIPP-RMC IIA (General), D-76-K-01, Rev 7.

Bechtel National, Inc., 1983. Waste Isolation Pilot Plant, Design Basis, Waste Shaft, D-31-R-01, Rev. 8.

Bechtel National, Inc., 1983. Waste Isolation Pilot Plant, Design Basis, Underground Excavations, D-51-W-01, Rev. 6.

Bechtel National, Inc., 1983. Waste Isolation Pilot Plant Preliminary Design Validation Report, San Francisco, California.

Bechtel National Inc., 1984. Waste Isolation Pilot Plant, Design Basis, Underground Shops and Facilities, D-54-E-01, Rev. 6.

Branstetter, L. J., R. D. Krieg, and C. M. Stone, 1982. The Effect of a Random Variation of Rock Salt Creep on Calculations of Storage Room Closure for the WIPP Project, SAND82-0024, Sandia National Laboratories, Albuquerque, New Mexico.

Branstetter, L. J., 1985. Second Reference Calculations for the WIPP, SAND83-2461, Sandia National Laboratories, Albuquerque, New Mexico.

DOE, (U.S. Department of Energy), 1980. Final Environmental Impact Statement: Waste Isolation Pilot Plant, DOE/EIS-0026, Washington, D.C.

DOE, (U.S. Department of Energy), 1983. Waste Isolation Pilot Plant, Design Validation Plan, Document No. 76B510AB-000, Rev. 6, Carlsbad, N.M.

DOE, (U.S. Department of Energy), 1986. Waste Isolation Pilot Plant, Design Validation Strategy, Carlsbad, N.M.

DOE, (U.S. Department of Energy), 1980. Waste Isolation Pilot Plant, Safety Analysis Report, Carlsbad, N.M.

Holt, R., and D. Powers. Geotechnical Activities in the Exhaust Shaft, DOE-WIPP-86-008, Westinghouse Electric Corp., Carlsbad, N.M.

Matalucci, R. V., C. L. Christensen, T. O. Hunter, M. A. Molecke, and D.E. Munson, 1982. WIPP Research and Development Program: In Situ Testing Plan, SAND81-2628, Sandia National Laboratories, Albuquerque, New Mexico.

Miller, J. D., C. M. Stone, L. J. Branstetter, 1982. Reference Calculations for Underground Rooms of the WIPP, SAND82-1176, Sandia National Laboratories, Albuquerque, New Mexico.

McKinney, R. F., and R. S. Newton, 1983. Site Validation Field Program Plan, Rev. 1.2, Westinghouse Electric Corp., Carlsbad, N.M.

Morgan, H.S., R. D. Grieg, and R. V. Matalucci, 1981. Comparative Analysis of None Structural Codes Used in the Second WIPP Benchmark Problem, SAND81-1389, Sandia National Laboratories.

Powers, D. W., S. J. Lambert, S.E. Shaffer, L. R. Hill, and W. D. Weart, ed., 1978. Geological Characterization Report, Waste Isolation Pilot Plant (WIPP) Site, Southeaster New Mexico, SAND78-1596, Sandia National Laboratories, Albuquerque, New Mexico.

Sandia National Laboratories, 1977. WIPP Conceptual Design Report, SAND77-0274.

Serata, S., 1979. Empirical Design Basis of Underground Salt Openings in the WIPP Project, DR-51-R-1.

Stormont, J.C., 1984. Plugging and Sealing Program for the Waste Isolation Pilot Plant (WIPP), SAND84-1057, Sandia National Laboratories, Albuquerque, New Mexico.

Weart, W. D., 1981. Reference Creep Law and Material Properties for WIPP, Memo to Distribution, Sandia National Laboratories, Albuquerque, New Mexico.

Weart, W. D., 1983. Summary Evaluation of the Waste Isolation Pilot Plant (WIPP Site Suitability, SAND83-0450, Sandia National Laboratories, Albuquerque, New Mexico.

Westinghouse Electric Corp., 1981. Design Criteria, Waste Isolation Pilot Plant (WIPP), Site and Preliminary Design Validation (SPDV), WIPP-DOE-72, Rev. 1, Carlsbad, N.M.

Westinghouse Electric Corp., 1982. Site Validation Program, WIPP-DOE-116, Rev. 1, Carlsbad, N.M.

Westinghouse Electric Corp., 1983. Results of Site Validation Experiments, Waste Isolation Pilot Plant (WIPP) Project, Southeastern New Mexico, Vols. 1 and 2, TME 3177.

Westinghouse Electric Corp., 1984. Design Criteria, Waste Isolation Pilot Plant (WIPP), Revised Mission Concept-IIA (RMC-IIa), WIPP-DOE-71, Rev. 4.

Westinghouse Electric Corp., 1984. Geotechnical Activities in the Waste Handling Shaft, WTSD-TME-038, Carlsbad, N.M.

J.3 **ENVIRONMENTAL**

Banz, I., P. Bradshaw, J. S. Cockman, N. T. Fischer, J. K. Prince, A. Rodriguez, and D. W. Uhland, 1987. Annual Site Environmental Monitoring Report for the Waste Isolation Pilot Plant Calendar Year 1986, DOE/WIPP-87-002, Waste Isolation Pilot Plant, Carlsbad, New Mexico.

Barnes, H., 1974. "Geologic and Hydrologic Background for Selecting Site of Pilot-Plant Repository for Radioactive Waste," Bulletin of the Association of Engineering Geologists, Vol. 11, No. 1, pp. 83-92.

Bednarz, J. C., 1987. The Los Medanos Cooperative Raptor Research and Management Program, 1986 Annual Report, Contract No. 59-WRK-90469-5D.

Bednarz, J. C., and T. J. Hayden, 1988. The Los Medanos Cooperative Raptor Research and Management Program Final Report, 1985-1987, Contract No. 59-WRK-90469-SD, U.S. Department of Energy, Carlsbad, New Mexico.

Best, T. L., and K. S. Neuhauser, ed., 1979. Report of Biological Investigations at the Los Medanos Waste Isolation Pilot Plant (WIPP) Area of New Mexico During FY 1978, SAND79-0368, Sandia National Laboratories, Albuquerque, New Mexico.

Bingham, F. W., and G. E. Barr, 1979. Scenarios for Long-Term Release of Radionuclides from a Nuclear-Waste Repository in the Los Medanos Region of New Mexico, SAND78-1730, Sandia National Laboratories, Albuquerque, New Mexico.

Blaney, H. F., and E. G. Hanson, 1965. Consumptive Use and Water Requirements in New Mexico, Technical Report 32, New Mexico State Engineer's Office.

Bradshaw, P. L., and E. T. Louderbough, 1987. Compilation of Historical Radiological Data Collected in the Vicinity of the WIPP Site, DOE/WIPP-87-004, Waste Isolation Pilot Plant, Carlsbad, New Mexico.

Braithwaite, J. W., and M. A. Molecke, 1980. "Nuclear Waste Canister Corrosion Studies Pertinent to Geologic Isolation," Nuclear and Chemical Waste, Vol. 1, (preprint: SAND79-1935J), Sandia National Laboratories, Albuquerque, New Mexico.

Brewer, L. W., and J. H. Metcalf, 1977. Environmental Monitoring at the WIPP Site, CY 1976, SAND77-1201, Sandia National Laboratories, Albuquerque, New Mexico.

Church, H. W. et al., 1978. Excerpts from WIPP Meterological, Air Quality, and Radiological Measurements Program Plan, SAND78-1144, Sandia National Laboratories, Albuquerque, New Mexico.

Dieckhoner, J. E., ed., 1978. "Report of the WIPP Waste Acceptance Criteria Steering Committee, Detailed Characterization of DOE Stored TRU Waste," internal memo, Office of Nuclear Waste Management, U.S. Department of Energy.

DOE (U.S. Department of Energy), 1979. Draft Environmental Impact Statement, Management of Commercially Generated Radioactive Waste, DOE/EIS-0046-D, two volumes, Washington, D.C.

DOE (U.S. Department of Energy), 1979. Environmental Aspects of Commercial Radioactive Waste Management, DOE/ET-0029, Vols. 1-3, Office of Nuclear Waste Management.

DOE (U.S. Department of Energy), 1980. Final Environmental Impact Statement, Waste Isolation Pilot Plant, DOE/EIS-0026, Vols. 1-2, U.S. Department of Energy, Washington, D.C.

DOE (U.S. Department of Energy), 1980. Safety Analysis Report, Waste Isolation Pilot Plant, Albuquerque, New Mexico.

DOE (U.S. Department of Energy) and State of New Mexico, 1981. Agreement for Consultation and Cooperation Between [the U.S.] Department of Energy and the State of New Mexico on the Waste Isolation Pilot Plant, as amended 1985.

DOE (U.S. Department of Energy), 1986. Safety Analysis Report for the Waste Isolation Pilot Plant, Amendment 9, Carlsbad, New Mexico.

DOE (U.S. Department of Energy), 1987. Environmental Protection, Safety, and Health Protection Information Reporting Requirements, DOE Order 5484.1, Change 3, Washington, D.C.

Dowhower, S. L., 1981. "Effects of Trampling and Salt Additions on Vegetation of Sandy Soils of the Los Medanos Area, New Mexico," unpublished thesis, New Mexico State University, Las Cruces, New Mexico.

EEG (Environmental Evaluation Group), 1979. Radiological Health Review of the Draft Environmental Impact Statement (DOE/EIS-0026-D) Waste Isolation Pilot Plant, U.S. Department of Energy, EEG-3, R.H. Neill, J. K. Channell, C. Wofsy, and M.A. Greenfield, ed., Health and Environment Department, State of New Mexico, Santa Fe, New Mexico.

EEG (Environmental Evaluation Group), 1980. Calculated Radiation Doses From Deposition of Material Released in Hypothetical Transportation Accidents Involving WIPP-Related Radioactive Wastes, J. K. Channell, Health and Environment Department, State of New Mexico, Santa Fe, New Mexico.

EEG (Environmental Evaluation Group), 1981. An Approach to Calculating Upper Bounds on Maximum Individual Doses From the Use of Contaminated Well Water Following a WIPP Repository Breach, EEG-9, P. Spiegler, Health and Environment Department, State of New Mexico, Santa Fe, New Mexico.

EEG (Environmental Evaluation Group), 1981. Radiological Health Review of the Final Environmental Impact Statement (DOE/EIS-0026) Waste Isolation Pilot Plant, U.S. Department of Energy, EEG-10, Health and Environment Department, State of New Mexico, Santa Fe, New Mexico.

EEG (Environmental Evaluation Group), 1982. Calculated Radiation Doses from Radionuclide Brought to the Surface if Future Drilling Intercepts the WIPP Repository and Pressurized Brine, EEG-11, J. K. Channell, Health and Environment Department, State of New Mexico, Santa Fe, New Mexico.

EEG (Environmental Evaluation Group), 1982. Estimated Radiation Doses Resulting if an Exploratory Borehole Penetrates a Pressurized Brine Reservoir Assumed to Exist Below the WIPP Repository Horizon - A Single Hole Scenario, EEG-15, S. T. Bard, Health and Environment Department, State of New Mexico, Santa Fe, New Mexico.

EEG (Environmental Evaluation Group), 1982. Radionuclide Release, Transport and Consequence Modeling for WIPP. A Report of a Workshop Held on September 16-17, 1981, EEG-16, Health and Environment Department, State of New Mexico, Santa Fe, New Mexico.

EEG (Environmental Evaluation Group), 1982. Review Comments on Environmental Analysis Cost Reduction Proposals (WIPP-DOE-136) July 1982, EEG-19, J. K. Channell, Health and Environment Department, State of New Mexico, Santa Fe, New Mexico.

EEG (Environmental Evaluation Group), 1983. An Evaluation of the Non-radiological Environmental Problems Relating to the WIPP, EEG-20, T. E. Baca, Health and Environment Department, State of New Mexico, Santa Fe, New Mexico.

EEG (Environmental Evaluation Group), 1983. Potential Problems from Shipment of High-Curie Content Contact-Handled Transuranic, (CH-TRU) Waste to WIPP, EEG-24, R. H. Neill and J. K. Channell, Health and Environment Department, State of New Mexico, Santa Fe, New Mexico.

EEG (Environmental Evaluation Group), 1984. Proposed Preoperational Environmental Monitoring Program For WIPP, EEG-26, P. Spiegler, Health and Environment Department, State of new Mexico, Santa Fe, New Mexico.

Emlen, J. T., 1971. "Population Densities of Birds Derived from Transect Counts," Auk 88:323-342.

Ewing, R. I., 1982. Environmental Gamma Ray Spectra from Selected Sites in Southeastern New Mexico, SAND82-0738, Sandia National Laboratories, Albuquerque, New Mexico.

Fischer, N. T., ed., 1985. Ecological Monitoring Program at the Waste Isolation Pilot Plant, Second Semi-Annual Report, DOE/WIPP-85-002, Carlsbad, New Mexico.

Fischer, N. T., ed., 1987. Ecological Monitoring Program at the Waste Isolation Pilot Plant Annual Report for FY 1986, DOE/WIPP-87-003, Carlsbad, New Mexico.

Fischer, N. T., E. T. Louderbough, A. L. Rodriguez, S. D. Prill, J. S. Cockman, and W. D. Byers, 1988. Ecological Monitoring Program at the Waste Isolation Pilot Plant Annual Report for Calendar Year 1987, DOE/WIPP-88-008, U.S. Department of Energy Report.

Flynn, D. T., 1988. Annual Site Environmental Monitoring Report for the Waste Isolation Pilot Plant Calendar Year 1987, DOE/WIPP-88-009, U.S. Department of Energy Report, Carlsbad, New Mexico.

Hansen, L. J., 1970. Engineering Evaluation of the Super Tiger Overpack Designed for the Shipment of Large Quantities of Hazardous Material, C2378, Mechanics Research, Inc., Tacoma, Washington.

Hart, J. S., 1981. Ecosystems Studies at the Los Medanos Site, Eddy County, New Mexico, Volume 1 of 2, TME-3106.

Hart, J. S., 1982. Ecosystems Studies at the Los Medanos Site, Eddy County, New Mexico, Volume 2 of 3, TME-3141.

Louderbough, E. T., 1986. Operational Environmental Permit Compliance Plan for the Waste Isolation Pilot Plant, DOE/WIPP 2-4.

MacLennan, R. B., and S. C. Schermer, 1979. "An Archaeological Survey for the Waste Isolation Pilot Plant: Access Roads and Railroad Right-of-Way," Agency for Conservation Archaeology, Eastern New Mexico University, Portales, New Mexico.

Magnani, N. J., and J. W. Braithwaite, 1979. Corrosion Resistant Metallic Canisters: An Important Element of a Multibarrier Disposal Program, SAND79-1429C, Sandia National Laboratories, Albuquerque, New Mexico, presented at the Materials Research Society Symposium, November 1979, Boston, Massachussets.

Matejka, D. O., 1977. Meteorological Data Quarterly Report, WIPP Site, Eddy County Summer Quarter, May-June 1976, New Mexico, SAND77-1146, Sandia National Laboratories, Albuquerque, New Mexico.

Metcalf, J. H., and L. W. Brewer, 1977. Environmental Monitoring at the WIPP Site, CY 1976, SAND77-1021, Sandia National Laboratories, Albuquerque, New Mexico.

Minnema, D. M., and L. W. Brewer, 1983. Background Radiation Measurements at the Waste Isolation Pilot Plant (WIPP) Site, Carlsbad, New Mexico, SAND83-1296, Sandia National Laboratories, Albuquerque, New Mexico.

Molecke, M. A., 1978. Waste Isolation Pilot Plant Transuranic Wastes Experimental Characterization Program, Executive Summary, SAND78-1356, Sandia National Laboratories, Albuquerque, New Mexico.

Molecke, M. A., 1979. Gas Generation from Transuranic Waste Degradation: Data Summary Interpretation, SAND79-1245, Sandia National Laboratories, Albuquerque, New Mexico.

Molecke, M. A., 1980. WIPP HLW Experimental Program: Preliminary Description of In Situ HLW Tests, SAND79-0510, Sandia National Laboratories, Albuquerque, New Mexico.

NCRP (National Council on Radiation Protection and Measurements), 1975. Natural Background Radiation in the United States, NCRP Report No. 45, Washington, D.C.

Nielsen, J., 1976. An Archaeological Reconnaissance of Sandia National Laboratories' Los Medanos Nuclear Waste Disposal Facility, Eddy County, New Mexico, SAND77-7024, Sandia National Laboratories, Albuquerque, New Mexico.

Nielsen, J., 1977. An Archaeological Reconnaissance of a Proposed Site for the Sandia National Laboratories, Albuquerque, New Mexico, SAND77-7024, Sandia National Laboratories, Albuquerque, New Mexico.

NOAA (National Oceanic and Atmospheric Administration), 1972-1976. Climatological Data, National Climatic Center, Asheville, North Carolina.

NOAA (National Oceanic and Atmospheric Administration), 1974. Climates of the United States, Vol. 2--Western States, Roswell, New Mexico, Water Information Center, Inc., Port Washington, New York, p. 883.

NUS Corporation, 1979. Environmental Characterization of Bedded Salt Formation and Overlying Areas of the Permian Basin, ONWI-27, prepared by NUS Corporation for the Office of Nuclear Waste Isolation, Battelle Memorial Institute, Columbus, Ohio.

Pocalujka, L. P. et al., 1979. Meteorological Data Quarterly Report, WIPP Site: Eddy County, New Mexico, Autumn Quarter, September through November 1976, SAND79-7041, Sandia National Laboratories, Albuquerque, New Mexico.

Pocalujka, L. P. et al., 1979. Meteorological and Air Quality Data Quarterly Report, WIPP Site: Eddy County, New Mexico, Winter Quarter, December 1976 through February 1977, Sandia National Laboratories, Albuquerque, New Mexico.

Pocalujka, L. P. et al., 1980. Meteorological and Air Quality Data Quarterly Report, WIPP Site: Eddy County, New Mexico, Spring Quarter, March 1977 through May 1977, SAND79-7109, Sandia National Laboratories, Albuquerque, New Mexico.

Pocalujka, L. P. et al., 1980. Meteorological and Air Quality Data Quarterly Report, WIPP Site: Eddy County, New Mexico, Summer Quarter, June 1977 through August 1977, SAND80-7107, Sandia National Laboratories, Albuquerque, New Mexico.

Pocalujka, L. P., and E. Babij, 1980. Meteorological and Air Quality Data Quarterly Report, WIPP Site Eddy County, New Mexico, Autumn Quarter, September 1977 through November 1977, SAND80-7121, Sandia National Laboratories, Albuquerque, New Mexico.

Pocalujka, L. P. et al., 1981. Meteorological and Air Quality Data Quarterly Report, WIPP Site: Eddy County, New Mexico, Winter Quarter, December 1977 through February 1978.

Pocalujka, L. P. et al., 1981. Final Meteorological and Air Quality Data Report, WIPP Site: Eddy County, New Mexico, Spring Quarter March 1978 through February 1980, SAND81-7052, Sandia National Laboratories, Albuquerque, New Mexico.

Prill, S. D., and G. R. Buckle, 1988. Guidance Manual, Surface Water and Sediment Sampling for the Environmental Monitoring Programs, Waste Isolation Pilot Plant, DOE/WIPP 88-007, U.S. Department of Energy, Carlsbad, New Mexico.

Reith, C. C., 1985. Environmental Data Acquisition at the Waste Isolation Pilot Plant: A Chronological Description and Justification Matrix, Contract No. DE-AC04-78AL05346, IT Corporation, Carlsbad, New Mexico.

Reith, C. C., and G. Daer, 1985. Radiological Baseline Program for the Waste Isolation Pilot Plant: Program Plan, WTSD-TME-057, Waste Isolation Pilot Plant, Carlsbad, New Mexico.

Reith, C. C., E. T. Louderbough, R. J. Eastmond, and A. L. Rodriguez, 1985. Ecological Monitoring Program for the Waste Isolation Pilot Plant, SemiAnnual Report: July-December 1984, WTSD-TME-058, Waste Isolation Pilot Plant, Carlsbad, New Mexico.

Reith, C. C., R. J. Eastmond, and R. F. Kehrman, 1986. "Preoperational Environmental Programs for the Waste Isolation Pilot Plant," Waste Isolation in the U.S., Technical Programs and Public Transportation, Vol. 1, pp. 81-87.

Reith, C. C., and E. T. Louderbough, 1986. "The Dispersal and Impact of Salt from Surface Storage Piles at WIPP," Proceedings of the Symposium of Waste Management '86, Tucson, Arizona.

Reith, C. C., J. K. Prince, N. T. Fischer, A. Rodriguez, D. W. Uhland, and D. J. Winstanley, 1986. Annual Site Environmental Monitoring Report for the Waste Isolation Pilot Plant, DOE/WIPP-86-002, Carlsbad, New Mexico.

Sandia National Laboratories, 1977. Preliminary Review Copy--Draft Environmental Impact Statement for Waste Isolation Pilot Plant, Eddy County, New Mexico, SAND77-0650, Albuquerque, New Mexico.

Sandia National Laboratories, 1979. Summary of Research and Development Activities in Support of Waste Acceptance Criteria for WIPP, SAND79-1305, Sandia National Laboratories, Albuquerque, New Mexico.

Santos, H., 1987. RADCOMP V1.5 User Reference Manual, Waste Isolation Pilot Plant, Carlsbad, New Mexico.

Shefelbine, H. C., 1978. Preliminary Evaluation of the Characteristics of Defense Transuranic Wastes, SAND78-1850, Sandia National Laboratories, Albuquerque, New Mexico.

Soil Conservation Service, 1971. Soil Survey of Eddy Area, New Mexico, Government Printing Office, Washington, D.C.

Stinebaugh, R. E., 1979. Retrieval of Canistered Experimental Waste at the Waste Isolation Pilot Plant, SAND79-1239, Sandia National Laboratories, Albuquerque, New Mexico.

Thompson, D. J., 1988. Environmental Thermoluminescent Dosimetry Measurements at the WIPP Site, 1976-1985, SAND87-0843, Sandia National Laboratories, Albuquerque, New Mexico.

Torres, B., and R. Balestri, 1978. Consequence Assessment of Radionuclide Release to the Environment from the WIPP Repository, BDM/TAC-78-497-TR, The BDM Corporation, Albuquerque, New Mexico.

Westinghouse Electric Corporation, 1980. Environmental Procedure and Instruction Manual, DOE/WIPP-02-3, Waste Isolation Pilot Plant, Carlsbad, New Mexico.

Wolfe, H. G. et al., ed., 1977. An Environmental Baseline Study of the Los Medanos Waste Isolation Pilot Plant (WIPP) Project Area of New Mexico: A Progress Report, SAND77-7017, Sandia National Laboratories, Albuquerque, New Mexico.

Wolfe, H. G. et al., ed., 1977. An Environmental Baseline Study of the Los Medanos Waste Isolation Pilot Plant (WIPP) Project Area of New Mexico: A Progress Report (Addendum), SAND77-7018, Sandia National Laboratories, Albuquerque, New Mexico.

J.4 GEOCHEMISTRY

Adams, S. S., 1967. "Bromine in the Salado Formation, Carlsbad Potash District, New Mexico," Unpublished Ph.D. Dissertation, Harvard University, Cambridge, Massachusetts, 202 pp.

Adams, S. S., 1969. "Bromine in the Salado Formation, Carlsbad Potash District, New Mexico," New Mexico Bureau of Mines and Mineral Resources Bulletin 93, 112 pp.

Barr, G. E., S. J. Lambert, and J. A. Carter, 1979. "Uranium-Isotope Disequilibrium in Groundwaters of Southeastern New Mexico and Implications Regarding Age-Dating of Waters," STI/PUB/403, Proceedings of the International Symposium on Isotope Hydrology, 1978, International Atomic Energy Agency, Vienna, Austria.

Barr, G. E., S. J. Lambert, and J. A. Carter, 1979. Uranium-Isotope Disequilibrium in Groundwaters of Southeastern New Mexico and Implications Regarding Age-Dating of Waters, SAND77-1799 (IAEA-SM-228/32), Sandia National Laboratories, Albuquerque, New Mexico.

Barr, G. E., and B. F. Jones, 1988. "Normative Analyses of Groundwater from the Rustler Formation, Associated with the Waste Isolation Pilot Plant (WIPP) in Southeastern New Mexico," U.S. Geological Survey, unpublished data.

Bodine, M. W., 1978. "Clay-Mineral Assemblages from Drill Core of Ochoan Evaporites, Eddy County," Geology and Mineral Deposits of Ochoan Rocks in the Delaware Basin and Adjacent Areas, New Mexico Bureau of Mines and Mineral Resources Circular 159, Socorro, New Mexico.

Bodine, M., and C. MacMillan, 1978. Investigation of Petrology, Mineralogy and Geochemistry of a Permian Basin Cone, interim report prepared for Sandia National Laboratories, Albuquerque, New Mexico.

Bodine, M. W., Jr., and B. F. Jones, 1986. "The Salt Norm: A Quantitative Chemical-Mineralogical Characterization of Natural Waters," U.S. Geological Survey Water-Resources Investigation Report 86-4086.

Bodine, M. W., Jr., B. F. Jones, and S. J. Lambert, 1988. "Normative Analysis of Groundwaters from the Rustler Formation," ed. M. D. Siegel, S. J. Lambert, and K. L. Robinson, Hydrogeochemical Studies of the Rustler Formation and Related Rocks in the WIPP Area, Southeastern New Mexico, SAND88-0196, Sandia National Laboratories, Albuquerque, New Mexico.

Brookins, D. G., J. K. Register, M. E. Register, and S. J. Lambert, 1980. "Long-Term Stability of Evaporite Minerals, Geochronological Evidence," SAND79-1283, in

Proceedings of International Symposium on Scientific Basis for Nuclear Waste Management, Materials Research Society, Vol. 2, pp. 479-486.

Brookins, D. G., 1981. "Geochronologic Studies Near the WIPP Site, Southeastern New Mexico," New Mexico Geological Society Special Publication No. 10, pp. 147-152.

Brookins, D. G., and J. K. Register, 1981. Potassium-Argon and Neutron Activation Analysis Studies of Polyhalites Near the WIPP Site, SAND81-7071, Sandia National Laboratories, Albuquerque, New Mexico.

Brookins, D. G., and S. J. Lambert, 1987. "Radiometric Dating of Ochoan (Permian) Evaporites, WIPP Site, Delaware Basin, New Mexico, USA," Materials Research Society Symposium Proceedings, Vol. 84, pp. 771-780.

Chapman, J. B., 1986. Stable Isotopes in Southeastern New Mexico Groundwater: Implications for Dating Recharge in the WIPP Area, EEG-35, State of New Mexico Environmental Evaluation Group, Santa Fe, New Mexico.

Colton, I. D., and J. G. Morse, 1985. Water Quality Sampling Plan, WIPP/DOE-215, Waste Isolation Pilot Plant, Carlsbad, New Mexico.

Dosch, R. G., and G. W. Lynch, 1978. Interaction of Radionuclides with Geomedia Associated with the Waste Isolation Pilot Plant (WIPP) Site in New Mexico, SAND78-0297, Sandia National Laboratories, Albuquerque, New Mexico.

EEG (Environmental Evaluation Group), 1983. The Geochemistry of Two Pressurized Brines From the Castile Formation in the Vicinity of the Waste Isolation Pilot Plant (WIPP) Site, EEG-21, S. Faith, P. Spiegler, and K. R. Rehfeldt, Health and Environment Department, State of New Mexico, Santa Fe, New Mexico.

EEG (Environmental Evaluation Group), 1984. Occurrence of Gases in the Salado Formation, EEG-25, L. Chaturvedi, Health and Environment Department, State of New Mexico, Santa Fe, New Mexico.

EEG (Environmental Evaluation Group), 1985. Chemistry of Rustler Fluids, EEG-31, D. S. Ramey, Health and Environment Department, State of New Mexico, Santa Fe, New Mexico.

Gonzalez, D. D., 1983. Hydrogeochemical Parameters of Fluid-Bearing Zones in the Rustler and Bell Canyon Formations: Waste Isolation Pilot Plant (WIPP), Southeastern New Mexico (SENM), SAND83-0210, Sandia National Laboratories, Albuquerque, New Mexico.

Gross, G. W., R. N. Hoy, and C. J. Duffy, 1976. Application of Environmental Tritium in the Measurement of Recharge and Aquifer Parameters in a Semi-Arid Limestone Terrain, Report No. 60, New Mexico Water Resources Research Institute, 212 pp.

Hoy, R. N., and G. W. Gross, 1982. A Baseline Study of Oxygen 18 and Deuterium in the Roswell, New Mexico, Groundwater Basin, Report No. 144, New Mexico Water Resources Research Institute, 95 pp.

Knauth, L. P., and M. A. Beeunas, 1986. "Isotope Geochemistry of Fluid Inclusions in Permian Halite, with Implications for the Isotopic History of Ocean Water and the Origin of Saline Formation Waters," Geochimica at Cosmochimica Acta, Vol. 50, pp. 419-434.

Kopp, O. D., and D. W. Combs, 1975. "Mineral Sources of Water in Evaporite Sequences Report," ORNL Subcontract No. 3670, Department of Geological Science, University of Tennessee.

Lambert, S. J., 1977. The Geochemistry of Delaware Basin Groundwaters, SAND77-0420, Sandia National Laboratories, Albuquerque, New Mexico.

Lambert, S. J., 1978. "The Geochemistry of Delaware Basin Groundwaters," Geology and Mineral Deposits of Ochoan Rocks in Delaware Basin and Adjacent Areas, New Mexico Bureau of Mines and Mineral Resources Circular 159, pp. 32-38.

Lambert, S. J., and K. L. Robinson, 1984. Field Geochemical Studies of Groundwaters in Nash Draw, Southeastern New Mexico, SAND83-1122, Sandia National Laboratories, Albuquerque, New Mexico.

Lambert, S. J., 1986. K-Ar and Rb-Sr Age Determinations from Clay Minerals and Related Minerals from the WIPP, Southeastern New Mexico, SAND86-0223J, Sandia National Laboratories, Albuquerque, New Mexico.

Lambert, S. J., 1986. "Radiometric Dating of Ochoan (Permian) Evaporites, WIPP Site, Delaware Basin, New Mexico," SAND86-2192C, Sandia National Laboratories, Albuquerque, New Mexico, published in the Proceedings of Materials Research Society Symposium, Boston, Massachusetts.

Lambert, S. J., 1987. Feasibility Study: Applicability of Geochronologic Methods Involving Radiocarbon and Other Nuclides to the Groundwater Hydrology of the Rustler Formation, SAND86-1054, Sandia National Laboratories, Albuquerque, New Mexico.

Lambert, S. J., 1987. "Stable-Isotope Studies of Groundwaters in Southeastern New Mexico," SAND85-1978, Sandia National Laboratories, Albuquerque, New Mexico, ed. L. Chaturvedi, The Rustler Formation at the WIPP Site, EEG-34, EEG-21, State of New Mexico Environmental Evaluation Group, Santa Fe, New Mexico.

Lambert, S. J., and J. A. Carter, 1987. Uranium-Isotope Systematics in Groundwaters of the Rustler Formation, Northern Delaware Basin, Southeastern New Mexico, SAND87-0388, Sandia National Laboratories, Albuquerque, New Mexico.

Lambert, S. J., and D. M. Harvey, 1987. Stable-Isotope Geochemistry of Groundwaters in the Delaware Basin of Southeastern New Mexico, SAND87-0138, Sandia National Laboratories, Albuquerque, New Mexico.

Lambert, S. J., 1988. "Isotopic Constraints on the Rustler and Dewey Lake Groundwater Systems," ed. M. D. Siegel, S. J. Lambert, and K. L. Robinson, Hydrogeochemical Studies of the Rustler Formation and Related Rocks in the WIPP Area, Southeastern New Mexico, SAND88-0196, Sandia National Laboratories, Albuquerque, New Mexico.

Lambert, S. J., and J. A. Carter, (in press). "Uranium-Isotope Disequilibrium in Brine Reservoirs of the Castile Formation, Northern Delaware Basin, Southeastern New Mexico," SAND83-0144, Sandia National Laboratories, Albuquerque, New Mexico.

Myers, J., P. James, and P. Drez, 1988. "The Redox State of the Culebra Member of the Rustler Formation," ed. M. D. Siegel, S. J. Lambert, and K. L. Robinson, Hydrogeochemical Studies of the Rustler Formation and Related Rocks in the WIPP Area, Southeastern New Mexico, SAND88-0196, Sandia National Laboratories, Albuquerque, New Mexico.

O'Neil, J. R., C. M. Johnson, L. D. White, and E. Roedder, 1986. "The Origin of Fluids in the Salt Beds of the Delaware Basin, New Mexico and Texas," Journal of Applied Geochemistry, Vol. 1.

Plummer, N. L., D. L. Parkhurst, G. W. Fleming, and S. A. Dunkle, 1988. "PHRWPITZ: A Computer Program for Geochemical Calculations in Brines," U.S. Geological Survey, unpublished data.

Potter, R. W., II, 1977. "Pressure Corrections for Fluid-Inclusion Homogenization Temperatures Based on the Volumetric Properties of the System NaCl-H2O," Journal of Research U.S. Geological Survey, Vol. 5, No. 5, pp. 603-607.

Rai, D., and M. J. Mason, 1977. Kd Measurements of Nuclides to Estimate Migration Potential at the Proposed Waste Isolation Pilot Plant in New Mexico, PNL-2448, Pacific Northwest Laboratory, Richland, Washington.

Randall, W. S., M. E. Crawley, and M. L. Lyon, 1988. Annual Water Quality Data Report for the Waste Isolation Pilot Plant, DOE/WIPP-88-006, U.S. Department of Energy.

Register, J. K. Rubedium-Strontium and Related Studies of the Salado Formation, Southeastern New Mexico, SAND81-7072, Sandia National Laboratories, Albuquerque, New Mexico.

Register, J. K., D. G. Brookins, M. E. Register, and S. J. Lambert, 1980. "Clay Mineral-Brine Interaction During Evaporite Diagenesis: Lanthanide Distribution in WIPP Samples," SAND79-1284C, Sandia National Laboratories, Albuquerque, New Mexico, presented in Proceedings of International Symposium on Scientific Basis for Nuclear Waste Management, Materials Research Society, Vol. 2, pp. 445-452.

Robinson, K. L., 1988. Analysis of Solutes in Groundwaters from the Rustler Formation at and Near the WIPP Site, SAND86-0917, Sandia National Laboratories, Albuquerque, New Mexico.

Roedder, E., and H. E. Belkin, 1980. "Thermal Gradient Migration of Fluid Inclusions in Single Crystals of Salt from the Waste Isolation Pilot Plant," Proceedings of International Symposium on Scientific Basis for Nuclear Waste Management, Materials Research Society, Vol. 2, pp. 453-464.

Sewards, T., M. L. Williams, C. L. Stein, and K. Keil, 1988. "Mineralogy of the Culebra Dolomite," ed. M. D. Siegel, S. J. Lambert, and K. L. Robinson, Hydrogeochemical Studies of the Rustler Formation and Related Rocks in the WIPP Area, Southeastern New Mexico, SAND88-0196, Sandia National Laboratories, Albuquerque, New Mexico.

Siegel, M. D., K. L. Robinson, and J. Myers, ed., 1988. "Solute Relationships in Groundwaters From the Culebra Member of the Rustler Formation Near the WIPP Site, Southeastern New Mexico," ed. M. D. Siegel, S. J. Lambert, and K. L. Robinson, Hydrogeochemical Studies of the Rustler Formation and Related Rocks in the WIPP Area, Southeastern New Mexico, SAND88-0196, Sandia National Laboratories, Albuquerque, New Mexico.

Stein, C. L., and J. L. Krumhansl, 1984. "Compositions of Brines in Halite from the Lower Salado Formation, Southeastern New Mexico," SAND84-1252A, Sandia National Laboratories, Albuquerque, New Mexico, presented at GSA Annual Meeting, Reno, Nevada, November 5-8, 1984, Abstracts with Programs, 97th Annual Meeting, Geological Society of America, Vol. 16, No. 6, p. 667.

Stein, C. L., 1985. Mineralogy in the Waste Isolation Pilot Plant (WIPP) Facility Stratigraphic Horizon, SAND85-0321, Sandia National Laboratories, Albuquerque, New Mexico.

Stein, C. L., 1985. Preliminary Report on Fluid Inclusions from Halites in the Castile and Lower Salado Formations of the Delaware Basin, Southeastern New Mexico, SAND83-0451, Sandia National Laboratories, Albuquerque, New Mexico.

Stein, C. L., and J. L. Krumhansl, 1985. An Interpretational Model for the Evolution of Brines in Salt from the Lower Salado Formation, Southeastern New Mexico, SAND85-1999J, Sandia National Laboratories, Albuquerque, New Mexico, submitted to Geochimica at Cosmochimica Acta.

Stein, C.L., and J.L. Krumhansl, 1986. Chemistry of Brines in Salt From the Waste Isolation Pilot Plant (WIPP), Southeastern New Mexico: A Preliminary Investigation, SAND85-0897, Sandia National Laboratories, Albuquerque, New Mexico.

Szabo, B. J., W. C. Gottschall, J. N. Rosholt, and C. R. McKinney, 1980. Part I: A Preliminary Study of Uranium-Thorium Systematics in Dissolution Residues at the Top of Salado Evaporites--Implications to Process and Time of the Last Vertical

Dissolution Cycle of Salt Beds Near the WIPP Site; Part II: Uranium Trend Dating of Surficial Deposits and Gypsum Spring Deposit Near WIPP Site, New Mexico, U.S. Geological Survey Open-File Report 80-879.

Uhland, D. W., and W. S. Randall, 1986. Annual Water Quality Data Report for the Waste Isolation Pilot Plant, DOE/WIPP-86-006, U.S. Department of Energy.

Uhland, D. W., W. S. Randall, and R. C. Carrascco, 1987. 1987 Annual Water Quality Data Report for the Waste Isolation Pilot Plant, DOE/WIPP 87-006, U.S. Department of Energy, Carlsbad, New Mexico.

J.5 GEOLOGY

Acton, R. V., 1977. "Thermal Conductivity of SE New Mexico Rocksalt and Anhydrite," Unpublished Sandia National Laboratories preliminary report, Albuquerque, New Mexico.

Adams, J. E., 1944. "Upper Permian Ochoa Series of the Delaware Basin, West Texas and Southeastern New Mexico," American Association of Petroleum Geologists Bulletin, Vol. 48, pp. 1596-1625.

Adams, J. E., 1965. "Stratigraphic-Tectonic Development of Delaware Basin," American Association of Petroleum Geologists Bulletin, Vol. 49, pp. 2140-2148.

Adams, J. E., 1972. "Semi-Cyclicity in the Castile Evaporite," in Cyclic Sedimentation in the Permian Basin, West Texas Geological Society Publication 72-60, pp. 196-202.

Anderson, R. Y., W. E. Dean, D. N. Kirkland, and H. I. Snyder, 1972. "Permian Castile Varved Evaporite Sequence, West Texas and New Mexico," Bulletin of the Geological Society of America, Vol. 83, pp. 59-86.

Anderson, R. Y., 1976. Correlation and Structural Relationships of the Castile Salado Evaporite Sequence in ERDA 6, AEC 7 and AEC 8 Boreholes, Eddy and Lea Counties, New Mexico, University of New Mexico, Albuquerque, New Mexico.

Anderson, R. Y., 1978. Deep Dissolution of Salt, Northern Delaware Basin, New Mexico, University of New Mexico, prepared for Sandia National Laboratories, Albuquerque, New Mexico.

Anderson, R. Y., K. K. Kietzke, and D. J. Rhodes, 1978. "Development of Dissolution Breccias, Northern Delaware Basin, New Mexico," Geology and Mineral Deposits of Ochoan Rocks in Delaware Basin and Adjacent Areas, New Mexico Bureau of Mines and Mineral Resources Circular 159, pp. 47-52.

Anderson, R. Y., and D. W. Powers, 1978. "Salt Anticlines in the Castile-Salado Evaporite Sequence, Northern Delaware Basin, New Mexico," Geology and Mineral Deposits of Ochoan Rocks in Delaware Basin and Adjacent Areas, Circular 159, New Mexico Bureau of Mines and Mineral Resources, Socorro, New Mexico.

Anderson, R. Y., 1979. "Notes on Dissolution and Brine Chambers Related to the WIPP," Memo submitted to State of New Mexico/Environmental Evaluation Group, Santa Fe, New Mexico, 15 pp.

Anderson, R. Y., and D. W. Kirkland, 1980. "Dissolution of Salt Deposits by Brine Density Flow," Geology, Vol. 8, pp. 66-69.

Anderson, R. Y., 1981. "Deep-Seated Dissolution in the Delaware Basin, Texas and New Mexico," Environmental Geology and Hydrology in New Mexico, ed. S. G. Wells, and W. Lambert, New Mexico Geological Society, Special Publication No. 10.

Algermissen, S. T., 1969. Seismic Risk Studies in the United States, Proceedings of the Fourth World Conference on Earthquake Engineering, Santiago, Chile, Vol. 1, pp. 14-27.

Algermissen, S. T., and D. M. Perkins, 1976. A Probabilistic Estimate of Maximum Acceleration in Rock in the Contiguous United States, U.S. Geological Survey Open-File Report 76-416.

Ash, S. R., and A. C. Clebsch, 1961. "Cretaceous Rocks in Lea County, New Mexico," U.S. Geological Survey Professional Paper 424-D, pp. 139-142.

Bachman, G. O., R. B. Johnson, and R. A. Swenson, 1972. "Stability of Bedded Salt in the Permian Basin, Colorado, Kansas, Oklahoma, Texas and New Mexico," Oak Ridge National Laboratories Pilot Plant Repository Staff, Alternative Geologic Formations for the Disposal of Radioactive Wastes, ORNL Report 72-6-42.

Bachman, G. O., 1973. Surficial Features and Late Cenozoic History in Southeastern New Mexico, U.S. Geological Survey Open-File Report 4339-8.

Bachman, G. O., and R. B. Johnson, 1973. Stability of Salt in the Permian Salt Basin of Kansas, Oklahoma, Texas, and New Mexico, Open-File Report 73-14, U.S. Geological Survey.

Bachman, G. O., R. B. Johnson, and F. A. Swenson, 1973. Stability of Salt in the Permian Salt Basin of Kansas, Oklahoma, Texas, and New Mexico, U.S. Geological Survey Open-File Report 4339-4.

Bachman, G. O., 1974. Geologic Processes and Cenozoic History Related to Salt Dissolution in Southeastern New Mexico, U.S. Geological Survey Open-File Report 74-194, 81 pp.

Bachman, G. O., 1976. "Cenozoic Deposits of Southeastern New Mexico and an Outline of the History of Evaporite Dissolution," U.S. Geological Survey Journal of Research, Vol. 4, No. 2, pp. 135-149.

Bachman, G. O., 1980. Regional Geology and Cenozoic History of Pecos Region, Southeastern New Mexico, U.S. Geological Survey Open-File Report 80-1099, 116 pp., 20 figs.

Bachman, G. O., 1981. Geology of Nash Draw, Eddy County, New Mexico, U.S. Geological Survey Open-File Report 81-31.

Bachman, G. O., 1985. Assessment of Near-Surface Dissolution At and Near the Waste Isolation Pilot Plant (WIPP), Southeastern New Mexico, SAND84-7178, Sandia National Laboratories, Albuquerque, New Mexico.

Bachman, G. O., 1985. Regional Geology of Ochoan Evaporites, Northern Part of Delaware Basin, New Mexico Bureau of Mines and Mineral Resources Circular 184, p. 22.

Bachman, G. O., 1986. Stratigraphy and Dissolution of the Rustler Formation, SAND86-7077C, Sandia National Laboratories, Albuquerque, New Mexico.

Bachman, G. O., 1987. Karst in Evaporites in Southeastern New Mexico, SAND86-7078, Sandia National Laboratories, Albuquerque, New Mexico.

Balazs, E. I., 1982. "Vertical Movement in the Los Medanos and Nash Draw Areas, New Mexico, as Indicated by 1977 and 1981 Leveling Surveys," NOAA Technical Memorandum No. NGS 37, National Geodetic Survey, Rockville, Maryland.

Barrows, L. J., 1982. "WIPP Geohydrology, The Implications of Karst," unpublished manuscript discussed in Neill et al., 1983, Evaluation of the Suitability of the WIPP Site, EEG-23, State of New Mexico Environmental Evaluation Group, Santa Fe, New Mexico.

Barnes, H., 1974. "Geologic and Hydrologic Background for Selecting Site of Pilot-Plant Repository for Radioactive Waste," Bulletin of the Association of Engineering Geologists, Vol. 11, No. 1, pp. 83-92.

Beauheim, R. L., B. W. Hassinger, and J. A. Klaiber, 1983. Basic Data Report for Borehole Cabin Baby-1 Deepening and Hydrologic Testing, DOE/TME-020, Albuquerque, New Mexico.

Bechtel, 1979. Geologic Data and Hole History for Borehole B-25, U.S. Department of Energy Document No. 22-V-510-02.

Bechtel, 1981. "Exploratory Shaft and Station, Instrument Location," Drawing No. 37-X-005, Rev. 5, October 3, 1980, prepared for U.S. Department of Energy Waste Isolation Pilot Plant, Carlsbad, New Mexico.

Bechtel, 1981. "Exploratory Shaft Key, Sections and Details," Drawing No. 37-R-012, Rev. 6, January 6, 1981, prepared for U.S. Department of Energy Waste Isolation Pilot Plant, Carlsbad, New Mexico.

Bechtel National Advanced Technology Division, 1985. Quarterly Geotechnical Field Data Report, December 1985, DOE/WIPP-221, U.S. Department of Energy Waste Isolation Pilot Plant Office, Carlsbad, New Mexico.

Bell and Murphy, and Associates, 1979. Geophysical Investigation of the Waste Isolation Pilot Plant, Eddy County, New Mexico, report to the Department of Energy.

Berg, R. R., 1979. "Reservoir Sandstones of the Delaware Mountain Group, Southeast New Mexico," Guadalupian Delaware Mountain Group of West Texas and Southeast New Mexico, Society of Economic Paleontologists and Mineralogists, Permian Basin Section Publication 79-18, pp. 75-95.

Bjorklund, L. J., and W. S. Motts, 1959. Geology and Water Resources of Carlsbad Area, New Mexico, U.S. Geolological Survey Open-File Report 59-9.

Borns, D. J., 1983. Petrographic Study of Evaporite Deformation Near the Waste Isolation Pilot Plant (WIPP), SAND83-0166, Sandia National Laboratories, Albuquerque, New Mexico.

Borns, D. J., L. J. Barrows, D. W. Powers, and R. P. Snyder, 1983. Deformation of Evaporites near the Waste Isolation Pilot Plant (WIPP) Site, SAND82-1069, Sandia National Laboratories, Albuquerque, New Mexico.

Borns, D. J., 1985. Marker Bed 139: A Study of Drillcore from a Systematic Array, SAND85-0023, Sandia National Laboratories, Albuquerque, New Mexico.

Borns, D. J., and S. E. Shaffer, 1985. Regional Well-Log Correlation in the New Mexico Portion of Delaware Basin, SAND83-1798, Sandia National Laboratories, Albuquerque, New Mexico.

Borns, D. J., 1987. The Geologic Structures Observed in Drillhole DOE-2 and Their Possible Origins: Waste Isolation Pilot Plant, SAND86-1495, Sandia National Laboratories, Albuquerque, New Mexico.

Borns, D. J., 1987. Rates of Evaporite Deformation: The Role of Pressure Solution, SAND85-1599, Sandia National Laboratories, Albuquerque, New Mexico.

Brokaw, A. L., C. L. Jones, M. E. Cooley, and W. H. Hays, 1972. Geology and Hydrology of the Carlsbad Potash Area, Eddy and Lea Counties, New Mexico, U.S. Geological Survey Open-File Report 72-49, 86 pp.

Brookins, D. G., and S. J. Lambert, 1988. "WIPP Site Studies: Secondary Selenite Veins in the Rustler Formation and Dewey Lake Red Beds," Material Resources Society Symposium Proceedings for 1987 (in press).

Callender, J. F., and T. Ingwell, 1977. Structural Petrology of Undeformed and Experimentally Deformed Halite Samples from USERDA Site #7 and #9, SAND78-7076, Department of Geology, University of New Mexico.

Calzia, J. P., and W. L. Hiss, 1978. "Igneous Rocks in Northern Delaware Basin, New Mexico and Texas," Geology and Mineral Deposits of Ochoan Rocks in Delaware Basin and Adjacent Areas, Circular 159, New Mexico Bureau of Mines and Mineral Resources, Socorro, New Mexico.

Caravella, F. J., and A. R. Sanford, 1977. An Analysis of Earthquakes North of the Los Medanos Site on July 26, 1972, and November 28, 1974, New Mexico Institute of Mining and Technology, Socorro, New Mexico.

Chaturvedi, Lokesh, 1984. "Occurrence of Gases in the Salado Formation."

Christensen, C. L., and T. O. Hunter, 1979. Waste Isolation Pilot Plant (WIPP) Borehole Plugging Program Description, January 1, 1979, SAND79-0640, Sandia National Laboratories, Albuquerque, New Mexico.

Chugg, J. C. et al., 1971. "Soil Survey of Eddy County Area, New Mexico," Photographs, U.S. Department of Agriculture 82:151.

Cooper, J. B., 1960. Geologic Section from Carlsbad Caverns National Park Through Project Gnome Site, Eddy and Lea Counties, New Mexico, U.S. Geological Survey Trace Element Investigation Report 767, 1 p.

Cooper, J. B., 1961. Test Holes Drilled in Support of Groundwater Investigations, Project Gnome, Eddy County, New Mexico, basic data report, U.S. Geological Survey Trace Element Investigation Report 786, 116 pp.

Cooper, J. B., 1962. "Ground Water in Cenozoic Fill in Collapse Structures, Southeastern Eddy County, New Mexico," Short Papers in Geology, Hydrology, and Topography, U.S. Geological Survey Professional Paper 450-B, pp. E152-E153.

Cooper, J. B., 1962. Groundwater Investigations of the Project Gnome Area, Eddy and Lea Counties, New Mexico, U.S. Geological Survey Trace Element Investigation Report 802, 67 pp.

Cooper, J. B. et al., 1962. Hydrologic and Geologic Studies for Project Gnome, preliminary report, U.S. Geological Survey Project Gnome Report PNE-130P, 54 pp.

Core Laboratories, 1977. "Special Core Analysis Study," for Sipes, Williamson and Aycock, Inc., unpublished consulting report to Sandia National Laboratories, Albuquerque, New Mexico.

Cox, E. R., 1967. "Geology and Hydrology between Lake McMillan and Carlsbad Springs, Eddy County, New Mexico," U.S. Geological Survey Water-Supply Paper 1828, 48 pp.

Cys, J. M., 1978. "Transitional Nature and Significance of the Castile-Bell Canyon Contact," Geology and Mineral Deposits of Ochoan Rocks in Delaware Basin and Adjacent Areas, New Mexico Bureau of Mines and Mineral Resources Circular 159, pp. 53-56.

D'Appolonia Consulting Engineers, Inc., 1982. Data File Report: ERDA-6 and WIPP-12 Testing, prepared for Westinghouse Electric Co. and U.S. Department of Energy, Albuquerque, New Mexico, 7 Vols.

D'Appolonia Consulting Engineers, Inc., 1983. Data File Report: ERDA-6 and WIPP-12 Testing, Addendum, prepared for Westinghouse Electric Co. and U.S. Department of Energy, Albuquerque, New Mexico.

Davies, P. B., 1983. "Assessing the Potential for Deep-Seated Salt Dissolution and Subsidence at the Waste Isolation Pilot Plant (WIPP)," unpublished manuscript presented at the State of New Mexico Environmental Evaluation Group Conference on WIPP Site Suitability for Radioactive Waste Disposal, Carlsbad, New Mexico.

Davies, P. B., 1983. "Structural Characteristics of a Deep-Seated Dissolution-Subsidence Chimney in Bedded Salt," Sixth International Symposium on Salt, Vol. 1, pp. 331-350.

Dawson, P. R., and P. F. Chavez, 1978. COUPLEFLO - A Computer Code for Coupled Creeping Viscous Flow and Conductive-Convective Heat Transfer, Part, I, Theoretical Background, SAND78-1406, Sandia National Laboratories, Albuquerque, New Mexico.

Dawson, P. R., and P. F. Chavez, 1978. COUPLEFLO - Computer Program for Coupled Creeping Viscous Flow and Conductive-Convective Heat Transfer, Part II, Users Manual, SAND78-1407, Sandia National Laboratories, Albuquerque, New Mexico.

Dean, W. E., Jr., 1967. "Petrologic and Geochemical Variations in the Permian Castile Varved Anhydrite, Delaware Basin, Texas and New Mexico," Ph.D. Dissertation, 326 pp. (University Microfilms Number 68-3463)."

Dean, W. E., and R. Y. Anderson, 1978. "Salinity Cycles: Evidence for Subaqueous Deposition of Castile Formation and Lower Part of Salado Formation, Delaware Basin, Texas and New Mexico," Geology and Mineral Deposits of Ochoan Rocks in Delaware Basin and Adjacent Areas, New Mexico Bureau of Mines and Mineral Resources Circular 159, pp. 15-20.

Djeddi, R., 1979. "An Integrated Geophysical and Geological Study of the Deep Structure and Tectonics of the Permian Basin of West Texas and Southeastern New Mexico," MS Thesis, University of Texas at El Paso.

Dobrin, M. B., P. L. Lawrence, and R. L. Sengbush, 1954. "Surface and Near-Surface Waves in the Delaware Basin," Geophysics, Vol. 19, pp. 695-715.

DOE (U.S. Department of Energy), 1983. Geotechnical Field Data Report No. 4 - Geologic Mapping and Water Inflow Testing in the SPDV Ventilation Shaft, Waste Isolation Pilot Plant, compiled for U.S. Department of Energy by TSC-D'Appolonia.

DOE (U.S. Department of Energy), 1983. Geotechnical Field Data Report No. 5 - Geologic Mapping of Access Drifts, Double Box Area, compiled for U.S. Department of Energy by TSC-D'Appolonia.

DOE (U.S. Department of Energy), 1983. Geotechnical Field Data Report No. 6 - Underground Excavation Field Instrumentation Data, compiled for U.S. Department of Energy by TSC-D'Appolonia.

DOE (U.S. Department of Energy), 1983. Geotechnical Field Data Report No. 7 - Geologic Mapping of Exploratory Drift.

DOE (U.S. Department of Energy), 1983. Geotechnical Field Data Report No. 9 - Logging of Vertical Coreholes "Double Box" Area and Exploratory Drift.

DOE (U.S. Department of Energy), 1983. Geotechnical Field Data Report No. 10 - Underground Excavation Field Instrumentation Data.

DOE (U.S. Department of Energy), 1983. Geotechnical Field Data Report, Part II, Gas Testing Data Update, WIPP/DOE-177.

DOE (U.S. Department of Energy), 1985. Geotechnical Field Data Report, DOE/WIPP-218.

DOE (U.S. Department of Energy), 1986. Interim Geotechnical Field Data Report, DOE/WIPP-86-012 (Bechtel National).

Drellack, S. L., Jr., 1979. "Geological Data," Basic Data Report for Drillhole WIPP-28, SAND79-0282, Sandia National Laboratories, Albuquerque, New Mexico, pp. 4-31, Fig. 2.

Drellack, S. L., Jr., and R. P. Snyder, 1979. "Geological Data," Basic Data Report for Drillhole WIPP-26, SAND79-0280, Sandia National Laboratories, Albuquerque, New Mexico, pp. 4-29, Fig. 2.

EEG (Environmental Evaluation Group), 1979. A Compilation of Site Slection Criteria, Considerations, and Concerns Appearing in the Literature on the Deep Geologic Disposal of Radioactive Wastes, D. Goad, Health and Environment Department, State of New Mexico, Santa Fe, New Mexico.

EEG (Environmental Evaluation Group), 1980. WIPP Site and Vicinity Geological Field Trip, A Field Trip to the Proposed Waste Isolation Pilot Plant Project in Southeastern New Mexico, June 16 to 18, 1980, EEG-7, L. Chaturvedi, Health and Environment Department, State of New Mexico, Santa Fe, New Mexico.

EEG (Environmental Evaluation Group), 1980. Geotechnical Considerations for Radiological Hazard Assessment of WIPP, A Report of a Meeting Held on January 17-18, 1980, EEG-6, Health and Environment Department, State of New Mexico, Santa Fe, New Mexico.

EEG (Environmental Evaluation Group), 1982. Analysis of the Potential Formation of a Breccia Chimney Beneath the WIPP Repository, EEG-13, P. Spiegler, Health and Environment Department, State of New Mexico, Santa Fe, New Mexico.

EEG (Environmental Evaluation Group), 1983. EEG Review Comments on the Geotechnical Reports Provided by DOE to EEG Under the Stipulated Agreement Through March 1, 1983, EEG-22, Health and Environment Department, State of New Mexico, Santa Fe, New Mexico.

EEG (Environmental Evaluation Group), 1983. Evaluation of the Suitability of the WIPP Site, EEG-23, R. H. Neill, J. K. Channell, L. Chaturvedi, M. S. Little, K. Rehfeldt, and P. Spiegler, Health and Environment Department, State of New Mexico, Santa Fe, New Mexico.

EEG (Environmental Evaluation Group), 1987. Exhaust Stack Monitoring Issues at the Waste Isolation Pilot Plant, EEG-37, J. C. Rodgers, Health and Environment Department, State of New Mexico, Santa Fe, New Mexico.

EEG (Environmental Evaluation Group), 1987. Post Burial Alteration of the Permian Rustler Formation Evaporites, WIPP Site, New Mexico: Textural, Stratigraphic and Chemical Evidence, EEG-36, T. K. Lowenstein, Health and Environment Department State of New Mexico, Santa Fe, New Mexico.

EEG (Environmental Evaluation Group), 1987. The Rustler Formation at the WIPP Site, EEG-34, L. Chatuverdi, Health and Environment Department, State of New Mexico, Santa Fe, New Mexico.

Elliot, C. L., 1976. An Experimental Detail Gravity Survey of Known or Suspected Breccia Pipes at Weaver Hill, Hills A and B, and Hills C and D, Eddy County, New Mexico, Elliot Geophysical Company report to Sandia National Laboratories, Albuquerque, New Mexico, for Waste Isolation Pilot Plant Program, Vol. 1, 23 pp.

Elliot, C. L., 1976. An Experimental Detail Resistivity Survey of Known or Suspected Breccia Pipes and Sinkholes, Eddy County, New Mexico, Elliot Geophysical Company report to Sandia National Laboratories, Albuquerque, New Mexico, for Waste Isolation Pilot Plant Program, 39 pp.

Elliot, C. L., 1976. A Preliminary Geophysical Study of a Trachyte Dike in Close Proximity to the Proposed Los Medanos Nuclear Waste Disposal Site, Eddy and Lea Counties, New Mexico, Elliot Geophysical Company, Tucson, Arizona, pp. 1-19.

Elliot, C. L., 1977. Evaluation of the Proposed Los Medanos Nuclear Waste Disposal Site by Means of Electrical Resistivity Surveys, Eddy and Lea Counties, New Mexico, Elliot Geophysical Company report to Sandia National Laboratories, Albuquerque, New Mexico, for Waste Isolation Pilot Plant Program, Vol. 1, 67 pp.

Elliot, C., 1977. Experimental Resistivity Soundings Near a Known Breccia Pipe, Weaver Area, Eddy County, New Mexico, report prepared for Sandia National Laboratories, Albuquerque, New Mexico.

Earth Technology Corp., 1987. Final Report for Time Domain Electromagnetic (TDEM) Surveys at the WIPP, SAND87-7144, Sandia National Laboratories, Albuquerque, New Mexico.

Ferrall, C. C., and J. F. Gibbons, 1980. Core Study of the Rustler Formation Over the WIPP Site, SAND79-7110, Sandia National Laboratories, Albuquerque, New Mexico.

Fournier, R. O., 1961. "Regular Interlayered Chlorite-Vermiculite in Evaporite of the Salado Formation, New Mexico," U.S. Geological Survey Professional Paper 424-D, pp. 323-327.

Gard, L. M., Jr., 1968. "Geologic Studies Project Gnome, Eddy County, New Mexico," U.S. Geological Survey Professional Paper 589, 33 pp.

Gera, F., 1974. On the Origin of the Small Hills in Nash Draw and Clayton Basin, Southeastern New Mexico, Oak Ridge National Laboratory, Report ORNL Central Files No. 74-2-29, Oak Ridge, Tennessee.

Gonzalez, D. D., 1983. Groundwater Flow in the Rustler Formation: Waste Isolation Pilot Plant (WIPP), Southeast New Mexico, SAND82-1012, Sandia National Laboratories, Albuquerque, New Mexico.

Gonzales, J. L., and C. L. Jones, 1979. Geological Data for Borehole WIPP-13, Basic Data Report for Drill Hole WIPP-1, SAND79-0273, Sandia National Laboratories, Albuquerque, New Mexico, pp. 4-15.

Gonzales, M. M., 1988. Compilation and Comparison of Test-Hole Location Surveys in the Vicinity of the Waste Isolation Pilot Plant (WIPP) Site, SAND-1065, Sandia National Laboratories, Albuquerque, New Mexico.

Griswold, G. B., 1977. Site Selection and Evaluation Studies of the Waste Isolation Pilot Plant (WIPP), Los Medanos, Eddy County, New Mexico, SAND77-0946, Sandia National Laboratories, Albuquerque, New Mexico.

Haigler, L. B., 1962. Geologic notes on the Delaware Basin, Circular 63, New Mexico Bureau of Mines and Mineral Resources, Socorro, New Mexico.

Haigler, L. B., and R. R. Cunningham, 1972. "Structure Contour Map on Top of the Undifferentiated Silurian and Devonian Rocks in Southeastern New Mexico," U.S. Geological Survey Map OM-218.

Haug, A., V. A. Kelley, A. M. LaVenue, and J. F. Pickens, 1987. Modeling of Groundwater Flow in the Culebra Dolomite at the Waste Isolation Pilot Plant

(WIPP) Site: Interim Report, SAND86-7167, Sandia National Laboratories, Albuquerque, New Mexico.

Hayes, P. T., 1964. "Geology of the Guadalupe Mountains, New Mexico," U.S. Geological Survey Professional Paper 446.

Hayes, P. T., and G. O. Bachman, 1979. Examination and Reevaluation of Evidence for the Barrera Fault, Guadalupe Mountains, New Mexico, U.S. Geological Survey Open-File Report 79-1520.

Hern, J. L., D. W. Powers, and L. J. Barrows, 1978. Seismic Reflection Data Report Waste Isolation Pilot Plant (WIPP) Site, Southeastern New Mexico, SAND79-0264, Sandia National Laboratories, Albuquerque, New Mexico, Vol. 2, 26 maps.

Hills, J. M., 1963. "Late Paleozoic Tectonics and Mountain Ranges, Western Texas to Southern Colorado," American Association of Petroleum Geologists Bulletin, Vol. 947, pp. 1709-1725.

Hills, J. M., 1976. "Late Paleozoic Structural Directions in Southern Permian Basin, West Texas and Southeastern New Mexico," American Association of Petroleum Geologists Bulletin, Vol. 54 (10), pp. 1809-1827.

Hills, J. M., 1979. "Delaware Basin Sedimentation Tectonism, and Hydrocarbon Generation, Guadalupian Delaware Mountain Group of West Texas and Southeast New Mexico," Society of Economic Paleontologists and Mineralogists, Permian Basin Section Publication, 79-18:1.

Hills, J. M., 1984. "Sedimentation, Tectonism, and Hydrocarbon Generation in Delaware Basin, West Texas and Southeastern New Mexico," American Association of Petroleum Geologists Bulletin, Vol. 68, pp. 250-267.

Hiss, W. L., 1976. "Structure of the Permian Capitan Aquifer, Southeast New Mexico and West Texas," Resource Map 6, New Mexico Bureau of Mines and Mineral Resources, Socorro, New Mexico.

Hiss, W. L., 1976. "Structure of the Permian Ochoan Rustler Formation, Southeast New Mexico and West Texas," Resource Map 7, New Mexico Bureau of Mines and Mineral Resources.

Holt, R. M., and D. W. Powers, 1984. Geotechnical Activities in the Waste-Handling Shaft, WTSD-TME-038, U.S. Department of Energy, Carlsbad, New Mexico.

Holt, R., and D. Powers, 1986. Geotechnical Activities in the Exhaust Shaft, DOE/WIPP-86-008, Waste Isolation Pilot Plant Project, Carlsbad, New Mexico.

Holt, R. M., and D. W. Powers, 1987. Rustler Formation, Waste-Handling and Exhaust Shafts, Waste Isolation Pilot Plant (WIPP) Site, EEG-34, State of New Mexico Environmental Evaluation Group, Santa Fe, New Mexico.

Hoy, R. N., and G. W. Gross, 1982. A Baseline Study of Oxygen 18 and Deuterium in the Roswell, New Mexico, Groundwater Basin, Report No. 144, New Mexico Water Resources Research Institute.

Jarolimek, L., M. J. Timmer, and R. F. McKinney, 1983. Geotechnical Activities in the Exploratory Shaft - Selection of the Facility Interval.

Jarolimek, L., M. J. Timmer, and D. W. Powers, 1983. Correlation of Drillhole and Shaft Logs, Waste Isolation Pilot Plant (WIPP) Project, Southeastern New Mexico, TME-3179, U.S. Department of Energy, Albuquerque, New Mexico.

Johnson, K. S., and S. Gonzales, 1978. Salt Deposits in the United States and Regional Geologic Characteristics Important for Storage of Radioactive Waste, Y/OWI/SUB-7414/1, Office of Waste Isolation, Union Carbide Corporation, Oak Ridge, Tennessee.

Johnson, K. S., 1981. "Dissolution of Salt on the East Flank of the Permian Basin in the Southwestern USA," Journal of Hydrology 54:75-93.

Jones, C. L., and B. M. Madsen, 1959. "Observations on Igneous Intrusions in Late Permian Evaporites, Southeastern New Mexico," Geological Society of America Bulletin, Vol. 70, pp. 1625-1626.

Jones, C. L., 1960. Thickness, Character and Structures of Upper Permian Evaporites in Part of Eddy County, New Mexico, TEM-1033, U.S. Geological Survey.

Jones, C. L., C. G. Bowles, and K. G. Bell, 1960. Experimental Drill Hole Logging in Potash Deposits of the Carlsbad District, New Mexico, U.S. Geological Survey Open-File Report 60-84.

Jones, C. L., M. E. Cooley, and G. O. Bachman, 1973. Salt Deposits of Los Medanos Area, Eddy and Lea Counties, New Mexico, sections on "Groundwater Hydrology," and "Surficial Geology," U.S. Geological Open-File Report 4339-7.

Jones, C. L., and A. F. McIntyre, 1979. Geological Data, Basic Data Report for Drillhole WIPP-27, SAND79-0281, Sandia National Laboratories, Albuquerque, New Mexico, pp. 5-18.

Jones, C. L., and J. L. Gonzales, 1980. Basic Data Report for Drillhole WIPP-19, SAND79-0276, Sandia National Laboratories and U.S. Geological Survey.

Jones, C. L., 1981. Geologic Data for Borehole ERDA-6, Eddy County, New Mexico, U.S. Geological Survey Open-File Report 81-468, 59 pp.

Jones, C. L., 1981. Geologic Data for Borehole ERDA-9, Eddy County, New Mexico, U.S. Geological Survey Open-File Report 81-469, 50 pp.

Kelley, V. C., 1971. Geology of the Pecos Country, Southeastern New Mexico, Memoir 24, New Mexico Bureau of Mines and Mineral Resources, Socorro, New Mexico.

King, P. B., 1948. Geology of the Southern Guadalupe Mountains, Texas, U.S. Geological Survey Professional Paper 215.

Kirkland, D. W., and R. Y. Anderson, 1970. "Microfolding in the Castile and Todilto Evaporite, Texas and New Mexico," Geological Society of America Bulletin, Vol. 81, pp. 3259-3282.

Lambert, S. J., 1980. Recommended Analysis Plan for the Borehole Plugging Program Potash Core Test, SAND80-0812, Sandia National Laboratories, Albuquerque, New Mexico.

Lambert, S. J., 1982. Interim report - Dissolution of Evaporites In and Around the Delaware Basin, Southeastern New Mexico and West Texas, SAND82-01461, Sandia National Laboratories Report, Albuquerque, New Mexico.

Lambert, S. J., 1983. Dissolution of Evaporites In and Around the Delaware Basin, Southeastern New Mexico, SAND82-01, Sandia National Laboratories Report, Albuquerque, New Mexico, 96 pp.

Lambert, S. J., 1983. Dissolution of Evaporites In and Around the Delaware Basin, Southeastern New Mexico and West Texas, SAND82-0461, Sandia National Laboratories, Albuquerque, New Mexico.

Lambert, S. J., 1983. "Evaporite Dissolution Relevant to the WIPP Site, Northern Delaware Basin, Southeastern New Mexico," Material Resources Society Symposium Proceedings, Vol. 15, pp. 291-298.

Lambert, S. J., and J. A. Carter, 1984. Uranium-Isotope Disequilibrium in Brine Reservoirs of the Castile Formation, Northern Delaware Basin, Southeastern New Mexico, I: Principles and Methods, SAND83-0144, Sandia National Laboratories, Albuquerque, New Mexico.

Lang, W. B., 1938. Geology of the Pecos River Between Laguna Grande de la Sal and Pierce Canyon, 12th and 13th Biennial Reports, New Mexico State Engineer, pp. 80-86.

Lappin, A. R., 1988. Summary of Site-Characterization Studies Conducted from 1983 through 1987 at the Waste Isolation Pilot Plant (WIPP), Southeastern New Mexico, SAND88-0157, Sandia National Laboratories, Albuquerque, New Mexico.

Long, G. J., and Associates, 1976. Interpretation of Geophysical Data, Los Medanos and Vicinity, Lea and Eddy Counties, New Mexico, prepared for Sandia National Laboratories, Albuquerque, New Mexico.

Lowenstein, T. K., 1987. Post-Burial Alteration of the Permian Rustler-Formation Evaporites, WIPP Site, New Mexico, EEG-36, State of New Mexico Environmental Evaluation Group, Santa Fe, New Mexico.

Maley, V. C., and R. M. Huffington, 1953. "Cenozoic Fill and Evaporite Solution in Delaware Basin, Texas, and New Mexico," Geological Society of America Bulletin, Vol. 64, No. 5, pp. 539-546.

Mansure, A., and M. Reiter, 1977. An Accurate Equilibrium Temperature Log in AEC #8, A Drill Test in the Vicinity of the Carlsbad Disposal Site, New Mexico Bureau of Mines and Mineral Resources Open-File Report #80.

McGlasson, E. H., 1968. "The Siluro-Devonian of West Texas and Southeast New Mexico," West Texas Geological Society-Delaware Basin Exploration Guidebook, Pub. 68-55, pp. 35-44.

Mercer, J. W., R. L. Beauheim, R. P. Snyder, and G. M. Fairer, 1986. Basic Data Report for Drillhole DOE-2 Drilling and Hydrologic Testing, SAND86-0611, Sandia National Laboratories, Albuquerque, New Mexico.

Mercer, J. W., R. L. Beauheim, R. P. Snyder, and G. M. Fairer, 1987. Basic Data Report for Drilling and Hydrologic Testing of Drillhole DOE-2 at the Waste Isolation Pilot Plant (WIPP) Site, SAND86-0611, Sandia National Laboratories, Albuquerque, New Mexico.

Meyer, R. F., 1966. Geology of Pennsylvania and Wolfcampian Rocks in Southeast New Mexico, Memoir 17, New Mexico Bureau of Mines and Mineral Resources, Socorro, New Mexico.

Morgan, A. M., 1941. "Solution-Phenomena in the Pecos Basin of New Mexico," Transcripts of the American Geophysics Union, pp. 27-35.

Motts, W. S., 1957. "Geology and Groundwater Resources of the Carlsbad Area, New Mexico", unpublished Ph.D. Thesis, University of Illinois, Urbana, Illinois.

Nicholson, A., Jr., and A. Clebsch, Jr., 1961. Geology and Groundwater Conditions in Southern Lea County, New Mexico: Groundwater Report 6, U.S. Geological Survey and State Bureau of Mines and Mineral Resources, New Mexico.

NOAA (U.S. National Oceanic and Atmospheric Administration) and USGS (U.S. Geological Survey). United States Earthquakes, Published jointly (annually since 1928).

Olive, W. W., 1957. "Solution-Subsidence Troughs Castile Formation of Gypsum Plain, Texas and New Mexico," Geological Society of America Bulletin, Vol. 68, pp. 351-358.

O'Neil, J. R., C. M. Johnson, L. D. White, and E. Roedder, 1986. "The Origin of Fluids in the Salt Beds of the Delaware Basin, New Mexico and Texas," Journal of Applied Geochemistry, Vol. 1, No. 2, pp. 265-271.

Peterson, E. W. et al., 1981. Analysis of Bell Canyon Test Results, S-CUBED Document No. SSS-R-80-4474-2.

Peterson, E. W., P. L. Langus, R. D. Broce, and K. Lie, 1981. In Situ Permeability Study of Rock Salt, SAND81-7073, Sandia National Laboratories, Albuquerque, New Mexico.

Peterson, E. W., P. L. Langus, R. D. Broce, and J. C. Stormont, 1986. Permeability Measurements at the Waste Isolation Pilot Plant (WIPP), paper presented at Waste Management 1986, Tucson, Arizona.

Pettigrew, R. R., and Associates, 1977. WIPP Conceptual Design Report (Soils and Foundation Investigation), prepared for Sandia National Laboratories, Albuquerque, New Mexico.

Pfeifer, M. C., 1987. "Multicomponent Underground DC Resistivity Study at the Waste Isolation Pilot Plant, Southeast New Mexico," MS Thesis T-3372, Colorado School of Mines, Golden, Colorado.

Pierce, W. G., and E. I. Rich, 1962. "Summary of Rock Salt Deposits in the United States as Possible Storage Sites for Radioactive Waste Materials," U.S. Geological Survey Bulletin 1148.

Piper, A. M., 1973. Subrosion In and About the Four-Township Study Area Near Carlsbad, New Mexico, ORNL Subcontract 3745, Oak Ridge National Laboratory, Oak Ridge, Tennessee.

Powers, D. W., S. J. Lambert, S. E. Shaffer, L. R. Hill, and W. D. Weart, ed., 1978. Geological Characterization Report, Waste Isolation Pilot Plant (WIPP) Site, Southeastern New Mexico, SAND78-1596, Vols. 1 and 2, Sandia National Laboratories, Albuquerque, New Mexico.

Powers, D. W., 1981. "Geologic Investigations of the WIPP Site--Overview and Issues," Environmental Geology and Hydrology in New Mexico, New Mexico Geological Society Special Publication No. 10, pp. 119-122.

Powers, D. W., and B. W. Hassinger, 1984. "Synsedimentary Dissolution Pits in Halite of the Salado Formation, Southeastern New Mexico," submitted to Journal of Sedimentary Petrology.

Powers, D. W., and R. M. Holt, 1984. "Depositional Environments and Dissolution in the Rustler Formation (Permian), Southeastern New Mexico," (Abstract) Geologic Society of America, 97th Annual Meeting Abstracts with Program, Vol. 16, No. 6, p. 627.

Pratt, W. E., 1954. "Evidences of Igneous Activity in the Northwestern Part of the Delaware Basin," New Mexico Geological Society Guidebook of Southeastern New Mexico Fifth Field Conference, pp. 143-147.

Pray, L. C., 1953. "Upper Ordovician and Silurian Stratigraphy of the Sacramento Mountains, Otero County, New Mexico," American Association of Petroleum Geologists Bulletin, Vol. 37, No. 8, pp. 1894-1918.

Pray, L. C., 1954. "Outline of the Stratigraphy and Structure of the Sacremento Mountain Escarpment," Fifth Field Conference, Southeastern New Mexico, New Mexico Geological Society, pp. 92-106.

Pray, L. C., 1959. "Stratigraphic and Structural Features of the Sacremento Mountain Escarpment, New Mexico," Guidebook for a Joint Field Conference in the Sacramento Mountains of Otero County, New Mexico, Permian Basin Section of Economic Paleontologists and Mineralogists and Roswell Geological Society, Alamogordo, New Mexico.

Pray, L. C., 1961. Geology of the Sacramento Mountains Escarpment, Otero County, New Mexico, New Mexico Bureau of Mines and Mineral Resources Bulletin 35, pp. 1-133.

Reddy, G. R., 1961. "Geology of the Queen Lake Domes Near Malaga, Eddy County, New Mexico," MS Thesis, University of New Mexico, Albuquerque, New Mexico.

Reddy, R. S., 1966. "Crustal Structure in New Mexico," MS Thesis, New Mexico Institute of Mining and Technology, Socorro, New Mexico, pp. 1-45.

Reeves, C. C., Jr., 1963. "Subterranean Natural Brines Produce Sodium Sulphate in West Texas," Groundwater, Vol. 1, pp. 35-36.

Register, J. K., 1981. Brine Pocket Occurrences in the Castile Formation, Southeastern New Mexico, U.S. Department of Energy TME-3080, 14 pp.

Robinson, T. W., and W. G. Lang, 1938. Geology and Groundwater Conditions of the Pecos River Valley in the Vicinity of Laguna Grande de la Sal, New Mexico, with Special Reference to the Salt Content of the River Water, 12th and 13th Biennial Reports, New Mexico State Engineer, pp. 77-100.

Roedder, E., and H. E. Belkin, 1978. Fluid Inclusions in Core Samples from ERDA No. 9 Borehole, WIPP Site, New Mexico, Status Report 2, prepared for Sandia National Laboratories, Albuquerque, New Mexico.

Rogers, A. M., and A. Malkiel, 1978. "A Study of Earthquakes in the Permian Basin, Texas - New Mexico," Draft of a U.S. Geological Survey Report for Open-File.

Ross, A. C., 1986. "Paleozoic Evolution of Southern Margin of Permian Basin," Geological Society of America Bulletin, 97 (5), pp. 536-554.

Roswell Geological Society, 1958. North-South Stratigraphic Cross-Section: Delaware Basin-Northwest Shelf.

Reynolds, C. B., and Associates, 1976. Summary and Final Report, Shallow Seismic Reflection Survey, Phases I and II, Los Medanos Area, Eddy County, New Mexico, report submitted to Sandia National Laboratories, Albuquerque, New Mexico.

Sandia National Laboratories, and U.S. Geological Survey, 1979. Basic Data Report for Drillhole WIPP-13, SAND79-0273, Albuquerque, New Mexico.

Sandia National Laboratories, and U.S. Geological Survey, 1979. Basic Data Report for Drillhole WIPP-25, SAND79-0279, Albuquerque, New Mexico.

Sandia National Laboratories, and U.S. Geological Survey, 1979. Basic Data Report for Drillhole WIPP-26, SAND78-0280, Albuquerque, New Mexico.

Sandia National Laboratories, and U.S. Geological Survey, 1979. Basic Data Report for Drillhole WIPP-27, SAND79-0281, Albuquerque, New Mexico.

Sandia National Laboratories, and U.S. Geological Survey, 1979. Basic Data Report for Drillhole WIPP-28, SAND79-0282, Albuquerque, New Mexico.

Sandia National Laboratories, and U.S. Geological Survey, 1979. Basic Data Report for Drillhole WIPP-29, SAND79-0283, Albuquerque, New Mexico.

Sandia National Laboratories, and U.S. Geological Survey, 1980. Basic Data Report for Drillhole WIPP-18, SAND79-0275, Albuquerque, New Mexico

Sandia National Laboratories, and U.S. Geological Survey, compilers, 1980. BasicData Report for Drillhole WIPP-19, SAND79-0276, Albuquerque, New Mexico.

Sandia National Laboratories, and U.S. Geological Survey, 1980. Basic Data Report for Drillhole WIPP-21, SAND79-0277, Albuquerque, New Mexico.

Sandia National Laboratories, and U.S. Geological Survey, 1980. Basic Data Report for Drillhole WIPP-22, SAND79-0278, Albuquerque, New Mexico.

Sandia National Laboratories, and U.S. Geological Society, 1980. Basic Data Report for Drillhole WIPP-30, SAND79-0284, Albuquerque, New Mexico.

Sandia National Laboratories, and U.S. Geological Society, 1980. Basic Data Report for Drillhole WIPP-32, SAND80-1102, Albuquerque, New Mexico.

Sandia National Laboratories, and University of New Mexico, 1981. Basic Data Report for Drillhole WIPP-15, SAND 79-0274, Albuquerque, New Mexico.

Sandia National Laboratories, and U.S. Geological Survey, 1981. Basic Data Report for Drillhole WIPP-33, SAND80-2011, Albuquerque, New Mexico.

Sandia National Laboratories, and U.S. Geological Survey, 1981. Basic Data Report for Drillhole WIPP-34, SAND81-2643, Albuquerque, New Mexico.

Sandia National Laboratories, and D'Appolonia Consulting Engineers, 1982. Basic Data Report for Drillhole AEC-7 WIPP, SAND79-0268, Albuquerque, New Mexico.

Sandia National Laboratories, and U.S. Geological Survey, 1982. Basic Data Report for Drillhole WIPP-11, SAND79-0272, Albuquerque, New Mexico.

Sandia National Laboratories, and D'Appolonia Consulting Engineers, 1982. Basic Data Report for Drillhole WIPP-12, SAND82-2336, Albuquerque, New Mexico.

Sandia National Laboratories, and D'Appolonia Consulting Engineers, 1982. Basic Data Report for Deepening of Drillhole WIPP-13, SAND82-1880, Albuquerque, New Mexico.

Sandia National Laboratories, and D'Appolonia Consulting Engineers, 1982. Basic Data Report for Drillhole WIPP-14, SAND82-1783, Albuquerque, New Mexico.

Sandia National Laboratories, and D'Appolonia Consulting Engineers, 1983. Basic Data Report for Drillhole AEC - WIPP, SAND79-0269, Albuquerque, New Mexico.

Sandia National Laboratories, and U.S. Geological Survey, 1983. Basic Data Report for Drillhole ERDA-6 - WIPP, SAND79-0267, Albuquerque, New Mexico.

Sandia National Laboratories, and U.S. Geological Survey, 1983. Basic Data Report for Drillhole ERDA-9 - WIPP, SAND79-0270, Albuquerque, New Mexico.

Sandia National Laboratories, and U.S. Geological Survey, 1983. Basic Data Report for Drillhole ERDA-10 - WIPP, SAND79-0271, Albuquerque, New Mexico.

Sanford, A. R., 1965. An Instrumental Study of New Mexico Earthquakes, New Mexico Bureau of Mines and Mineral Resources Circular 78, pp. 1-12.

Sanford, A. R., and T. R. Toppozada, 1974. Seismicity of Proposed Radioactive Waste Disposal Site in Southeastern New Mexico, New Mexico Bureau of Mines and Mineral Resources Circular 143, Socorro, New Mexico.

Sanford, A. R., S. J. Johnson, F. Caravella, and R. Ward, 1976. A Report on Seismic Recording at the Los Medanos Area in Southeastern New Mexico, 1974-1975, New Mexico Institute of Mining and Technology, Socorro, New Mexico.

Sanford, A. R., S. Sandford, F. Caravella, L. Merritt, J. Sheldon, and R. Ward, 1978. A Report on Seismic Studies of the Los Medanos Area in Southeastern New Mexico, New Mexico Institute of Mining and Technology, interim report prepared for Sandia National Laboratories, Albuquerque, New Mexico.

Sares, S. W., and S. G. Wells, 1986. "Geomorphic and Hydrogeologic Development of the Gypsum Plain Karst, Delaware Basin, New Mexico," National Speleological Society Geology Field Trip Guidebook.

Schreiber, J. R., Jr., 1981. A Thin Section Petrographic Study of Rustler Formation Dolomites from the WIPP Site, Eddy County, New Mexico, Hydro Geo Chem., Inc., Tech Report No. 5 as a contractor report to Sandia National Laboratories, Albuquerque, New Mexico.

Semmes, D. R., 1920. "Notes on the Tertiary Intrusives of the Lower Pecos Valley, New Mexico," American Journal of Science, 4th Series, Vol. 50, pp. 415-430.

Seward, P. D., 1982. Abridged Borehole Histories for the Waste Isolation Pilot Plant (WIPP) Studies, SAND82-0080, Sandia National Laboratories, Albuquerque, New Mexico.

Shaffer, S. E., and D. W. Powers, 1977. Survey of Background Geology for WIPP Project in Southeastern New Mexico, SAND77-0448, Sandia National Laboratories, Albuquerque, New Mexico.

Shaffer, S. E., 1982. Bibliography of Geology of Southeastern New Mexico, SAND82-0770, Sandia National Laboratories, Albuquerque, New Mexico.

Shelby, J. E., 1978. "Permeability of Sodium Chloride," interoffice memo, Sandia National Laboratories, Albuquerque, New Mexico.

Shell Exploration and Production Research Center, 1973. "Potassium-Argon Dates on Permian Potash Minerals from Southeastern New Mexico," Isochron/West, No. 6, p. 37.

Silver, B. A., and R. G. Todd, 1969. "Permian Cyclic Strata, Northern Midland and Delaware Basins, West Texas and Southeast New Mexico," American Association of Petroleum Geologists Bulletin, 1966, Vol. 53, No. 11, pp. 2223-2251.

Snider, H. I., 1966. "Stratigraphy and Associated Tectonics of the Upper Permian Castile-Salado-Rustler Evaporite Complex, Delaware Basin, West Texas and Southeast New Mexico," Ph.D. Dissertation, University of New Mexico, Albuquerque, New Mexico.

Snyder, R. P., and L. M. Gard, Jr., 1982. Evaluation of Breccia Pipes in Southeastern New Mexico and Their Relation to the Waste Isolation Pilot Plant (WIPP) Site (with a section on drill-stem tests, WIPP-31, by J. W. Mercer), U.S. Geological Survey Open-File Report 82-968.

Snyder, R. P., 1985. Dissolution of Halite and Gypsum, and Hydration of Anhydrite to Gypsum, Rustler Formation, in the Vicinity of the Waste Isolation Pilot Plant, Southeastern New Mexico, U.S. Geological Survey Open-File Report 85-229, Denver, Colorado.

Spiegler, P., 1982. Hydrologic Analyses of Two Brine Encounters in the Vicinity of the Waste Isolation Pilot Plant (WIPP) Site.

Spiegler, P., 1983. Origin of the Brines Near WIPP from the Drill Holes ERDA-6 and WIPP-12 Based on Stable Isotope Concentrations of Hydrogen and Oxygen.

Stewart, S. W., and L. C. Pakiser, 1962. "Crustal Structure in Eastern New Mexico Interpreted from the Gnome Explosion," Seismological Society of American Bulletin, Vol. 52, pp. 1017-1030.

Stipp, T. F., 1960. Major Structural Features and Geologic History of Southeastern New Mexico, A Symposium of the Gas and Oil Fields of Southeastern New Mexico, Roswell Geological Society.

Swenson, F. A., 1973. Dissolved Salts in Surface Water, U.S. Geological Survey Open-File Report 73-14.

Szabo, B. J., W. C. Gottschall, J. N. Rosholt, and C. R. McKinney, 1980. Part I: A Preliminary Study of Uranium-Thorium Systematics in Dissolution Residues at the Top of Salado Evaporites--Implications to Process and Time of the Last Vertical Dissolution Cycle of Salt Beds Near the WIPP Site; Part II: Uranium Trend Dating of Surficial Deposits and Gypsum Spring Deposit Near WIPP Site, New Mexico, U.S. Geological Survey Open-File Report 80-879.

Teufel, L. W., 1981. Mechanical Properties of Anhydrite and Polyhalite in Quasi-Static Triaxial Compression, SAND81-0858, Sandia National Laboratories, Albuquerque, New Mexico.

Toppozada, T. R., and A. R. Sanford, 1976. "Crustal Structure in Central New Mexico Interpreted from the Gasbuggy Explosion," Seismological Society of American Bulletin, Vol. 66, pp. 877-886.

Unterberger, R. R., 1981. Subsurface Radar Applications in the Delaware Basin, SAND81-7153, Sandia National Laboratories, Albuquerque, New Mexico.

U.S. Geological Survey, 1973. "Aeromagnetic Map of the Carlsbad Area, New Mexico and Texas," U.S. Geological Survey Geophysical Investigations Map GP-861.

Van Devender, T. R., 1980. "Holocene Plant Remains from Rocky Arroyo and Last Chance Canyon, Eddy County, New Mexico," The Southwestern Naturalist, Vol. 25.

Vine, J. D., 1960. "Recent Domal Structures in Southeastern New Mexico," American Association of Petroleum Geologists Bulletin, Vol. 44, No. 12, pp. 1903-1911.

Vine, J. D., 1963. "Surface Geology of the Nash Draw Quadrangle, Eddy County, New Mexico," U.S. Geological Survey Bulletin 1141-B, Government Printing Office, Washington, D.C.

Vine, J. D., 1976. "Breccia Pipes and Burial Metamorphism in Permian Evaporites of the Delaware Basin New Mexico," Geological Society of American Abstracts, Vol. 8, No. 6.

Walter, J. C., Jr., 1953. "Paleontology of the Rustler Formation, Culberson County, Texas." Journal of Paleontology, Vol. 27, No. 5, pp. 279-702.

Watson, W. G., 1979. "Inhomogeneities of the Ramsey Member of the Permian Bell Canyon Formation, Geraldine Ford Field, Culberson and Reeves Counties, Texas, Guadalupian Delaware Mountain Group of West Texas and Southeast New Mexico," Permian Basin Society Section of Economic Paleontologists and Mineralogists Publication, 79-18, pp. 2-38.

West, R. E., and W. G. Wieduwilt, 1976. Experimental Geophysical Survey of the Los Medanos Site and Surrounding Areas for Waste Isolation Pilot Plant Program, Eddy and Lea Counties, New Mexico, Project 0611, Mining Geophysical Surveys report to Sandia National Laboratories.

Widdicombe, R., 1980. "Quaternary Surficial Features in the Delaware Basin, Eddy and Lea Counties, New Mexico," unpublished MS Thesis, University of New Mexico, Albuquerque, New Mexico.

Wood, B. G., R. E. Snow, D. J. Cosler, and S. Haji-Djafari, 1982. Delaware Mountain Group (DMG) Hydrology--Salt Removal Potential, DOE/TME-3166.

J.6 HYDROLOGY

Allison, G. B., W. J. Stone, and M. W. Hughes, 1985. "Recharge in Karst and Dune Elements of a Semi-Arid Landscape as Indicated by Natural Isotopes and Chloride," Journal of Hydrology, Vol. 76, pp. 1-25.

Anderson, R. Y., 1982. Upper Castile Brine Aquifer, Northern Delaware Basin, New Mexico.

Antevs, E., 1954. "Climate of New Mexico During the Last Glacio-Pluvial," Journal of Geology, Vol. 62, pp. 182-191.

Barr, G. E., and D. D. Gonzalez, 1980. "Current Status of the Hydrogeology for the WIPP," SAND80-1539C, in Proceedings of ONWI/LBL Workshop on Thermomechanical-Hydrochemical Modeling for a Hardrock Waste Repository, LBL-1120, pp. 89-94.

Barr, G. E., W. B. Miller, and D. D. Gonzalez, 1983. Interim Report on the Modeling of the Regional Hydraulics of the Rustler Formation, SAND83-0391, Sandia National Laboratories, Albuquerque, New Mexico.

Barrows, L. J., 1982. "WIPP Geohydrology--The Implications of Karst," Unpublished manuscript, 21 pp., (Reproduced in Appendix 1 of this report).

Basler, J. A, 1983. Instrumentation Used for Hydraulic Testing of Potential Water-Bearing Formations at the Waste Isolation Pilot Plant Site in Southeastern New Mexico, U.S. Geological Survey Open-File Report 83-144, 29 pp.

Beauheim, R. L., B. W. Hassinger, and J. A. Klaiber, 1983. Basic Data Report for Borehole Cabin Baby-1 Deepening and Hydrologic Testing, Waste Isolation Pilot Plant (WIPP) Project, Southeastern New Mexico, WTSD-TME-020, U.S. Department of Energy, Albuquerque, New Mexico.

Beauheim, R. L., 1985. Effects of Borehole History on Well-Test Analysis, SAND85-2008A, Sandia National Laboratories, Albuquerque, New Mexico, presented at 1985 AGU Fall Meeting.

Beauheim, R. L., 1986. Hydraulic-Test Results for Well DOE-2 at the Waste Isolation Pilot Plant (WIPP) Site, SAND86-1364, Sandia National Laboratories, Albuquerque, New Mexico.

Beauheim, R. L., 1987. Analysis of Pumping Tests of the Culebra Dolomite Conducted at the H-3 Hydropad at the Waste Isolation Pilot Plant (WIPP) Site, SAND86-2311, Sandia National Laboratories, Albuquerque, New Mexico.

Beauheim, R. L., 1987. Interpretations of Single-Well Hydraulic Tests Conducted At and Near the Waste Isolation Pilot Plant (WIPP) Site, 1983-1987, SAND87-0039, Sandia National Laboratories, Albuquerque, New Mexico.

Beauheim, R. L., 1987. Interpretation of the WIPP-13 Multipad Pumping Test of the Culebra Dolomite at the Waste Isolation Pilot Plant (WIPP) Site, SAND87-2456, Sandia National Laboratories, Albuquerque, New Mexico.

Bentley, H. W., J. J. Ward, G. R. Walter, S. J. Alweis, and D. D. Gonzalez, 1981. "H-6 Convergent Tracer Test, the WIPP, Southeast New Mexico," (in preparation).

Bentley, H. W., 1983. "Development and Features of Groundwater Tracers at the Waste Isolation Pilot Plant (WIPP), New Mexico," Transactions, AGU Fall Meeting, Hydrology Section, p. 714.

Bjorklund, L. J., and W. S. Motts, 1959. Geology and Water-Resources of the Carlsbad Area, New Mexico, U.S. Geological Survey Open-File Report 59-9, 322 pp.

Brokaw, A. L., C. L. Jones, M. E. Cooley, and W. H. Hays, 1972. Geology and Hydrology of the Carlsbad Potash Area, Eddy and Lea Counties, New Mexico, U.S. Geological Survey, Open-File Report 4339-1.

Buck, A. D., J. E. Rhoderick, J. P. Burkes, K. Mather, R. E. Reinhold, and J. A. Boa, 1983. Modification of Bell Canyon Test (BCT) 1-FF Grout, SAND83-7097, Sandia National Laboratories, Albuquerque, New Mexico.

Bureau of Land Management (BLM), 1978. Groundwater Study for the Proposed Expansion of Potash Mining Near Carlsbad, New Mexico.

Canfield, T. R., 1983. Stress Near Waste Canisters Buried in Salt, SAND82-0525, Sandia National Laboratories, Albuquerque, New Mexico.

Chaturvedi, L., and K. Rehfeldt, 1984. "Groundwater Occurrence and the Dissolution of Salt at the WIPP Radioactive Waste Repository Site," EOS, American Geophysical Union Trans 65(31):457-459.

Chaturvedi, L., and J. K. Channell, 1985. The Rustler Formation as a Transport Medium for Contaminated Groundwater, EEG-32, State of New Mexico Environmental Evaluation Group, Santa Fe, New Mexico.

Christensen, C. L., and E. W. Peterson, 1981. The Bell Canyon Test Summary Report, SAND80-1375, Sandia National Laboratories, Albuquerque, New Mexico.

Cole, C. R., and F. W. Bond, 1980. Assessment of the Effectiveness of Geologic Isolation Systems, Comparison of INTERA and WISAP Model Application, Pacific Northwest Laboratory, PNL-3070, 50 pp.

Colton, I. D., and J. G. Morse, 1985. Water Quality Sampling Plan, DOE/WIPP-215, Waste Isolation Pilot Plant, Carlsbad, New Mexico.

Cooper, J. B., 1962. Groundwater in Cenozoic Fill in Collapse Structures, Southeastern Eddy County, New Mexico, U.S. Geological Survey Professional Paper 450-E, Art 225.

Cooper, J. B., 1962. Groundwater Investigations of the Project Gnome Area, Eddy and Lea Counties, New Mexico, U.S. Geological Survey TEI-802, 67 pp., 17 figs.

Cooper, J. B., and V. M. Glanzman, 1971. Geohydrology of Project Gnome Site, Eddy County, New Mexico, U.S. Geological Survey Professional Paper 712-A, 24 pp.

Cox, E. R., and J. L. Kunkler, 1962. Feasibility of Injecting Brine from Malaga Bend into the Delaware Mountain Group, Eddy County, New Mexico, U.S. Geological Survey Open-File Report, 69 pp., 5 figs.

Cox, E. R., and J. S. Havens, 1965. A Progress Report on the Malaga Bend Experimental Salinity Alleviation Project, Eddy County, New Mexico, U.S. Geological Survey Open-File Report 65-35, 91 pp.

Crawley, M. E., 1985. Hydrostatic Pressure Fluid Density Distribution of the Culebra Dolomite Member of the Rustler Formation Near the Waste Isolation Pilot Plant Site, Southeastern New Mexico, U.S. Department of Energy, Carlsbad, New Mexico.

Crawley, M. E., 1987. Initial Data Release Report for the Pressure-Density Survey Program, WID, WS:87:00002.

Crawley, M. E., 1987. Pressure-Density Survey Program Plan, Waste Isolation Pilot Plant, Carlsbad, New Mexico, IT Corporation, 41 pp.

Crawley, M. E., 1987. Second Data Release Report for the Pressure-Density Survey Program, WID, WS:87:00015.

Crawley, M. E., 1988. Third Data Release Report for the Pressure-Density Survey Program, WID, WS:88:00005.

D'Appolonia Consulting Engineers, 1981. Modeling Verification Studies Long-Term Waste Isolation Assessment, Waste Isolation Pilot Plant (WIPP) Project, Southeastern New Mexico, Consultant's Report to U.S. Department of Energy, var. pp.

Davies, P. B., 1986. "Pleistocene-to-Present Flow-System Evolution in the Northern Delaware Basin, Southeastern New Mexico--Analysis Using Transient Cross-Sectional Flow Simulations," Geological Society of America, Abstracts with Programs, Vol. 18, No. 6, pp. 580.

Davies, P. B., 1987. "Modeling Area, Variable-Density Groundwater Flow Using Equivalent Freshwater Head--Analysis of Potentially Significant Errors,"

Proceedings of the NWWA Conference on Solving Groundwater Problems with Models, February 10-12, 1987, Denver, Colorado, pp. 888-903.

Davies, P. B., 1988. Variable Density Groundwater Flow and Paleohydrology in the Region Surrounding the Waste Isolation Pilot Plant (WIPP), Southeastern New Mexico, U.S. Geological Survey Open-File Report 88-490.

Dennehy, K. F., 1982. "Results of Hydrologic Tests and Water-Chemistry Analyses, Wells H-6A, H-6B, and H-6C at the Proposed Waste Isolation Pilot Plant Site in Southeastern New Mexico," U.S. Geological Survey Water-Resources Investigations 82-8, 68 pp.

Dennehy, K. F., and J. W. Mercer, 1982. "Results of Hydrologic Tests and Water-Chemistry Analyses, Wells H-5A, H-5B, and H-5C at the Proposed Waste Isolation Pilot Plant Site in Southeastern New Mexico," U.S. Geological Survey Water-Resources Investigations 82-19, 83 pp.

Dillon, R. T., R. B. Lantz, and S. B. Pahwa, 1977. Risk Methodology for Geologic Disposal of Radioactive Waste: The Sandia Waste Isolation Flow and Transport (SWIFT) Model, SAND78-1267, Sandia National Laboratories, Albuquerque, New Mexico.

Dosch, R. G., 1978. "Radionuclide Migration Studies associated with the WIPP Site in Southeastern New Mexico," SAND78-1178J, Sandia National Laboratories, Albuquerque, New Mexico, presented at the Symposium on Science Underlying Radioactive Waste Materials Research Society, Boston, Massachusetts, published in a Proceedings Volume, Science Underlying Radioactive Waste Management, by Plenum Publishing Co.

Dosch, R. G., and A. W. Lynch, 1979. Radionuclide Transport in a Dolomite Aquifer, SAND79-1016C, Sandia National Laboratories, Albuquerque, New Mexico, presented at Materials Research Society Meeting, Boston, Massachusetts.

Dosch, R. G., 1980. Assessment of Potential Radionuclide Transport in Site-Specific Geologic Formations, SAND79-2468, Sandia National Laboratories, Albuquerque, New Mexico.

Dosch, R. G., 1981. Solubility and Sorption Characteristics of Uranium (VI) Associated with Rock Samples and Brines/Groundwaters from WIPP and NTS, SAND80-1595, Sandia National Laboratories, Albuquerque, New Mexico.

Duffey, T. A., 1980. The Salt Block I Test: Experimental Details and Comparison with Theory, Final Report, SAND79-7050, Sandia National Laboratories, Albuquerque, New Mexico.

Eaton, R. R., and D. B. Hayes, 1981. Analytical and Numerical Analyses of Hydrologic Well-Bore Experiments, SAND80-1120, Sandia National Laboratories, Albuquerque, New Mexico.

EEG (Environmental Evaluation Group), 1980. The Significance of Certain Rustler Aquifer Parameters for Predicting Long-Term Radiation Doses from WIPP, EEG-8, C. Wofsy, Health and Environment Department, State of New Mexico, Santa Fe, New Mexico.

EEG (Environmental Evaluation Group), 1982. Hydrologic Analyses of Two Brine Encounters in the Vicinity of the Waste Isolation Pilot Plant, (WIPP) Site EEG-17, P. Spiegler Health and Environment Department, State of New Mexico, Santa Fe, New Mexico.

EEG (Environmental Evaluation Group), 1983. Origin of the Brines Near WIPP from the Drill Holes ERDA-6 and WIPP-12 Based on Stable Isotope Concentrations of Hydrogen and Oxygen, EEG-18, P. Spiegler and D. Updegraff, Health and Environment Department, State of New Mexico, Santa Fe, New Mexico.

EEG (Environmental Evaluation Group), 1984. Sensitivity Analysis of Solute Transport in Fractures and Determination of Anisotrophy Within the Culebra Dolomite, EEG-27, K. Rehfeldt, Health and Environment Department, State of New Mexico, Santa Fe, New Mexico.

EEG (Environmental Evaluation Group), 1986. Stable Isotopes in Southeastern New Mexico Groundwater: Implications for Dating Recharge in the WIPP, EEG-35, J. B. Chapman, Health and Environment Department, State of New Mexico, Santa Fe, New Mexico.

EEG (Environmental Evaluation Group), 1988. Chemical and Radiochemical Characteristics of Groundwater in the Culebra Dolomite, Southeastern New Mexico, EEG-39, J. B. Chapman, Health and Environment Department, State of New Mexico, Santa Fe, New Mexico.

Federal Water Pollution Control Administration (FWPCA), 1967. Immediate Water Pollution Control Needs, Pecos River Basin, New Mexico and Texas, PB-266-387, South Central Region, Dallas, Texas.

Fortney, D. R., 1979. Sensitivity of the Consequences of Pu Migration in the WIPP Environment on Kd Values Used in Current Transport Models, SAND79-1305, Summary of Research and Development Activities in Support of Waste Acceptance Criteria for WIPP, Sandia National Laboratories, Albuquerque, New Mexico.

Fried, S. et al., 1981. "The Radiolytic Oxidation and Reduction of Plutonium, Argonne National Laboratories, 1979," SAND80-2577, Sandia National Laboratories, Albuquerque, New Mexico, presented at Materials Research Society Meeting Symposium, on Scientific Basis for Nuclear Waste Management, Boston, Massachusetts, published in Subseabed Disposal Program Annual Report, ed. D. M. Talbert, Vol. 2, pp. 271-284.

Geohydrology Associates, Inc., 1978. Groundwater Study Related to Proposed Expansion of Potash Mining Near Carlsbad, New Mexico, prepared for U.S. Bureau of Land Management, Denver, Colorado.

Geohydrology Associates, Inc., 1979. Water-Resources Study of the Carlsbad Potash Area, New Mexico, Albuquerque, New Mexico.

Gonzalez, D. D., and L. R. Hill, 1979. "Tracer Tests Performed in the Field for WIPP in Southeastern New Mexico," SAND79-0981C, in Proceedings of the International Symposium on Scientific Basis for Nuclear Waste Management, Materials Research Society, Vol. 2, pp. 487-489.

Gonzalez, D. D., 1983. Fracture Flow in the Rustler Formation, Waste Isolation Pilot Plant (WIPP), Southeastern New Mexico (SENM): Interim Report, SAND82-1012, Sandia National Laboratories, Albuquerque, New Mexico.

Gonzalez, D. D., 1983. Groundwater Flow in the Rustler Formation, Waste Isolation Pilot Plant (WIPP), Southeast New Mexico (SENM): Interim Report, SAND82-1012, Sandia National Laboratories, Albuquerque, New Mexico.

Gonzalez, D. D., 1983. Hydrogeochemical Parameters of Fluid-Bearing Zones in the Rustler and Bell Canyon Formations: Waste Isolation Pilot Plant (WIPP), Southeast New Mexico (SENM), SAND83-0210, Sandia National Laboratories, Albuquerque, New Mexico.

Gonzalez, D. D., 1983. "Hydrogeologic Characterization of Radioactive Waste Repositories: The WIPP Example," SAND83-2029A, in Transactions, AGU Fall Meeting Hydrology Screen, p. 713.

Gonzalez, D. D., and H. W. Bentley (Hydro Geo Chem, Inc.), 1984. "Field Test for Effective Porosity and Dispersivity in Fractured Dolomite, the WIPP, Southeastern New Mexico," Water Resources Monograph 9, American Geophysical Union, pp. 207-221.

Gonzalez, D. D., H. W. Bentley, and G. R. Walter. "Dispersion and Porosity Determinations at the H-2 Site, the WIPP, Southeastern New Mexico," Symposium of Ferris Water Resources Monograph Series, (in preparation).

Grove, D. B., and W. A. Beetum, 1971. "Porosity and Dispersion-Constant Calculations for a Fractured Carbonate Aquifer Using the Two-Well Tracer Method," Water Resources Research, Vol. 7.

Hale, W. E., 1945. "Groundwater Conditions in the Vicinity of Carlsbad, New Mexico," 16th and 17th Biennial Reports, New Mexico State Engineer, pp. 195-250.

Hale, W. E., L. S. Hughes, and E. R. Cox, 1954. Possible Improvement of Quality of Water of the Pecos River by Diversion of Brine at Malaga Bend, Eddy County, New Mexico, Pecos River Commission, New Mexico and Texas, in cooperation with U.S. Geological Survey Water Resources Division, Carlsbad, New Mexico.

Hale, W. E., and A. Clebsch, Jr., 1958. "Preliminary Appraisal of Groundwater Conditions in Southeastern Eddy County and Southwestern Lea County, New Mexico," U.S. Geological Survey Trace Element Memorandum Report 1045, 23 pp.

Hale, W. E., 1961. "Availability of Groundwater in New Mexico," Sixth Annual New Mexico Water Conference, November 1-2, 1961, New Mexico State University, Las Cruces, New Mexico, pp. 11-22.

Haug, A., V. A. Kelley, A. M. LaVenue, and J. F. Pickens, 1987. Modeling of Groundwater Flow in the Culebra Dolomite at the Waste Isolation Pilot Plant (WIPP) Site, Interim Report, SAND86-7167, Sandia National Laboratories, Albuquerque, New Mexico.

Havens, J. S., 1972. Malaga Bend Experimental Salinity Alleviation Project--A Comprehensive Interim Report--Eddy County, New Mexico, U.S. Geological Survey Water Resources Division, in cooperation with the Pecos River Commission.

Havens, J. S., and D. W. Wilkins, 1980. "Experimental Salinity Alleviation at Malage Bend of the Pecos River, Eddy County, New Mexico," U. S. Geological Survey Water-Resources Investigations 80-4, 65 pp.

Henrickson, G. E., and R. S. Jones, 1952. "Geology and Groundwater Resources of Eddy County, New Mexico," New Mexico Bureau of Mines and Mineral Resources Groundwater Report 3, 169 pp.

Herkenhoff, Gordon, and Associates, Inc., 1975. Water and Wastewater Master Plan, 1975-1995, Water Supply Study, City of Hobbs, New Mexico.

Hiss, W. L., 1971. "Capitan Aquifer Observation-Well Network, Carlsbad to Jal, New Mexico," New Mexico State Engineer Technical Report 38, 76 pp.

Hiss, W. L., 1975. "Chloride-Ion Concentration in Groundwater in Permian Guadalupian Rocks, Southeast New Mexico and West Texas," Resource Map 5, New Mexico Bureau of Mines and Mineral Resources, Socorro, New Mexico.

Hiss, W. L., 1975. "Stratigraphy and Groundwater Hydrology of the Capitan Aquifer, Southeastern New Mexico and Western Texas," Ph.D. Thesis, University of Colorado, Boulder, Colorado.

Hiss, W. L., 1975. "Thickness of the Permian Guadalupian Aquifer, Southeastern New Mexico and West Texas," Resource Map 5, New Mexico Bureau of Mines and Mineral Resources, Socorro, New Mexico.

Hiss, W. L., 1975. Water Quality Data from Oil and Gas Wells in Part of the Permian Basin, Southeastern New Mexico and Western Texas, U.S. Geological Survey Open-File Report 75-579.

Hiss, W. L., 1976. "Structure of the Permian Guadalupian Aquifer, Southeastern New Mexico and Western Texas," Resource Map 6, New Mexico Bureau of Mines and Mineral Resources, Socorro, New Mexico.

Hiss, W. L., 1980. "Movement of Groundwater in Permian Guadalupian Aquifer Systems, Southeastern New Mexico and Western Texas, Trans-Pecos Region," New Mexico Geological Society, 31st Field Conference, pp. 289-294.

Hohlfelder, J. J., and G. R. Hadley, 1979. "Laboratory Studies of Water Transport in Rock Salt," SAND79-1044J, Letters in Heat and Mass Transfer, Pergamon Press, Great Britain, Vol. 6, p. 271.

Hohlfelder, J. J., A. C. Beattie, and H. C. Shefelbine, 1982. Water Release and Mechanical Failure in Heated Geologic Salt, SAND81-1488, Sandia National Laboratories, Albuquerque, New Mexico.

Hohlfelder, J. J., and W. M. McMurtry, 1983. Water Sources in Southeast New Mexico (SENM) Rock Salt, SAND82-0530, Sandia National Laboratories, Albuquerque, New Mexico.

Hunter, R. L., 1985. A Regional Water Balance for the Waste Isolation Pilot Plant (WIPP) Site and Surrounding Area, SAND84-2233, Sandia National Laboratories, Albuquerque, New Mexico.

Hydro Geo Chem, Inc., 1985. WIPP Hydrology Program Waste Isolation Pilot Plant, SENM: Hydrology Data Report No. 1, SAND85-7206, Sandia National Laboratories, Albuquerque, New Mexico.

Hydro Geo Chem, Inc., 1986. Two-Well Recirculation Tracer Test at the H-2 Hydropad, Waste Isolation Pilot Plant (WIPP), Southeastern New Mexico, SAND86-7092, Sandia National Laboratories, Albuquerque, New Mexico.

Intera Environmental Consultants, Inc., 1981. Consequence Assessment of Hydrological Communications Through Borehole Plugs, SAND81-7164, Sandia National Laboratories, Albuquerque, New Mexico.

Intera Technologies, Inc., and Hydro Geo Chem, Inc., 1985. WIPP Hydrology Program, Waste Isolation Pilot Plant, Southeastern New Mexico, Hydrologic Data Report No. 2, SAND85-7263, Sandia National Laboratories, Albuquerque, New Mexico.

Intera Technologies, Inc., 1986. WIPP Hydrology Program Waste Isolation Pilot Plant, Southeastern New Mexico, Hydrologic Data Report No. 3, SAND86-7109, Sandia National Laboratories, Albuquerque, New Mexico.

Jennings, A. H., 1963. "Maximum Recorded U.S. Point Rainfall, Weather Bureau Technical Paper No. 2 (revised)," U.S. Department of Commerce, Washington, D.C.

Kelley, V. A., and J. F. Pickens, 1986. Interpretation of the Convergent-Flow Tracer Tests Conducted in the Culebra Dolomite at the H-3 and H-4 Hydropads at the Waste Isolation Pilot Plant (WIPP) Site, SAND86-7161, Sandia National Laboratories, Albuquerque, New Mexico.

Kunkler, J. L., 1980. Evaluation of the Malaga Bend Salinity Alleviation Project, Eddy County, New Mexico, U.S. Geological Survey Open-File Report 80-1111, 31 pp.

Lambert, S. J., and J. W. Mercer, 1977. Hydrologic Investigations of Los Medanos Area, Southeast New Mexico, SAND77-1401, Sandia National Laboratories, Albuquerque, New Mexico, 56 pp.

Lambert, S. J., and J. W. Mercer, 1978. Hydrologic Investigations of the Los Medanos Area, Southeastern New Mexico, 1977, SAND77-1401, Sandia National Laboratories, Albuquerque, New Mexico.

Lambert, S. J., 1980. Mineralogical Aspects of Fluid Migration in the Salt Block II Experiment, SAND79-2423, Sandia National Laboratories, Albuquerque, New Mexico.

Lambert, S. J., 1980. Proposed Standards, Controls and Procedures for the Collection of Hydrologic Data for the Waste Isolation Pilot Plant (WIPP), Southeastern New Mexico, SAND80-0436, Sandia National Laboratories, Albuquerque, New Mexico, (Internal Distribution Only).

Lambert, S. J., and H. C. Shefelbine, 1980. A Strategy for Investigation of Fluid Migration in Evaporites (Waste Isolation Pilot Plant WIPP), SAND79-1889, Sandia National Laboratories, Albuquerque, New Mexico.

Lappin, A. L., 1988. Summary of Site-Characterization Studies Conducted from 1983 through 1987 at the Waste Isolation Pilot Plant (WIPP) Site, Southeastern New Mexico, SAND88-0157, Sandia National Laboratories, Albuquerque, New Mexico.

LaVenue, A. M., A. Haug, and V. A. Kelley, 1988. Numerical Simulation of Groundwater Flow in the Culebra Dolomite at the Waste Isolation Pilot Plant (WIPP) Site, Second Interim Report, SAND88-7002, Sandia National Laboratories, Albuquerque, New Mexico.

Lynch, A. W., 1978. Migration of Cesium in Dolomite from the Rustler Formation in the Los Medanos Area in Southeastern New Mexico, SAND78-1179C, Sandia National Laboratories, Albuquerque, New Mexico, presented at the Materials Research Society - Science Underlying Radioactive Waste Management, Boston, Massachusetts.

Lynch, A. W., and R. G. Dosch, 1980. Cesium Migration Through Solid Cores of Magenta Dolomite, SAND80-1335C, Sandia National Laboratories, Albuquerque, New Mexico, presented at Materials Research Society Meeting, Boston, Massachusetts.

Lynch, A. W., and R. G. Dosch, 1980. Sorption Coefficients for Radionuclides on Samples from the Water-Bearing Magenta and Culebra Members of the Rustler Formation, SAND80-1064, Sandia National Laboratories, Albuquerque, New Mexico.

Lynch, A. W., R. G. Dosch, and C. R. Hills, 1981. Migration of Cesium-137 Through a Solid Core of Magenta Dolomite Taken from the Rustler Formation in SENM, SAND80-1259, Sandia National Laboratories, Albuquerque, New Mexico.

Magara, K., 1971. "Permeability Considerations in Generation of Abnormal Pressures," Journal of the Society of Petroleum Engineers, Vol. 11, pp. 236-242.

Mercer, J. W., and B. R. Orr, 1977. Review and Analysis of Geohydrology Conditions Near the Site of a Potential Nuclear-Waste Repository, Eddy and Lea Counties, New Mexico, U.S. Geological Survey Open-File Report, 77-123, 35 pp.

Mercer, J. W., and B. R. Orr, 1978. "Geohydrology of the Proposed Waste Isolation Pilot Plant, Southeastern New Mexico," U.S. Geological Survey, Preliminary Water-Resources Investigations.

Mercer, J. W., and B. R. Orr, 1979. "Interim Data Report on the Geohydrology of the Proposed Waste Isolation Pilot Plant Site, Southeastern New Mexico," U.S. Geological Survey Water-Resources Investigations 79-98, 178 pp.

Mercer, J. W., and D. D. Gonzalez, 1981. "Geohydrology of the Proposed Waste Isolation Pilot Plant in Southeastern New Mexico," in Environmental Geology and Hydrology in New Mexico, New Mexico Geological Society Special Publication No. 10, pp. 123-131.

Mercer, J. W., and D. D. Gonzalez, 1981. "Geohydrology of the Proposed Waste Isolation Pilot Plant Site in Southeastern New Mexico," SAND81-0197C, in Environmental Geology and Hydrology in New Mexico, New Mexico Geological Society Special Publication No. 10, pp. 123-131.

Mercer, J. W., P. Davis, K. F. Dennehy, and C. L. Geotz, 1981. "Results of Hydrologic Tests and Water-Chemistry Analyses, Wells H-4A, H-4B, and H-4C at the Proposed Waste Isolation Pilot Plant Site, Southeastern New Mexico," U.S. Geological Plant Site, Southeastern New Mexico," U.S. Geological Survey, Water-Resources Investigations, 81-3666, 92 pp.

Mercer, J. W., 1983. "Geohydrology of the Proposed Waste Isolation Pilot Plant Site, Los Medanos Area, Southeastern New Mexico," U.S. Geological Survey Water-Resources Investigations Report 83-4016, 113 pp.

Mercer, J. W., 1987. Compilation of Hydrologic Data from Drilling the Salado and Castile Formations Near the WIPP Site, Southeastern New Mexico, SAND86-0954, Sandia National Laboratories, Albuquerque, New Mexico.

Mercer, J. W., R. L. Beauheim, R. P. Snyder, and G. M. Fairer, 1987. Basic Data Report for Drilling and Hydrologic Testing of Drillhole DOE-2 at the Waste Isolation Pilot Plant (WIPP) Site, SAND86-0611, Sandia National Laboratories, Albuquerque, New Mexico.

Mercer, J. W., and B. R. Orr. Interim Data Report on the Geohydrology of the Proposed Waste Isolation Pilot Plant Site, Southeastern New Mexico, U.S. Geological Survey.

Mercer, J. W., and B. R. Orr. Interim Data Report on the Geohydrology of the Proposed Waste Isolation Pilot Plant Site, Los Medanos Area, Southeastern New Mexico, U.S. Geological Survey Water Investigations Report 83-4016, U.S. Geological Survey, (Not funded through Sandia.)

Motts, W. S., 1968. "The Control of Groundwater Occurrence by Lithofacies in the Guadalupian Reef Complex Near Carlsbad, New Mexico," Geological Society of America Bulletin 79:283-298.

Nash, K., S. Fried, and A. Friedman, 1981. "Radiolysis of Np in Environmental Solutions, Argonne National Laboratories, 1979," SAND80-2577, Sandia National Laboratories, Albuquerque, New Mexico, published in Subseabed Disposal Program Annual Report, ed. D. M. Talbert, Vol. 2, pp. 271-284.

New Mexico Interstate Stream Commission, and New Mexico State Engineer's Office, 1975. County Profile for Eddy County and County Profile for Lea County.

New Mexico State Engineer's Office, 1967. Water Resources of New Mexico Occurrence, Development and Use.

Nowak, J. E., 1984. Diffusion of Plutonium in Compacted, Brine-Saturated Bentonite, SAND84-1118C, Sandia National Laboratories, Albuquerque, New Mexico.

Nowak, J. E. The Migration of Eu Through Geologic Media, SAND70-1746J, Sandia National Laboratories, Albuquerque, New Mexico.

Pearson, F. J., V. A. Kelley, and J. F. Pickens, 1986. Preliminary Design for A Sorbing Tracer Test in the Culebra Dolomite at the H-3 Hydropad at the Waste Isolation Pilot Plant, SAND86-7177, Sandia National Laboratories, Albuquerque, New Mexico.

Pearson, F. J., V. A. Kelley, and J. F. Pickens, 1987. Preliminary Design for a Sorbing Tracer Test in the Culebra Dolomite at the H-3 Hydropad at the Waste Isolation Pilot Plant (WIPP) Site, SAND86-7177, Sandia National Laboratories, Albuquerque, New Mexico.

Popielak, R. S., R. L. Beauheim, S. R. Black, W. E. Coons, C. T. Ellingson, and R. L. Olsen, 1983. "Brine Reservoirs in the Castile Formation, Waste Isolation Pilot Plant (WIPP) Project, Southeastern New Mexico," TME 3153, U.S. Department of Energy.

Randall, W. S., M. E. Crawley, and M. L. Lyon, 1988. 1988 Annual Water Quality Data Report for the Waste Isolation Pilot Plant, DOE/WIPP 88-006, Carlsbad, New Mexico.

Reeves, M., D. S. Ward, N. D. Johns, and R. M. Cranwell, 1986. Data Input Guide for SWIFT II, the Sandia Waste Isolation Flow and Transport Model for Fractured Media, Release 4.84, SAND84-1586, Sandia National Laboratories, Albuquerque, New Mexico (also NUREG/CR-3925).

Reeves, M., D. S. Ward, N. D. Johns, and R. M. Cranwell, 1986. Theory and Implementation for SWIFT II, the Sandia Waste Isolation Flow and Transport Model, Release 4.84, SAND83-1159, Sandia National Laboratories, Albuquerque, New Mexico (also NUREG/CR-3328).

Reeves, M., V. A. Kelley, and J. F. Pickens, 1987. Regional Double-Porosity Solute Transport in the Culebra Dolomite: An Analysis of Parameter Sensitivity and Importance at the Waste Isolation Pilot Plant (WIPP) Site, SAND87-7105, Sandia National Laboratories, Albuquerque, New Mexico.

Register, J. K., 1980. "Subsurface Hydrology of Strata Overlying the Salado Formation at the Waste Isolation Pilot Plant Site, Eddy County, New Mexico," TME-3059, Waste Isolation Pilot Plant, Carlsbad, New Mexico.

Register, J. K., 1981. "Brine Pocket Occurrences in the Castile Formation, Southeastern New Mexico," TME-3080, U.S. Department of Energy, Albuquerque, New Mexico.

Richey, S. F., J. G. Wells, and K. T. Stephens, 1985. "Geohydrology of the Delaware Basin and Vicinity, Texas and New Mexico," U.S. Geological Survey Water Resources Investigation Report 84-4077, (Albuquerque, New Mexico).

Richey, S. F., 1986. Hydrologic-Test Data from Wells at Hydrologic-Test Pads H-7, H-8, H-9 and H-10 Near the Proposed Waste Isolation Pilot Plant, Southeastern New Mexico, U.S. Geological Survey Open-File Report 86-413.

Richey, S. F., 1987. Preliminary Hydrologic Data for Wells Tested in Nash Draw, Near the Proposed Waste Isolation Pilot Plant, Southeastern New Mexico, U.S. Geological Survey Open-File Report 87-37, (Albuquerque, New Mexico).

Rose, W., 1977. "Development of a Conceptual Model to Explain Brine Flowage into Wells Drilled Through the Salado-Castile Formation: Contact in Locations such as the ERDA #6 Site Near Carlsbad in Southeastern New Mexico," Report to Sandia National Laboratories, Albuquerque, New Mexico.

Sares, S. W., 1984. "Hydrologic and Geomorphic Development of a Low Relief Evaporite Karst Drainage Basin, Southeastern New Mexico," University of New Mexico, MS Thesis.

Saulnier, G. J., Jr., 1987. Analysis of Pumping Tests of the Culebra Dolomite Conducted at the H-11 Hydropad at the Waste Isolation Pilot Plant (WIPP) Site, SAND87-7124, Sandia National Laboratories, Albuquerque, New Mexico.

Saulnier, G. J., Jr. et al., 1987. Program Waste Isolation Pilot Plant Southeastern New Mexico, Hydrologic Data Report No. 4, SAND86-7166, Sandia National Laboratories, Albuquerque, New Mexico.

Saulnier, G. J., Jr., G. A. Freeze, and W. A. Stensrud, 1987. WIPP Hydrology Program, Waste Isolation Pilot Plant, Southeastern New Mexico, Hydrologic Data Report No. 4, SAND86-7166, Sandia National Laboratories, Albuquerque, New Mexico.

Saulnier, G. J., Jr., and J. D. Avis, 1988. Interpretation of Hydraulic Tests Conducted in the Waste-Handling Shaft at the Waste Isolation Pilot Plant (WIPP) Site, SAND87-7001, Sandia National Laboratories, Albuquerque, New Mexico.

Seitz, M. G., D. Bowers, and D. R. Fortney, 1981. A Groundwater Stream Experiment for the Waste Isolation Pilot Plant, ANL-81-28, Argonne National Laboratory, Argonne, Illinois.

Serne, R. J., D. Rai, M. J. Mason, and M. A. Molecke, 1977. "Batch Kd Measurements of Nuclides to Estimate Migration Potential at the Proposed Waste Isolation Pilot Plant in New Mexico," Battelle Pacific Northwest Laboratories Report PNL-2448.

Shefelbine, H. C., 1982. Brine Migration: A Summary Report, SAND82-0152, Sandia National Laboratories, Albuquerque, New Mexico.

Stensrud, W. A., M. A. Bame, K. D. Lantz, A. M. LaVenue, J. B. Palmer, and G. J. Saulnier, Jr., 1987. WIPP Hydrology Program, Waste Isolation Pilot Plant Site, Southeastern New Mexico, Hydrologic Data Report No. 5, SAND87-7125, Sandia National Laboratories, Albuquerque, New Mexico.

Stensrud, W. A., M. A. Bame, K. D. Lantz, T. L. Cauffman, J. B. Palmer, and G. J. Saulnier, Jr., 1988. WIPP Hydrology Program, Waste Isolation Pilot Plant Site, Southeastern New Mexico, Hydrologic Data Report No. 6, SAND87-7166, Sandia National Laboratories, Albuquerque, New Mexico.

Tomasko, D., 1986. The Effect of Side-Wall Boundary Conditions on Convective Heat Transfer in a Porous Medium Heated from Below, SAND86-1549A, Sandia National Laboratories, Albuquerque, New Mexico, presented at CUBE Symposium, Livermore, California.

Tomasko, D., 1987. The Effects of a Bimodel Pore Distribution on Matrix Diffusion in a Fractured Porous Medium, SAND87-0265, Sandia National Laboratories, Albuquerque, New Mexico.

Tomasko, D., 1987. Optimally Orienting a Parallel-Strip Aquifer Using Multiwell Test Data, SAND86-1440J, Sandia National Laboratories, Albuquerque, New Mexico, presented at Solving Groundwater Problems with Models, Denver, Colorado.

Tomasko, D., and A. L. Jensen, 1987. A Linear-Flow Interpretation of the H-3 Multiwell Pumping Test Conducted at the Waste Isolation Pilot Plant (WIPP) Site, SAND87-0630, Sandia National Laboratories, Albuquerque, New Mexico.

Trucano, T. G., 1981. Computer Modeling of Stress States Association with Fluid Migration Experiments, SAND81-2008, Sandia National Laboratories, Albuquerque, New Mexico.

U.S. Army Corps of Engineers, 1976. "Hydrology, Pecos River and Tributaries at and in the Vicinity of Carlsbad, New Mexico," Feasibility Report for the Water Resources Development, Albuquerque, New Mexico.

Uhland, D. W., and W. S. Randall, 1986. Annual Water Quality Data Report, DOE/WIPP-86-006, Waste Isolation Pilot Plant, Carlsbad, New Mexico.

Uhland, D. W., W. S. Randall, and R. C. Carrasco, 1987. Annual Water Quality Data Report, DOE/WIPP-87-007, Waste Isolation Pilot Plant, Carlsbad, New Mexico.

USGS (U.S. Geological Survey), 1976. Water Resources Data for New Mexico, Water Year 1975, NM-75-1, Department of the Interior, Albuquerque, New Mexico.

USGS (U.S. Geological Survey), 1977. Water Resources Data for New Mexico, Water Year 1976, NM-76-1, Albuquerque, New Mexico.

Walter, G. R., 1983. Aquifer Tests to Determine the Principal Components of Transmissivity in the Culebra Dolomite at Hydropads H-4, H-5 and H-6: Waste Isolation Pilot Plant (WIPP) Southeastern New Mexico, SAND83-7009, Sandia National Laboratories, Albuquerque, New Mexico.

Walter, G. R., H. W. Bentley, and J. J. Ward, Hydro Geo Chem, Inc., and D. D. Gonzalez, 1983. "Continuum and Non-Continuum Aspects of Groundwater Movement at the Waste Isolation Pilot Plant, Southeastern New Mexico," Sandia National Laboratories, Albuquerque, New Mexico, in Transactions, AGU Fall Meeting Hydrology Section, p. 713.

Walter, G. R., and Hydro Geo Chem, Inc., 1983. A Three-Well Technique for Determining Formation Anisotropy at the Waste Isolation Pilot Plant (WIPP) Southeastern New Mexico, SAND83-7011, Sandia National Laboratories, Albuquerque, New Mexico.

Walter, G. R. "Convergent-Flow Tracer Test at H-6: Waste Isolation Pilot Plant (WIPP), Southeastern New Mexico," SAND83-7015, (in preparation), Sandia National Laboratories, Albuquerque, New Mexico.

Ward, J. J., and D. D. Gonzales, 1981. "Anisotrophy Tests in the Culebra Dolomite at F-4, H-5, and H-6 Sites, The WIPP, Southeast New Mexico," (in preparation).

Ward, J. J., and G. R. Walter, 1983. A Three Well Technique for Determining Formation Anisotropy at the Waste Isolation Pilot Plant (WIPP) Southeast New Mexico, SAND83-7011, Sandia National Laboratories, Albuquerque, New Mexico.

Ward, J. J., G. R. Walter, Hydro Geo Chem Inc., and D. D. Gonzalez, 1983. "Heterogeneity and Anisotrophy of a Groundwater System in Carbonate Rocks at the Waste Isolation Pilot Plant (WIPP)," Sandia National Laboratories, Albuquerque, New Mexico, in Transactions AGU Fall Meeting Hydrology Section.

Welder, G. E, 1983. "Geohydrologic Framework of the Roswell Groundwater Basin, Chavez and Eddy Counties, New Mexico," New Mexico State Engineer Technical Report 42, 28 pp.

Winstanley, D. J., and R. C. Carrasco, 1986. Annual Hydrogeologic Data Report 1985/1986, DOE/WIPP-004, Waste Isolation Pilot Plant, Carlsbad, New Mexico.

Wofsy, C., 1980. The Significance of Certain Rustler Aquifer Parameters for Predicting Long-Term Radiation Doses from WIPP, EEG-8, State of New Mexico Environmental Evaluation Group, Santa Fe, New Mexico.

Wood, B. J., R. E. Snow, D. J. Cosler, and S. Haji-Djafari, 1982. "Delaware Mountain Group (DMG) Hydrology - Salt Removal Potential," TME-3166, U.S. Department of Energy, Albuquerque, New Mexico.

J.7 REPOSITORY TECHNOLOGY

Abrego, L., and J. W. Braithwaite, 1980. Corrosion of Titanium in Saline Nuclear Waste Isolation Environments, SAND80-0325A, Sandia National Laboratories, Albuquerque, New Mexico, presented at the American Nuclear Society Annual Meeting, Las Vegas, Nevada.

Abrego, L., and H. J. Rack, 1981. The Slow Strain Rate Behavior of TiCode 12 (ASTM Gr. 12) in Aqueous Chloride Solutions, SAND80-1738C, Sandia National Laboratories, Albuquerque, New Mexico, presented at Corrosion/81, National Association of Corrosion Engineers Meeting, Toronto, Canada.

Acton, R. V., 1977. "Thermal Conductivity of SE New Mexico Rock Salt and Anhydrite," unpublished Sandia National Laboratories preliminary report, Albuquerque, New Mexico.

Adcock, L., 1978. An Outline of the Input-Output Model and the Impact Projections Methodology, Tech Document Socioeconomic Portion Waste Isolation Pilot Environmental Impact Report, SAND78-7061, Sandia National Laboratories, Albuquerque, New Mexico.

Adcock & Associates, 1980. Sociocultural Analysis for the Proposed Waste Isolation Pilot Plant, SAND80-7155, Sandia National Laboratories, Albuquerque, New Mexico.

Adcock & Associates, 1980. Socioeconomics Study for Proposed Waste Isolation Pilot Plant, SAND80-7123, Sandia National Laboratories, Albuquerque, New Mexico.

Arguello, J. G., and R. Beraum, 1986. Numerical Simulation of Drift Response Resulting from the Emplacement of RH TRU Waste in an Array of Horizontal Long Boreholes in a Separate Panel, SAND86-2224A, Sandia National Laboratories, Albuquerque, New Mexico, presented at the U.S. Symposium on Rock Mechanics, Tucson, Arizona.

Arguello, J. G., and H. S. Morgan, 1986. Numerical Simulation of the Creep Response of Model Salt Pillars, SAND85-2429, Sandia National Laboratories, Albuquerque, New Mexico.

Arguello, J. G., 1987. Numerical Simulation of WIPP Panel Entryway Seal/Formation Structural Interaction, SAND87-2257A, Sandia National Laboratories, Albuquerque, New Mexico, presented at the Ninth U.S. Symposium on Rock Mechanics at Minneapolis, Minnesota.

Arguello, J.G., 1987. WIPP Panel Entryway Seal—Numerical Simulation of Seal Composite Interaction for Preliminary Seal Design Evaluation, SAND87-2804, Sandia National Laboratories, Albuquerque, New Mexico.

Arguello, J. G., and R. Beraun, 1987. Numerical Simulation of Drift Response in Rock Salt Resulting From the Emplacement of RH TRU Waste in an Array of Horizontal Long Boreholes in a Separate Panel at the WIPP, SAND86-2224C, Sandia National Laboratories, Albuquerque, New Mexico.

Arguello, J. G., D. E. Munson, and D. S. Preece, 1987. Preliminary Results of the Three-Dimensional Modeling of the WIPP Room D Excavation Sequence, SAND86-2380C, Sandia National Laboratories, Albuquerque, New Mexico, presented at U.S. Symposium on Rock Mechanics, Tucson, Arizona.

Arguello, J. G., and T. M. Torres, 1987. WIPP Panel Entryway Seal—Numerical Simulation of Seal Component/Formation Interaction for Preliminary Seal Design Evaluation, SAND87-2591, Sandia National Laboratories, Albuquerque, New Mexico.

Anderson, H. M., J. Pietz, and D. Smith, 1983. Solutions to Radionuclide Migration with Nonlinear Retardation Mechanisms in Backfill Material, Interim Progress Report, June-December 1982, SAND82-7089, Sandia National Laboratories, Albuquerque, New Mexico.

Anderson, H. M., J. M. Pietz, and D. M. Smith, 1984. "Radionuclide Transport Modeling of Diffusion Cell Experiments Specific to a Backfill Barrier in a Salt Repository," Scientific Basis for Nuclear Waste Management VII, Materials Research Society Symposia Proceedings, Vol. 26, ed. G. L. McVay, North-Holland, New York.

Arnold, G. W., 1980. Radiation Hardening of Rock Salt, SAND80-1566C, Sandia National Laboratories, Albuquerque, New Mexico, presented at Annual Meeting of the Materials Research Society, Boston, Massachusetts.

Baes, C. F., Jr., L. O. Gilpatrick, F. G. Kitts, H. R. Bronstein, and A. J. Shor, 1983. The Effect of Water in Salt Repositories: Final Report, ORNL-5950, Oak Ridge National Laboratory, Oak Ridge, Tennessee.

Bard, S. T., 1982. Estimated Radiation Doses Resulting if an Exploratory Borehole Penetrates a Pressurized Brine Reservoir Assumed to Exist Below the WIPP Repository Horizon—A Single Borehole Scenario, EEG-15, New Mexico Environmental Evaluation Group, Santa Fe, New Mexico.

Barnhart, B. J., D. E. Caldwell et al. (Los Alamos Scientific Laboratory and University of New Mexico), 1978-79. Potential Microbial Impact on Transuranic Wastes Under Conditions Expected in the Waste Isolation Pilot Plant (WIPP), Progress Reports: LA-7788-PR, LA-7839-PR, LA-7918-PR, LA-8297-PR.

Barr, G. E., F. W. Bingham, and M. S. Tierney, 1980. The Use and Misuse of Generic Scenarios, SAND80-1537A, Sandia National Laboratories, Albuquerque, New

Mexico, presented at OECD Workshop on Radionuclide Release Scenarios for Geologic Repositories in Paris, France.

Barrows, L. J., and C. W. Cook, 1980. WIPP Statement of Work for Subsurface Geophysical Survey of the Hill C Breccia Pipe, Sandia National Laboratories, Albuquerque, New Mexico.

Beall, G. W., draft, April 1982. Chemistry and Solution Effects on Radionuclides in Backfill Materials, Final Report, SAND82-7222, Sandia National Laboratories, Albuquerque, New Mexico.

Beall, G. W., draft, April 1982. A Literature Survey of Near-Field Effects in a Bedded Salt Nuclear Waste Repository Site, SAND81-7218, Sandia National Laboratories, Albuquerque, New Mexico.

Beauheim, R. L., S. R. Black, C. L. Christensen, T. O. Hunter, L. Jarolimek, A. K. Kuhn, S. J. Lambert, R. F. McKinney, D. Meyer, J. B. Murray, R. S. Newton, D. W. Powers, C. L. Stein, D. E. Stephenson, B. R. Sullivan, M. J. Timmer, and W. D. Weart, 1983a. Results of Site Validation Experiments, Waste Isolation Pilot Plant (WIPP) Project, Southeastern New Mexico, TME-3177, U.S. Department of Energy, Albuquerque, New Mexico (2 Vols.).

Beauheim, R. L., 1988. Salado Permeability Measurements in Holes Drilled from the Surface and the Waste-Handling Shaft, presentation to the National Research Council/National Academy of Science WIPP Panel.

Bechtel National, Inc., 1983. "Waste Isolation Pilot Plant, Preliminary Design Validation Report," compiled for U.S. Department of Energy, Albuquerque, New Mexico.

Beraun, R., and M. A. Molecke, 1987. Numerical Thermal Modeling of the WIPP In Situ Room A1 Simulated DHLW Experiments, SAND87-0467C, Sandia National Laboratories, Albuquerque, New Mexico, presented at Waste Management 1987, Tucson, Arizona.

Beraun, R., and M. A. Molecke, 1987. Thermal Analysis of the WIPP In Situ Room A1 DHLW Package Experiments, SAND86-0681, Sandia National Laboratories, Albuquerque, New Mexico.

Bibler, N. E., 1977. TRU Waste Form and Package Criteria Meeting, Sheraton Old Town, Albuquerque, New Mexico, (cassettes only), SAND77-1178, Sandia National Laboratories, Albuquerque, New Mexico.

Bibler, N. E., 1978-81. Gas Production from Alpha Radiolysis of Concrete Containing TRU Incineratory Ash, Progress Reports: DPST-78-150-1, DPST-78-150-2, DPST-80-150-1, DPST-80-150-2, Savannah River Laboratory, Aiken, South Carolina.

Bibler, N. E., 1979. Radiolytic Gas Generation in Concrete Made with Incinerator Ash Containing Transuranium Nuclides, DP-MS-79-25, Savannah River Laboratory,

Aiken, South Carolina, presented at Materials Research Society, Boston, Massachusetts, November, 1979, published in Scientific Basis for Nuclear Waste Management, Volume 2.

Biffle, J. H., 1981. Second Benchmark Problem for WIPP Structural Computation with the JAC Computer Program, SAND81-0767, Sandia National Laboratories, Albuquerque, New Mexico.

Biffle, J. H., 1984. JAC—A Two-Dimensional Finite Element Computer Program for the Non-Linear Quasistatic Response of Solids with the Conjugate Gradient Method, SAND81-0998, Sandia National Laboratories, Albuquerque, New Mexico.

Bingham, F. W., and G. E. Barr, 1979. "Development of Scenarios for the Long-Term Release of Radionuclides from the Proposed Waste Isolation Pilot Plant in Southeastern New Mexico," SAND79-0955c, Sandia National Laboratories, Albuquerque, New Mexico, published in Proceedings of International Symposium on Scientific Basis for Nuclear Waste Management, Materials Research Society, Vol. 2, pp. 771-778.

Black, S. R., R. S. Newton, and D. K. Shukla, ed., 1983. Results of Site Validation Experiments, Volumes I and II, TME-3177, prepared for U.S. Department of Energy by TSC-D'Appolonia.

Boa, J. A., Jr., 1978. Borehole Plugging Program (Waste Disposal), Report 1, Initial Investigations and Preliminary Data, SAND77-7005, Sandia National Laboratories, Albuquerque, New Mexico.

Boa, J. A., Jr., 1981. Borehole Plugging Program (Waste Disposal), Report 2, Petrographic Examination of Several Four-Year-Old Laboratory-Developed Grout Mixtures, MPC-78-1, prepared for Sandia National Laboratories, Albuquerque, New Mexico.

Borns, D. J., and J. C. Stormont, 1987. "Delineation of the Disturbed Rock Zone Around Excavations in Salt, Waste Isolation Pilot Plant (WIPP), Southeastern New Mexico," Geological Society of America Abstracts with Programs, Vol. 19, No. 6.

Borns, D. J., and J. C. Stormont, 1987. "Delineation of the Disturbed Rock Zone Around Excavations in Salt," Geological Society of America Abstracts with Programs, Vol. 19, No. 7.

Borns, D. J., and J. C. Stormont, 1988. "An Interim Report on Excavation Effects Studies at the Waste Isolation Pilot Plant," SAND86-xxx, (in preparation), Sandia National Laboratories, Albuquerque, New Mexico.

Boyd, R. D., 1978. Forced-Air Cooling of a WIPP Mine Drift, SAND78-1122, Sandia National Laboratories, Albuquerque, New Mexico.

Bradshaw, R. L., and F. Sanchez, 1969. "Migration of Brine Cavities in Rock Salt," Journal of Geophysical Research, Vol. 74, pp. 4209-4212.

Bradshaw, R. L., and W. C. McClain, 1971. Project Salt Vault, A Demonstration of the Disposal of High-Activity Solidified Waste in Underground Salt Mines, Oak Ridge National Laboratories, No. 4555, Oak Ridge, Tennessee.

Braithwaite, J. W., and M. A. Molecke, 1978. High-Level Waste Canister Corrosion Studies Pertinent to Geologic Isolation, SAND78-2111, Sandia National Laboratories, Albuquerque, New Mexico.

Braithwaite, J. W., and N. J. Magnani, 1979. "Corrosion Considerations for Nuclear Waste Isolation Canisters," SAND78-1093C, Sandia National Laboratories, Albuquerque, New Mexico, presented at Materials Research Society, Boston, Massachusetts, published in Scientific Basis for Nuclear Waste Management, Vol. 1, ed. G. J. McCarthy, Plenum Press, New York.

Braithwaite, J. W., and M. A. Molecke, 1979. Corrosion and Anti-Corrosion Coatings Studies for TRU Waste Containers, Section 7 in Summary of Research and Development Activities in Support of Waste Acceptance Criteria for WIPP, SAND79-1305, Sandia National Laboratories, Albuquerque, New Mexico.

Braithwaite, J. W., N. J. Magnani, and J. W. Munford, 1979. Corrosion of Candidate Nuclear Waste Canister Alloys, SAND79-1560C, Sandia National Laboratories, Albuquerque, New Mexico, presented at AIME Meeting, Las Vegas, Nevada.

Braithwaite, J. W., 1980. "Brine Chemistry Effects on the Durability of a Simulated Nuclear Waste Glass," SAND79-0900C, Sandia National Laboratories, Albuquerque, New Mexico, presented at Materials Research Society, Boston, Massachusetts, published in Scientific Basis for Nuclear Waste Management, Vol. 2, ed. C. J. Northrup, Plenum Press, New York.

Braithwaite, J. W., and J. K. Johnstone, 1980. "Chemical Durability and Characterization of Nuclear Waste Forms in a Hydrothermal Environment," SAND78-2259C, Sandia National Laboratories, Albuquerque, New Mexico, presented at American Ceramic Society Conference, Cincinnati, Ohio, published in Ceramics in Nuclear Waste Management, (CONF-79420).

Braithwaite, J. W., N. J. Magnani, and J. W. Munford, 1980. Titanium Alloy Corrosion in Nuclear Waste Environments, SAND79-2023C, Sandia National Laboratories, Albuquerque, New Mexico, presented at Corrosion 80, National Association of Corrosion Engineers, Chicago, Illinois.

Braithwaite, J. W., and M. A. Molecke, 1980. "Nuclear Waste Canister Corrosion Studies Pertinent to Geologic Isolation," SAND79-1935J, Sandia National Laboratories, Albuquerque, New Mexico, published in Nuclear and Chemical Waste Management, Vol. 1, No. 1, pp. 37-50.

Braithwaite, J. W., 1987. The Corrosion Behavior of Metals in Terminal Nuclear Waste Storage Environments, SAND77-1812C, Sandia National Laboratories, Albuquerque, New Mexico, presented at Corrosion/78, National Association of Corrosion Engineers, Houston, Texas.

Brandshaug, Terje (RE/SPEC, Inc.), 1986. A Thermomechanical Analysis of WIPP DHLW Experiments: Waste Container/Borehole Interactions, SAND85-7210, Sandia National Laboratories, Albuquerque, New Mexico.

Branstetter, L. J., R. D. Krieg, and C. M. Stone, 1981. A Method for Modeling Regional Scale Deformation and Stresses Around Radioactive Waste Depositories in Bedded Salt, SAND81-0237, Sandia National Laboratories, Albuquerque, New Mexico.

Branstetter, L. J., C. M. Stone, and R. D. Krieg, 1981. WIPP Benchmark II Results Using SANCHO, SAND81-0853, Sandia National Laboratories, Albuquerque, New Mexico.

Branstetter, L. J., R. D. Krieg, and C. M. Stone, 1982. The Effect of a Random Variation of Rock Salt Creep on Calculations of Storage Room Closure for the WIPP Project, SAND82-0024, Sandia National Laboratories, Albuquerque, New Mexico.

Branstetter, L. J., 1983. Pretest Parametric Calculations for the Heated Pillar Experiment in the WIPP In Situ Experimental Area, SAND82-2781, Sandia National Laboratories, Albuquerque, New Mexico.

Branstetter, L. J., R. D. Krieg, and C. M. Stone, 1983. The Effects of a Random Variation of Rock Salt Creep on Closure Calculations for an Excavated Opening in a Complex Stratigraphy, SAND82-2256A, presented at ASCE Engineering Mechanics Division, Specialty Conference, Purdue University.

Branstetter, L. J., 1985. Second Reference Calculation for the WIPP, SAND82-2461, Sandia National Laboratories, Albuquerque, New Mexico.

Brausch, L. M., J. S. Hart, K. R. Porter, and J. K. Register, 1980. Technical and Environmental Analyses, Development of the Site and Preliminary Design Validation Program, Los Medanos Site, Southeastern New Mexico, TME 3058, WIPP Technical Support Contractor, Albuquerque, New Mexico.

Brunton, G. D., and W. C. McClain, 1977. Geological Criteria for Radioactive Waste Repositories, Y/OWI/TM-47, Office of Waste Isolation, Union Carbide Corporation, Oak Ridge, Tennessee.

Buck, A. D., J. P. Burkes, and J. E. Rhoderick, 1981. Examination of ERDA-10 Grout Specimens at Different Ages, USAE Waterways Experiment Station Miscellaneous Paper SL-81-20, (also issued as ONWI-341).

Buck, A. E. et al., 1983. Modification of Bell Canyon Test (BCT) 1-FF Grout, miscellaneous paper SL-83-18, SAND83-7097, U.S. Army Engineer Waterways.

Buck, A. D., 1985. Development of a Sanded Expansive Salt Grout for Repository Sealing Application, SL-85-6, Office of Nuclear Waste Isolation, Columbus, Ohio.

Buck, A. D., 1985. Development of Two Candidate Concrete Mixtures (Salt, Nonsalt) for Repository Sealing Applications, SL-85-8, Office of Nuclear Waste Isolation, Columbus, Ohio.

Buck, A. D., J. A. Boa, and D. M. Walley, 1985. Development of a Sanded Expansive Salt Grout for Repository Sealing Application, SL-85-11, Office of Nuclear Waste Isolation, Columbus, Ohio.

Buck, A. D., 1987. Effect of Salt-Saturated Mixing Water on Long-Term Durability of Hydraulic-Cement Mixtures, Structures Laboratory, USAE Waterways Experiment Station Draft Report to Sandia National Laboratories, Albuquerque, New Mexico.

Burkes, J. P., and J. E. Rhoderick, 1983. Petrographic Examination of Bell Canyon Tests (BCT) 1-FF Field Grouts Over a Three-Year Period, SL-83-12, Office of Nuclear Waste Isolation, Columbus, Ohio.

Burkes, J. P., and J. E. Rhoderick, 1983. Petrographic Examination of Bell Canyon Tests (BCT) 1-FF Field Grouts Over a Three-Year Period, miscellaneous paper SL-83-12, SAND83-7115, Sandia National Laboratories, Albuquerque, New Mexico.

Butcher, B. M., 1980. Creep Consolidation of Nuclear Depository Backfill Materials, SAND79-22-12, Sandia National Laboratories, Albuquerque, New Mexico.

Butcher, B. M., 1981. An Elastic-Plastic Mechanical Constitutive Description for Rock Salt Triaxial Compression, SAND80-1935, Sandia National Laboratories, Albuquerque, New Mexico.

Butcher, B. M., and J. P. Hill, 1984. A Method for Defining the Distribution of Triaxial Stress States in Underground Structures, SAND83-2506, Sandia National Laboratories, Albuquerque, New Mexico.

Caldwell, D. E., M. A. Molecke, R. C. Hallet, E. Martinez, and B. J. Barnhart, 1987. Rates of CO_2 Production from the Microbial Degradation of Transuranic Wastes Under Simulated Geologic Isolation Conditions, SAND87-7170, Sandia National Laboratories, Albuquerque, New Mexico.

Canfield, T. R., 1983. Stresses Near Waste Canisters Buried in Salt, SAND82-0525, Sandia National Laboratories, Albuquerque, New Mexico.

Case, J. B., S. M. Dass, J. G. Franzone, and A. K. Kuhn, 1982. Analysis of Potential Impacts of Brine Flow Through Boreholes Penetrating the WIPP Storage Facility, TME-3155, U.S. Department of Energy, Albuquerque, New Mexico.

Case, J. B., P. C. Kelsall, and J. L. Withiam, 1987. "Laboratory Investigation of Crushed Salt Consolidation," Proceedings of the 28th U.S. Rock Mechanics Symposium, Tucson, Arizona, Pub. A. A. Balkema, ed. I. W. Farmer, J. K. Daemen, C. S. Desai, C. E. Glass, and S. P. Neuman, pp. 189-196.

Channell, J. K., 1982. Calculated Radiation Doses from Radionuclides Brought to the Surface if Future Drilling Intercepts the WIPP Repository and Pressurized Brine, EEG-11, New Mexico Environmental Evaluation Group, Santa Fe, New Mexico.

Christensen, C. L., 1979. Bell Canyon Test, WIPP Experimental Program Borehole Plugging, Sandia National Laboratories, Albuquerque, New Mexico.

Christensen, C. L., 1979. Field Test Programs of Borehole Plugs in Southeastern New Mexico, SAND79-1634C, Sandia National Laboratories, Albuquerque, New Mexico, presented at ONWI, Columbus, Ohio.

Christensen, C. L., 1979. Potash Core Test, WIPP Experimental Program Borehole Plugging, Sandia National Laboratories, Albuquerque, New Mexico.

Christensen, C. L., 1979. Test Plan—Bell Canyon Test, WIPP Experimental Program Borehole Plugging, SAND79-0739, Sandia National Laboratories, Albuquerque, New Mexico.

Christensen, C. L., 1979. Test Plan—Potash Core Test, WIPP Experimental Program Borehole Plugging, SAND79-0739, Sandia National Laboratories, Albuquerque, New Mexico.

Christensen, C. L., C. W. Cook, and C. W. Gulick, 1979. Borehole Plugging Program Status Report, October 1, 1978 - September 30, 1979 (January 1980), SAND79-2141, Sandia National Laboratories, Albuquerque, New Mexico.

Christensen, C. L., 1980. Results from the Bell Canyon Borehole Plugging Test, SAND80-2376C, presented at 1980 National Waste Terminal Storage Program Information Meeting, Columbus, Ohio.

Christensen, C. L., 1980. Sandia Borehole Plugging Program for the Waste Isolation Pilot Plant (WIPP), SAND80-0390C, Sandia National Laboratories, Albuquerque, New Mexico, presented at Workshop on Borehole and Shaft Plugging, Columbus, Ohio.

Christensen, C. L. 1980. Thermal Conductivity Probe Repeatability Assessment, Sandia National Laboratories, Albuquerque, New Mexico.

Christensen, C. L., and T. O. Hunter, 1980. Bell Canyon Test and Results, SAND80-2414C, presented at Materials Research Society Meeting, Boston, Massachusetts.

Christensen, C. L., and T. O. Hunter, 1980. The Bell Canyon Test and Results, SAND80-1557A, Sandia National Laboratories, Albuquerque, New Mexico, presented at Scientific Basis for Nuclear Waste Management Symposium, Boston, Massachusetts.

Christensen, C. L., R. D. Statler, and E. W. Peterson, 1980. Downhole Television Applications in Borehole Plugging, SAND80-0459, Sandia National Laboratories, Albuquerque, New Mexico.

Christensen, C. L., 1981. Trapped Gas Experiment, Sandia National Laboratories, Albuquerque, New Mexico.

Christensen, C. L., C. W. Gulick, and S. J. Lambert, 1981. Sealing Concepts for the Waste Isolation Pilot Plant (WIPP) Site, SAND81-2195, Sandia National Laboratories, Albuquerque, New Mexico.

Christensen, C. L., and E. W. Peterson, 1981. "Field-Test Programs of Borehole Plugs in Southeastern New Mexico," in Advances in the Science and Technology of the Management of High-Level Nuclear Waste, Vol. I, Office of Nuclear Waste Isolation (ONWI), DOE/Tic-4621-Vol. 1, pp. 354-369.

Christensen, C. L., and E. W. Peterson, 1981. Bell Canyon Test Summary Report, SAND80-1375, Sandia National Laboratories, Albuquerque, New Mexico.

Christensen, C. L., 1984. Compliance with Prescribed Plugging Criteria for Reentry, Preparation, and Cementing of the B-25 Borehole at the WIPP Site, SAND83-2189A, Sandia National Laboratories, Albuquerque, New Mexico, presented at Waste Management 1984, Tucson, Arizona.

Christensen, C. L., and J. C. Stormont, 1984. Compliance with Prescribed Plugging Critera for the Reentry, Preparation, and Cementing of the B-25 Borehole at the WIPP Site, Memorandum of Record, Sandia National Laboratories, Albuquerque, New Mexico.

Claiborne, H. C., and F. Gera, 1974. Potential Containment Failure Mechanisms and Their Consequences at a Radioactive Waste Repository in Bedded Salt in New Mexico, ORNL-TM-4639, Oak Ridge National Laboratory, Oak Ridge, Tennessee.

Claiborne, H. C. et al., 1980. Expected Environments in High-Level Nuclear Waste and Spent Fuel Repositories in Salt, ORNL/TM-7201, Oak Ridge National Laboratory, Oak Ridge, Tennessee.

Comes, G. D., L. D. Wakeley, and E. F. O'Neil, 1987. Laboratory-Tested Specimens of Concrete from Small Scale Seal Performance Tests at the Waste Isolation Pilot Plant, MP SL-87-9, prepared for Sandia National Laboratories, Albuquerque, New Mexico.

Cook, C. W., 1979. Instrumentation Development for the Waste Isolation Pilot Plant (WIPP) Borehole Plugging Program, SAND79-1902, Sandia National Laboratories, Albuquerque, New Mexico.

Cook, C. W. and E. S. Ames, 1979. "Borehole-Inclusion Stressmeter Measurements in Bedded Salt," SAND79-0377C, Sandia National Laboratories, Albuquerque, New

Mexico, presented at Proceedings of the 20th U.S. National Symposium in Rock Mechanics, Austin, Texas.

Cook, C. W., and A. R. Sattler, 1979. Scanning of Intact Salt in the Avery Island Mine with Radar, Sandia National Laboratories, Albuquerque, New Mexico.

Cook, C. W., 1980. Impulse Radar Scanning of Intact Salt at the Avery Island Mine, SAND80-0632, Sandia National Laboratories, Albuquerque, New Mexico.

Cook, C. W., and E. S. Ames, 1980. Borehole-Inclusion Stressmeter Measurements in Bedded Salt, SAND79-0377, Sandia National Laboratories, Albuquerque, New Mexico.

Cook, C. W., C. B. Kinabrew, P. L. Lagus, and R. D. Broce, 1980. Bell Canyon Test (BCT) Instrumentation Development, SAND80-0408C, Sandia National Laboratories, Albuquerque, New Mexico, presented at the International BHP Symposium, Columbus, Ohio.

Cook, C. W., 1982. Underground Scanning with an Impulse Radar, SAND82-0470, Sandia National Laboratories, Albuquerque, New Mexico.

Cooley, C. H., S. W. Butters, and A. H. Jones, 1978. Permeability of Rock Salt to Gases and Liquids, TR78-62, prepared for Sandia National Laboratories, Albuquerque, New Mexico.

Cooley, C. H., and S. W. Butters, 1979. Pressure Time Effects on Permeability of Salt Cores, TR79-45, prepared for Sandia National Laboratories, Albuquerque, New Mexico.

Costin, L. S., 1979. Summary of Research and Development Activities in Support of Waste Acceptance Criteria for WIPP, SAND79-1305, Sandia National Laboratories, Albuquerque, New Mexico.

Costin, L. S., and W. R. Wawersik, 1980. Creep Healing of Fractures in Rock Salt, SAND80-0392, Sandia National Laboratories, Albuquerque, New Mexico.

D'Appolonia Consulting Engineers, Inc., 1979. Repository Sealing Design Approach--1979, ONWI-55, Office of Nuclear Waste Isolation, Columbus, Ohio.

D'Appolonia Consulting Engineers, Inc. 1981. Sealing Consideration for Repository Shafts in Bedded and Dome Salt, ONWI-255, Office of Nuclear Waste Isolation, Columbus, Ohio.

Dawson, P. R., and J. R. Tillerson, 1977. Comparative Evaluations of the Thermo-mechanical Responses for Three High-Level Waste Canister Emplacement Alternatives, SAND77-0388, Sandia National Laboratories, Albuquerque, New Mexico.

Dawson, P. R., and J. R. Tillerson, 1978. Nuclear Waste Canister Thermally Induced Motion, SAND78-0566, Sandia National Laboratories, Albuquerque, New Mexico.

Dawson, P. R., and J. R. Tillerson, 1978. Salt Motion Following Nuclear Waste Disposal, SAND77-1226C, Sandia National Laboratories, Albuquerque, New Mexico, presented at the Conference of Evaluation and Prediction of Subsidence, Pensacola, Florida.

Dawson, P. R., 1979. Constitutive Models Applied in the Analysis of Creep of Rock Salt, SAND79-0137, Sandia National Laboratories, Albuquerque, New Mexico.

Dawson, P. R., and D. E. Munson, 1983. "Numerical Simulation of Creep Deformations Around a Room in a Deep Potash Mine," SAND82-0184J, Sandia National Laboratories, Albuquerque, New Mexico, published in International Journal of Rock Mechanics & Mineral Science, Vol. 20, pp. 33-42.

Deal, D. E., and J. B. Case, 1987. Brine Sampling and Evaluation Program, Phase I Report, DOE/WIPP-87-008, U.S. Department of Energy, Carlsbad, New Mexico.

Dennis, A. W. et al., 1978. Revised Concept for the Waste Isolation, SAND78-1429, Sandia National Laboratories, Albuquerque, New Mexico.

DOE (U.S. Department of Energy), 1980. "Statement of the Position of the United States Department of Energy in the Matter of Proposed Rulemaking on the Storage and Disposal of Nuclear Waste (NRC Waste Confidence Rulemaking)," DOE/NE-0007, Washington, D.C.

DOE (U.S. Department of Energy), 1981. "Waste Isolation Pilot Plant Safety Assessment: DOE Report," Vol. 1, Chap. 2, pp. 2.6-2 to 2.6-7.

DOE (U.S. Department of Energy), 1982. "Site Validation Program," DOE/WIPP-116, Revision 1, Waste Isolation Pilot Plant Project Office.

DOE (U.S. Department of Energy), 1983. DOE Responses to the State of New Mexico's Comments on Summary of Results of the Evaluation of the WIPP Site and Preliminary Design Validation Program, DOE/WIPP-161, DOE/WIPP-174, Albuquerque, New Mexico.

DOE (U.S. Department of Energy), 1983. "Geotechnical Activities in the Exploratory Shaft," TME-3178.

DOE (U.S. Department of Energy), 1983. "Results of Site Validation Experiments," Vol. II, supporting documents 5 through 14, Technical Support Contract DE-AC04-78AL05346, TME-3177 DOE/AL, Albuquerque, New Mexico.

DOE (U.S. Department of Energy), 1984. "Geotechnical Activities in the Waste Handling Shaft," WSTD-TME-038.

DOE (U.S. Department of Energy), 1984. "Radioactive Waste Management," DOE Order 5820.2.

DOE (U.S. Department of Energy), 1985. "Radioactive Waste Management," DOE Order, AL 5820.2.

DOE (U.S. Department of Energy), 1986. "Design Validation Final Report," WIPP/DOE 86-010, DOE Carlsbad, New Mexico.

DOE (U.S. Department of Energy), 1987. "Exhaust Shaft Grouting Program 'C', Report for Week Ending June 21," WIPP, Carlsbad, New Mexico.

DOE (U.S. Department of Energy), 1988. "Final Safety Analysis Report, Waste Isolation Pilot Plant, (Draft)," DOE/WIPP 87-013, DOE Carlsbad, New Mexico.

DOE (U.S. Department of Energy), 1988. "Panel One Monitoring Plan for the Waste Isolation Pilot Plant (Draft)," DOE Carlsbad, New Mexico.

Duffy, T. A., 1980. The Salt Block I Test: Experimental Details and Comparison with Theory, Los Alamos Technical Associates, Inc. (LATA 102), SAND79-7050, Sandia National Laboratories, Albuquerque, New Mexico.

Dunn, L. A., 1981. Development Report for Contact-Handled Waste Container and Handling System, SAND81-0141, Sandia National Laboratories, Albuquerque, New Mexico.

Eaton, R. R., 1984. Three-Dimensional Thermal Analysis for the WIPP In Situ Test Room A Heater Configuration, SAND84-2220, Sandia National Laboratories, Albuquerque, New Mexico.

EEG (Environmental Evaluation Group), 1980. "Geotechnical Considerations for Radiological Hazard Assessment of WIPP: A Report of a Meeting Held on January 17-18, 1980."

EEG (Environmental Evaluation Group), 1980. Review Comments on the Report of the Steering Committee on Waste Acceptance Criteria for the Waste Isolation Pilot Plant, M. S. Little, EEG-4, Health and Environment Department, State of New Mexico, Santa Fe, New Mexico.

EEG (Environmental Evaluation Group), 1981. "Radionuclide Release, Transport and Consequence Modeling for WIPP: A Report of a Workshop Held on September 16-17, 1981", EEG-27.

EEG (Enviromental Evaluation Group), 1983. "Review Comments on the Geotechnical Reports Provided by DOE to EEG Under the Stipulated Agreement through March 1, 1983", EEG-22.

EEG (Environmental Evaluation Group), 1984. Radiation Shielding in the Hot Cell Facility at the Waste Isolation Pilot Plant: A Review, H. B. Knowles, EEG-28,

Health and Environment Department, State of New Mexico, Santa Fe, New Mexico.

EEG (Environmental Evaluation Group), 1985. Evaluation of the Safety Analysis Report for the Waste Isolation Pilot Plant Project, M. S. Little, EEG-29, Health and Environment Department, State of New Mexico, Santa Fe, New Mexico.

EEG (Environmental Evaluation Group), 1985. Evaluation of the Waste Isolation Pilot Plant Classification of Systems, Structures, and Components, EEG-30, Submitted by the Tenera Corporation, Health and Environment Department, State of New Mexico, Santa Fe, New Mexico.

EEG (Environmental Evaluation Group), 1987. Exhaust Stack Monitoring Issuses at the Waste Isolation Pilot Plant, EEG-37, Health and Environment Department, State of New Mexico, Santa Fe, New Mexico.

EEG (Environmental Evaluation Group), 1988. A Critical Assessment of Continuous Air Monitoring Systems at the Waste Isolation Pilot Plant, J. C. Rodgers and J.W. Kenney, EEG-38, Health and Environment Department, State of New Mexico, Santa Fe, New Mexico.

Ekren, E. B. et al., 1974. Geologic and Hydrologic Considerations for Various Concepts of High-Level Radioactive Waste Disposal in Conterminous United States, U.S. Geological Survey Open-File Report 74-158.

Evans, B., 1983. "Alteration of Porosity and Permeability by Plastic Flow Processes in Rocks," No. 27664, Geological Society of America Abstracts with Programs, Vol. 15, No. 6.

Ewing, R. I., and A. R. Sattler, 1979. Measurement of Gamma Radiation Background at Avery Island Mine, Sandia National Laboratories, Albuquerque, New Mexico.

Ewing, R. I., 1979. Test of a Radiant Heater in the Avery Island Salt Mine, Sandia National Laboratories, Albuquerque, New Mexico.

Ewing, R. I., 1981. Preliminary Moisture Release Experiment in a Potash Mine in Southeastern New Mexico, SAND81-1318, Sandia National Laboratories, Albuquerque, New Mexico.

Ewing, R. I., 1982. Environmental Gamma Ray Spectra from Selected Sites in Southeastern New Mexico, SAND82-0738, Sandia National Laboratories, Albuquerque, New Mexico.

Ewing, R. I., and H. C. Shefelbine, 1980. Preliminary Moisture Release Experiment in the Mississippi Chemical Potash Mine, Sandia National Laboratories, Albuquerque, New Mexico.

Ewing, R. I., and H. C. Shefelbine, 1981. Test Plan for Three Heater Moisture Release Experiment, Sandia National Laboratories, Albuquerque, New Mexico.

Fenix & Scisson, Inc., 1978. WIPP 18, 19, 21, and 22 Field Engineering Summary, Vols. I and II, Sandia National Laboratories, Albuquerque, New Mexico.

Ferrall, C., and J. F. Gibbons (Civil Systems, Inc.), 1980. Core Study of Rustler Formation Over the WIPP Site, CSI-2055-03, SAND79-7110, Sandia National Laboratories, Albuquerque, New Mexico.

Fortney, D. R., and M. G. Seitz, 1981. Test Plan: Development of Dynamic Stream Simulation Methodology, Sandia National Laboratories, Albuquerque, New Mexico.

Fossum, A. F., 1986. Computer Calculations to Develop Quality Assurance (QA) Methodology for Nuclear Waste Repository Design Calculations: Isothermal Parallel Calculations, SAND85-7262, Sandia National Laboratories, Albuquerque, New Mexico.

Franke, C., 1987. "Excavation Effects and Fracture Mapping," Input to 1987 GFDAR, August 18 Memorandum to R. McKinney, International Technology Corporation WIPP Site, Carlsbad, New Mexico.

Gartling, D. K., 1981. MERLIN: A Computer Program to Transfer Data Between Finite Element Meshes, SAND81-0463, Sandia National Laboratories, Albuquerque, New Mexico.

George, O. L., Jr., 1980. Computer Thermal Modeling for the Salt Block II Experiment, SAND79-2250, Sandia National Laboratories, Albuquerque, New Mexico.

George, O. L., Jr., 1980. Predicted Temperature/Time Histories Resulting from the Burial of Nuclear Waste Canisters in Bedded Salt, SAND79-1773, Sandia National Laboratories, Albuquerque, New Mexico.

Gerstle, W. H., and A. K. Jones, 1986. Mechanical Properties of Crushed Salt/Bentonite Blocks, SAND86-0707, Sandia National Laboratories, Albuquerque, New Mexico.

Glass, R. S., 1981. Effects of Radiation on the Chemical Environment Surrounding Waste Canisters in Proposed Repository Sites and Possible Effects on the Corrosion Process, SAND81-1677, Sandia National Laboratories, Albuquerque, New Mexico.

Glass, R. S., J. A. Ruppen, and R. B. Diegle, 1982. Sensitization to Corrosion of Heat Treated TiCode-12, SAND82-1021A, Sandia National Laboratories, Albuquerque, New Mexico, presented at the Electrochemical Society Meeting, Detroit, Michigan.

Glass, R. S., 1983. "Effect of Intermetallic Ti2Ni on the Electrochemistry of TiCode-12 in Hydrochloric Acid," SAND83-0053J, Sandia National Laboratories, Albuquerque, New Mexico, published in Electrochimica Acta, Vol. 28, No. 11, pp. 1507-13.

Glass, R. S., and Y. K. Hong, 1983. Mechanism of Transpassive Dissolution of Titanium-Molydenum Alloys, SAND82-2757A, Sandia National Laboratories,

Albuquerque, New Mexico, presented at the Electrochemical Society Meeting, San Francisco, California.

Glass, R. S., 1984. "Technical Note: The Interpretation of Weight-Loss Measurements for Alloys Showing Time-Delay Activation," SAND83-0053J, Sandia National Laboratories, Albuquerque, New Mexico, published in Corrosion, Vol. 40, No. 6, pp. 322-323.

Glass, R. S., and Y. K. Hong, 1984. "Transpassive Behavior of Titanium-Molybdenum Alloys in H2SO4," SAND83-1901J, Sandia National Laboratories, Albuquerque, New Mexico, published in Electrochimica Acta, Vol. 29, No. 10, pp. 1465-70.

Glass, R. S., 1985. "Passivation of Titanium by Molybdate Ion," SAND83-2541J, Sandia National Laboratories, Albuquerque, New Mexico, presented at Electrochemical Society Meeting, Fall 1983, published in Corrosion, Vol. 41, No. 2, pp. 89-93.

Gnirk, P. F., W. G. Pariseau, J. E. Russel, W. R. Wawersik, and H. V. Hovland, 1973. Analysis and Evaluation of the Rock Mechanics Aspects of the Proposed Salt Mine Repository, RE/SPEC Report RSI-005.

Gnirk, P. F. 1978. "Deformation and Strength Characteristics of Granulated Salt from Laboratory Consolidation Tests," Technical Letter Memorandum, RSI-0020, RE/SPEC, Inc.

Gnirk, P. F., K. D. Mellegard, and H. Waldman, 1978. "Deformation and Strength Characteristics of Granulated Salt from Laboratory Consolidation Tests," RE/SPEC Technical Letter Memorandum, RSI-0020, P.O. Box 725, Rapid City, South Dakota, 57709.

Gnirk, P. F. et al., 1981. State-of-the-Art Review of Brine Migration Studies in Salt, SAND81-7054, prepared for Sandia National Laboratories, Albuquerque, New Mexico, by RE/SPEC, Inc.

Griswold, G. B., 1977. Site Selection and Evaluation Studies of the Waste Isolation Pilot Plant (WIPP), Los Medanos, Eddy County, New Mexico, SAND77-0946, Sandia National Laboratories, Albuquerque, New Mexico.

Griswold, G., 1980. "Summary of Brine Flow," Geotechnical Consideration for Radiological Hazard Assessment of WIPP, State of New Mexico Environmental Evaluation Group Report EEG-6, pp. 16-22.

Gulick, C. W., Jr., 1978. Borehole Plugging Materials Development Program, SAND78-0715, Sandia National Laboratories, Albuquerque, New Mexico.

Gulick, C. W., Jr., 1979. Borehole Plugging Program—Plugging of ERDA No. 10 Drill Hole, SAND79-0789, Sandia National Laboratories, Albuquerque, New Mexico.

Gulick, C. W., Jr., J. A. Boa, Jr., and A. D. Buck, 1980. Bell Canyon Test (BCT) Cement Development Report, SAND80-0358C, Sandia National Laboratories, presented at the International BHP Symposium, Columbus, Ohio.

Gulick, C. W., Jr., J. A. Boa, Jr., and A. D. Buck, 1980. Bell Canyon Test (BCT) Cement Grout Development Report, SAND80-1928, Sandia National Laboratories, Albuquerque, New Mexico.

Gulick, C. W., Jr., J. A. Boa, Jr., D. M. Walley, and A. D. Buck, 1980. Borehole Plugging Materials Development Program—Report No. 2, SAND79-1514, Sandia National Laboratories, Albuquerque, New Mexico.

Gulick, C. W., Jr., J. A. Boa, Jr., and A. D. Buck, 1982. Borehole Plugging Materials Development Program—Report 3, SAND81-0065, Sandia National Laboratories, Albuquerque, New Mexico.

Gulick, C. W., Jr., 1984. Test Plan: Plug Test Matrix, Sandia National Laboratories, Albuquerque, New Mexico.

Gulick, C. W., and L. D. Wakeley, 1988. "Reference Properties of Cement-Based Plugging and Sealing Materials for Waste Isolation Pilot Plant (WIPP)," SAND87-2817, (in preparation), Sandia National Laboratories, Albuquerque, New Mexico.

Hadley, G. R., and G. W. Faris, 1981. Revised Theory of Water Transport in Rock Salt, SAND80-2398, Sandia National Laboratories, Albuquerque, New Mexico.

Hadley, G. R., 1981. Salt Block II: Brine Migration Modeling, SAND81-0438, Sandia National Laboratories, Albuquerque, New Mexico.

Hansen, F. D., and P. F. Gnirk, 1975. Design Aspects of Radioactive Waste Repository; III Uniaxial Quasi-Static and Creep Properties of the Site Rock, Technical Memorandum Report RSI-0029, Sandia National Laboratories, Albuquerque, New Mexico.

Hansen, F. D., 1976. Experimental Consolidation of Granulated Rock Salt with Application to Sleeve Buckling, ORNL/Sub-42-69/21, prepared for U.S. Department of Energy by Oak Ridge National Laboratory, Oak Ridge, Tennessee.

Hansen, F. D., and K. D. Mellegard, 1977. Creep Behavior for Bedded Salt from Southeastern New Mexico at Elevated Temperatures, Technical Memorandum Report, RSI-0062, Sandia National Laboratories, Albuquerque, New Mexico.

Hansen, F. D., 1977. Triaxial Quasi-Static Compression and Creep Behavior of Bedded Salt from Southeastern New Mexico, Technical Memorandum Report, RSI-0055, Sandia National Laboratories, Albuquerque, New Mexico.

Hansen, F. D., and K. D. Mellegard, 1980. Further Creep Behavior of Bedded Salt from Southeastern New Mexico at Elevated Temperature, SAND80-7114, Sandia National Laboratories, Albuquerque, New Mexico.

Henderson, J. T., 1982. Waste-Management QA Training and Motivation, SAND82-0358C, Sandia National Laboratories, Albuquerque, New Mexico, presented at 1982 ASQC Western Region Conference, Phoenix, Arizona.

Herrmann, W., W. R. Wawersik, and H. S. Lauson, 1980. Analysis of Steady State Creep of Southeastern New Mexico Bedded Salt, SAND80-0558, Sandia National Laboratories, Albuquerque, New Mexico.

Herrmann, W., W. R. Wawersik, and H. S. Lauson, 1980. Creep Curves and Fitting Parameters for Southeastern New Mexico Bedded Salt, SAND80-0087, Sandia National Laboratories, Albuquerque, New Mexico.

Herrmann, W., W. R. Wawersik, and H. S. Lauson, 1980. A Model for Transient Creep of Southeastern New Mexico Rock Salt, SAND80-2172, Sandia National Laboratories, Albuquerque, New Mexico.

Herrmann, W., and H. S. Lauson, 1981. Analysis of Creep Data for Various Natural Rock Salts, SAND81-2567, Sandia National Laboratories, Albuquerque, New Mexico.

Herrmann, W., and H. S. Lauson, 1981. Analysis of Stress Drop in Multistage Creep Experiments: Predictions of Exponential Creep Law, SAND81-1612, Sandia National Laboratories, Albuquerque, New Mexico.

Herrmann, W., and H. S. Lauson, 1981. Review and Comparison of Transient Creep Laws Used for Natural Rock Salt, SAND81-0738, Sandia National Laboratories, Albuquerque, New Mexico.

Herrmann, W., W. R. Wawersik, and S. T. Montgomery, 1982. Review of Creep Modeling for Rock Salt, SAND82-2178C, Sandia National Laboratories, Albuquerque, New Mexico, presented at the International Conference on Constitutive Laws for Engineering Materials: Theory and Application, Toronto, Canada.

Hill, L. R., 1980. "Characterization of a Site in Bedded Salt for Isolation of Radioactive Wastes," in IAEA-SM243/38, 20, Underground Disposal of Radioactive Wastes, Vol. 1, pp. 269-287.

Hohlfelder, J. J., and G. R. Hadley, 1979. Laboratory Studies of Water Transport in Rock Salt, SAND79-1519, Sandia National Laboratories, Albuquerque, New Mexico.

Hohlfelder, J. J., 1979. Measurement of Water Lost from Heated Geologic Salt, SAND79-0462, Sandia National Laboratories, Albuquerque, New Mexico.

Hohlfelder, J. J., 1980. Salt Block II: Description and Results, SAND79-2226, Sandia National Laboratories, Albuquerque, New Mexico.

Hohlfelder, J. J., 1981. Volatile Content of Rock Salt, SAND79-2349, Sandia National Laboratories, Albuquerque, New Mexico.

Holcomb, D. J., and D. W. Hannum, 1982. Consolidation of Crushed Salt Backfill Under Conditions Appropriate to the WIPP Facility, SAND82-0630, Sandia National Laboratories, Albuquerque, New Mexico.

Holcomb, D. J., 1985. "Results of the 55-Day Consolidation Test," internal memo to J. Stormont, 6332, Sandia National Laboratories, Albuquerque, New Mexico.

Holcomb, D. J., and M. Shields, 1987. Hydrostatic Creep Consolidation of Crushed Salt with Added Water, SAND87-1990, Sandia National Laboratories, Albuquerque, New Mexico.

Holcomb, D. J., 1988. Time-Dependent Changes in Velocity and Attenuation in Salt at the Waste Isolation Pilot Plant, SAND87-3016, Sandia National Laboratories, Albuquerque, New Mexico, presented at the 29th U.S. Symposium on Rock Mechanics, Minneapolis, Minnesota.

Holcomb, D. J., and A. K. Jones. Data Acquisition for the Rock Mechanics Laboratory, SAND83-0646, Sandia National Laboratories Report, Albuquerque, New Mexico.

Holdoway, K. A., 1974. "Behavior of Fluid Inclusions in Salt During Heating and Irradiation," Fourth Symposium on Salt, Vol. 1, ed. A. H. Coogan, Northern Ohio Geological Society, Cleveland, Ohio, pp. 303-312.

Hong, Y. K., and R. S. Glass, 1983. Active-Passive Transition Study of Titanium-Molybdenum Alloys, SAND82-2884A, Sandia National Laboratories, Albuquerque, New Mexico, presented at the Electrochemical Society Meeting, San Francisco, California.

Hudson, T., 1987. Preliminary Personal Communication to J. S. Stormont (Sandia) on USGS Moisture and Density Measurements in Bedded Rock Salt at the WIPP Site.

Hughes, P. S., and L. D. Rigdon, 1980. Waste Isolation Pilot Plant Title I Operator Dose Calculations, LATA Report No. 90, SAND79-7107, Sandia National Laboratories, Albuquerque, New Mexico.

Hunter, T. O., 1979. Summary of Research and Development Activities in Support of Waste Acceptance Criteria for WIPP, SAND79-1305, Sandia National Laboratories, Albuquerque, New Mexico.

Hunter, T. O., 1979. Summary of Results and Plans of the Experimental Program for the Waste Isolation Pilot Plant, SAND79-1305, Sandia National Laboratories, Albuquerque, New Mexico.

Hunter, T. O., 1979. Technical Issues of Nuclear Waste Isolation in the Waste Isolation Pilot Plant WIPP, SAND79-1117C, Sandia National Laboratories, Albuquerque, New Mexico.

Hunter, T. O., 1980. Borehole Plugging Test Activities in Southeastern New Mexico, SAND80-2462C, Sandia National Laboratories, Albuquerque, New Mexico, presented at 1980 NWTS Annual Information Meeting, Columbus, Ohio.

Hunter, T. O., 1980. The Perspective of Waste Isolation Research Issues and Assessment of Consequences for Radionuclide Release, SAND79-1076C, Sandia National Laboratories, Albuquerque, New Mexico, presented at the Materials Research Society International Symposium on the Scientific Basis for Nuclear Waste Management, Boston, Massachusetts, November 26-29, 1979.

Hunter, T. O., 1980. Role of Borehole Plugging Program in the Evaluation of the Waste Isolation Pilot Plant, SAND80-0502C, Sandia National Laboratories, Albuquerque, New Mexico, presented at the International BHP Symposium, Columbus, Ohio.

Hunter, T. O., C. L. Christensen, R. V. Matalucci, W. R. Wawersik, and M. A. Molecke, 1980. Summary of Research and Development Activities Related to the US/FRG Cooperative Program on Nuclear Waste Mangement, SAND81-1204C, Sandia National Laboratories, Albuquerque, New Mexico, presented at the US/FRG Bilateral Meeting, Bonn, Federal Republic of Germany.

Hunter, T. O., 1982. Borehole and Facility Sealing Activities for the Waste Isolation Pilot Plant, SAND81-2034, Sandia National Laboratories, Albuquerque, New Mexico.

Hunter, T. O., 1982. Nuclear Waste Disposal: Technical Issues & Status, SAND82-2238C, Sandia National Laboratories, Albuquerque, New Mexico, presented at the Spent Fuel Management and Waste Disposal Seminar by the Institute for Nuclear Materials Management, Washington, D.C.

Hunter, T. O., 1982. A Summary of Research & Development for Disposal of U.S. Defense Wastes in the Waste Isolation Pilot Plant (WIPP), SAND82-2313C, Sandia National Laboratories, Albuquerque, New Mexico.

Hunter, T. O., 1983. The WIPP Research and Development Program: Providing the Technical Basis for Defense Waste Disposal, SAND83-0178C, Sandia National Laboratories, Albuquerque, New Mexico.

Hunter, T. O., 1984. Engineering and Construction Management Strategies on the WIPP, SAND83-2118A, Sandia National Laboratories, Albuquerque, New Mexico, presented at the Waste Management 1984 Conference, Tucson, Arizona.

Intera Environmental Consultants, Inc., 1978. Radiological Waste Storage Analysis, Intera Environmental Consultants, Inc., prepared for Sandia National Laboratories, Albuquerque, New Mexico.

Intera Environmental Consultants, Inc., 1981. Consequence Assessment of Hydrological Communications through Borehole Plugs, SAND81-7164, Sandia National Laboratories, Albuquerque, New Mexico.

INTERA Technologies, Inc., 1985. Field Operations Plan for the H-8 Hydropad Pumping Test at the WIPP Site, Sandia National Laboratories, Albuquerque, New Mexico.

INTERA Technologies, Inc., 1985. Field Operations Plan for the Southern Long-Term Multipad Interference Test at the WIPP Site, Sandia National Laboratories, Albuquerque, New Mexico.

INTERA Technologies, Inc., 1986. Field Operations Plan for the H-7 Hydropad Pumping Test at the WIPP, Sandia National Laboratories, Albuquerque, New Mexico.

INTERA Technologies, Inc., 1986. Field Operations Plan for Hydrologic Testing at P-14, P-15, P-17, H-14, H-15, ERDA-9 and Cabin Baby-1, Sandia National Laboratories, Albuquerque, New Mexico.

INTERA Technologies, Inc., 1986. Field Operations Plan for Well Development and Pumping Tests at DOE-2, and WIPP-12, WIPP-13, WIPP-18, WIPP-19, WIPP-21, and WIPP-2A, Sandia National Laboratories, Albuquerque, New Mexico.

INTERA Technologies, Inc., 1987. Field Operations Plan for Monitoring of Ground-Water Observation Wells at the Waste Isolation Pilot Plant (WIPP) Site, Sandia National Laboratories, Albuquerque, New Mexico.

INTERA Technologies, Inc., 1987. Field Operations Plan for the Northern Long-Term Multipad Interference Test at the WIPP Site, Sandia National Laboratories, Albuquerque, New Mexico.

INTERA Technologies, Inc., 1987. Field Operations Plan for Permeability Testing in the Waste-Handling Shaft at the Waste Isolation Pilot Plant (WIPP) Site, Sandia National Laboratories, Albuquerque, New Mexico.

INTERA Technologies, Inc., 1987. Field Operations Plan for Well Development and Hydrologic Testing at H-1, H-12, P-18 and WIPP, Sandia National Laboratories, Albuquerque, New Mexico.

International Atomic Energy Agency, 1977. Site Selection Factors for Repositories of Solid High-Level and Alpha-Bearing Waste in Geological Formations, Technical Report Series No. 177, Vienna, Austria.

IT Corporation, 1984. Assessment of Crushed Salt Consolidation and Fracture Healing Processes in a Nuclear Waste Repository in Salt, BMI/ONWI-546, prepared for the Office of Nuclear Waste Isolation, Columbus, Ohio.

IT Corporation, 1987. Laboratory Investigation of Crushed Salt Consolidation and Fracture Healing, BMI/ONWI-631, Office of Nuclear Waste Isolation, Columbus, Ohio.

Jacobson, A., and R. Pusch, 1977. Deposition of High-Level Radioactive Waste Products in Boreholes with Buffer Substance, KBS Report 03, KBS, Stockholm, Sweden.

Jenks, G. H., 1979. Effects of Temperature, Temperature Gradients, Stress, and Irradiation on Migration of Brine Inclusions in a Salt Repository, ORNL-5526, Oak Ridge National Laboratory, Oak Ridge, Tennessee.

Kelsall, P. C., J. B. Case, D. Meyer, and W. E. Coons, 1982. Schematic Designs for Penetration Seals for a Reference Repository in Bedded Salt, ONWI-405, Office of Nuclear Waste Isolation, Columbus, Ohio.

Kent, D., and W. R. Wawersik, 1976. "Laboratory Velocity Measurements on Rock Salt Core Samples," interoffice memo, Sandia National Laboratories, Albuquerque, New Mexico.

Key, S. W., C. M. Stone, and R. D. Krieg, 1980. Dynamic Relaxation Applied to the Quasi-Static, Large Deformation, Inelastic Response of Axisymmetric Solids, SAND80-1605C, Sandia National Laboratories, Albuquerque, New Mexico, proceedings of U.S. European Workshop, Non-Linear Finite Element Analysis and Structural Mechanics, West Germany.

Kircher, J. F., R. G. Easterling, N. Hubbard, J. Krager, N. J. Magnani, D. P. Moak, R. E. Westerman, B. J. Woodand, and M. A. Molecke (U.S. Department of Energy), 1981. Nuclear Waste Package Material Degeneration Modes and Accelerated Testing, DOE/NWTS-13.

Knorovsky, G. A., and T. J. Headley, 1985. Evaluation of Titanium Alloy Resistance Upset Welds for Defense High-Level Waste Canisters, SAND85-0735, Sandia National Laboratories, Albuquerque, New Mexico.

Kosiewicz, S. T., A. Zerwekh, and B. Barraclough (Los Alamos Scientific Laboratory), 1978-80. Studies of Transuranic Waste Storage Under Conditions Expected in the Waste Isolation Pilot Plant (WIPP), Progress Reports: LA-7582-PR, LA-7649-PR, LA-7775-PR, LA-7931-PR, LA-8106-PR, LA-8224-PR, LA-8345-PR.

Kosiewicz, S. T., and A. Zerwekh (Los Alamos Scientific Laboratory), 1979. "Transuranic Waste Degradation Under Waste Isolation Pilot Plant Conditions," published in the Transactions of 1979 Winter Meeting, American Nuclear Society 33, San Francisco, California, p. 426.

Kosiewicz, S. T. (Los Alamos Scientific Laboratory), 1980. "Cellulose Thermally Decomposes at 70°C," Thermochimica Acta, 40, pp. 319-326.

Kosiewicz, S. T. (Los Alamos Scientific Laboratory), 1980. "Gas Generation from the Alpha Radiolysis of Bitumen," Nuclear and Chemical Waste Management, (2) pp. 139-141.

Kosiewicz, S. T. (Los Alamos Scientific Laboratory), 1981. "Gas Generation from Organic Transuranic Wastes, I. Alpha Radiolysis at Atmospheric Pressure," Nuclear Technology, Vol. 54, No. 1, pp. 92-99.

Koski, J. A., and D. F. McVey, 1981. Application of Parameter Estimation Techniques to Thermal Conductivity Probe Data Reduction, SAND80-2601C, Sandia National Laboratories, Albuquerque, New Mexico, presented at the International Joint Conferences on Thermophysical Properties, Gaithersburg, Maryland.

Krieg, R. D., and T. O. Hunter, 1980. Geomechanics Activities Conducted at Sandia National Laboratories in Support of the Waste Isolation Pilot Plant, SAND80-1592C, Sandia National Laboratories, Albuquerque, New Mexico, presented at ONWI/LBL Workshop on Thermomechanical Hydrochemical Modeling for a Hardrock Waste Repository, Berkeley, California.

Krieg, R. D., H. S. Morgan, and T. O. Hunter, 1980. Second Benchmark Problem for WIPP Structural Computations, SAND80-1331, Sandia National Laboratories, Albuquerque, New Mexico.

Krieg, R. D., 1980. A Unified Creep-Plasticity Model for Halite, SAND80-1195, Sandia National Laboratories, Albuquerque, New Mexico, presented at the Mechanical Testing for Deformation Model Development Symposium by ASTM, Bal Harbor, Florida.

Krieg, R. D., 1983. "Implementation of Creep Equations for a Metal Into a Finite Element Computer Program," Computer Methods for Nonlinear Solids and Structural Mechanics, ed. S. Atluri and N. Perrone, ASME Special Publication AMD, Vol. 54.

Krieg, R. D., 1984. Reference Stratigraphy and Rock Properties for the Waste Isolation Pilot Plant (WIPP) Project, SAND83-1908, Sandia National Laboratories, Albuquerque, New Mexico.

Krieg, R. D., C. M. Stone, and S. W. Key, 1981. Comparisons of the Structural Behavior of Three Storage Room Designs for the WIPP Project, SAND80-1629, Sandia National Laboratories, Albuquerque, New Mexico.

Krumhansl, J. L., 1982. "Mineralogic Stability of a Bentonite Backfill in a Bedded Salt Repository," SAND82-0951A, Sandia National Laboratories, Albuquerque, New Mexico, Geological Society of America Abstracts, Vol. 14, No. 7.

Krumhansl, J., 1984. Observations Regarding the Stability of Bentonite-Based Backfills in a High-Level Waste Repository in Rock Salt, SAND83-1293, Sandia National Laboratories, Albuquerque, New Mexico.

Labreche, D. A., and L. L. Van Sambeek, 1988. "Analysis of Data from Expansive Salt-Water Concrete Seals in Series B Small Scale Seal Performance Tests," SAND87-7155, (in preparation), Sandia National Laboratories, Albuquerque, New Mexico.

Lambert, S. J., 1980. Mineralogical Aspects of Fluid Migration in the Salt Block II Experiment, SAND79-2423, Sandia National Laboratories, Albuquerque, New Mexico.

Lambert, S. J., 1980. Recommended Analysis Plan for the Borehole Plugging Program Potash Core Test, SAND80-0812, Sandia National Laboratories, Albuquerque, New Mexico.

Lambert, S. J., 1980. A Strategy for Evaluating the Long-Term Stability of Hole-Plugging Materials in Their Geological Environments, SAND80-0359C, Sandia National Laboratories, Albuquerque, New Mexico, presented at the International Workshop on Borehole and Shaft Plugging, Columbus, Ohio.

Lambert, S. J., and H. C. Shefelbine, 1980. A Strategy for Investigation of Fluid Migration in Evaporites (Waste Isolation Pilot Plant (WIPP), SAND79-1889, Sandia National Laboratories, Albuquerque, New Mexico.

Long, G. J., and Associates, Inc., 1977. Waste Isolation Pilot Plant (WIPP), Los Medanos Area, Eddy and Lea Counties, New Mexico, Final Report submitted to Sandia National Laboratories, Albuquerque, New Mexico.

Loukota, J. J., 1986. Software to Obtain Polonomial Coefficients from Gage Calibration Data, SAND85-1796, Sandia National Laboratories, Albuquerque, New Mexico.

.Loukota, J. J., 1986. Technical Manual Data Reduction Software for Gage Comparison Experiments in the WIPP, SAND85-1795, Sandia National Laboratories, Albuquerque, New Mexico.

Lucas, J. P., 1984. Analysis of Rock Bolt Material Failures at the WIPP Site, SAND84-0224, Sandia National Laboratories, Albuquerque, New Mexico.

Magnani, N. J., and J. W. Braithwaite, 1980. "Corrosion Resistant Metallic Canisters for Nuclear Waste Isolation," SAND79-1429C, Sandia National Laboratories, Albuquerque, New Mexico, presented at Materials Research Society, Boston, Massachusetts, published in Scientific Basis for Nuclear Waste Management, Vol. 2, ed. C. J. Northrup, Plenum Press, New York.

Magnani, N. J., 1983. "Corrosion Resistant Canisters for Nuclear Waste Isolation," SAND82-1384C, Sandia National Laboratories, Albuquerque, New Mexico, presented at Materials Research Society, Boston, Massachusetts, published in Scientific Basis for Nuclear Waste Management VI, Vol. 15, ed. D. Brookins, North-Holland, New York.

Matalucci, R. V., C. L. Christensen, T. O. Hunter, M. A. Molecke, and D. M. Munson, 1979. Waste Isolation Pilot Plant (WIPP) Research and Development Program: In Situ Testing Plan, SAND81-2628, Sandia National Laboratories, Albuquerque, New Mexico.

Matalucci, R. V., and T. O. Hunter, 1981. Geomechanical Applications for the Waste Isolation Pilot Plant (WIPP) Project, SAND81-1203C, Sandia National Laboratories, Albuquerque, New Mexico, presented at the First Conference on the Mechanical Behavior of Salt, University Park, Pennsylvania.

Matalucci, R. V., H. S. Morgan, and R. D. Krieg, 1981. The Role of Bench-marking in Assessing the Capability to Predict Room Response in Bedded Salt Repositories, SAND81-1293C, Sandia National Laboratories, Albuquerque, New Mexico, presented at the OECD Nuclear Energy Workshop on Near-Field Phenomena in Geologic Repositories for Radioactive Waste, Seattle, Washington.

Matalucci, R. V., 1982. Simulated-Waste Experiments Planned for Waste Isolation Pilot Plant (WIPP), SAND82-0547, Sandia National Laboratories, Albuquerque, New Mexico.

Matalucci, R. V., 1983. Field Evaluation of Strain Gaged Stressmeter and USBM Hydraulic Pressure Cells at WIPP, Sandia National Laboratories, Albuquerque, New Mexico.

Matalucci, R. V., 1984. The Waste Isolation Pilot Plant (WIPP) In Situ Testing Program, SAND84-0661A, Sandia National Laboratories, Albuquerque, New Mexico, presented at the Geotechnical Group, New Mexico, Section of the American Society of Civil Engineers.

Matalucci, R. V., 1986. Planning, Developing, and Organizing In Situ Tests for the Waste Isolation Pilot Plant (WIPP), SAND84-1390, Sandia National Laboratories, Albuquerque, New Mexico, presented at the Second Conference on Mechanical Behavior of Salt, Hannover, Federal Republic of Germany.

Matalucci, R. V., 1987. Summary Report: The Integrated In Situ Testing Program for the Waste Isolation Pilot Plant (WIPP), SAND86-2716, Sandia National Laboratories, Albuquerque, New Mexico.

Matalucci, R. V., 1987. Test Plan: WIPP Air Intake Shaft Performance Tests, Sandia National Laboratories, Albuquerque, New Mexico.

Matalucci, R. V., J. R. Ball, and L. K. Shepard, 1987. User's Manual for the UNDERDOG Data Reduction Software, SAND87-7149, Sandia National Laboratories, Albuquerque, New Mexico.

Matalucci, R. V. and F. G. Yost, 1987. The Scientific Program at the Waste Isolation Pilot Plant, SAND85-1699, Sandia National Laboratories, Albuquerque, New Mexico.

Maxwell, D. E., K. K. Wahi, and B. Dial, 1980. The Thermomechanical Response of WIPP Repositories, SAND79-7111, Sandia National Laboratories, Albuquerque, New Mexico.

McClain, W. C. et al., 1975. Geologic Disposal Program Semi-Annual Report for Period Ending March 31, 1975, Chemical Technology Division, Oak Ridge National Laboratory, Oak Ridge, Tennessee.

McIlmoyle, J. T., R. V. Matalucci, and C. O. Harvey, 1987. The Data Acquisition System for the Waste Isolation Pilot Plant In Situ Tests, SAND86-1031, Sandia National Laboratories, Albuquerque, New Mexico.

McIlmoyle, J. T., R. V. Matalucci, and H. C. Ogden, 1986. "Developing a Data Acquisition System for the Waste Isolation Pilot Plant In Situ Tests," SAND85-2505C, Sandia National Laboratories, Albuquerque, New Mexico, Proceedings of the 32nd International Instrumentation Symposium, pp. 445-456, Seattle, Washington.

McKinney, R. F., and R. S. Newton, 1983. "Site Validation Field Program Plan," Revision 1.2, January 3, 1983, prepared for the U.S. Department of Energy by the WIPP Technical Support Contractor.

McTigue, D. F., 1985. A Linear Theory for Porous Thermoelastic Materials, SAND85-1159, Sandia National Laboratories, Albuquerque, New Mexico.

McTigue, D. F., and E. J. Nowak, 1987. Brine Transport Studies in the Bedded Salt of the Waste Isolation Pilot Plant (WIPP), SAND87-1274C, Sandia National Laboratories, Albuquerque, New Mexico, presented at the 1987 Fall Meeting of the Materials Research Society, Boston, Massachusetts.

McTigue, D. F., and E. J. Nowak, 1988. "Brine Transport in the Bedded Salt of the Waste Isolation Pilot Plant (WIPP) Field Measurements and a Darcy Flow Model," Scientific Basis for Nuclear Waste Management X, Materials Research Society Symposia Proceedings, Vol. 84, Materials Research Society, Pittsburgh, Pennsylvania.

McVey, D. F., 1981. Analysis of Data from Line Source Thermal Conductivity Measurments Taken In Situ and Dome Salt at the Avery Island Mine, SAND81-1232, Sandia National Laboratories, Albuquerque, New Mexico.

Mercer, J. W., 1986. Field Operations Plan of Sandia National Laboratories WIPP Site Investigations Hydrologic Test Holes H-14 and H-15, Sandia National Laboratories, Albuquerque, New Mexico.

Mercer, J. W., 1987. Field Operations Plant of Sandia National Laboratories WIPP Site Investigations Hydrologic Test Holes H-3B4 and H-3B5, Sandia National Laboratories, Albuquerque, New Mexico.

Mercer, J. W., 1987. Field Operations Plan of Sandia National Laboratories WIPP Site Investigations Hydrologic Test Holes H-17 and H-18, Sandia National Laboratories, Albuquerque, New Mexico.

Mercer, J. W., and R. L. Beauheim, 1987. Field Operations Plan of Sandia National Laboratories WIPP Site Investigations Hydrologic Test Hole H-16, Sandia National Laboratories, Albuquerque, New Mexico.

Meyer, D., and J. J. Howard, Eds., 1983. Evaluation of Clays and Clay Minerals for Application to Repository Sealing, ONWI-486, Office of Nuclear Waste Isolation, Columbus, Ohio.

Miller, J. D., C. M. Stone, and L. J. Branstetter, 1982. Reference Calculations for Underground Rooms of the WIPP, SAND82-1176, Sandia National Laboratories, Albuquerque, New Mexico.

Mogford, J. A., and W. L. Garner, 1977. Waste Isolation Pilot Plant (WIPP), Southeastern New Mexico, SAND77-0701, Sandia National Laboratories, Albuquerque, New Mexico.

Molecke, M. A., 1977. "Waste Isolation Pilot Plant (WIPP) Transuranic Waste Experimental Program," SAND77-1300, Sandia National Laboratories, Albuquerque, New Mexico, published in Transactions of the ANS, 27, p. 441.

Molecke, M. A., 1977. The Waste Isolation Pilot Plant High-Level Waste Experimental Program, SAND77-1301A, Sandia National Laboratories, Albuquerque, New Mexico, presented at the American Nuclear Society National Meeting, San Francisco, California, published in Transactions of the ANS, Vol. 27, p. 440.

Molecke, M. A., 1977. "WIPP In Situ Experimental Program for HLW," Sandia National Laboratories, Albuquerque, New Mexico, published in Proceedings of the NWTS Program Conference on Waste-Rock Interactions, Pennsylvania State University, Y/OWI/SUB-77/142.

Molecke, M. A., 1978. Waste Isolation Pilot Plant Transuranic Wastes Experimental Characterization Program: Executive Summary, SAND78-1356, Sandia National Laboratories, Albuquerque, New Mexico.

Molecke, M. A., 1979. Gas Generation from Transuranic Waste Degradation: Data Summary of Interpretation, SAND79-1245, Sandia National Laboratories, Albuquerque, New Mexico.

Molecke, M. A., 1979. Gas Generation from Transuranic Waste Degradation: Interim Assessment, SAND79-0117, Sandia National Laboratories, Albuquerque, New Mexico.

Molecke, M. A., 1979. "WIPP Waste Characterization and Experimental Programs," Sandia National Laboratories, Albuquerque, New Mexico, published in Proceedings of the Task 2 Workshop Waste Isolation Safety Assessment Program, D. J. Bradley, Chairman, Seattle, Washington, PNL-SA-7992, pp. 205-229.

Molecke, M. A., 1980. Gas Generation from Transuranic Waste Degradation, SAND79-0911C, Sandia National Laboratories, Albuquerque, New Mexico, presented at Materials Research Society, Boston, Massachusetts, November 1979, published in Scientific Basis for Nuclear Waste Management, Vol. 2, Plenum Press, New York.

Molecke, M. A., and L. Abrego, 1980. "Status of Sandia HLW Canister/Overpack Program Studies," SAND80-2191C, Sandia National Laboratories, Albuquerque, New Mexico, presented at 1980 NWTS Annual Information Meeting, Columbus, Ohio, published in Proceedings of the National Waste Terminal Storage Program Information Meeting, ONWI-212, p. 230.

Molecke, M. A., and E. J. Nowak, 1980. Applicability of a Backfill-Getter Barrier for Radioactive Waste Isolation: Chemical and Physical Functions, SAND80-0838A, Sandia National Laboratories, Albuquerque, New Mexico, presented at American Chemical Society Annual Meeting, San Francisco, California.

Molecke, M. A., and E. J. Nowak, 1980. "Status of Sandia Backfill-Getter Development Studies," SAND80-2190C, Sandia National Laboratories, Albuquerque, New Mexico, presented at 1980 NTWTS Annual Information Meeting, Columbus, Ohio, published in Proceedings of the National Waste Terminal Storage Program Information Meeting, ONWI-22, p. 212.

Molecke, M. A., 1981. "Degradation of Transuranic-Contaminated Wastes Under Geologic Isolation Conditions," SAND79-2216, Sandia National Laboratories, Albuquerque, New Mexico, published in Management of Alpha-Contaminated Wastes, Proceedings of an International Symposium on the Management of Alpha-Contaminated Wastes, International Atomic Energy Commission, Vienna, Austria, 1983, IAEA-SM-246/37, pp. 653-666.

Molecke, M. A., and G. H. Miller, 1981. Waste Package Materials Test in SENM Salt, CFT/WPMT/CIA, Sandia National Laboratories, Albuquerque, New Mexico.

Molecke, M. A., D. J. Bradley, and J. W. Shade, 1982. "PNL-Sandia HLW Package Interactions Test: Phase One," SAND80-1442C, Sandia National Laboratories, Albuquerque, New Mexico, published in Scientific Basis for Nuclear Waste Management, Vol. 6, ed. S. V. Topp, North-Holland, New York.

Molecke, M. A., 1983. A Comparison of Brines Relevant to Nuclear Waste Experimentation, SAND83-0516, Sandia National Laboratories, Albuquerque, New Mexico.

Molecke, M. A., J. A. Ruppen, and R. B. Diegle, 1983. "Materials for High-Level Waste Canister/Overpacks in Salt Formations," SAND82-0429, Sandia National Laboratories, Albuquerque, New Mexico, published in Nuclear Technology, Vol. 63, pp. 476-506.

Molecke, M. A., D. W. Schaefer, R. S. Glass, and J. A. Ruppan, 1983. "Sandia HLW Canister/Overpack Studies Applicable for a Salt Repository," SAND81-1584, Sandia National Laboratories, Albuquerque, New Mexico, published in Advances

in Science and Technology of the Management of High-Level Nuclear Waste, Vol. 1, ed. P. Hofmann, Battelle Press.

Molecke, M. A., 1984. Test Plan: Waste Package Performance Technology Experiments for Simulated DHLW, Sandia National Laboratories, Albuquerque, New Mexico.

Molecke, M. A., 1984. WIPP Waste Package Testing on Simulated DHLW: Emplacement, SAND84-1263A, Sandia National Laboratories, Albuquerque, New Mexico, presented at MRS Symposium, Boston, Massachusetts.

Molecke, M. A., and R. V. Matalucci, 1984. Preliminary Requirements for the Emplacement and Retrieval of Defense High-Level Waste (DHLW) Tests in the Waste Isolation Pilot Plant (WIPP), SAND84-1444, Sandia National Laboratories, Albuquerque, New Mexico.

Molecke, M. A., and T. M. Torres, 1984. "The Waste Package Materials Field Test in S. E. New Mexico Salt," SAND83-1516C, Sandia National Laboratories, Albuquerque, New Mexico, presented at Materials Research Society Symposium, Boston, Massachusetts, published in Scientific Basis for Nuclear Waste Management, Vol. 26, pp. 69-76.

Molecke, M. A., 1985. "WIPP Waste Package Testing on Simulated DHLW: Emplacement," SAND84-1263C, Sandia National Laboratories, Albuquerque, New Mexico, presented at Materials Research Sumposium, Boston, Massachusetts, published in Scientific Basis for Nuclear Waste Management VIII, p. 44.

Molecke, M. A., 1986. "Overview of Waste Package Performance Experiments in WIPP," SAND86-2024C, Sandia National Laboratories, Albuquerque, New Mexico, presented at the Third International Symposium on Ceramics in Nuclear Waste Management, Chicago, Illinois, published in Advances in Ceramics (20).

Molecke, M. A., 1986. Test Plan: WIPP CH and RH TRU Waste Technology Experiments, Sandia National Laboratories, Albuquerque, New Mexico.

Molecke, M. A., 1986. "WIPP Waste Package Performance Testing on Simulated DHLW: Early Data," SAND85-0559C, Sandia National Laboratories, Albuquerque, New Mexico, presented at the High-Level Waste Meeting, Pasco, Washington, published in High-Level Nuclear Waste Disposal, ed. H. C. Burkholder, Battelle Press.

Molecke, M. A., and R. Beraun, 1986. WIPP Simulated DHLW Tests: Status and Initial In Situ Backfill Thermal Conductivities, SAND86-0489C, Sandia National Laboratories, Albuquerque, New Mexico, presented at the Waste Management 1986 Meeting.

Molecke, M. A., and T. Brandshang, 1986. A Comparison of Measured and Predicted Stresses on Simulated DHLW Package Tests Emplaced in WIPP Bedded Salt, SAND86-1165, Sandia National Laboratories, Albuquerque, New Mexico.

Molecke, M. A., and G. G. Wicks, 1986. Test Plan: WIPP Materials Interface Interactions Test (MIIT), Sandia National Laboratories, Albuquerque, New Mexico.

Molecke, M. A., and D. E. Munson, 1987. Test Plan Appendix: WIPP Simulated RH TRU Waste Add-On Tests, Sandia National Laboratories, Albuquerque, New Mexico.

MMolecke, M. A., and J. A. Van Den Avyle, 1987. FY 1985 Annual Summary of WIPP Waste Package Corrosion and Metallurgy Laboratory Research, SAND86-2636, Sandia National Laboratories, Albuquerque, New Mexico.

Molecke, M. A., 1988. WIPP/SRI International In Situ Testing Program, SAND87-2654A, Sandia National Laboratories, Albuquerque, New Mexico, presented at Waste Management 1988, Tucson, Arizona.

Monsees, J. E., and D. E. Munson, 1982. Design Considerations for a Nuclear Waste Repository in Salt, Tunneling Technology, Sandia National Laboratories, Albuquerque, New Mexico, presented at National Academy of Sciences.

Montgomery, S. T., 1981. Implementation of a Transient Creep Model for Natural Rock Salt as a Material-Response Subroutine for SANCHO, SAND81-1163, Sandia National Laboratories, Albuquerque, New Mexico.

Moody, N. R., and S. L. Robinson, 1982. The Effect of Hydrogen on TiCode-12 Ti-0.3 Mo-0.8Ni, SAND82-8705A, Sandia National Laboratories, Albuquerque, New Mexico.

Moody, N. R., and S. L. Robinson, 1982. "Internal Hydrogen Effects in TiCode-12 Canister/Overpack Materials," SAND82-8732A, presented at the Materials Research Society, Boston, Massachusetts, published in Scientific Basis for Nuclear Waste Management VI, Vol. 15, ed. D. Brookins, North-Holland, New York.

Moody, N. R., S. L. Robinson, and F. A. Greulich, 1985. Hydrogen Effects on TiCode-12 Properties and Microstructure, SAND85-8203, Sandia National Laboratories, Albuquerque, New Mexico.

Moody, N. R., and S. L. Robinson, 1986. Compositional and Microstructural Effects on Hydrogen Embrittlement of ASTM Grade 12 Titanium (T1 0.3 Mo—0.8 Ni), SAND85-8247, Sandia National Laboratories, Albuquerque, New Mexico.

Morgan, H. S., 1981. MARC Calculations for the Second WIPP Structural Benchmark Problem, SAND81-0925, Sandia National Laboratories, Albuquerque, New Mexico.

Morgan, H. S., R. D. Krieg, and R. V. Matalucci, 1981. Comparative Analysis of Nine Structural Codes Used in the Second WIPP Benchmark Problem, SAND81-1389, Sandia National Laboratories, Albuquerque, New Mexico.

Morgan, H. S., 1982. Analysis of Borehole Inclusion Stress Measurement Concepts Proposed for Use in the Waste Isolation Pilot Plant In Situ Testing Program, SAND82-1192, Sandia National Laboratories, Albuquerque, New Mexico.

Morgan, H. S., 1984. Analysis of Borehole Inclusion Stress Measurement Concepts Proposed for Use in the Waste Isolation Pilot Plant (WIPP), SAND83-2342C, Sandia National Laboratories, Albuquerque, New Mexico, presented at the 25th U.S. Symposium on Rock Mechanics, Northwestern University, Evanston, Illinois.

Morgan, H. S., and C. M. Stone, 1985. Pretest Reference Calculation for the 18-W/M2 Mockup for Defense High-Level Waste (WIPP Room A In Situ Experiment), SAND85-0807, Sandia National Laboratories, Albuquerque, New Mexico.

Morgan, H. S., and C. M. Stone, 1985. Pretest Reference Calculation for the Heated Axisymmetric Pillar (WIPP Room H In Situ Experiment), SAND85-1146, Sandia National Laboratories, Albuquerque, New Mexico.

Morgan, H. S., and C. M. Stone, 1985. Pretest Reference Calculation for the Overtest for Simulated Defense High-Level Waste (WIPP Room B In Situ Experiment), SAND85-0213, Sandia National Laboratories, Albuquerque, New Mexico.

Morgan, H. S., and C. M. Stone, 1985. Pretest Reference Calculation for the 6.1 Meter (20 ft) Wide Drifts for the Geomechanical Evaluation (WIPP Room G In Situ Experiment), SAND85-0893, Sandia National Laboratories, Albuquerque, New Mexico.

Morgan, H. S., C. M. Stone, and R. D. Krieg, 1985. The Use of Field Data to Evaluate and Improve Drift Response Models for the Waste Isolation Pilot Plant (WIPP), SAND84-2126C, Sandia National Laboratories, Albuquerque, New Mexico, presented at 26th U.S. Symposium on Rock Mechanics, Rapid City, South Dakota.

Morgan, H. S., C. M. Stone, and R. D. Krieg, 1986. A Comparison of Computed and Measured Responses for a Long Isolated Excavation at the Waste Isolation Pilot Plant (WIPP) Facility Computers and Geotechnics, SAND86-223858J, Sandia National Laboratories, Albuquerque, New Mexico.

Morgan, H. S., C. M. Stone, and R. D. Krieg, 1986. An Evaluation of WIPP Structural Modeling Capabilities Based on Comparisons with South Drift Data, SAND85-0323, Sandia National Laboratories, Albuquerque, New Mexico.

Morgan, H. S., C. M. Stone, R. D. Krieg, and D. E. Munson, 1986. Thermal/Structural Modeling of a Large Scale In Situ Overtest Experiment for Defense High-Level Waste at the WIPP Facility, SAND85-1926C, Sandia National Laboratories, Albuquerque, New Mexico, presented at the Second International Symposium on Numerical Models in Geomechanics, Ghent, Belgium.

Morgan, H. S., W. Wallner, and D. E. Munson, 1987. Results of an International Parallel Calculations Exercise Comparing Creep Responses Predicted with Three

Computer Codes for Two Excavations in Rock Salt, SAND87-2125, Sandia National Laboratories, Albuquerque, New Mexico.

Morse, J. G., and B. W. Hassinger, 1985. "Brine Testing Program Plan: Waste Isolation Pilot Plant (WIPP) Project, Carlsbad, New Mexico, Revision 22," Internal Document WD:85:01214, transmitted as a letter from W. R. Cooper to R. H. Neill, WIPP:AEH:85:086.

Moss, M., 1980. Energy of Gamma-Irradiated 97% Pure Rock Salt, SAND80-1616C, Sandia National Laboratories, Albuquerque, New Mexico, presented at ASME Symposium on Thermophysical Properties of Composite Materials, Chicago, Illinois, Paper 80-WA/HT-53.

Moss, M., 1980. Stored Energy of Gamma Irradiated WIPP Salt, SAND80-0416, Sandia National Laboratories, Albuquerque, New Mexico.

Moss, M., and G. M. Haseman, 1981. Thermal Conductivity of Polyhalite and Anhydrite from the Site of the Proposed Waste Isolation Pilot Plant, SAND81-0856, Sandia National Laboratories, Albuquerque, New Mexico.

Moss, M., and M. A. Molecke, 1983. "Thermal Conductivity of Bentonite/Quartz High-Level-Waste-Package Backfill," SAND82-1274C, Sandia National Laboratories, Albuquerque, New Mexico, presented at the Materials Research Society Meeting, Boston, Massachusetts, published in Scientific Basis for Nuclear Waste Management, Vol. 15, ed. D. Brookins, North-Holland, New York.

Munson, D. E., 1979. Preliminary Deformation-Mechanism Map for Salt (With Application to WIPP), SAND79-0076, Sandia National Laboratories, Albuquerque, New Mexico.

Munson, D. E., and P. R. Dawson, 1979. Constitutive Model for the Low Temperature Creep of Salt (With Application to WIPP), SAND79-1853, Sandia National Laboratories, Albuquerque, New Mexico.

Munson, D. E., and P. R. Dawson, 1980. Numerical Simulation of Creep Closure of Deep Potash Mine (With Application to Waste Isolation), SAND80-0467, Sandia National Laboratories, Albuquerque, New Mexico.

Munson, D. E., 1981. Establishing Parametric Bounds for Groundwater Transport of Nuclides from a Mine Geologic Repository, SAND81-2626J, Sandia National Laboratories, Albuquerque, New Mexico.

Munson, D. E. and P. R. Dawson, 1981. Salt-Constitutive Modeling Using Mechanism Maps, SAND81-2196C, Sandia National Laboratories, Albuquerque, New Mexico, presented at first Conference on the Mechanical Behavior of Salt, Pennsylvania State University, University Park, Pennsylvania.

Munson, D. E., 1982. Application of Mechanism Maps to Response of Storage Caverns in Salt, SAND82-1218A, Sandia National Laboratories, Albuquerque, New Mexico, presented at 6th International Symposium on Salt, Toronto, Canada.

Munson, D. E., 1982. "Rock Mechanics Considerations for Design of a Nuclear Waste Repository in Salt," SAND82-0185J, Sandia National Laboratories, Albuquerque, New Mexico, published in NAS Tunneling Technology Journal.

Munson, D. E., 1982. "A Work Hardening/Recovery Model of Transient Creep of Salt During Stress Loading and Unloading, "SAND82-0810J, Sandia National Laboratories, Albuquerque, New Mexico, Proceedings 23rd U.S. Symposium on Rock Mechanics, University of California, Berkeley, California, pp. 299-306.

Munson, D. E., and P. R. Dawson, 1982. A Transient Creep Model for Salt During Stress Loading and Unloading, SAND82-0962, Sandia National Laboratories, Albuquerque, New Mexico.

Munson, D. E., and P. R. Dawson, 1982. "A Work Hardening/Recovery Model of Transient Creep of Salt During Stress Loading and Unloading", SAND82-0370A, Sandia National Laboratories, Albuquerque, New Mexico, presented at the 23rd U.S. Symposium on Rock Mechanics, University of California, Berkeley, California.

Munson, D. E., 1983. Geomechanical Evaluation, Sandia National Laboratories, Albuquerque, New Mexico.

Munson, D. E., 1983. Overtest for Simulated Defense High-Level Waste (DHLW), Sandia National Laboratories, Albuquerque, New Mexico.

Munson, D. E., 1983. 12-w/m2 Mockup for Defense High-Level Waste (DHLW), Sandia National Laboratories, Albuquerque, New Mexico.

Munson, D. E., and R. V. Matalucci, 1984. "Planning, Developing, and Fielding of Thermal/Structural Interactions In Situ Tests for the Waste Isolation Pilot Plant (WIPP)," SAND84-0379J, Sandia National Laboratories, Albuquerque, New Mexico, presented in Proceedings of the Symposium on Waste Management, Tucson, Arizona.

Munson, D. E., and R. V. Matalucci, 1984. Planning, Developing, and Fielding of the WIPP Thermal/Structural Interactions In Situ Tests, SAND83-2048C, Sandia National Laboratories, Albuquerque, New Mexico, presented at Waste Management 1984, Tucson, Arizona.

Munson, D. E., R. V. Matalucci, and T. M. Torres, 1984. Implementation of Thermal/ Structural Interactions In Situ Tests at the Waste Isolation Pilot Plant Facility, SAND 84-0804C, Sandia National Laboratories, Albuquerque, New Mexico, Second Conference on Mechanical Behavior of Salt, Hannover, Federal Republic of Germany.

Munson, D. E., R. V. Matalucci, and T. M. Torres, 1984. Thermal Structural Interactions In Situ Tests Implementation at the Waste Isolation Pilot Plant Facility, SAND84-0807A, Sandia National Laboratories, Albuquerque, New Mexico, Second Conference on Mechanical Behavior of Salt, Hannover, Federal Republic of Germany.

Munson, D. E., and A. F. Fossom, 1986. "Comparison Between Predicted and Measured South Drift Closures at the WIPP Using a Transient Creep Model for Salt," Rock Mechanics: Key to Energy Production, Proceedings of the 27th U.S. Symposium on Rock Mechanics, University of Alabama, Tuscaloosa, Alabama.

Munson, D. E., and R. V. Matalucci, 1986. Planning, Developing, and Fielding of Thermal/Structural Interactions In Situ Tests for the Waste Isolation Pilot Plant (WIPP), SAND83-2048, Sandia National Laboratories, Albuquerque, New Mexico.

Munson, D. E., and H. S. Morgan, 1986. Methodology for Performing Parallel Design Calculations (Nuclear Waste Repository Application), SAND85-0324, Sandia National Laboratories, Albuquerque, New Mexico.

Munson, D. E., T. M. Torres, and D. Blankenship, 1986. Early Results from the Thermal/Structural In Situ Test Series at the WIPP, SAND85-2237C, Sandia National Laboratories, Albuquerque, New Mexico, presented at the 27th U.S. Rock Mechanics Symposium.

Munson, D. E., T. M. Torres, and R. L. Jones, 1987. Pseudostrain Representation of Multipass Excavations in Salt, SAND86-22397C, Sandia National Laboratories, Albuquerque, New Mexico, presented at the U.S. Symposium on Rock Mechanics.

Munson, D. E., T. M. Torres, and R. L. Jones, 1987. Results of a Large, In Situ, Heated Axisymmetric Pillar Test at the Waste Isolation Pilot Plant (WIPP), SAND87-2257A, Sandia National Laboratories, Albuquerque, New Mexico, presented at the 29th U.S. Symposium on Rock Mechanics, Minneapolis, Minnesota.

NAS/NRC, 1970. "Report by the Committee on Radioactive Waste Management, Disposal of Solid Radioactive Waste in Bedded Salt Deposits."

Neill, R. H., J. K. Channell, L. Chaturvedi, M. S. Little, K. Rehfeldt, and P. Spiegler, 1983. Evaluation of the Suitability of the WIPP Site, EEG-23, New Mexico Environmental Evaluation Group, Santa Fe, New Mexico.

Nowak, E. J., 1978. "Migration of Eu Through Geologic Media," Sandia National Laboratories, Albuquerque, New Mexico, published in the American Geophysics Union, Vol. 59, p. 1224.

Nowak, E. J., 1979. The Backfill Barrier as a Component in a Multiple Barrier Nuclear Waste Isolation System, SAND79-1109, Sandia National Laboratories, Albuquerque, New Mexico.

Nowak, E. J., and M. A. Molecke, 1979. WIPP Radionuclide Getter Development Study Thermal Transport Properties of Backfill Materials, Sandia National Laboratories, Albuquerque, New Mexico.

Nowak, E. J., 1980. "The Backfill as an Engineered Barrier for Nuclear Waste Management," ed. C. J. Northrup, Scientific Basis for Nuclear Waste Management, Vol. 2, Plenum Press, New York.

Nowak, E. J., 1980. "Diffusion of Colloids and Other Waste Species in Brine Saturated Backfill Materials," SAND83-1843C, Sandia National Laboratories, Albuquerque, New Mexico, published in Scientific Basis for Nuclear Waste Management, Vol. 2.

Nowak, E. J., 1980. Radionuclide Sorption and Migration Studies of Getters for Backfill Barriers, SAND79-1110, Sandia National Laboratories, Albuquerque, New Mexico.

Nowak, E. J., and I. Hayden, 1980. "Measurements of Thermal Transport Properties of Backfill Barrier Materials for the Waste Isolation Pilot Plant," (unpublished memorandum), Sandia National Laboratories, Albuquerque, New Mexico.

Nowak, E. J., 1981. Backfill Barriers for Nuclear Waste Repositories in Salt, SAND81-0377A, Sandia National Laboratories, Albuquerque, New Mexico, presented at the International Seminar on Chemistry and Process Engineering for High-Level Liquid Waste Solidification, Julich, Federal Republic of Germany.

Nowak, E. J., 1981. "Composite Backfill Materials for Radioactive Waste Isolation by Deep Burial in Salt," ed. J. G. Moore, Scientific Basis for Nuclear Waste Management, Vol. 3, Plenum Press, New York.

Nowak, E. J., 1981. Predicting the Performance of a Backfill Barrier to Radionuclide Migration for a Repository in Salt, SAND80-2565A, Sandia National Laboratories, Albuquerque, New Mexico, presented at the NRC Symposium on Uncertainties Associated with the Regulation of the Geologic Disposal of High-Level Radioactive Waste, Gatlinburg, Tennessee.

Nowak, E. J., 1982. The Diffusion of Cs(I) and Sr(II) in Liquid-Saturated Beds of Backfill Materials, SAND82-0750, Sandia National Laboratories, Albuquerque, New Mexico.

Nowak, E. J., 1982. The Diffusion of Leached Constituents in Backfill Barriers, SAND82-1156A, Sandia National Laboratories, Albuquerque, New Mexico, Second Semiannual Workshop on the Leaching Mechanisms of Nuclear Waste Forms.

Nowak, E. J., and J. L. Krumhansl, 1982. Backfill Barriers for Radioactive Waste Isolation: Effectiveness and Research Needs, SAND82-2158J, Sandia National Laboratories, Albuquerque, New Mexico.

Nowak, E. J., 1983. "Diffusion of Radionuclides in Brine-Saturated Backfill Barrier Materials," SAND82-1258C, Sandia National Laboratories, Albuquerque, New Mexico, presented at the Materials Research Society Meeting, Boston,

Massachusetts, published in Scientific Basis for Nuclear Waste Management VI, Vol. 15, ed. D. Brookins, North-Holland, New York, pp. 735-744.

Nowak, E. J., 1984, "Diffusion of Colloids and Other Waste Species in Brine-Saturated Backfill Materials," Scientific Basis for Nuclear Waste Management VII, ed. G. L. McVay, Materials Research Society Symposium Proceedings, Vol. 26, pp. 59-68.

Nowak, E. J., 1985. "Diffusion of Plutonium in Compacted, Brine-Saturated Bentonite," Scientific Basis for Nuclear Waste Management VIII, ed. C. M. Jantzen, J. A. Stone, and R. C. Ewing, Materials Research Society Symposium Proceedings, Pittsburgh, Pennsylvania, Vol. 44, pp. 351-358.

Nowak, E. J., 1985. Test Plan Moisture Release Experiment for Rooms AI and B, Sandia National Laboratories, Albuquerque, New Mexico.

Nowak, E. J., 1986. "Brine Migration Studies in the Waste Isolation Pilot Plant (WIPP)," SAND85-1987c, Sandia National Laboratories, Albuquerque, New Mexico, in Waste Management 1986--Waste Isolation in the U.S. Technical Programs and Public Education, Proceedings of the Symposium on Waste Management, Tuscon, Arizona, Vol. 2, pp. 53-158.

Nowak, E. J., 1986. "Brine Movement in Waste Isolation Pilot Plant (WIPP) Tests," SAND86-1094A, Sandia National Laboratories, Albuquerque, New Mexico, presented at the Symposium on Origin & Evaluation of Brines in the Subsurface, American Chemical Society National Meeting, Anaheim, California.

Nowak, E. J., 1986. Preliminary Results of Brine Migration Studies in the Waste Isolation Pilot Plant (WIPP), SAND86-0720, Sandia National Laboratories, Albuquerque, New Mexico.

Nowak, E. J., and D. F. McTigue, 1987. Interim Results of Brine Transport Studies in the Waste Isolation Pilot Plant (WIPP), SAND87-0880, Sandia National Laboratories, Albuquerque, New Mexico.

Nowak, E. J., and J. C. Stormont, 1987. Scoping Model Calculations of the Reconsolidation of Crushed Salt in the WIPP Shafts, SAND87-0879, Sandia National Laboratories, Albuquerque, New Mexico.

Nowak, E. J., 1988. "Assessment of Brine Inflow to WIPP Disposal Rooms," Memo from Experimental Programs Division, Sandia National Laboratories, Albuquerque, New Mexico.

Nowak, E. J., 1988. Test Plan: Brine Inflow and Humidity Experiments in Room D, Sandia National Laboratories, Albuquerque, New Mexico.

Nowak, E. J. The Diffusion of Cs(I) and Sr(II) in Liquid-Saturated Backfill Materials, SAND82-0750, Sandia National Laboratories, Albuquerque, New Mexico.

Nowak, E. J., D. F. McTigue, and R. Beraun. "Brine Inflow to WIPP Disposal Rooms: Data Modeling and Assessment," SAND88-0112, (in preparation), Sandia National Laboratories, Albuquerque, New Mexico.

Oak Ridge National Laboratory, 1973. Site Selection Factors for the Bedded Salt Pilot Plant, ORNL-TM-4219, Oak Ridge, Tennessee.

Olander, D. R. et al., 1980. Thermal Gradient Migration of Brine Inclusions in Salt, ONWI-208, Office of Nuclear Waste Isolation, Columbus, Ohio.

ONWI (Office of Nuclear Waste Isolation), 1980. NWTS Criteria for the Geologic Disposal of Nuclear Wastes: Site-Qualification Criteria, ONWI-33(2) (draft), Battelle Memorial Institute, Columbus, Ohio.

OSTP (Office of Science and Technology Policy), 1978. Isolation of Radioactive Wastes in Geologic Repositories: Status of Scientific and Technological Knowledge (draft), Executive Office of the President, Washington, D.C.

Pace, C. E., and C. W. Gulick, 1985. Expansive Grout Plug Effects in Restrained Environments, TR SL-85-?, prepared for Sandia National Laboratories, Albuquerque, New Mexico.

Pahwa, S. B., and J. R. Wayland, 1979. Far Field Thermal Calculations for the WIPP Site in SENM, SAND79-1013C, Sandia National Laboratories, Albuquerque, New Mexico, presented at Materials Research Society Meeting, Boston, Massachusetts.

Peterson, E. W., 1980. Analysis of Borehole Plug Performance, presented at 1980 NWTS Annual Information Meeting, Columbus, Ohio.

Peterson, E. W., and C. L. Christensen, 1980. Analysis of Bell Canyon Test Results, SAND80-7044C, Sandia National Laboratories, Albuquerque, New Mexico, presented at the International BHP Symposium, Columbus, Ohio.

Peterson, E., and S. Kelkar, 1983. Laboratory Tests to Determine Thermal and Hydraulic Properties of Bentonite-Based Backfill Systems, SAND82-7221, Terra Tek, Inc., Albuquerque, New Mexico.

Peterson, E. W., and J. C. Stormont, 1984. Test WIPP Horizon In Situ Permeability Measurements, Sandia National Laboratories, Albuquerque, New Mexico.

Peterson, E. W., and P. L. Lagus, 1985. "WIPP Horizon In Situ Permeability Measurements/Permeability Test System," S-CUBED Document No. 31062-08-01.

Peterson, E. W., P. L. Lagus, J. Brown, and K. Lie, 1985. WIPP Horizon In Situ Permeability Measurements, SAND85-7166, prepared for Sandia National Laboratories, Albuquerque, New Mexico.

Peterson, E. W., P. L. Lagus, and J. C. Stormont, 1986. Permeability Measurements at the Waste Isolation Pilot Plant (WIPP), SAND85-1988A, Sandia National Laboratories, Albuquerque, New Mexico, presented at Waste Management '86 Conference.

Peterson, E. W., 1987. Summary of N1100 Drift Tracer Gas Travel Time Tests, SSS-LR-88-9078, prepared for Sandia National Laboratories, Albuquerque, New Mexico.

Peterson, E. W., P. L. Lagus, and K. Lie. Fluid Flow Measurements of Test Series A and B for the Small Scale Seal Performance Tests, SAND87-7041, Sandia National Laboratories, Albuquerque, New Mexico.

Peterson, E. W., P. L. Lagus, and K. Lie. WIPP Horizon Free Field Fluid Transport Characteristics, SAND87-7164, Sandia National Laboratories, Albuquerque, New Mexico.

Pettigrew, R., and Associates, 1977. WIPP Conceptual Design Report (Soils and Foundation Investigation), prepared for Sandia National Laboratories, Albuquerque, New Mexico.

Pfeifle, T. W., and P. E. Senseny, 1981. Elastic-Plastic Deformation of Anhydrite and Polyhalite as Determined from Quasi-Static Triaxial Compressions Tests, SAND81-7063, RE/SPEC, Inc., for Sandia National Laboratories, Albuquerque, New Mexico.

Pfeifle, T. W., 1985. Mechanical Properties and Consolidation of Potential DHLW Backfill Materials: Crushed Salt and 70/30 Bentonite/Sand, SAND85-7208, RE/SPEC, Inc., for Sandia National Laboratories, Albuquerque, New Mexico.

Pfeifle, T. W., and P. E. Senseny, 1985. Permeability and Consolidation of Crushed Salt from the WIPP Site, RE/SPEC Topical Report RSI-0278.

Pfeifle, T. W., 1987. Backfill Material Specifications and Requirements for the WIPP Simulated DHLW and TRU Waste Technology Experiments, SAND85-7209, RE/SPEC, Inc., for Sandia National Laboratories, Albuquerque, New Mexico.

Pfeifle, T. W., 1987. Mechanical Properties and Consolidation of Potential DHLW Backfill Materials: Crushed Salt and 70/30 Bentonite/Sand, SAND85-7208, RE/SPEC, Inc., for Sandia National Laboratories, Albuquerque, New Mexico.

Pietz, J., 1983. "An Integral Equation Approach to Modeling Radionuclide Migration in the Backfill Barrier," MS Thesis, University of New Mexico, Albuquerque, New Mexico.

Powers, D. W. et al., 1978. Geological Characterization Report, Waste Isolation Pilot Plant (WIPP) Site, Southeastern New Mexico, SAND78-1596, Sandia National Laboratories, Albuquerque, New Mexico.

Powers, D. W., 1979. WIPP Statement of Work for Deepening WIPP 13, Sandia National Laboratories, Albuquerque, New Mexico.

Powers, D. W., and W. D. Weart, 1979. Status of Siting for the Waste Isolation Pilot Plant (WIPP), SAND79-1329A, Sandia National Laboratories, Albuquerque, New Mexico.

Powers, D. W., and W. D. Weart, 1979. "Status of Siting for the Waste Isolation Pilot Plant," SAND79-1329A, Trans ANS, Vol. 33, pp. 141-142.

Powers, D. W., 1980. Markov Processes and Cycles in the Evaporites of the Upper Salado Formation, Southeastern New Mexico, SAND80-2530A, Sandia National Laboratories, Albuquerque, New Mexico, presented at University of Utah Seminar, University of Utah.

Powers, D. W., 1981. "Geologic Investigation of the WIPP Site: Overview and Issues," SAND81-0201C, in Environmental Geology and Hydrology in New Mexico, New Mexico Geological Society Special Publication 10, pp. 199-123.

Preece, D. S., 1987. Pretest 3-D Finite Modeling of the Wedge Pillar Portion of the WIPP Geomechanical Evaluation (Room G) In Situ Experiment, SAND87-0472, Sandia National Laboratories, Albuquerque, New Mexico.

Price, R. H., 1980. Effects of Anhydrite and Pressure on the Mechanical Behavior of Synthetic Rock Salt, SAND80-2005J, Sandia National Laboratories, Albuquerque, New Mexico, presented at the Fall 1980 AGU Meeting, San Francisco, California.

Rack, H. J., L. Abrego, and M. A. Molecke, 1981. Titanium Utilization in Long-Term Nuclear Waste Storage, SAND80-2129A, Sandia National Laboratories, Albuquerque, New Mexico, presented at the Annual AIME Meeting, Chicago, Illinois.

Ratigan, J. L., and R. A. Wagner, 1978. "Thermomechanical Analysis of Crushed-Salt Backfilled Disposal Rooms in a Conceptual Radioactive Waste Repository in Dome Salt," in Conceptual Design Report, National Waste Terminal Storage Repository for Storing Reprocessing Wastes in a Dome Salt Formation, Special Study No. 2, Vol. XVIII, Stearns-Roger Services, Denver, Colorado.

Ratigan, J. L., 1987. A Sensitivity Study of Brine Transport into a Borehole Containing a Commercial High-Level Waste Canister, ONWI-384, prepared for the Office of Nuclear Waste Isolation, Battelle Memorial Institute, Columbus, Ohio.

Rhoderick, J. E., and A. D. Buck, 1981. Borehole Plugging Program (Waste Disposal), Report 2, Petrographic Examination of Several Four-Year-Old Laboratory-Developed Grout Mixtures, USAE Waterways Experiment Station Miscellaneous Paper C-78-1 (also issued as ONWI-342).

Rhoderick, J. E., and A. D. Buck, 1981. Examination of Simulated Borehole Specimens, SL-81-7, SAND81-7109, ONWI-247, Structures Laboratory, U.S. Army Engineers, Waterways Experiment Station, Vicksburg, Mississippi.

Rhoderick, J. E., and A. D. Buck, 1981. Petrographic Examination of Several Four-Year-Old Laboratory-Developed Grant Mixtures, C-78-1 Waterways Experiment Station, ONWI-342, Sandia National Laboratories, Albuquerque, New Mexico.

Rhoderick, J. E., G. W. Wong, and A. D. Buck, 1981. Examination of Samples of Bell Canyon Test 1-FF Grout, SAND81-7110, Sandia National Laboratories, Albuquerque, New Mexico, SL-81-5, ONWI-246, Structures Laboratory, U.S. Army Engineers, Waterways Experiment Station, Vicksburg, Mississippi.

Rigdon, S. D., and P. S. Hughes, 1979. Waste Isolation Pilot Plant (WIPP) Operator Dose Calculations Final Report, SAND79-7028, Sandia National Laboratories, Albuquerque, New Mexico.

Roedder, E., and H. E. Belkin, 1979. "Application of Studies of Fluid Inclusions in Permian Salado Salt, New Mexico, to Probems of Siting the Waste Isolation Pilot Plant," ed. G. J. McCarthy, Scientific Basics for Nuclear Waste Management, Vol. 1, Plenum Press, New York, pp. 313-321.

Roy, D. M., M. W. Grutzeck, K. Mather, and A. D. Buck, 1981. PSU/WES Interlaboratory Comparative Methodology Study of an Experimental Cementitious Repository Seal Material, Report 2, Final Results, USAE Waterways Experiment Station Miscellaneous Paper SL-81-2 (also published as ONWI-324).

Ruppen, J. A., M. A. Molecke, and R. S. Glass, 1981. "Titanium Utilization in Long-Term Nuclear Waste Storage," SAND81-2466J, Sandia National Laboratories, Albuquerque, New Mexico, published in Titanium for Energy and Industrial Applications, ed. D. Eylon, TMS-AIME Publications, pp. 355-69.

Ruppen, J. A., R. B. Diegle, R.S. Glass, and T. J. Headley, 1983. "Some Effects of Microstructure and Chemistry on Corrosion and Hydrogen Embrittlement of TiCode-12," SAND82-1279C, Sandia National Laboratories, Albuquerque, New Mexico, presented at Materials Research Society, Boston, Massachusetts, published in Scientific Basis for Nuclear Waste Management VI, Vol. 15. ed. D. Brookins, North-Holland, New York.

Sandia National Laboratories, 1977. A Study of the Nuclear Regulatory Commission Quality Assurance Program, SAND77-1009, Sandia National Laboratories, Albuquerque, New Mexico.

Sandia National Laboratories, 1977. WIPP Conceptual Design Report, SAND77-0274, Albuquerque, New Mexico.

Sandia National Laboratories, 1978. Review Comments on Geological Characterization Report, Waste Isolation Pilot Plant (WIPP) Site, Southeastern New Mexico, SAND78-1596, Volumes I and II, Albuquerque, New Mexico.

Sandia National Laboratories, 1979. Summary of Research and Development Activities in Support of Waste Acceptance Criteria for WIPP, SAND79-1305, Albuquerque, New Mexico.

Sandia National Laboratories, 1979. Waste Isolation Pilot Plant (WIPP) Program for FY 1980, SAND79-1771, Albuquerque, New Mexico.

Sandia National Laboratories, 1979. Waste Isolation Pilot Plant (WIPP) Program Plan for FY 1979, SAND79-0098, Albuquerque, New Mexico.

Sandia National Laboratories, 1980. Waste Isolation Pilot Plant (WIPP) Program Plan for FY 1981, SAND79-1771, Albuquerque, New Mexico.

Sandia National Laboratories, 1982. Waste Isolation Pilot Plant (WIPP) Program Plan for FY 1982, SAND82-0597, Albuquerque, New Mexico.

Sandia National Laboratories, 1983. Waste Isolation Pilot Plant (WIPP) Program Plan for FY 1983, SAND83-0127, Albuquerque, New Mexico.

Sandia National Laboratories, 1983. Waste Isolation Pilot Plant (WIPP) Program Plan for FY 1984, Sandia National Laboratories, Albuquerque, New Mexico.

Sandia National Laboratories, 1984. Waste Isolation Pilot Plant (WIPP) Program Plan for FY 1985, Albuquerque, New Mexico.

Sandia National Laboratories, 1985. Waste Isolation Pilot Plant (WIPP) Program Plan for FY 1986, Albuquerque, New Mexico.

Sandia National Laboratories, 1987. Waste Isolation Pilot Plant (WIPP) Program Plan for FY 1987, Albuquerque, New Mexico.

Sandia National Laboratories, 1987. Waste Isolation Pilot Plant (WIPP) Program Plan for FY 1988, Albuquerque, New Mexico.

Sandia National Laboratories, 1987. WIPP Conceptual Design Report, SAND77-0274: Part I, II, III, Addendum C-F, Addendum A thru J, L, and M (Addendum K was never published), Albuquerque, New Mexico.

Sarkar, A. K., M. W. Barnes, and D. M. Roy, 1982. Longevity of Borehole and Shaft Sealing Materials: I. Thermodynamic Properties of Cement and Related Phases Applied to Repository Sealing, ONWI-201, Office of Nuclear Waste Isolation, Columbus, Ohio.

Sattler, A. R., H. C. Walker, and T. O. Hunter, 1979. In Situ Experiments to Support Development of the Waste Isolation Pilot Plant (WIPP), SAND79-0905C, Sandia National Laboratories, Albuquerque, New Mexico, presented at Materials Research Society, Boston, Massachusetts.

Sattler, A. R., and C. L. Christensen, 1980. Measurements of Very Large Deformations in "Potash Salt" in Conjunction with an Ongoing Mining Operation, SAND79-2254, Sandia National Laboratories, Albuquerque, New Mexico.

Sattler, A. R., and T. O. Hunter, 1987. Pre-WIPP In Situ Experiments in Salt Part I, Executive Summary; Part II, Program Description, SAND79-0625, Sandia National Laboratories, Albuquerque, New Mexico.

Schutz, R. W., and J. A. Hall, 1984. Optimization of Mechanical/Corrosion Properties of TICODE-12 Plate and Sheet, Part I: Compositional Effects, Stage I Final Report, SAND83-7438, TIMET Titanium Metals Corporation of America, Henderson Technical Laboratory, Henderson, Nevada.

Schutz, P. W., and J. A. Hall, Titanium Metals Corp of America, 1987. Optimization of Mechanical/Corrosion Properties of Ti-Code 12 Plate and Sheet--Part II: Thermomechanical Processing Effects, State II Final Report, SAND87-7171, Sandia National Laboratories, Albuquerque, New Mexico.

Senseny, P. E., 1986. Triaxial Compression Creep Tests on Salt from the Waste Isolation Pilot Plant, SAND85-7261, Sandia National Laboratories, Albuquerque, New Mexico.

Serata, S., S. Sakuri, and T. Adachi, 1972. "Theory of Aggregate Rock Behavior Based on Absolute Three-Dimensional Testing (ATT) of Rock Salt," Basic and Applied Rock Mechanics, Proceedings 10th U.S. Symposium Rock Mechanics, ed. K. E. Gray, AIME.

Serata, S., and T. E. Cundey, 1978. Rheological Method of Salt County Design for Underground Storage of Solid Liquid and Gaseous Matters, 19th U.S. Symposium on Rock Mechanics, ed. Y. S. Kim, Reno, Nevada.

Serne, R. J. et al., and M. A. Molecke, 1977. Batch Kd Measurements of Nuclides to Estimate Migration Potential at the Proposed Waste Isolation Pilot Plant in New Mexico, PNL-2448, Battelle Pacific Northwest Laboratories.

Seward, P. O., 1982. Abridged Borehole Histories for the Waste Isolation Pilot Plant (WIPP) Studies, SAND82-0080, Sandia National Laboratories Albuquerque, New Mexico.

Shade, J. W., D. J. Bradley, and M. A. Molecke, 1980. "Joint PNL0WIPP High-Level Total System Test," PNL-SA-8716, published in Proceedings of the 1980 National Waste Terminal Storage Program Information Meeting, ONWI-212, p. 234.

Shaffer, S. E., 1982. Bibliography of Geology of Southeastern New Mexico, SAND82-0-770, Sandia National Laboratories, Albuquerque, New Mexico.

Shefelbine, H. C., 1979. Test of Thermal Conductivity Probe in the Avery Island Salt Mine, Sandia National Laboratories, Albuquerque, New Mexico.

Shefelbine, H. C., 1979. WIPP Statement of Work for Deepening WIPP 13, Sandia National Laboratories, Albuquerque, New Mexico.

Shefelbine, H. C., 1982. Brine Migration: A Summary Report, SAND82-0152, Sandia National Laboratories, Albuquerque, New Mexico.

Shor, A. J., C. F. Baes, and C. M. Canonico, 1981. Consolidation and Permeability of Salt in Brine, ORNL-5774, Oak Ridge National Laboratory, Oak Ridge, Tennessee.

Sisson, C. E., 1978. Predicted Temperatures in a Bedded-Salt Repository Resulting from Burial of DOE High-Level Nuclear Waste Canisters, SAND78-0924, Sandia National Laboratories, Albuquerque, New Mexico.

Sjaardema, G. D., and R. D. Krieg, 1987. A Constitutive Model for the Consolidation of WIPP Crushed Salt and Its Use in Analyses of Backfilled Shaft Drift Configurations, SAND87-1977, Sandia National Laboratories, Albuquerque, New Mexico.

Sorensen, N. R., J. A. Ruppen, and R. W. Schutz, 1984. The Environmental Cracking of TiCode 12 in a Repository Brine, SAND83-2207J, NACE Corrosion 1984 International Forum and Exhibition, New Orleans, Louisiana.

Spiegler, P., 1981. An Approach to Calculating Upper Bounds on Maximum Individual Doses from the Use of Contaminated Well Water Following a WIPP Repository Breach.

St. John, C. M., 1978. "Computer Models and the Design of Underground Radioactive Waste Repositories," M.I.T. Special Summer Session on Rock Engineering.

Statler, R. D., 1978. Field Operations Program for WIPP H5A, B, C, H6A, B and C, Sandia National Laboratories, Albuquerque, New Mexico.

Statler, R. D., 1978. Hydro Test Wells H-4, H-5 and H-6, Vol. II, Sandia National Laboratories, Albuquerque, New Mexico.

Statler, R. D., 1979. Experimental Coreholes into Breccia Pipe from Mississippi Chemical Potash Mine, Sandia National Laboratories, Albuquerque, New Mexico.

Statler, R. D., 1979. Field Engineering Summary for Hydro Test Wells H-4, H-5, and H-6, Vols. 1 and 2, Sandia National Laboratories, Albuquerque, New Mexico.

Statler, R. D., 1979. Field Engineering Summary for Nash Draw Holes WIPP 25, 26, 27, 28, 29, and 30, Vols. 1 and 2, Sandia National Laboratories, Albuquerque, New Mexico.

Statler, R. D., 1979. Field Operations Plan for Hydrologic Study Wells WIPP H-7A, B&C, H-9A, B7c and H-10A, B&C, Sandia National Laboratories, Albuquerque, New Mexico.

Statler, R. D., 1979. Field Operations Program of Sandia Laboratories WIPP Site Investigations: Resistivity Anomaly WIPP 13, Sandia National Laboratories, Albuquerque, New Mexico.

Statler, R. D., 1979. Site Investigations for WIPP 32, Sandia National Laboratories, Albuquerque, New Mexico.

Statler, R. D., 1979. Site Investigations for WIPP 33, Sandia National Laboratories, Albuquerque, New Mexico.

Statler, R. D., 1979. Well Completion of H-4, 5 & 6 for WIPP Tracer Program Revision No. 1, Sandia National Laboratories, Albuquerque, New Mexico.

Statler, R. D., 1980. Field Operation Plan for Hydrologic Testing Nash Draw Wells WIPP-25 Through 30, Sandia National Laboratories, Albuquerque, New Mexico.

Statler, R. D., 1980. Field Operations Program of Sandia National Laboratories WIPP Site Investigations Resistivity Anomaly, WIPP 31, Sandia National Laboratories, Albuquerque, New Mexico.

Statler, R. D., 1980. Field Operations Program of Sandia National Laboratories WIPP Site Investigations WIPP 25-30, Sandia National Laboratories, Albuquerque, New Mexico.

Statler, R. D., 1980. Site Investigations for WIPP 31 Re-Entry and Deepening, Sandia National Laboratories, Albuquerque, New Mexico.

Stein, C. L., 1985. Mineralogy in the Waste Isolation Pilot Plant (WIPP) Facility Stratigraphic Horizon, SAND85-0321, Sandia National Laboratories, Albuquerque, New Mexico.

Stickney, R. G., and A. R. Sattler, 1979. In Situ Performance Evaluation of Stress Gages at Avery Island, Sandia National Laboratories, Albuquerque, New Mexico.

Stinebaugh, R. E., 1979. Compressibility of Granulated Rock Salt, SAND79-1119, Sandia National Laboratories, Albuquerque, New Mexico.

Stinebaugh, R. E., 1979. Retrieval of Canistered Experimental Waste at the Waste Isolation Pilot Plant, SAND79-1239, Sandia National Laboratories, Albuquerque, New Mexico.

Stone, L. M., R. D. Krieg, and L. J. Branstetter, 1981. The Effect of Clay-Seam Behavior on WIPP Repository Design, SAND81-0768, Sandia National Laboratories, Albuquerque, New Mexico.

Stone, C. M., R. D. Krieg, and Z. E. Beisinger, 1985. SANCHO--A Finite Element Computer Program for the Quasistatic, Large Deformation, Inelastic Response of Two-Dimensional Solids, SAND84-2618, Sandia National Laboratories, Albuquerque, New Mexico.

Stormont, J. C., 1983. Field Evaluation of Stress Measurement Techniques at the WIPP Site, Sandia National Laboratories, Albuquerque, New Mexico.

Stormont, J. C., 1984. Plugging and Sealing Program for the Waste Isolation Pilot Plant (WIPP), SAND84-1057, Sandia National Laboratories, Albuquerque, New Mexico.

Stormont, J. C., 1984. "Recommendation to Reduce Width of Certain Drifts in the WIPP to Facilitate Repository Sealing," Memorandum, Sandia National Laboratories, Albuquerque, New Mexico.

Stormont, J. C., and E. W. Peterson, 1984. Test Plan: WIPP Horizon In Situ Permeability Measurement, Sandia National Laboratories, Albuquerque, New Mexico.

Stormont, J. C., R. V. Matalucci, and H. S. Morgan, 1984. Field Evaluation of Stress Measurement Techniques in Rock Salt, SAND83-2051A, Sandia National Laboratories, Albuquerque, New Mexico, presented at 30th International Instrumentation Symposium, Denver, Colorado, (report entered under SAND83-2507).

Stormont, J. C., R. V. Matalucci, and H. S. Morgan, 1984. Field Tests of Stress Measurement Techniques in Rock Salt, SAND83-2507, Sandia National Laboratories, Albuquerque, New Mexico.

Stormont, J. C., 1985. Operations Plan: Test Series B of the Small Scale Seal Performance Tests, Sandia National Laboratories, Albuquerque, New Mexico.

Stormont, J. C., 1985. Test Plan: Appendix B, Small Scale Seal Performance Tests, Sandia National Laboratories, Albuquerque, New Mexico.

Stormont, J. C., 1986. Development and Implementation: Test Series A of the Small Scale Seal Performance Tests, SAND85-2602, Sandia National Laboratories, Albuquerque, New Mexico.

Stormont, J. C., 1986. Development and Implementation: Test Series B of the Small Scale Seal Performance Tests, SAND86-1329, Sandia National Laboratories, Albuquerque, New Mexico.

Stormont, J. C., 1986. In Situ Seal Tests at the Waste Isolation Pilot Plant (WIPP), SAND85-1989C, Sandia National Laboratories, Albuquerque, New Mexico, presented at the Waste Management 1986, Tucson, Arizona.

Stormont, J. C., 1986. Operations Plan: Test Series C of the Small Scale Seal Performance Tests, Sandia National Laboratories, Albuquerque, New Mexico.

Stormont, J. C., 1986. Permeability Measurements at the Waste Isolation Pilot Plant (WIPP), SAND85-1988C, Sandia National Laboratories, Albuquerque, New Mexico, presented at the Waste Management 1986, Tucson, Arizona.

Stormont, J. C., 1986. Test Plan: Appendix C, Small Scale Seal Performance Tests, Sandia National Laboratories, Albuquerque, New Mexico.

Stormont, J. C., and C. L. Howard, 1986. Development, Implementation and Early Results: Test Series B of the Small Scale Seal Performance Tests, SAND86-1329, Sandia National Laboratories, Albuquerque, New Mexico.

Stormont, J. C., and C. L. Howard, 1986. Development, Implementation and Early Results: Test Series C of the Small Scale Seal Performance Tests, SAND87-2203, Sandia National Laboratories, Albuquerque, New Mexico.

Stormont, J. C., 1987. Small Scale Seal Performance Test Series A Thermal/Structural Data Through the 180th Day, SAND87-0178, Sandia National Laboratories, Albuquerque, New Mexico.

Stormont, J. C., and C. L. Howard, 1987. Development, Implementation and Early Results: Test Series C of the Small Scale Seal Performance Tests, SAND87-2203, Sandia National Laboratories, Albuquerque, New Mexico.

Stormont, J. C., E. W. Peterson, and P. L. Lagus, 1987. Summary of and Observations About WIPP Facility Horizon Flow Measurements Through 1986, SAND87-0176, Sandia National Laboratories, Albuquerque, New Mexico.

Stormont, J. C., 1988. Preliminary Seal Design Evaluation for the Waste Isolation Pilot Plant, SAND87-3083, Sandia National Laboratories, Albuquerque, New Mexico.

Stormont, J. C. Test Plan for the AEC-7 Re-Entry Test, Sandia National Laboratories, Albuquerque, New Mexico.

Stormont, J. C. Test Plan: Small Scale Seal Performance Tests, Sandia National Laboratories, Albuquerque, New Mexico.

Stormont, J. C., and J. G. Arguello. Model Calculations of Flow Through Shaft Seals in the Rustler Formation, SAND87-2859 (in preparation), Sandia National Laboratories, Albuquerque, New Mexico.

Stroup, D. E., and P. E. Senseny, 1987. Influence of Bentonite Content on Consolidation and Permeability of Crushed Salt from the WIPP, Topical Report RSI-0309, RE/SPEC, Inc., Albuquerque, New Mexico.

Sullivan, B. R., 1983. Results of the SPDV Site Validation Experiment Waste Isolation Pilot Plant, TME-3177, ed. S. Black, R. Nausten, and D. Shukla, prepared for U.S. Department of Energy.

Sumlin, H. A., 1981. A Report on the Development of Equipment and Techniques for Drilling and Machining Bedded Salt, SAND80-2603, Sandia National Laboratories, Albuquerque, New Mexico.

Sutherland, H. J., 1978. "Permeability of SENM Rock Salt," Interoffice Memo, Sandia National Laboratories, Albuquerque, New Mexico.

Sutherland, S. H., and D. E. Bennet, 1979. Defense High-Level Waste and Spent Fuel Characterization for Geologic Waste Repositories, SAND79-0172, Sandia National Laboratories, Albuquerque, New Mexico.

Sutherland, H. J., and S. P. Cave, 1979. Gas Permeability of SENM Rock Salt, SAND78-2287, Sandia National Laboratories, Albuquerque, New Mexico.

Sutherland, H. J., and S. P. Cave, 1980. "Argon Gas Permeability of New Mexico Rock Salt Under Hydrostatic Compression," International Journal of Rock Mechanic Mineral Science & Geomechanical Abstracts, 17, pp. 281-288.

Sutherland, H. J., 1982. Subsidence Prediction of High Extraction Mining Using Complementary Influence Functions, SAND82-2949, Sandia National Laboratories, Albuquerque, New Mexico.

Sweet, J. N., and J. E. McCreight, 1979. Thermal Conductivity of Rock Salt and Other Geologic Materials from the Site of the Proposed Waste Isolation Pilot Plant, SAND79-1665C, Sandia National Laboratories, Albuquerque, New Mexico, presented at Thermal Conductivity Conference, Chicago, Illinois.

Sweet, J. N., and J. E. McCreight, 1980. Thermal Conductivity of Rock Salt and Other Geologic Materials from the Site of the Proposed Waste Isolation Pilot Plant, SAND79-1665, Sandia National Laboratories, Albuquerque, New Mexico.

Sweet, J. N., and J. E. McCreight, 1980. Thermal Properties Measurement on Rock Salt Samples from the Site of the Proposed Waste Isolation Pilot Plant, SAND80-0709, Sandia National Laboratories, Albuquerque, New Mexico.

Sweet, J. N., and J. E. McCreight, 1980. Thermal Properties Measurements on Rock Salt Samples from the Site of the Proposed Waste Isolation Pilot Plant, SAND80-0799, Sandia National Laboratories, Albuquerque, New Mexico.

Szeki, A., 1978. Influence of Volume on Creep Behavior of Rock Salt Pillars, Fifth International Salt Symposium, Hamburg, Federal Republic of Germany.

Terra Tek Inc., 1978. "Gas Permeabilities of SENM Salt," consulting memo to Sandia National Laboratories, Albuquerque, New Mexico.

Teufel, L. W., 1981. Mechanical Properties of Anhydrite and Polyhalite in Quasi-Static Triaxial Compression, SAND81-0858, Sandia National Laboratories, Albuquerque, New Mexico.

Thomas, R. L., C. V. Char, and W. J. Bergeron, 1973. "Finite Element Analysis of Creep in Rock Salt Pillar Models," Proceedings, 14th Symposium Rock Mechanics, ed. H. R. Hardy, and R. Stefanko, AIME.

Thorne, B. J., 1980. Drift Response to Elevated Temperatures, SAND80-7086, Sandia National Laboratories, Albuquerque, New Mexico.

Thorne, B. J., 1981. Calculations of the Uplift of an Elastic Model of the Rustler Formation over a 75 K Watt/Acre Repository at the WIPP Site, SAND80-7166, Sandia National Laboratories, Albuquerque, New Mexico.

Thorne, B. J., and D. K. Rudeen, 1981. Regional Effects of TRU Repository Heat, SAND80-7161, Sandia National Laboratories, Albuquerque, New Mexico.

Tillerson, J. R., and M. M. Madsen, 1978. Thermoelastic Capabilities for the SAND-BMINES Program, SAND77-0378, Sandia National Laboratories, Albuquerque, New Mexico.

Tillerson, J. R., and P. R. Dawson, 1981. "Heated Mine Room and Pillar Secondary Creep Response," SAND79-1199, Sandia National Laboratories, Albuquerque, New Mexico, published in International Journal for Numerical and Analytical Methods in Geomechanics, Vol. 5, pp. 177-193.

Torres, T. M., 1983. Heated Axisymmetric Pillar, Sandia National Laboratories, Albuquerque, New Mexico.

Torres, T. M., 1985. Scope of Work for Gas Testing, Sandia National Laboratories, Albuquerque, New Mexico.

Torres, T. M., 1986. Preliminary Evaluation of Drift Closure and Closure Rate Response with Respect to the Effects of Gas Occurrences Within the Waste Isolation Pilot Plant, SAND86-1059, Sandia National Laboratories, Albuquerque, New Mexico.

Torres, T. M., 1986. Two-Dimensions Axisymmetric and Plane Strain Scoping Calculations for the Small Scale Seal Performance Test, Series A, SAND86-0488, Sandia National Laboratories, Albuquerque, New Mexico.

Torres, T. M., 1987. Design Evaluation: Structural Calculations for the Construction and Salt Handling Shaft and the Waste Handling Shaft at the Waste Isolation Pilot Plant (WIPP), SAND87-2230, Sandia National Laboratories, Albuquerque, New Mexico.

Trucano, T. G., 1981. Computer Modeling of Stress States Associated with Fluid Migration Experiments, SAND81-2008, Sandia National Laboratories, Albuquerque, New Mexico.

Tyler, L. D., 1984. In Situ Tests and Instrumentation in the WIPP Facility, SAND84-0986C, Sandia National Laboratories, Albuquerque, New Mexico, presented at CEC/NEA Workshop, Brussels, Belgium.

Tyler, L. R., R. V. Matalucci, M. A. Molecke, D. E. Munson, E. J. Nowak, and J. C. Stormont, 1988. Summary Report for the WIPP Technology Development

Program for the Isolation of Radioactive Waste, SAND88-0844, Sandia National Laboratories, Albuquerque, New Mexico.

Urai, J. L., C. J. Spiers, J. Zwart, and G. S. Lister, 1986. "Weakening of Rock Salt by Water During Long-Term Creep," Nature, Vol. 324, pp. 554-557.

Van Sambeek, L. L., 1987. Thermal and Thermomechanical Analyses of WIPP Shaft Seals, SAND87-7039, Sandia National Laboratories, Albuquerque, New Mexico.

Van Sambeek, L. L., and J. C. Stormont, 1987. Thermal/Structural Modeling of Test Series A of the Small Scale Seal Performance Tests, SAND87-7037, Sandia National Laboratories, Albuquerque, New Mexico.

Wagner, R. A., 1979. "Ambient Drillhole Closure in a Mined Drift," RSI-024/7/79/15, Technical Letter.

Wagner, R. A., and J. L. Ratigan, 1979. Thermo/Viscoelastic Analysis of a Heated Room with Crushed Salt Backfill in the Pre-WIPP Dedicated Area, RSI-0081.

Wakeley, L. D., and D. M. Roy, 1985. Cementatious Mixtures for Sealing Evaporite and Clastic Rocks in a Radioactive-Waste Repository, MP SL-85-16, prepared for Sandia National Laboratories, Albuquerque, New Mexico.

Wakeley, L. D., M. D. Walley, and A. D. Buck, 1986. Development of Fresh-Grout Subsequent to the Bell Canyon Tests (BCT), SL-86-2, Sandia National Laboratories, Albuquerque, New Mexico.

Wakeley, L. D., 1987. "Results of Laboratory Test of Specimens Cast at the Waste Isolation Pilot Plant (WIPP) in 1983 and 1984," letter to J. C. Stormont, Sandia National Laboratories, Albuquerque, New Mexico.

Wawersik, W. R., J. F. Callender, R. Weaver, and R. K. Dropek, 1976. Preliminary Determination of Mechanical Properties on Rock Salt from Southeastern New Mexico, Pre-Proc., 17th U.S. Symposium Rock Mechanics, University of Utah.

Wawersik, W. R., 1978. Effects of Pressure, Deviator Stress and Temperature on Transient Creep of Rock Salt at Low Confining Pressure AGU, Vol. 59, No. 4, p. 376.

Wawersik, W. R., and D. W. Hannum, 1978. Mechanical Behavior of New Mexico Rock Salt in Triaxial Compression Up to 200°C, 5th International Salt Symposium, Hamburg, Federal Republic of Germany.

Wawersik, W. R., 1979. Creep Fracture in Compression, in Chapter 3 in Summary of Research and Development Activities in Support of Waste Acceptance Criteria for WIPP, SAND79-1305, Sandia National Laboratories, Albuquerque, New Mexico.

Wawersik, W. R., 1979. Indirect Deformation (Strain) Measurements and Calibrations in Sandia Triaxial Apparatus for Rock Testing to 250°C, SAND79-0114, Sandia National Laboratories, Albuquerque, New Mexico.

Wawersik, W. R., and D. W. Hannum, 1979. Interim Summary of Sandia Creep Experiments on Rock Salt from the WIPP Study Area, Southeastern New Mexico, SAND79-0115, Sandia National Laboratories, Albuquerque, New Mexico.

Wawersik, W. R., and D. W. Hannum, 1979. "Mechanical Behavior of New Mexico Rock Salt in Triaxial Compression up to 200°C," SAND77-1192, Sandia National Laboratories, Albuquerque, New Mexico, published in the Journal of Geophysical Research, Vol. 85, No. 1, pp. 891-900.

Wawersik, W. R. and D. W. Hannum, 1980. "Mechanical Behavior of New Mexico Rock Salt in Triaxial Compression Up to 200°C," Journal of Geophysical Research, Vol. 85, No. B2, pp. 891-900.

Wawersik, W. R., 1981. Recent Measurements of Power Law Stress Exponents, Activation Energies and Creep Transients, SAND81-1117C, Sandia National Laboratories, Albuquerque, New Mexico, presented at the First Conference on the Mechanical Behavior of Salt, The Pennsylvania State University, University Park, Pennsylvania.

Wawersik, W. R., W. Herrmann, S. T. Montgomery, and H. S. Lauson, 1981. Evacuation Design in Rock Salt: Laboratory Experiments, Material Modeling and Validations, SAND81-1167C, Sandia National Laboratories, Albuquerque, New Mexico, presented at International Symposium on Rock Mechanics Related to Caverns and Pressure Shafts, Aachen, Federal Republic of Germany.

Wawersik, W. R., 1982. Low Temperature Creep Mechanisms in Rock Salt, SAND82-2071A, Sandia National Laboratories, Albuquerque, New Mexico, presented at AGU Fall Meeting, San Francisco, California.

Wawersik, W. R., and D. W. Preece, 1982. Creep Testing of Salt: Procedures, Problems and Suggestions, SAND81-1116C, Sandia National Laboratories, Albuquerque, New Mexico, presented at the First Conference on the Mechanical Behavior of Salt, The Pennsylvania State University, University Park, Pennsylvania.

Wawersik, W. R., 1983. Determination of Steady State Creep Rates and Activation Parameters for Rock Salt, SAND82-2731J, Sandia National Laboratories, Albuquerque, New Mexico.

Wawersik, W. R., 1983. Scope of Work for Gas Testing, Sandia National Laboratories, Albuquerque, New Mexico.

Wawersik, W. R., 1984. Comparison of Creep and Creep Models for Rock Salt, SAND84-0888A, Sandia National Laboratories, Albuquerque, New Mexico.

Wawersik, W. R., 1984. Hydraulic Fracturing Tests in Salt, SAND84-0390A, Sandia National Laboratories, Albuquerque, New Mexico, presented at Second Conference on the Mechanical Behavior of Salt, Hannover, Federal Republic of Germany.

Wawersik, W. R., 1984. On the Evolution of Texture and Microstructure in Laboratory Deformed Salt, SAND84-0889A, Sandia National Laboratories, Albuquerque, New Mexico, presented at Second Conference on the Mechanical Behavior of Salt, Hannover, Federal Republic of Germany.

Wawersik, W. R., and C. M. Stone, 1985. Application of Hydraulic Fracturing to Determine Virgin In Situ Stress State Around Waste Isolation Pilot Plant—In Situ Measurements, SAND85-1776, Sandia National Laboratories, Albuquerque, New Mexico.

Wawersik, W. R., 1986. Microstructures in Deformed Rock Salt from Around Old Mine Workings, SAND86-2187A, Sandia National Laboratories, Albuquerque, New Mexico, presented at the Fall AGU Meeting, San Francisco, California.

Wawersik, W. R., and C. M. Stone, 1986. "Experience with Hydraulic Fracturing Tests for Stress Measurements in WIPP," SAND85-2273C, Sandia National Laboratories, Albuquerque, New Mexico, published in the Proceedings of the 27th U.S. Symposium on Rock Mechanics.

Wawersik, W. R., and H. S. Morgan, 1987. "Evaluating Design Procedures for Structures in Rock Salt," SAND86-2597C, Sandia National Laboratories, Albuquerque, New Mexico, published in the Proceedings of the 28th U.S. Symposium on Rock Mechanics, presented at the University of Arizona, Tucson, Arizona.

Wawersik, W. R., and C. M. Stone, 1988. "Character and Interpretation of Pressure Records in Anelastic Rock with Examples of Hydraulic Fracturing Tests in Salt," SAND87-2569A, proposed for presentation at the Second International Workshop on Hydraulic Fracturing Stress Measurements, Minneapolis, Minnesota.

Wayland, J. R., and L. Bertholf, 1980. A Comparison of Thermomechanical Calculations for Highly Non-Linear Quasistatic Drift Formations, SAND80-0149, Sandia National Laboratories, Albuquerque, New Mexico.

Wayland, J. R., and S. B. Pahua, 1979. Far Field Thermal Calculations for the WIPP Site in Southeastern New Mexico, SAND79-1013C, Sandia National Laboratories, Albuquerque, New Mexico, presented at the Symposium on the Scientific Basis for Nuclear Waste Management, Boston, Massachusetts.

Weart, W. D., 1977. Beneficial Uses and Disposal of Radioactive Wastes, SAND77-0375C, Sandia National Laboratories, Albuquerque, New Mexico.

Weart, W. D., 1977. New Mexico Waste Isolation Pilot Plant, Mid 1977, Status Report, SAND77-0994, Sandia National Laboratories, Albuquerque, New Mexico.

Weart, W. D., 1978. Evaluation of Salt Beds in New Mexico as a Geologic Repository for Nuclear Waste, SAND78-2086, Sandia National Laboratories, Albuquerque, New Mexico.

Weart, W. D., 1978. Geotechnical Evaluation of the Proposed WIPP Site in Southeast New Mexico, SAND78-2194C, Sandia National Laboratories, Albuquerque, New Mexico.

Weart, W. D., 1979. Meeting Evaluation of the Proposed WIPP Site in Southeast New Mexico, SAND79-1113C, Sandia National Laboratories, Albuquerque, New Mexico, presented at the 87th National American Institute of Chemical Engineers, Boston, Massachusetts.

Weart, W. D., 1979. Status Report on the Waste Isolation Pilot Plant, SAND79-0323A, Sandia National Laboratories, Albuquerque, New Mexico, presented at Trans ANS Special Session on Geologic Repositories, Atlanta, Georgia.

Weart, W. D., 1979. "Status Report on the Waste Isolation Pilot Plant," SAND79-1992A, published in BASALT 79 Annual Report, Second Annual Meeting, Basalt Waste Isolation Program, Richland, Washington.

Weart, W. D., 1979. Status of the WIPP: A Bedded Salt Repository for Defense Radioactive Waste in Southeastern New Mexico, SAND79-1904A, Sandia National Laboratories, Albuquerque, New Mexico, presented to the 1979 Fall Meeting of the Rio Grande Chapter Health Physics Society, Santa Fe, New Mexico.

Weart, W. D., 1979. WIPP: A Bedded Salt Repository for Defense Radioactive Waste in Southeastern New Mexico, SAND78-0934C, Sandia National Laboratories, Albuquerque, New Mexico, presented at the Chemical Society Meeting, Miami, Florida.

Weart, W. D., 1979. WIPP: A Repository for Defense Radioactive Waste in Southeastern New Mexico Salt Beds, SAND79-1207A, Sandia National Laboratories, Albuquerque, New Mexico.

Weart, W. D., 1980. Status of the Waste Isolation Pilot Plant Project, SAND80-0134A, Sandia National Laboratories, Albuquerque, New Mexico, presented at AIME Meeting, Carlsbad Potash Section of the AIME, Carlsbad, New Mexico.

Weart, W. D., 1980. Supplement No. 1 to Field Operations Plan for WIPP 31 Re-entry, Sandia National Laboratories, Albuquerque, New Mexico.

Weart, W. D., 1980. Technical Developments in the WIPP Program, SAND80-1599C, Sandia National Laboratories, Albuquerque, New Mexico, presented at Association of Engineering Geologists 1980 Annual Meeting, Dallas, Texas.

Weart, W. D., and D. W. Powers, 1980. Geologic Issues for the Waste Isolation Pilot Plant (WIPP), A Revised Abstract for the Geological Society of America

Symposium, SAND80-1269C, Sandia National Laboratories, Albuquerque, New Mexico.

Weart, W. D., 1980. "Technical Issues in the Geologic Disposal of Radioactive Wastes," SAND80-03233C, Sandia National Laboratories, Albuquerque, New Mexico, published in Institute of Environmental Sciences 1980 Proceedings 26th Annual Technical Meeting, Life Cycle Problems and Environmental Technology, Philadelphia, Pennsylvania.

Weart, W. D., and D. W. Powers, 1981. "Geologic Issues for the Waste Isolation Pilot Plant (WIPP)," Abstract, Geological Society of America, Vol. 12, No. 7, p. 546.

Weart, W. D., 1983. Conclusions Regarding Geotechnical Acceptability of the WIPP Site, SAND83-0226C, Sandia National Laboratories, Albuquerque, New Mexico, presented at the Waste Management 1983 Symposium, Tucson, Arizona.

Weart, W. D., 1983. Summary of Evaluation of the Waste Isolation Pilot Plant (WIPP) Site Suitability, SAND83-0450, Sandia National Laboratories, Albuquerque, New Mexico.

Weart, W. D., 1983. WIPP: the Solution to Disposal of Defense Transuranic Waste, SAND83-0062A, Sandia National Laboratories, Albuquerque, New Mexico, presented at the 1983 Annual Meeting, American Nuclear Society, Detroit, Michigan.

Weart, W. D., 1985. Status of the WIPP, a Defense Transuranic Waste Isolation Facility, SAND85-0736J, Sandia National Laboratories, Albuquerque, New Mexico, Proceedings of the National Council on Radiation Protection and Measurements.

Wicks, G. G., 1985. WIPP/SRL In Situ and Laboratory Testing Programs—Part I: MIIT Overview, Nonradioactive Waste Glass Studies, DP-1706, Savannah River Laboratory, Aiken, South Carolina.

Wicks, G. G., M. E. Weinle, and M. A. Molecke, 1987. WIPP/SRL In Situ Tests Part II: Pictorial History of MIIT and Final MIIT Matrices, Assemblies, and Sample Listings, DP-1733 (also SAND86-2720), Savannah River Laboratory, Aiken, South Carolina.

Wilson, W. C., 1980. Field Operations Plan of Sandia National Laboratories Potash Core Test, Sandia National Laboratories, Albuquerque, New Mexico.

Winslow, C. D., 1981. The Sorption of Cesium and Strontium from Concentrated Brines by Backfill Barrier Materials, SAND80-2046, Sandia National Laboratories, Albuquerque, New Mexico.

Woolfolk, S. W., 1982. Radiological Consequences of Brine Release by Human Intrusion into WIPP, TME-3151, U.S. Department of Energy, Albuquerque, New Mexico.

Wowak, W. E., and A. R. Sattler, 1979. Criteria and Preliminary Design for WIPP Exploratory Program Experiments, SAND79-2077, Sandia National Laboratories, Albuquerque, New Mexico.

Wowak, W. E., 1979. Early In Situ Measurements Program for the Waste Isolation Pilot Plant, SAND79-0362, Sandia National Laboratories, Albuquerque, New Mexico.

Yost, F. G., and E. A. Aronson, 1987. Crushed Salt Consolidation Kinetics, SAND87-0264, Sandia National Laboratories, Albuquerque, New Mexico.

Zerwekh, A., S. T. Kosiewicz, and B. Barraclough (Los Alamos Scientific Laboratory), 1977-78. Experimental Studies of the Degradation of RAD-Wastes for the Sandia Laboratories Waste Isolation Pilot Plant, Progress Reports: LA-7246-PR, LA-7259-PR, LA-7478-PR.

Zeuch, D. H., 1984. Analysis of Consolidation of Crushed Rock Salt Backfill Using a Plastic Flow Model for Isostatic Hot Pressing, SAND84-1599A, Sandia National Laboratories, Albuquerque, New Mexico, presented at American Geophysical Union Fall Meeting, San Francisco, California.

Zeuch, D. H., D. J. Holcomb, and H. S. Lauson, 1985. Analysis of Consolidation of Granulated Rock Salt Using a Plastic Flow Model for Isostatic Hot Pressing, SAND84-1106, Sandia National Laboratories, Albuquerque, New Mexico.

ZoBell, C. E., and M. A. Molecke, 1978. Survey of Microbial Degradation of Asphalts with Notes on Relationship to Nuclear Waste Management, SAND78-1371, Sandia National Laboratories, Albuquerque, New Mexico.

J.8 **RESOURCES**

AIM (Agricultural and Industrial Minerals, Inc.), 1979. Resource Study for the Waste Isolation Pilot Plant Eddy County, New Mexico, AIM, Inc., San Carlos, California.

Biederman, P.L., 1984. National Resources of the Waste Isolation Pilot Plant Site, Energy and Minerals Department, Task Force on National Resources, State of New Mexico, 33pp.

Braush, L. M., A. K. Kuhn, and J. K. Register, 1982. Natural Resources Study, TME 3156, prepared for U.S. Department of Energy, WIPP Project Office.

Cheeseman, R. J., 1978. "Geology and Oil/Potash Resources of Delaware Basin, Eddy and Lea Counties," in Geology and Mineral Deposits of Ochoan Rocks in Delaware Basin and Adjacent Areas, New Mexico Bureau of Mines and Mineral Resources Circular 159, pp. 7-14.

EEG (Environmental Evaluation Group), 1982. Potential Release Scenario and Radiological Consequence Evaluation of Mineral Resources at WIPP, EEG-12, M. S. Little, Contract No. AF (401)-4423 OROWL, Health and Environment Department, State of New mexico, Santa Fe, New Mexico.

Foster, R. W., 1974. Oil and Gas Potential of a Proposed Site for Disposal of High-Level Radioactive Waste, New Mexico Bureau of Mines Mineral Resource Open-File Report, 296 pp.

Hendrickson, G. E., and R. J. Jones, 1952. Geology and Ground Water Resources of Eddy County, New Mexico, Ground Water Report 3, Bureau of Mines and Mineral Resources, New Mexico Institute of Mining and Technology.

John, C. B., R. J. Cheeseman, J. C. Lorenz, and M. L. Millgate, 1978. Potash Ore Reserves in the Proposed Waste Isolation Pilot Plant Area, Eddy County, Southeastern New Mexico, U.S. Geological Survey Open-File Report 78-828.

Jones, C. L., 1954. "The Occurrence and Distribution of Potassium Minerals in Southeastern New Mexico," ed. T. F. Stiff, New Mexico Geological Society Guidebook, 5th Field Conference, Southeastern New Mexico.

Jones, C. L., C. G. Bowles, and K. G. Bell, 1960. Experimental Drill Hole Logging in Potash Deposits of the Carlsbad District, New Mexico, U.S. Geological Survey Open-File Report 60-84.

Jones, C. L., 1972. "Permian Basin Potash Deposits, Southwestern United States," in Geology of Saline Deposits, UNESCO, Earth Science Series No. 7, pp. 191-101.

Jones, C. L., 1975. Potash Resources in Part of Los Medanos Area of Eddy and Lea Counties, New Mexico, U.S. Geological Survey Open-File Report 75-407, 37 pp.

Jones, C. L., 1978. Test Drilling for Potash Resources, Waste Isolation Pilot Plant Site, Eddy County, New Mexico, U.S. Geological Survey Open-File Report 78-592, 2 Vols., 431 pp.

Keesey, J. J., 1976. Hydrocarbon Evaluation, Proposed Southeastern New Mexico Radioactive Storage Site, Eddy County, New Mexico, 2 Vols., report to Sandia National Laboratories, Albuquerque, New Mexico.

Keesey, J. J., 1979. Evaluation of Directional Drilling for Oil and Gas Reserves Underlying the WIPP Site Area, Eddy County, New Mexico, Sipes, Williamson, & Associates, Midland, Texas.

McMillan, C., 1976. Los Medanos Area: Permian Exploration Co., report to Sandia National Laboratories, Albuquerque, New Mexico.

Netherland, Sewell, and Associates, Inc., 1974. Evaluation of Hydrocarbon Potential, AEC Study Area, Southeastern New Mexico, prepared for Oak Ridge National Laboratory, Oak Ridge, Tennessee.

Netherland, Sewell, and Associates, Inc., 1974. Hydrocarbon Distribution Map, ORNL Project 78X 382 84V, Eddy and Lea Counties, New Mexico.

Schaller, W. T., and E. P. Henderson, 1932. "Mineralogy of Drill Cores From the Potash Field of New Mexico and Texas," U.S. Geological Survey Bulletin No. 833, 124 pp.

Sipes, Williamson, and Aycock, Inc., 1976. "Hydrocarbon Evaluation, Proposed Southeastern New Mexico Radioactive Material Storage Site, Eddy County, New Mexico," report submitted to Sandia National Laboratories, Albuquerque, New Mexico.

Siemers, W. T., J. W. Hawley, C. Rautman, and C. Austin, 1978. "Evaluation of the Mineral Potential (Excluding Hydrocarbons, Potash and Water) of the Waste Isolation Pilot Plant Site, Eddy County, New Mexico," New Mexico Bureau of Mines and Mineral Resources, report to Sandia National Laboratories, Albuquerque, New Mexico.

Smith, A. R., 1978. "Sulfur Deposits in Ochoan Rocks of Southeast New Mexico and West Texas," in Geology and Mineral Deposits of Ochoan Rocks in Delaware Basin and Adjacent Areas, New Mexico Bureau of Mines and Mineral Resources Circular 159, pp. 71-76.

U.S. Bureau of Land Management, 1975. Preliminary Regional Environmental Analysis Record--Potash Leasing in Southeastern New Mexico, Department of the Interior, New Mexico State Office.

U.S. Bureau of Land Management, 1977. East Eddy Planning Unit; Unit Resource Analysis, Department of the Interior, Roswell, New Mexico.

U.S. Bureau of Land Management (U.S. Bureau of Mines), 1977. Valuation of Potash Occurrences Within the Waste Isolation Pilot Plant Site in Southeastern New Mexico, report to the Energy Research and Development Administration.

U.S. Geological Survey, 1979. Preliminary Map Showing Distribution of Potash Resources, Carlsbad Mining District, Eddy and Lea Counties, New Mexico, OFR 79-1579.

U.S. Soil Conservation Service, 1971. Soil Survey of Eddy Area, New Mexico, U.S. Department of Agriculture, Government Printing Office, Washington, D.C.

U.S. Soil Conservation Service, 1974. Soil Survey of Lea County, New Mexico, U.S. Department of Agriculture, Government Printing Office, Washington, D.C.

APPENDIX K

DOE READING ROOMS AND PUBLIC LIBRARIES

Harvard University, Library of the Museum of Comparative Zoology

TABLE OF CONTENTS

Section		Page
K.1	INTRODUCTION	K-1

LIST OF TABLES

Table		Page
K.1.1	Location of DOE Public Reading Rooms Receiving SEIS Documents and References	K-2
K.1.2	Location of Public Libraries Receiving SEIS Documents	K-3

Digitized by the Internet Archive in 2011 with funding from Boston Public Library

K.1 INTRODUCTION

This appendix contains lists of the DOE public reading rooms and public libraries that will receive copies of this SEIS, including appendices; the 1980 FEIS; the 1980 Executive Summary; and the 1981 Record of Decision (Table K.1.1 and K.1.2). As

Appendix K	K-1	Third line	"As noted on the tables, the DOE public reading rooms plus the city libraries of Carlsbad, Albuquerque, and Santa Fe, New Mexico have available complete sets of the supporting documents referenced in the Draft SEIS," should read, "As noted on the tables, the DOE public reading rooms plus the city libraries of Carlsbad and Santa Fe, New Mexico; the Zimmerman Library on the UNM Campus in Albuquerque, New Mexico; and the New Mexico State Library in Santa Fe, New Mexico have available complete sets of the supporting documents referenced in this Draft SEIS."

UNIVERSITY OF CALIFORNIA
LIBRARY

K.1 INTRODUCTION

This appendix contains lists of the DOE public reading rooms and public libraries that will receive copies of this SEIS, including appendices; the 1980 FEIS; the 1980 Executive Summary; and the 1981 Record of Decision (Table K.1.1 and K.1.2). As noted on the tables, the DOE public reading rooms plus the city libraries of Carlsbad, Albuquerque, and Santa Fe, New Mexico have available complete sets of the supporting documents referenced in this Draft SEIS (Table K.1.2).

TABLE K.1.1 Location of DOE public reading rooms receiving SEIS documents and References[a]

U.S. Department of Energy-HQ
Public Reading Room
Room 1E-190 Forrestal Building
1000 Independence Ave SW
Washington, DC 20585
(202-586-6020)

U.S. Department of Energy-ID
Public Reading Room
University Place
1776 Science Center Drive
Idaho Falls, ID 83402
(208-526-1144)

U.S. Department of Energy-NV
Public Reading Room
2753 South Highland Street
Las Vegas, NV 89109
(702-295-1274)

U.S. Department of Energy-OR
Public Reading Room
Federal Building
200 Administration Road
Oak Ridge, TN 37830
(615-576-1216)

National Atomic Museum
Public Reading Room
Wyoming Boulevard South
Kirtland Air Force Base
Albuquerque, NM 87115
(505-844-4378)

U.S. Department of Energy-RL
Public Reading Room
Hanford Science Center
825 Jadwin Avenue
Richland, WA 99352
(509-376-8583)

U.S. Department of Energy-SR
FOI Publication/Document Room
University of South Carolina - Aiken
Gregg - Graniteville Library
171 University Parkway
Aiken, SC 29801
(803-725-1408)

U.S. Department of Energy-SFO
Public Reading Room
1333 Broadway, 7th Floor
Oakland, CA 94612
(415-273-4428)

U.S. Department of Energy-CH
Public Reading Room
9800 South Cass Avenue, Building 201
Argonne, IL 60439
(312-972-2010)

[a] Complete sets of the supporting documents referenced in this SEIS are available at these locations.

TABLE K.1.2 Location of public libraries receiving SEIS documents

Alabama Public Library Service
6030 Monticello Drive
Montgomery, AL 36104
(205-277-7330)

Arkansas State Library
1 Capitol Mall
Little Rock, AR 72201
(501-682-1527)

Arizona Library, Archives and Public Records
1700 W. Washington
Phoenix, AZ 85701
(602-542-4159)

California Libraries Division
Library and Courts Building

Add: Denver Public Library
Government Publications
Department
1357 Broadway
Denver, CO 80203
(303) 571-2000

Boulder, CO 80309
(303-492-7511)

Denver Public Library
Government Documents Room
Second Floor
1357 Broadway
Denver, CO 80203-2165
(303-571-2000)

Georgia State Library
301 Judicial Building
Atlanta, GA 30334
(404-656-3468)

Library - Region 2
U.S. Nuclear Regulatory Commission
101 Marietta Street, Suite 3100
Atlanta, GA 30303
(404-331-5518)

Idaho State Library
325 W. State Street
Boise, ID 83702
(208-334-5124)

Indiana State Library
140 N. Senate Avenue
Indianapolis, IN 46204
(317-232-3675)

Illinois Department of Nuclear Safety
1035 Outer Park Drive
Springfield, IL 62704
(217-524-5968)

Illinois State Library Division
275 Centennial Building
Springfield, IL 62756
(271-782-2994)

Legislative Research Library

Missouri State Library
2002 Missouri Blvd.
Jefferson City, MO 65102
(314-751-3615)

Mississippi Library Commission
1221 Ellis Avenue
Jackson, MS 39209
(601-359-1036)

Nevada State Library and Archives
Federal Documents
Capitol Complex
401 N. Carson Street
Carson City, NV 89710
(702-885-5160) (800-922-2880)

Mississippi Bureau of Geology
2525 N. West Street
Jackson, MS 39216
(601-354-6228)

TABLE K.1.1 Location of DOE public reading rooms receiving SEIS documents and References[a]

U.S. Department of Energy-HQ
Public Reading Room
Room 1E-190 Forrestal Building
1000 Independence Ave SW
Washington, DC 20585
(202-586-6020)

U.S. Department of Energy-ID
Public Reading Room
University Place
1776 Science Center Drive
Idaho Falls, ID 83402
(208-526-1144)

U.S. Department of Energy-NV
Public Reading Room
2753 South Highland Street
Las Vegas, NV 89109
(702-295-1274)

U.S. Department of Ene
Public Reading Room
Federal Building
200 Administration Road
Oak Ridge, TN 37830
(615-576-1216)

National Atomic Museum
Public Reading Room
Wyoming Boulevard South
Kirtland Air Force Base
Albuquerque, NM 87115
(505-844-4378)

U.S. Department of Energy-RL
Public Reading Room
Hanford Science Center
825 Jadwin Avenue
Richland, WA 99352
(509-376-8583)

U.S. Department of Energy-SR
FOI Publication/Document Room
University of South Carolina - Aiken
Gregg - Graniteville Library
171 University Parkway
Aiken, SC 29801
(803-725-1408)

U.S. Department of Energy-SFO
Public Reading Room
1333 Broadway, 7th Floor
Oakland, CA 94612

[a] Complete sets of the supporting documents referenced in this SEIS are available at these locations.

TABLE K.1.2 Location of public libraries receiving SEIS documents

Alabama Public Library Service
6030 Monticello Drive
Montgomery, AL 36104
(205-277-7330)

Arkansas State Library
1 Capitol Mall
Little Rock, AR 72201
(501-682-1527)

Arizona Library, Archives and Public Records
1700 W. Washington
Phoenix, AZ 85701
(602-542-4159)

California Libraries Division
Library and Courts Building
914 Capitol Mall
Sacramento, CA 95814
(916-445-8833)

Government Publications
Norlin Library
University of Colorado/Boulder
18th and Colorado Streets
Campus Box 184
Boulder, CO 80309
(303-492-7511)

Denver Public Library
Government Documents Room
Second Floor
1357 Broadway
Denver, CO 80203-2165
(303-571-2000)

Georgia State Library
301 Judicial Building
Atlanta, GA 30334
(404-656-3468)

Library - Region 2
U.S. Nuclear Regulatory Commission
101 Marietta Street, Suite 3100
Atlanta, GA 30303
(404-331-5518)

Idaho State Library
325 W. State Street
Boise, ID 83702
(208-334-5124)

Indiana State Library
140 N. Senate Avenue
Indianapolis, IN 46204
(317-232-3675)

Illinois Department of Nuclear Safety
1035 Outer Park Drive
Springfield, IL 62704
(217-524-5968)

Illinois State Library Division
275 Centennial Building
Springfield, IL 62756
(271-782-2994)

Legislative Research Library
State Capitol Building
13th Floor
Baton Rouge, LA 70804
(504-342-4923)

State Library of Louisiana
760 Riverside North
Baton Rouge, LA 70821
(504-342-4923)

Missouri State Library
2002 Missouri Blvd.
Jefferson City, MO 65102
(314-751-3615)

Mississippi Library Commission
1221 Ellis Avenue
Jackson, MS 39209
(601-359-1036)

Nevada State Library and Archives
Federal Documents
Capitol Complex
401 N. Carson Street
Carson City, NV 89710
(702-885-5160) (800-922-2880)

Mississippi Bureau of Geology
2525 N. West Street
Jackson, MS 39216
(601-354-6228)

TABLE K.1.2 Concluded

Zimmerman Library [a]
Government Publications
University of New Mexico
Roma Avenue and Yale Boulevard
Albuquerque, NM 87131
(505-277-5441)

Carlsbad Public Library [a]
Public Document Room
101 South Halagueno Street
Carlsbad, NM 88220
(505-885-6776)

New Mexico State Library
325 Don Gaspar
Santa Fe, NM 87503
(505-827-3800)

Santa Fe Public Library [a]
145 Washington Avenue
Santa Fe, NM 87501
(505-984-6780)

Ohio Library Board
65 S. Front Street
Columbus, OH 43266
(614-644-7061)

Oklahoma Libraries Department
200 NE 18th Street
Oklahoma City, OK 73105
(405-521-2502)

Oregon State Library
State Library Building
Court and Summer Streets
Salem, OR 97310
(503-378-4277)

South Carolina State Library
1500 Senate Street
Columbia, SC 29201
(803-734-8666)

Silas Mason Company Inc.
East Highway 60
Amarillo, TX 79177
(806-477-3000)

Texas Library and Archives Commission
1201 Brazos Street
Austin, TX 78701
(512-463-5460)

Utah State Library
2150 South 300 West
Suite 16
Salt Lake City, UT 84115
(801-466-5888)

State of Washington
Department of Ecology Library
Abbott Raphael Building
St. Martins College Campus
Olympia, WA 98504
(206-459-6150)

Washington State Library
State Library Building
16th and Water Streets
Olympia, WA 98504
(206-753-5590)

Wyoming Library Department
Supreme Court Building
Capitol Avenue, between 22nd and 24th
Cheyenne, WY 82002
(307-777-6333)

[a] Complete sets of the supporting documents referenced in this SEIS are available at these locations.

☆U.S. GOVERNMENT PRINTING OFFICE: 1989-674-580

Digitized by the Internet Archive in 2010 with funding from Boston Public Library

UNIVERSITY OF ILLINOIS-URBANA
3 0112 075681137